Fisheries and Oceans Canada | Pêches et Océans Canada
Ecosystems and Oceans Science | Sciences des écosystèmes et des océans

Canadian Science Advisory Secretariat (CSAS)

Research Document 2021/004

Pacific Region

Walleye Pollock (*Theragra chalcogramma*) stock assessment for British Columbia in 2017

Paul J. Starr[1] and Rowan Haigh[2]

[1]Canadian Groundfish Research and Conservation Society
1406 Rose Ann Drive
Nanaimo, British Columbia, V9T 4K8

[2]Pacific Biological Station
Fisheries and Oceans Canada
3190 Hammond Bay Road
Nanaimo, British Columbia, V9T 6N7

June 2021

Foreword

This series documents the scientific basis for the evaluation of aquatic resources and ecosystems in Canada. As such, it addresses the issues of the day in the time frames required and the documents it contains are not intended as definitive statements on the subjects addressed but rather as progress reports on ongoing investigations.

Published by:

Fisheries and Oceans Canada
Canadian Science Advisory Secretariat
200 Kent Street
Ottawa ON K1A 0E6

http://www.dfo-mpo.gc.ca/csas-sccs/
csas-sccs@dfo-mpo.gc.ca

ISSN 1919-5044
ISBN 978-0-660-38449-8 Cat. No. Fs70-5/2021-004E-PDF

Correct citation for this publication:

Starr, P.J. and Haigh, R. 2021. Walleye Pollock (*Theragra chalcogramma*) stock assessment for British Columbia in 2017. DFO Can. Sci. Advis. Sec. Res. Doc. 2021/004. vii + 265 p.

Aussi disponible en français :

*Starr, P.J. et Haigh, R. 2021. Évaluation du stock de goberge de l'Alaska (*Theragra chalcogramma*) pour la Colombie-Britannique en 2017. Secr. can. de consult. sci. du MPO. Doc. de rech. 2021/004. viii +294 p.*

TABLE OF CONTENTS

LIST OF MAIN TABLES

LIST OF MAIN FIGURES

ABSTRACT

A new stock assessment is presented for two British Columbia (BC) stocks of Walleye Pollock (*Theragra chalcogramma*, WAP), with the BC North stock encompassing the three most northerly Pacific Marine Fisheries Commission (PMFC) major areas (5C, 5D, 5E) and the BC South stock including the remaining four outside PMFC major areas (3C, 3D, 5A, 5B plus minor areas 12 & 20). These stock definitions were selected on the basis of a difference in observed mean weights, with BC North mean weights estimated near 1.0 kg/fish while the equivalent BC South mean weights averaged near 0.5 kg/fish. A delay-difference production model was used to assess each stock, using data from fishery-independent surveys, a CPUE series derived from commercial bottom trawl catch rates, and an annual mean weight series derived from unsorted commercial catch samples. Because there are no useable BC ageing data, we used survey age samples from the Gulf of Alaska (GoA) to specify growth for the BC North stock. The BC South stock proved more problematic, with the GoA growth model unable to fit the BC South observed mean weights, eventually requiring us to use a published WAP growth model from the Asian Sea of Okhotsk. Each stock assessment explored a range of plausible natural mortality values as well as a range of ages for the knife-edge selectivity assumption because the biomass indices and the mean weight data used in the delay-difference model were not informative for these parameters. The stock assessment was conducted in a Bayesian framework, where the best fit to the data was used as the starting point for a search across the joint posterior parameter distributions using the Monte Carlo Markov Chain (MCMC) procedure. Twelve runs were made for the BC North stock and 11 for the BC South stock, with each run consisting of 60 million MCMC iterations, sampling every 50,000th iteration, discarding the first 200 draws for burn-in, leaving 1,000 draws to comprise the posterior. Composite reference (model averaged) scenarios were used to represent each stock, with the model average for both stocks consisting of eight model runs selected on the basis of a subjective evaluation of the quality of the MCMC posterior. Each composite reference scenario included three values for instantaneous natural mortality (M=0.25, 0.30, 0.35) and covered two or three ages at which knife-edge recruitment (k) to the fishery occurred (k=3, 4 in BC North and including k=5 in BC South). The MCMC posteriors for the two composite scenarios were constructed by pooling the 1000 MCMC samples from each of the selected runs to give a posterior of 3,000 samples for BC North and 6,000 samples for BC South, thus giving equal weight to each run. The composite reference scenario was evaluated against historical reference points (HRPs) based on the reconstructed spawning biomass trajectory due to concerns about the stability of estimating B_0 and B_{2017}. The HRP B_{avg}, the average spawning biomass from 1967-2016, was used as a proxy for B_{MSY}, and B_{min}, the minimum spawning biomass from which it subsequently recovered to B_{avg}, was used in place of 0.4B_{MSY}. Twice B_{min} was used in place of 0.8B_{MSY}. The average exploitation rate over the period 1967-2016 (u_{avg}) was used in place of u_{MSY}. The biomass at the beginning of 2017 for the model average BC North stock was evaluated as being primarily above the USR while the 2017 beginning year biomass for the BC South stock was evaluated as being entirely above the USR. For each stock, the assessment provides a decision table which evaluates the probability of the model average case staying above five reference points across a wide range of 22 constant catches. However, the paper warns that the probabilities in these decision tables should be viewed cautiously as the delay-difference model used in this stock assessment is not capable of making reliable multi-year projections because it has no latent age structure to inform predictions and the stock-recruitment function is poorly determined.

1. INTRODUCTION

Walleye Pollock (*Theragra chalcogramma*, acronym WAP) shares an evolutionary lineage with the Pacific, Atlantic, and Greenland Cods (*Gadus macrocephalus*, *G. morhua*, and *G. ogac*, respectively). The Alaskan stock assessment group currently uses the 2013 taxonomic nomenclature change for this species, adopting the new name *Gadus chalcogrammus* (masculine genus name) over *Theragra chalcogramma* (feminine). In this assessment, we use *Theragra chalcogramma*.

Walleye Pollock's appearance features an olive green to brown colour dorsally, often mottled or blotched; silvery on its sides, and pale ventrally; the fins are darker (Cohen et al. 1990). In Alaska, the species has been observed to reach a maximum length of 105 cm, a maximum weight of 6.05 kg, and a maximum age of 22 years (NOAA 2010). In British Columbia (BC), the observed maximum length was also 105 cm for a male specimen caught off the southeast coast of Moresby Island (PMFC major 5C, minor 6, locality 2) at 94 m in June 2015 (DFO GFBio database, accessed Dec 13, 2016).

This species is a semi-demersal (30-400 m) schooling fish that performs diurnal vertical migrations and becomes increasingly associated with the bottom as the fish ages (Cohen et al. 1990, NOAA 2010). It reaches first maturity at 3-4 years (30 to 38 cm total length); fecundity varies with age (Cohen et al. 1990). Fish congregate in dense schools to spawn, usually at 50-250 m depth; spawning in the Strait of Georgia occurs from January to March (Cohen et al. 1990). In BC, Walleye Pollock prey upon shrimps, sand lance, and herring (Cohen et al. 1990); predation on juvenile pollock (cannibalism) and other bony fish is reported in the eastern Bering Sea (NOAA 2010).

The Alaskan Walleye Pollock fisheries support the largest landings of any single species in the USA, and possibly in the world. The highest concentrations of pollock occur in the Eastern Bering Sea (annual catches > 1 million tonnes, Ianelli et al. 2015) with lesser amounts caught in the Gulf of Alaska (annual catches > 100,000 tonnes, Dorn et al. 2015). These Alaskan fisheries are supported by complex age-structured stock assessment models, reflecting a strong investment by government in acoustic and trawl surveys, catch sampling and an intensive ageing program. In BC, the annual 2016 coastwide TAC was 4225 t comprising 1320 t in PMFC 5CDE, 1790 t in 5AB, and 1115 t in the Strait of Georgia. No TAC has ever been set for 3CD other than a 270 t quota set in 1997 only Appendix A. In this assessment, we consider two stocks: "BC North" (PMFC 5CDE) and "BC South" (PMFCs 5AB+3CD + minor areas 12 & 20), for reasons outlined below.

The last stock assessment of Walleye Pollock (WAP) was conducted in 1997 (Saunders and Andrews 1998[1]). This was a qualitative assessment that did not estimate stock status with respect to established reference points, partially because the DFO Precautionary Approach reference points had not been set. Harvest advice is required for this species to determine if current harvest levels are sustainable and are compliant with the DFO Fishery Decision-Making Framework Incorporating the Precautionary Approach (DFO 2006, 2009). A request was submitted to Science by staff in the Fisheries and Aquaculture Management's Groundfish Management Unit (GMU) in 2013 but was considered unachievable due to data limitations. In 2016, a review of the available data suggested that Science could potentially assess Walleye Pollock using a delay-difference model similar to the approach used to assess Shortspine

[1] Saunders, M.W. and Andrews, W. 1998. Walleye pollock stock assessment for 1997 and recommended yield options for 1998. PSARC Working Paper G:97-7, 18 pp, Pacific Biological Station, DFO, Nanaimo BC, Canada.

Thornyhead (*Sebastolobus alascanus*) in 2016 (Starr and Haigh 2017). Initial runs treated the entire offshore region of BC as a single stock (excluding the Strait of Georgia, Figure 1); however, after some exploration, it became clear that a more tenable hypothesis was that there were at least two separate stocks, given the large difference in observed mean weight in the respective fisheries: BC North (1.056 kg/fish) vs. BC South (0.521 kg/fish).

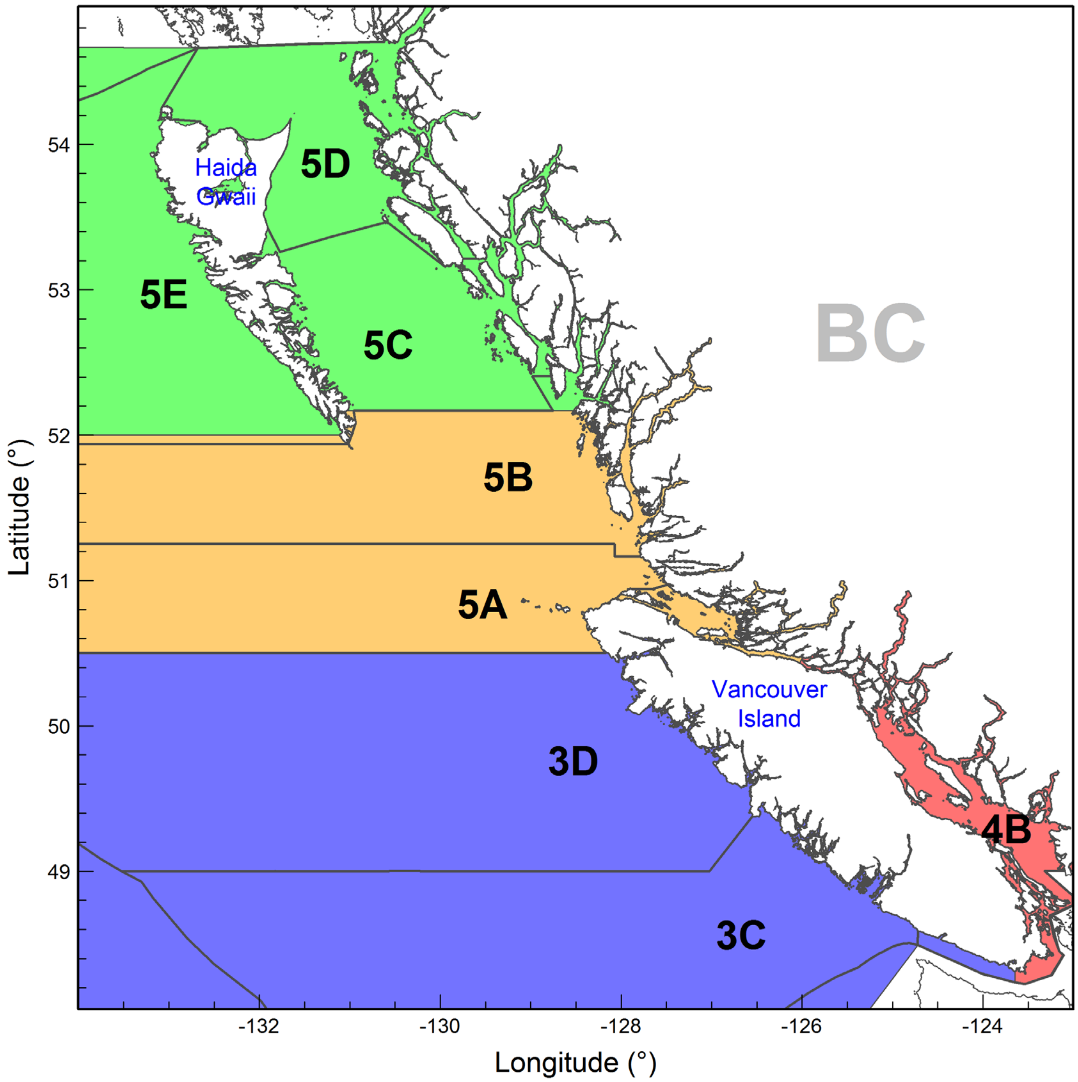

Figure 1. Walleye Pollock assessment areas comprising Pacific Marine Fisheries Commission (PMFC) major and minor areas – green for 5CDE, orange for 5AB + minor area 12, blue for 3CD + minor area 20, and red for 4B less minor areas 12 and 20. The Groundfish Management Unit area boundaries, which differ from PMFC area, are superimposed for comparison. This assessment is for areas called 'BC North' (5CDE, green) and 'BC South' (5AB3CD, orange + blue).

The modelling of these stocks presented many difficulties, primarily associated with a scarcity of usable data. In particular, there were almost no age data for BC pollock with the small amount of available data determined using an ageing methodology known to be biased. We were forced to go outside of BC to obtain usable age-length data, using survey derived data from the eastern Gulf of Alaska (Martin Dorn, pers. comm.) for BC North (see Appendix D). Suitable growth data for BC South pollock proved harder to find, requiring us to use a growth model from the Sea of Okhotsk (Janusz and Horbowy 1997), which lies between the eastern Russian mainland and Kamchatka Peninsula, just west of the Bering Sea. A further problem was the generation of unstable reference points based on maximum sustainable yield (MSY) calculations. This issue necessitated the adoption of historical-based reference points (HRPs), specifically the average estimated spawning biomass over the full time period of the model (1967-2016), denoted B_{avg} and a limit reference point (LRP) set to the minimum estimated spawning biomass in a year from which the biomass trajectory recovered to above B_{avg}. The mode of the posterior distribution (MPD) for this year was B_{2001} for BC North and B_{2008} for BC South. The upper stock reference (USR) was set to twice the LRP. The advice is provided in decision tables that give the probability that $B_{2018,\,2019}$ (1- and 2-year projected spawning biomass) will be greater than the various reference points (Appendix F).

1.1. RANGE AND DISTRIBUTION

Walleye Pollock occur along the North Pacific rim, ranging from the Sea of Japan, extending north into Russian and Alaskan waters, then down through BC and southward to southern California (FAO Aquatic Species Distribution Map Viewer, accessed May 8, 2017). The species primarily hugs the coastline in this range, but form two large population centres in the Sea of Okhotsk and the Bering Sea. In BC, there are four primary spawning grounds – Dixon Entrance/northern Hecate Strait, Queen Charlotte Sound, SW Vancouver Island, and the Strait of Georgia (Saunders et al. 1989). These are reflected by high CPUE density in Figure 2, which also shows an additional hotspot in upper Moresby Gully. The bulk (98%) of the commercial captures from the BC North population lies between depths 55 m and 457 m while those from BC South lie between 90 m and 401 m in 5AB and between 64 m and 470 m in 3CD (Appendix D).

1.2. ASSESSMENT BOUNDARIES

This assessment includes Pacific Marine Fisheries Commission (PMFC) major areas 5CDE for the BC North stock and PMFC major areas 5AB and 3CD plus minor areas 12 (Queen Charlotte Strait) and 20 (entrance to Juan de Fuca Strait) for the BC South stock (Figure 1). These assessed areas are similar to the GMU TAC (total allowable catch) areas, so managers can divide any recommended catch, delimited by brackets [ ], using simple TAC ratios:

$$\mathrm{TAC}_{5CDE} = [\mathrm{BC\ North}];$$

$$\mathrm{TAC}_{5AB} = [\mathrm{BC\ South}]\left(\frac{\mathrm{TAC}_{5AB}}{\mathrm{TAC}_{5AB} + \mathrm{TAC}_{3CD}}\right);$$

$$\mathrm{TAC}_{3CD} = [\mathrm{BC\ South}]\left(\frac{\mathrm{TAC}_{3CD}}{\mathrm{TAC}_{5AB} + \mathrm{TAC}_{3CD}}\right).$$

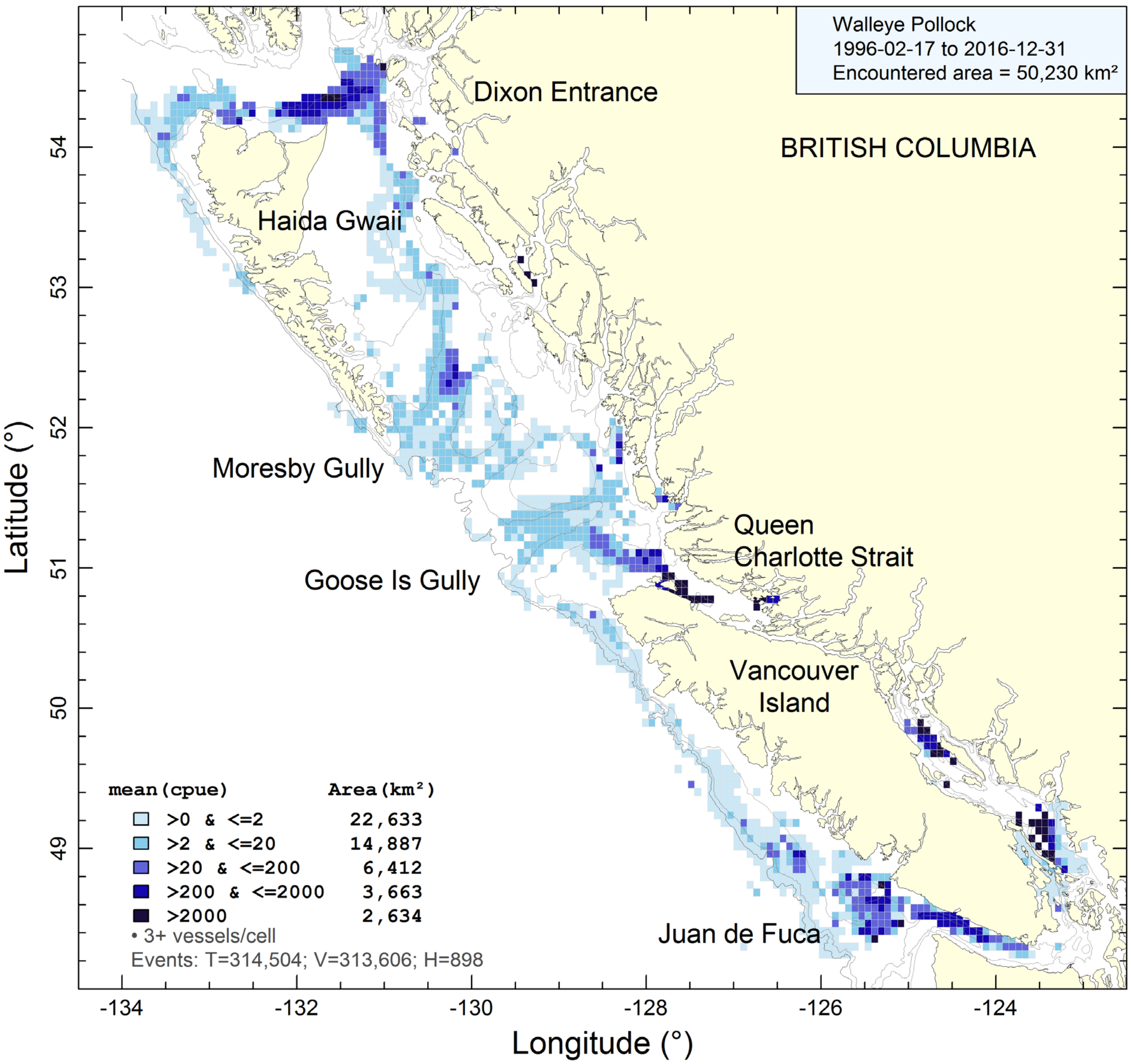

Figure 2. Aerial distribution of Walleye Pollock mean trawl (combined bottom and midwater trawl) tow catch per unit effort (kg/hour) from Feb 17, 1996 to Dec 31, 2016 (accessed May 3, 2017). Isobaths show the 100, 200, and 500 m depth contours. Note that cells with <3 fishing vessels are not displayed. Each cell represents, on average, 32 km².

2. CATCH DATA

The preparation methods and a full catch history for the assessment of the two Walleye Pollock stocks are presented in detail in Appendix A. The catch used in the model appears in Table A.7. The 5-year average catch (over 2011-15) was 992 t in BC North and 3,256 t for BC South. Information about species caught concurrently with WAP commercial catches are presented in Appendix D.

3. FISHERIES MANAGEMENT

Table A.2 summarises all management actions taken for Walleye Pollock since 1981. The last assessment of Walleye Pollock was conducted in 1997 (Saunders and Andrews 1998[1]) – an assessment that did not estimate stock status with respect to DFO Precautionary Approach reference points. Harvest advice is required for this species to determine if current harvest levels are sustainable and are compliant with the DFO Sustainable Fisheries Framework's Decision-making Framework incorporating the Precautionary Approach. A request was submitted to Science by staff in the Fisheries and Aquaculture Management's Groundfish Management Unit in 2013 but was considered unachievable due to data limitations.

One of the conditions from the 2014 Marine Stewardship Council (MSC) Canadian hake fishery certification was that a Pollock assessment be completed by 2018. In response to this MSC condition, the December 5, 2014 GTAC (Groundfish Trawl Advisory Committee) Summary states: "*GTAC recommended that DFO ensure that redstripe, pollock and rougheye be assessed by 2018 to ensure compliance with the MSC conditions*".

4. SURVEY DESCRIPTIONS

Four sets of fishery independent survey indices have been used to track changes in the biomass of the BC North population (Appendix B):

1. Goose Island Gully (GIG) Historical[2] – an early series of 9 indices extending from 1967 to 1995. Most of these surveys were performed by the research vessel *G.B. Reed*, but two commercial vessels (*Eastward Ho* and *Ocean Selector*) were used in 1984 and 1994 respectively. The 1995 survey used both the *Ocean Selector* and the *Frosti*. Only tows located in GIG were used to ensure continuity across all surveys.
2. HS Assemblage – a series of 11 indices spanning 1984 to 2003. The original design of this survey assigned fishing locations by 10-fathom depth intervals within a 10 nautical mile grid of Hecate Strait (HS). The HS Assemblage survey was designed as a systematic fixed-station survey. In 2004, this survey series was discontinued in favour of the HS Synoptic survey.
3. HS Synoptic – a random-stratified "synoptic" (species comprehensive) trawl survey covering all of Hecate Strait and extending into Dixon Entrance and across the top of Graham Island. This survey has been repeated 6 times between 2005 to 2015 using two vessels and a consistent design, including targeting a wide range of finfish species.
4. WCHG Synoptic – a random-stratified synoptic trawl survey covering the west coast (WC) of Graham Island in Haida Gwaii (HG) and western part of Dixon Entrance. This survey has been repeated 6 times between 2006 to 2016 using three vessels and a consistent design, including targeting a wide range of finfish species.

Three sets of fishery independent survey indices have been used to track changes in the biomass of the BC South population (Appendix B):

1. Goose Island Gully (GIG) Historical– an early series of 9 indices extending from 1967 to 1995. Most of these surveys were performed by the research vessel *G.B. Reed*, but two commercial vessels (*Eastward Ho* and *Ocean Selector*) were used in 1984 and 1994

[2] Strictly speaking, this survey did not operate in the stock definition area for the BC North stock. However, because this series is the only set of early abundance information, two blocks of stock assessment runs were made for this stock, one with and one without this survey.

respectively. The 1995 survey used both the *Ocean Selector* and the *Frosti*. Only tows located in GIG were used to ensure continuity across all surveys.

2. WCVI Synoptic – a random-stratified synoptic trawl survey covering the west coast of Vancouver Island (WCVI). This survey has been repeated 7 times between 2004 to 2016 using the same vessel and a consistent design, including targeting a wide range of finfish species.
3. QCS Synoptic – a random-stratified synoptic trawl survey covering all of Queen Charlotte Sound (QCS) and targeting a wide range of finfish species. This survey has been repeated 8 times between 2003 to 2015, using three different vessels (see Table B.10) but with a consistent design.

The relative biomass survey indices were used as data in the model to index abundance, along with their associated relative errors to weight each index value inversely proportional to its variance. All surveys in the Synoptic series use the same net, an Atlantic Western IIA box trawl net.

5. COMMERCIAL TRAWL CPUE

Commercial catch and effort data from the bottom trawl fishery were used to generate indices of abundance for Walleye Pollock in this stock assessment (Figure 3, Figure 4). This was done for several reasons, with the primary reason being the lack of long-term abundance information for use in this model. In addition, it was hoped that the nature of the bottom trawl fishery, with all of the WAP catches taken while targeting other groundfish species, would result in an index series that was not unduly affected by economic considerations.

The theoretical basis for the analysis is described in Appendix C, Section C.2. The analysis (Sections C.3 and C.4) is based on tow-by-tow data which reported Walleye Pollock landings or discards or which operated in a depth range where WAP would be expected to be caught. The period analysed was from 1996, when compulsory onboard observer coverage began, to 2015, the last complete year of data. Three analyses were performed for each stock:

- a regression analysis on all positive catch records which assumed a log-normal distribution, where the effect on catch rates by DFO locality, fishing depth, month, 0.1° latitude bands, hours fished and vessel were estimated and removed from the trend, leaving a standardised annual abundance trend;
- a similar analysis using the presence/absence of WAP in the data set, which assumed a binomial distribution and which removed the effects of DFO locality, fishing depth, month, 0.1° latitude bands and hours fished, resulting in an alternative annual abundance trend; and
- an analysis which combined the log-normal and binomial series using the delta-lognormal method of Vignaux (1994; see Equation C.4).

The combined series was used as input to the WAP stock assessment models for the BC North (Figure 3) and the BC South (Figure 4) stocks. The initial decline in the index may have been partly influenced by the adjustment to a new regulatory regime (onboard observers, transferrable individual vessel quotas). Model sensitivity runs which dropped this series were made to investigate the impact of the CPUE series in the stock assessment.

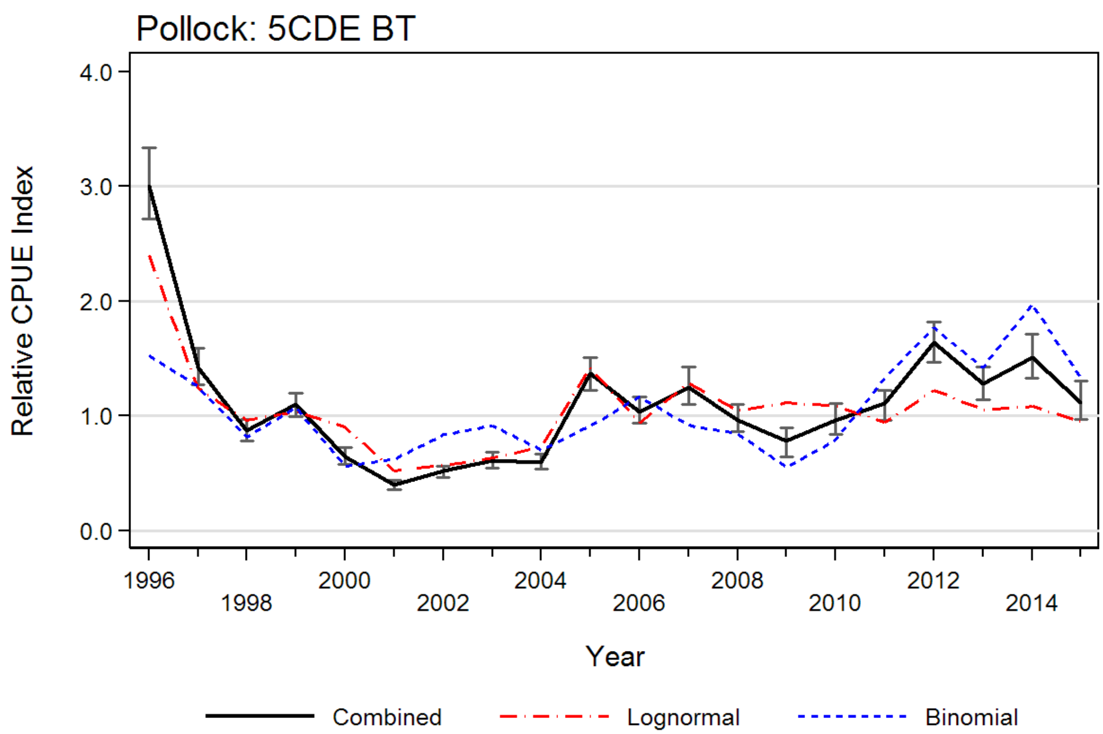

Figure 3. Combined index series for the BC North bottom trawl fishery along with the contributing lognormal and binomial index series, all normalised on their respective geometric means. The 95% confidence bounds are based on 500 bootstrap replicates.

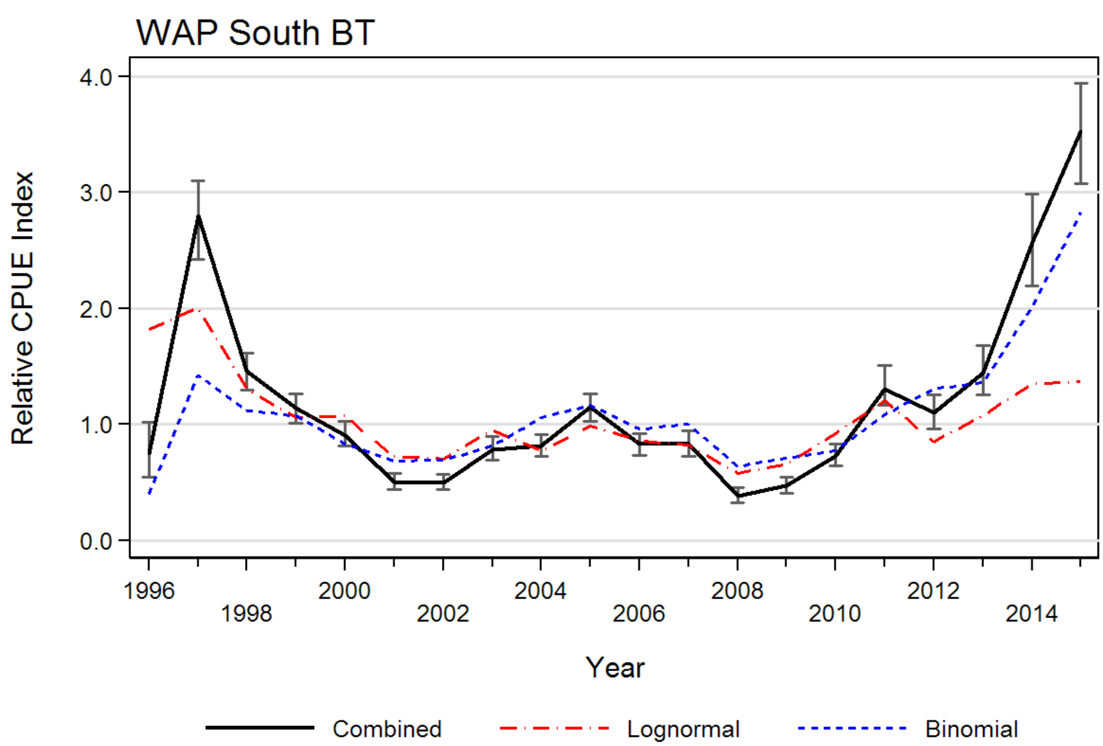

Figure 4. Combined index series for the BC South bottom trawl fishery. Details in Figure 3 caption.

6. BIOLOGICAL INFORMATION

6.1. NATURAL MORTALITY

Although the Alaskan fisheries stock assessments use age-specific mortality rates for Walleye Pollock, the underlying assumption is that M = 0.30 at full maturity (Dorn et al. 2015). Age-specific M values of 0.90, 0.45, and 0.30 for ages 1, 2 and 3+, respectively, have been used in Alaskan Eastern Bering Sea catch-age models since 1982 (Ianelli et al. 2015). The delay-difference model (Section 7) assumes that maturity matches selectivity, i.e., all recruited fish are mature with a single natural mortality rate. Runs were made with M=0.25, M=0.30 and M=0.35 to bracket plausible values for this parameter.

6.2. KNIFE-EDGE SELECTIVITY

Dorn et al. (2012) provide a range of selectivity ogives for the Gulf of Alaska (GoA) fisheries and surveys, with the median age selected to these commercial fisheries ranging from age 3 to age 5 (see columns 5 to 7 in Table D.8). Based on the ogives in this table, ages 3 and 4 were selected as the most likely ages to use for the age of knife-edge recruitment in the WAP delay-difference model. Knife-edge selectivity at age 5 was also run as an additional sensitivity for the BC South stock because of the lower maximum size in the growth model used for this stock.

6.3. GROWTH PARAMETERS

Growth parameters were estimated from WAP length and age data from DFO biological samples collected from 1976 to 1995 (Appendix D); however, ages determined by the break and burn method (MacLellan 1997) existed for only 17 specimens from commercial trips (16 in BC North, 1 in BC South). Otoliths from commercial sources and aged by surface readings were more abundant (230 in BC North, 399 in BC South) but are known to be biased (Stanley 1987), at least for Pacific rockfish species. The remaining processed otoliths came from research surveys but were aged using pectoral fin ray counts (638 in BC South) or an unknown method (210 in BC South). Unfortunately, pectoral fin ageing is thought to be biased, especially at older ages (MacLellan et al. 1990[3]), because fin ray deposition slows down or ceases at older ages.

As the DFO age data were insufficient to derive growth parameters not biased by ageing methodology, we approached an Alaskan colleague, Martin Dorn (Research Fish Biologist, NOAA Fisheries, Sand Point, Seattle), who supplied 8,882 age-length pairs randomly selected from six biannual surveys conducted in the Gulf of Alaska (GoA) between 2005 and 2015. These fish had all been aged from otoliths prepared using the “break & burn” method and he advised us to use the samples from the Eastern GoA as growth varied across the GoA. We used these data to estimate a growth function (L_{∞} = 66.944 cm, K = 0.212, t_0 = -1.136, Figure 5) for the BC North stock that adequately fit the mean weight data for three knife-edge ages 3, 4, and 5 (Appendix D). However, we could not use this function for the BC South stock because fish sampled from Dixon Entrance were, on average, twice as large as those sampled from more southern BC waters. This North stock likely belongs to a larger stock that includes Dixon Entrance, northern Hecate Strait, and waters off of Southeast Alaska (Gustafson et al. 2000).

For the BC South stock, other sources were explored. Growth functions based on fin ray ages published by Saunders et al. (1989) for the west coast of Vancouver Island (3CD) and the Strait

[3] MacLellan, S.E., Gillespie, D., Janz, S., Charles, K., Little, D. and Rankin, J. 1990. Age determination of various freshwater fish species being analyzed for dioxin and furan studies in B.C., 1989. Unpub. tech. rep., Pacific Biological Station, DFO, Nanaimo BC, Canada.

of Georgia (apparently derived from age-length pairs not available in the general DFO database) were tested but featured growth rate coefficients that were so steep that neither function could fit the South mean weight data satisfactorily. NOAA colleagues, who work on pelagic fish off the west coasts of Washington and Oregon, indicated that age-length pairs from fisheries off Washington or Oregon were non-existent. In the end, we found a growth function published by Janusz and Horbowy (1997) for Walleye Pollock in the central Sea of Okhotsk (*L*¥ = 50.827 cm, *K* = 0.199, t_0 = -1.790, Figure 5), which provided satisfactory fits to the observed BC South mean weight data for knife-edge ages 3 and 4 (Appendix D). We have no reason to believe that the Sea of Okhotsk (OS) relationship represents BC South (BCS) other than the estimated OS growth (1991-94) was consistent with our mean weight data. Although the study region in the Sea of Okhotsk sits at higher latitudes (54-55°N) than BC South (48-52°N) and experiences cooler temperatures (8-12°C in summer vs. ~15°C), the two populations of pollock share comparable length compositions: mean = 40 cm (OS) vs. 37 cm (BCS), maximum = 75 cm (OS) vs. 78 cm (BCS), predominant lengths = 35-45 cm (OS) vs. 23-50 cm (BCS) for ~76% of the lengths.

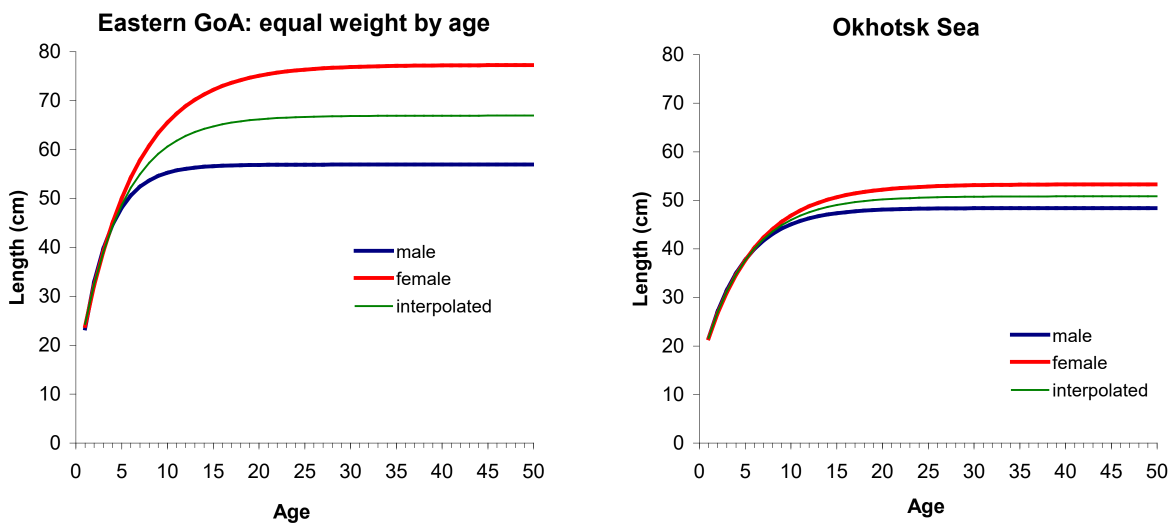

Figure 5. Interpolated combined-sex growth models used to estimate the Walford parameters used in the WAP delay-difference stock assessment model. [left panel]: Eastern Gulf of Alaska model; [right panel]: Okhotsk Sea model.

Growth and length-weight parameters (Section D.1.1) appropriate for each stock were used to prepare Walford plots (Figure D.16) which provide the growth parameter values used as input to the WAP delay-difference model. The Walford parameters are calculated from the knife-edge recruitment age to 30 y for the each growth model. The Walford parameters will vary slightly with changing age assumptions at knife-edge recruitment for both growth models (GoA in the North, Sea of Okhotsk in the South). Table D.9 presents the Walford parameters used in the stock assessment along with the mean length and mean weight associated with each of the knife-edge age at recruitment assumptions.

6.4. MEAN WEIGHT

In excess of 50,000 WAP length observations, taken from unsorted samples, were available from the combined offshore trawl fisheries (see Appendix D), 18,873 in the North (1973-2016) and 32,125 in the South (1972-2016). All lengths were converted to weights using combined-sex, stock-specific parameters in Section D.1.1. Although females attain larger sizes than males

(Figure 5), the allometric relationship between length and weight remains similar between the sexes (Figure D.4). To remove some of the variance due to influential factors in the data, an additive lognormal model (Schnute et al. 2004) was used to adjust the annual index of fish weight for each BC pollock stock (Section D.2.1). The only explanatory variable that had an observable effect on the series was the minor PMFC area. Additional explanatory variables (e.g., season, depth, sex) were explored but their effects on the annual index series were minimal and consequently not used. The most striking feature between the North and South is that fish are roughly twice as large in the North with a geometric mean weight of 1.056 kg/fish vs. 0.521 kg/fish in the South (see Appendix D). This observation may be due to a number of possible hypotheses:

A. True differences in growth exist between two discrete populations;

B. Older (and larger fish) migrate north;

C. Exploitation rates in the south are higher, cropping off all the big fish.

Hypothesis C seems unlikely, given the spotty exploitation history in the south. We prefer hypothesis A; the modal age in the GoA survey data, which we use to represent the BC North stock, can be either age 1 or age 3 (i.e., many young fish); however, these data do not rule out hypothesis B. To eliminate migration, we would need age samples from the BC South stock.

6.5. MATURITY

Maturity is not used as input into a delay-difference model. Instead, the model assumes that the age at knife-edge recruitment also defines maturity, resulting in a population where all recruited fish are fully mature. Maturity ogives based on the available DFO age and length data were constructed to test the consistency of the available data with the assumption that all fish from the knife-edge age were mature (see Section D.1.3).

The resulting analysis indicated that the median age at full maturity for WAP is 3.4 y using pectoral fins and 4.6 y using surface-read otoliths (Figures D.5 & D.6). Median lengths at full maturity using unsorted research, unsorted commercial, and sorted commercial are 49.7 cm, 56.6 cm, 57.3 cm, respectively (Figure D.15). These values are consistent with the ages (3 to 5 y) used in this stock assessment as candidates for knife-edge recruitment. These analyses indicate that the assumption that vulnerable fish are fully mature is not wholly satisfied, particularly when knife-edge selectivity equals age three. Dorn et al. (2012) report that estimates of the 50% maturity age in the Gulf of Alaska *"..are highly variable and range from 3.5 years in 1983 to 6.1 years in 1991, with an average of 4.9 years*".

6.6. STEEPNESS

A Beverton-Holt (BH) stock-recruitment function was used to generate average recruitment estimates in each year, based on the biomass of recruited WAP (Equation E.22). Recruitment deviations from this average (Equation E.23) were estimated to improve the fit to the model data and to introduce variability in the Bayesian estimation phase. The BH function was parameterised using a steepness parameter, h, which specifies the proportion of the maximum recruitment available at $0.2B_0$ (Mace and Doonan 1988). The parameter h was estimated in the model, constrained by a prior that took the form of a beta distribution with mean 0.7 and standard deviation 0.15. This prior was the same one used by Forrest et al. (2015) for Pacific Cod (*Gadus macrocephalus*), and is very similar to the prior developed for west coast rockfish by Forrest et al. (2010; mean=0.674; standard deviation=0.168). Myers et al. (1999) reported median h = 0.55 for *T. chalcogramma* (with 20 and 80 percentiles of 0.53 and 0.58); however, this estimate is based on only two fish. Estimated *h* for *G. morhua* was 0.84 (0.76. 0.90) based on 21 fish, and *h* = 0.79 (0.67, 0.87) for the family Gadidae based on 49 fish (Myers et al. 1999).

7. DELAY-DIFFERENCE MODEL

Delay difference models represent an intermediate approach between aggregated surplus production models and age-structured models. The delay-difference structure tracks the effects of recruitment, survival and growth on biomass, without requiring an explicit age-structured framework, and can perform well as long as its major assumptions are met (Hilborn and Walters 1992). Difference equations, which allow for a time-delay between spawning and recruitment, are used to build population models in discrete time-steps (generally 1 year), in which the surviving biomass for next year is predicted from the surviving biomass from the previous year, after adjusting for growth and mortality and adding next year's recruitment. An advantage of delay difference models over simpler production models is that they do not assume constant recruitment over time.

The key assumptions of the delay difference model are:

- Growth in mean body weight follows the linear relationship described by the Ford-Walford equation (E.1).
- Knife-edge selectivity, i.e., all fish aged *k* and older are equally vulnerable to the fishing gear. A corollary to the assumption of knife-edge selectivity is that maturity is also knife-edge and the same as selectivity. All fish in the model are mature and fully selected.
- Constant natural mortality at age, i.e., all fish aged *k* and older have the same natural mortality rate.

This model is described with equations in Appendix E (see also Forrest et al. 2015). The model was fit to the annual catch data (Table A.7), three or four survey series in the North and three in the South (Appendix B), a series of CPUE biomass indices from commercial bottom trawls (Appendix C), and a series of fishery mean weights described in Section D.2. We did not attempt to alter the relative weighting of the component data series, instead using the observation error CVs estimated by the surveys without modification. An arbitrary CV=0.3 was used for the CPUE data and CV=0.15 for the mean weight data. We decided not to explore sensitivity to the variance components of the model because, in our previous work with a Shortspine Thornyhead delay-difference model, we had not found much effect on model estimates other than to raise or lower model uncertainty (Starr and Haigh 2017). Given limited resources, we opted to concentrate on sensitivity runs which would directly affect model conclusions.

We describe an “example case” run in detail for each of the BC North and BC South stocks. We then present a range of alternative runs for each stock which explore the effect of key model assumptions (age at knife-edge selectivity, *M* and the effect of some of the series indices). Each example case is not more likely than the other runs (12 in total for the BC North and 11 for the BC South). It is simply one run in the group of 12 or 11 runs presented for each BC stock. These alternative analyses were run (with full MCMC simulations) to see how model results differed when input assumptions were changed. Specifications for these runs are given in Table 1 for both Walleye Pollock stocks.

Table 1. Summary of the analyses performed to test the sensitivity of the delay-difference model to variations in natural mortality M, knife-edge recruitment age k and included series indices. All runs for the BC North stock use the eastern Gulf of Alaska growth function (Martin Dorn, pers. comm.); all runs for the BC South stock use the Okhotsk Sea growth function (Janusz and Horbowy 1997). The column marked 'MCMC rank' provides a subjective ranking of the MCMCs, where 1 = good, 2 = acceptable, and 3 = poor.

	Case	Run ID	Run #	M	k	MCMC rank
BC North example	S00	M.30+k3	1	0.30	3	1.25
4 surveys + CPUE	S01	M.25+k3	16	0.25	3	3
	S02	M.30+k4	4	0.30	4	2.5
	S03	M.35+k3	2	0.35	3	1.5
	S04	M.35+k4	12	0.35	4	1.5
No GIG survey	S05	M.25+k3-GIG	9	0.25	3	3
	S06	M.25+k4-GIG	7	0.25	4	2
	S07	M.30+k3-GIG	3	0.30	3	3
	S08	M.30+k4-GIG	5	0.30	4	1.5
	S09	M.35+k4-GIG	10	0.35	4	1.25
No GIG or CPUE	S10	M.30+k3-GIG-CPUE	8	0.30	3	2
	S11	M.30+k4-GIG-CPUE	6	0.30	4	2
BC South example	S00	M.30+k3	4	0.30	3	2
k at M=0.30	S01	M.30+k4	5	0.30	4	2
	S02	M.30+k5	15	0.30	5	2
k at M=0.25	S03	M.25+k3	11	0.25	3	1
	S04	M.25+k4	9	0.25	4	1.5
	S05	M.25+k5	14	0.25	5	2
k at M=0.35	S06	M.35+k3	12	0.35	3	2
	S07	M.35+k4	13	0.35	4	2
	S08	M.35+k5	16	0.35	5	2
No CPUE	S09	M.30+k3-CPUE	10	0.30	3	1
	S10	M.30+k4-CPUE	8	0.30	4	3

The MPD (mode of the posterior distribution) "best fit" was used as the starting point for a Bayesian search across the joint posterior distributions of the parameters using the Monte Carlo Markov Chain (MCMC) procedure. All models were run for 60,000,000 iterations, sampling every 50,000th, to give 1,200 draws (1,000 samples after dropping the first 200 as a "burn-in").

The range of model exploration represented in Table 1 was undertaken because there is substantial uncertainty in specifying the productivity of these stocks (represented by *M* and *h* in the growth model), as well as selecting the age at full knife-edge recruitment (*k*), when making the assumptions that are mandatory when using a delay difference model. Because the available data are not informative with respect to these key model parameters, it is not possible to objectively rule out most of these alternative hypotheses. Instead, after covering a range of plausible values for the key parameter assumptions, we chose model runs for advice based on a subjective ranking of the MCMC diagnostics (e.g., autocorrelation, stability of traces) using a simple ranking system (1 = good, 2 = acceptable, 3 = poor), selecting only those runs that ranked ≤ 2 (using the mean ranking assigned by each author independently). This stock assessment adopted a "Model Averaging" approach, using selected model runs for each stock that represent a range of hypotheses based on plausible F values (see Sections 8.1.2 and 8.2.2) to construct a "Model Average Composite" for providing advice to managers (Section 9).

8. MODEL RESULTS

8.1. BC NORTH

8.1.1. Model Example

Results for an example model run for BC North (Case S00, Table 1), which assumed *M*=0.30 and *k*=3 years, are presented to illustrate model behaviour, particularly in how these models fit the available data, the shape of the biomass trajectory and the predictions of stock status. This example case was chosen because the model estimated fishing mortality rates (*F*) less than 2 (≈ maximum harvest rate *u* < 0.86) in the MCMC runs (Table 2). However, there are other plausible model runs that could be used as the example case, regardless of the assumptions made regarding key productivity parameters, because the available data are not informative with respect to productivity and age at knife-edge selectivity.

Table 2. Median values for select MCMC-derived parameters and quantities for the 12 runs described for BC North in Table 1. The historical reference points use averages from 1967-2016. Projections to 2018 were made assuming TAC=1000 t, a value near to the 2011-2015 average catch of 992 t. Shaded rows highlight runs contributing to the Model Average.

Case	h	B_{avg} (tonnes)	B_{2017}/B_{avg}	B_{2018}/B_{avg}	Yr_{min}	B_{2017}/B_{min}	P[B_{2018}> B_{2017}]	u_{avg}	u_{2016}/u_{avg}	Median F_{max} by MCMC	# Years median $F_t > 2$
S00: M.30+k3	0.74	7,568	0.57	0.42	2001	1.9	0	0.14	2.0	0.71	0
S01: M.25+k3	0.75	4,962	0.48	0.28	1986	2.3	0	0.21	2.0	1.69	0
S02: M.30+k4	0.78	3,377	0.44	0.21	1986	3.1	0.06	0.35	1.7	19.4	7
S03: M.35+k3	0.73	10,270	0.60	0.47	2001	1.9	0.02	0.11	2.0	0.51	0
S04: M.35+k4	0.77	3,695	0.46	0.24	1986	3.1	0.05	0.33	1.6	16.1	6
S05: M.25+k3-GIG	0.78	4,628	0.54	0.39	1986	2.7	0.09	0.26	1.8	9.97	1
S06: M.25+k4-GIG	0.81	3,272	0.51	0.35	1986	2.9	0.12	0.36	1.6	19.0	6
S07: M.30+k3-GIG	0.77	5,325	0.65	0.53	1986	3.7	0.10	0.24	1.6	8.01	0
S08: M.30+k4-GIG	0.80	3,438	0.58	0.43	1986	3.5	0.14	0.35	1.5	18.9	6
S09: M.35+k4-GIG	0.80	3,725	0.62	0.49	1986	3.5	0.16	0.34	1.5	17.5	5
S10: M.30+k3-GIG-CPUE	0.75	6,986	1.3	1.1	2000	9.9	0.05	0.20	0.80	18.4	1
S11: M.30+k4-GIG-CPUE	0.80	4,248	1.1	0.92	1986	8.9	0.07	0.31	0.87	19.9	8

The MPD fits in the example model run to the survey and CPUE indices are generally acceptable although the model is incapable of fitting the abrupt changes in some series like the HS assemblage (Figure 6). The model is also not capable of fitting the mean weights near the end of the time series; generally, the fit fluctuates without trend (Figure 7). The fit to the catch series is tight (Figure 7). The MCMC spawning biomass trajectory in relation to B_{avg} appears in Figure 7 and shows the median limit reference point B_{2001}=0.30B_{avg}. The MCMC recruitment of age 3 fish shows that 10 recruitment-year medians exceed the mean recruitment Figure 7.

Observing the alternative runs for BC North, the MPD fits to the data series (Figure F.13: mean weight, Figure F.14: HS assemblage, Figure F.15: HS synoptic, Figure F.16 WCHG synoptic, and Figure F.17: North CPUE), demonstrate that this model has little power to distinguish among hypotheses. Figure F.17 suggests that some combinations of *M* and *k* are better able to fit the high 1996 CPUE index point. In general, model runs with *k*=4 fit the mean weight data better than the models with *k*=3 or *k*=5. However, models with *k*=3 tend to have lower maximum exploitation rates because the estimated stock size is larger. Models with *k*=4 tend to reach the model's maximum fishing mortality rate (constrained at *F*=20) in some years because there are too few fish available to match the observed catch. This is likely due to a failure in the model assumption of knife-edge selectivity at a specified age.

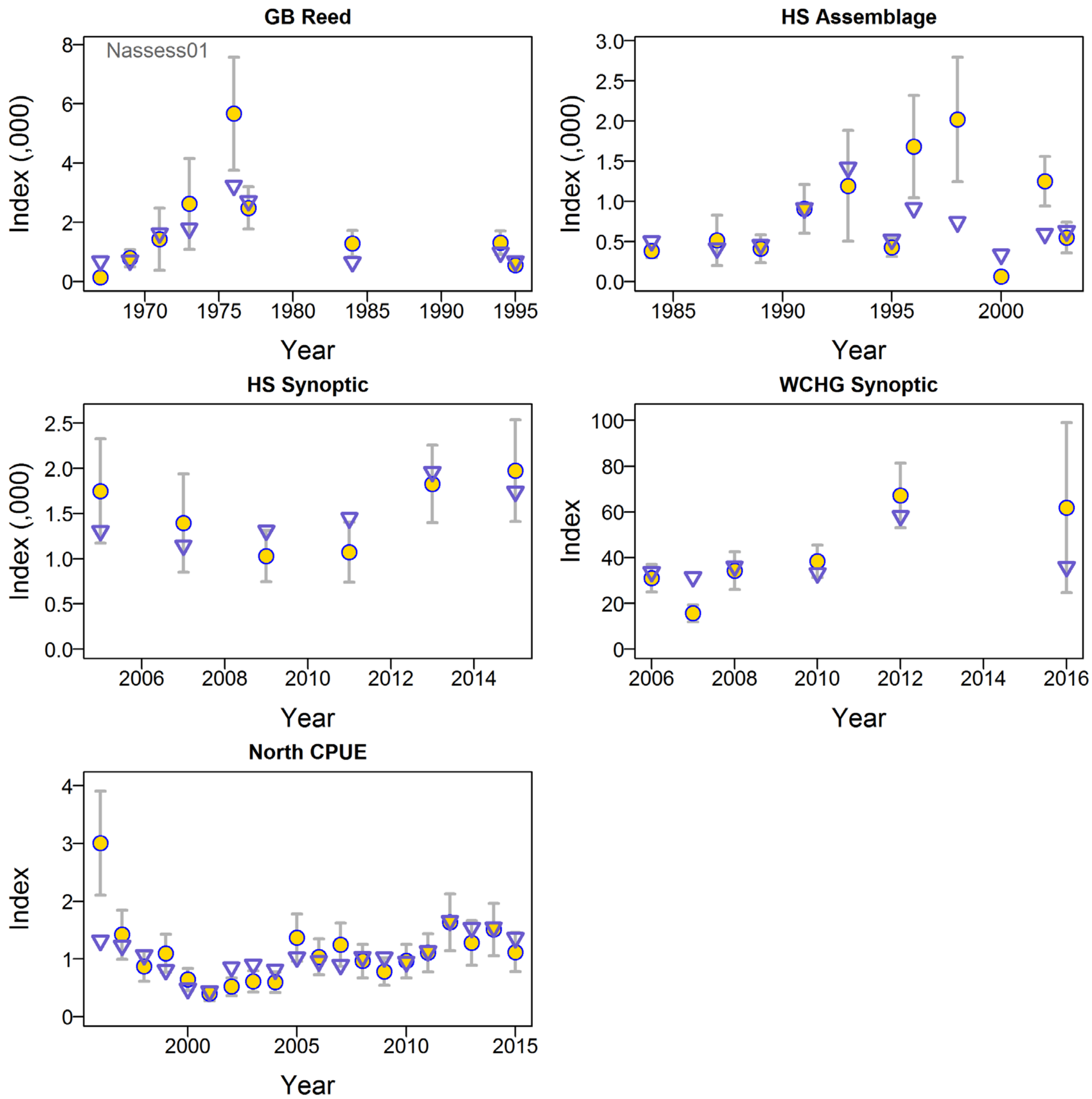

Figure 6. BC North MPD fits (triangles) to the four survey abundance series and to the CPUE index series for the example model Case S00.

When the MCMC traces of the alternative run hypotheses are examined (Figure F.18), they appear to be relatively well-behaved with smooth running quantiles; however, the autocorrelation plots (Figure F.19) point to roughly half of the MCMC chains containing important lagged correlation effects. The example case (S00) shows some serial correlation at the beginning, but this dissipates over time. Some of the cases (e.g., S02 and S11) show periodic correlation and two cases (S01 and S07) show high positive serial correlation through most of the time series. Visually, the best cases (S06, S08, S09) all feature k=4, regardless of M, and no GIG survey.

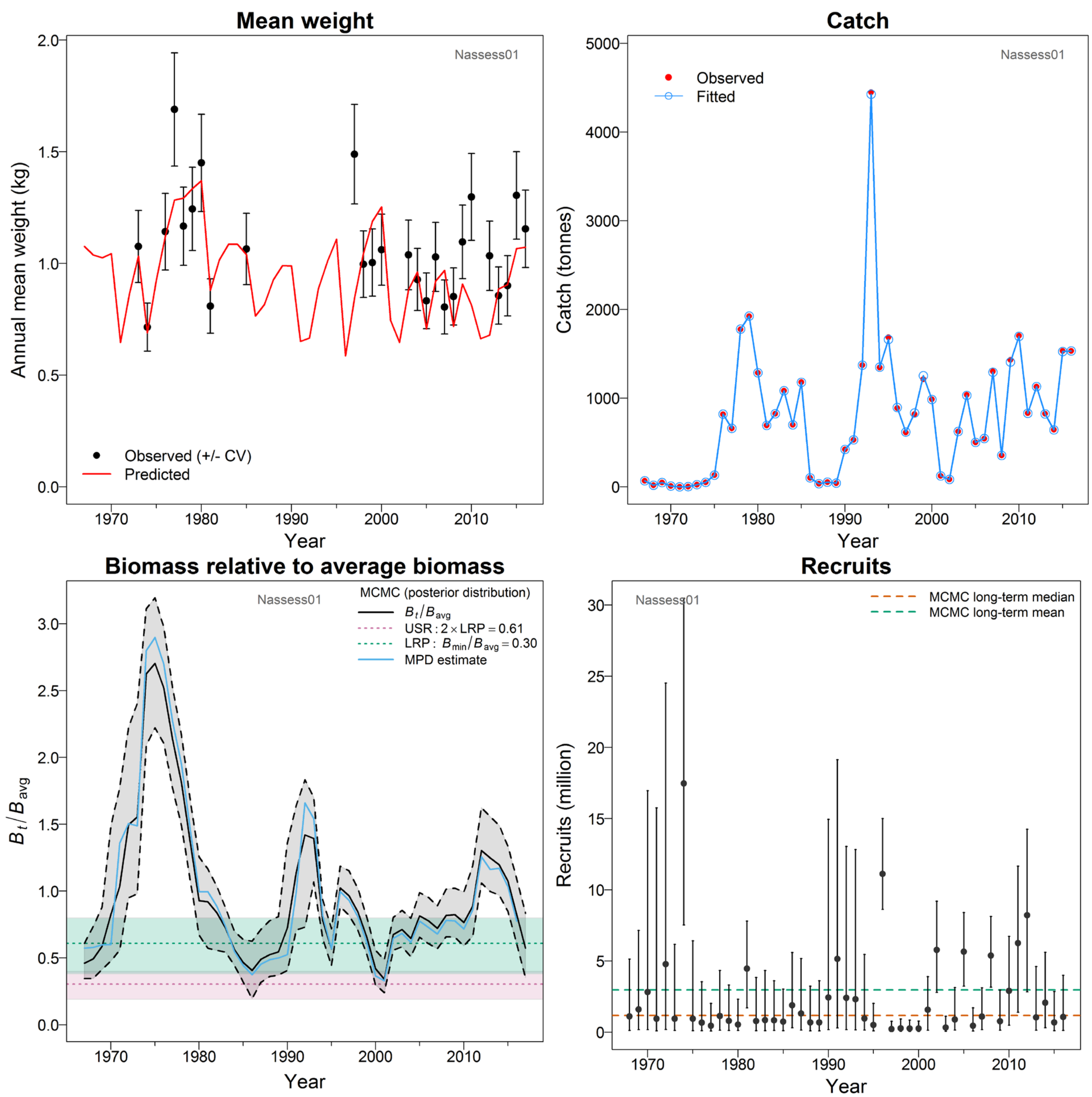

*Figure 7. BC North example model case S00: **[top left]** MPD fit to the mean weight data; **[top right]** MPD fit to the catch data; [**bottom left**] MCMC time trend of B_t/B_{avg}, showing the median (heavy black line), 5% and 95% quantiles (dashed lines) from the posterior distribution, as well as showing the MPD trend and the historical reference points LRP=B_{min}/B_{avg} and USR = 2LRP; [**bottom right**] MCMC time trend of recruitment showing 90% credibility intervals.*

Table F.3, which gives the negative log likelihoods (NLLs) for alternative model fits, provides a more quantitative basis to make comparisons. This table shows that there are some big differences in the component NLLs, indicating how well the models fit the various data components. These likelihoods can be use to select models among similar alternative runs, depending on which components are deemed important. For instance, case S10 had the lowest NLL for mean weight, but suffered from periodic autocorrelation in the log R_0 MCMC traces (Figure F.19). The objective function value (OFV) can be compared within three clusters where model components are symmetrical – {S00, ... S04}, {S05, ..., S09}, and {S10, S11}. Within the second cluster, S08 has the lowest OFV, the best fit to mean weight, and the lowest NLLs for all survey components. These results suggest that a model without the GIG survey featuring M=0.35 and k=4 offers the best fit to the data with little autocorrelation. Unfortunately, choosing k>3 results in unrealistically high fishing mortality rates in some years (see $F_{\max}$ in Table 2). These high fishing mortality rates are likely a by-product of the assumed knife-edge recruitment made by the delay-difference model, which sometimes results in insufficient biomass available to accommodate catch levels in some years when k>3.

Median estimates for current biomass lie well above the LRP=$B_{\min}$ reference point across the full range of alternative runs (Table 2). Additionally, current (2017) spawning biomass only falls below 0.5B_{avg} three times (cases S01, S02, and S04). Projected spawning biomass has a high probability of being lower than the current spawning biomass under a catch strategy of 1000 t/y. Generally, assumptions of higher knife-edge selectivity produce higher rates of fishing mortality and lower estimates of standing stock. Regardless of the alternative run, the BC North stock is not large and most likely represents the southern extreme of a larger SE Alaska population. If this is correct, the existence of this larger (and mostly unfished) population of Pollock may provide a rescue effect for the BC portion of the population in situations of low abundance.

Seven of the alternative BC North runs removed the GIG survey abundance index estimates, resulting in model runs with a lower average biomass (B_{avg}) and higher average removal rates ($u_{\text{avg}}B_{\text{avg}}$, Figures F21 & F.22); however, estimated stock status (B_{2017}/B_{avg}) for the first five cases remains similar across these runs and to the example case (Figure F21). Removing the commercial CPUE series and the GIG survey increases stock status (B_{2017}/B_{avg}) and reduces current exploitation rate (u_{2016}/u_{avg}) relative to the example run (Figure F22).

8.1.2. Model Average

Initially, model runs used for a Model Average were selected based on MCMC diagnostics alone. However, the RPR participants further restricted the initial selection based on aspects of the estimated fishing mortality in the MCMC samples (Figure 8). The following criteria (also see Table 1 and Table 2) were used for selecting model runs for inclusion to the Model Average posterior for this assessment:

- use model runs where the median $F_{\max}$ for MCMC samples was < 2;
- add model runs where median annual F_t was > 2 only once;
- remove model runs with poor MCMC diagnostics (rank > 2).

Three alternative BC North runs were selected for inclusion to the Model Average posterior based on the above criteria. Table 3 gives the model-based and HRP-based quantities (0.05, 0.50, 0.95 quantiles) from the Model Average posterior based on the 3000 pooled MCMC samples (runs S00, S03, S10). This table shows that the BC North composite stock is evaluated to be 68% of B_{avg} (90% credibility range: 38% to 162%) and to be 231% above $B_{\min}$ (90% credibility range: 129% to 1610%). There is a high degree of positive skewness in the estimates of current and average stock size because, while the lower bounds of stock size are determined by the catch history and the assumed model maximum exploitation rate, there is little information in the data to constrain the upper bounds of stock size.

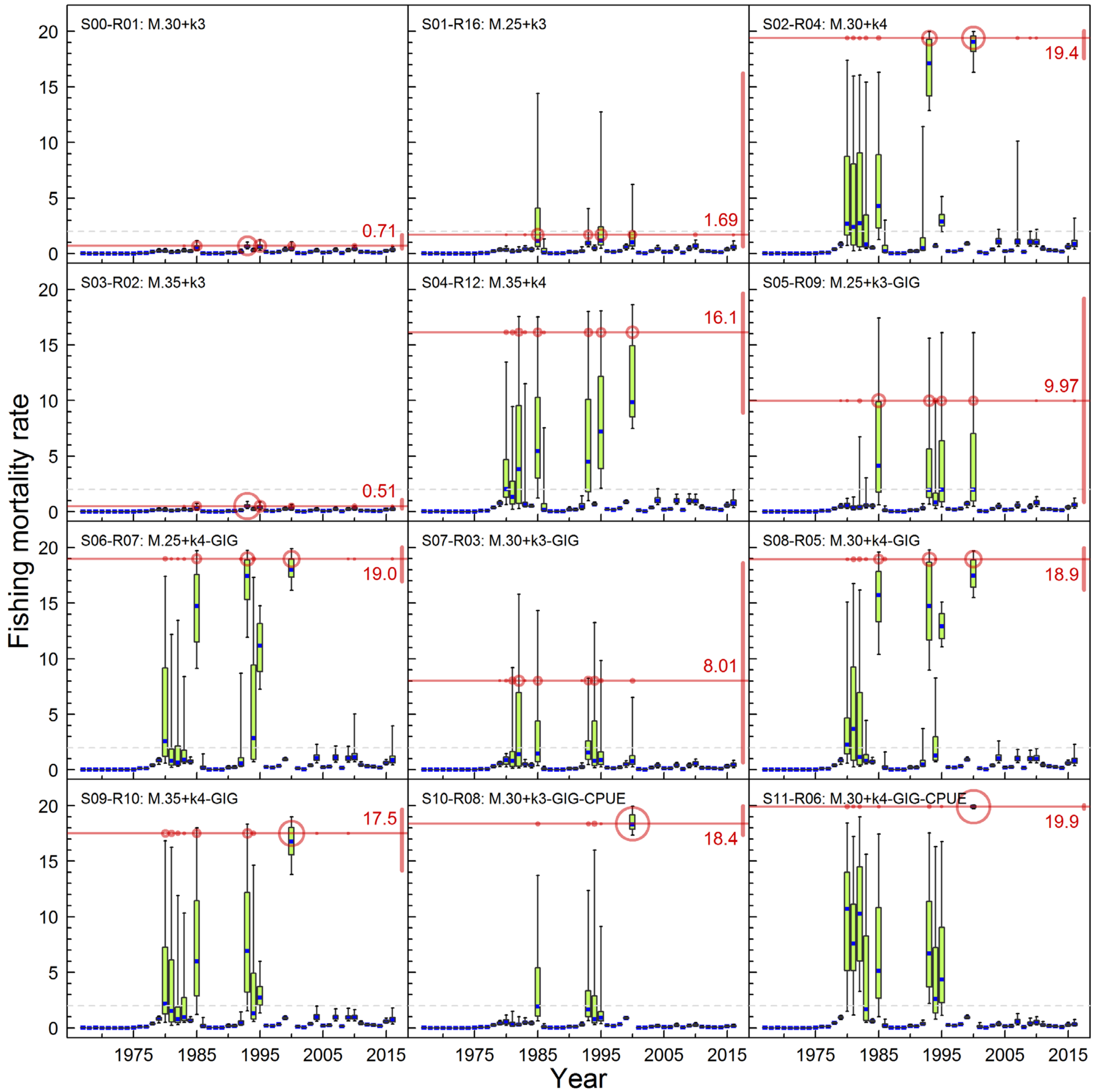

Figure 8. BC North: Fishing mortality rate (F_t) for the alternative model runs (see Table 1). Annual boxplots show the 5, 25, 50, 75 and 95% quantiles. The horizontal dashed line indicates F=2, the horizontal solid line with number above/below indicates the median of 1000 F_{max} estimates, the vertical bar to the right of the F_{max} line shows the 90% credibility interval for F_{max}, and the annual circles along the F_{max} line indicate the frequency of MCMC runs that reached F_{max} in that year.

Table 3. BC North: the 0.05, 0.50, and 0.95 quantiles of MCMC-derived quantities from 3000 MCMC samples comprising the Model Average Composite scenario. Definitions: B_{2017}: current beginning year spawning biomass, B_{avg}: average biomass from 1967 to 2016, B_{min}: minimum biomass that acts as the LRP (USR = 2LRP), u_{2016}: harvest rate (ratio of total catch to vulnerable biomass) in the middle of 2016, and u_{avg}: average harvest rate from 1967 to 2016. All biomass values are in tonnes. For reference, the average catch over the last 5 years (2011-2015) is 992 t.

	Quantile		
	5%	50%	95%
Model based			
B_{2017}	2,621	6,185	13,927
B_{avg}	5,634	7,837	14,626
B_{2017}/B_{avg}	0.385	0.683	1.62
u_{2016}	0.106	0.214	0.406
HRP-based			
B_{min}	654	2,051	4,818
$2B_{min}$	1,307	4,101	9,636
B_{min}/B_{avg}	0.0921	0.27	0.388
$2B_{min}/B_{avg}$	0.184	0.54	0.775
B_{2017}/B_{min}	1.29	2.31	16.1
u_{avg}	0.0744	0.15	0.234
u_{2016}/u_{avg}	0.602	1.79	2.52

8.2. BC SOUTH

8.2.1. Model Example

Results for an example model run for BC South (Case S00, Table 1), which assumed M=0.30 and k=3 years, are presented to illustrate model behaviour, particularly in how these models fit the available data, the shape of the biomass trajectory and the predictions of stock status. This example case was chosen because the model estimated low fishing mortality rates (F) in the MCMC runs (Table 4).

Table 4. Median values for select MCMC-derived parameters and quantities for the 11 runs described for BC South in Table 1. The historical reference points use averages from 1967-2016. Projections to 2020 were made assuming TAC=3250 t, a value below the 2011-2015 average catch of 3,256 t. Shaded rows highlight runs contributing to the Model Average.

Case	h	B_{avg} (tonnes)	B_{2017}/B_{avg}	B_{2020}/B_{avg}	Yr_{min}	B_{2017}/B_{min}	P[$B_{2020}>B_{2017}$]	u_{avg}	u_{2016}/u_{avg}	Median F_{max} by MCMC	# Years median $F_t > 2$
S00: M.30+k3	0.75	89,549	1.0	0.88	2008	5.8	0.01	0.04	0.73	0.28	0
S01: M.30+k4	0.77	21,257	0.79	0.64	2008	8	0.02	0.16	0.82	18.3	1
S02: M.30+k5	0.79	14,835	0.72	0.53	2008	8.3	0.01	0.24	0.82	17.9	4
S03: M.25+k3	0.76	54,998	1.0	0.87	2008	6.4	0	0.06	0.74	0.49	0
S04: M.25+k4	0.78	20,412	0.85	0.64	2008	8.5	0	0.16	0.80	18.3	1
S05: M.25+k5	0.81	13,022	0.84	0.64	2008	8.7	0.01	0.24	0.82	19.4	5
S06: M.35+k3	0.74	183,563	1.0	0.86	2008	5.5	0.01	0.02	0.74	0.12	0
S07: M.35+k4	0.78	21,814	0.75	0.54	2008	7.6	0.01	0.17	0.82	14.2	1
S08: M.35+k5	0.79	14,623	0.72	0.45	2008	7.9	0.01	0.23	0.85	19.7	3
S09: M.30+k3-CPUE	0.75	33,336	0.62	0.48	2008	18	0.01	0.14	0.81	19.2	2
S10: M.30+k4-CPUE	0.76	19,971	0.90	0.65	2008	17	0.01	0.18	0.69	18.4	2

The MPD fits in the example case to the survey and CPUE indices are generally acceptable, although the model is incapable of fitting the abrupt changes in some series like the

WCVI synoptic in 2010 (Figure 9). The model is also not capable of fitting the high mean weights in the first half of the time series (Figure 10). It is not possible to know if the early (pre-1980) mean weight samples, which seem to be inconsistent with the later mean weights in the series, are truly representative the BC South population. Apart from the poor fit to these early data, the fit to the remainder of the mean weight series fluctuates with a slight dome-shaped trend. The fit to the catch series is tight (Figure 10). The MCMC spawning biomass trajectory in relation to B_{avg} appears in Figure 10 and shows the median limit reference point B_{2008}=0.18B_{avg}. The MCMC recruitment of age 3 fish shows that only four recruitment-year medians exceed the mean recruitment Figure 10.

Observing the alternative runs for BC South, the MPD fits to the data series (Figure F.36: mean weight, Figure F.37: GB Reed, Figure F.38: WCVI synoptic, Figure F.39 QCS synoptic, and Figure F.40: South CPUE) demonstrate that this model has little power to distinguish among hypotheses. The MCMC traces of the alternative hypotheses (Figure F.41) appear to be generally well-behaved with smooth running quantiles for most cases.

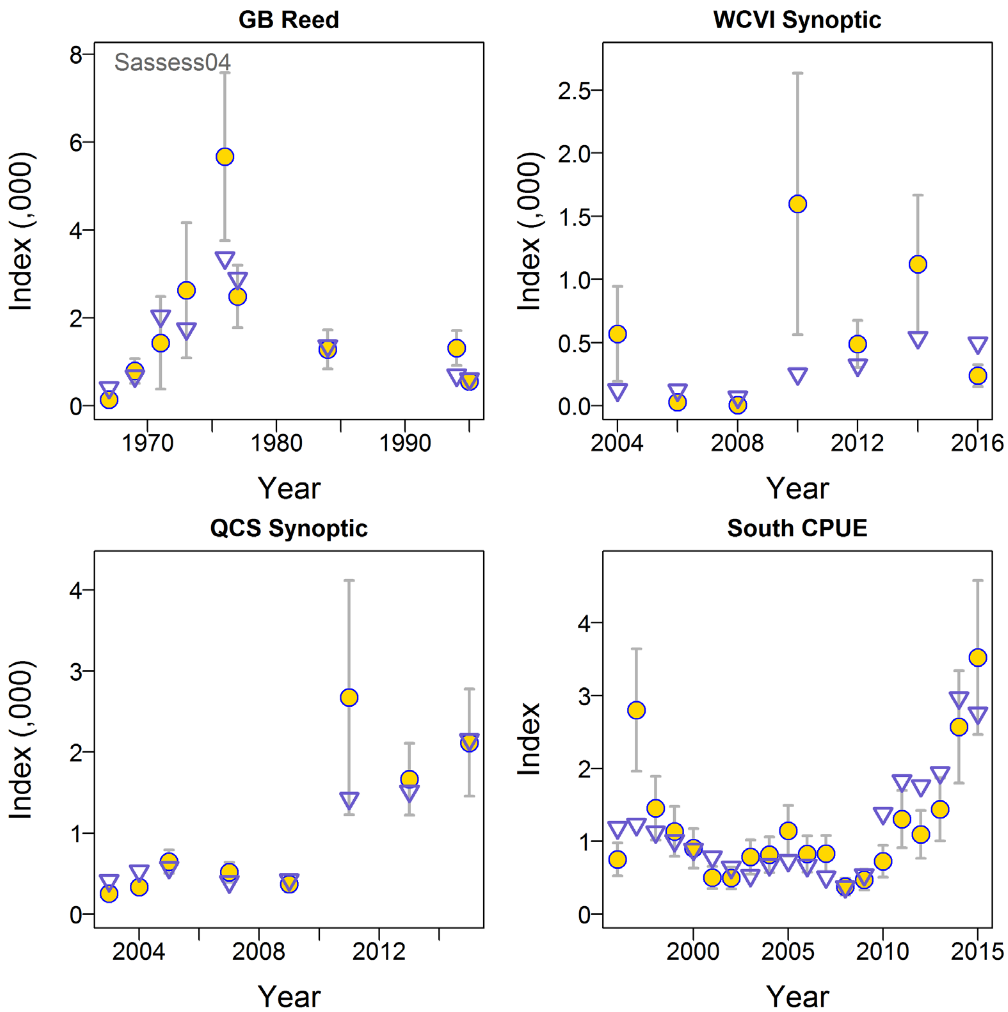

Figure 9. BC South MPD fits (triangles) to the three survey abundance series and to the CPUE index series for the example model Case S00.

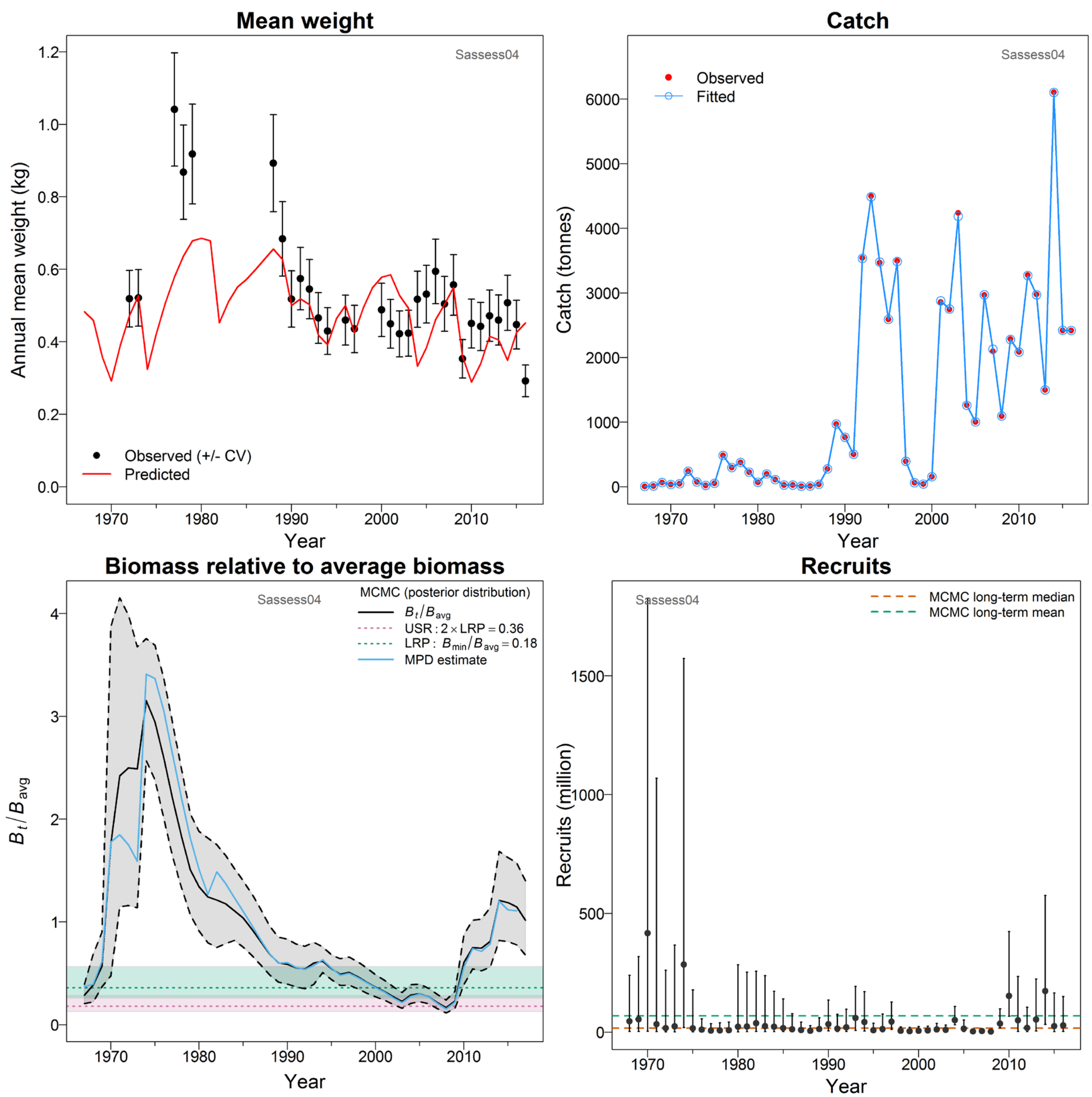

*Figure 10. BC South example model case S00: **[top left]** MPD fit to the mean weight data; **[top right]** MPD fit to the catch data; [**bottom left**] MCMC time trend of B_t/B_{avg}, showing the median (heavy black line), 5% and 95% quantiles (dashed lines) from the posterior distribution, as well as showing the MPD trend and the historical reference points LRP=B_{min}/B_{avg} and USR = 2LRP; [**bottom right**] MCMC time trend of recruitment showing 90% credibility intervals.*

Table F.22, which gives the negative log likelihoods (NLLs) for the alternative model fits, provides a more quantitative basis to make comparisons. This table shows that there are some large differences in the component NLLs, indicating how well the models fit the various data components. These likelihoods can be used to select models among the alternative runs, depending on which components are deemed important and as long as the comparisons are made for models with the same data components. Excluding the cases that drop CPUE, almost all components show the smallest NLL for case S08, which suggests that this case provides the best fit to the data. However, case S08 features a high *k* of 5y and the MCMC chains have unacceptable levels of autocorrelation (Figure F.42). Also, at k=5, the median F_{max} is hitting a model constraint of F=20 (Table 4), i.e., the complete removal of spawning biomass. Generally, the higher the k, the better the fit to mean weight, but the overall stock size is estimated to be smaller, resulting in very high levels of F in some years. This latter result is caused by the assumption of knife-edge recruitment at a specified age that is made by the delay-difference model, sometimes resulting in insufficient biomass to accommodate catch levels in some years when k>3.

The example case (S00) demonstrates a step-wise increase in the 95th quantile and S05 appears to have a downward trend in median log R_0. The autocorrelation plots (Figure F.42) point to substantial lagged correlation effects in many of the MCMC chains. The example case shows serial correlation for at least 20 lags before dissipating, but it re-appears at later lags. Case S06, a variation on the example case with M=0.35, demonstrates substantial periodic correlation. The only cases to show low auto-correlation are S01 (M=0.30, k=4), S03 (M=0.25, k=3), S04 (M=0.25, k=4), and S09 (M=0.30, k=3, no CPUE). It appears that the model is sensitive to combinations of M and k with a tendency for better MCMC diagnostics when M is low with low k. When the CPUE series is removed, the example combination of moderate M and k yields MCMC chains with low autocorrelation.

Median estimates for current biomass lie well above the LRP=B_{min} reference point across the full range of alternative runs (Table 4). Additionally, the minimum median current spawning biomass depletion is only 0.62B_{avg} (case S09). Projected spawning biomass has a high probability of being lower than the current spawning biomass under a catch strategy of 3250 t/y. Unlike the BC North stock, all cases find the same year for a biomass minimum (in 2008). The southern stock is at least an order of magnitude larger in population than the northern one. The two runs which discard the CPUE series also estimate levels of biomass which result in very high estimates for F_{max}, even when k=3.

8.2.2. Model Average

Initially, model runs used for a Model Average were selected based on MCMC diagnostics alone. However, the RPR participants further restricted the initial selection based on aspects of the estimated fishing mortality in the MCMC samples (Figure 11). The following criteria (also see Table 1 and Table 4) were used for selecting model runs for inclusion to the Model Average posterior for this assessment:

- use model runs where the median F_{max} for MCMC samples was < 2;
- add model runs where median annual F_t was > 2 only once;
- remove model runs with poor MCMC diagnostics (rank > 2).

Six alternative BC South runs were selected for inclusion to the Model Average posterior based on the above criteria. Table 5 gives the model-based and HRP-based quantities (0.05, 0.50, 0.95 quantiles) from the Model Average posterior based on the 6000 pooled MCMC samples (runs S00, S01, S03, S04, S06, S07). This table shows that the composite stock is evaluated to be 90% of B_{avg} (90% credibility range: 59% to 135%) and to be 677% above B_{min} (90% credibility range: 233% to 1080%). There is a high degree of positive skewness in the estimates of current and average stock size because, while the lower bounds of stock size are determined by the catch history and the assumed model maximum exploitation rate, there is little information in the data to constrain the upper bounds of stock size.

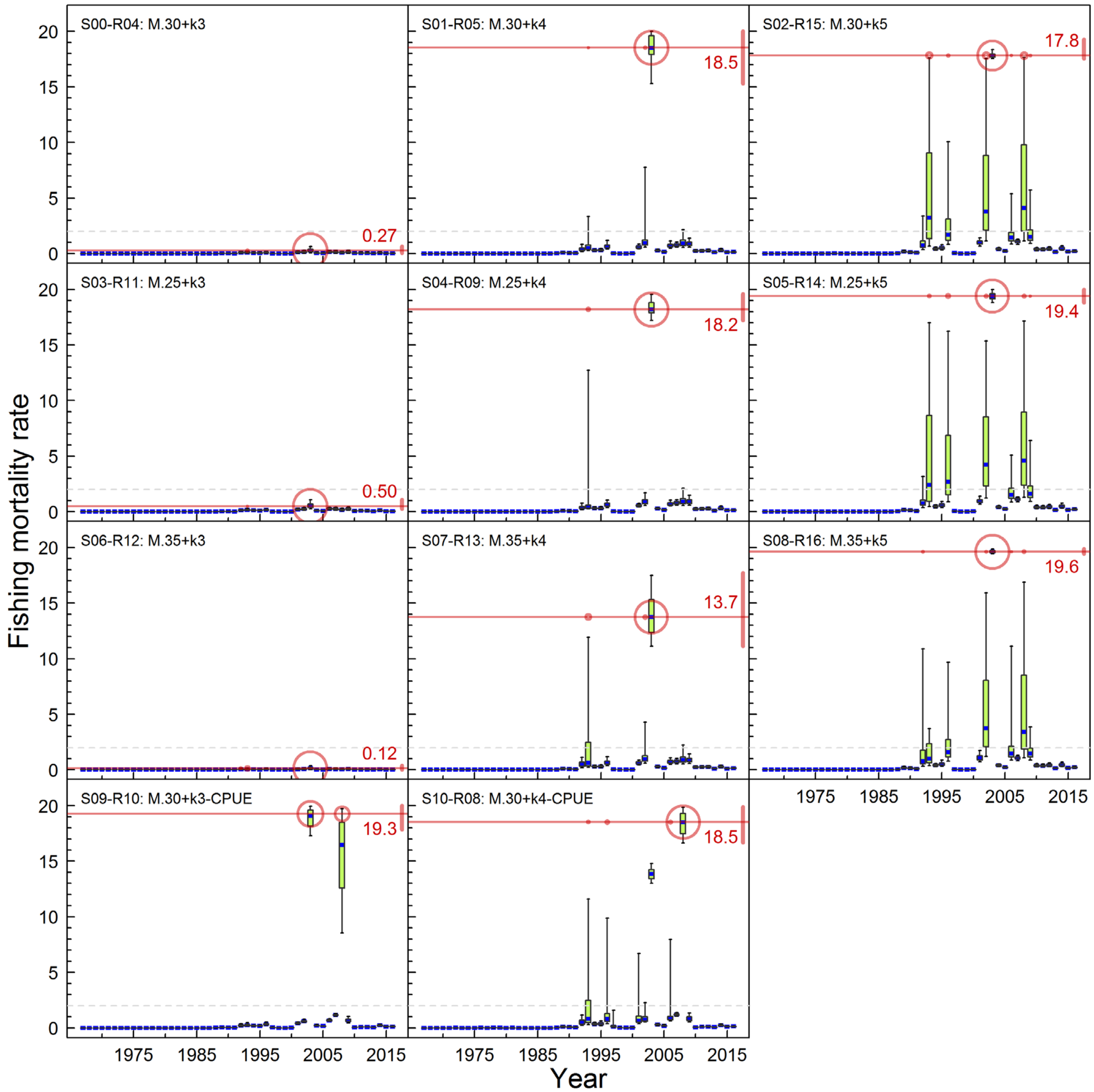

Figure 11. BC South: Fishing mortality rate (F_t) for the alternative model runs (see Table 1). Annual boxplots show the 5, 25, 50, 75 and 95% quantiles. The horizontal dashed line indicates F=2, the horizontal solid line with number above/below indicates the median of 1000 F_{max} estimates, the vertical bar to the right of the F_{max} line shows the 90% credibility interval for F_{max}, and the annual circles along the F_{max} line indicate the frequency of MCMC runs that reached F_{max} in that year.

*Table 5. BC South: The 0.05, 0.50, and 0.95 quantiles of MCMC-derived quantities from 6000 MCMC samples comprising the Model Average Composite scenario. Definitions: B_{2017}: current beginning year spawning biomass, B_{avg}: average biomass from 1967 to 2016, B_{min}: minimum biomass that acts as the LRP (USR = 2*LRP), u_{2016}: harvest rate (ratio of total catch to vulnerable biomass) in the middle of 2016, and u_{avg}: average harvest rate from 1967 to 2016. All biomass values are in tonnes. For reference, the average catch over the last 5 years (2011-2015) is 3,256 t.*

	Quantiles		
	5%	50%	95%
Model based			
B_{2017}	12,737	28,923	317,629
B_{avg}	16,938	33,487	292,976
B_{2017}/B_{avg}	0.589	0.899	1.35
u_{2016}	0.00787	0.0829	0.171
HRP-based			
B_{min}	1,543	6,520	58,110
$2B_{min}$	3,086	13,041	116,219
B_{min}/B_{avg}	0.0753	0.138	0.296
$2B_{min}/B_{avg}$	0.150	0.277	0.593
B_{2017}/B_{min}	2.33	6.77	10.8
u_{avg}	0.0113	0.119	0.195
u_{2016}/u_{avg}	0.589	0.772	1.00

9. ADVICE FOR MANAGERS

9.1. MANAGEMENT TARGETS

The Sustainable Fisheries Framework (SFF, DFO 2009) established provisional reference points to guide management and assess harvest in relation to sustainability. These reference points are the Limit Reference Point (LRP) of $0.4B_{MSY}$ and the upper stock reference point (USR) of $0.8B_{MSY}$, which have not been adopted in this assessment due to concerns about the stability of estimating B_0 and B_{2017} using the iSCAM delay-difference model (see Appendix E for discussion). In their stead, this assessment adopted historical reference points (HRPs): B_{avg} (average spawning biomass from 1967-2016) as a proxy for B_{MSY}, and B_{min} (spawning biomass in the year when the reconstructed biomass reached a minimum from which it subsequently recovered to B_{avg}) in place of $0.4B_{MSY}$. The current (B_{2017}) spawning biomass is used as an indicator for the probability of an increase or decrease. Therefore, the following reference points are used:

- Current spawning biomass: B_{2017}
- Limit Reference Point (LRP): B_{min}
- Upper Stock Reference (USR): $2B_{min}$
- B_{MSY} proxy: B_{avg} (average over the years 1967-2016)
- Average removal rate: u_{avg} (average over the years 1967-2016)

9.2. HARVEST ADVICE

9.2.1. BC North

Figure 12 shows the current stock status (B_{2017}/B_{avg}) relative to two historical-based reference points (B_{min}/B_{avg} = LRP and $2B_{min}/B_{avg}$ = USR) for the BC North Model Average Composite posterior and for each of the component runs comprising the Model Average Composite posterior. This plot shows that the 2017 biomass for the Model Average run is evaluated to be primarily above the USR.

A decision table of probabilities, based on Model Average Composite posterior (Table 6), forms the basis of the advice to managers. Note that the probabilities for 2017 cannot change as the 2016 catches have already been taken. The probability that the estimated spawning biomass at the beginning of 2017 (B_{2017}) is greater than the LRP (B_{min}) is 0.99, greater than the USR ($2B_{min}$) is 0.62 and greater than B_{avg} is 0.27. The estimated harvest rate u_{2016} has a probability of 0.74 of being greater than the average removal rate (u_{avg}), indicating that the 2016 harvest rate is likely above this indicator.

Table 6. BC North: Decision table for the Model Average Composite scenario for 5 reference points: the current year spawning biomass, the limit reference point B_{min}, the upper stock reference $2B_{min}$, the average spawning stock biomass from 1967 to 2016, and the average harvest rate over the same time period; for projection-year biomass B_{2018} and mid-year harvest rate u_{2017} for a range of constant catch strategies (in tonnes). Each value is the probability that projected biomass or harvest rate is greater than the indicated reference point. The probabilities are the proportion of MCMC samples from ***three*** *pooled scenarios chosen for their acceptable MCMC diagnostics. The probabilities that current-year spawning biomass (or harvest rate) is greater than the reference points are: $P(B_{2017} > B_{min}) = 0.99$, $P(B_{2017} > 2B_{min}) = 0.62$, $P(B_{2017} > B_{avg}) = 0.27$, and $P(u_{2016} > u_{avg}) = 0.74$. For reference, the average catch over the last 5 years (2011-2015) is 992 t.*

Catch (t)	$P(B_{2018} > B_{2017})$	$P(B_{2018} > B_{min})$	$P(B_{2018} > 2B_{min})$	$P(B_{2018} > B_{avg})$	$P(u_{2017} > u_{avg})$
0	0.23	0.99	0.58	0.26	0
100	0.17	0.99	0.56	0.26	0
200	0.13	0.98	0.54	0.25	0
300	0.10	0.98	0.53	0.25	0.01
400	0.08	0.97	0.51	0.24	0.08
500	0.07	0.96	0.50	0.23	0.24
600	0.06	0.95	0.49	0.22	0.45
700	0.05	0.94	0.47	0.22	0.59
800	0.04	0.93	0.46	0.21	0.65
900	0.03	0.91	0.45	0.21	0.68
1000	0.03	0.90	0.43	0.20	0.70
1200	0.02	0.87	0.42	0.19	0.74
1400	0.01	0.84	0.40	0.18	0.80
1600	0.01	0.80	0.39	0.16	0.85
1800	0.01	0.76	0.38	0.15	0.90
2000	0.01	0.71	0.37	0.13	0.93
2500	0	0.62	0.35	0.11	0.98
3000	0	0.54	0.34	0.09	0.99
3500	0	0.48	0.32	0.07	1
4000	0	0.43	0.30	0.05	1
4500	0	0.40	0.28	0.04	1
5000	0	0.37	0.26	0.03	1

The average annual removals by the trawl fishery over the last five years (2011-2015) from the BC North stock were 992 t. This value can guide a manager by locating a similar catch strategy

(1000 t) in Table 6 (shaded row). If this annual catch were maintained over one year, the probability that B_{2018} will be greater than B_{2017} is 0.03, i.e., a decline in stock abundance is expected with a high probability. Additionally, the probability that B_{2018} will be greater than the LRP and USR is 0.90 and 0.43, respectively, which should be seen as a cautionary indicator. However, managers should keep in mind that projections (Figure 13) from this simple delay-difference model are uncertain because it has no latent age structure to inform predictions and the stock-recruitment function is poorly determined. Appendix F supplies an additional table for projections to 2019.

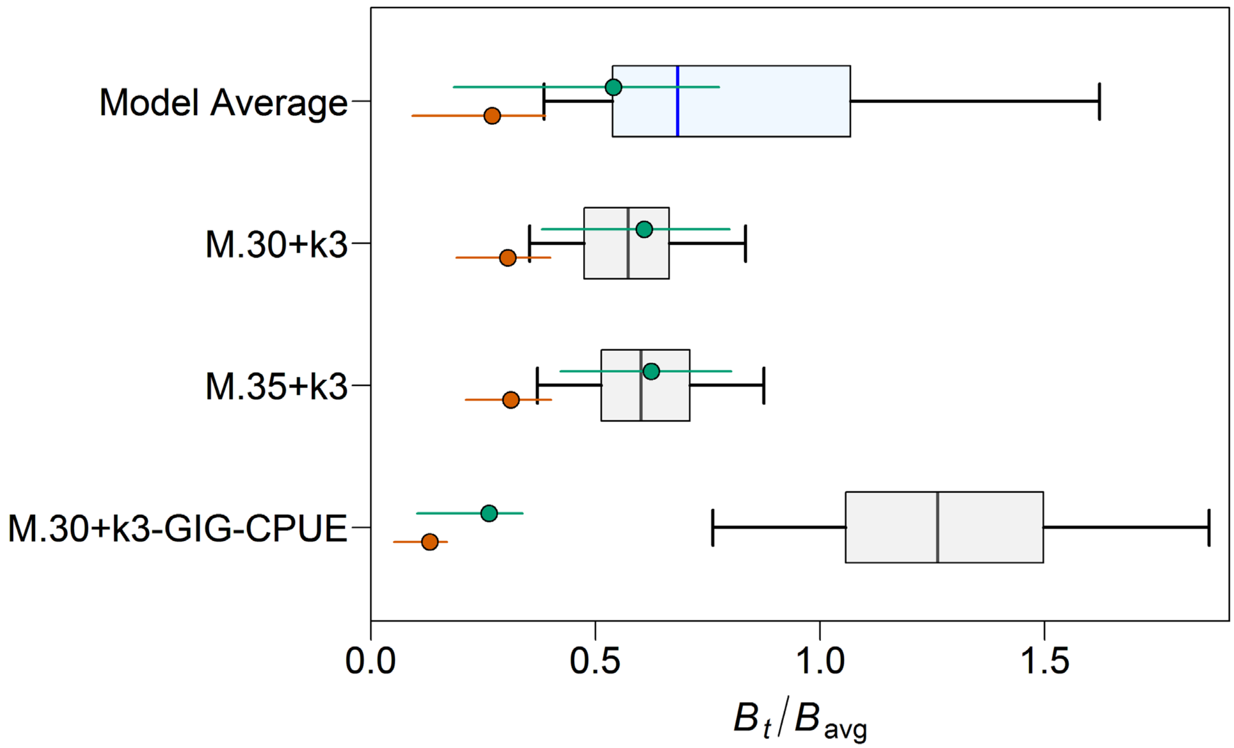

Figure 12. BC North: Status of the current stock B_{2017} relative to B_{avg} with the circles showing median biomass reference points (B_{min}/B_{avg} [red], $2B_{min}/B_{avg}$ [green]), where B_{avg} is a proxy for B_{MSY}, B_{min} is the limit reference point (LRP), and $2B_{min}$ is the upper stock reference point (USR). The 90% credibility range is shown for the LRP and USR. Stock status is shown for the Model Average Composite scenario comprising three pooled model runs (see Table 1 for definitions of these model runs). Box plots show the 5, 25, 50, 75 and 95 percentiles from the MCMC posteriors. M = instantaneous natural mortality(y^{-1}); k = age (y) at knife-edge recruitment.

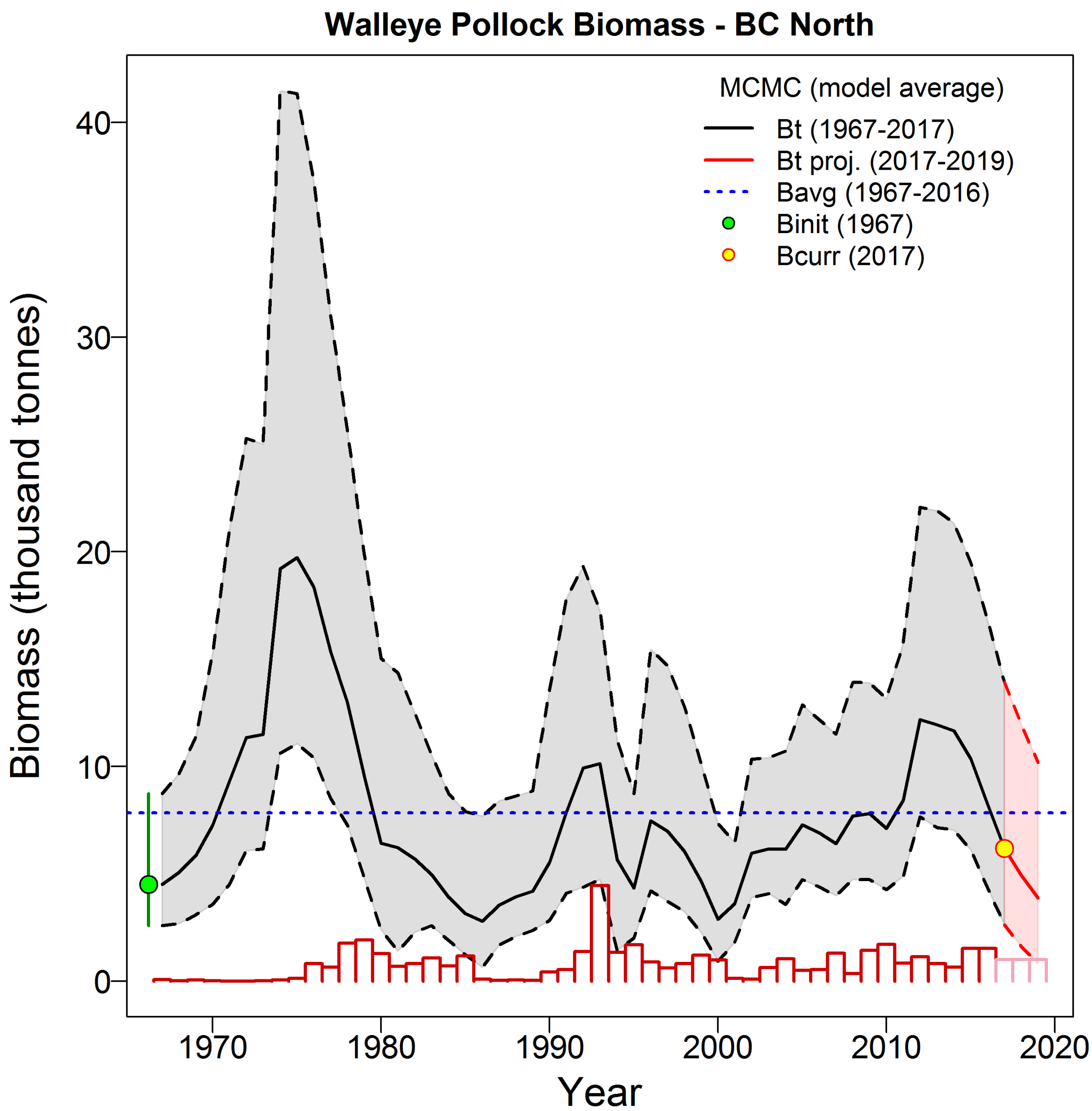

Figure 13. BC North. Median estimates (solid black line) and 90% credibility intervals (black dashed lines, grey fill) for the model-average B_t (biomass in year t in tonnes) for Walleye Pollock. Also shown are the initial biomass B_{1967} (green circle), current biomass B_{2017} (yellow circle), two-year projections $B_{2018\text{-}19}$ (pink fill), the median of average biomass B_{avg} (blue dotted line), the historical catch (red bars) and the catch strategy (pink bars, 1000 t).

9.2.2. BC South

Figure 14 shows the current stock status (B_{2017}/B_{avg}) relative to two historical-based reference points (B_{min}/B_{avg} = LRP and $2B_{min}/B_{avg}$ = USR) for the BC South Model Average Composite posterior and for each of the component runs comprising the Model Average Composite posterior. This plot shows that the Model Average run is evaluated to be above the 90% credibility interval of the USR, as are all of the component runs where k=3.

A decision table of probabilities, based on the Model Average Composite posterior (Table 7), forms the basis of the advice to managers for this stock. Note that the probabilities for 2017 cannot change as the 2016 catches have already been taken. The probability that the estimated spawning biomass at the beginning of 2017 (B_{2017}) is greater than the LRP (B_{min}) is 1, greater than the USR ($2B_{\mathrm{min}}$) is 0.96 and greater than B_{avg} is 0.34. The estimated harvest rate u_{2016} has a probability of 0.05 of being greater than the estimated average removal rate (u_{avg}), indicating that the current harvest rate is likely below this indicator.

*Table 7. BC South: Decision table for the Model Average scenario for 5 reference points: the current year spawning biomass, the limit reference point B_{min}, the upper stock reference $2B_{min}$, the average spawning stock biomass from 1967 to 2016, and the average harvest rate over the same time period; for projection-year biomass B_{2018} and mid-year harvest rate u_{2017} for a range of constant catch strategies (in tonnes). Each value is the probability that projected biomass or harvest rate is greater than the indicated reference point. The probabilities are the proportion of MCMC samples from **six** pooled scenarios chosen for their acceptable MCMC diagnostics. The probabilities that current-year spawning biomass (or harvest rate) is greater than the reference points are: $P(B_{2017} > B_{min}) = 1$, $P(B_{2017} > 2B_{min}) = 0.96$, $P(B_{2017} > B_{avg}) = 0.34$, and $P(u_{2016} > u_{avg}) = 0.05$. For reference, the average catch over the last 5 years (2011-2015) is 3,256 t.*

Catch (t)	$P(B_{2018} > B_{2017})$	$P(B_{2018} > B_{\mathrm{min}})$	$P(B_{2018} > 2B_{\mathrm{min}})$	$P(B_{2018} > B_{\mathrm{avg}})$	$P(u_{2017} > u_{\mathrm{avg}})$
0	0.05	1	0.96	0.20	0
500	0.03	1	0.95	0.19	0
1000	0.02	1	0.95	0.18	0
1500	0.01	1	0.95	0.17	0
1750	0.01	1	0.95	0.16	0.02
2000	0.01	1	0.95	0.16	0.07
2250	0.01	1	0.95	0.15	0.20
2500	0.01	1	0.95	0.15	0.38
2750	0.01	0.99	0.95	0.15	0.56
3000	0	0.99	0.95	0.14	0.73
3250	0	0.99	0.95	0.14	0.85
3500	0	0.99	0.95	0.13	0.93
4000	0	0.99	0.95	0.13	0.99
4500	0	0.99	0.94	0.12	1
5000	0	0.98	0.94	0.11	1
5500	0	0.98	0.94	0.11	1
6000	0	0.98	0.94	0.11	1
6500	0	0.98	0.93	0.10	1
7000	0	0.97	0.93	0.10	1
8000	0	0.97	0.91	0.09	1
9000	0	0.96	0.87	0.09	1
10000	0	0.94	0.82	0.08	1

The average annual removals by the trawl fishery over the last five years (2011-2015) from the BC South stock were 3,256 t. A catch strategy of 3250 t in Table 7 (shaded row) indicates that if this annual catch were maintained over one year, the probability that B_{2018} will be greater than B_{2017} is 0, i.e., a decline in stock abundance is expected (Figure 14). The probability that B_{2018} will be greater than the LRP and USR is 0.99 and 0.95, which indicates that the stock should remain above these reference points (Figure 14), lying well above the two B_{min} reference points. Again it should be noted that the projections (Figure 15) by this model are uncertain because it has no latent age structure to inform predictions and the stock-recruitment function is poorly determined. Appendix F supplies an additional table for projections to 2019.

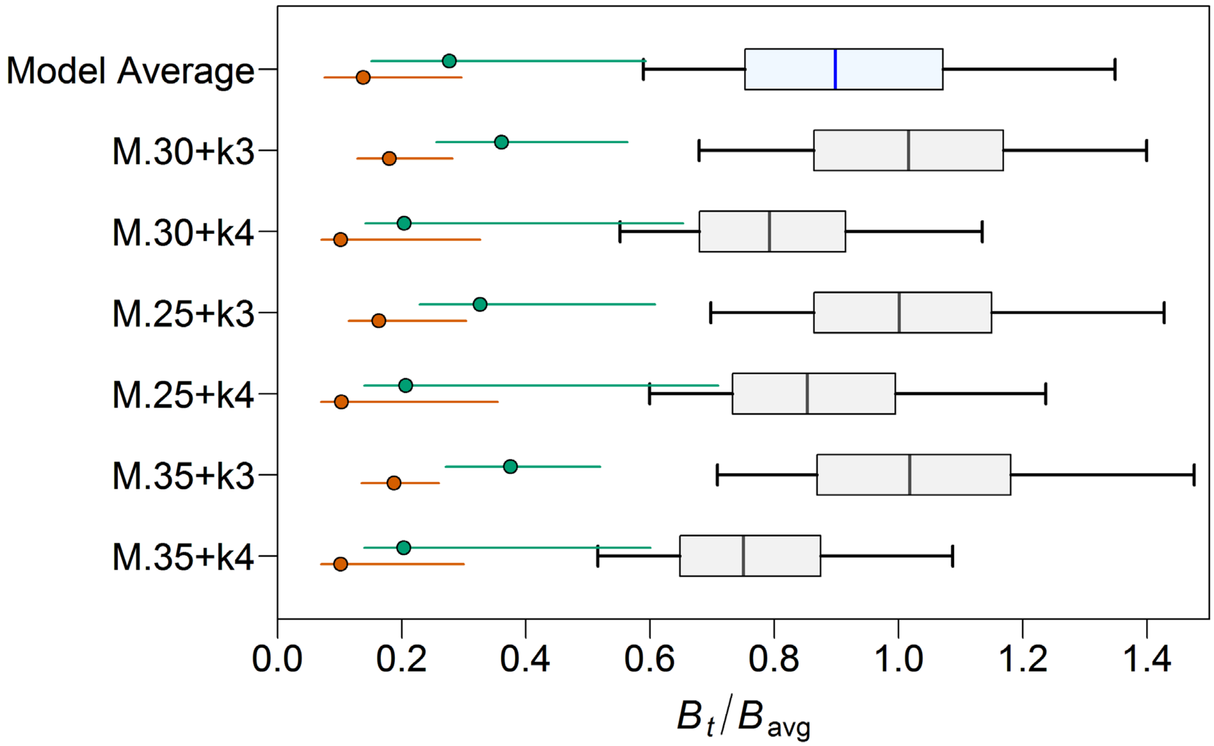

Figure 14. BC South: Status of the current stock B_{2017} relative to B_{avg} with the circles showing median biomass reference points (B_{min}/B_{avg} [red], $2B_{min}/B_{avg}$ [green]), where B_{avg} is a proxy for B_{MSY}, B_{min} is the limit reference point (LRP), and $2B_{min}$ is the upper stock reference point (USR). The 90% credibility range is shown for the LRP and USR. Stock status is shown for the Model Average Composite scenario comprising six pooled model runs (see Table 1 for definitions of these model runs). Box plots show the 5, 25, 50, 75 and 95 percentiles from the MCMC posteriors. M = instantaneous natural mortality(y^{-1}); k = age (y) at knife-edge recruitment

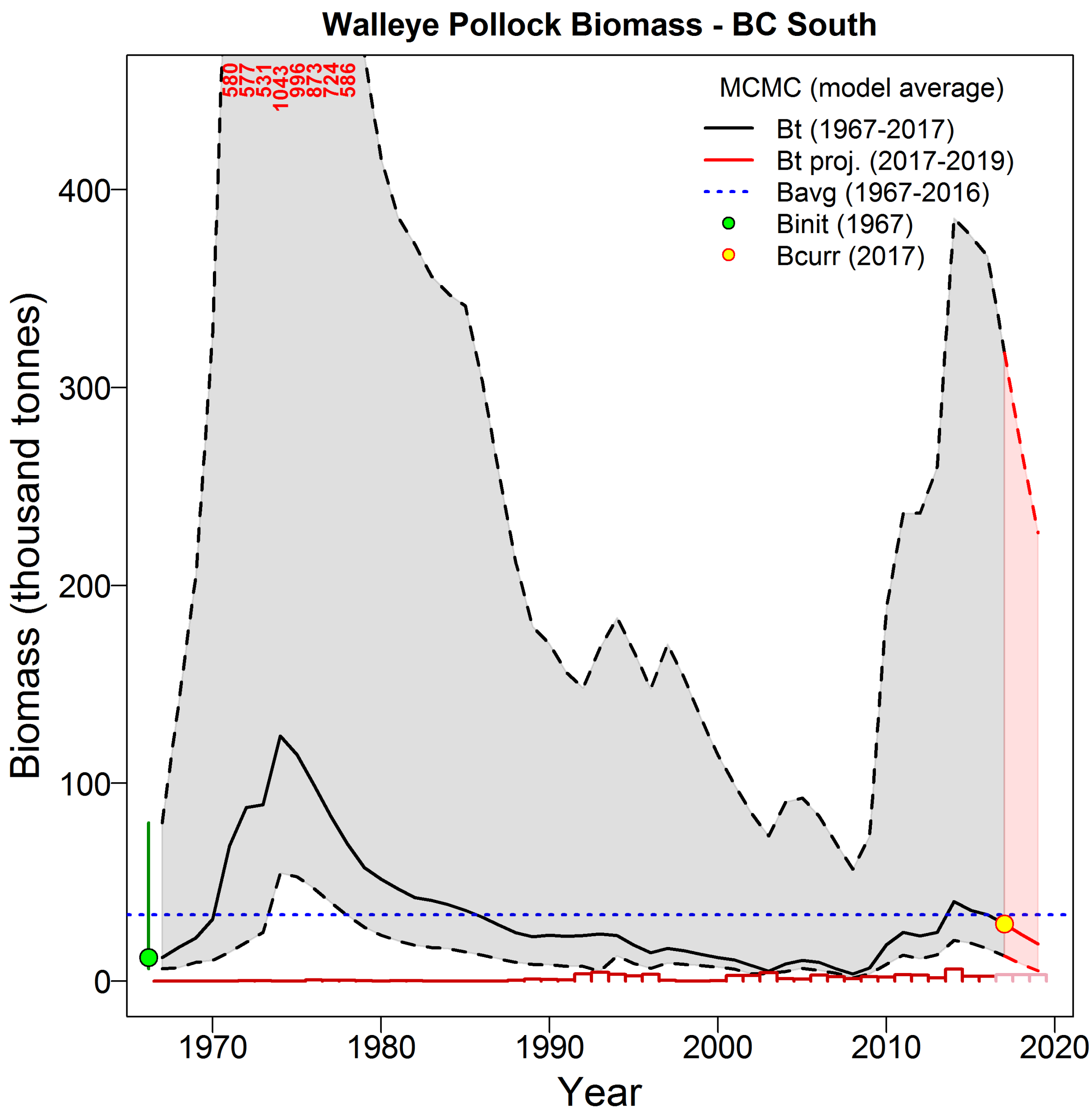

Figure 15. BC South. Median estimates (solid black line) and 90% credibility intervals (black dashed lines, grey fill) for the model-average B_t (biomass in year t in tonnes) for Walleye Pollock. Also shown are the initial biomass B_{1967} (green circle), current biomass B_{2017} (yellow circle), two-year projections $B_{2018\text{-}19}$ (pink fill), the median of average biomass B_{avg} (blue dotted line), the historical catch (red bars) and the catch strategy (pink bars, 3250 t).

9.3. ASSESSMENT SCHEDULE

Advice was also requested concerning the appropriate time interval between future assessments and, for the interim years between assessments, potential values of indicators that could trigger a full assessment earlier than usual (as per DFO, 2016). We suggest the next full stock assessment be scheduled for 2022, such that there will be new indices available from the synoptic surveys (three for HS, two for WCHG, three for QCS, and two for WCVI). By then, otoliths aged by break-and burn should be available to determine growth functions for the

BC North and BC South stocks of Walleye Pollock. Having considered the possible indicators that could be monitored in the interim years, we conclude that none are suitable for triggering an earlier-than-scheduled full assessment. Although *advice* for the interim years is explicitly included in this assessment in the form of decision tables (see Table 6 and Table 7), the predictions in these tables should be viewed cautiously as the delay-difference model used in this stock assessment has no latent age structure to inform predictions and the stock-recruitment function is poorly determined.

10. DISCUSSION AND CONCLUSIONS

The median estimate for current stock status (B_{2017}/B_{avg}) for the Model Average Composite stock is estimated to be 0.68 for BC North (Table 3) and 0.90 for BC South (Table 5). Both stocks are expected to decline over the next one to two years at a level of catch consistent with the 2011-2015 average catch in each region (North = 1000 t/year, South = 3250 t/year). These declines will affect the two stocks similarly with respect to stock status – in the North there is a high probability (0.90) that B_{2018} will be greater than the LRP B_{min} (Table 6) while in the South the probability is almost certain (0.99) that B_{2018} will be greater than the LRP B_{min} (Table 7)

This stock assessment is not capable of giving advice on equilibrium levels of yield, nor does it provide confidence in the absolute stock size, given that the available data can be fit reasonably well across a wide range of stock production hypotheses and that equilibrium calculations can vary depending on the definition of the equilibrium biomass. Following the examples of Pacific Cod (Forrest et al. 2015) and Rock Sole (Holt et al. 2016), this assessment uses historical reference points to guide managers on the sustainability of the Walleye Pollock removals by the trawl fleets (bottom and midwater). There was no simulation performed to determine the suitability of these reference points, but B_{min} as a limit reference point is thought to be a reasonable benchmark because the stock has declined to this level in the past and has recovered from it.

The stock assessment projections indicate that recent catches will reduce the biomass over the next three years once the information from biomass indices is no longer available. This drop indicates that stock abundance has been maintained in the past through good recruitment or possibly stock productivity is too low. Projections are always less reliable than stock reconstruction results, but these limitations should increase the caution when considering the projection probabilities presented in Table 6 and Table 7 compared to the stock status results presented in Figure 12 and Figure 14.

We are aware that the assessment of this species has a number of important limitations. These are mainly related to the lack of reliable ageing of this species from BC waters. It is possible that this lack could be remedied in advance of the next stock assessment for this species as there exists a large number of unprocessed ageing structures in storage at the Pacific Biological Station.

It is suspected that the BC North stock may be part of a larger SE Alaska stock (Gustafson et al. 2000, and references therein), which suggests that it should not be evaluated as a unit stock. This possibility should be further explored, because concepts such as stock status and long-term yields need to be evaluated for the total stock, not just the part of it that appears in BC waters. The SE Gulf of Alaska stock is lightly exploited, given the long-term prohibition of trawling in the SE Alaskan panhandle, which may possibly provide a “rescue effect” (i.e. replenishment of the BC part of the population) from this larger, less exploited parent population.

Within BC waters, there is uncertainty with respect to the stock structure adopted by this stock assessment. While there is a clear difference in mean size between northern and southern Pollock, it is unclear how this large difference has been maintained. The simplest explanation is that the stocks are distinct, which is the hypothesis adopted here. However, there are other processes which could cause this observation, including migration of older fish from south to north and differential exploitation rates. Without reliable ageing, it is not possible to rule out the first alternative hypothesis, although the NOAA survey data indicate the presence of younger age classes in the Eastern Gulf of Alaska. The hypothesis of differential harvest rates seems less likely, given the relative equivalence of the catch histories over much of the recent 25 years.

This assessment of Walleye Pollock touches on a number of issues and concerns. Table 8 attempts to summarise them.

Table 8. Summary table of issues encountered in the stock assessment of Walleye Pollock.

Concern	Issue	Solution
Boundary stocks	BC North may only represent the southern edge of a larger SE Gulf of Alaska stock; therefore, sustainable fishing may be irrelevant if there is an ongoing rescue effect.	Acknowledge that perceived changes in stock may be due to factors other than population dynamics.
Migration	Delay-difference model assumes that signals in mean weight trend result from recruitment, not spatial movement of the fishery.	Investigate other possible stock structure hypotheses.
Size at age	If there are annual trends in length-at-age in the data used to estimate a growth model, the estimates of growth may be biased.	Eastern GoA survey lengths-at-age remained fairly constant over the years of data used to estimate the BC North growth model.
Reference points	If the estimated value for B_{min} is very low, USR=2B_{min} may not provide a management reference point that is sufficiently precautionary.	Use an additional USR = 0.8B_{avg} ≈ 0.8B_{MSY}.
Sampling protocol	Mean weights based on a small number of samples could easily misrepresent mean weight for any given year.	Ensure that every year has at least two samples.
Projections	Unreliable because they are only driven by random average recruitment generated by a poorly determined stock-recruitment function.	Develop more dynamic recruitment functions; collect age data for use in catch-age models.
Model uncertainty	Parameter uncertainty can only be explored using alternative models. Structural uncertainty is not addressed.	Run enough alternative runs to bracket realistic stock parameter values and merge the MCMC results to create a Model Average Composite run for management advice.
Biological information	With data-limited stocks, reliable age data (via break-and-burn) are often not available.	Use data/models from other regions/stocks until stock-specific data can be obtained.
MCMC diagnostics	Goodness-of-fit criteria (e.g., NLL, AIC) alone are not always the best means of identifying suitable model runs for use in the Model Average.	Rank MCMCs using diagnostics such as autocorrelation, split-chain consistency, and quantile drift in traces, where 1=good, 2=acceptable, and 3=poor. Use rank <=2.
Priors	Priors can pre-determine parameter estimates if the data do not contain enough information to update the prior.	Check previous stock assessment work in Alaska or Washington for suitable priors and/or fixed parameter values; check Myers et al. (1999) for information on steepness.

11. FUTURE RESEARCH AND DATA REQUIREMENT

The following issues should be considered when planning future stock assessments and management evaluations for Walleye Pollock.

1. Determine the most reliable method for ageing this species in BC. While the Alaskan Pollock are aged using otolith break and burn methodology, there is uncertainty whether this procedure is suitable for BC Pollock.
2. Available BC Pollock ageing data (currently only available on paper) from the 1980s should be entered into the DFO data system.
3. Review the existing otolith repository and begin break-and-burn ageing if this ageing method is deemed reliable and where there exist sufficient samples/specimens to yield useful stock assessment data.
4. If otolith ageing is deemed reliable, review the otolith sampling plans for Walleye Pollock in the commercial fishery and in the synoptic surveys, and adjust as needed to ensure that stocks are adequately represented.
5. Collect length-stratified biological samples from the commercial fishery and from research surveys to ensure that age structures represent the full size range of WAP in BC.
6. Reassess the growth curves for BC WAP stocks when reliable ages become available.

12. ACKNOWLEDGEMENTS

We thank Martin Dorn (NOAA) for his initial advice on conducting this analysis and his extremely useful and thoughtful data set of 9,000 randomly selected Pollock otoliths drawn from six recent years of Gulf of Alaska trawl survey data. We thank the two reviewers of the working paper, Doug Swain and Sean Anderson, who provided useful feedback and commentary. We thank Steve Martell for the original iSCAM code and Robyn Forrest for supplying the iSCAM delay-difference model software and documentation as well as helping to make changes to the TPL code. We also thank Chris Grandin for his original GUI and output R code, which we subsequently modified to suit our needs. We thank the members of the Walleye Pollock Technical Working Group (Robyn Forrest, Chris Grandin, Bruce Turris, Brian Mose, Greg Workman, Norm Olsen, and Rob Tadey) for their information and advice during the preparation of the assessment. Finally, we thank Stephen Wischniowski, Pacific Biological Station Sclerochronology Laboratory, for supplying us with aged otolith data that had been buried in paper archives and for making some of these data available in GFBio.

13. REFERENCES

Cohen, D.M., Inada, T., Iwamoto, T. and Scialabba, N. 1990. FAO species catalogue. Vol. 10. Gadiform fishes of the world (Order Gadiformes). An annotated and illustrated catalogue of cods, hakes, grenadiers and other gadiform fishes known to date. FAO Fisheries Synopsis, Rome FAO 10(125): 442 p.

DFO, 2006. A Harvest Strategy Compliant with the Precautionary Approach. DFO Can. Sci. Advis. Sec. Sci. Advis. Rep. 2006/023.

DFO. 2009. A fishery decision-making framework incorporating the precautionary approach. (Accessed 18 March 2015).

DFO. 2016. Guidelines for providing interim-year updates and science advice for multi-year assessments. DFO Can. Sci. Advis. Sec. Sci. Advis. Rep. 2016/020.

Dorn, M., Aydin, K., Barbeaux, S., Jones, D., Spalinger, K. and Palsson, W. 2012. Chapter 1. Assessment of the Walleye Pollock stock in the Gulf of Alaska. In NPFMC Gulf of Alaska SAFE, p. 53-182. North Pacific Fisheries Management Council.

Dorn, M., Aydin, K., Jones, D., McCarthy, A., Palsson, W. and Spalinger, K. 2015. Chapter 1. Assessment of the Walleye Pollock stock in the Gulf of Alaska. In NPFMC Gulf of Alaska SAFE, p. 49-172. North Pacific Fisheries Management Council.

Forrest, R.E., McAllister, M.K., Dorn, M.W., Martell, S.J.D. and Stanley, R.D. 2010. Hierarchical Bayesian estimation of recruitment parameters and reference points for Pacific rockfishes (*Sebastes* spp.) under alternative assumptions about the stock-recruit function. Can. J. Fish. Aquat. Sci. 67: 1611-1634.

Forrest, R.E., Rutherford, K.L., Lacko, L., Kronlund, A.R., Starr, P.J., and McClelland, E.K. 2015. Assessment of Pacific Cod (*Gadus macrocephalus*) for Hecate Strait (5CD) and Queen Charlotte Sound (5AB) in 2013. DFO Can. Sci. Advis. Sec. Res. Doc. 2015/052. xii + 197 p.

Gustafson, R.G., Lenarz, W.H., McCain, B.B., Schmitt, C.C., Grant, W.S., Builder, T.L. and Methot, R.D. 2000. Status review of Pacific Hake, Pacific Cod, and Walleye Pollock from Puget Sound, Washington. NOAA Technical Memorandum NMFS-NWFSC-44: 275 pp.

Hilborn, R. and Walters, C.J. 1992. Quantitative Fisheries Stock Assessment: Choice, Dynamics and Uncertainty. Chapman and Hall, New York NY.

Holt, K.R., Starr, P.J., Haigh, R., and Krishka, B. 2016. Stock assessment and harvest advice for Rock Sole (*Lepidopsetta* spp.) in British Columbia. DFO Can. Sci. Advis. Sec. Res. Doc. 2016/009. ix + 256 p.

Ianelli, J.N., Honkalehto, T., Barbeaux, S. and Kotwicki, S. 2015. 1. Assessment of the walleye pollock stock in the Eastern Bering Sea. In NPFMC Bering Sea and Aleutian Islands SAFE, p. 53-152. North Pacific Fisheries Management Council.

Janusz, J. and Horbowy, J. 1997. The state of the walleye pollock in the northern part of the Okhotsk Sea, North Pacific. Fish. Res. 30(1-2): 87–102.

Mace, P.M. and Doonan, I.J. 1988. A generalized bioeconomic simulation model for fish population dynamics. NZ Fish. Assess. Res. Doc. 88/4: 51 pp.

MacLellan, S.E. 1997. How to age rockfish (*Sebastes*) using *S. alutus* as an example – the otolith burnt section technique. Can. Tech. Rep. Fish. Aquat. Sci. 2146: 39 pp.

Myers, R.A., Bowen, K.G. and Barrowman, N.J. 1999. Maximum reproductive rate of fish at low population sizes. Can. J. Fish. Aquat. Sci. 56(12): 2404-2419.

NOAA Fisheries Service, A.F.S.C. 2010. Walleye Pollock Fact Sheet.

Saunders, M.W., McFarlane, G.A. and Shaw, W. 1989. Delineation of Walleye Pollock (*Theragra chalcogramma*) stocks off the Pacific Coast of Canada. In Proc. Int. Symp. Biol. Mgmt. Walleye Pollock, Anchorage, AK, Nov 14-16, 1988, Lowell Wakefield fisheries symposia series 7, Alaska sea grant rep. 89-1, p. 379-401. Alaska Sea Grant College Program, University of Alaska, Fairbanks, AK.

Schnute, J.T., Haigh, R., Krishka, B.A., Sinclair, A. and Starr, P.J. 2004. The British Columbia Longspine Thornyhead fishery: analysis of survey and commercial data (1996-2003). DFO Can. Sci. Advis. Sec. Res. Doc. 2004/059. iii + 75 p.

Stanley, R.D. 1986. A comparison of age estimates derived from the surface and cross-section methods of otolith reading for Pacific ocean perch (*Sebastes alutus*). In Proceedings of the International Rockfish Symposium, Anchorage, Alaska USA, October 20-22, 1986, Lowell Wakefield Fisheries Symposium, Alsk. Sea Grant Rep. No. 87-2, 187–196.

Starr, P.J. and Haigh, R. 2017. Stock assessment of the coastwide population of Shortspine Thornyhead (*Sebastolobus alascanus*) in 2015 off the British Columbia coast. DFO Can. Sci. Advis. Sec. Res. Doc. 2017/015. ix + 174 p.

Vignaux, M. 1994. Catch per unit effort (CPUE) analysis of west coast South Island and Cook Strait spawning hoki fisheries, 1987-93. N.Z. Fish. Ass. Res. Doc. 94/11: 29 pp.

APPENDIX A. CATCH DATA

A.1. BRIEF HISTORY OF THE FISHERY

The early history of the British Columbia (BC) trawl fleet is discussed by Forrester and Smith (1972); however, the document focuses on major stocks of flatfish, cod, and rockfish with no mention of Walleye Pollock. Saunders et al. (1989) noted that aside from market demand for Walleye Pollock, Canadian landings of this species followed its abundance in the northeast Pacific Ocean.

A Pollock fishery in Queen Charlotte Strait (PMFC minor area 12) reportedly started in 1992 to target spawning fish in the first quarter of the year (Saunders and Andrews 1998[4]). Saunders et al. (1989) identify four primary spawning grounds for Walleye Pollock in BC waters:

- Dixon Entrance/northern Hecate Strait,
- Queen Charlotte Sound,
- South West Vancouver Island, and
- the Strait of Georgia,

which are broadly outlined in Figure A.1 as the adopted areas for assessing this species. A summary of BC spawning areas appears in Gustafson et al. (2000).

The highest capture rates by the bottom trawl commercial fishery (averaged over 1996-2017, Figure A.2) occur in:

- Dixon Entrance (perhaps as part of a larger South East Alaska population, Thompson 1981),
- upper Moresby Gully,
- lower Queen Charlotte Sound outside Queen Charlotte Strait, and
- off Juan de Fuca Strait (gyre in summer).

The midwater trawl data (Figure A.3) show catch rates 10 times higher than those for the bottom trawl data, and more likely correspond to the spawning grounds (e.g., Queen Charlotte Strait). The Strait of Georgia (or Gulf) spawning stock shows up as two discrete patches (north and south) in Figure A.3.

Starting in April, 2012, groundfish bottom trawl activities were confined to a trawl footprint agreed to by the commercial fishing industry, DFO management, and the David Suzuki Foundation (Wallace et al. 2015; DFO 2016).

[4] Saunders, M.W. and Andrews, W. 1998. Walleye Pollock stock assessment for 1997 and recommended yield options for 1998. PSARC Working Paper G:97-7, 18 pp., Department of Fisheries and Oceans, Pacific Biological Station.

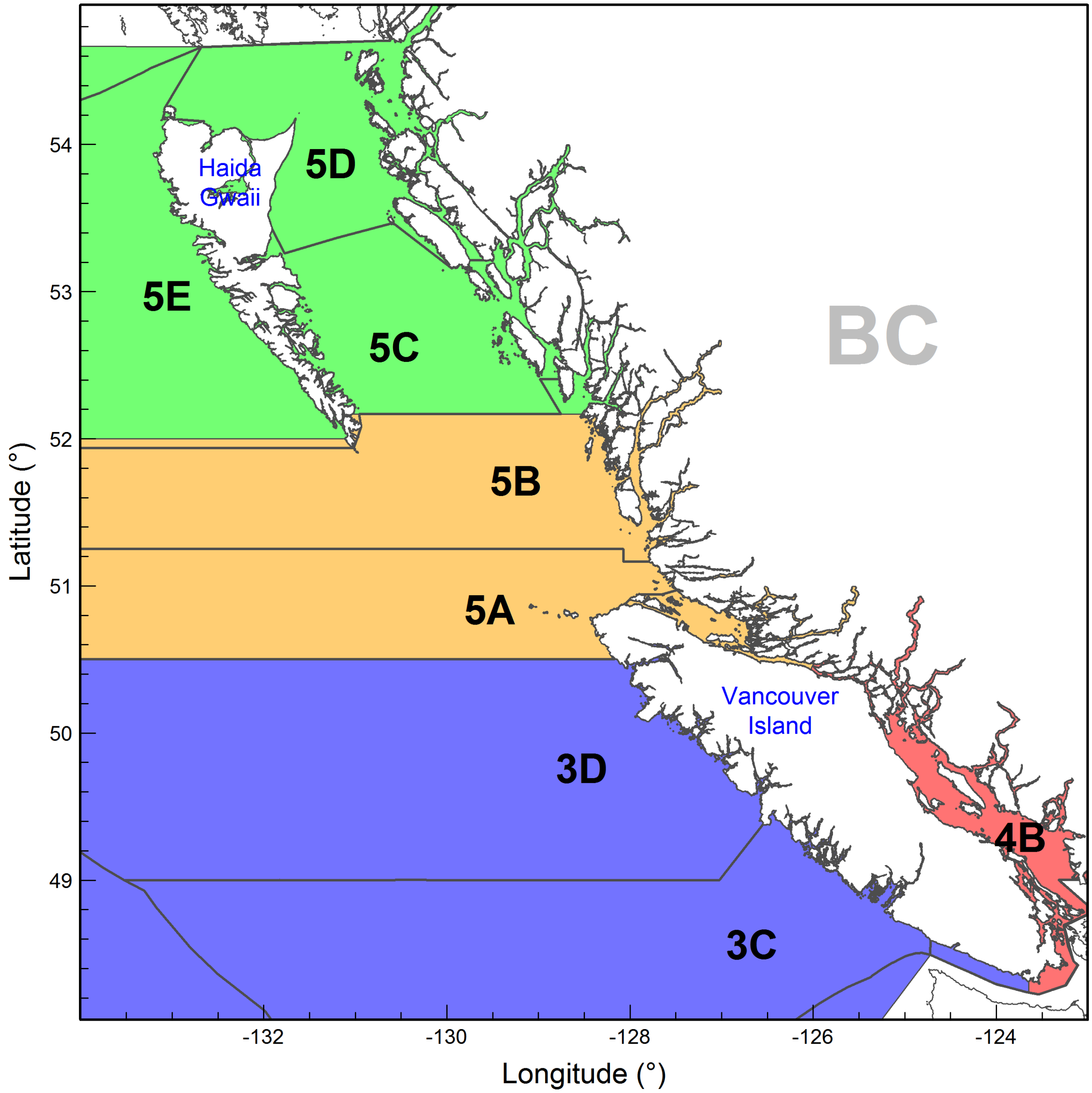

Figure A.1. Walleye Pollock assessment areas comprising Pacific Marine Fisheries Commission (PMFC) major and minor areas – green for 5CDE, orange for 5AB + minor area 12, blue for 3CD + minor area 20, and red for 4B less minor areas 12 and 20. The Groundfish Management Unit area boundaries, which differ from PMFC area, are superimposed for comparison. This assessment is for areas called 'North' (5CDE, green) and 'South' (5AB3CD, orange + blue).

Table A.1. Annual trawl Total Allowable Catches (TACs) in tonnes for Walleye Pollock in groundfish management areas. Entries '---' denote no TAC set; empty cells denote unknown TAC. Note: year can either be calendar year (1994-1996) or fishing year (1997 on).

Year	Start	End	5CDE	5AB	3CD	Gulf	Coast	Outside	Notes
1981	1/1/1981	12/31/1981	-	-	-	3400	3400	-	a
1982	1/1/1982	12/31/1982	-	-	-	3400	3400	-	-
1983	1/1/1983	12/31/1983	-	-	-	3400	3400	-	-
1984	1/1/1984	12/31/1984	-	-	-	3400	3400	-	-
1985	1/1/1985	12/31/1985	-	-	-	3400	3400	-	-
1986	1/1/1986	12/31/1986	-	-	-	3400	3400	-	-
1987	1/1/1987	12/31/1987	-	-	-	3400	3400	-	-
1988	1/1/1988	12/31/1988	-	-	-	3400	3400	-	-
1989	1/1/1989	12/31/1989	-	-	-	3400	3400	-	-
1990	1/1/1990	12/31/1990	-	-	-	3400	3400	-	-
1991	1/1/1991	12/31/1991	-	-	-	3700	3700	-	-
1992	1/1/1992	12/31/1992	-	-	-	3700	3700	-	-
1993	1/1/1993	12/31/1993	-	-	-	3700	3700	-	-
1994	1/1/1994	12/31/1994	-	-	-	2000	2000	-	b
1995	1/1/1995	12/31/1995	2900	1750	-	2260	6910	4650	c
1996	2/6/1996	3/31/1997	3190	1898	-	1490	6578	5088	d,e
1997	4/1/1997	3/31/1998	825	1790	270	1115	4000	2885	f
1998	4/1/1998	3/31/1999	825	1790	-	1115	3730	2615	-
1999	4/1/1999	3/31/2000	1320	1790	-	1115	4225	3110	-
2000	4/1/2000	3/31/2001	1320	1790	-	1115	4225	3110	-
2001	4/1/2001	3/31/2002	1320	1790	-	1115	4225	3110	-
2002	4/1/2002	3/31/2003	1320	1790	-	1115	4225	3110	g,h
2003	4/1/2003	3/31/2004	1320	1790	-	1115	4225	3110	-
2004	4/1/2004	3/31/2005	1320	1790	-	1115	4225	3110	-
2005	4/1/2005	3/31/2006	1320	1790	-	1115	4225	3110	-
2006	4/1/2006	3/31/2007	1320	1790	-	1115	4225	3110	i
2007	3/10/2007	3/31/2008	1320	1790	-	1115	4225	3110	-
2008	3/8/2008	2/20/2009	1320	1790	-	1115	4225	3110	-
2009	2/21/2009	2/20/2010	1320	1790	-	1115	4225	3110	-
2010	2/21/2010	2/20/2011	1320	1790	-	1115	4225	3110	-
2011	2/21/2011	2/20/2013	1320	1790	-	1115	4225	3110	-
2012	2/21/2011	2/20/2013	1320	1790	-	1115	4225	3110	j
2013	2/21/2013	2/20/2014	1320	1790	-	1115	4225	3110	k
2014	2/21/2014	2/20/2015	1320	1790	-	1115	4225	3110	-
2015	2/21/2015	2/20/2016	1320	1790	-	1115	4225	3110	l
2016	2/21/2016	2/20/2017	1320	1790	-	1115	4225	3110	m

*See Table A.2 for management actions indicated by note letter.

Table A.2. Codes to notes on management actions and quota adjustments that appear in Table A.1. Abbreviations under 'Management Actions': WAP = Walleye Pollock, DMP = dockside monitoring program, IVQ = individual vessel quota, lbs = pounds (0.4536 kg/lb).

	Year	Management Actions*
a	1981	Pollock TAC (1981-1994): only 4B=Areas 13-18, 29
b	1994	Started DMP for Trawl fleet.
c	1995	Pollock TAC areas: 5CDE=5CD; 5AB=Area 12; 4B=Areas 13-18, 29
d	1996	Started 100% onboard observer program for offshore Trawl fleet.
e	1996	Pollock TAC areas: 5CDE=5CD; 5AB=Areas 11,12; 4B=Areas 13-18, 29
f	1997	Started IVQ system for Trawl *Total Allowable Catch* (TAC) species (April 1, 1997)
g	2002	Established the inshore rockfish conservation strategy.
h	2002	Closed areas to preserve four hexactinellid (glassy) sponge reefs.
i	2006	Introduced an *Integrated Fisheries Management Plan* (IFMP) for most groundfish fisheries.
j	2012	Freeze the footprint of where groundfish bottom trawl activities can occur (all vessels under the authority of a valid Category "T" commercial groundfish trawl license selecting Option A as identified in the IFMP).
k	2013	To support groundfish research the Groundfish Trawl Industry agreed to the trawl TAC offsets to account for unavoidable mortality incurred in during the 2013 DFO and Trawl industry agreed upon Groundfish Trawl Multi-species surveys: WAP in 5CDE=2.2 t, 5AB=1.2 t.
l	2015	Research allocations for 2015 to account for the mortalities associated with survey catches within TACs: WAP=4.3 t.
m	2016	Research allocations for 2016 to account for the mortalities associated with survey catches within TACs: WAP=0.3 t.

* see Archived Integrated Fisheries Management Plans - Pacific Region.

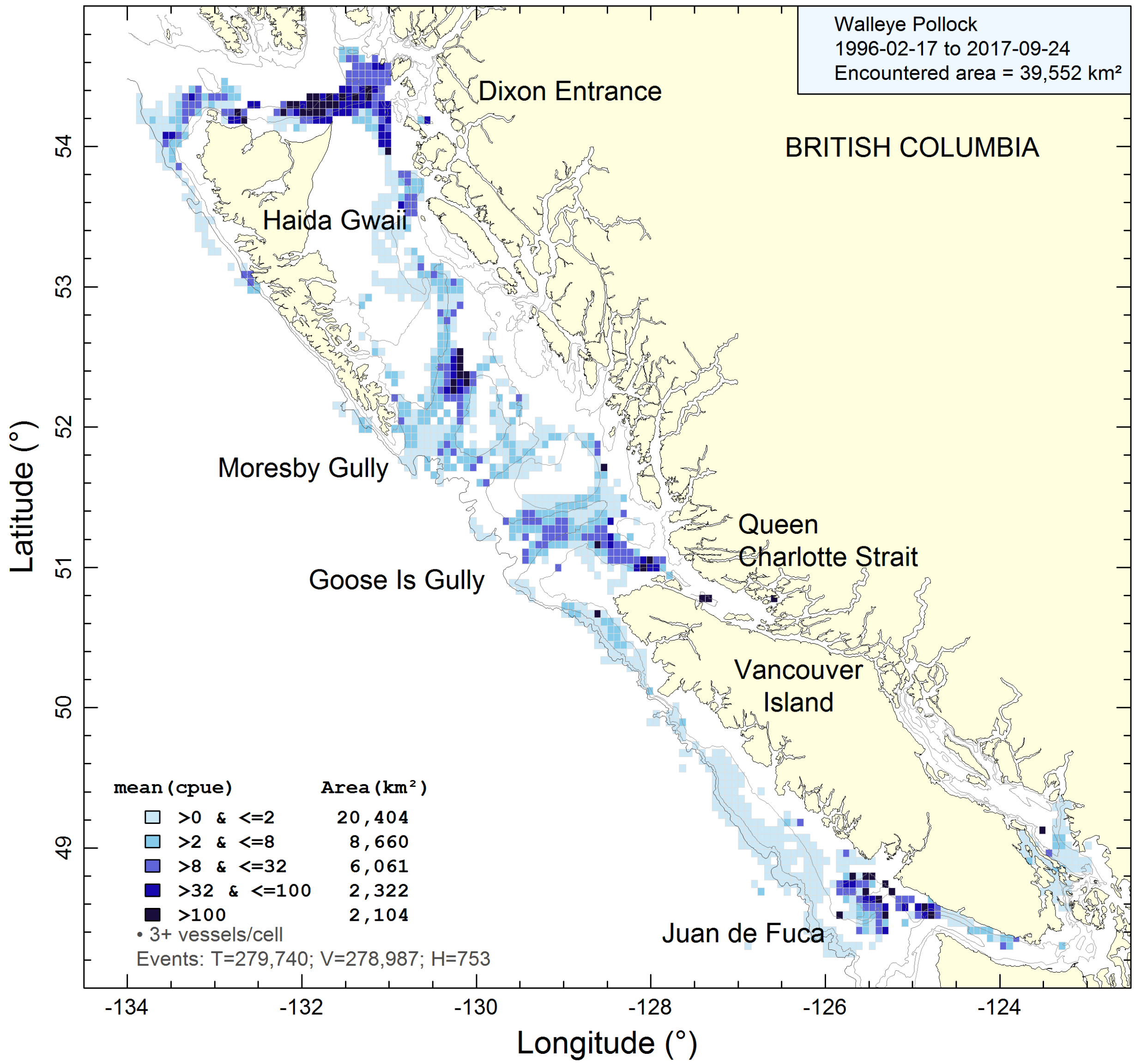

Figure A.2. Aerial distribution of Walleye Pollock bottom trawl tow mean catch per unit effort (kg/hour) from Feb 17, 1996 to Sep 24, 2017. Isobaths show the 100, 200, and 500 m depth contours. Note that cells with <3 fishing vessels are not displayed. Each cell represents, on average, 32 km².

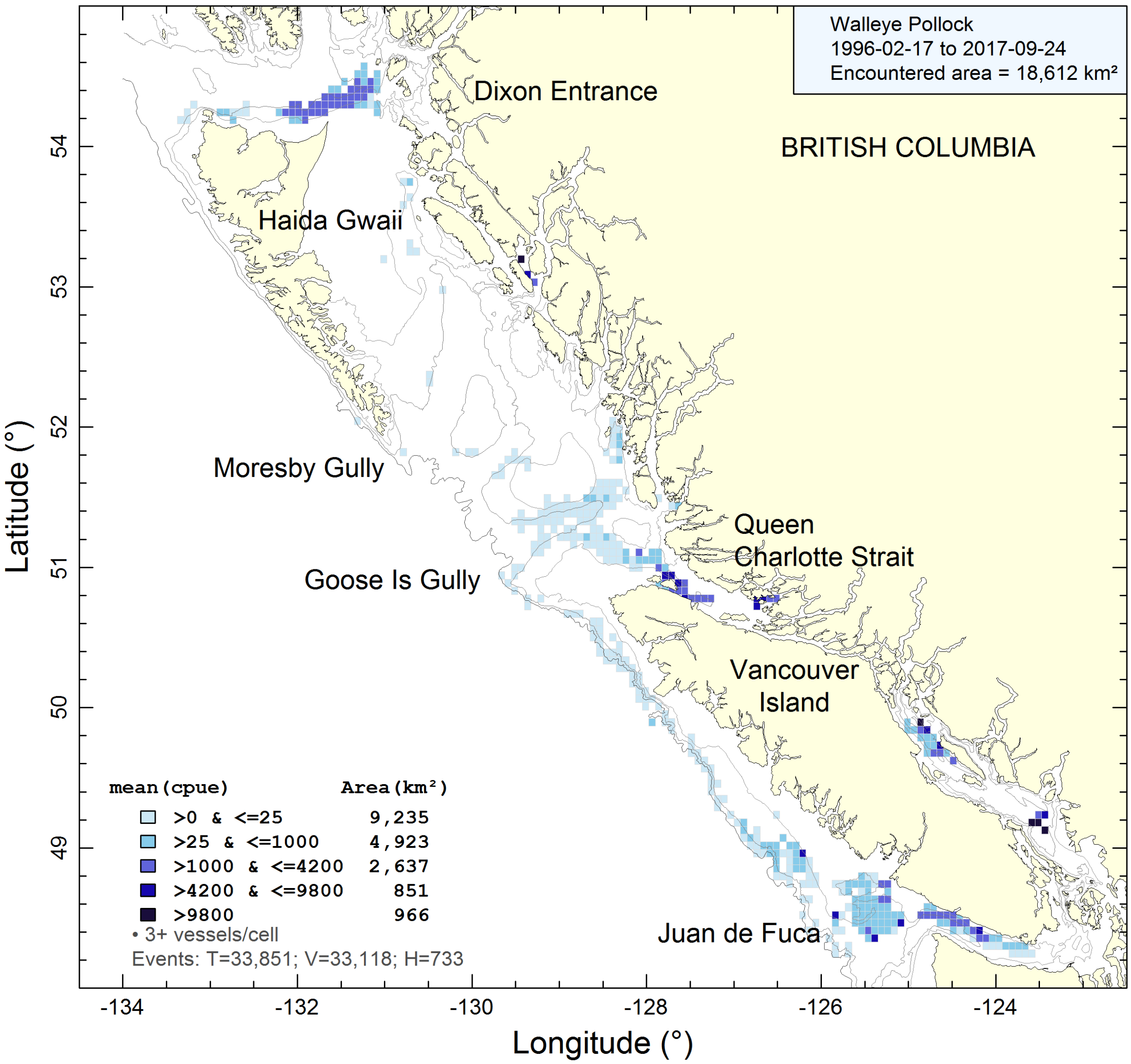

Figure A.3. Aerial distribution of Walleye Pollock midwater trawl tow mean catch per unit effort (kg/hour) from Feb 17, 1996 to Sep 24, 2017. Isobaths show the 100, 200, and 500 m depth contours. Note that cells with <3 fishing vessels are not displayed. Each cell represents, on average, 32 km².

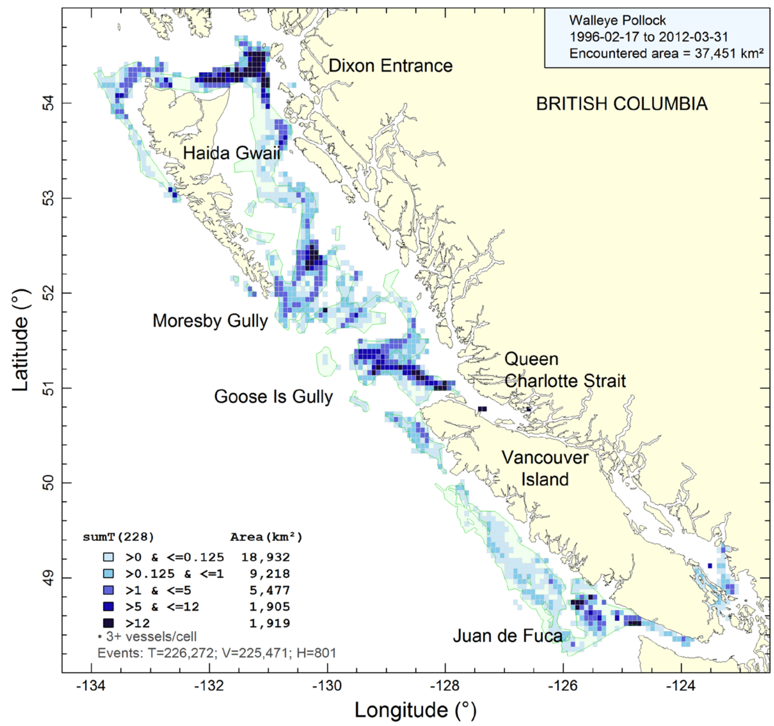

Figure A.4. Aerial distribution of accumulated Walleye Pollock catch (tonnes) from bottom trawls before the introduction of the trawl footprint (green polygons) in April 2012, limiting areas in which trawl vessels can operate. Note that cells with <3 fishing vessels are not displayed. Each cell represents, on average, 32 km².

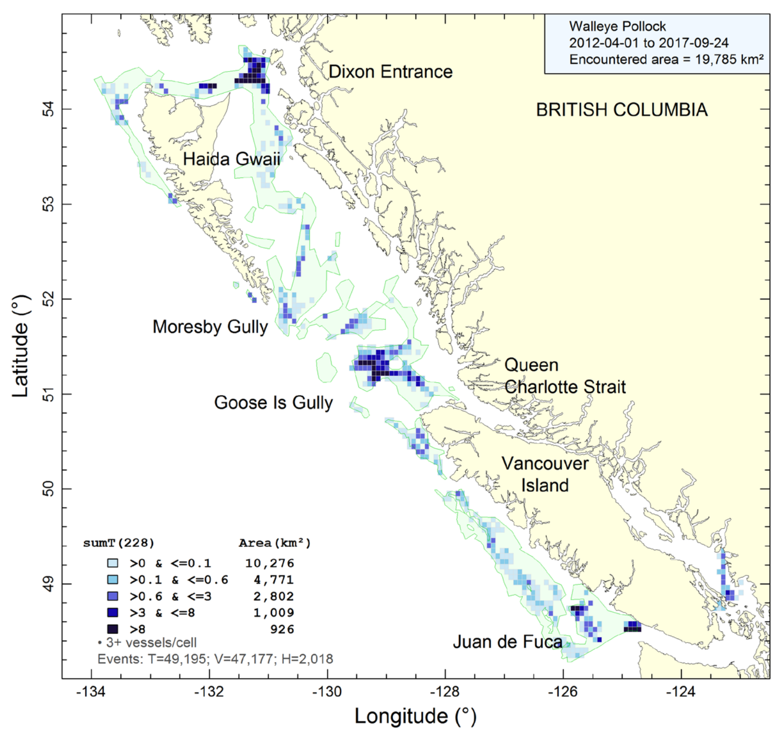

Figure A.5. Aerial distribution of accumulated Walleye Pollock catch (tonnes) from bottom trawls after the introduction of the trawl footprint (green polygons) in April 2012. See Figure A.2 captions for details.

A.2. CATCH HISTORY

This assessment collects reported catches back to 1954 but considers the start of the fishery to be 1967 (Figure A.6, Table A.3) when the Canadian domestic fleet started to increase the capture of Walleye Pollock.

Starting in 2015, all official catch tables from the databases below have been merged into one table called "GF_MERGED_CATCH", which is available in DFO's GFFOS database. All groundfish DFO databases are now housed on the DFBCV9TWVASP001 server (formerly on the SVBCPBSGFIIS server). Walleye Pollock catch by fishery sector ultimately comes from the following four DFO databases:

- GFCatch (1954-1995) – trawl and trap (Rutherford 1999);
- PacHarvest observer trawl (1996-2007) – trawl;
- GFFOS groundfish subset from Fishery Operation System (2006-2016) – all fisheries, gear types, and modern surveys; and
- GFBio joint-venture hake and research survey catches (1947-2016) – multiple gear types.

However, all these data sources are superseded by GFFOS from 2007 on because this latter repository was designed to record all landings and discards from commercial fisheries and research activities. Prior to this, midwater landings of pollock only appeared in either GFCatch or GFBio. The latter was designed primarily to hold biological information from fish samples but also served to record catch from J-V hake fishing events and research survey activity.

A.2.1. Coastwide Stock

Total annual catches used in the delay-difference population model comprised those from bottom and midwater trawls in three offshore areas – 5CDE (around Haida Gwaii), 5AB (Queen Charlotte Sound and Strait), and 3CD (west coast Vancouver Island plus the entrance to Juan de Fuca Strait) – and areas unknown (Table A.3, Figure A.6). Only catches in the Strait of Georgia (4B) were excluded from this assessment. Additionally, catches not in 4B are presented by fishing gear (Table A.4) and by DFO database (Table A.5). These include records from non-trawl fisheries; however, the amounts from these sources are so minor that the population assessment only considered removals by trawl gear.

Table A.3. Reported catches (in tonnes, landings + releases) of WAP in PMFC 5CDE + 5AB+ 3CD by coastal region. Catches from the trawl fishery explicitly excluding the Gulf region (4B) were used in the population model (see Table A.7). Catch for 2016 is not complete.

Year	5CDE	5AB	3CD	UNK	Total	Year	5CDE	5AB	3CD	UNK	Total
1954	0	14.9	5.93	0	21	1986	99.7	8.39	3.74	0	112
1955	2.77	1.4	5.55	0	10	1987	34.7	35.3	3.62	0	74
1956	14.5	20.6	52.8	0	88	1988	52.1	13.3	265	0	330
1957	7.26	3.16	4.35	0	15	1989	42.5	27.6	944	0	1014
1958	14.4	3.38	15.9	0	34	1990	422	142	625	0	1189
1959	1.72	2.24	18.6	0	23	1991	529	48.5	454	0	1032
1960	9.47	5.87	12.1	0	27	1992	1372	1772	1769	0	4913
1961	6.2	1	3.46	0	11	1993	4447	3828	671	0	8946
1962	11.8	0	20.3	0	32	1994	1344	3279	192	0.005	4815
1963	3.54	5.87	11.9	0	21	1995	1685	2574	16.3	0	4275
1964	2.08	5.56	22.9	0	31	1996	887	685	2812	52.9	4437
1965	9.21	0	30.2	0	39	1997	612	128	268	11.4	1019
1966	134	1.27	26.5	0	162	1998	819	61	3.14	5.46	889
1967	68	2.38	4.27	1	76	1999	1213	34.7	6.22	4.52	1258
1968	17.6	6.67	3.68	0	28	2000	987	57.5	99.6	4.57	1149
1969	47.2	33.2	32.5	0	113	2001	122	6.8	2854	50	3033
1970	7.5	0	34.9	0	42	2002	84	19.5	2726	246	3076
1971	0	0	47.4	0	47	2003	625	1723	2516	65	4929
1972	1.03	172	70.1	0	243	2004	1036	590	675	71.4	2372
1973	23.5	70.4	4.98	0	99	2005	501	851	154	277	1783
1974	49.8	19.4	0	0	69	2006	543	2863	105	113	3624
1975	132	34.4	18.1	0	185	2007	1302	2095	2.24	30.7	3430
1976	818	469	17.4	0	1304	2008	354	1090	4.96	21.6	1471
1977	659	244	55.3	0	958	2009	1430	2004	283	139	3856
1978	1776	324	51.6	0	2152	2010	1702	1976	112	26.5	3817
1979	1923	164	63.6	0	2151	2011	831	1935	1341	31	4138
1980	1285	41	27.2	0	1353	2012	1129	1751	1226	41.6	4148
1981	693	15	184	0	892	2013	824	1345	154	25.7	2349
1982	824	7.38	105	0	936	2014	643	2013	4092	33	6781
1983	1084	20.8	6.99	0	1112	2015	1532	1858	563	121	4074
1984	699	18.7	7.52	0	725	2016	170	714	20.5	52	957
1985	1180	1.38	8.56	0	1190	-	-	-	-	-	-

Table A.4. Reported catches (in tonnes, landings + releases) of WAP in PMFC 5CDE + 5AB+ 3CD by fishing gear. Catch for 2016 is not complete.

Year	Bottom Trawl	Midw. Trawl	Trap	Hook& Line	Total	Year	Bottom Trawl	Midw. Trawl	Trap	Hook& Line	Total
1954	20.9	0	0	0	21	1986	43.9	67.9	0	0	112
1955	9.71	0	0	0	10	1987	72.4	1.17	0	0	74
1956	87.8	0	0	0	88	1988	75.9	254	0	0	330
1957	14.8	0	0	0	15	1989	76.5	938	0	0	1015
1958	33.6	0	0	0	34	1990	556	633	0	0	1189
1959	22.5	0	0	0	23	1991	538	493	0	0	1031
1960	27.5	0	0	0	28	1992	1089	3825	0	0	4914
1961	10.5	0	0	0	11	1993	2753	6192	0	0	8945
1962	32.1	0	0	0	32	1994	1102	3713	0	0	4815
1963	21.3	0	0	0	21	1995	815	3460	0	0.008	4275
1964	30.6	0	0	0	31	1996	1026	3410	0	0	4436
1965	39.4	0	0	0	39	1997	311	708	0	0.001	1019
1966	162	0	0	0	162	1998	203	686	0	0.023	889
1967	75.6	0	0	0	76	1999	278	980	0	0.004	1258
1968	28	0	0	0	28	2000	172	977	0	0.009	1149
1969	113	0	0	0	113	2001	194	2840	0	0.004	3034
1970	42.4	0	0	0	42	2002	135	2940	0	0	3075
1971	47.4	0	0	0	47	2003	186	4742	0	0	4928
1972	243	0.02	0	0	243	2004	145	2227	0	0.005	2372
1973	97.5	1.42	0	0	99	2005	446	1336	0	0.006	1782
1974	66.7	2.53	0	0	69	2006	143	3481	0	0.049	3624
1975	123	61.5	0	0	185	2007	142	3288	0	0	3430
1976	899	406	0	0	1305	2008	74.6	1396	0	0	1471
1977	904	54.2	0	0	958	2009	110	3746	0	0	3856
1978	1313	839	0	0	2152	2010	117	3699	0	0	3816
1979	1378	772	0.005	0	2150	2011	175	3963	0	0.059	4138
1980	831	522	0	0	1353	2012	155	3993	0	0.041	4148
1981	576	316	0	0	892	2013	162	2186	0	0.053	2348
1982	254	682	0	0	936	2014	153	6628	0	0.054	6781
1983	239	872	0	0	1111	2015	284	3790	0	0.046	4074
1984	158	567	0	0	725	2016	96.6	860	0	0.013	957
1985	65.5	1125	0	0	1191	-	-	-	-	-	-

Table A.5. Reported catches (in tonnes, landings + releases) of WAP in PMFC 5CDE + 5AB+ 3CD reported by DFO database. Catch for 2016 is not complete.

Year	GF Catch	GFBio	Pac Harvest	GF FOS	Total	Year	GF Catch	GFBio	Pac Harvest	GF FOS	Total
1954	20.9	0	0	0	21	1986	112	0	0	0	112
1955	9.71	0	0	0	10	1987	73.6	0	0	0	74
1956	87.8	0	0	0	88	1988	78.6	252	0	0	331
1957	14.8	0	0	0	15	1989	109	905	0	0	1014
1958	33.6	0	0	0	34	1990	605	584	0	0	1189
1959	22.5	0	0	0	23	1991	602	429	0	0	1031
1960	27.5	0	0	0	28	1992	3476	1437	0	0	4913
1961	10.5	0	0	0	11	1993	8339	607	0	0	8946
1962	32.1	0	0	0	32	1994	4650	166	0	0	4816
1963	21.3	0	0	0	21	1995	4265	9.83	0	0	4275
1964	30.6	0	0	0	31	1996	0	2314	2122	0	4436
1965	39.4	0	0	0	39	1997	0	162	857	0	1019
1966	162	0	0	0	162	1998	0	0	888	0	888
1967	75.6	0	0	0	76	1999	0	0	1258	0	1258
1968	28	0	0	0	28	2000	0	143	1006	0	1149
1969	113	0	0	0	113	2001	0	1325	1708	0	3033
1970	42.4	0	0	0	42	2002	0	0	3075	0	3075
1971	47.4	0	0	0	47	2003	0	0	4928	0	4928
1972	243	0	0	0	243	2004	0	43.9	2329	0	2373
1973	98.9	0	0	0	99	2005	0	0	1781	0	1781
1974	69.2	0	0	0	69	2006	0	22.7	3602	0	3625
1975	184	0	0	0	184	2007	0	0	1436	1994	3430
1976	1304	0	0	0	1304	2008	0	0	0	1470	1470
1977	958	0	0	0	958	2009	0	0	0	3856	3856
1978	2152	0	0	0	2152	2010	0	0	0	3817	3817
1979	2150	0	0	0	2150	2011	0	0	0	4138	4138
1980	1353	0	0	0	1353	2012	0	0	0	4148	4148
1981	892	0	0	0	892	2013	0	0	0	2349	2349
1982	867	68.8	0	0	936	2014	0	0	0	6781	6781
1983	1111	0	0	0	1111	2015	0	0	0	4074	4074
1984	725	0	0	0	725	2016	0	0	0	956	956
1985	1190	0	0	0	1190	-	-	-	-	-	-

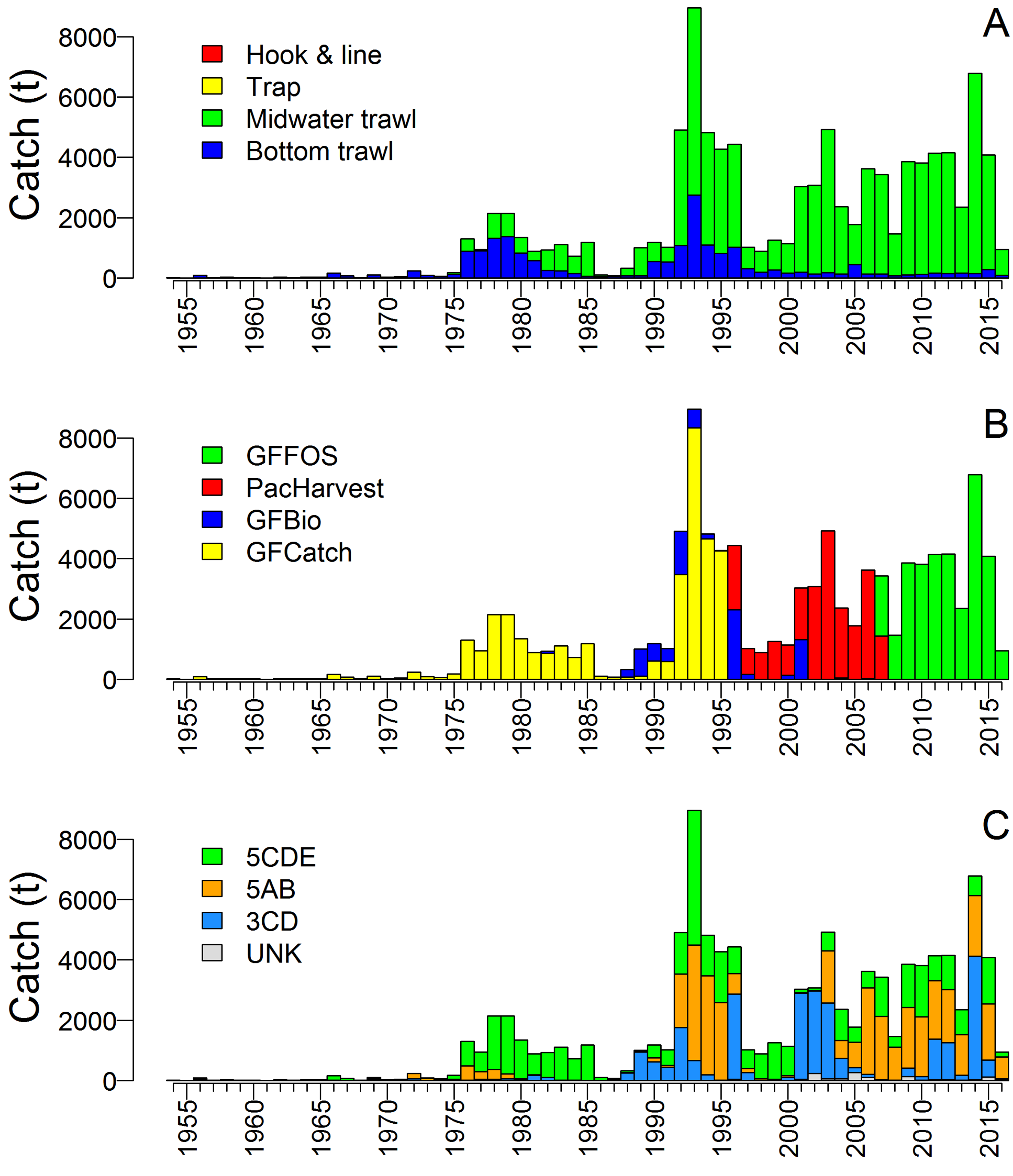

Figure A.6. Reported total (landed + released) catch (t) for Walleye Pollock in PMFC major areas 5CDE + 5AB + 3CD from (A) all gear types, (B) DFO databases, and (C) the three regions and areas unknown (trawl fishery only). Note that catches in panels A and B include those from non-trawl fisheries; however, these are negligible.

A.2.2. North vs. South Stocks

Initially, the assessment focused on a coastwide stock; however, after some exploration it became evident that Walleye Pollock in the North were twice as big, on average, as those in the South (1.04 kg/fish vs. 0.51 kg/fish, respectively, Table A.6, Figure A.7.). A meeting of the Technical Working Group on Mar 23, 2016, facilitated the decision to model the North (PMFC 5CDE) separately from the South (PMFC 5AB3CD + minor areas 12 & 20). The catch inputs to the model appear in Table A.7. We note that catch by gear type differs by region (Figure A.8).

Table A.6. Annual mean weight (kg) of Walleye Pollock by PMFC minor areas roughly arrange in a North-to-South direction. The final row gives the geometric mean of the fish by minor area (see Figure A.7). Headers in blue indicate areas for the North stock, those in pink indicate areas for the South stock.

Year	35	3	4	1	5	6	2	7	8	11	12	23	21	20
1972	---	---	---	---	---	---	---	---	0.611	1.227	---	---	---	---
1973	---	---	---	---	0.643	0.300	0.302	---	---	1.229	---	---	---	1.227
1974	---	---	---	---	---	---	0.832	---	---	---	---	---	---	---
1976	---	---	1.157	---	1.293	---	1.727	---	---	---	---	---	---	---
1977	1.562	1.058	1.323	1.478	1.037	---	---	---	1.679	---	---	---	0.868	---
1978	---	1.348	1.263	---	---	1.369	0.425	---	1.740	0.907	---	---	---	---
1979	1.481	1.563	1.423	1.482	0.981	1.167	---	---	---	---	---	---	---	1.021
1980	---	---	0.827	---	---	---	---	---	---	---	---	---	---	---
1981	---	---	1.100	---	---	---	---	---	---	---	---	---	---	---
1985	---	---	1.434	---	---	---	---	---	---	---	---	---	---	---
1988	---	---	---	---	---	---	---	---	---	---	---	0.709	---	---
1989	---	---	---	---	---	---	---	---	---	---	---	0.395	0.820	---
1990	---	---	---	---	---	---	---	---	---	---	---	0.536	0.585	---
1991	---	---	---	---	---	---	---	---	---	---	---	0.481	---	---
1992	---	---	---	---	---	---	---	---	---	---	---	0.332	0.356	---
1993	---	---	---	---	---	---	---	---	---	---	---	0.285	0.271	---
1994	---	---	---	---	---	---	---	---	---	---	---	---	0.374	---
1996	---	---	---	---	---	---	---	---	---	---	---	0.271	0.294	---
1997	---	0.994	1.179	---	---	---	---	---	---	---	---	0.377	0.401	---
1998	---	1.024	1.148	---	---	---	0.720	---	---	---	---	---	---	---
1999	---	1.236	0.930	---	---	---	---	---	---	---	---	---	---	---
2000	---	1.269	0.833	---	---	---	---	---	---	---	---	---	0.352	---
2001	---	---	---	---	---	---	---	---	---	---	---	0.230	0.271	---
2002	---	---	---	---	---	---	---	---	---	---	---	0.057	0.479	---
2003	---	1.008	1.014	---	---	---	---	---	---	---	0.698	0.394	---	---
2004	---	---	0.856	---	---	---	---	---	---	---	0.700	---	0.497	---
2005	---	---	1.067	---	---	---	---	---	---	0.633	0.857	---	---	---
2006	---	---	0.822	---	---	---	---	---	---	0.608	0.632	---	---	---
2007	---	---	0.878	---	---	---	---	---	---	0.782	0.732	---	---	---
2008	---	1.225	---	---	---	---	---	---	---	---	0.282	---	---	---
2009	---	1.409	1.279	---	---	---	---	---	---	---	0.394	0.596	---	0.322
2010	---	1.018	1.212	---	---	---	---	---	---	---	0.508	---	---	---
2011	---	---	---	---	---	---	---	---	0.336	---	0.527	0.592	0.448	0.503
2012	---	---	0.914	1.066	---	---	---	---	---	0.601	0.575	---	---	0.276
2013	---	0.908	0.974	---	---	---	---	---	---	0.853	0.609	---	---	0.243
2014	---	---	---	---	---	1.067	---	---	---	0.550	0.571	---	0.414	0.286
2015	---	---	1.084	---	---	0.974	---	0.95426	0.501	---	---	---	---	---
2016	---	---	1.606	---	---	---	---	---	---	---	0.570	---	---	---
Geomean	1.521	1.157	1.085	1.327	0.959	0.870	0.668	0.954	0.786	0.787	0.569	0.352	0.430	0.453

Table A.7. Catches used in the 2016 Walleye Pollock delay-difference model. Columns labelled 'North' include catches from PMFC area 5CDE, 'South' includes catches from PMFC areas 5AB (+ minor area 12) and 3CD (+ minor area 20), and 'Coast' includes catches from 'North', 'South', and unknown areas (see Table A.3). The coastwide equivalent catch from Saunders and Andrews (1998[4]), excluding 4B, is reported in the column labelled 'WP G07-7' for comparison purposes only.

Year	North	South	Coast	WP G97-7	Year	North	South	Coast
1967	68	7	76	56	1997	612	396	1019
1968	18	10	28	26	1998	819	64	889
1969	47	66	113	94	1999	1213	41	1259
1970	8	35	42	8	2000	987	157	1149
1971	0	47	47	5	2001	122	2861	3034
1972	1	242	243	173	2002	84	2746	3075
1973	23	75	99	85	2003	625	4239	4928
1974	50	19	69	61	2004	1036	1265	2373
1975	132	52	184	102	2005	501	1004	1782
1976	818	487	1304	1296	2006	543	2968	3624
1977	659	299	958	841	2007	1302	2097	3430
1978	1776	376	2152	2031	2008	354	1095	1470
1979	1923	227	2150	2045	2009	1430	2287	3856
1980	1285	68	1353	2932	2010	1702	2088	3817
1981	693	199	892	1640	2011	831	3276	4138
1982	824	112	936	1706	2012	1129	2977	4148
1983	1084	28	1111	1064	2013	824	1499	2349
1984	699	26	725	758	2014	643	6106	6781
1985	1180	10	1190	1263	2015	1532	2420	4074
1986	100	12	112	195	2016	1532	2420	4074
1987	35	39	74	1389	-	-	-	-
1988	52	278	330	269	-	-	-	-
1989	42	972	1014	975	-	-	-	-
1990	422	767	1189	1086	-	-	-	-
1991	529	503	1031	948	-	-	-	-
1992	1372	3541	4913	3501	-	-	-	-
1993	4447	4498	8945	5410	-	-	-	-
1994	1344	3471	4815	1717	-	-	-	-
1995	1685	2590	4275	2390	-	-	-	-
1996	887	3497	4436	3907	-	-	-	-

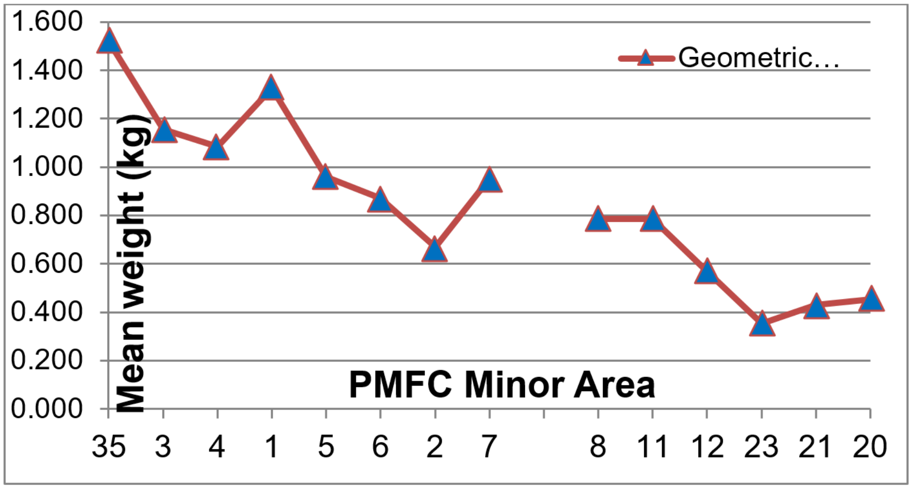

Figure A.7. Trend in mean weight of Walleye Pollock by PMFC minor area arranged from North to South (see Table A.6).

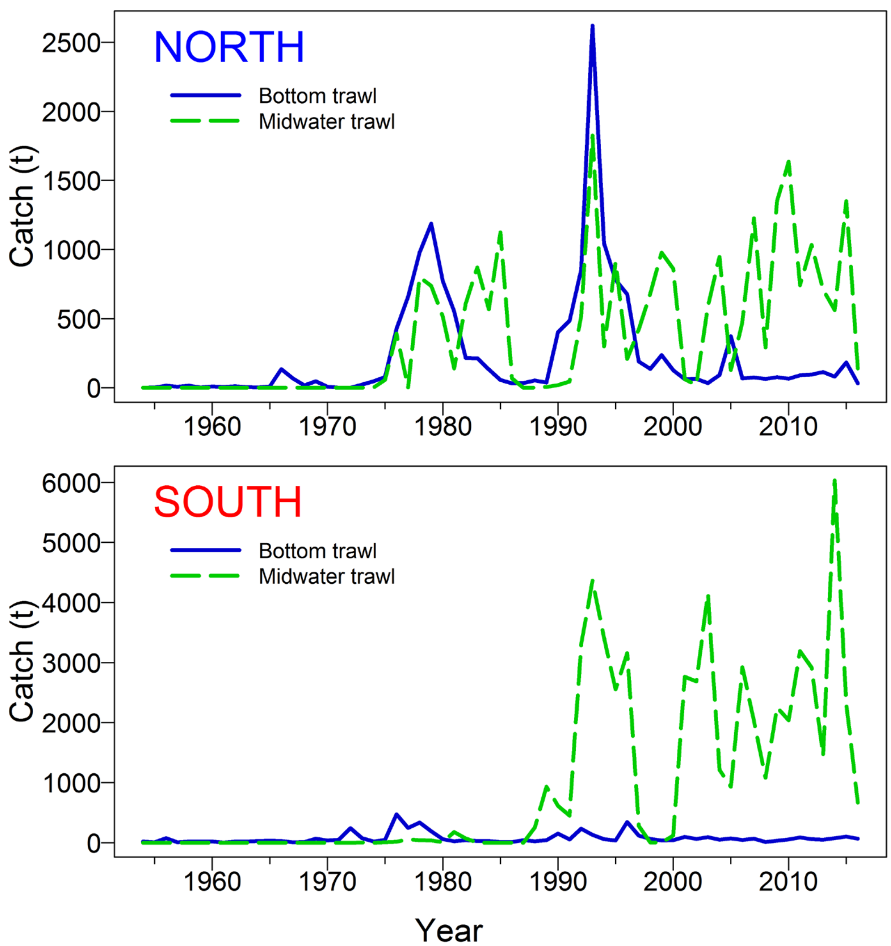

Figure A.8. Annual catch (t) of Walleye Pollock by gear type in the North and South areas.

A.3. REFERENCES – CATCH

DFO. 2016. Pacific Region Integrated Fisheries Management Plan – Groundfish: Effective February 21, 2016 (Version 1.5).

Forrester, C.R. et Smith, J.E. 1972. The British Columbia groundfish fishery in 1971, some aspects of its investigation and related fisheries. Fish. Res. Board Can. Tech. Rep. 338: 67 pp.

Gustafson, R.G., Lenarz, W.H., McCain, B.B., Schmitt, C.C., Grant, W.S., Builder, T.L. and Methot, R.D. 2000. Status review of Pacific Hake, Pacific Cod, and Walleye Pollock from Puget Sound, Washington. NOAA Technical Memorandum NMFS-NWFSC-44: 275 pp.

Rutherford, K.L. 1999. A brief history of GFCatch (1954-1995), the groundfish catch and effort database at the Pacific Biological Station. Can. Tech. Rep. Fish. Aquat. Sci. 2299: v + 66 pp.

Saunders, M.W., McFarlane, G.A. and Shaw, W. 1989. Delineation of Walleye Pollock (*Theragra chalcogramma*) stocks off the Pacific Coast of Canada. In Proc. Int. Symp. Biol. Mgmt. Walleye Pollock, Anchorage, AK, Nov 14-16, 1988, Lowell Wakefield Fisheries Symposia Series 7, Alaska Sea Grant Rep. 89-1, p. 379-401. Alaska Sea Grant College Program, University of Alaska, Fairbanks, AK.

Thompson, J.M. 1981. Preliminary report on the population biology and fishery of walleye pollock (*Theragra chalcogramma)* off the Pacific Coast of Canada. Can. Tech. Rep. Fish. Aquat. Sci. 1031: v + 157 pp.

Wallace, S., Turris, B., Driscoll, J., Bodtker, K., Mose, B. and Munro, G. 2015. Canada's Pacific groundfish trawl habitat agreement: A global first in an ecosystem approach to bottom trawl impacts. Mar. Pol. 60: 240–248.

APPENDIX B. TRAWL SURVEYS

B.1. INTRODUCTION

This appendix summarizes the derivation of relative Walleye Pollock (WAP) abundance indices from the following bottom trawl surveys:

- a set of historical surveys operated in the Goose Island Gully (GIG) of Queen Charlotte Sound (Section B.3);
- Hecate Strait assemblage or multi-species survey (Section B.4);
- Hecate Strait synoptic survey (Section B.5);
- Queen Charlotte Sound synoptic survey (Section B.6);
- west coast Vancouver Island synoptic survey (Section B.7);
- west coast Haida Gwaii synoptic survey (Section B.8).

Only surveys which were used in the WAP stock assessment are presented. The NMFS Triennial, WCVI shrimp and QC Sound shrimp surveys have been omitted because the presence of WAP in these surveys has been sporadic, rendering these surveys poor candidates to provide reliable abundance series for this species.

B.2. ANALYTICAL METHODS

Catch and effort data for strata i in year y yield catch per unit effort (CPUE) values U_{yi}. Given a set of data $\left\{C_{yij}, E_{yij}\right\}$ for tows $j = 1,\ldots,n_{yi}$,

Eq. B.1 $$U_{yi} = \frac{1}{n_{yi}} \sum_{j=1}^{n_{yi}} \frac{C_{yij}}{E_{yij}},$$

where C_{yij} = catch (kg) in tow j, stratum i, year y;
E_{yij} = effort (h) in tow j, stratum i, year y;
n_{yi} = number of tows in stratum i, year y.

CPUE values U_{yi} convert to CPUE densities δ_{yi} (kg/km^2) using:

Eq. B.2 $$\delta_{yi} = \frac{1}{vw} U_{yi},$$

where v = average vessel speed (km/h);
w = average net width (km).

Alternatively, if vessel information exists for every tow, CPUE density can be expressed

Eq. B.3 $$\delta_{yi} = \frac{1}{n_{yi}} \sum_{j=1}^{n_{yi}} \frac{C_{yij}}{D_{yij} w_{yij}},$$

where C_{yij} = catch weight (kg) for tow j, stratum i, year y;

D_{yij} = distance travelled (km) for tow j, stratum i, year y;

w_{yij} = net opening (km) for tow j, stratum i, year y;

n_{yi} = number of tows in stratum i, year y.

The annual biomass estimate is then the sum of the product of CPUE densities and bottom areas across m strata:

Eq. B.4 $$B_y = \sum_{i=1}^{m} \delta_{yi} A_i = \sum_{i=1}^{m} B_{yi} \ ,$$

where δ_{yi} = mean CPUE density (kg/km^2) for stratum i, year y;

A_i = area (km^2) of stratum i;

B_{yi} = biomass (kg) for stratum i, year y;

m = number of strata.

The variance of the survey biomass estimate V_y (kg^2) follows:

Eq. B.5 $$V_y = \sum_{i=1}^{m} \frac{\sigma_{yi}^2 A_i^2}{n_{yi}} = \sum_{i=1}^{m} V_{yi} \ ,$$

where σ_{yi}^2 = variance of CPUE density (kg^2/km^4) for stratum i, year y;

V_{yi} = variance of the biomass estimate (kg^2) for stratum i, year y.

The coefficient of variation (CV) of the annual biomass estimate for year y is

Eq. B.6 $$CV_y = \frac{\sqrt{V_y}}{B_y} .$$

B.3. EARLY GIG SURVEYS IN QUEEN CHARLOTTE SOUND

B.3.1. Data selection

Tow-by-tow data from a series of historical trawl surveys were available for 12 years spanning the period from 1965 to 1995. The first two surveys, in 1965 and 1966, were wide-ranging, with the 1965 survey extending from near San Francisco to halfway up the Alaskan Panhandle (Westrheim 1966a, 1967b). The 1966 survey was only slightly less ambitious, ranging from the southern US-Canada border in Juan de Fuca Strait into the Alaskan Panhandle (Westrheim 1966b, 1967b). It was apparent that the design of these two early surveys was exploratory and that these surveys would not be comparable to the subsequent Queen Charlotte Sound (QCS) surveys which were much narrower in terms of area covered and which had a much higher density of tows in the Goose Island Gully (GIG). This can be seen in the small number of tows used by the first two surveys in GIG (Table B.1). As a consequence, these surveys are not included in this series.

The 1967 ([left panel]: Figure B.1) and 1969 ([left panel]: Figure B.2) surveys (Westrheim 1967a, 1969; Westrheim et al. 1968) also performed tows on the west coast of Vancouver Island, the west coast of Haida Gwaii and SE Alaska, but both of these surveys had a reasonable number of tows in the GIG grounds (Table B.1). The 1971 survey ([left panel]:

Figure B.3) was entirely confined to GIG (Harling et al. 1971) while the 1973 ([left panel]: Figure B.4), 1976 ([left panel]: Figure B.5) and 1977 ([left panel]: Figure B.6) surveys covered both Goose Island and Mitchell Gullies in QCS (Harling et al. 1973; Westrheim et al. 1976; Harling and Davenport 1977).

A 1979 survey (Nagtegaal and Farlinger 1980) was conducted by a commercial fishing vessel (*Southward Ho*, Table B.1), with the distribution of tows being very different from the preceding and succeeding surveys (plot not provided; see Figure C5 in Edwards et al. 2012). As well, the distribution of tows by depth was also different from the other surveys (Table B.2). These observations imply a substantially different survey design and consequently this survey was not included in the time series.

The 1984 survey was conducted by two vessels: the *G.B. Reed* and the *Eastward Ho* (Nagtegaal et al. 1986). Part of the design of this survey was to compare the catch rates of the two vessels (one was a commercial fishing vessel and the other a government research vessel – Greg Workman, DFO, pers. comm.), thus they both followed similar design specifications, including the configuration of the net. Unfortunately, the tows were not distributed similarly in all areas, with the *G.B. Reed* fishing mainly in the shallower portions of the GIG, while the *Eastward Ho* fished more in the deeper and seaward parts of the GIG ([left panel]: Figure B.7) although the two vessels fished more contiguously in Mitchell Gully (immediately to the north). When the depth-stratified catch rates for POP (the main design species of the surveys) of the two vessels were compared within the GIG only (using a simple ANOVA), the *Eastward Ho* catch rates were significantly higher ($p=0.049$) than those observed for the *G.B. Reed*. However, the difference in catch rates was no longer significant when tows from Mitchell's Gully were added to the analysis ($p=0.12$). Given the lack of significance when the full suite of available tows were compared, along with the uneven spatial distribution of tows among vessels within the GIG (although the ANOVA was depth-stratified, it is possible that the depth categories were too coarse), the most parsimonious conclusion was that there was no detectable difference between the two vessels. Consequently, all the GIG tows from both vessels were pooled for this survey year.

The 1994 survey (Hand et al. 1995), also conducted by a commercial vessel (the *Ocean Selector*, Table B.2) ([left panel]: Figure B.8), was modified by the removal of 19 tows which were part of an acoustic experiment and therefore were not considered appropriate for biomass estimation (they were tows used to estimate species composition for ensonified schools). Although this survey was designed to emulate as closely as possible the previous *G.B. Reed* surveys in terms of tow location selection (same fixed tow locations, G. Workman, DFO, pers. comm.), the timing of this survey was about two to three months earlier than the previous surveys (starting in mid-June rather than August or September, Table B.3).

The 1995 survey (Yamanaka et al, 1996), conducted by two commercial fishing vessels: the *Ocean Selector* and the *Frosti* (Table B.2), used a random stratified design with each vessel duplicating every tow (G. Workman, DFO, pers. comm.). This type of design was entirely different from that used in the previous surveys. As well, the focus of this survey was on Pacific Ocean Perch (POP), with tows optimised to capture this species. Given the difference in design (random stations rather than fixed locations), this survey was not used in the stock assessment.

Table B.1. Number of tows in GIG and in other areas (Other) by survey year and vessel conducting the survey for the 12 historical (1965 to 1995) surveys. Survey years in grey were not used in the assessment.

Survey	GB Reed		Southward Ho		Eastward Ho		Ocean Selector		Frosti	
Year	Other	GIG	Other	GIG	Other	GIG	Other	GIG	Other	GIG
1965	76	8	-	-	-	-	-	-	-	-
1966	49	15	-	-	-	-	-	-	-	-
1967	17	33	-	-	-	-	-	-	-	-
1969	3	32	-	-	-	-	-	-	-	-
1971	3	36	-	-	-	-	-	-	-	-
1973	13	33	-	-	-	-	-	-	-	-
1976	23	33	-	-	-	-	-	-	-	-
1977	15	47	-	-	-	-	-	-	-	-
1979	-	-	20	59		-	-	-	-	-
1984	19	42	-	-	15	27	-	-	-	-
1994	-	-	-	-	-	-	2	69	-	-
1995	-	-	-	-	-	-	2	55	1	57

Table B.2. Total number of tows by 20 fathom depth interval (in metres) in GIG and in other areas (Other) by survey year for the 12 historical (1965 to 1995) surveys. Survey years in grey were not used in the assessment. There are more tows in the GIG portion of this table than in Table B.3 because some of the tows in this table were not suitable for index calculations.

Areas other than GIG

Survey	20 fathom depth interval (m)									Total
year	66-146	147-183	184-219	220-256	257-292	293-329	330-366	367-402	440-549	Tows
1965	3	15	26	17	6	6	1	1	1	76
1966	3	11	18	8	2	1	3	2	1	49
1967	1	-	6	1	2	1	1	4	-	16
1969	-	1	-	1	-	1	-	-	-	3
1971	-	-	-	-	-	-	-	-	-	-
1973	-	-	4	3	2	2	2	-	-	13
1976	-	-	4	4	4	4	4	-	-	20
1977	-	-	3	2	2	3	2	-	-	12
1979	11	2	1	5	1	-	-	-	-	20
1984	-	-	4	10	7	7	6	-	-	34
1994	-	-	-	-	-	-	-	-	-	-
1995	-	-	-	-	-	-	-	-	-	-

GIG

Survey	20 fathom depth interval (m)									Total
year	66-146	147-183	184-219	220-256	257-292	293-329	330-366	367-402	440-549	Tows
1965	-	2	4	1	1	-	-	-	-	8
1966	3	2	3	5	2	-	-	-	-	15
1967	1	6	11	6	10	-	-	-	-	34
1969	-	9	11	6	6	-	-	-	-	32
1971	-	5	15	9	10	-	-	-	-	39
1973	-	7	11	7	8	-	-	-	-	33
1976	-	7	15	8	6	-	-	-	-	36
1977	1	12	14	14	9	-	-	-	-	50
1979	23	12	18	6	-	-	-	-	-	59
1984	-	13	25	17	13	1	-	-	-	69
1994	-	15	18	20	18	-	-	-	-	71
1995	2	23	47	22	15	6	-	-	-	115

Given that the only area that was consistently monitored by these surveys was the GIG grounds, tows lying between 50.9°N and 51.6°N latitude from the seven acceptable survey years, covering the period from 1967 to 1984, were used to index the WAP population (Table B.1).

The original depth stratification of these surveys was in 20 fathom (36.1 m) intervals, with the important strata for WAP ranging from 70 fathoms (183 m) to 160 fathoms (300 m). For the GIG survey series, the shallowest tow capturing WAP was 121 m. Similarly, the deepest tow capturing WAP was 282 m. These depth strata were combined for analysis into three ranges: 70–100 fm, 100–120 fm and 120–160 fm, for a total of 333 tows from the eight accepted survey years (Table B.3).

Table B.3. Number of tows available by survey year and depth stratum for the analysis of the historical GIG trawl survey series. Survey year in grey was not used in the WAP stock assessment.

	Depth stratum					
Survey Year	**120-183 m (70–100 fm)**	**184-218 m (100–120 fm)**	**219-300 m (120–160 fm)**	**Total**	**Start Date**	**End Date**
1967	7	11	15	33	07-Sep-67	03-Oct-67
1969	9	11	12	32	14-Sep-69	24-Sep-69
1971	4	15	17	36	14-Oct-71	28-Oct-71
1973	7	11	15	33	07-Sep-73	24-Sep-73
1976	7	13	13	33	09-Sep-76	26-Sep-76
1977	13	14	20	47	24-Aug-77	07-Sep-77
1984	13	23	33	69	05-Aug-84	08-Sep-84
1994	10	16	24	50	21-Jun-94	06-Jul-94
1995	22	45	45	112	11-Sep-95	22-Sep-95

Table B.4. Biomass estimates for Walleye Pollock from the historical Goose Island Gully trawl surveys for the years 1967 to 1995. Biomass estimates are based on three depth strata (Table B.3), assuming that the survey tows were randomly selected within these areas. Bootstrap bias corrected confidence intervals and CVs are based on 1000 random draws with replacement.

Survey Year	**Biomass (t) (**Eq. B.4**)**	**Mean bootstrap biomass (t)**	**Lower bound biomass (t)**	**Upper bound biomass (t)**	**Bootstrap CV**	**Analytic CV (**Eq. B.6**)**
1967	141	143	32	289	0.467	0.465
1969	792	779	367	1,495	0.358	0.359
1971	1,432	1,417	109	4,283	0.735	0.740
1973	2,628	2,553	544	6,386	0.584	0.588
1976	5,669	5,678	2,220	9,918	0.336	0.346
1977	2,486	2,532	1,226	4,083	0.286	0.292
1984	1,284	1,290	522	2,356	0.345	0.346
1994	1,312	1,324	634	2,186	0.304	0.305

A doorspread density (Eq. B.3) was calculated for each tow based on the catch of WAP, using a fixed doorspread value of 61.6 m (Yamanaka et al. 1996) for every tow and the recorded distance travelled. Unfortunately, the speed, effort and distance travelled fields were not well populated for these surveys. Therefore, missing values for these fields were filled in with the mean values for the survey year. This resulted in the majority of the tows having distances towed near 3 km, which was the expected result given the design specification of ½ hour tows at an approximate speed of 6 km/h (about 3.2 knots).

B.3.2. Results

Maps showing the locations where WAP were caught in the Goose Island Gully (GIG) indicate that this species is found throughout the GIG in most years, excepting 1967 and 1969 (see Figure B.1 to Figure B.8). WAP was taken relatively frequently in small amounts, with 277 of the 444 valid tows capturing WAP with a median catch weight of 16 kg. The largest WAP tow in terms of catch weight was 2370 kg in 1971. WAP were mainly taken at depths from 159 to 276 m (5% and 95% quantiles of the starting depth empirical distribution), with the minimum and maximum observed depths at 148 and 296 m respectively (Figure B.9).

Estimated biomass levels in the GIG for Walleye Pollock from the historical GIG trawl surveys were variable, with the maximum biomass recorded in 1976 (at 5669 t) and the minimum biomass in 1967 (at 141 t) (Figure B.10; Table B.4). Survey relative errors are moderate to high for this species, ranging from a low of 0.29 in 1977 to 0.74 in 1971 (Table B.4). The proportion of tows which caught WAP was variable between years, ranging between 33% and 96% of the tows (Figure B.11). Overall, 277 tows from a total 444 valid tows (62%) contained WAP.

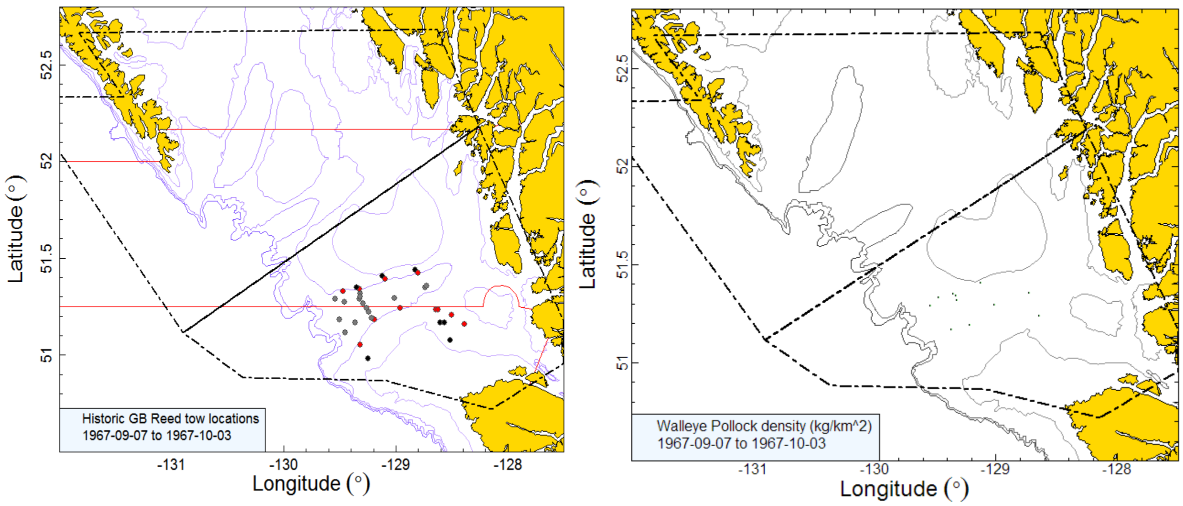

Figure B.1. Valid tow locations and density plots for the historic 1967 Goose Island Gully (GIG) survey. Tow locations are colour-coded by depth range: black=120–183m; red=184-218m; grey=219-300m. Circle sizes in the right-hand density plot scaled across all years (1967, 1969, 1971, 1973, 1976, 1977, 1984, and 1994), with the largest circle = 12,825 kg/km² in 1971. Black boundary lines show the extent of the modern Queen Charlotte Sound synoptic survey and the red solid lines indicate the boundaries between PMFC areas 5A, 5B and 5C.

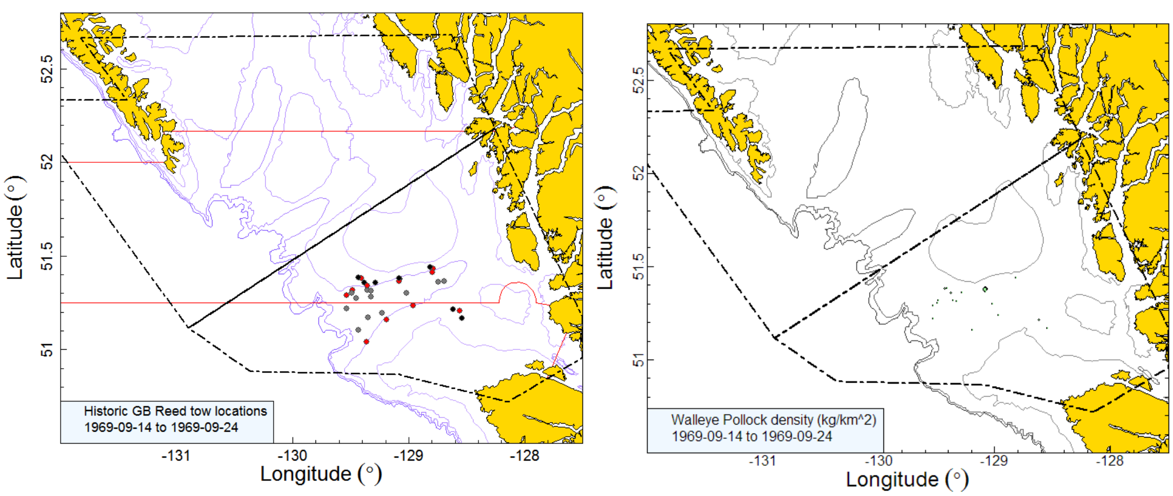

Figure B.2. Tow locations and density plots for the historic 1969 Goose Island Gully (GIG) survey (see Figure B.1 caption).

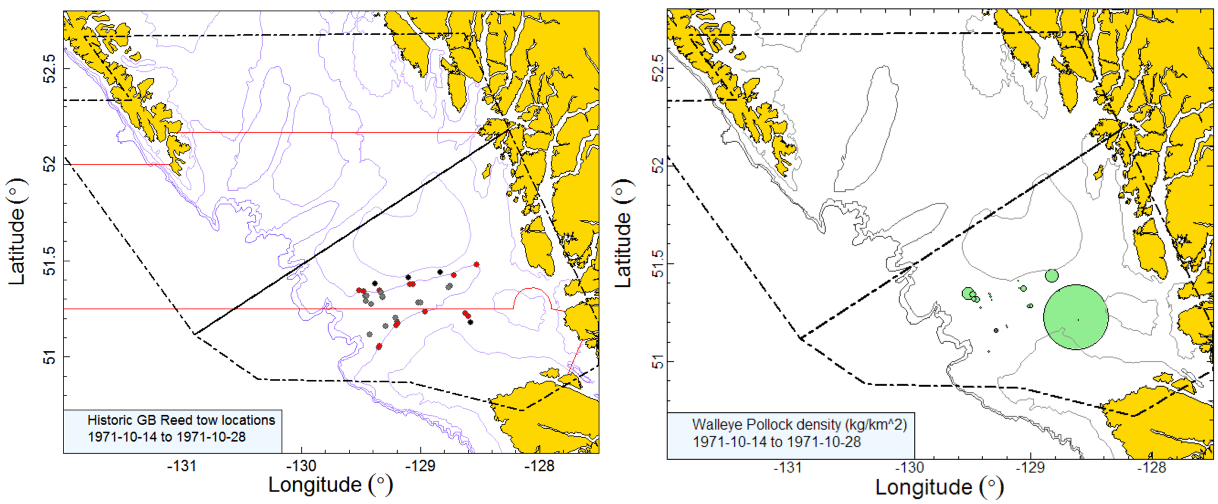

Figure B.3. Tow locations and density plots for the historic 1971 Goose Island Gully (GIG) survey (see Figure B.1 caption).

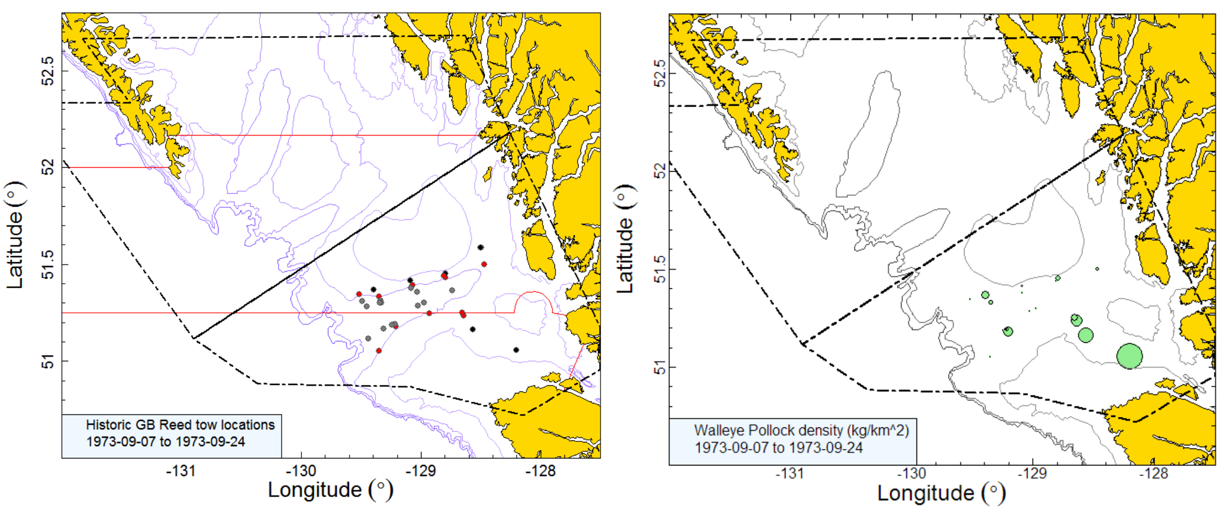

Figure B.4. Tow locations and density plots for the historic 1973 Goose Island Gully (GIG) survey (see Figure B.1 caption).

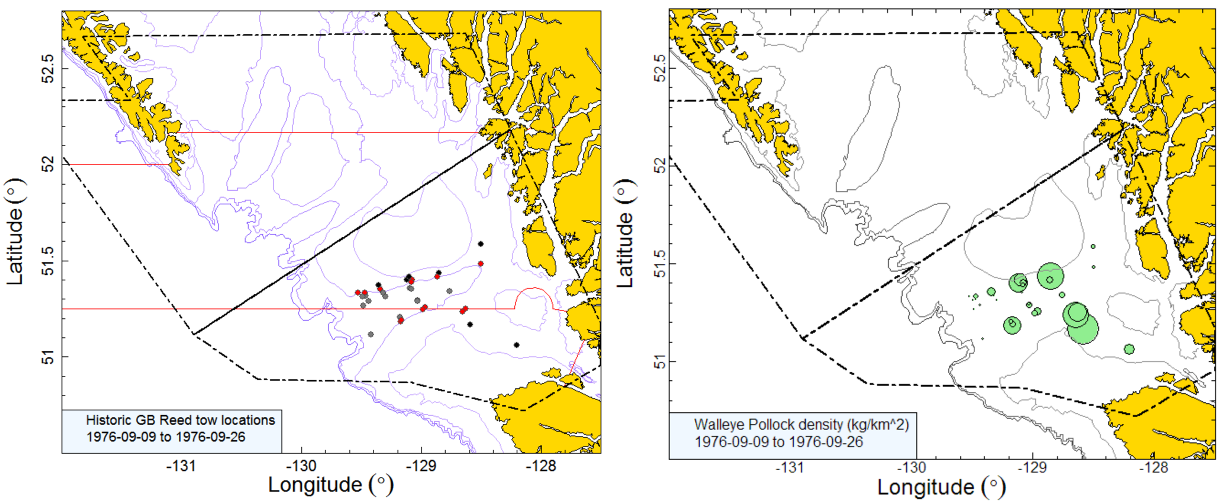

Figure B.5. Tow locations and density plots for the historic 1976 Goose Island Gully (GIG) survey (see Figure B.1 caption).

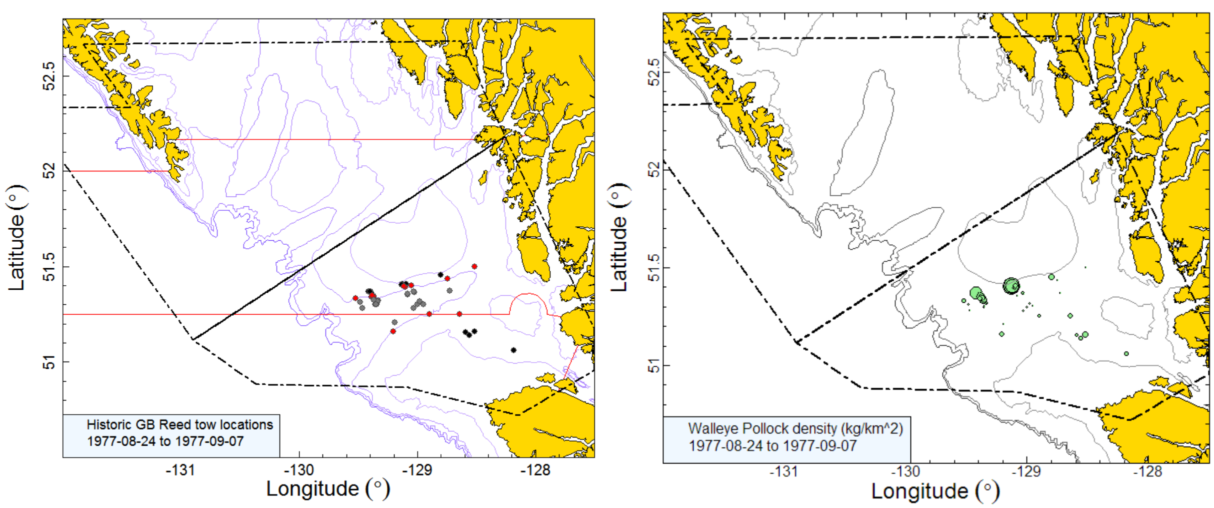

Figure B.6. Tow locations and density plots for the historic 1977 Goose Island Gully (GIG) survey (see Figure B.1 caption).

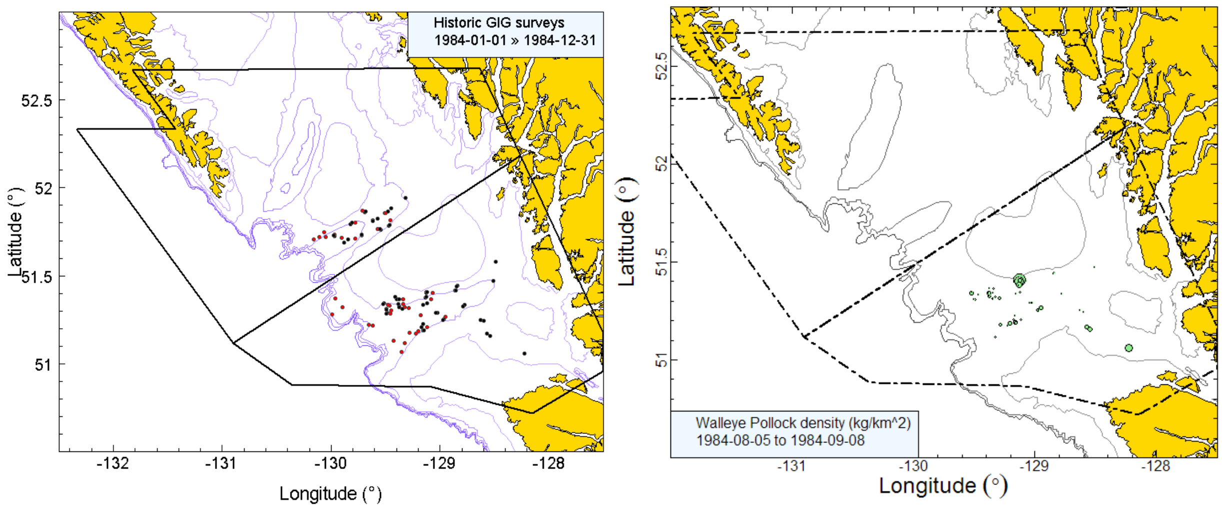

Figure B.7. [left panel]: Tow location colours indicate the vessel fishing rather than depth: black=G.B. Reed; red=Eastward Ho. Additional locations fished by vessel in Mitchell Gully are also shown; [right panel]: density plot for the historic 1984 Goose Island Gully (GIG) survey (see Figure B.1 caption).

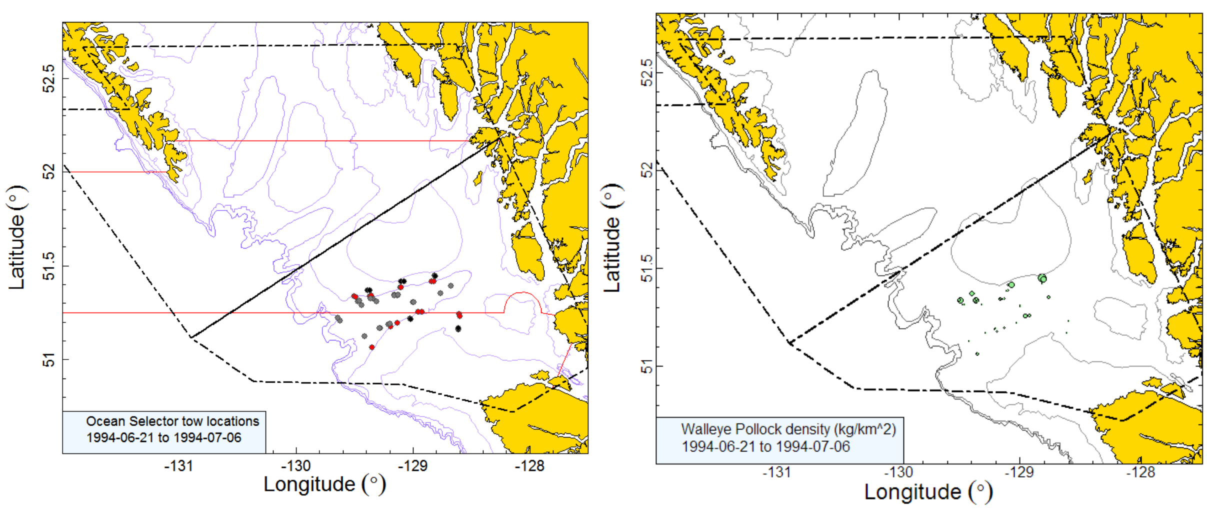

Figure B.8. Tow locations and density plots for the historic 1994 Goose Island Gully (GIG) survey (see Figure B.1 caption).

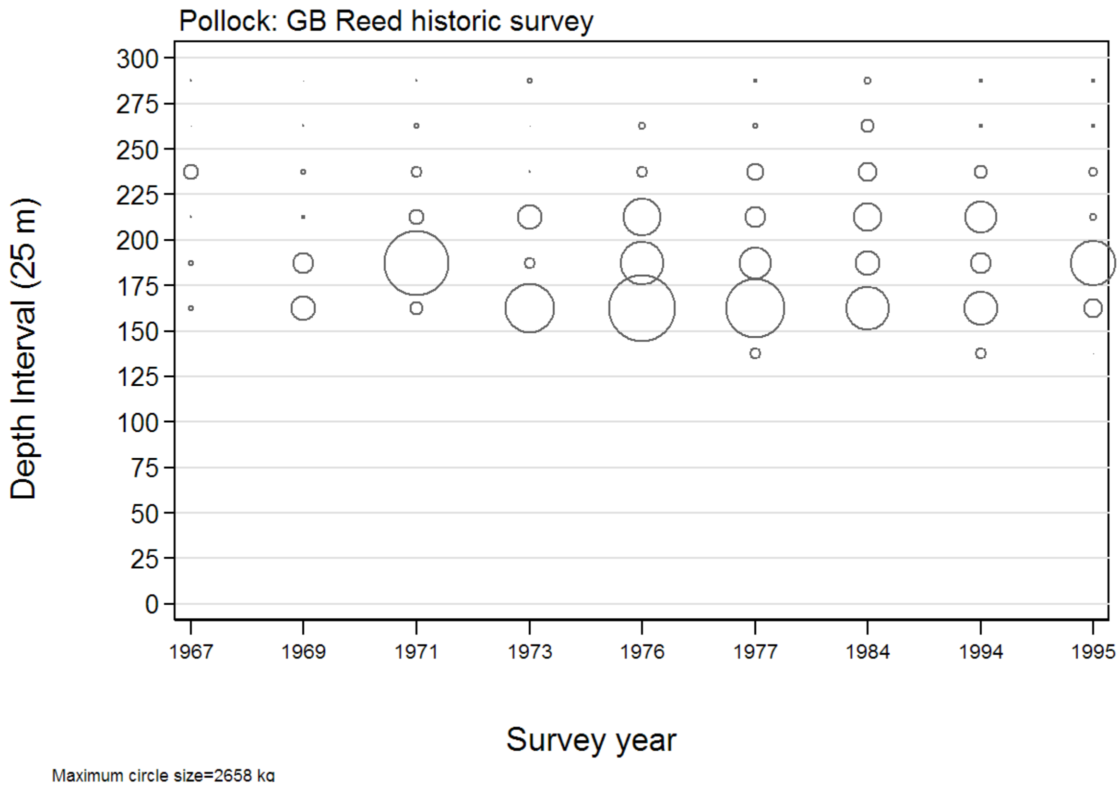

Figure B.9. Distribution of observed catch weights of Walleye Pollock (WAP) for the historic Goose Island Gully (GIG) surveys (Table B.3) by survey year and 25 m depth zone. Depth zones are indicated by the mid point of the depth interval and circles in the panel are scaled to the maximum value (2658 kg) in the 150–175 m interval in 1976. The 1% and 99% quantiles for the WAP empirical start of tow depth distribution= 148 m and 282 m respectively.

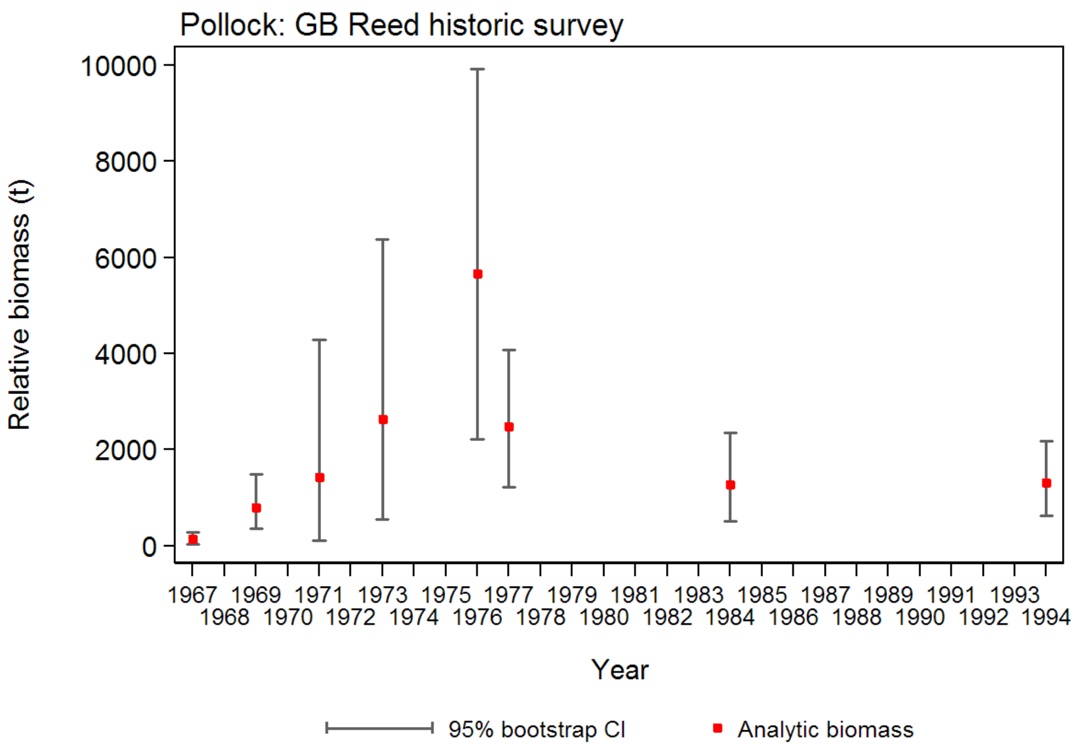

Figure B.10. Plot of biomass estimates for the WAP historic Goose Island Gully (GIG) surveys: 1967 to 1994 (values provided in Table B.4). Bias corrected 95% confidence intervals from 1000 bootstrap replicates are plotted.

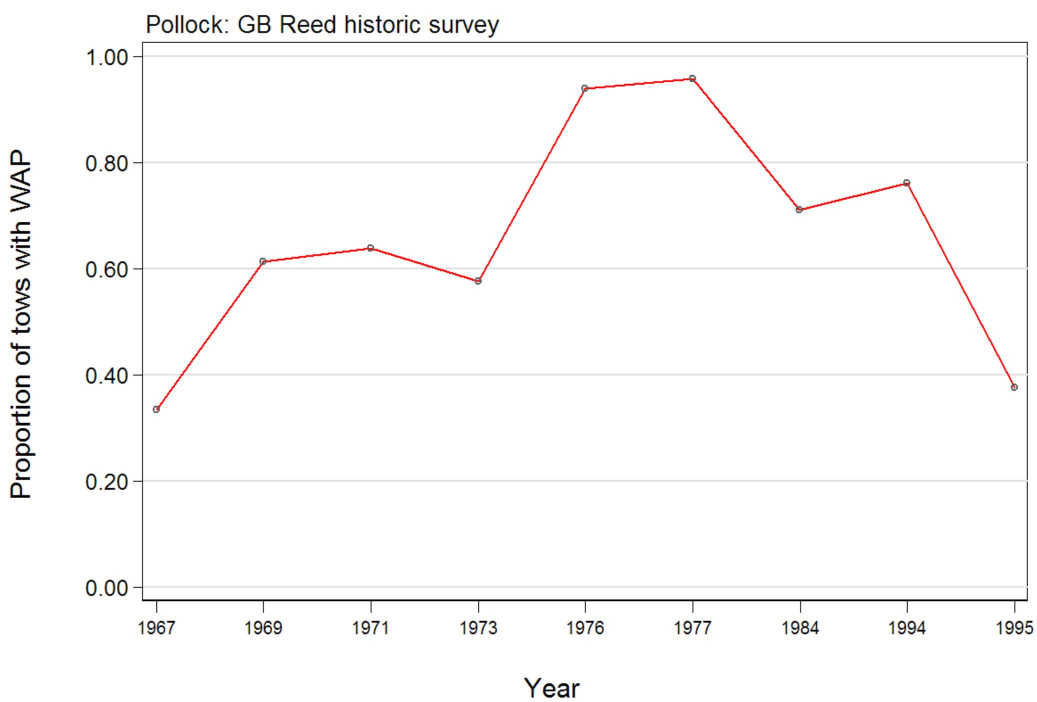

Figure B.11. Proportion of tows by year which contain WAP from the historic Goose Island Gully (GIG) surveys: 1967 to 1995.

B.4. HECATE STRAIT ASSEMBLAGE SURVEY

B.4.1. Data selection

This survey was conducted 11 times over the period 1984 to 2003 in Hecate Strait (HS) between Moresby and Graham Islands and the mainland (all valid tow starting positions are shown by survey year in Figure B.12 to Figure B.22 (Sinclair 1999). The design overlaid a 10 nm square grid over Hecate Strait and placed one tow per grid square in each 10-fathom depth interval over the range of 10 to 80 fathoms (18 to 146 m). Strata deeper than 80 fathoms were sampled in some survey years, but these were excluded from the analysis because the deeper strata were not sampled in all survey years. Tow positions were selected non-randomly by substrate type and were fixed after the first survey, although there was some variation in how tow positions were revisited, and new tow positions were added over the years. There were 85 to 105 valid tows in each survey year after the initial year, which had over 140 tows (Table B.5). Sinclair (1999) chose to analyze these data using the 10 fathom depth intervals as depth strata, without reference to the overlaid grid pattern by assuming that the tow locations had been selected randomly.

Table B.5. Number of usable tows for biomass estimation by year and depth stratum for the Hecate Strait assemblage survey over the period 1984 to 2003. Also shown is the area of each depth stratum and the vessel conducting the survey by survey year.

		Depth stratum							Total
Year	**Vessel**	**10-19fm**	**20-29fm**	**30-39fm**	**40-49fm**	**50-59fm**	**60-69fm**	**70-79fm**	**tows**
1984	G.B. Reed/ Arctic Ocean	19	19	23	25	23	23	14	146
1987	Southward Ho	15	12	12	11	16	10	9	85
1989	Southward Ho	17	12	12	15	12	9	13	90
1991	Southward Ho	18	12	15	10	21	15	7	98
1993	W.E. Ricker	16	20	11	15	10	15	7	94
1995	W.E. Ricker	17	19	15	16	14	14	7	102
1996	W.E. Ricker	25	24	21	10	11	10	4	105
1998	W.E. Ricker	14	11	17	13	13	14	4	86
2000	W.E. Ricker	18	22	19	14	15	11	6	105
2002	Viking Storm	17	17	15	16	11	10	6	92
2003	W.E. Ricker	15	17	16	18	15	9	5	95
Area (km^2)	-	2,657	1,651	908	828	912	792	612	8,360 [1]

[1] total area for survey

Table B.6. Biomass estimates for Walleye Pollock from the Hecate Strait assemblage trawl survey for the survey years 1984 to 2003, using the method of Starr et al. (2006[5]) (see text for explanation). Bootstrap bias corrected confidence intervals and CVs are based on 1000 random draws with replacement.

Survey Year	**Biomass (t)** (Eq. B.4)	**Mean bootstrap biomass (t)**	**Lower bound biomass (t)**	**Upper bound biomass (t)**	**Bootstrap CV**	**Analytic CV** (Eq. B.6)
1984	383	382	229	569	0.216	0.227
1987	514	505	114	1,268	0.611	0.618
1989	410	417	114	807	0.420	0.430
1991	907	885	429	1,602	0.337	0.340
1993	1,193	1,227	303	3,111	0.579	0.555
1995	425	429	251	703	0.260	0.262
1996	1,684	1,684	747	3,240	0.379	0.372
1998	2,022	2,031	848	4,058	0.383	0.393
2000	62	62	30	114	0.335	0.322
2002	1,253	1,251	736	1,925	0.247	0.242
2003	549	536	243	970	0.348	0.355

Two methods have been used to generate a doorspread density value (Eq. B.3) for each survey tow, given that there are no estimates of doorspread or wingspread for this survey and there only exist estimates of [**distance_travelled**] and [**speed**] for the final three survey years. The method proposed by Sinclair (1999) was to calculate a CPUE (kg/h) for each tow and to convert this value to biomass per area swept (kg/km^2) by assuming a constant area swept by each tow, with 0.0486 km^2/h as the constant. A second method was proposed by Starr et al. (2006), who assumed a constant doorspread value of 43 m and a constant speed of 5.1 km/h (Eq. B.2). There was little practical difference between these methods when the resulting biomass indices are treated as relative, as was demonstrated by Starr et al. (2006).

B.4.2. Results

Catch densities of WAP from this survey were generally highest in the northern half of Hecate Strait, rarely extending to the top of Graham Island or the southern part of Hecate Strait (Figure B.12 to Figure B.22). WAP were mainly taken at depths from 57 to 139 m (5% and 95% quantiles of the empirical depth distribution), with observations down to depths deeper than 200 m in the years that the deep strata were sampled (Figure B.23).

Estimated WAP biomass indices from this trawl survey showed no trend from 1984 to 2003 (Table B.6; Figure B.24). The estimated relative errors were moderate to high, ranging from 23 to 62% (Table B.6). These estimates of variability may be biased low, given the non-random selection of tow locations. On average, one third of the survey tows captured WAP (ranging from 0.20 to 0.45) (Figure B.25). Overall, 362 of the 1,098 valid survey tows contained WAP.

[5] Starr, P.J., Kronlund, A.R., Workman, G., Olsen, N. and Fargo, J. 2006. Rock sole (*Lepidopsetta* spp.) in BC, Canada: Stock assessment for 2005 and advice to managers for 2006/2007. Pacific Scientific Advice Review Committee (PSARC) Working Paper, unpublished manuscript, Pacific Biological Station, DFO, Nanaimo BC, Canada.

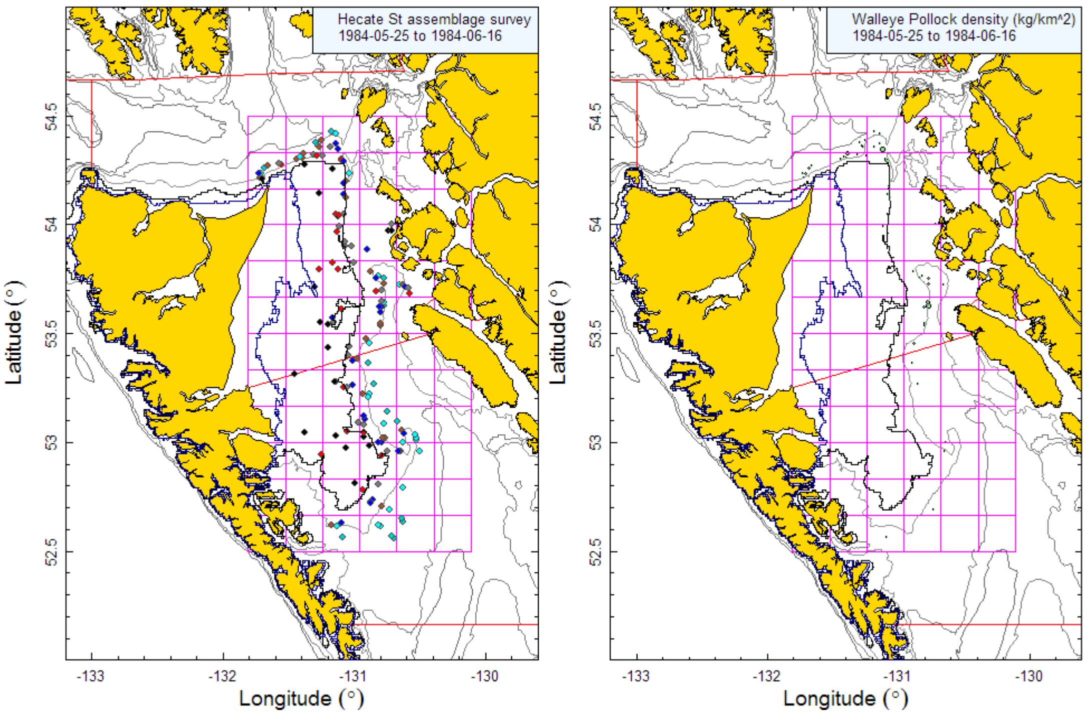

Figure B.12. Valid tow locations and density plots for the 1984 Hecate Strait assemblage survey with strata in fathoms: 10-19 (black), 20-29 (red), 30-39 (grey), 40-49 (blue), 50-59 (sienna), 60-69 (cyan), 70-79 (turquoise); and density plots for the 1984 Hecate Strait assemblage survey. Circle sizes in the right-hand density plot scaled across all years (1984, 1987, 1989, 1991, 1993, 1995, 1996, 1998, 2000, 2002, 2003), with the largest circle = 12,777 kg/km² in 1996.

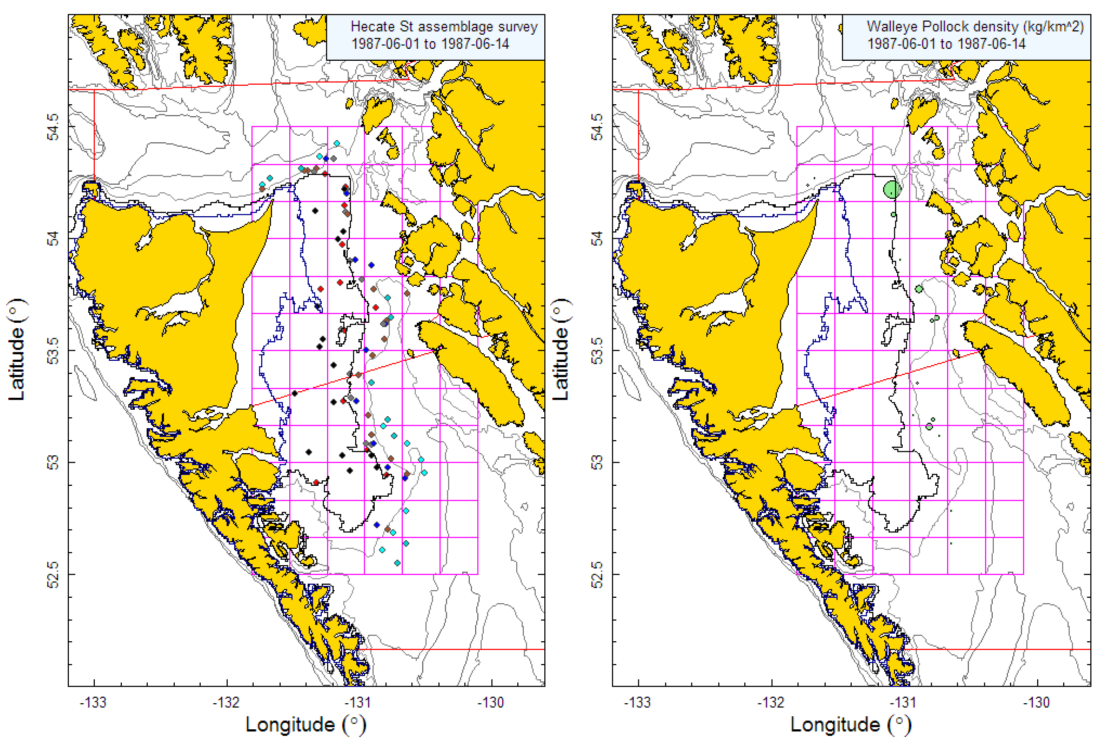

Figure B.13. Tow locations and density plots for the 1987 Hecate Strait assemblage survey (see Figure B.12 caption).

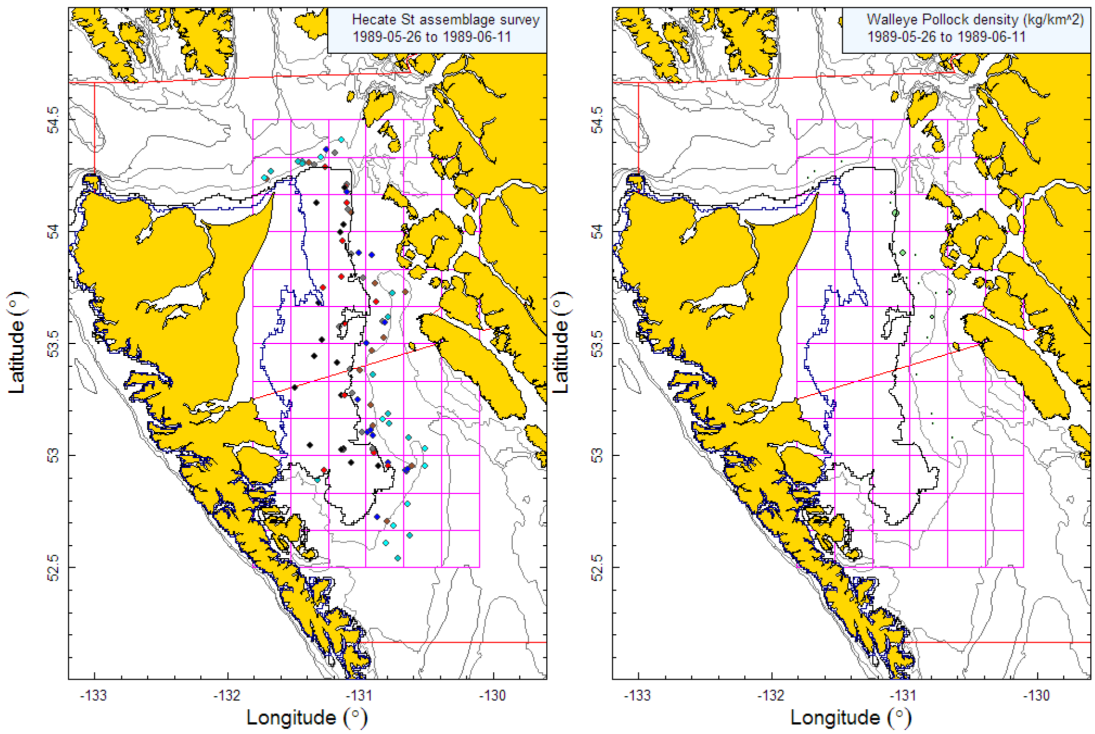

Figure B.14. Tow locations and density plots for the 1989 Hecate Strait assemblage survey (see Figure B.12 caption).

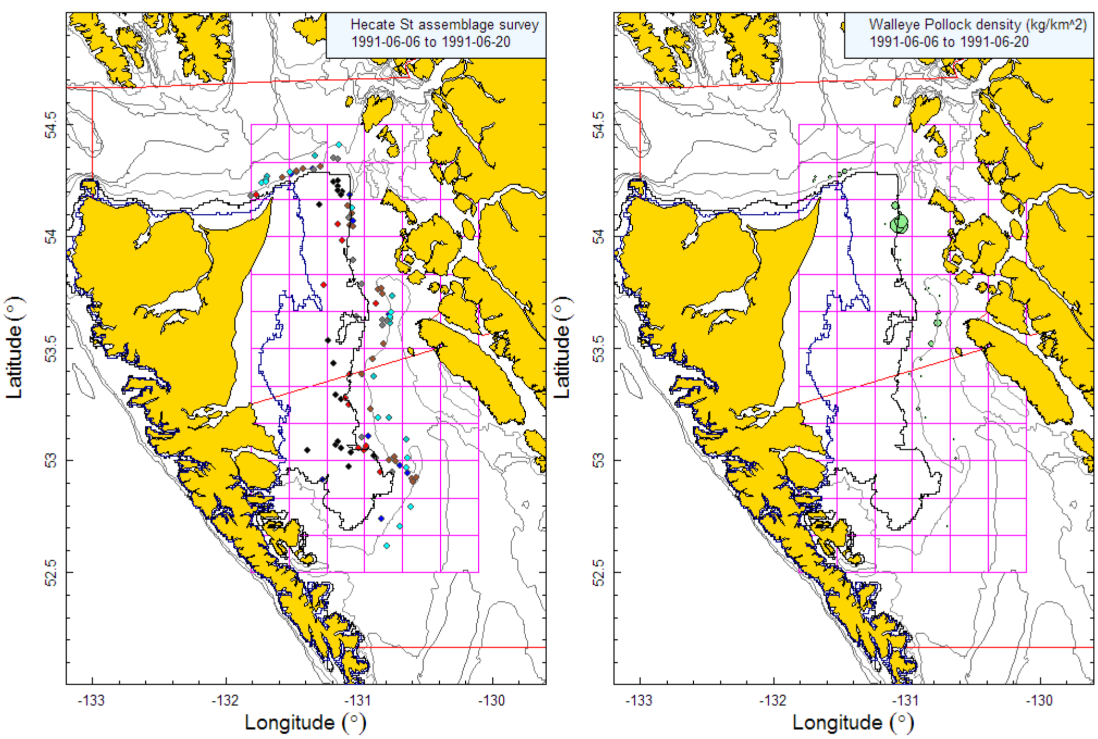

Figure B.15. Tow locations and density plots for the 1991 Hecate Strait assemblage survey (see Figure B.12 caption).

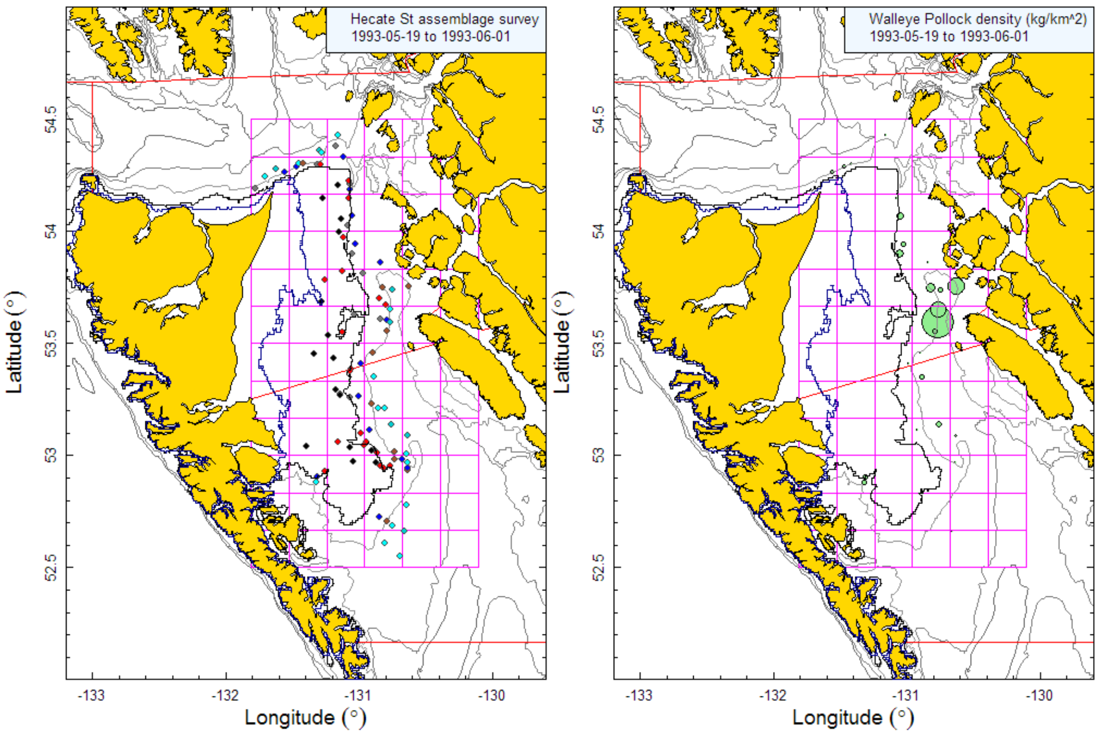

Figure B.16. Tow locations and density plots for the 1993 Hecate Strait assemblage survey (see Figure B.12 caption).

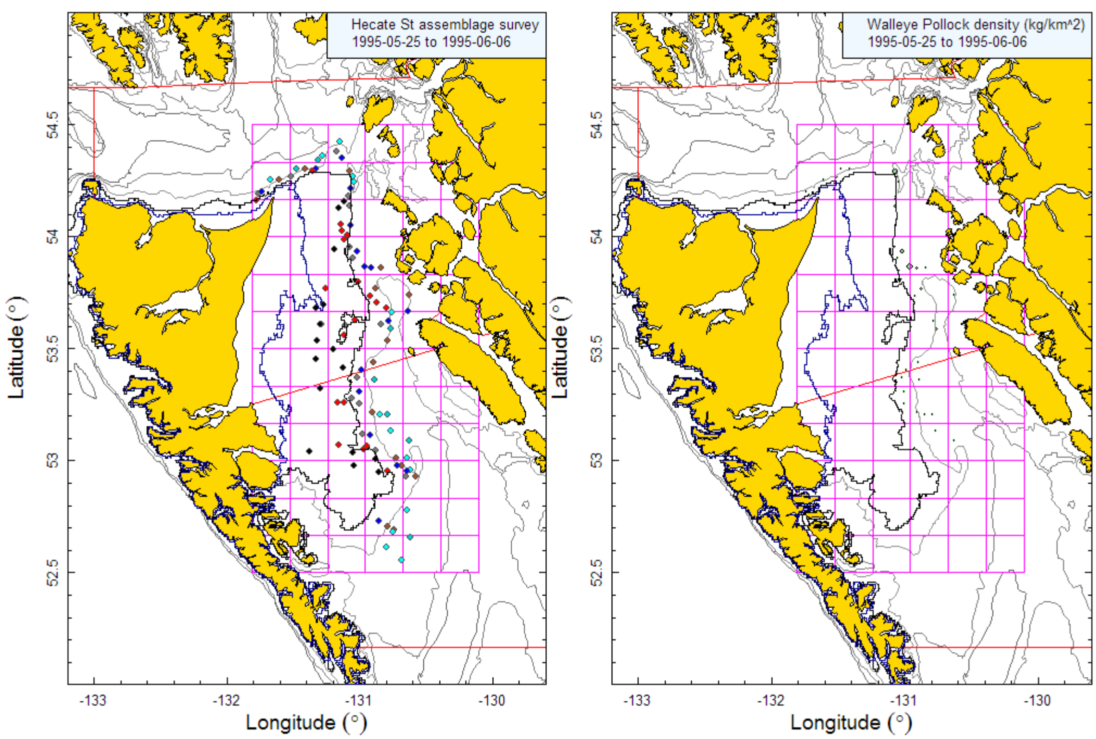

Figure B.17. Tow locations and density plots for the 1995 Hecate Strait assemblage survey (see Figure B.12 caption).

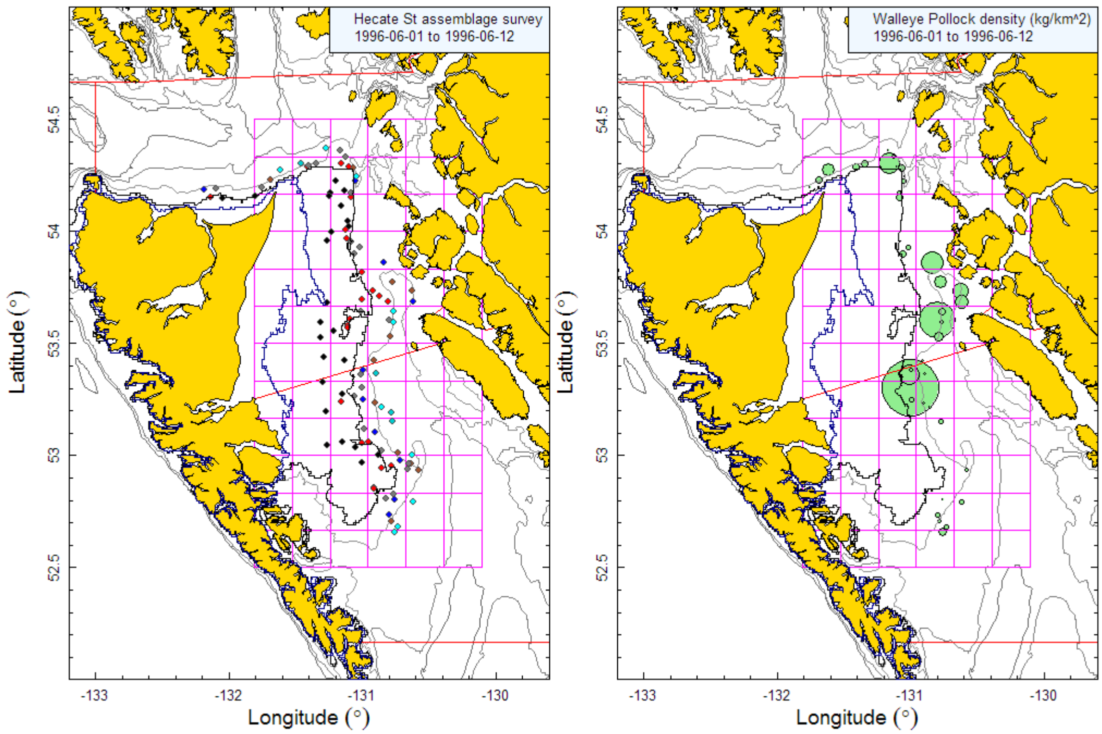

Figure B.18. Tow locations and density plots for the 1996 Hecate Strait assemblage survey (see Figure B.12 caption).

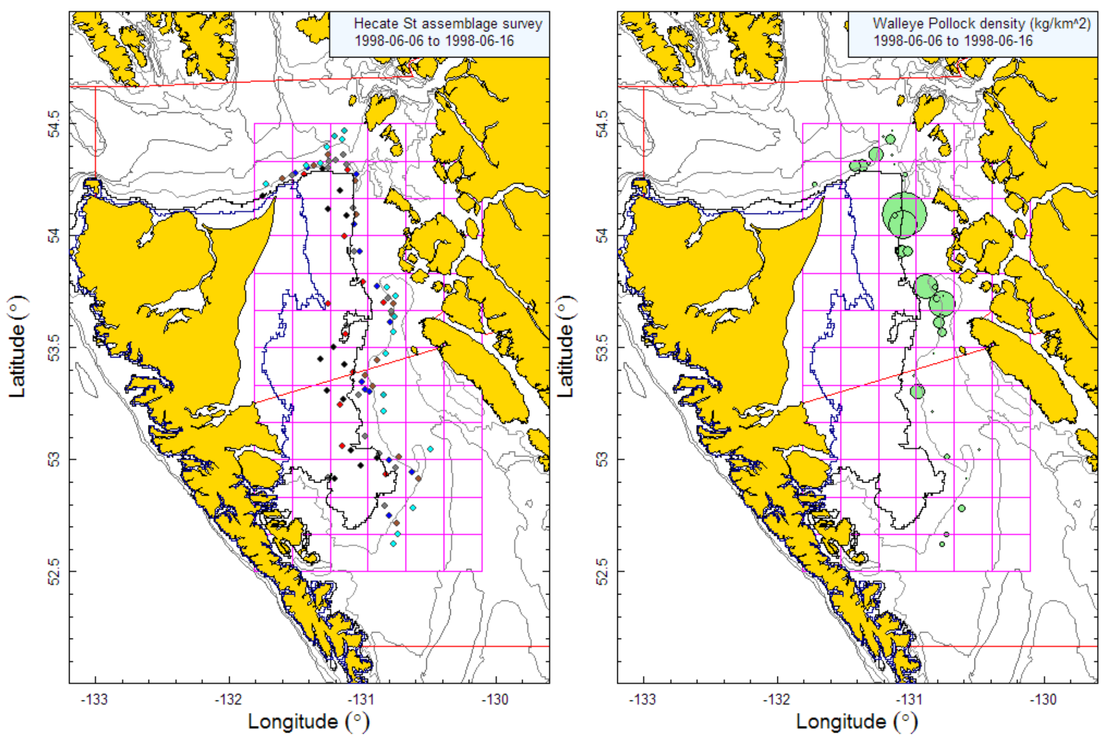

Figure B.19. Tow locations and density plots for the 1998 Hecate Strait assemblage survey (see Figure B.12 caption).

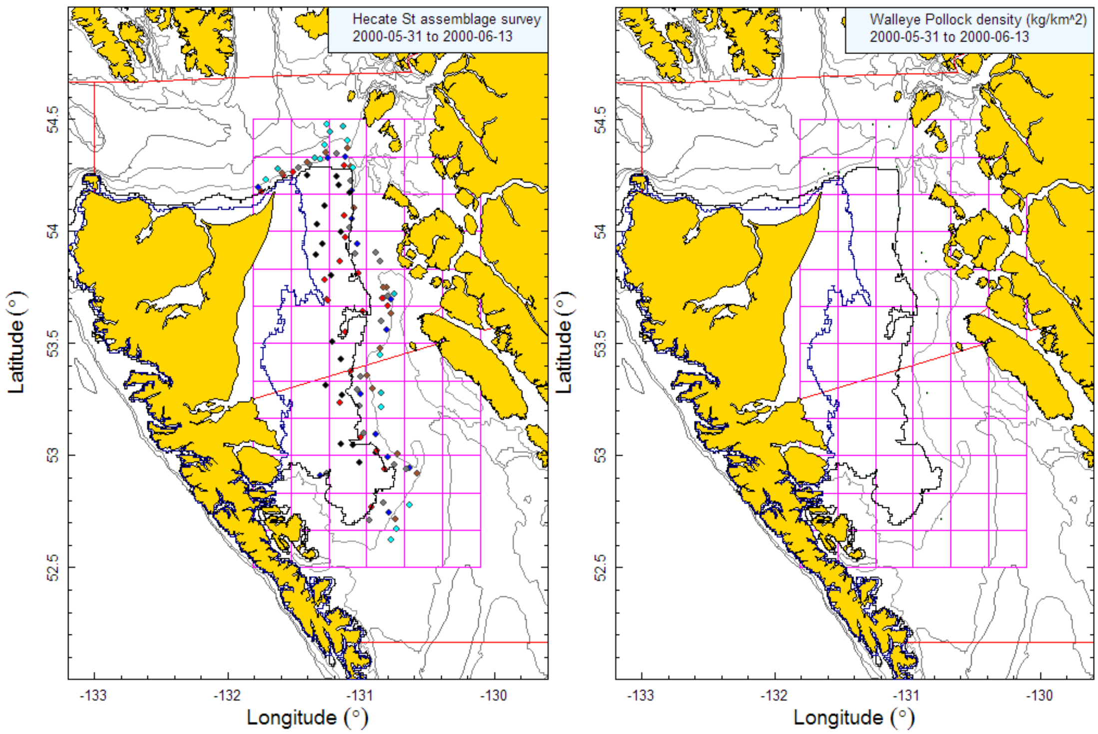

Figure B.20. Tow locations and density plots for the 2000 Hecate Strait assemblage survey (see Figure B.12 caption).

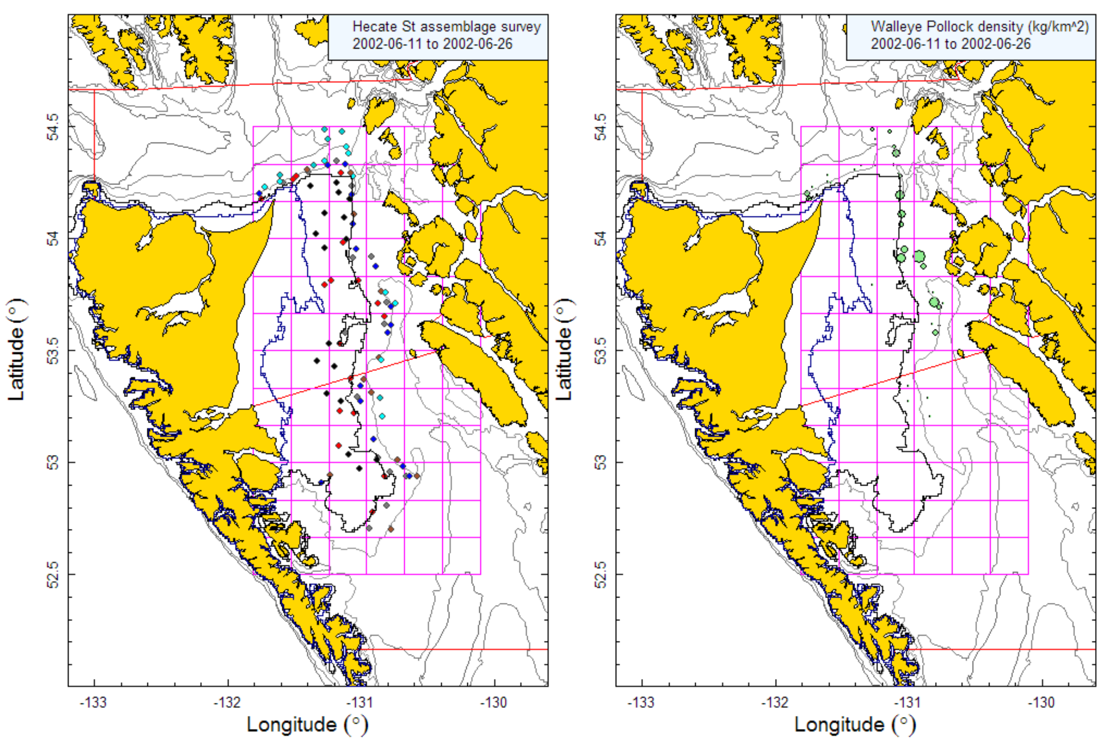

Figure B.21. Tow locations and density plots for the 2002 Hecate Strait assemblage survey (see Figure B.12 caption).

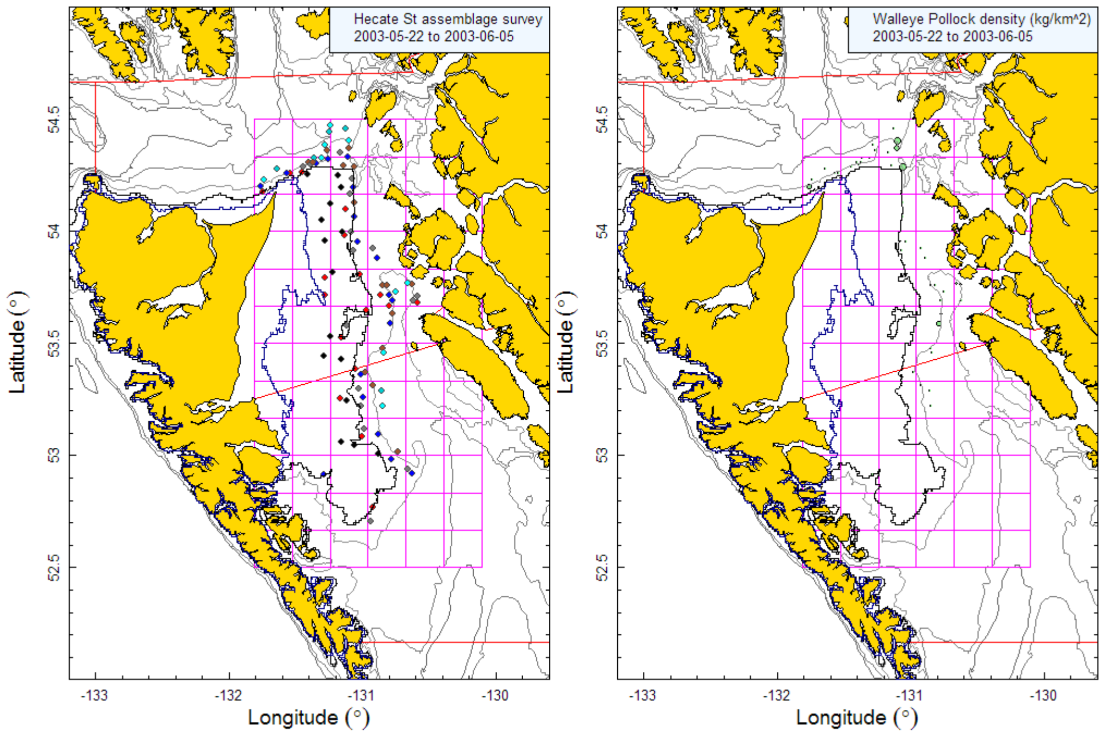

Figure B.22. Tow locations and density plots for the 2003 Hecate Strait assemblage survey (see Figure B.12 caption).

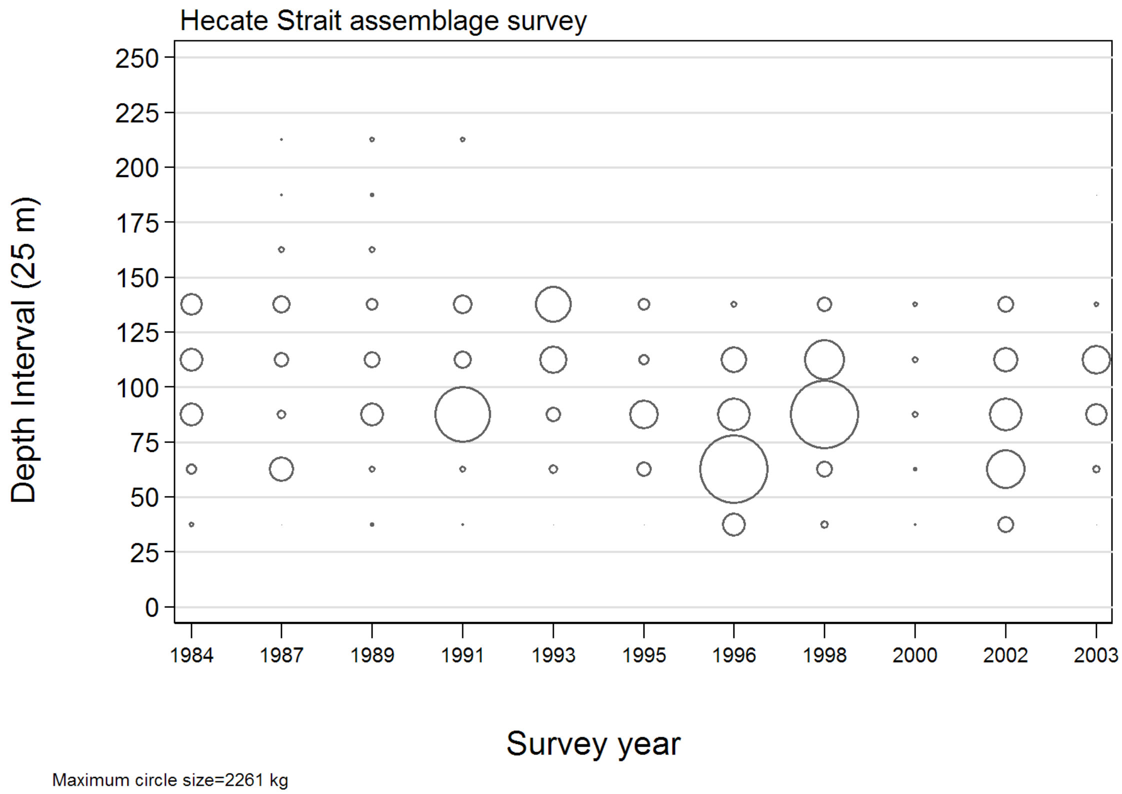

Figure B.23. Distribution of observed catch weights of Walleye Pollock for the Hecate Strait assemblage survey (Table B.5) by survey year and 25 m depth zone. Depth zones are indicated by the mid point of the depth interval and circles in the panel are scaled to the maximum value (2,261 kg) in the 50–75 m interval in 1996. The 1% and 99% quantiles for the WAP empirical start of tow depth distribution= 37 m and 203 m respectively. Note that tows deeper than 148 m (80 fm) are presented here when available but were excluded from the biomass analysis because the deeper strata were not sampled consistently in all survey years.

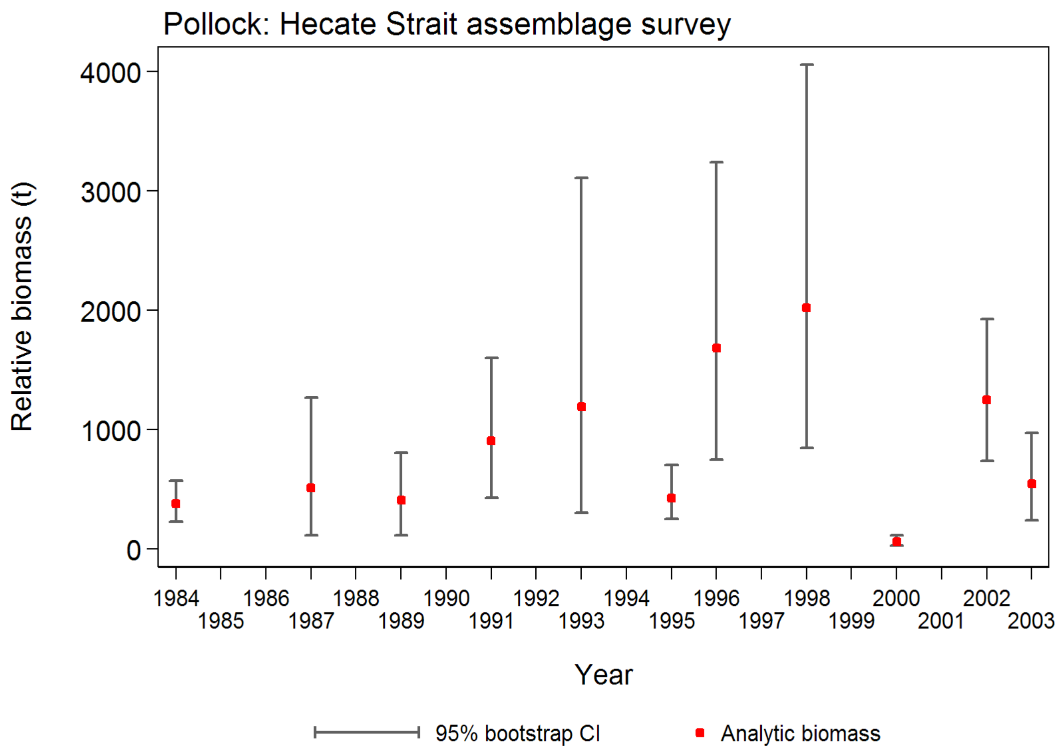

Figure B.24. Plot of biomass estimates for WAP (values provided in Table B.6) from the Hecate Strait assemblage survey over the period 1984 to 2003 . Bias corrected 95% confidence intervals from 1000 bootstrap replicates are plotted.

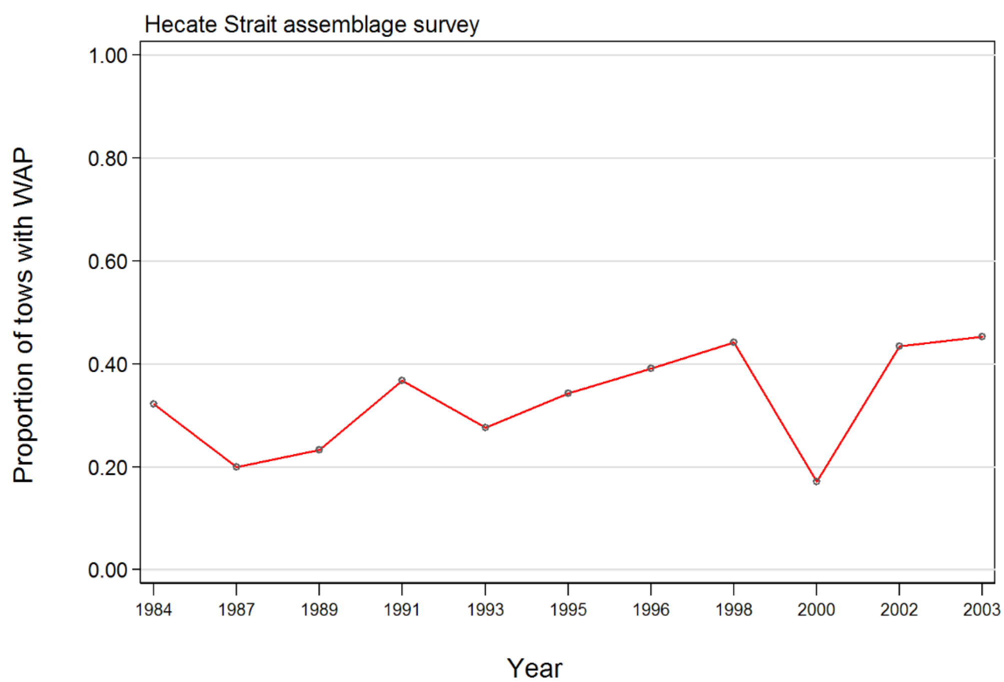

Figure B.25. Proportion of tows by year which contain WAP from the Hecate Strait assemblage survey over the period 1984 to 2003.

B.5. HECATE STRAIT SYNOPTIC SURVEY

B.5.1. Data selection

This survey has been conducted in six alternating years over the period 2005 to 2015 in Hecate Strait (HS) between Moresby and Graham Islands and the mainland and in Dixon Entrance at the top of Graham Island (all valid tow starting positions by survey year are shown in Figure B.26 to Figure B.31). This survey treats the full spatial coverage as a single areal stratum divided into four depth strata: 10–70 m; 70–130 m; 130–220 m; and 220–500 m (Table B.7).

A doorspread density value (Eq. B.3) was generated for each tow based on the catch of Walleye Pollock (WAP), the mean doorspread for the tow and the distance travelled; [**distance_travelled**] is a database field which is calculated directly from the tow track. This field is used preferentially for the variable D_{yij} in Eq. B.3. A calculated value ([**vessel_speed**] X [**tow_duration**]) is used for this variable if [**distance_travelled**] is missing, but there were no instances of this occurring in the 6 trawl surveys. Missing values for the [**doorspread**] field were filled in with the mean doorspread for the survey year (217 values over all years: Table B.8).

Table B.7. Number of usable tows for biomass estimation by year and depth stratum for the Hecate Strait synoptic survey over the period 2005 to 2015. Also shown is the area of each depth stratum and the vessel conducting the survey by survey year.

Year	Vessel	Depth stratum 10-70	70-130	130-220	220-500	Total tows
2005	Frosti	79	88	26	9	202
2007	W.E. Ricker	48	43	36	7	134
2009	W.E. Ricker	53	43	48	12	156
2011	W.E. Ricker	70	51	50	14	185
2013	W.E. Ricker	74	42	43	16	175
2015	W.E. Ricker	47	46	40	15	148
Area (km^2)	-	5,958	3,011	2,432	1,858	13,259[1]

[1] total area for survey

Table B.8. Number of missing doorspread values by year for the Hecate Strait synoptic survey over the period 2005 to 2015 as well as showing the number of available doorspread observations and the mean doorspread value for the survey year.

Year	Number tows with missing doorspread [1]	Number tows with doorspread observations [2]	Mean doorspread (m) used for tows with missing values [2]
2005	7	217	64.4
2007	98	37	59.0
2009	93	70	54.0
2011	13	186	54.8
2013	6	169	51.7
2015	0	151	59.4
Total	217	830	57.6

[1] valid biomass estimation tows only
[2] includes tows not used for biomass estimation

Table B.9. Biomass estimates for Walleye Pollock from the Hecate Strait synoptic trawl survey for the survey years 2005 to 2015. Bootstrap bias corrected confidence intervals and CVs are based on 1000 random draws with replacement.

Survey Year	Biomass (t) (Eq. B.4)	Mean bootstrap biomass (t)	Lower bound biomass (t)	Upper bound biomass (t)	Bootstrap CV	Analytic CV (Eq. B.6)
2005	1750	1741	919	3293	0.330	0.321
2007	1394	1422	568	2776	0.391	0.391
2009	1028	1032	604	1798	0.275	0.267
2011	1073	1069	561	1856	0.308	0.308
2013	1828	1816	1113	2851	0.234	0.232
2015	1972	1974	1062	3293	0.285	0.273

B.5.2. Results

Catches of WAP from this survey are concentrated along the 100 m depth contour in Dixon Entrance and then follow that contour into upper Hecate Strait (Figure B.26 to Figure B.31). WAP are mainly taken at depths from 43 to 239 m (5–95% quantiles), but there are sporadic observations to depths up to about 330 m and down to about 20 m (Figure B.32).

Estimated WAP doorspread biomass from this trawl survey showed no overall trend over the period 2005 to 2015, with the highest estimates recorded in 2005, 2013 and 2015 and the lowest estimate in 2009 (Table B.9; Figure B.33). The estimated relative errors were moderate, ranging from 23 to 39% (Table B.9). On average, 55% of the survey tows captured WAP (ranging from 0.52 to 0.60 by year) (Figure B.34). Overall, 549 of the 1000 valid survey tows contained WAP with a low median catch weight for positive tows (3.3 kg/tow) and a maximum catch weight across all six surveys of 1622 kg (in 2005).

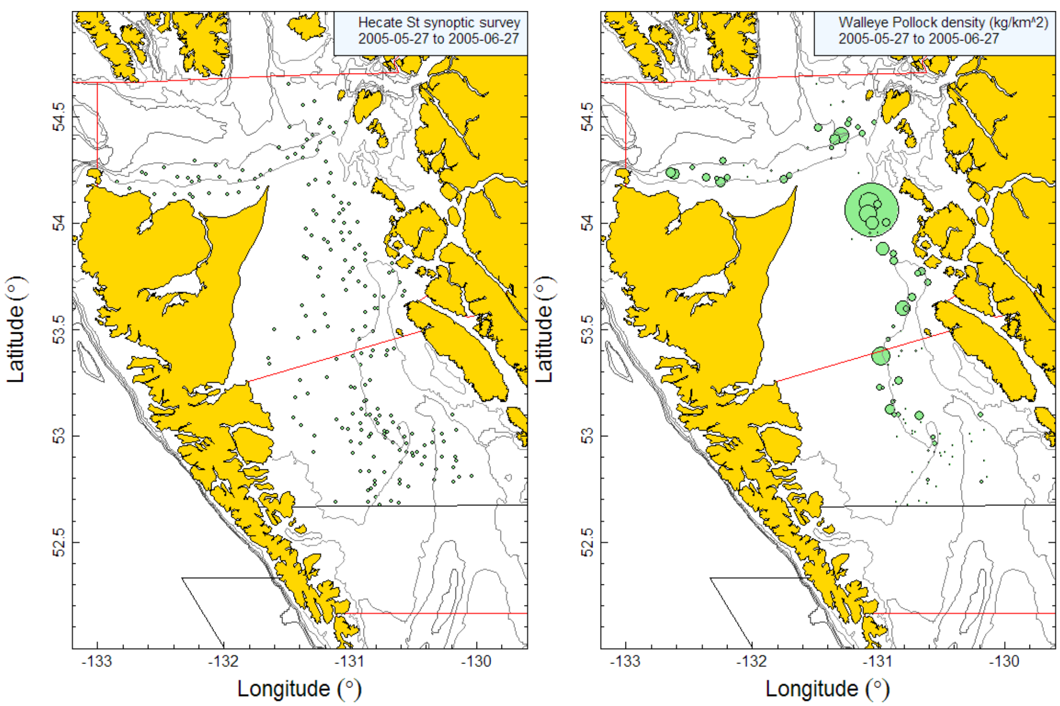

Figure B.26. Valid tow locations and density plots for the 2005 Hecate Strait synoptic survey. Circle sizes in the right-hand density plot scaled across all years (2005, 2007, 2009, 2011, 2013, 2015), with the largest circle = 14,373 kg/km² in 2005. Red lines indicate boundaries for PMFC major statistical areas 5C, 5D and 5E.

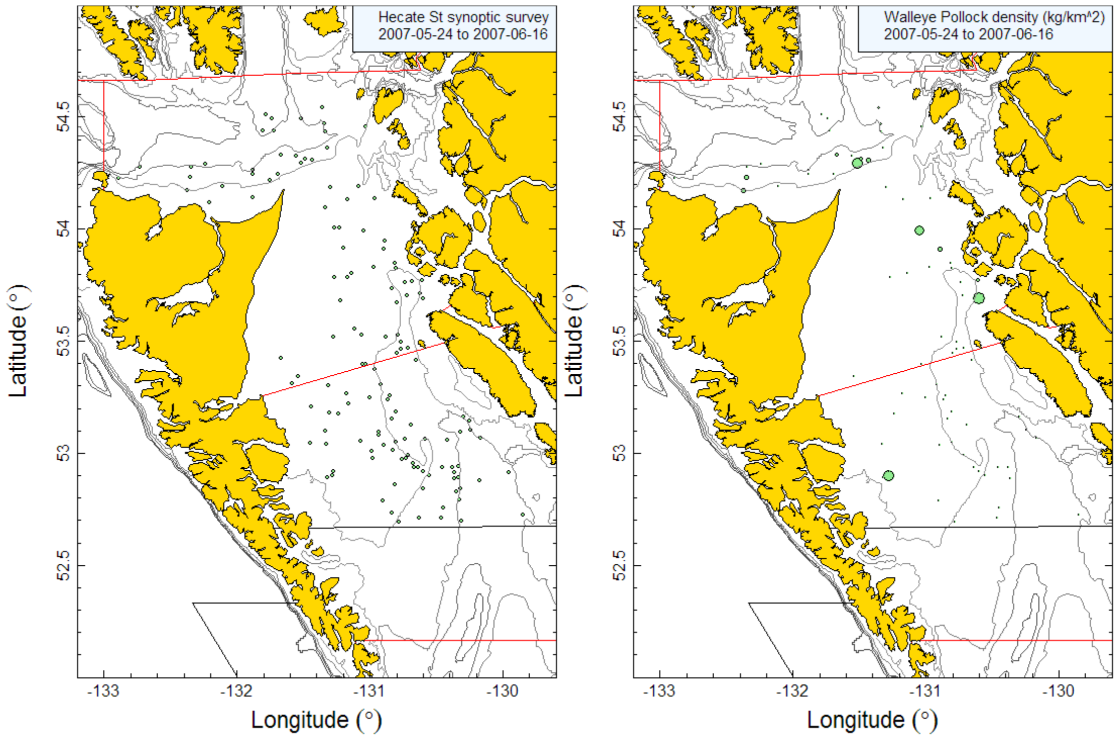

Figure B.27. Tow locations and density plots for the 2007 Hecate Strait synoptic survey (see Figure B.26 caption).

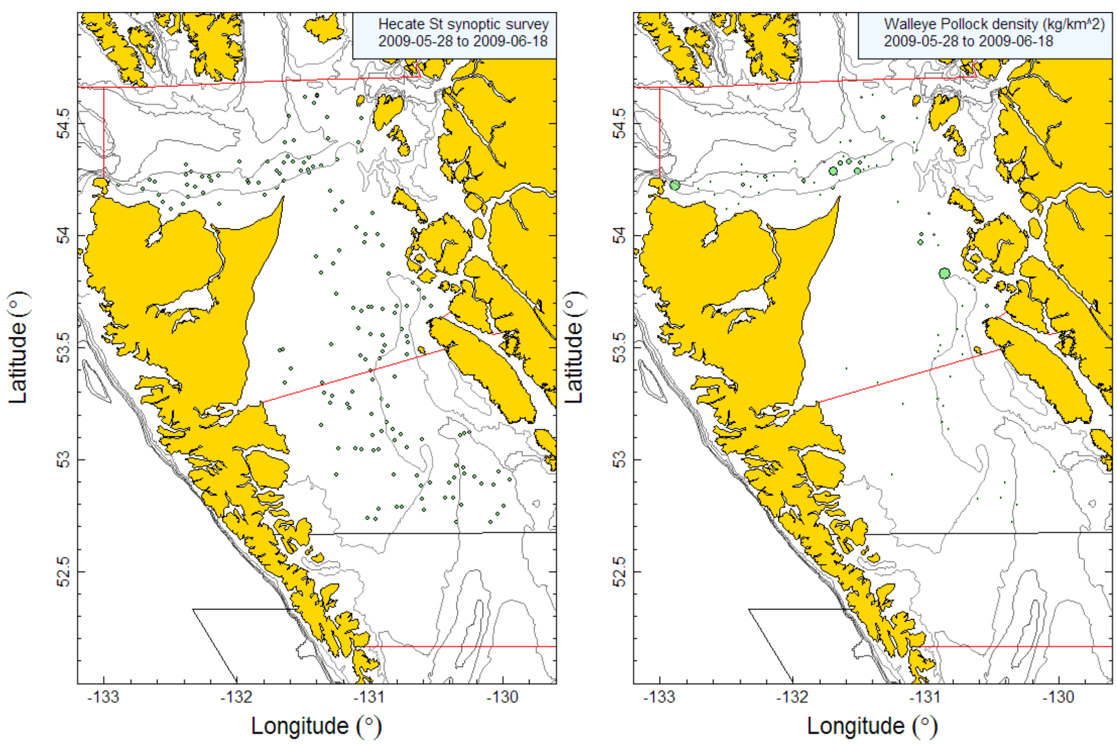

Figure B.28. Tow locations and density plots for the 2009 Hecate Strait synoptic survey (see Figure B.26 caption).

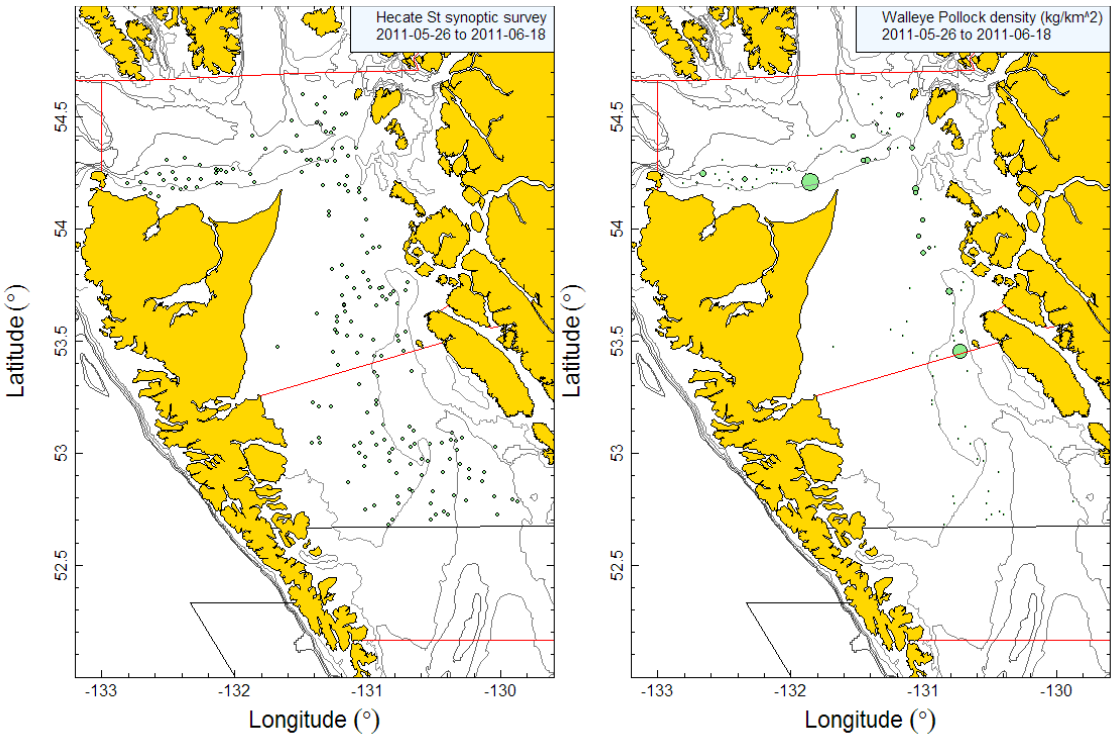

Figure B.29. Tow locations and density plots for the 2011 Hecate Strait synoptic survey (see Figure B.26 caption).

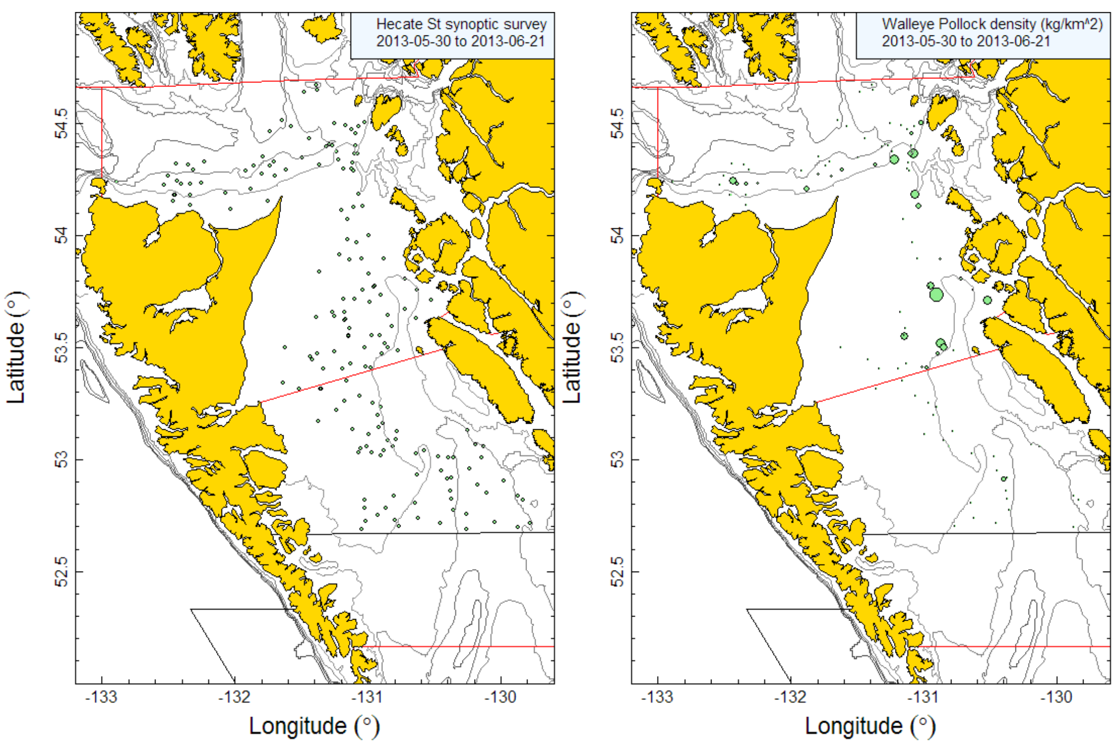

Figure B.30. Tow locations and density plots for the 2013 Hecate Strait synoptic survey (see Figure B.26 caption).

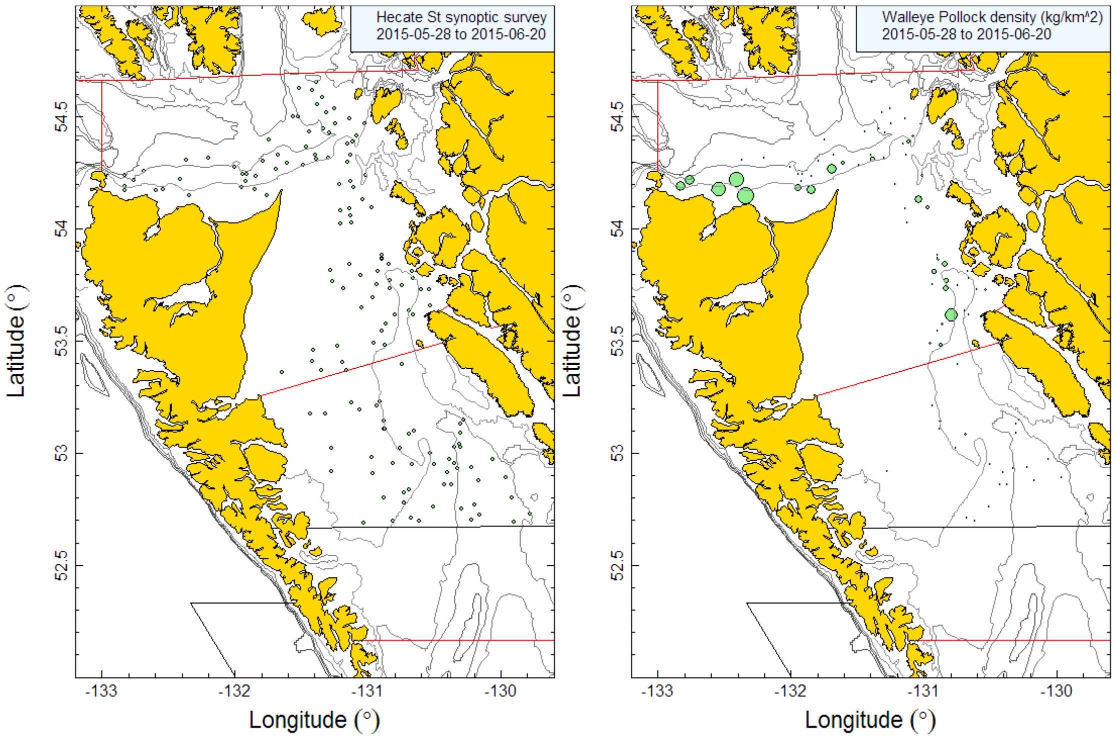

Figure B.31. Tow locations and density plots for the 2015 Hecate Strait synoptic survey (see Figure B.26 caption).

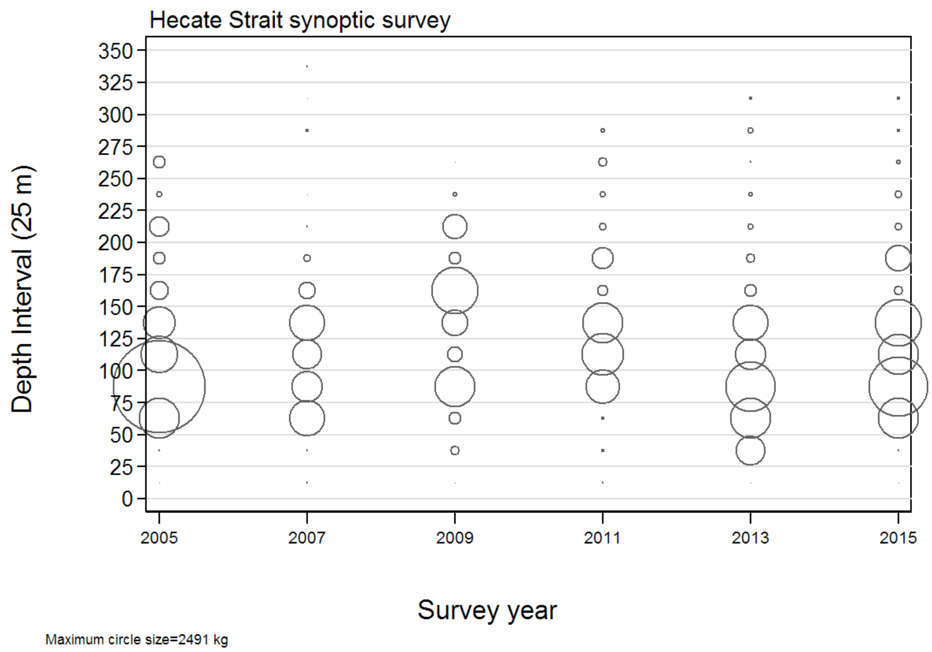

Figure B.32. Distribution of observed catch weights of Walleye Pollock for the Hecate Strait synoptic survey (Table B.7) by survey year and 25 m depth zone. Catches are plotted at the mid-point of the interval and circles in the panel are scaled to the maximum value (2491 kg) in the 75-100 m interval in 2005. The 1% and 99% quantiles for the WAP empirical start of tow depth distribution= 25 m and 288 m respectively.

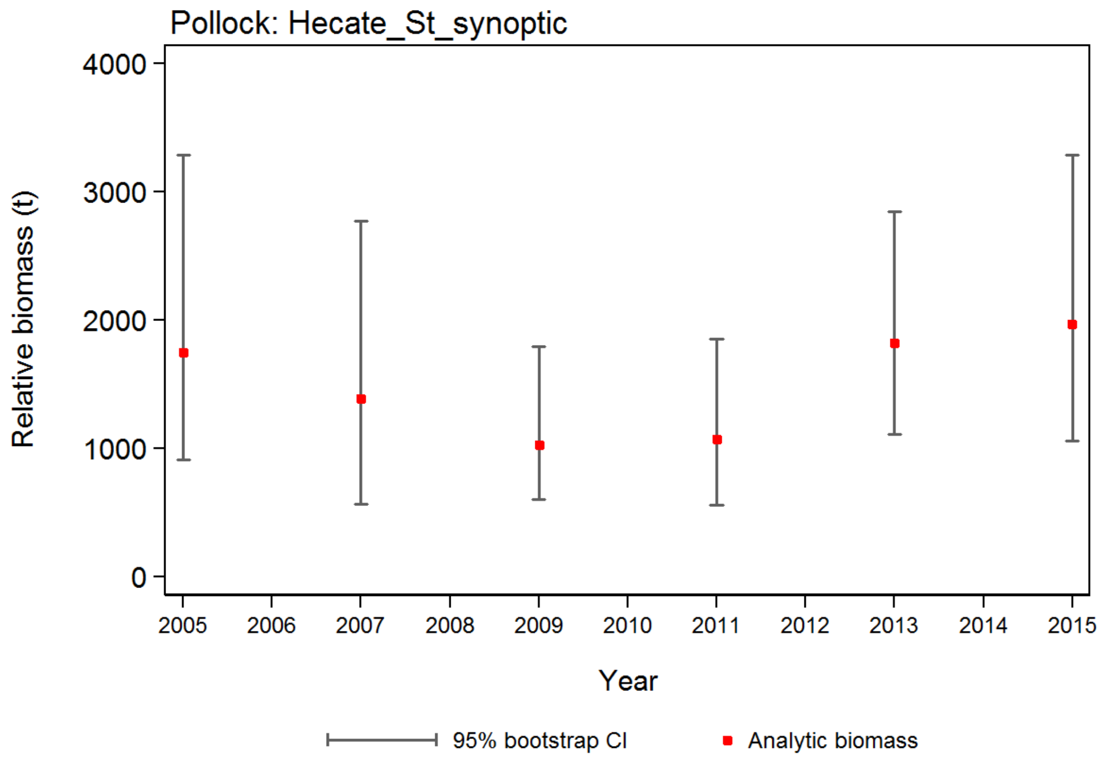

Figure B.33. Plot of biomass estimates for Walleye Pollock values provided in Table B.9 from the Hecate Strait synoptic survey over the period 2005 to 2015 . Bias corrected 95% confidence intervals from 1000 bootstrap replicates are plotted.

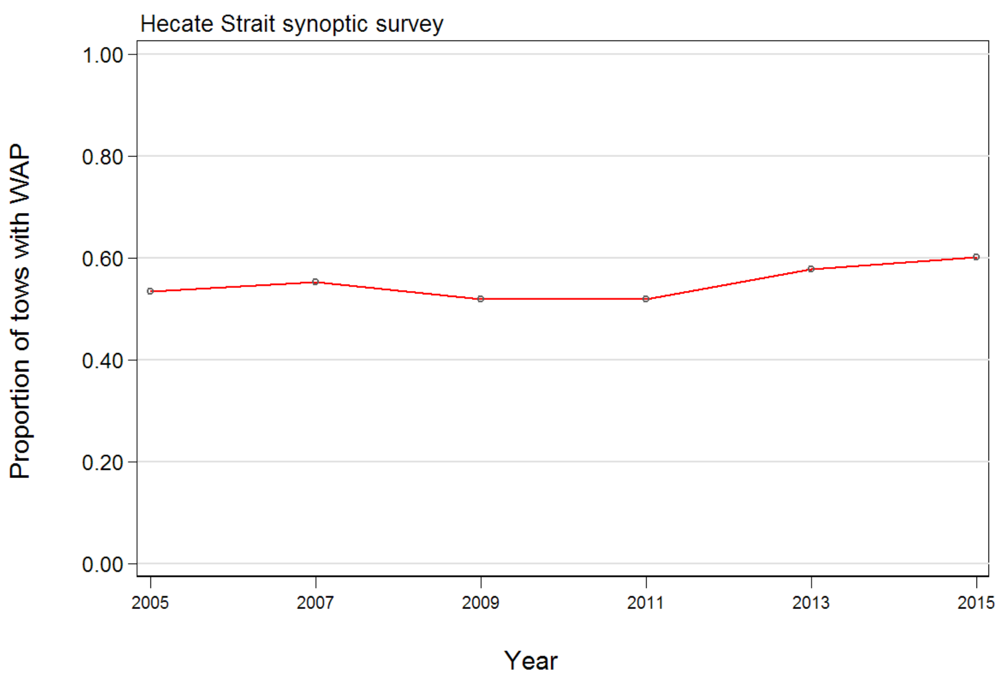

Figure B.34. Proportion of tows by year which contain Walleye Pollock from the Hecate Strait synoptic survey over the period 2005 to 2015.

B.6. QUEEN CHARLOTTE SOUND SYNOPTIC TRAWL SURVEY

B.6.1. Data selection

This survey has been conducted in eight years over the period 2003 to 2015 in Queen Charlotte Sound (QCS), which lies between the top of Vancouver Island and the southern portion of Moresby Island and extends into the lower part of Hecate Strait between Moresby Island and the mainland. The design divided the survey into two large areal strata which roughly correspond to the PMFC regions 5A and 5B while also incorporating part of 5C (all valid tow starting positions are shown by survey year in Figure B.35 to Figure B.42). Each of these two areas was divided into four depth strata: 50–125 m; 125–200 m; 200–330 m; and 330–500 m (Table B.10).

A doorspread density value (Eq. B.3) was generated for each tow based on the catch of Walleye Pollock (WAP), the mean doorspread for the tow and the distance travelled. [**distance_travelled**] is a database field which is calculated directly from the tow track. This field is used preferentially for the variable D_{yij} in Eq. B.3. A calculated value ([**vessel_speed**] X [**tow_duration**]) is used for this variable if [**distance_travelled**] is missing, but there were only two instances of this occurring in the 8 trawl surveys. Missing values for the [**doorspread**] field were filled in with the mean doorspread for the survey year (101 values over all years, Table B.11).

Table B.10. Number of usable tows for biomass estimation by year and depth stratum for the Queen Charlotte Sound synoptic survey over the period 2003 to 2015. Also shown is the area of each stratum for the 2015 survey and the vessel conducting the survey by survey year.

		South depth strata				North depth strata				Total
Year	**Vessel**	**50-125**	**125-200**	**200-330**	**330-500**	**50-125**	**125-200**	**200-330**	**330-500**	**tows**[1]
2003	Viking Storm	29	56	29	6	5	39	50	19	233
2004	Viking Storm	42	48	31	8	20	38	37	6	230
2005	Viking Storm	29	60	29	8	8	45	37	8	224
2007	Viking Storm	33	62	24	7	19	57	48	7	257
2009	Viking Storm	34	60	28	8	10	44	43	6	233
2011	Nordic Pearl	38	67	25	8	10	51	45	8	252
2013	Nordic Pearl	32	66	29	10	9	46	44	5	241
2015	Frosti	30	65	26	4	12	50	44	8	239
Area (km^2)[2]		5,072	5,432	2,712	548	1,804	4,060	3,748	1,252	24,628

[1] GFBio usability codes=0,1,2,6 [2] Total area (km^2) for 2015 synoptic survey

Table B.11. Number of missing doorspread values by year for the Queen Charlotte Sound synoptic survey over the period 2003 to 2015 as well as showing the number of available doorspread observations and the mean doorspread value for the survey year.

Year	Number tows with missing doorspread [1]	Number tows with doorspread observations [2]	Mean doorspread (m) used for tows with missing values [2]
2003	13	236	72.1
2004	8	267	72.8
2005	1	258	74.5
2007	5	262	71.8
2009	2	248	71.3
2011	30	242	67.0
2013	42	226	69.5
2015	0	249	70.5
Total	101	1,988	71.2

[1] valid biomass estimation tows only
[2] includes tows not used for biomass estimation

Table B.12. *Biomass estimates for Walleye Pollock from the Queen Charlotte Sound synoptic trawl survey for the survey years 2003 to 2015. Bootstrap bias corrected confidence intervals and CVs are based on 1000 random draws with replacement.*

Survey Year	Biomass (t) (Eq. B.4)	Mean bootstrap biomass (t)	Lower bound biomass (t)	Upper bound biomass (t)	Bootstrap CV	Analytic CV (Eq. B.6)
2003	254	254	176	370	0.183	0.188
2004	335	335	224	492	0.198	0.194
2005	648	649	423	1020	0.221	0.219
2007	518	518	305	796	0.240	0.243
2009	372	375	209	563	0.239	0.239
2011	2671	2639	926	6745	0.541	0.539
2013	1667	1689	874	2605	0.266	0.265
2015	2114	2116	1066	3669	0.313	0.315

B.6.2. Results

Catch densities of WAP were very low for the first five surveys, resulting in low incidence for this species (Figure B.35 to Figure B.39). However, the incidence of this species in this survey increased after 2009, particularly in the 2011 survey (Figure B.40), but was also higher in the 2013 (Figure B.41) and 2015 surveys (Figure B.42). The tows that captured WAP in these three surveys were generally located in Queen Charlotte Strait near the northern end of Vancouver Island, which is also the location of one of the three targeted midwater fisheries for this species. WAP were mainly taken at depths from 112 to 291 m (5–95% quantiles), but there were sporadic observations up to depths near 400 m and down to about 60 m (Figure B.43).

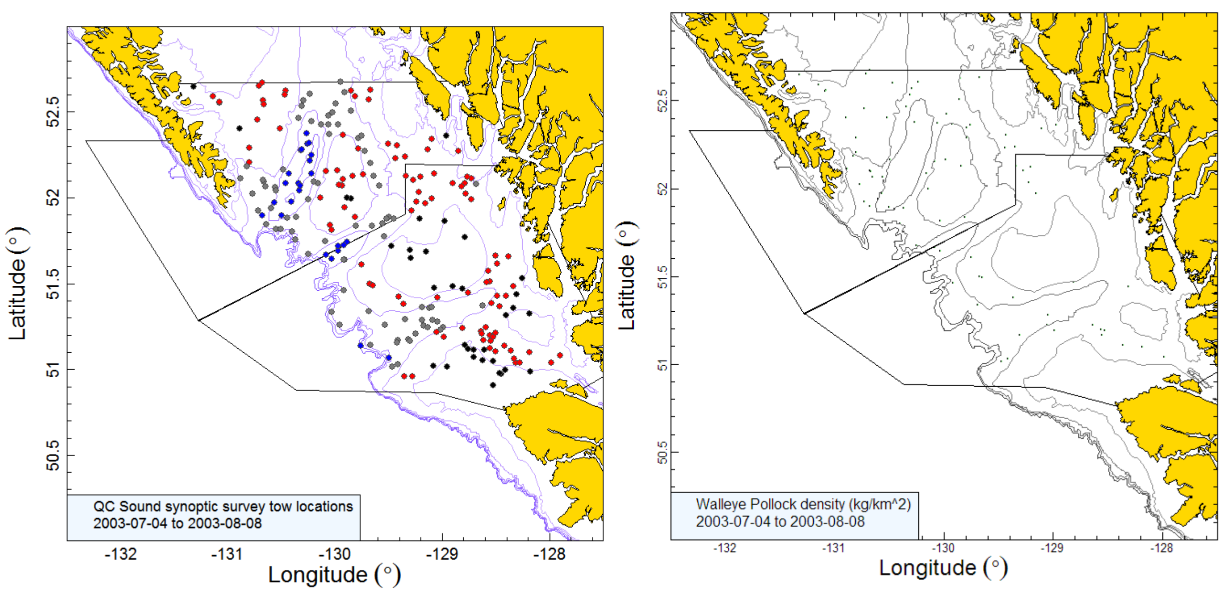

Figure B.35. Valid tow locations (50-125m stratum: black; 126-200m stratum: red; 201-330m stratum: grey; 331-500m stratum: blue) and density plots for the 2003 QC Sound synoptic survey. Circle sizes in the right-hand density plot scaled across all years (2003–2005, 2007, 2009, 2011, 2013, 2015), with the largest circle = 17,403 kg/km^2 in 2011. Boundaries delineate the North and South areal strata.

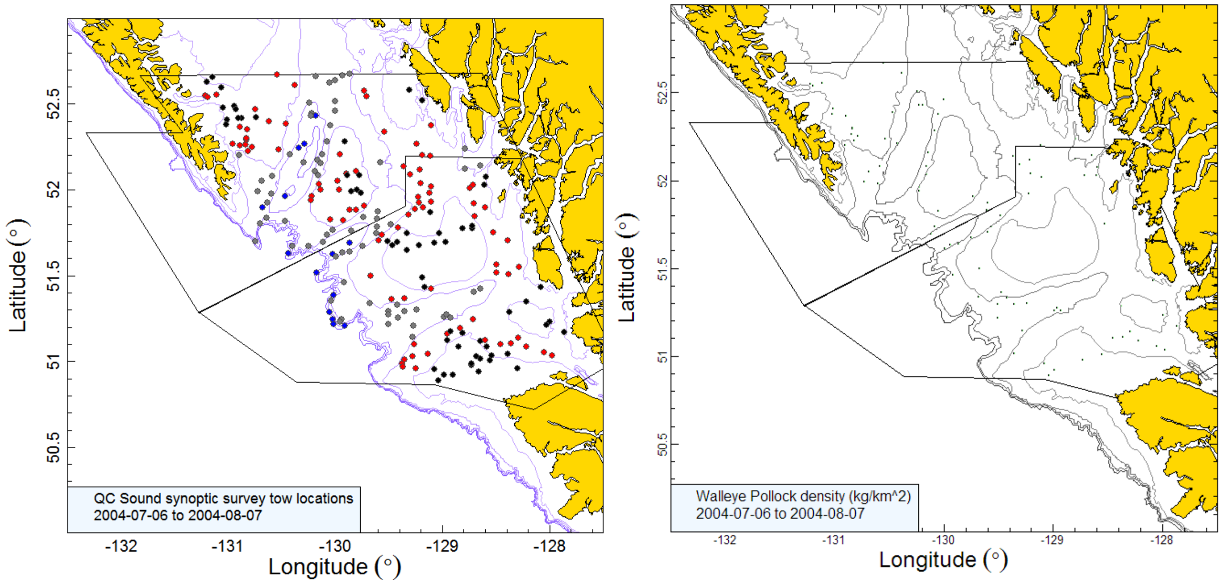

Figure B.36. Tow locations and density plots for the 2004 Queen Charlotte Sound synoptic survey (see Figure B.35 caption).

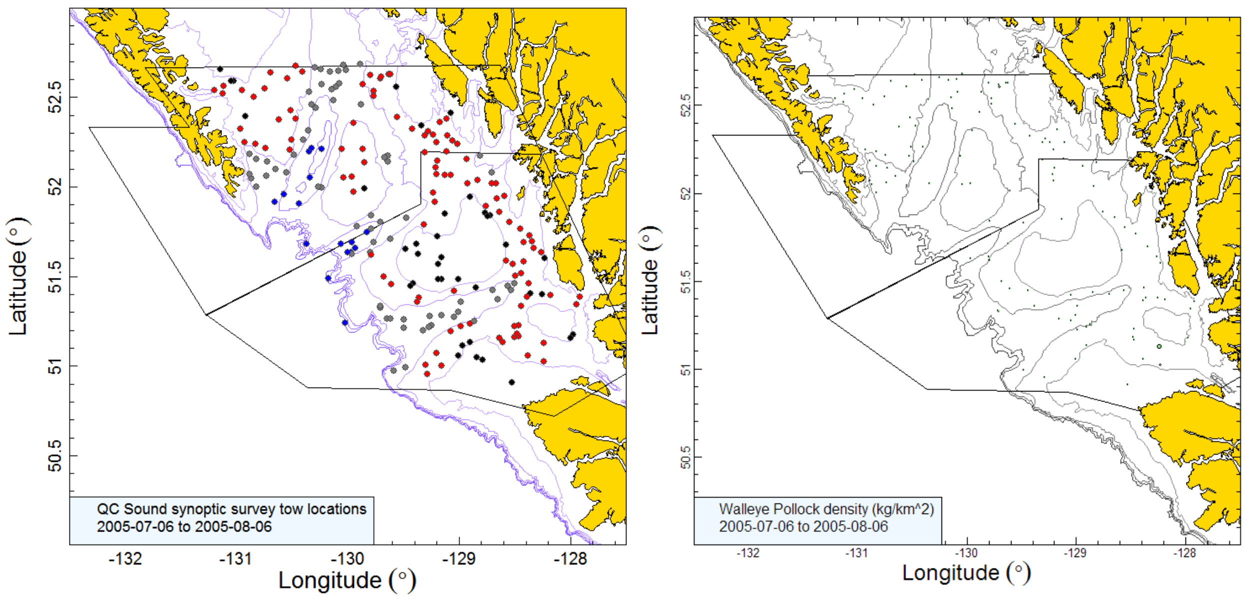

Figure B.37. Tow locations and density plots for the 2005 Queen Charlotte Sound synoptic survey (see Figure B.35 caption).

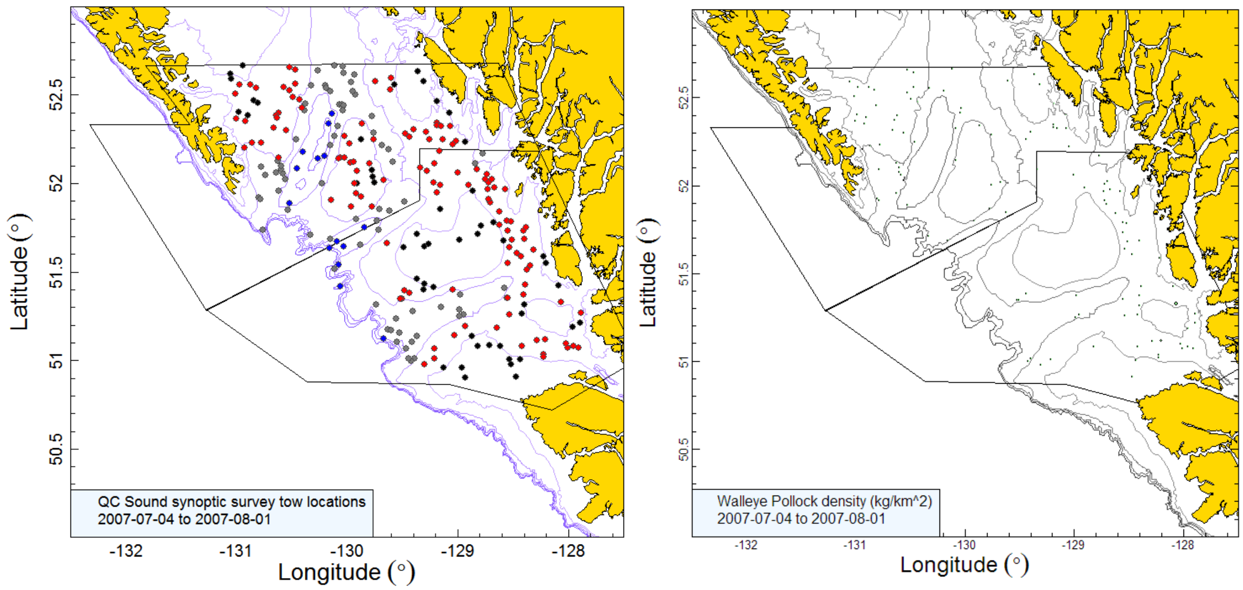

Figure B.38. Tow locations and density plots for the 2007 Queen Charlotte Sound synoptic survey (see Figure B.35 caption).

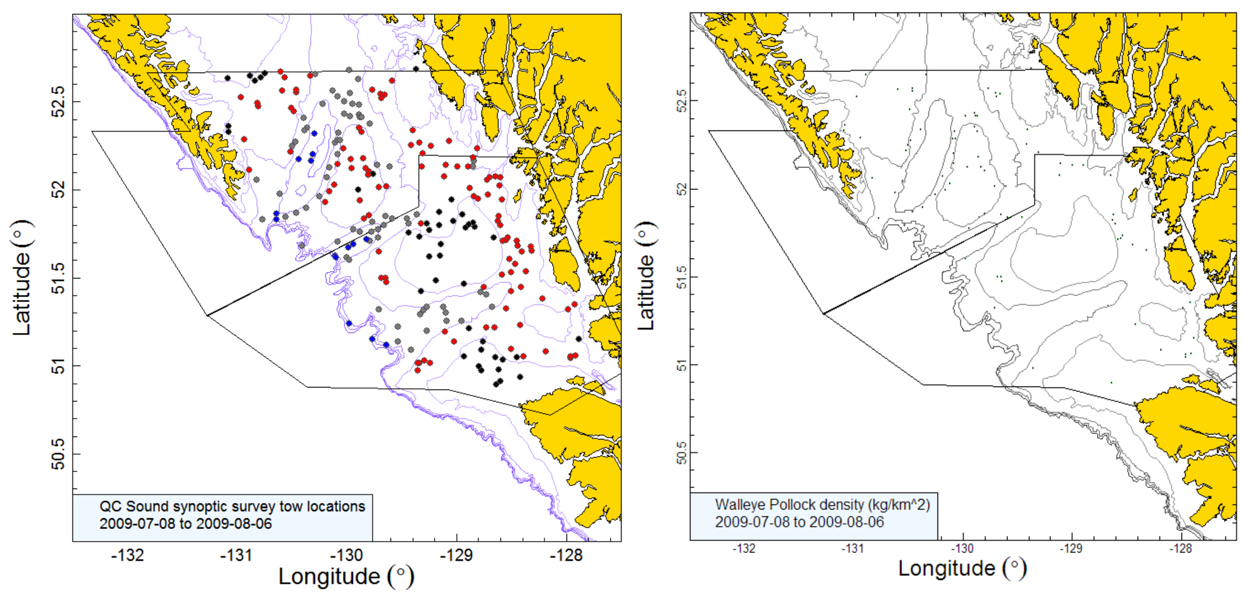

Figure B.39. Tow locations and density plots for the 2009 Queen Charlotte Sound synoptic survey (see Figure B.35 caption).

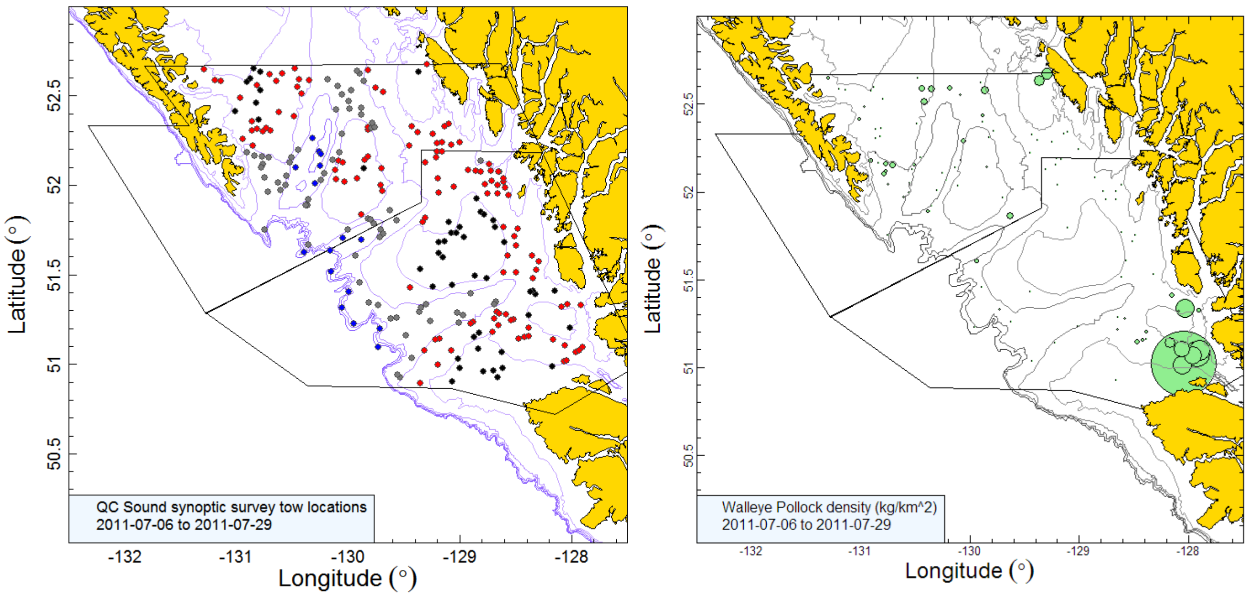

Figure B.40. Tow locations and density plots for the 2011 Queen Charlotte Sound synoptic survey (see Figure B.35 caption).

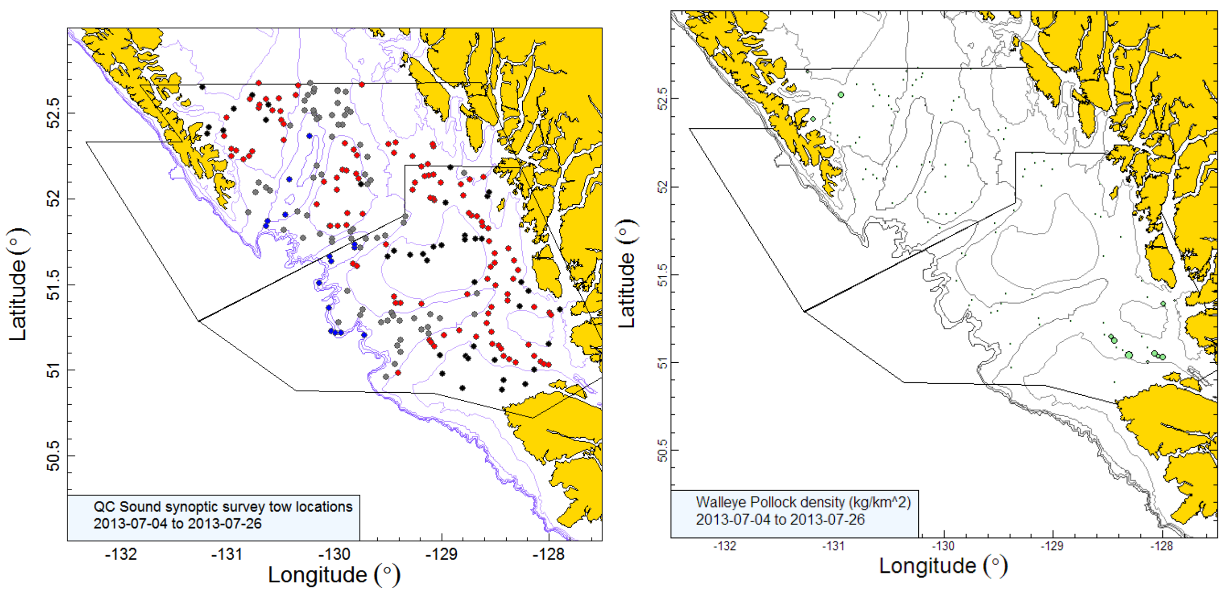

Figure B.41. Tow locations and density plots for the 2013 Queen Charlotte Sound synoptic survey (see Figure B.35 caption).

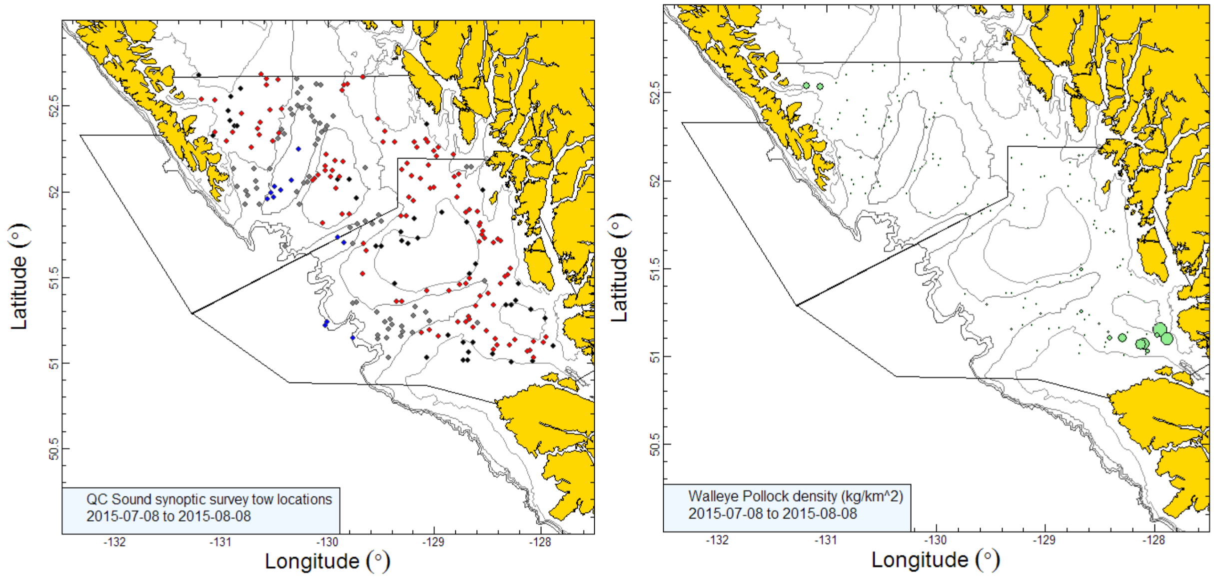

Figure B.42. Tow locations and density plots for the 2015 Queen Charlotte Sound synoptic survey (see Figure B.35 caption).

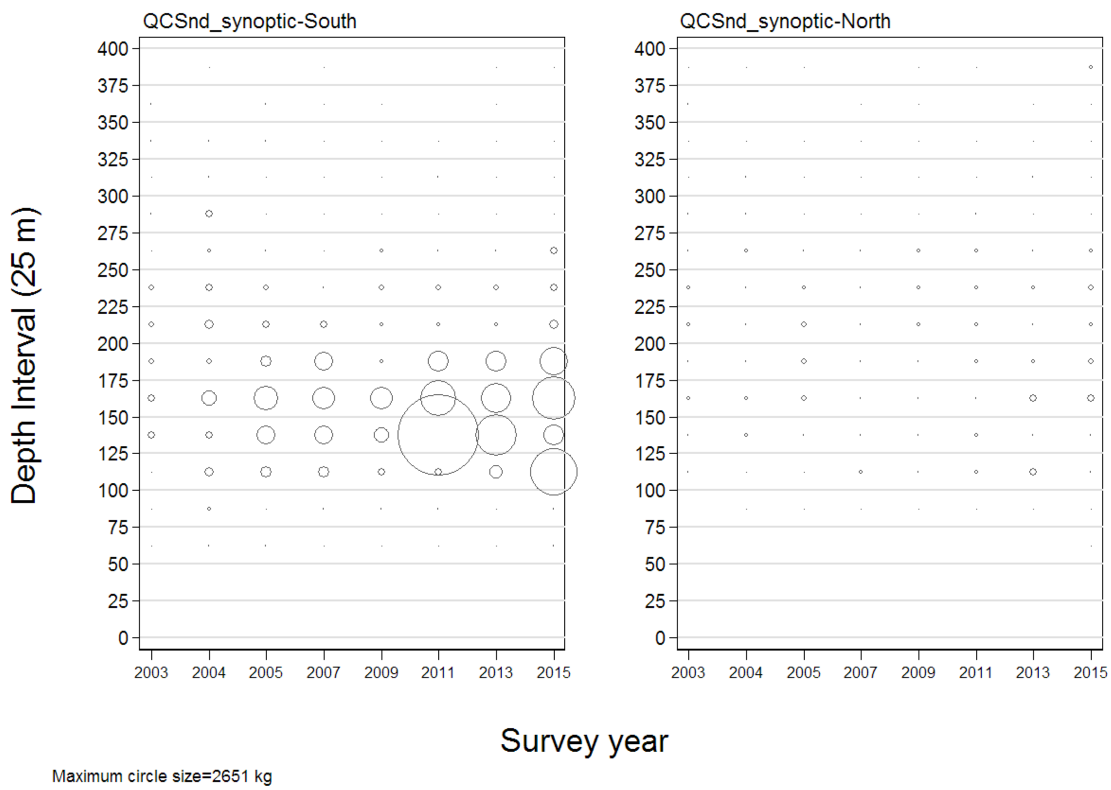

Figure B.43. Distribution of observed catch weights of Walleye Pollock for the two main Queen Charlotte Sound synoptic survey areal strata (Table B.10) by survey year and 25 m depth zone. Catches are plotted at the mid-point of the interval and circles in the panel are scaled to the maximum value (2651 kg) in the 125–150 m interval in the 2011 southern stratum. The 1% and 99% quantiles for the WAP empirical start of tow depth distribution= 76 m and 353 m respectively.

Estimated WAP doorspread biomass from this trawl survey were low from 2003 to 2009, followed by a step up in biomass beginning with the 2011 survey (Table B.12; Figure B.44). The estimated relative errors were variable for this species, lying between 19 and 24% when the survey biomass estimates were low, but jumping to higher values after 2009 (Table B.12). Between 23 and 62% of the South stratum tows and 39 to 62% of the North stratum tows captured some WAP (Figure B.45). Overall, 858 of the 1909 valid survey tows (45%) contained WAP, with the North stratum having a 53% average proportion non-zero tows while the equivalent South stratum proportion was 38%. Although this species occurs frequently in this survey, catch weights tend to be low, with the median catch weight for positive tows around 1.8 kg/tow across all 8 surveys, but the maximum catch weight was 2127 kg in the 2011 survey.

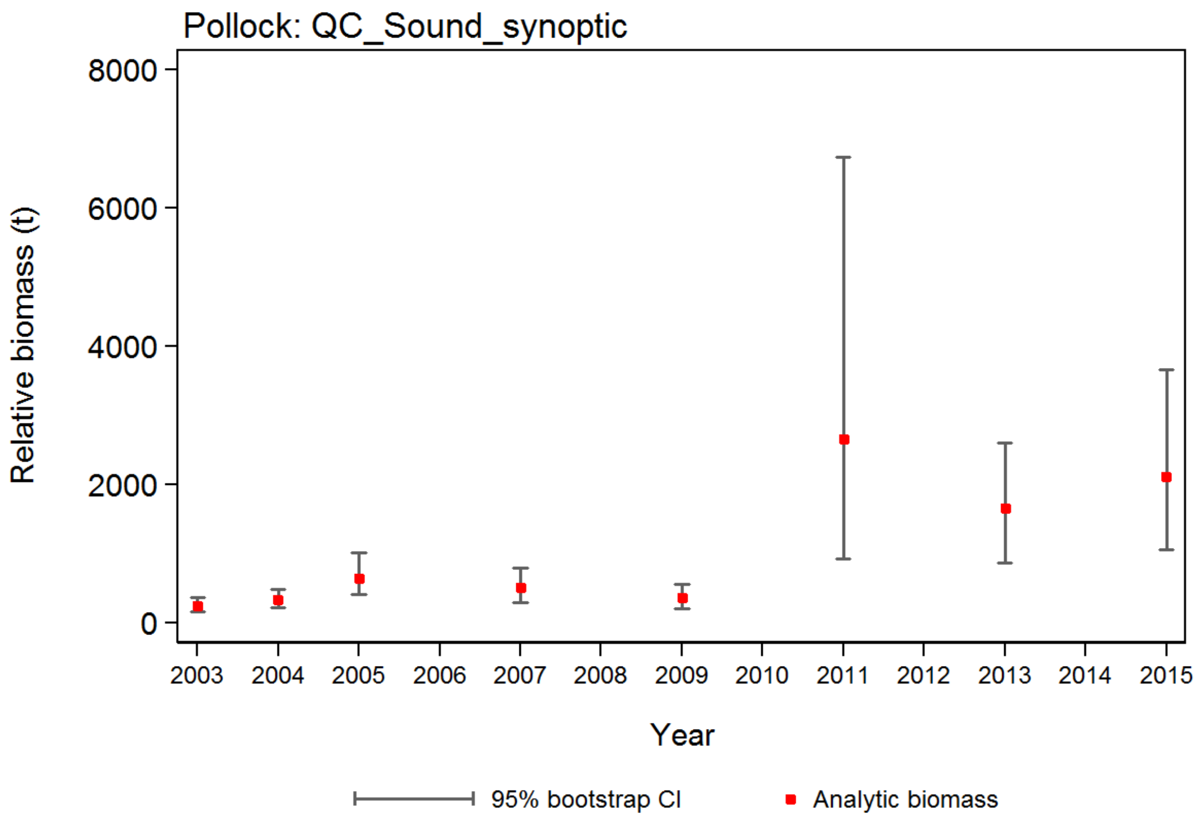

Figure B.44. Plot of biomass estimates for WAP (values provided in Table B.12) from the Queen Charlotte Sound synoptic survey over the period 2003 to 2015. Bias corrected 95% confidence intervals from 1000 bootstrap replicates are plotted.

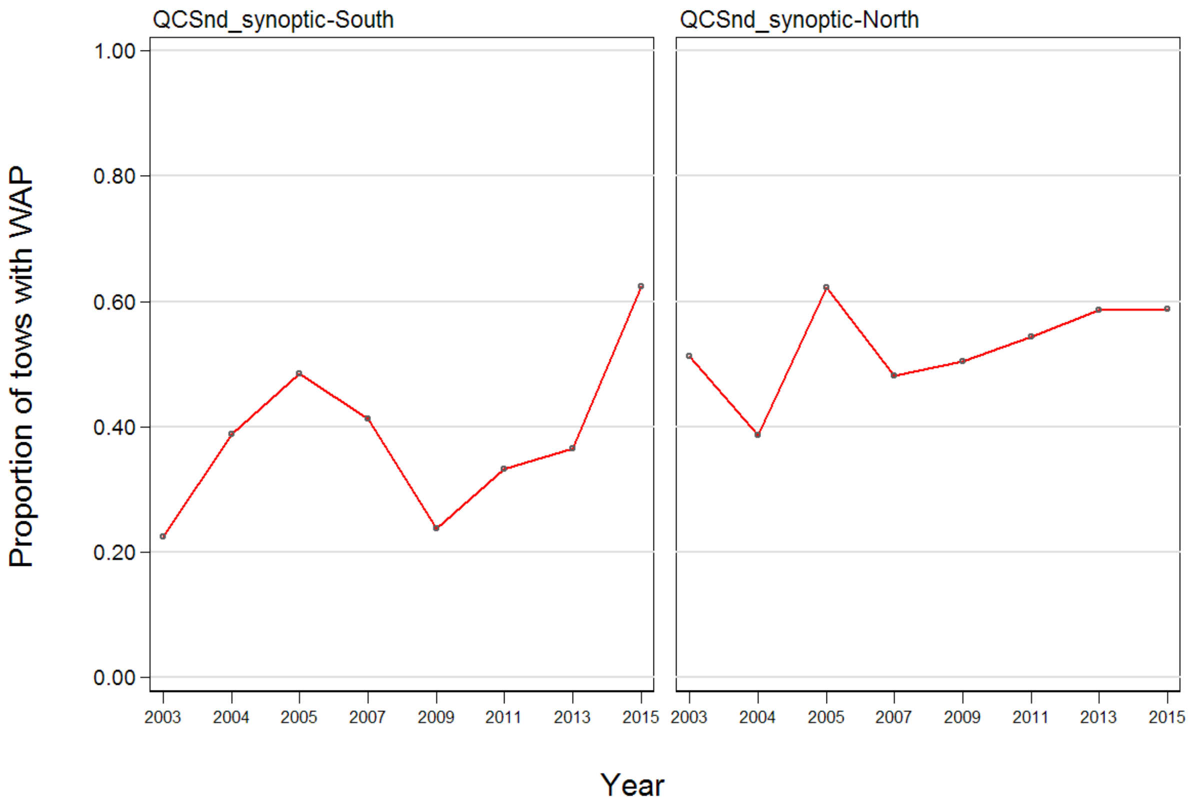

Figure B.45. Proportion of tows by stratum and year which contain WAP from the Queen Charlotte Sound synoptic survey over the period 2003 to 2015.

B.7. WEST COAST VANCOUVER ISLAND SYNOPTIC TRAWL SURVEY

B.7.1. Data selection

This survey has been conducted seven times in the period 2004 to 2016 off the west coast of Vancouver Island by RV *W.E. Ricker*. It comprises a single areal stratum, separated into four depth strata: 50-125 m; 125-200 m; 200-330 m; and 330-500 m (Table B.13). Approximately 150 to 180 2-km^2 blocks are selected randomly among the four depth strata when conducting each survey (Olsen et. al. 2008).

A doorspread density value was generated for each tow based on the catch of Walleye Pollock, the mean doorspread for the tow and the distance travelled (Eq. B.3). The distance travelled was provided as a data field, determined directly from vessel track information collected during the tow. There were only two missing values in this field which were filled in by multiplying the vessel speed by the time that the net was towed. There were a large number of missing values for the doorspread field, which were filled in using the mean doorspread for the survey year or a default value of 64.7 m for the three years with no doorspread data (Table B.14). The default value is based on the mean of the observed doorspread from the net mensuration equipment, averaged across the years with doorspread estimates.

Table B.13. Stratum designations, number of usable and unusable tows, for each year of the west coast Vancouver Island synoptic survey. Also shown is the area of each stratum in 2016 and the start and end dates for each survey.

Survey	Stratum depth zone				Total	Unusable	Start	End
year	50-125 m	125-200 m	200-330 m	330-500 m	Tows[1]	tows	date	date
2004	34	34	13	8	89	17	26-May-04	09-Jun-04
2006	61	62	28	13	164	12	24-May-06	18-Jun-06
2008	54	50	32	23	159	19	27-May-08	21-Jun-08
2010	58	47	22	9	136	8	08-Jun-10	28-Jun-10
2012	61	46	26	20	153	4	23-May-12	15-Jun-12
2014	55	49	29	14	147	6	29-May-14	20-Jun-14
2016	54	41	26	19	140	7	25-May-16	15-Jun-16
Area (km^2)	5804	3796	708	608	10,916[2]	–	–	–

[1] GFBio usability codes=0,1,2,6
[2] Total area (km^2) for 2016 synoptic survey

Table B.14. Number of tows with and without doorspread measurements by survey year for the WCVI synoptic survey. Mean doorspread values for those tows with measurements are provided.

	Number tows		Mean
	Without doorspread	With doorspread	doorspread (m)
2004	89	0	–
2006	96	69	64.3
2008	58	107	64.5
2010	136	0	–
2012	153	0	–
2014	14	139	64.3
2016	0	147	65.5
All surveys	546	462	64.7

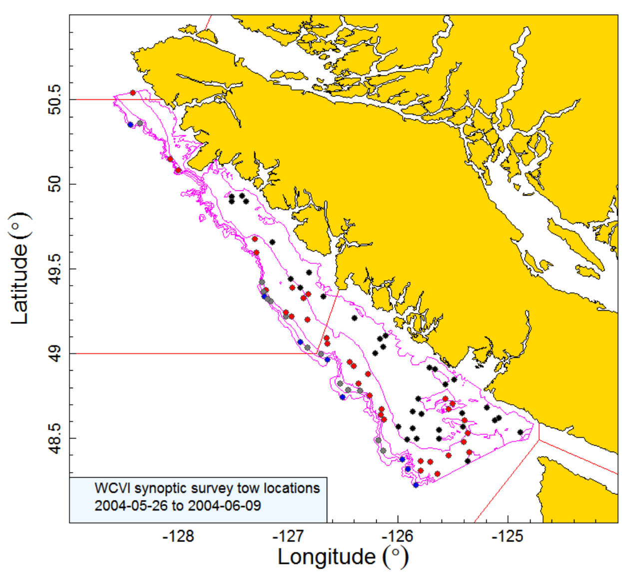

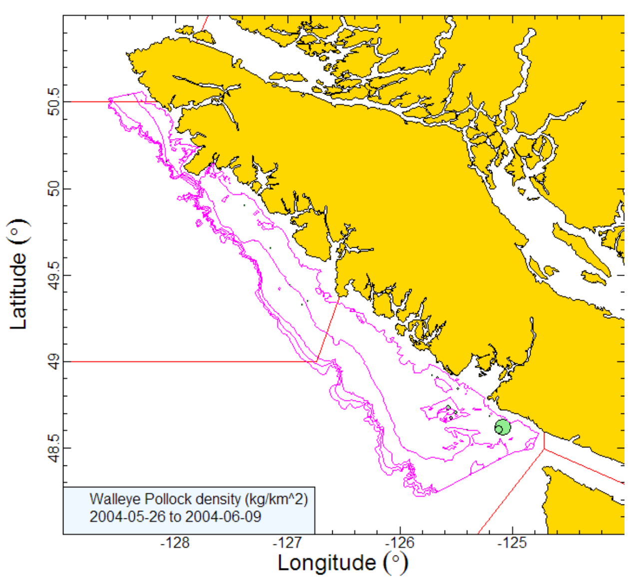

Figure B.46. Valid tow locations (50-125m stratum: black; 126-200m stratum: red; 201-330m stratum: grey; 331-500m stratum: blue) and density plots for the 2004 west coast Vancouver Island synoptic survey. Circle sizes in the right-hand density plot scaled across all years (2004, 2006, 2008, 2010, 2012, 2014), with the largest circle = 8962 kg/km² in 2010. The red solid lines indicate the boundaries for PMFC areas 3C, 3D and 5A.

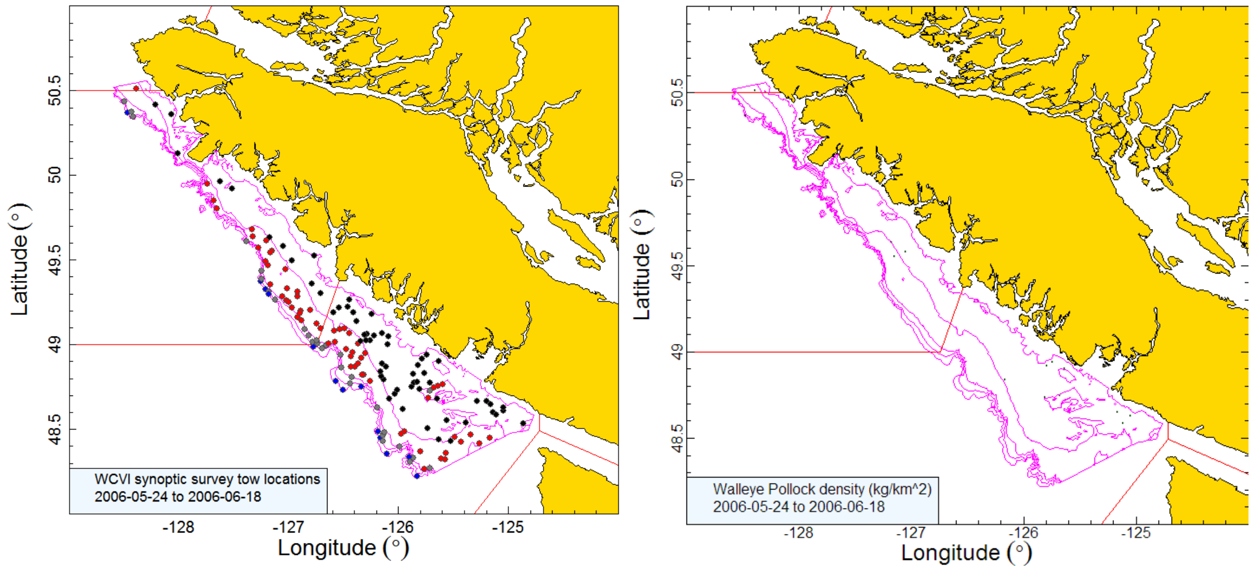

Figure B.47. Tow locations and density plots for the 2006 west coast Vancouver Island synoptic survey (see Figure B.46 caption).

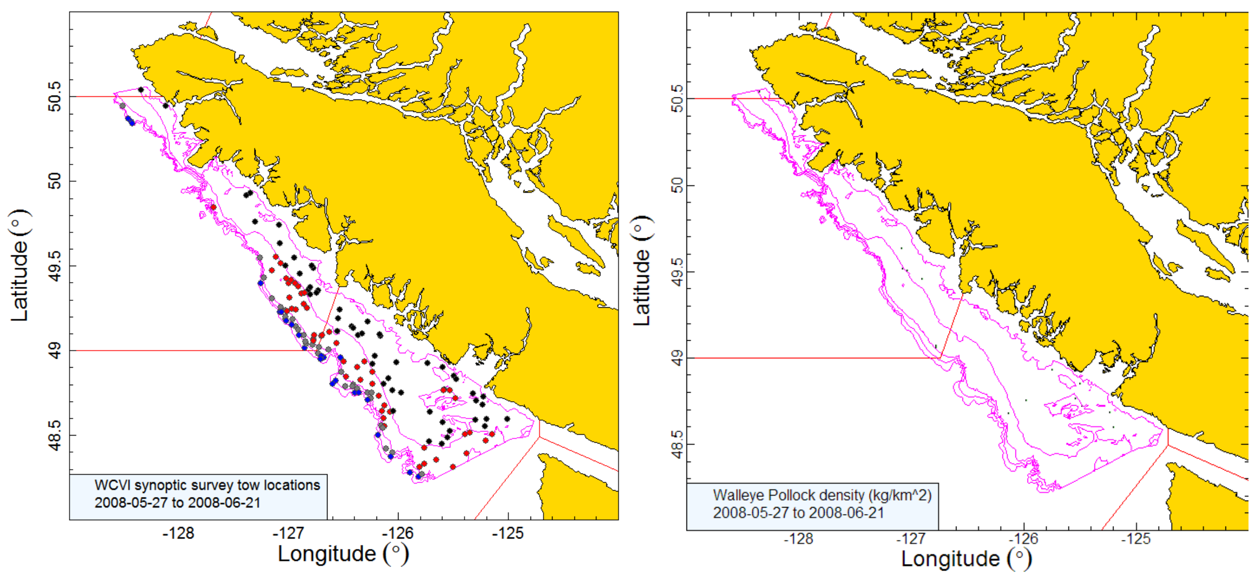

Figure B.48. Tow locations and density plots for the 2008 west coast Vancouver Island synoptic survey (see Figure B.46 caption).

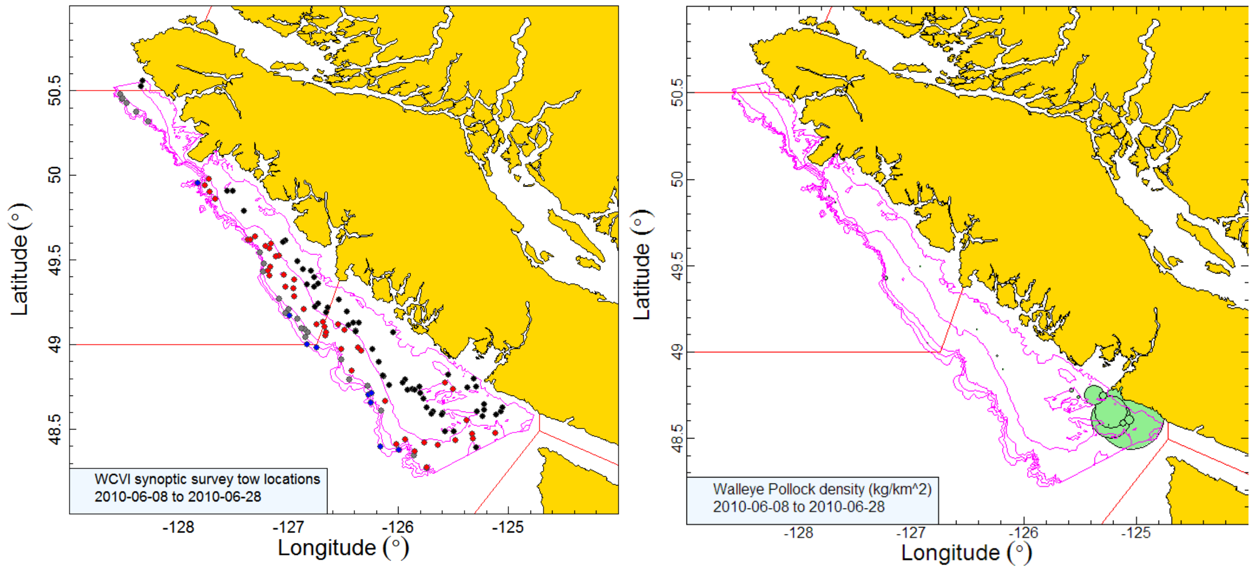

Figure B.49. Tow locations and density plots for the 2010 west coast Vancouver Island synoptic survey (see Figure B.46 caption).

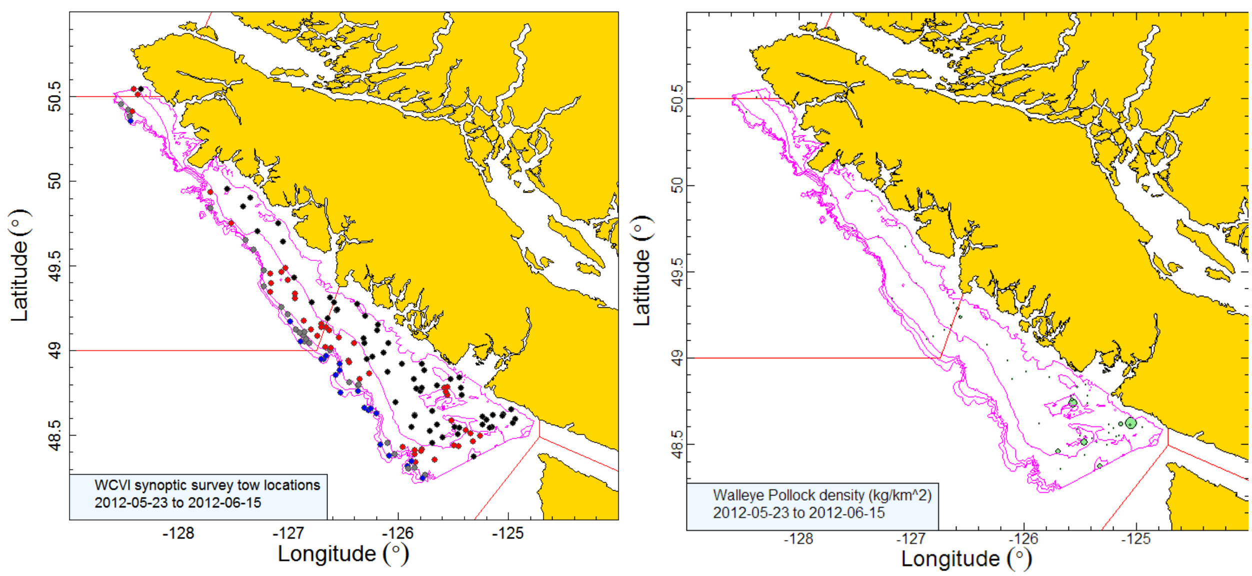

Figure B.50. Tow locations and density plots for the 2012 west coast Vancouver Island synoptic survey (see Figure B.46 caption).

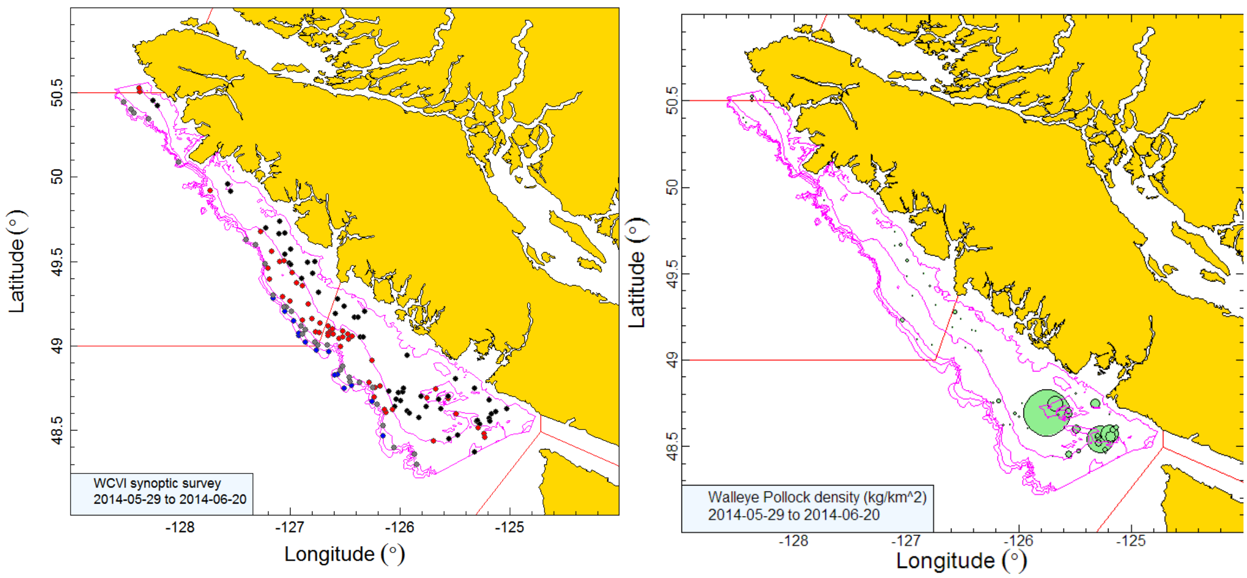

Figure B.51. Tow locations and density plots for the 2014 west coast Vancouver Island synoptic survey (see Figure B.46 caption).

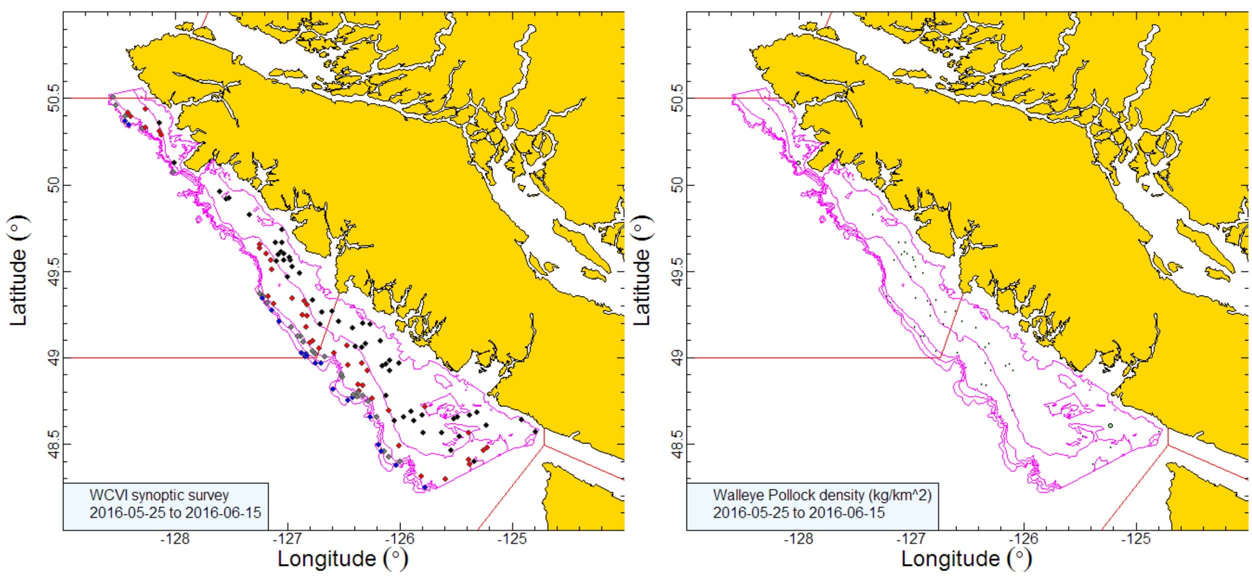

Figure B.52. Tow locations and density plots for the 2016 west coast Vancouver Island synoptic survey (see Figure B.46 caption).

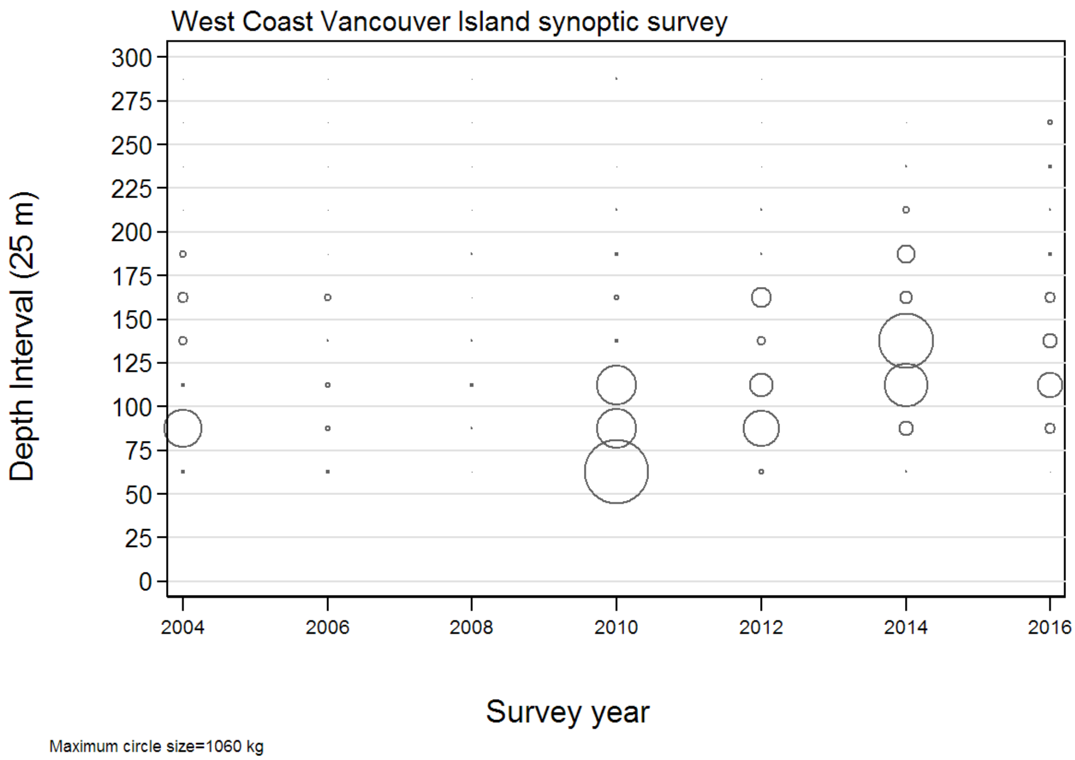

Figure B.53. Distribution of observed weights of Walleye Pollock by survey year and 25 m depth zone. Catches are plotted at the mid-point of the interval and circles in the panel are scaled to the maximum value (1060 kg) in the 50-75 m interval in 2010. The 1% and 99% quantiles for the WAP empirical start of tow depth distribution= 61 m and 270 m respectively.

B.7.2. Results

Walleye Pollock are mainly taken near the entrance of Juan de Fuca Strait, although the incidence of these encounters appears to vary between years (Figure B.46 to Figure B.51). There is an important midwater trawl fishery for this species in Juan de Fuca Strait, but much of it occurs further in the Strait, although there are also catches in the same location where WAP are taken in this survey (see Figure A.2). Walleye Pollock were mainly taken at depths from 75 to 213 m (5–95% quantiles) and there were almost no observations at depths greater than 300 m (Figure B.53). Estimated biomass levels for Walleye Pollock from this trawl survey show elevated biomass levels beginning with 2010, but there is no apparent trend after that year. Relative errors are high, ranging from 36 to 66% across the seven surveys (Figure B.54; Table B.15).

The proportion of tows capturing Walleye Pollock ranged between 9 and 41% for the seven surveys, with a mean value of 25% (Figure B.55). About one quarter of the tows from this survey contain WAP, but as in the QC Sound synoptic survey, the median catch weight for positive tows was low (around 1.3 kg/tow) and the maximum catch weight across all six surveys was 1060 kg (in 2010).

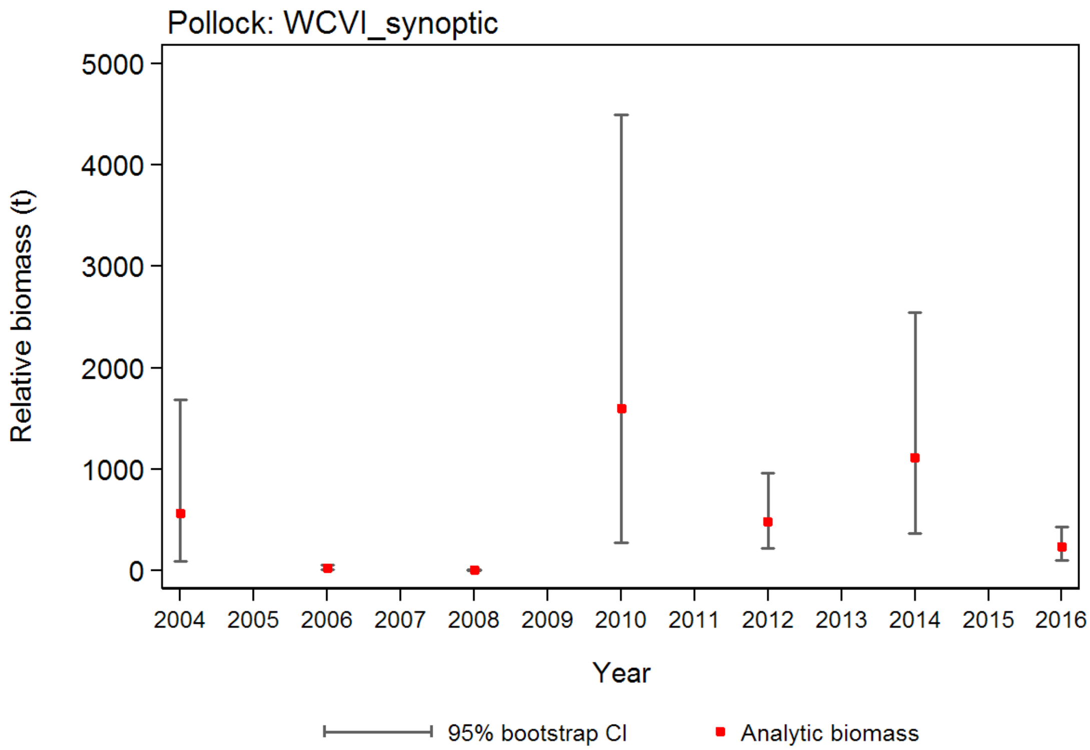

Figure B.54. Plot of biomass estimates for Walleye Pollock from the 2004 to 2016 west coast Vancouver Island synoptic trawl surveys (Table B.15). Bias-corrected 95% confidence intervals from 1000 bootstrap replicates are plotted.

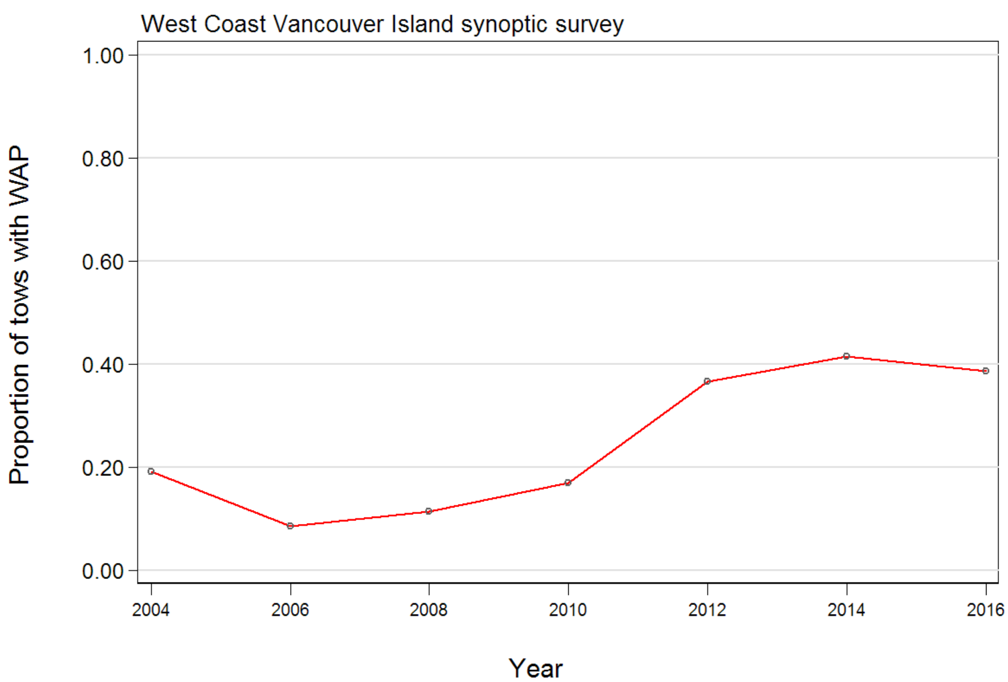

Figure B.55. Proportion of tows by stratum and year capturing Walleye Pollock in the WCVI synoptic trawl surveys, 2004–2016.

Table B.15. Biomass estimates for Walleye Pollock from the WCVI synoptic trawl survey for the survey years 2004 to 2016. Bootstrap bias-corrected confidence intervals and CVs are based on 1000 random draws with replacement.

Survey Year	Biomass (t) (Eq. B.4)	Mean bootstrap biomass (t)	Lower bound biomass (t)	Upper bound biomass (t)	Bootstrap CV	Analytic CV (Eq. B.6)
2004	569	561	92	1684	0.662	0.669
2006	28	28	8	61	0.473	0.490
2008	7	7	3	14	0.408	0.419
2010	1598	1551	274	4493	0.648	0.609
2012	489	482	221	968	0.380	0.378
2014	1121	1112	365	2542	0.486	0.490
2016	237	231	104	438	0.364	0.383

B.8. WEST COAST HAIDA GWAII SYNOPTIC TRAWL SURVEY

B.8.1. Data selection

The west coast Haida Gwaii (WCHG) survey has been conducted six times in the period 2006 to 2016 off the west coast of Haida Gwaii. A survey conducted in 2014 did not complete a sufficient number of tows for it to be considered completed. The survey comprises a single areal stratum extending from about 53°N to the BC-Alaska border and east to 133°W (e.g., Olsen et al. 2008). The 2006 survey used a different depth stratification scheme compared to the later synoptic surveys: 150–200 m, 200–330 m, 330–500 m, 500–800 m, and 800–1300 m (Workman et al. 2007). All tows from this survey were re-stratified into the four depth strata used from 2007 onwards: 180–330 m; 330–500 m; 500–800 m; and 800–1300 m, based on the mean of the beginning and end depths of each tow (Table B.16). Plots of the locations of all valid tows by year and stratum are presented in Figure B.56 (2006), Figure B.57 (2007), Figure B.58 (2008), Figure B.59 (2010), Figure B.60 (2012) and Figure B.61 (2016). Note that the depth stratum boundaries for this survey differ from those used for the Queen Charlotte Sound (Edwards et al., 2012) and west coast Vancouver Island (Edwards et al., 2014) synoptic surveys due to the considerable difference in the seabed topography of the area being surveyed. The deepest stratum (800–1300 m) was omitted from this analysis because of lack of coverage in 2007.

Table B.16. Stratum designations, vessel name, number of usable and unusable tows, for each year of the west coast Haida Gwaii synoptic survey. Also shown are the area of each stratum and the dates of the first and last survey tow in each year.

Survey year	Vessel	Depth stratum 180-330m	330-500m	500-800m	800-1300m	Total tows[1]	Unusable tows	Start date	End date
2006	Viking Storm	55	26	16	13	110 [2]	13	30-Aug-06	22-Sep-06
2007	Nemesis	68	34	9	0	111	5	14-Sep-07	12-Oct-07
2008	Frosti	71	31	8	8	118	9	28-Aug-08	18-Sep-08
2010	Viking Storm	82	29	12	6	129	2	28-Aug-10	16-Sep-10
2012	Nordic Pearl	75	29	10	16	130	11	27-Aug-12	16-Sep-12
2016	Frosti	69	28	5	10	112	8	28-Aug-16	24-Sep-16
Area (km^2)	-	1104	1024	956	2248	5332 [3]	-	-	-

[1] GFBio usability codes=0,1,2,6; [2] excludes 2 tows S of 53°N; [3] Total area in 2016 (km^2)

Table B.17. Number of valid tows with doorspread measurements, the mean doorspread values (in m) from these tows for each survey year and the number of valid tows without doorspread measurements.

Year	Tows with doorspread	Tows missing doorspread	Mean doorspread (m)
2006	93	30	77.7
2007	113	3	68.5
2008	123	4	80.7
2010	129	2	79.1
2012	92	49	73.8
2016	105	15	74.1
Total/Average	655	103	75.8[1]

[1] average 2006–2016: all observations

A doorspread density (Eq. B.3) was generated for each tow based on the catch of Walleye Pollock (WAP), the mean doorspread for the tow and the distance travelled. [**distance_travelled**] is a database field which is calculated directly from the tow track. This field is used preferentially for the variable D_{yij} in Eq. B.3. A calculated value ([**vessel_speed**] X [**tow_duration**]) is used for this variable if [**distance_travelled**] is missing, but there were no instances of this occurring in the six trawl surveys. Missing values for the [**doorspread**] field were filled in with the mean doorspread for the survey year (103 values over all years, Table B.17).

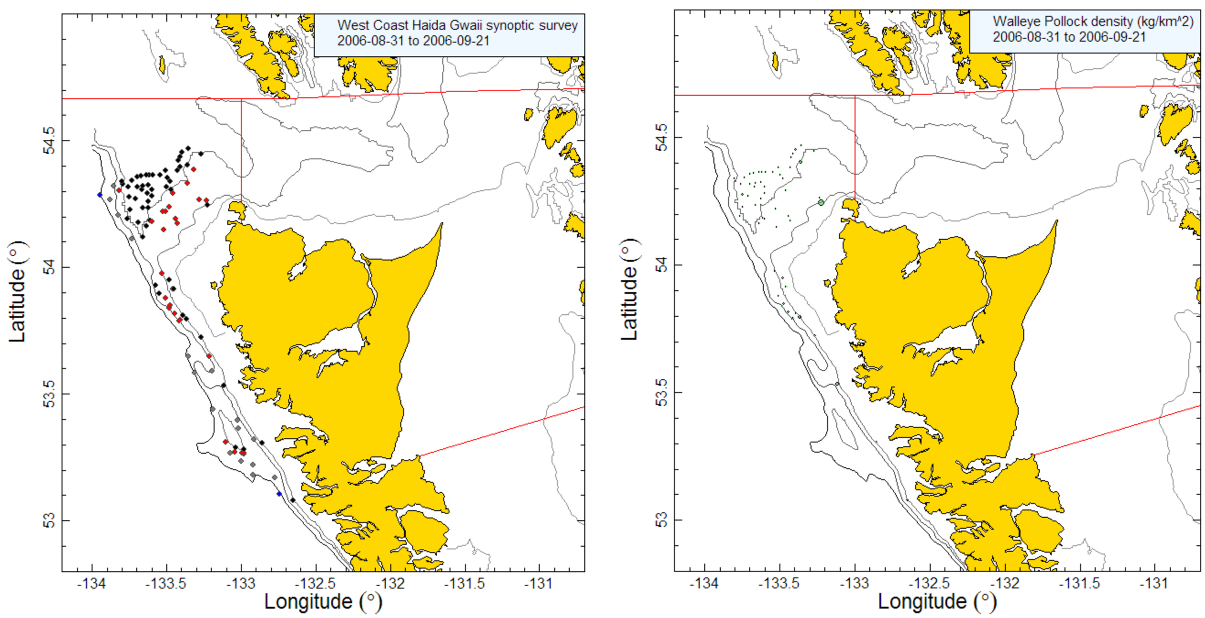

Figure B.56. Valid tow locations by stratum (180-330m: black; 330-500m: red; 500-800m: grey; 800-1300m: blue) and density plots for the 2006 Viking Storm synoptic survey. Circle sizes in the right-hand density plot scaled across all years (2006–2016), with the largest circle =2384 kg/km² in 2016. The red lines show the Pacific Marine Fisheries Commission 5E and 5D major area boundaries.

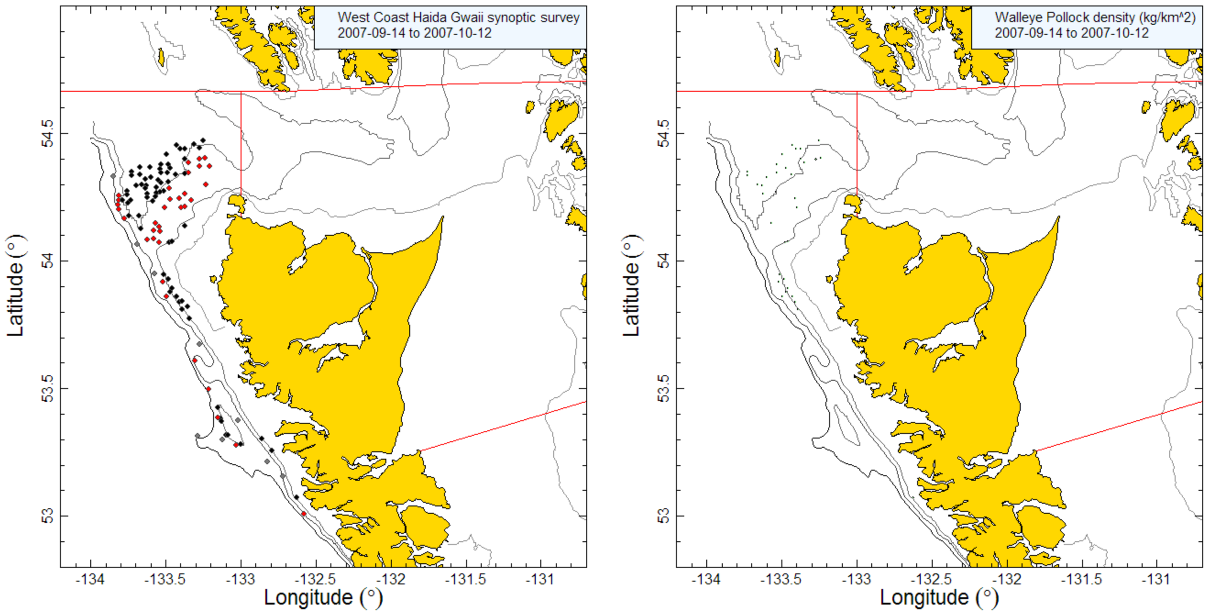

Figure B.57. Tow locations and density plots for the 2007 Nemesis synoptic survey (see Figure B.56 caption).

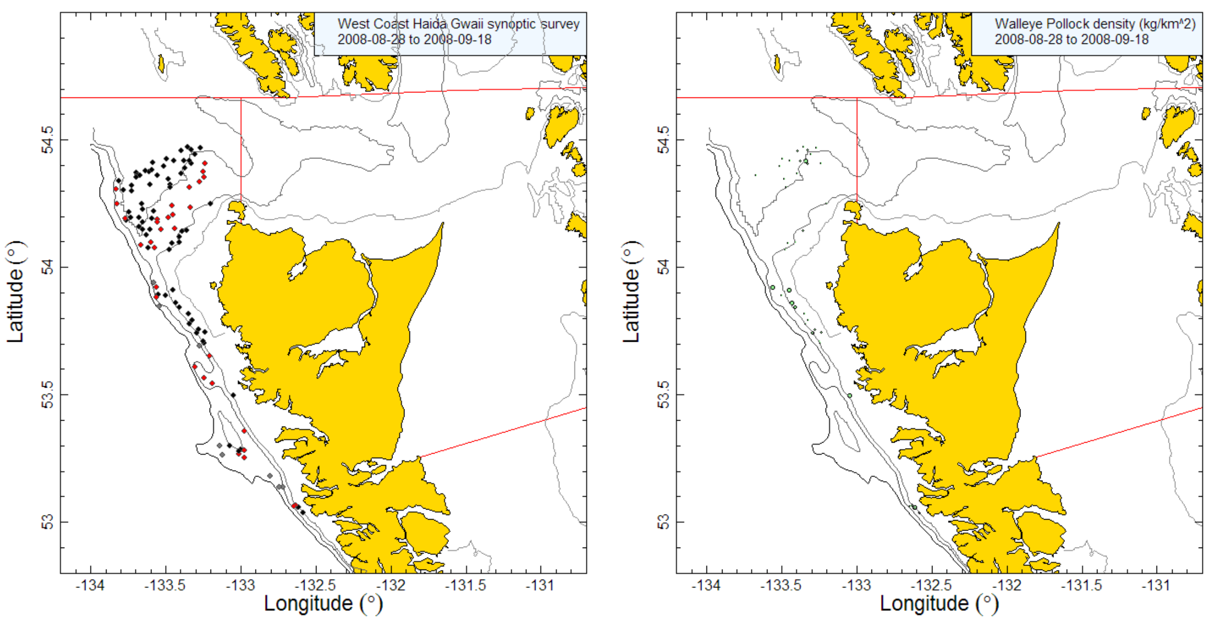

Figure B.58. Tow locations and density plots for the 2008 Frosti synoptic survey (see Figure B.56 caption).

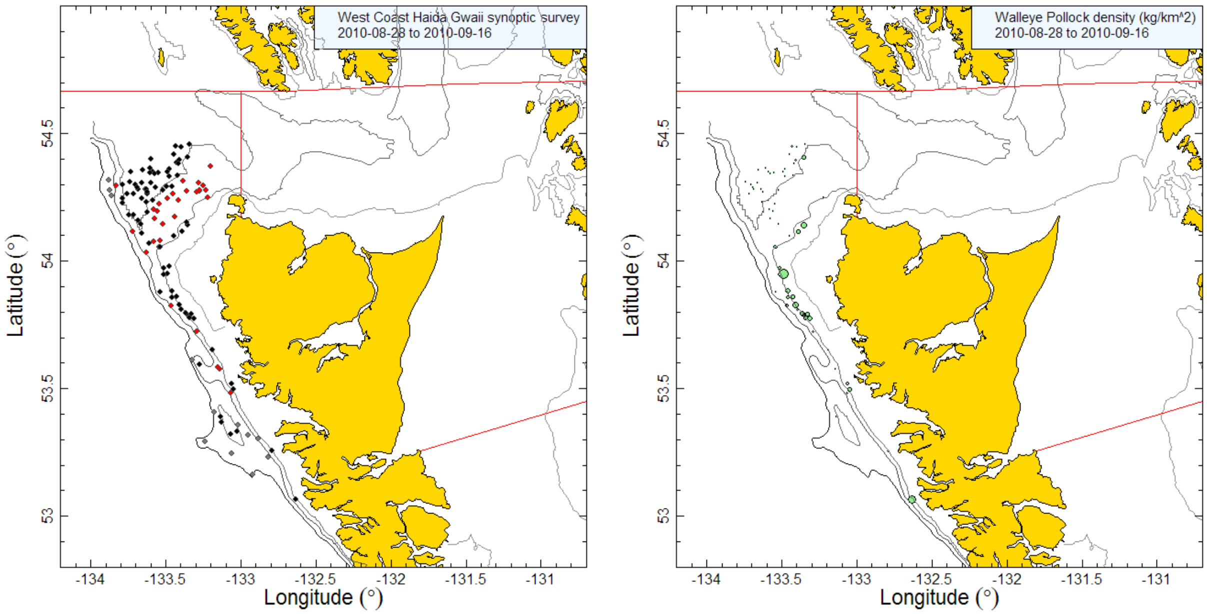

Figure B.59. Tow locations and density plots for the 2010 Viking Storm synoptic survey (see Figure B.56 caption).

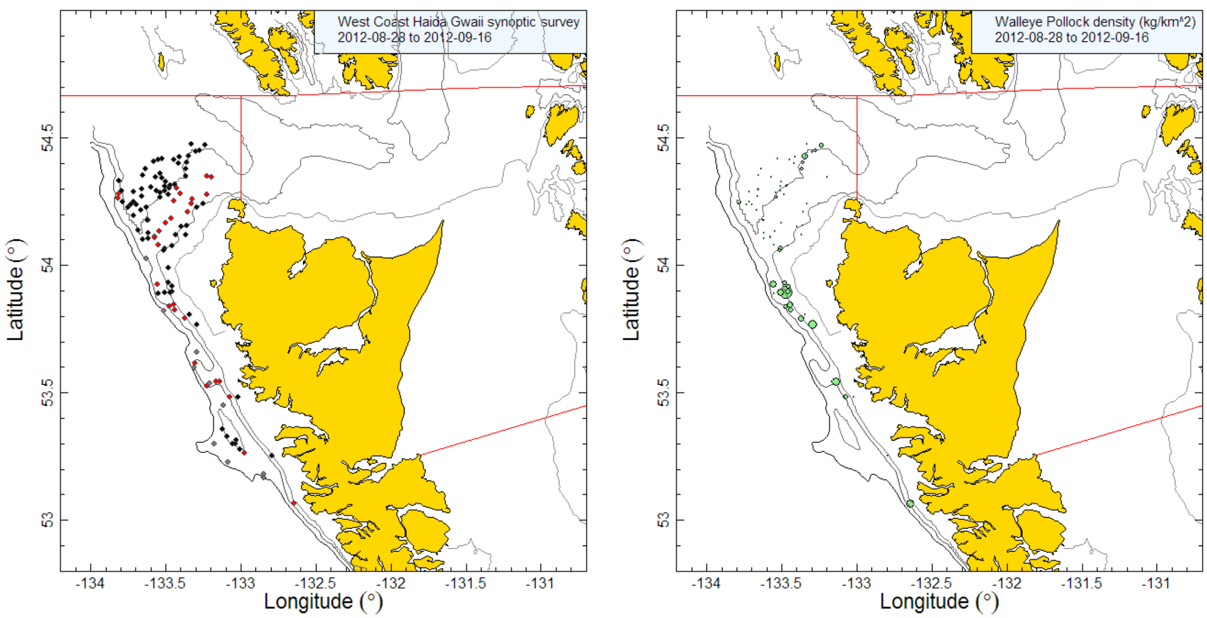

Figure B.60. Tow locations and density plots for the 2012 Viking Storm synoptic survey (see Figure B.56 caption).

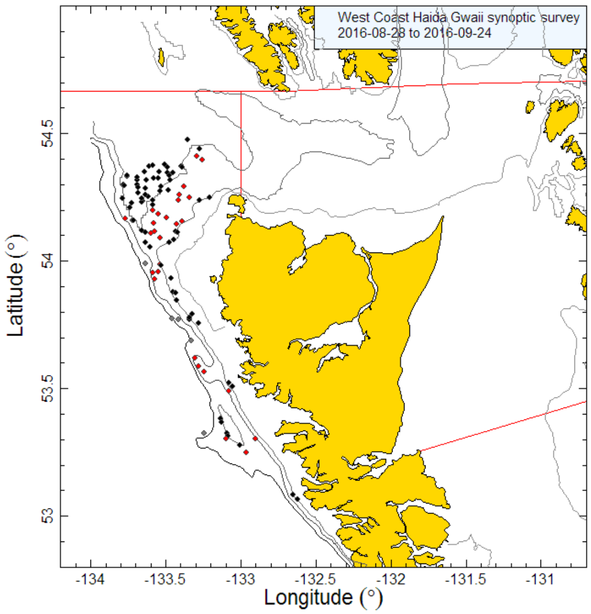

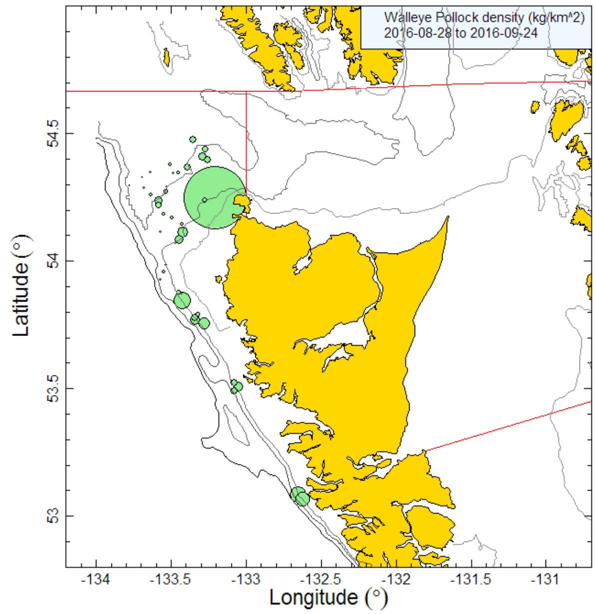

Figure B.61. Tow locations and density plots for the 2016 Frosti synoptic survey (see Figure B.56 caption).

B.8.2. Results

WAP was taken in small amounts off the north coast of Graham Island, into the western part of Dixon Entrance and down the west side of Graham in most of the first five surveys [Figure B.56 (2006), Figure B.57 (2007), Figure B.58 (2008), Figure B.59 (2010), Figure B.60 (2012)]. WAP catches in the 2016 survey (Figure B.61) were distributed down the west coast of Graham Island down to 53 N (the southern limit of the survey) and there was one large tow west of Langara Island. Walleye Pollock were mainly taken at depths from 210 to 394 m (5 to 95% quantiles), with the majority of the observations lying between 220 and 370 m depth (Figure B.62).

Table B.18. Biomass estimates for Walleye Pollock from the six west coast Haida Gwaii synoptic surveys. Bootstrap bias-corrected confidence intervals and coefficients of variation (CVs) are based on 1000 random draws with replacement.

Survey Year	Biomass (t) (Eq. B.4)	Mean bootstrap biomass (t)	Lower bound biomass (t)	Upper bound biomass (t)	Bootstrap CV	Analytic CV (Eq. B.6)
2006	31.0	31.0	21.8	45.9	0.194	0.191
2007	15.7	15.9	9.4	24.2	0.236	0.237
2008	34.3	34.5	20.0	54.7	0.242	0.238
2010	38.4	38.6	26.8	53.8	0.183	0.191
2012	67.2	67.3	41.7	96.9	0.210	0.212
2016	61.8	62.0	18.5	159.3	0.600	0.618

Estimated biomass levels for Walleye Pollock from these trawl surveys may show a weak ascending trend (ranging from 31 t in 2010 to 60+ t in 2012 and 2016) (Figure B.63; Table B.18). The estimated relative errors (RE) for these surveys were low (compared to other WAP surveys) up to 2016, ranging from 18 to 24%, but the 2016 RE was 60% (Table B.18).

The proportion of tows that captured Walleye Pollock ranged from 32 to 53% of tows over the six synoptic survey years, with an overall mean of 43% (Figure B.64). The median WAP catch weight for positive tows was low (<2 kg/tow) and the maximum catch weight across all six surveys was 308 kg (in 2016). This tow was the largest of the series, with the next largest tow being 69 kg, which explains the high variance observed in the 2016 biomass estimate.

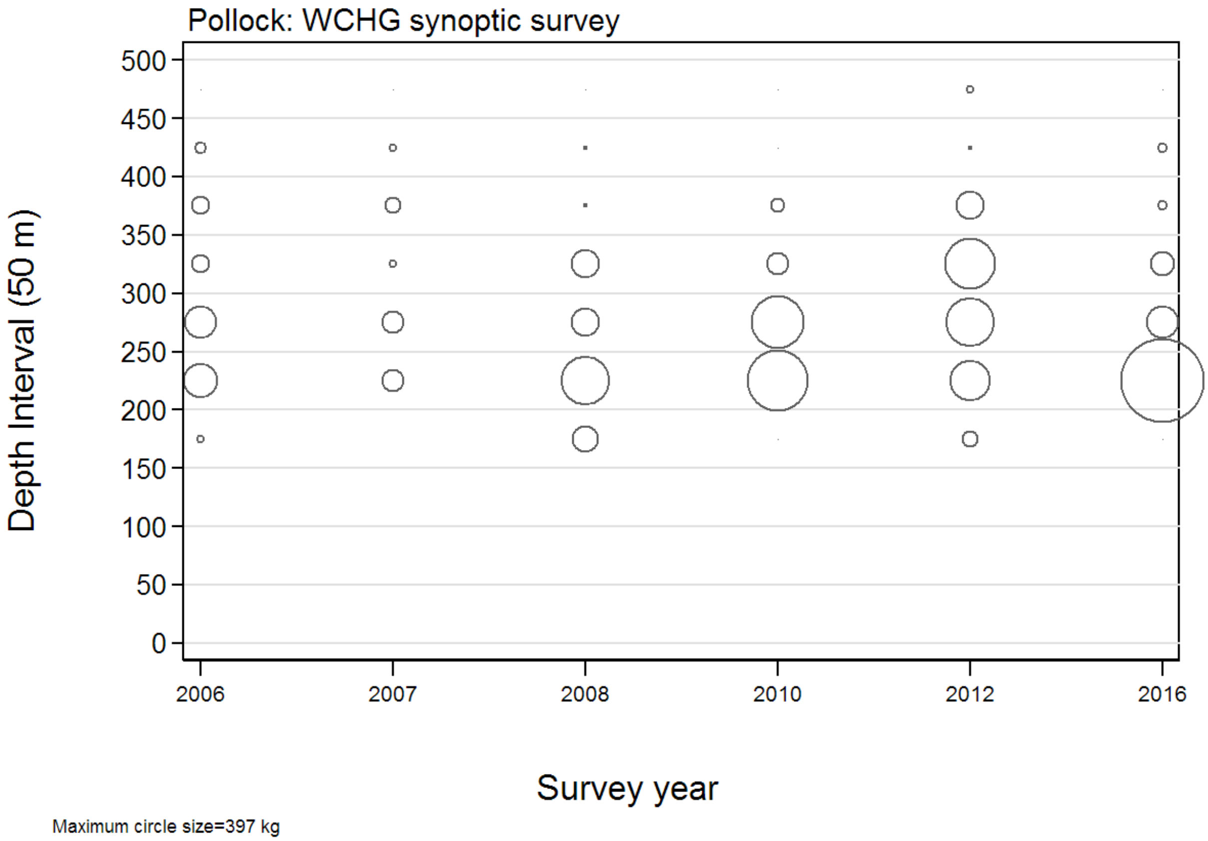

Figure B.62. Distribution of observed weights of Walleye Pollock by survey year and 50 m depth zone intervals. Catches are plotted at the mid-point of the interval and circles in the each panel are scaled to the maximum value (397 kg – 200-250 m interval in 2016). Minimum and maximum depths observed for WAP: 157 m and 473 m, respectively. Depth is taken at the start position for each tow.

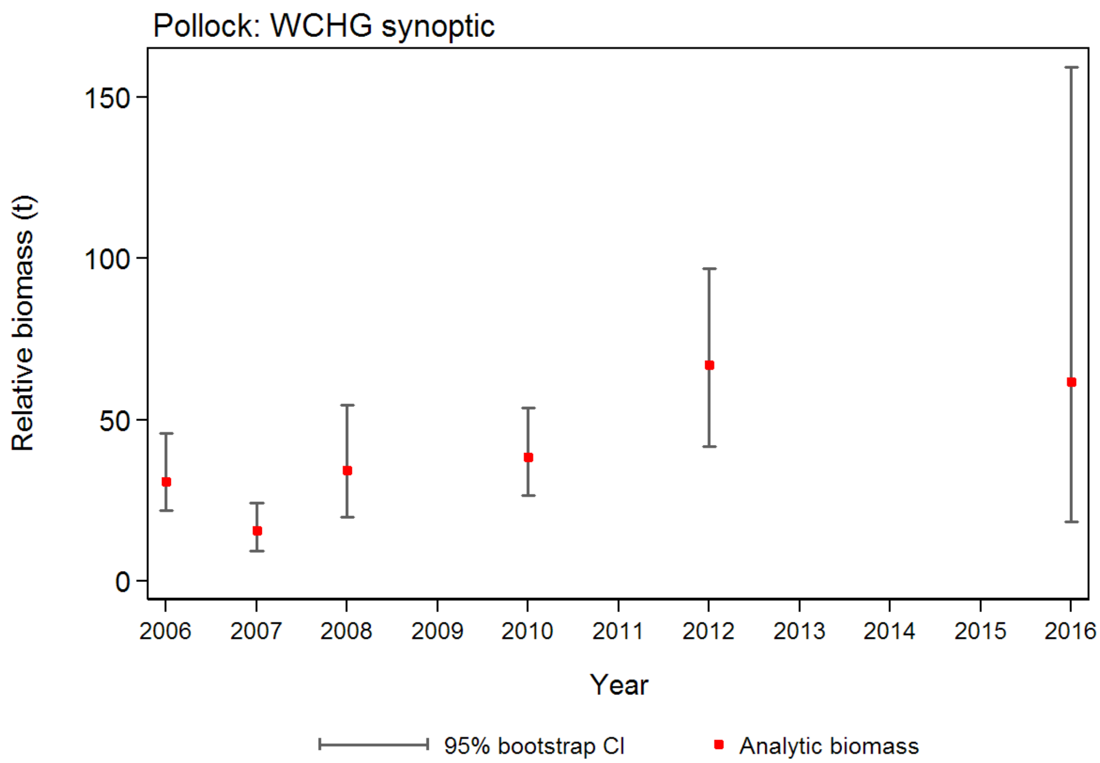

Figure B.63. Biomass estimates for Walleye Pollock from the six west coast Haida Gwaii synoptic surveys (Table B.18). Bias-corrected 95% confidence intervals from 1000 bootstrap replicates are plotted.

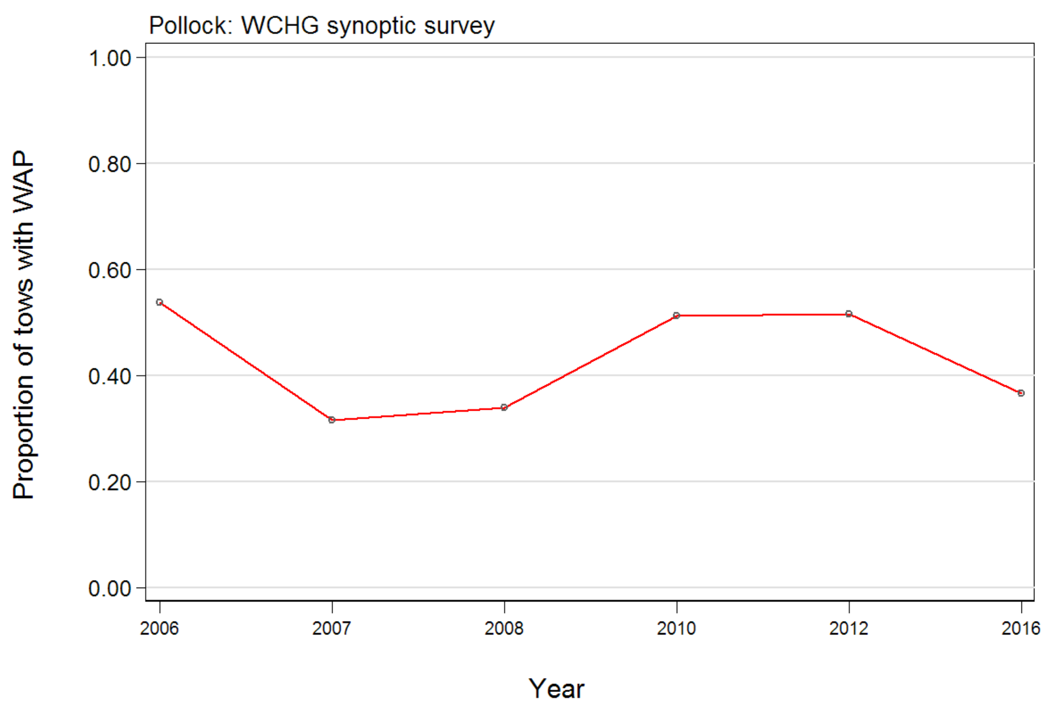

Figure B.64. Proportion of tows by year that contain Walleye Pollock for the six west coast Haida Gwaii synoptic surveys.

B.9. REFERENCES – SURVEYS

Edwards, A.M., Haigh, R. and Starr, P.J. 2014. Pacific Ocean Perch (*Sebastes alutus*) stock assessment for the west coast of Vancouver Island, British Columbia. DFO Can. Sci. Advis. Sec. Res. Doc. 2013/093. vi + 135 p.

Edwards, A.M., Starr, P.J. and Haigh, R. 2012. Stock assessment for Pacific ocean perch (*Sebastes alutus*) in Queen Charlotte Sound, British Columbia. DFO Can. Sci. Advis. Sec. Res. Doc. 2011/111. viii + 172 p.

Hand, C.M., Workman, G.D., Richards, L.J., Kieser, R. and Perry, R.I. 1995. Bottom trawl and exploratory hydroacoustic survey for rockfish in Queen Charlotte Sound, June 20 to July 7, 1994. Can. Manuscr. Rep. Fish. Aquat. Sci. 2300: iv + 87 pp.

Harling, W.R. and Davenport, D. 1977. *G.B. Reed* Groundfish Cruise No. 77-3 August 22 to September 8, 1977. Fish. Mar. Serv. Data Rep. 42: 46 pp.

Harling, W.R., Davenport, D., Smith, H.S., Wowchuk, R.H. and Westrheim, S.J. 1971. *G.B. Reed* Groundfish Cruise No. 71-3, October 1-29, 1971. Fish. Res. Board Can. Tech. Rep. 290: 35 pp.

Harling, W.R., Davenport, D., Smith, M.S., Phillips, A.C. and Westrheim, S.J. 1973. *G.B. Reed* Groundfish Cruise No. 73-2, September 5-25, 1973. Fish. Res. Board Can. Tech. Rep. 424: 37 pp.

Nagtegaal, D.A. and Farlinger, S.P. 1980. Catches and trawl locations of the M/V SOUTHWARD HO during a rockfish exploration and assessment cruise to Queen Charlotte Sound, September 7-27, 1979. Can. Data Rep. Fish. Aquat. Sci. 216: 95 pp.

Nagtegaal, D.A., Leaman, B.M. and Stanley, R.D. 1986. Catches and trawl locations of R/V *G.B. Reed* and M/V EASTWARD HO during the Pacific Ocean Perch assessment cruise to Queen Charlotte Sound, August-September, 1984. Can. Data Rep. Fish. Aquat. Sci. 611: 109 pp.

Olsen, N., Rutherford, K.L. and Stanley, R.D. 2008. West Coast Queen Charlotte Islands groundfish bottom trawl survey, August 25th to September 21st , 2008. Can. Manuscr. Rep. Fish. Aquat. Sci. 2858: vii + 50 p.

Sinclair, A. 1999. Survey design considerations for Pacific Cod in Hecate Strait. DFO Can. Sci. Advis. Sec. Res. Doc. 1999/196. 42 pp.

Westrheim, S.J. 1966a. Report on the trawling operations of the Canadian Research Vessel *G.B. Reed* from Queen Charlotte Sound, British Columbia to Cape Spencer, Alaska, August 23 to September 7, 1965. Fish. Res. Board Can. Manuscr. Rep. 890: 27 pp.

Westrheim, S.J. 1966b. Report on the trawling operations of the Canadian Research Vessel *G.B. Reed* from Queen Charlotte Sound, British Columbia to Sitka Sound, Alaska, August 24 to September 15, 1966. Fish. Res. Board Can. Manuscr. Rep. 891: 27 pp.

Westrheim, S.J. 1967a. Report on the trawling operations of the Canadian Research Vessel *G.B. Reed* off British Columbia and Southeastern Alaska, September 6 - October 4, 1967. Fish. Res. Board Can. Manuscr. Rep. 934: 8 pp.

Westrheim, S.J. 1967b. *G.B. Reed* groundfish cruise reports, 1963-66. Fish. Res. Board Can. Tech. Rep. 30: ii + 286 pp.

Westrheim, S.J. 1969. Report of the trawling operations of the Canadian Research Vessel *G.B. Reed* off British Columbia, September 1969. Fish. Res. Board Can. Manuscr. Rep. 1063: 6 pp.

Westrheim, S.J., Harling, W.R. and Davenport, D. 1968. *G.B. Reed* Groundfish Cruise No. 67-2, September 6 to October 4, 1967. Fish. Res. Board Can. Tech. Rep. 46: 45 pp.

Westrheim, S.J., Leaman, B.M., Harling, W.R., Davenport, D., Smith, M.S. and Wowchuk, R.M. 1976. *G.B. Reed* Groundfish Cruise No. 76-3, September 8-27, 1976. Fish. Mar. Serv. Data Rec. 21: 47 pp.

Workman, G.D., Olsen, N. and Rutherford, K.L. 2007. West Coast Queen Charlotte Islands groundfish bottom trawl survey, August 28th to September 25th , 2006. Can. Manuscr. Rep. Fish. Aquat. Sci. 2804: vii + 44 p.

Yamanaka, K.L., Richards, L.J. and Workman, G.D. 1996. Bottom trawl survey for rockfish in Queen Charlotte Sound, September 11 to 22, 1995. Can. Manuscr. Rep. Fish. Aquat. Sci. 2362: iv + 116 pp.

APPENDIX C. COMMERCIAL TRAWL CPUE

C.1. INTRODUCTION

Commercial catch and effort data have been used to generate indices of abundance in several ways. The simplest indices are derived from the arithmetic mean or geometric mean of catch divided by an appropriate measure of effort (Catch Per Unit Effort or CPUE) but such indices make no adjustments for changes in fishing practices or other non-abundance factors which may affect catch rates. Consequently, methods to standardise for changes to vessel configuration, the timing or location of catch and other possible effects have been developed to remove potential biases to CPUE that may result from such changes. In these models, abundance is represented as a “year effect” and the dependent variable is either an explicitly calculated CPUE represented as catch divided by effort, or an implicit CPUE represented as catch per tow or catch per record. In the latter case, additional effort terms can be offered as explanatory variables, allowing the model to select the effort term with the greatest explanatory power. It is always preferable to standardise for as many factors as possible when using CPUE as a proxy for abundance. Unfortunately, it is often not possible to adjust for factors that might affect the behaviour of fishers, particularly economic factors, resulting in indices that may not entirely reflect the underlying stock abundance.

C.2. METHODS

C.2.1. Arithmetic and Unstandardised CPUE

Arithmetic and unstandardised CPUE indices provide potential measures of relative abundance, but are generally considered unreliable because they fail to take into account changes in the fishery, including spatial and temporal changes as well as behavioural and gear changes. They are frequently calculated because they provide a measure of the overall effect of the standardisation procedure.

Arithmetic CPUE (A_y) in year y was calculated as the total catch for the year divided by the total effort in the year using Eq. C.1:

Eq. C.1 $$A_y = \sum_{i=1}^{n_y} C_{i,y} \Big/ \sum_{i=1}^{n_y} E_{i,y}$$

where $C_{i,y}$ is the [catch], $E_{i,y} = T_{i,y}$ ([*tows*]) or $E_{i,y} = H_{i,y}$ ([*hours_fished*]) for record i in year y, and n_y is the number of records in year y.

Unstandardised (geometric) CPUE assumes a log-normal error distribution. An unstandardised index of CPUE (G_y) in year y was calculated as the geometric mean of the ratio of catch to effort for each record i in year y, using Eq. C.2:

Eq. C.2 $$G_y = \exp\left[\sum_{i=1}^{n_y} \ln\left(\frac{C_{i,y}}{E_{i,y}} \right) \Big/ n_y \right]$$

where $C_{i,y}$, $E_{i,y}$ and n_y are as defined for Eq. C.1

C.2.2. Standardised CPUE

These models are preferred over the unstandardised models described above because they can account for changes in fishing behaviour and other factors which may affect the estimated abundance trend, as long as the models are provided with adequate data. In the models described below, catch per record is used as the dependent variable and the associated effort is treated as an explanatory variable.

C.2.2.1. Lognormal Model

Standardised CPUE assumes a lognormal error distribution, with explanatory variables used to represent changes in the fishery. A standardised CPUE index (Eq. C.3) is calculated from a generalised linear model (GLM) (Quinn and Deriso 1999) using a range of explanatory variables including [*year*], [*month*], [*depth*], [*vessel*] and other available factors:

Eq. C.3 $$\ln\left(I_i\right) = B + Y_{y_i} + \alpha_{a_i} + \beta_{b_i} + \ldots + f\left(\chi_i\right) + f\left(\delta_i\right) + \ldots + \varepsilon_i$$

where I_i = C_i or catch;

B = the intercept;

Y_{y_i} = year coefficient for the year corresponding to record i;

α_{a_i} and β_{b_i} = coefficients for factorial variables a and b corresponding to record i;

$f\left(\chi_i\right)$ and $f\left(\delta_i\right)$ are polynomial functions (to the 3rd order) of the continuous variables χ_i and δ_i corresponding to record i;

ε_i = an error term.

The actual number of factorial and continuous explanatory variables in each model depends on the model selection criteria. Because each record represents a single tow, C_i has an implicit associated effort of one tow. Hours fished for the tow is represented on the right-hand side of the equation, usually as a continuous (polynomial) variable.

Note that calculating standardised CPUE with Eq. C.3 without additional explanatory variables is equivalent to using Eq. C.2, provided the same definition for $E_{i,y}$ is used.

Canonical coefficients and standard errors were calculated for each categorical variable (Francis 1999). Standardised analyses typically set one of the coefficients to 1.0 without an error term and estimate the remaining coefficients and the associated error relative to the fixed coefficient. This is required because of parameter confounding. The Francis (1999) procedure rescales all coefficients so that the geometric mean of the coefficients is equal to 1.0 and calculates a standard error for each coefficient, including the fixed coefficient.

Coefficient-distribution-influence (CDI) plots are visual tools to facilitate understanding of patterns which may exist in the combination of coefficient values, distributional changes, and annual influence (Bentley et al. 2012). CDI plots were used to illustrate each explanatory variable added to the model.

C.2.2.2. Binomial Logit Model

The procedure described by Eq. C.3 is necessarily confined to the positive catch observations in the data set because the logarithm of zero is undefined. Observations with zero catch were modelled by fitting a logit regression model based on a binomial distribution and using the presence/absence of Walleye Pollock as the dependent variable (where 1 is substituted for

$\ln(I_i)$ in Eq. C.3 if it is a successful catch record and 0 if it is not successful) and using the same data set. Explanatory factors are estimated in the model in the same manner as described in Eq. C.3. Such a model provides an alternative series of standardised coefficients of relative annual changes that is analogous to the series estimated from the lognormal regression.

C.2.2.3. Combined Model

A combined model, integrating the two sets of relative annual changes estimated by the lognormal and binomial models, can be estimated using the delta distribution, which allows zero and positive observations (Vignaux 1994). Such a model provides a single index of abundance which integrates the signals from the positive (lognormal) and binomial series. This approach uses the following equation to calculate an index based on the two contributing indices:

Eq. C.4 $$^{C}Y_y = {^{L}Y_y} \bigg/ \left(1 - P_0\left[1 - \frac{1}{^{B}Y_y}\right]\right)$$

where $^{C}Y_y$ = combined index for year y,

$^{L}Y_y$ = lognormal index for year y,

$^{B}Y_y$ = binomial index for year y, and

P_0 = proportion zero for base year 0.

Francis (2001) suggests that a bootstrap procedure is the appropriate way to estimate the variability of the combined index. Therefore, confidence bounds for the combined model were estimated using a bootstrap procedure based on 500 replicates, drawn with replacement.

The index series plots below present normalised values, i.e., each series is divided by its geometric mean so that the series is centred on 1. This facilitates comparison among series.

C.3. PRELIMINARY INSPECTION OF THE DATA

The analyses reported in this Appendix is based on tow-by-tow total catch (landings + discards) data collected over the period 1996–2015 for which detailed positional data for every tow are available and there is an estimate of discarded catch for the tow because of the presence of an observer on board the vessel. These data are held in the DFO PacHarvTrawl (PacHarvest) and GFFOS databases (Fisheries and Oceans Canada, Pacific Region, Groundfish Data Unit).

Tow-by-tow catch and effort data for Walleye Pollock (WAP) from the BC trawl fishery operating from Juan de Fuca Strait to the Dixon Entrance from 1996 to 2015 were selected using the following criteria:

- Tow start date between 1 January 1996 and 31 December 2015;
- Bottom trawl type (includes ‘unknown’ gear) or Midwater trawl type (includes ‘unspecified trawl’ for vessels fishing in the ‘HAKE’ fishing sector);
- Fished in PMFC regions: 3C, 3D, 4B, 5A, 5B, 5C, 5D or 5E;
- Fishing success code <=1 (code 0= unknown; code 1= useable);
- Catch of at least one fish or invertebrate species (no water hauls or inanimate object tows);
- Valid depth field;

- Valid latitude and longitude co-ordinates;
- Valid estimate of time towed that was > 0 hours and <= 24 hours.

Each record represents a single tow, which results in equivalency between the number of records and number of tows. Catch per record can therefore be used to represent CPUE, because each record (tow) has an implicit effort component.

The catch and effort data for WAP were sub-divided into two areas (BC North and BC South) based on the localised distribution of midwater trawl catches (see Appendix A). The data were further sub-divided into two gear types for each area: midwater trawl and bottom trawl, on the premise that fishing for this species will differ, with the midwater fishery largely targeting WAP while the bottom trawl fishery catches WAP while targeting other species (Thompson 1981). Furthermore, the catch rates for the two gear types differ greatly and it would be inappropriate to combine the two capture methods in a single analysis.

Figure C.1 plots the distribution of depth for all successful WAP tows for each of two areas and two gear types per area. A depth range for each analysis was selected from these plots and are summarised in Table C.1.

Table C.1. Depth bins used in CPUE analyses of stock by gear.

Analysis	Gear	First year	Depth range (m)	Upper bound effort (h)	Minimum bin records	N depth bins	N latitude bins	N locality bins
Area 5CDE	Midwater trawl	1996	50–550	10	35	20	5	9
	Bottom trawl	1996	50–450	8	150	16	18	15
Area 3CD5AB + Minors 12&20	Midwater trawl	2003	50-450	10	30	16	16	25
	Bottom trawl	1996	50–400	8	75	14	28	31

Vessel qualification criteria for the bottom trawl fisheries were based on number of trips per year and number of years fishing to avoid including vessels which only occasionally captured Walleye Pollock. However, this was not possible to do for the equivalent midwater trawl fisheries because of the small number of participating vessels and the relatively small amount of available catch information (see table below). For the 5CDE fishery, only two midwater trawl vessels provided data in 2014 and there were only four in 2015 ([upper left panel] Figure C.2). Vessel numbers are higher for the southern fishery, but the overlap of vessels over time is poor in this fishery ([lower left panel] Figure C.2). Consequently the [vessel] explanatory variable was not offered to the midwater models. The vessel qualification criteria used in each analysis appear in Table C.2 and the distribution of tows by vessel and fishery is presented in Figure C.2. Once a vessel was selected, all data for the qualifying vessel were included, regardless of the number of trips in a year. All vessels were included (i.e., no year restriction) in the 5CDE and 5AB3CD analyses but [vessel] was not selected as a categorical explanatory variable in these analyses.

Table C.2. Vessel qualification criteria used in CPUE analyses of stock by gear.

		Vessel selection criteria			Data set characteristics				
Analysis	Trawl Gear	N years	N trips	Minimum Records	N vessels	% catch	catch (t)	Total records	Positive records
Area 5CDE	Midwater	NA	NA	NA	NA	100	12,218	2,771	1,722
	Bottom	4	4	0	22	82	2,347	54,836	16,344
Area 3CD5AB +Minors12&20	Midwater	NA	NA	NA	NA	100	27,448	25,139	3,492
	Bottom	5	5	100	40	77	1,317	125,538	16,393

Table C.2 shows the number of vessels used in each analysis and the fraction of the total catch represented in each core fleet. There were considerably more vessels participating in the bottom trawl analyses, with good vessel overlap across years ([right column] Figure C.2). Table C.3 reports the explanatory variables offered to the models, based on the tow-by-tow information in each record, with the number of available categories varying as indicated in Table C.1 and Table C.2Table C.4, Table C.5, Table C.6, and Table C.7 summarise the data used in each analysis by calendar year, including the number of records, the total hours fished and the associated WAP catch.

Table C.3. Explanatory variables offered to the CPUE model, based on the tow-by-tow information.

Variable	Data type
Year	20 categories (calendar years)
Hours_fished	continuous: 3rd order polynomial
Month	12 categories
DFO_locality	Fishing locality areas identified by Rutherford (1995) (includes a final aggregated category)
Latitude_bands	Latitude aggregated by 0.1° bands starting at 48°N (includes a final aggregated category)
Vessel	See Table C.2 for number of categories by analysis (no final aggregated category)
Depth_bands	See Table C.1 for number of categories by analysis (no final aggregated category)

Table C.4. Summary data for the Walleye Pollock midwater trawl fishery in 5CDE by year for the core data set (after applying all data filters).

Year	Number vessels[1]	Number trips[1]	Number tows[1]	Number records[1]	Number records[2]	% zero records[2]	Total catch (t)[1]	Total hours[1]	CPUE (kg/h) (Eq. C.1)
1996	18	37	94	94	131	28.2	156.5	281	557.1
1997	10	20	54	54	60	10.0	395.8	162	2,445.7
1998	7	12	49	49	59	16.9	238.8	135	1,765.1
1999	10	24	85	85	95	10.5	617.5	284	2,170.8
2000	6	8	43	43	59	27.1	258.0	138	1,867.8
2001	6	11	28	28	144	80.6	56.7	115	492.2
2002	7	14	38	38	145	73.8	20.1	97	208.4
2003	7	16	60	60	140	57.1	566.8	201	2,824.5
2004	5	26	112	112	185	39.5	920.8	321	2,868.3
2005	6	11	90	90	151	40.4	127.5	151	844.8
2006	6	23	90	90	147	38.8	440.1	267	1,648.1
2007	8	45	230	230	341	32.6	1,172.4	765	1,533.5
2008	10	25	115	115	266	56.8	286.2	275	1,041.4
2009	6	24	116	116	181	35.9	1,238.5	402	3,084.0
2010	5	25	153	153	205	25.4	1,627.9	488	3,338.6
2011	5	17	70	70	106	34.0	742.1	222	3,338.9
2012	5	18	82	82	95	13.7	1,033.1	307	3,366.9
2013	5	15	76	76	88	13.6	705.5	320	2,206.2
2014	3	10	42	42	59	28.8	470.7	182	2,588.2
2015	4	16	95	95	114	16.7	1,143.2	352	3,251.2

[1] calculated for tows with Walleye Pollock catch >0
[2] calculated for all tows

Table C.5. Summary data for the Walleye Pollock bottom trawl fishery in 5CDE by year for the core data set (after applying all data filters and selection of core vessels).

Year	Number vessels[1]	Number trips[1]	Number tows[1]	Number records[1]	Number records[2]	% zero records[2]	Total catch (t)[1]	Total hours[1]	CPUE (kg/h) (Eq. C.1)
1996	20	139	1,091	1,091	2,434	55.2	388.4	2,407	161.4
1997	19	162	909	909	2,538	64.2	131.9	1,870	70.5
1998	18	189	1,002	1,002	3,520	71.5	122.2	2,195	55.7
1999	20	221	1,299	1,299	3,908	66.8	177.7	2,736	64.9
2000	19	189	926	926	4,202	78.0	121.2	2,010	60.3
2001	20	163	837	837	3,310	74.7	56.3	1,831	30.8
2002	19	176	988	988	3,593	72.5	60.1	1,764	34.1
2003	17	158	730	730	2,851	74.4	29.2	1,334	21.9
2004	17	185	838	838	3,152	73.4	89.2	1,539	57.9
2005	17	228	1,092	1,092	3,206	65.9	344.9	1,803	191.3
2006	15	157	763	763	2,493	69.4	65.7	1,584	41.5
2007	15	123	578	578	2,106	72.6	65.4	1,076	60.8
2008	13	129	587	587	2,151	72.7	62.1	1,036	60.0
2009	14	107	407	407	2,465	83.5	75.5	746	101.2
2010	12	122	473	473	2,265	79.1	49.9	873	57.1
2011	13	168	829	829	2,474	66.5	88.5	1,419	62.3
2012	11	139	916	916	2,359	61.2	93.1	1,604	58.0
2013	12	146	841	841	2,409	65.1	112.9	1,628	69.4
2014	10	129	686	686	1,721	60.1	81.2	1,364	59.6
2015	10	107	552	552	1,679	67.1	131.9	932	141.5

[1] calculated for tows with Walleye Pollock catch >0
[2] calculated for all tows

Table C.6. Summary data for the Walleye Pollock midwater trawl fishery in 3CD5AB+Minor Areas 12&20 by year for the core data set (after applying all data filters, including vessel filter).

Year	Number vessels[1]	Number trips[1]	Number tows[1]	Number records[1]	Number records[2]	% zero records[2]	Total catch (t)[1]	Total hours[1]	CPUE (kg/h) (Eq. C.1)
2003	35	110	293	293	1,135	74.2	1,772.1	753	2,354.7
2004	22	42	100	100	818	87.8	611.3	254	2,408.4
2005	26	59	417	417	1,431	70.9	828.6	1,015	816.4
2006	16	64	578	578	1,675	65.5	2,444.8	1,502	1,628.1
2007	20	56	358	358	2,591	86.2	1,980.0	1,024	1,933.8
2008	12	35	143	143	2,669	94.6	1,050.5	571	1,840.4
2009	18	58	266	266	2,099	87.3	2,186.8	672	3,255.1
2010	9	37	179	179	2,125	91.6	1,832.0	839	2,184.8
2011	18	58	228	228	2,123	89.3	2,835.3	737	3,846.4
2012	17	54	224	224	2,115	89.4	2,772.2	644	4,302.8
2013	14	37	116	116	2,319	95.0	1,433.3	418	3,427.2
2014	23	101	338	338	2,125	84.1	5,557.0	1,008	5,514.1
2015	21	75	252	252	1,914	86.8	2,143.9	528	4,059.4

[1] calculated for tows with Walleye Pollock catch >0
[2] calculated for all tows

Table C.7. *Summary data for the Walleye Pollock bottom trawl fishery in 3CD5AB+Minor Areas 12&20 by year for the core data set (after applying all data filters and selection of core vessels).*

Year	Number vessels[1]	Number trips[1]	Number tows[1]	Number records[1]	Number records[2]	% zero records[2]	Total catch (t)[1]	Total hours[1]	CPUE (kg/h) (Eq. C.1)
1996	34	102	237	237	4,111	94.2	81.8	626	130.5
1997	36	238	988	988	5,157	80.8	68.9	2,294	30.0
1998	36	253	969	969	5,885	83.5	40.9	2,297	17.8
1999	36	310	1,041	1,041	6,892	84.9	33.3	2,539	13.1
2000	37	311	958	958	8,407	88.6	34.1	2,128	16.0
2001	37	273	728	728	7,825	90.7	93.2	1,430	65.2
2002	37	276	834	834	8,983	90.7	55.1	1,763	31.3
2003	37	313	856	856	9,054	90.5	55.0	1,677	32.8
2004	37	340	1,057	1,057	8,424	87.5	38.9	2,340	16.6
2005	35	319	1,128	1,128	8,462	86.7	68.9	2,474	27.8
2006	29	260	963	963	6,871	86.0	42.1	2,318	18.1
2007	29	221	852	852	5,871	85.5	62.9	2,068	30.4
2008	27	163	479	479	4,834	90.1	11.3	1,117	10.1
2009	27	208	602	602	5,685	89.4	28.2	1,340	21.1
2010	25	227	762	762	5,925	87.1	50.7	1,914	26.5
2011	25	198	780	780	5,709	86.3	86.3	1,892	45.6
2012	26	205	713	713	4,719	84.9	47.9	1,610	29.8
2013	22	189	691	691	4,529	84.7	45.5	1,603	28.4
2014	22	202	750	750	4,077	81.6	285.5	1,699	168.1
2015	21	219	1,005	1,005	4,118	75.6	86.1	2,240	38.4

[1] calculated for tows with Walleye Pollock catch >0; [2] calculated for all tows

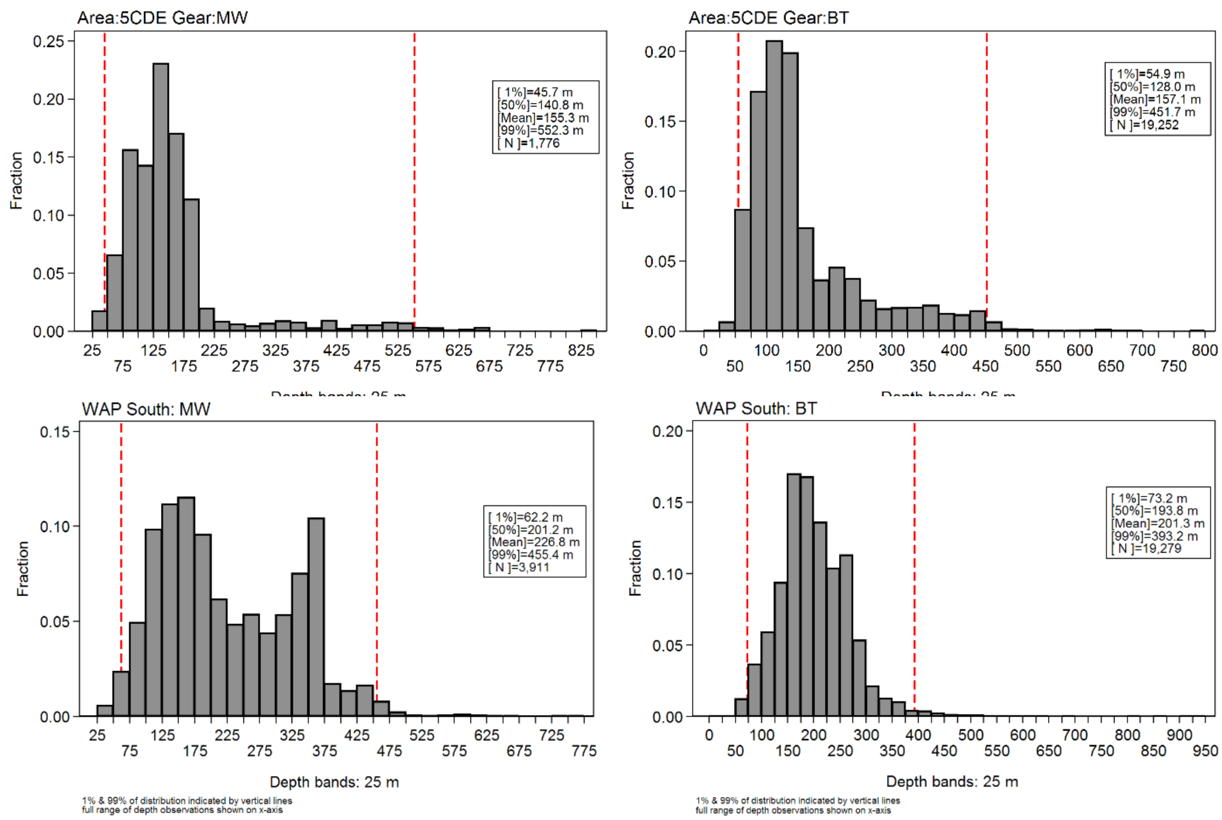

Figure C.1. Depth distribution of tows capturing WAP for the four GLM analyses from 1996 to 2015 using 25m intervals (each bin is labelled with the upper bound of the interval). Vertical lines indicate the 1% and 99% quantiles.

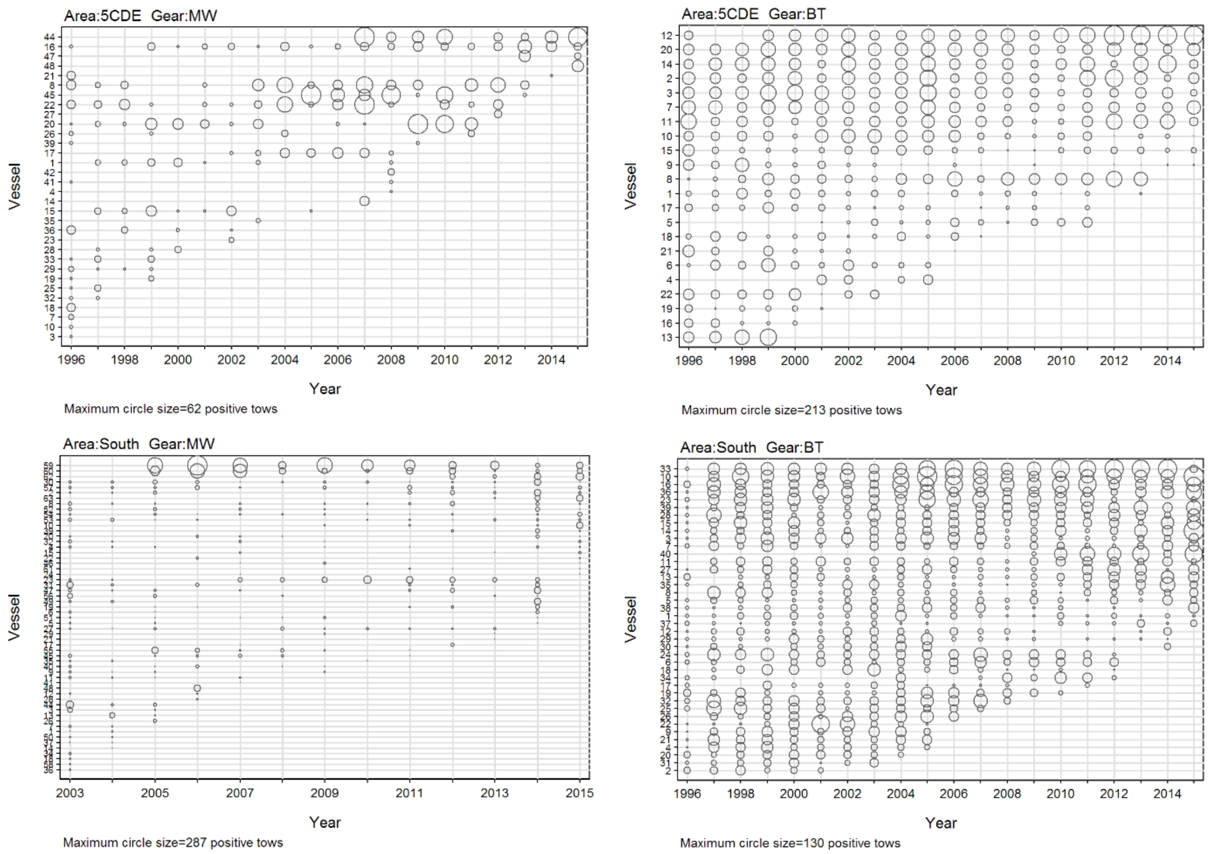

Figure C.2. Bubble plot showing vessel participation (number tows) by the core fleets in the four GLM analyses. Vessels are coded in ascending order total catch by year.

C.4. RESULTS

C.4.1. Areas 5CDE (North)

C.4.1.1. Midwater trawl fishery

A standardised lognormal General Linear Model (GLM) analysis was performed on positive catch records from the midwater trawl tow-by-tow data set generated as described in Section C.3. Six explanatory variables (described in Section C.3 above) were offered to the model and *ln(catch)* was used as the dependent variable, where catch is the total by weight of landed plus discarded Walleye Pollock in each record (tow) (Eq. C.3). The resulting CPUE index series is presented in Figure C.3.

The **[Year]** categorical variable was forced as the first variable in the model without regard to its effect on the model deviance. The remaining five variables were offered sequentially, with a stepwise acceptance of the remaining variables with the best AIC. This process was continued until the improvement in the model R^2 was less than 1% (Table C.8). This model selected three of the five remaining explanatory variables, including **[DFO_locality]**, **[Month]**, and **[Hours_fished]** in addition to **[Year]**. The final lognormal model accounted for 61% of the total model deviance (Table C.8), with the year variable explaining 28% of the model deviance.

Model residuals do not fit the underlying lognormal distributional assumption very well, with deviations at the tails and in the body of the residual distribution (Figure C.4).

A stepwise plot showing the effect on the year indices as each explanatory variable was introduced into the model shows that the standardisation procedure brought down the unstandardised year indices from peaks observed in 1997, 1999, 2004, 2010, 2012 and 2015 (Figure C.5).

CDI plots of the three explanatory variables introduced to the model in addition to **[Year]** show a strong standardisation effect with the addition of the **[DFO_locality]** variable (Figure C.6). Unfortunately, two locations, which have no previous history in the model, dominate in 2014 and 2015. This means that these location coefficients will be poorly estimated and confounded with the year effect. The variables **[Month]** (Figure C.7) and **[Hours_fished]** (Figure C.8) show high annual variability, with strong shifts in the resulting indices. This is evidence of poor consistency in the underlying data.

The year indices show a rising index from the mid- to late-2000s (Figure C.3) but this model has poor residual diagnostics, strong abrupt annual shifts in data and is consequently not reliable.

*Table C.8. Order of acceptance of variables into the lognormal model of positive total mortalities (verified landings plus discards) of Walleye Pollock 5CDE midwater trawl fishery with the amount of explained deviance (R^2) for each variable. Variables accepted into the model are marked in bold with an *. Year was forced as the first variable and vessel was not offered to this model.*

Variable	1	2	3	4	5
Year*	**0.2846**	-	-	-	-
DFO_locality*	0.4278	**0.5313**	-	-	-
Month*	0.2004	0.4082	**0.5887**	-	-
Hours_fished*	0.1463	0.3380	0.5611	**0.6065**	-
Latitude_bands	0.1003	0.3731	0.5344	0.5906	0.6087
Depth_bands	0.0466	0.3094	0.5377	0.5944	0.6115
Improvement in deviance	0	0.2467	0.0574	0.0178	0.0022

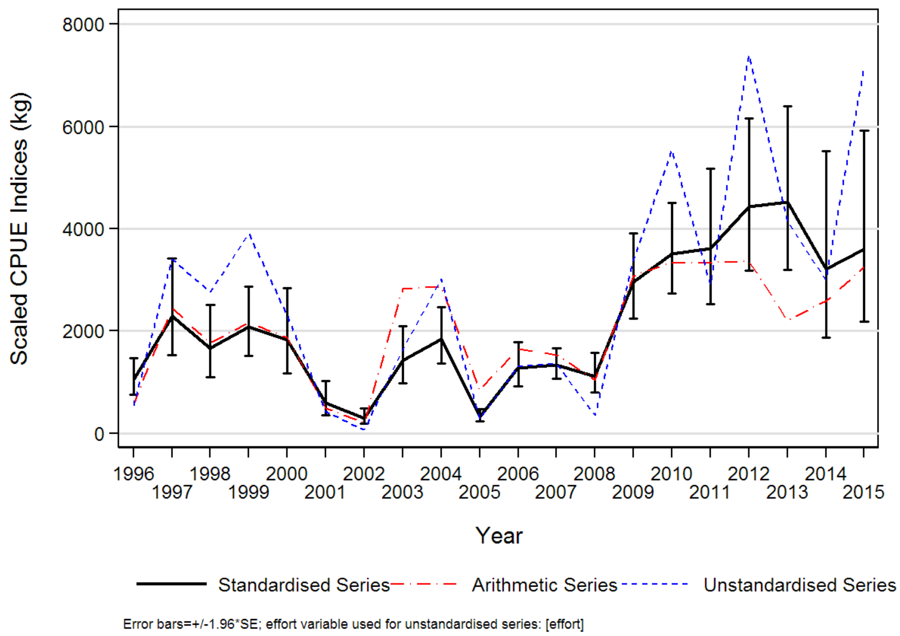

Figure C.3. Three CPUE series for WAP from 1996 to 2015 in 5CDE midwater trawl fishery. The solid line is the standardised CPUE series from the lognormal model (Eq. C.3). The arithmetic (Eq. C.1) and the unstandardised series (Eq. C.2) are also presented. All series are scaled to same geometric mean.

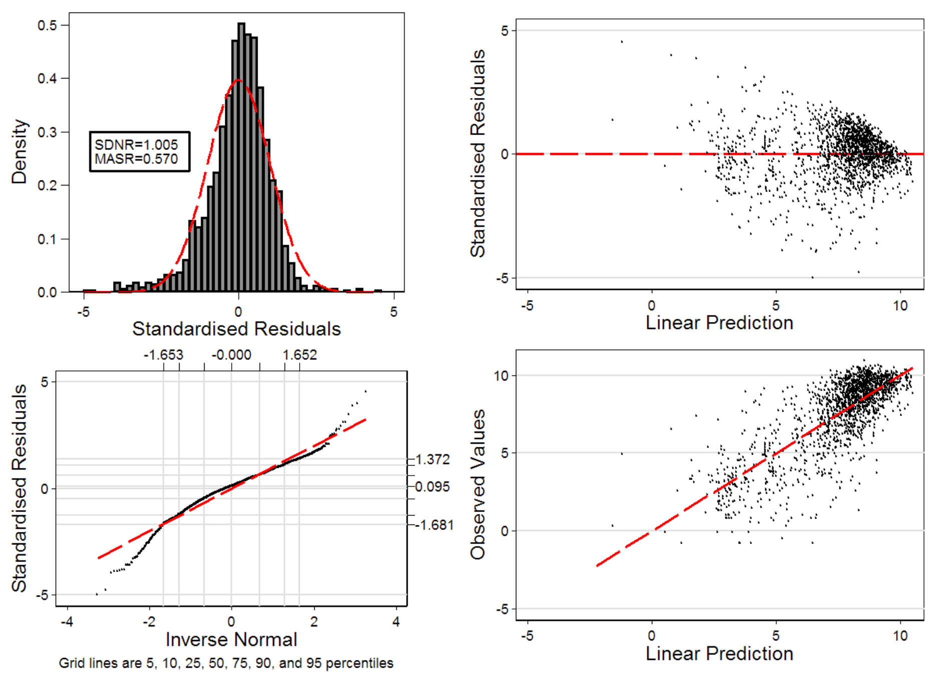

Figure C.4. Residual diagnostic plots for the GLM lognormal analysis for Walleye Pollock in 5CDE midwater trawl fishery. Upper left: histogram of the standardised residuals with overlaid lognormal distribution (SDNR = standard deviation of normalised residuals. MASR = median of absolute standardised residuals). Lower left: Q-Q plot of the standardised residuals with the outside horizontal and vertical lines representing the 5th and 95th percentiles of the theoretical and observed distributions. Upper right: standardised residuals plotted against the predicted CPUE. Lower right: observed CPUE plotted against the predicted CPUE.

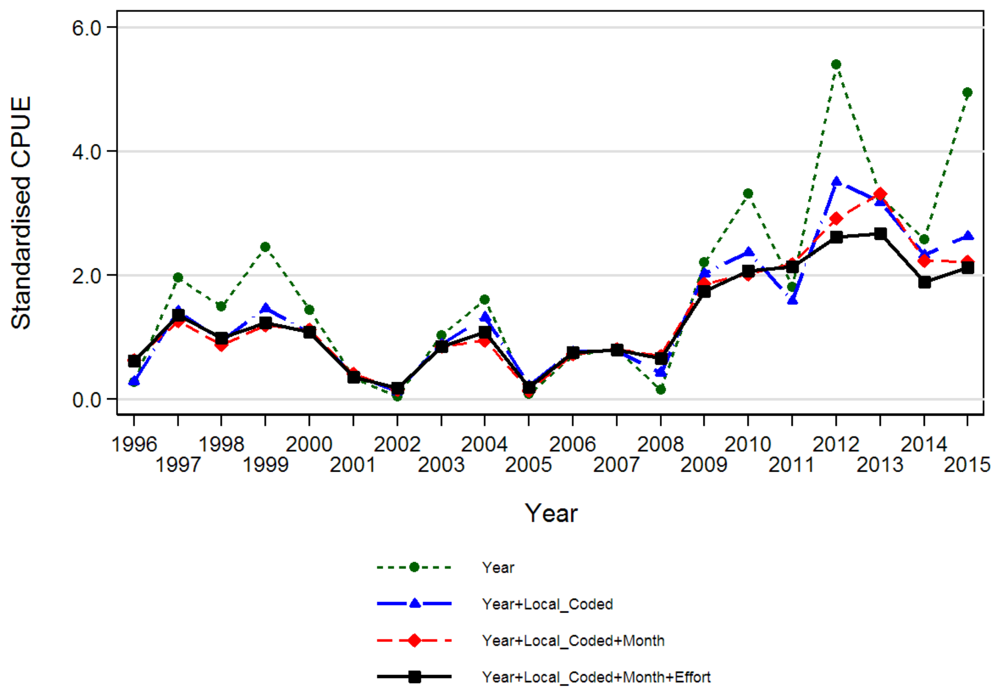

Figure C.5. Plot showing the year coefficients after adding each successive term of the standardised lognormal regression analysis for Walleye Pollock in the 5CDE midwater trawl fishery. The final model is shown with a thick solid black line. Each line has been scaled so that the geometric mean equals 1.0.

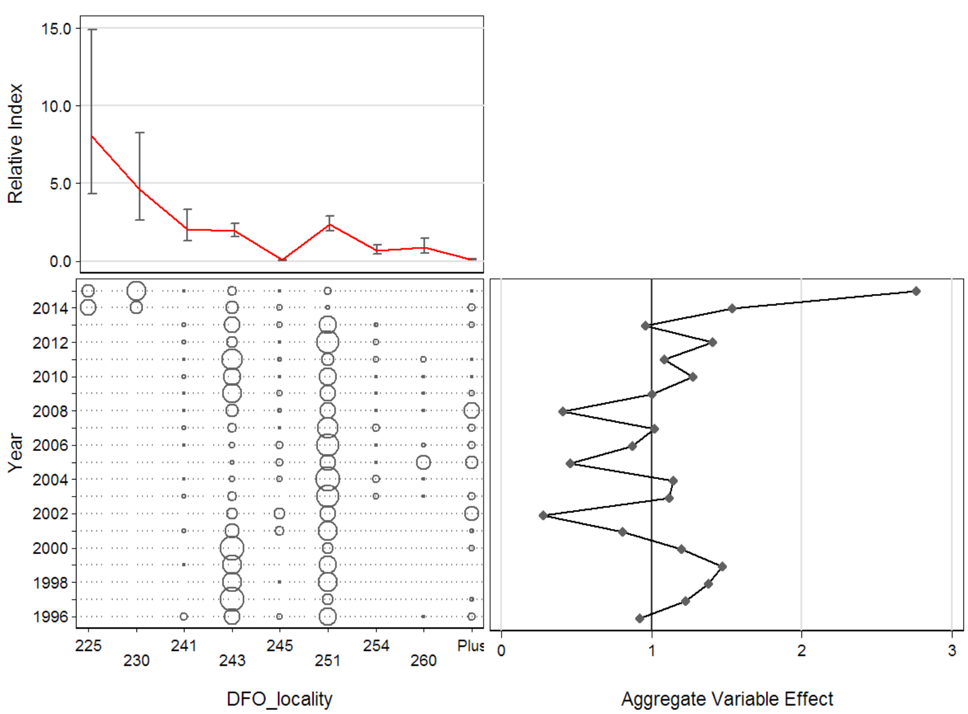

Figure C.6. CDI plot showing the effect of introducing the categorical variable [DFO_locality] to the lognormal regression model for Walleye Pollock in the 5CDE midwater trawl fishery. Each plot consists of subplots showing the effect by level of variable (top left), the relative distribution by year of variable records (bottom left), and the cumulative effect of variable by year (bottom right).

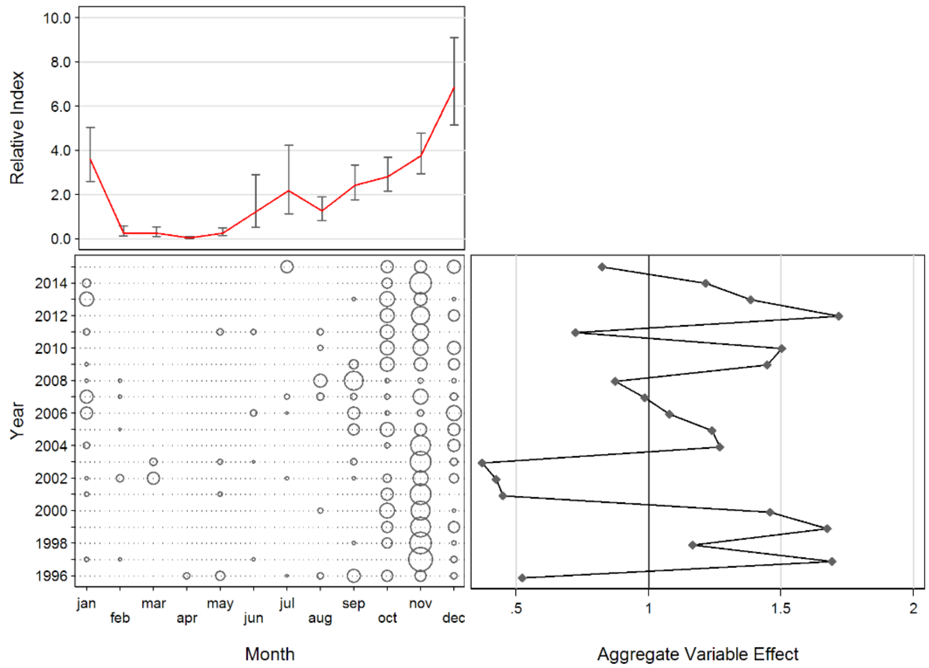

Figure C.7. CDI plot showing the effect of introducing the categorical variable [Month] to the lognormal regression model for Walleye Pollock in the 5CDE midwater trawl fishery. Each plot consists of subplots showing the effect by level of variable (top left), the relative distribution of variable records by year (bottom left), and the cumulative effect of variable by year (bottom right).

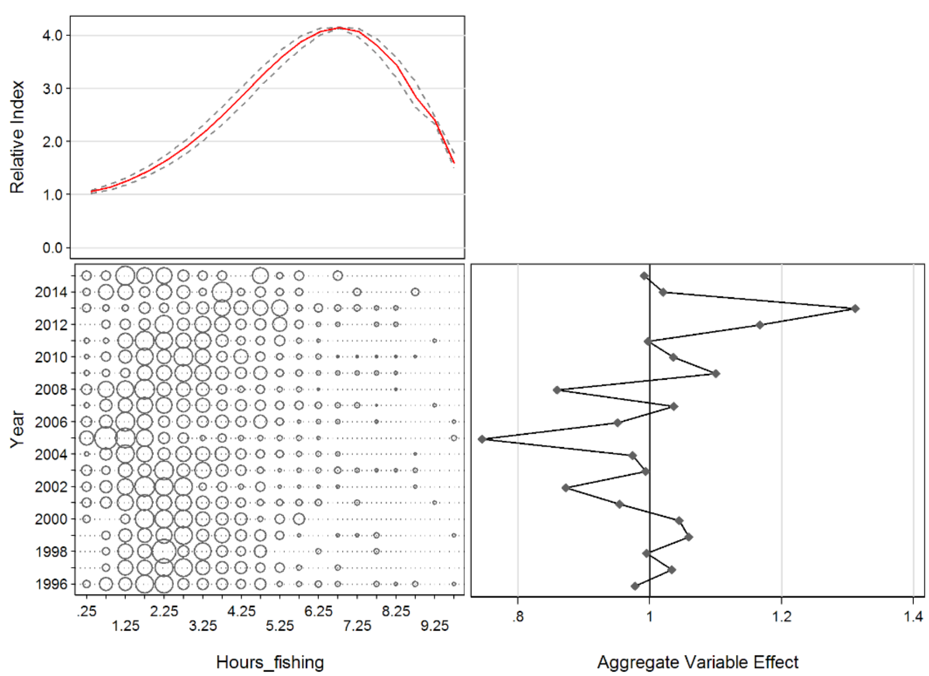

Figure C.8. CDI plot showing the effect of introducing the continuous variable [Hours_fished] to the lognormal regression model for Walleye Pollock in the 5CDE midwater trawl fishery. Each plot consists of subplots showing the effect by level of variable (top left), the relative distribution by year of variable records (bottom left), and the cumulative effect of variable by year (bottom right).

C.4.1.2. Bottom trawl fishery: positive lognormal model

A standardised lognormal General Linear Model (GLM) analysis was performed on positive catch records from the bottom trawl tow-by-tow data set generated as described in Section C.3. Seven explanatory variables (described in Section C.3 above) were offered to the model and *ln(catch)* was used as the dependent variable, where catch is the total by weight of landed plus discarded Walleye Pollock in each record (tow) (Eq. C.3). The resulting CPUE index series is presented in Figure C.9.

The **[Year]** categorical variable was forced as the first variable in the model without regard to its effect on the model deviance. The remaining six variables were offered sequentially, with a stepwise acceptance of the remaining variables with the best AIC. This process was continued until the improvement in the model R^2 was less than 1% (Table C.9). This model selected all six of the remaining explanatory variables, including **[DFO_locality]**, **[Depth_bands]**, **[Month]**, **[Vessel]**, **[Hours_fished]** and **[Latitude_bands]** in addition to **[Year]**. The final lognormal model accounted for 29% of the total model deviance (Table C.9), with the year variable explaining 5% of the model deviance.

Model residuals show an excellent fit with the underlying lognormal distributional assumption, with no deviation at the tails or in the body of the residual distribution (Figure C.10).

A stepwise plot showing the effect on the year indices as each explanatory variable was introduced into the model shows that the standardisation procedure did not modify the underlying annual indices, except for a small drop at the beginning of the series (Figure C.11). This is indicative of stability in the underlying data, with few annual shifts.

CDI plots of the six explanatory variables introduced to the model in addition to **[Year]** show a strong standardisation effect at the beginning of the series with the addition of **[DFO_locality]** variable (Figure C.12). There is a trend in the standardisation effect from the addition of the **[Depth_bands]** variable (Figure C.13), but the effect is relatively small. The variables **[Month]** (Figure C.14), **[Vesssel]** (Figure C.15), **[Hours_fished]** (Figure C.16) and **[Latitude_bands]** (Figure C.17) all show some standardisation effects, but the overall model impact is small.

The year indices show a decline at the beginning of the series, followed by no change to 2015 (Figure C.9). This model has excellent diagnostics and shows little change from the unstandardised series.

*Table C.9. Order of acceptance of variables into the lognormal model of positive total mortalities (verified landings plus discards) of Walleye Pollock 5CDE bottom trawl fishery with the amount of explained deviance (R^2) for each variable. Variables accepted into the model are marked in bold with an *. Year was forced as the first variable.*

Variable	1	2	3	4	5	6	7
Year*	**0.0519**	-	-	-	-	-	-
DFO_locality*	0.1237	**0.1774**	-	-	-	-	-
Depth_bands*	0.0635	0.1114	**0.2147**	-	-	-	-
Month*	0.0504	0.1018	0.2048	**0.2474**	-	-	-
Vessel*	0.0225	0.0746	0.2043	0.2383	**0.2692**	-	-
Hours_fished*	0.0137	0.0630	0.1946	0.2304	0.2623	**0.2810**	-
Latitude_bands*	0.1211	0.1710	0.2013	0.2291	0.2634	0.2820	**0.2945**
Improvement in deviance	0	0.1255	0.0373	0.0327	0.0218	0.0118	0.0134

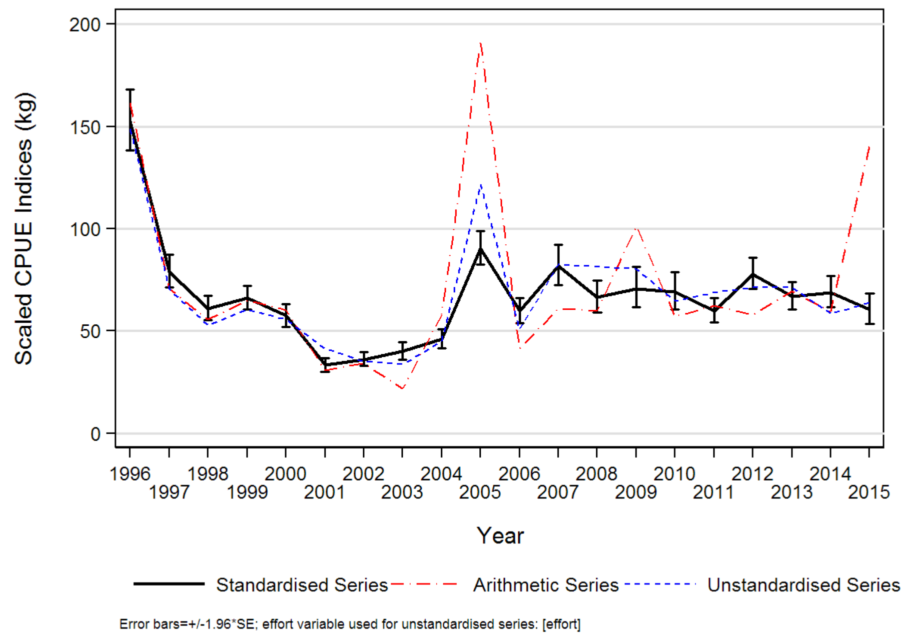

Figure C.9. Three CPUE series for Walleye Pollock from 1996 to 2015 in 5CDE bottom trawl fishery. The solid line is the standardised CPUE series from the lognormal model (Eq. C.3). The arithmetic series (Eq. C.1) and the unstandardised series (Eq. C.2) are also presented. All three series have been scaled to same geometric mean.

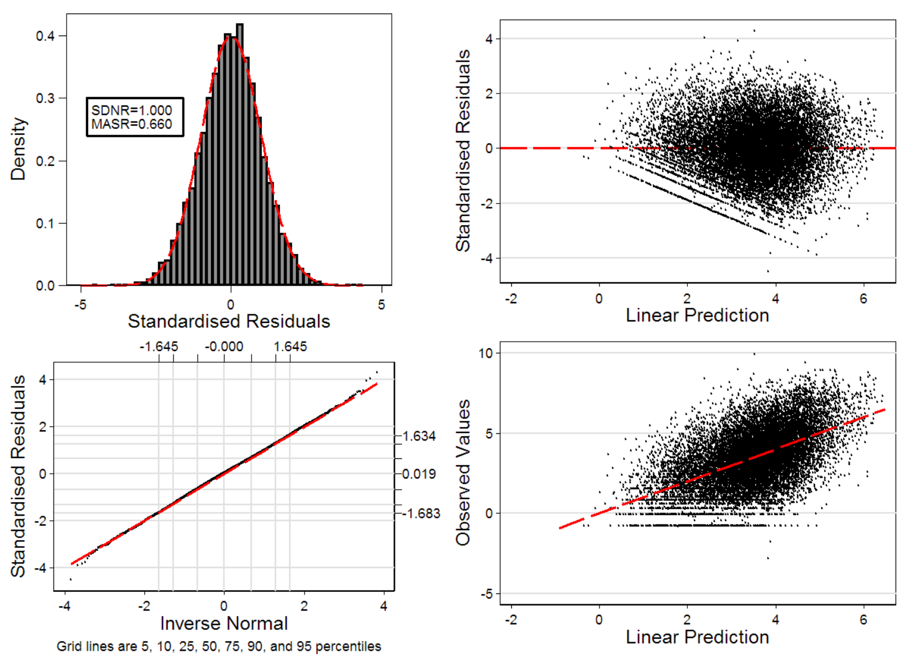

Figure C.10. Residual diagnostic plots for the GLM lognormal analysis for Walleye Pollock in 5CDE bottom trawl fishery. Upper left: histogram of the standardised residuals with overlaid lognormal distribution (SDNR = standard deviation of normalised residuals. MASR = median of absolute standardised residuals). Lower left: Q-Q plot of the standardised residuals with the outside horizontal and vertical lines representing the 5th and 95th percentiles of the theoretical and observed distributions. Upper right: standardised residuals plotted against the predicted CPUE. Lower right: observed CPUE plotted against the predicted CPUE.

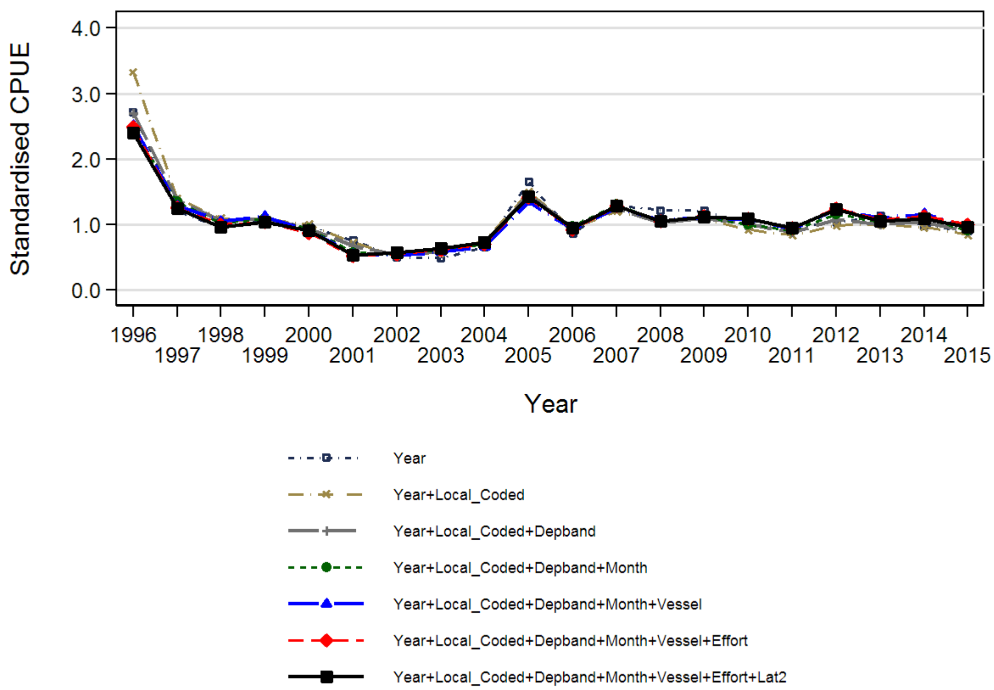

Figure C.11. Plot showing the year coefficients after adding each successive term of the standardised lognormal regression analysis for Walleye Pollock in the 5CDE bottom trawl fishery. The final model is shown with a thick solid black line. Each line has been scaled so that the geometric mean equals 1.0.

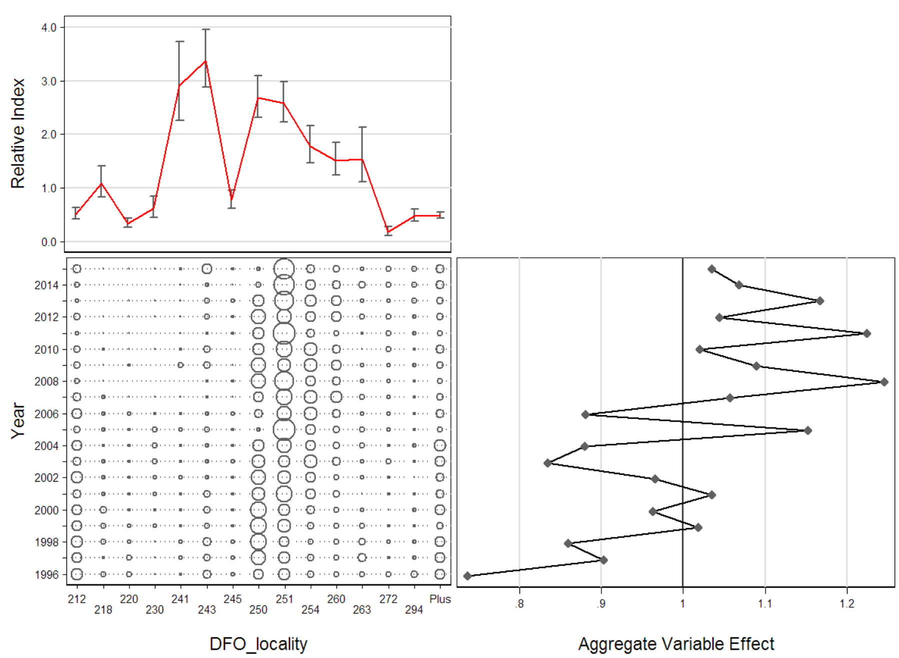

Figure C.12. CDI plot showing the effect of introducing the categorical variable [DFO_locality] to the lognormal regression model for Walleye Pollock in the 5CDE bottom trawl fishery. Each plot consists of subplots showing the effect by level of variable (top left), the relative distribution by year of variable records (bottom left), and the cumulative effect of variable by year (bottom right).

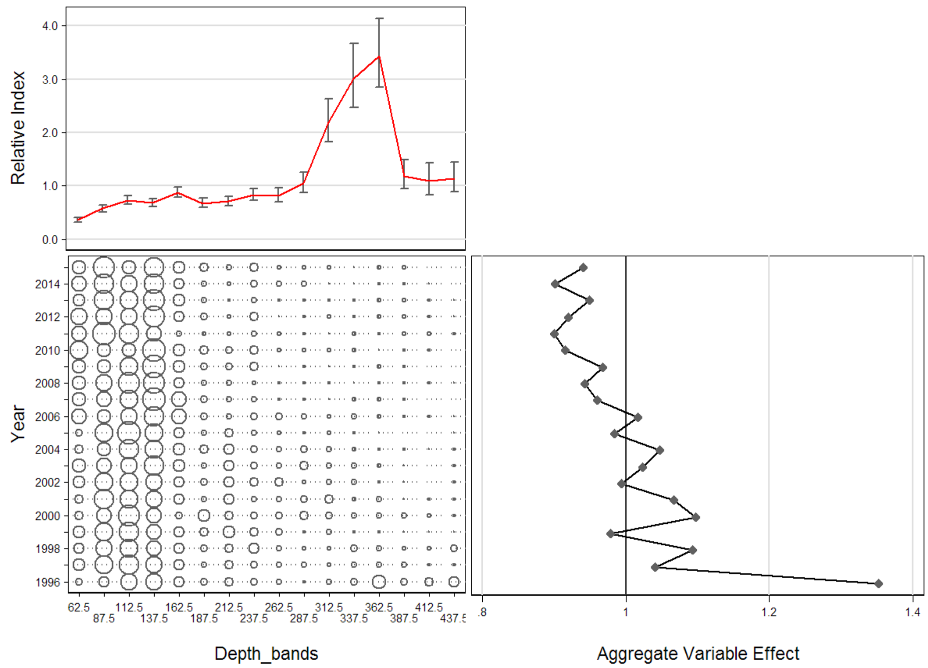

Figure C.13. CDI plot showing the effect of introducing the categorical variable [Depth_bands] to the lognormal regression model for Walleye Pollock in the 5CDE bottom trawl fishery. Each plot consists of subplots showing the effect by level of variable (top left), the relative distribution of variable records by year (bottom left), and the cumulative effect of variable by year (bottom right).

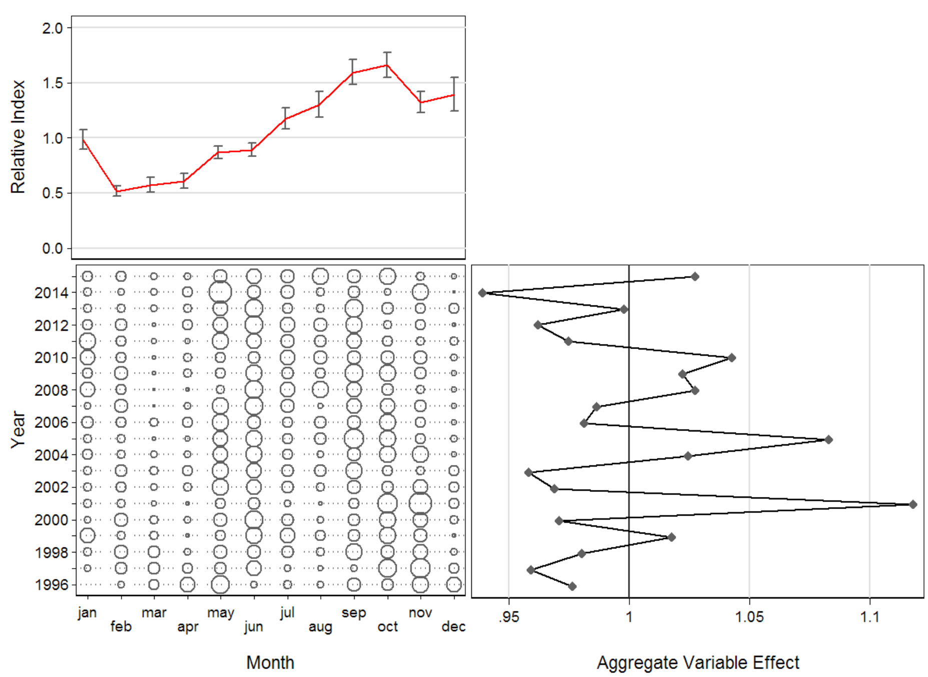

Figure C.14. CDI plot showing the effect of introducing the categorical variable [Month] to the lognormal regression model for Walleye Pollock in the 5CDE bottom trawl fishery. Each plot consists of subplots showing the effect by level of variable (top left), the relative distribution by year of variable records (bottom left), and the cumulative effect of variable by year (bottom right).

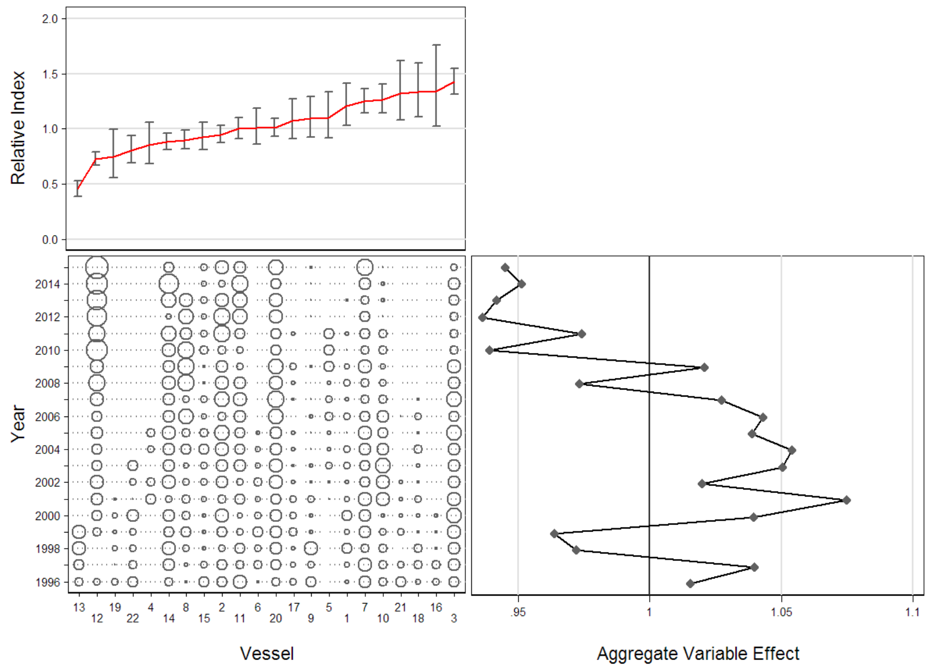

Figure C.15. CDI plot showing the effect of introducing the categorical variable [Vessel] to the lognormal regression model for Walleye Pollock in the 5CDE bottom trawl fishery. Each plot consists of subplots showing the effect by level of variable (top left), the relative distribution by year of variable records (bottom left), and the cumulative effect of variable by year (bottom right).

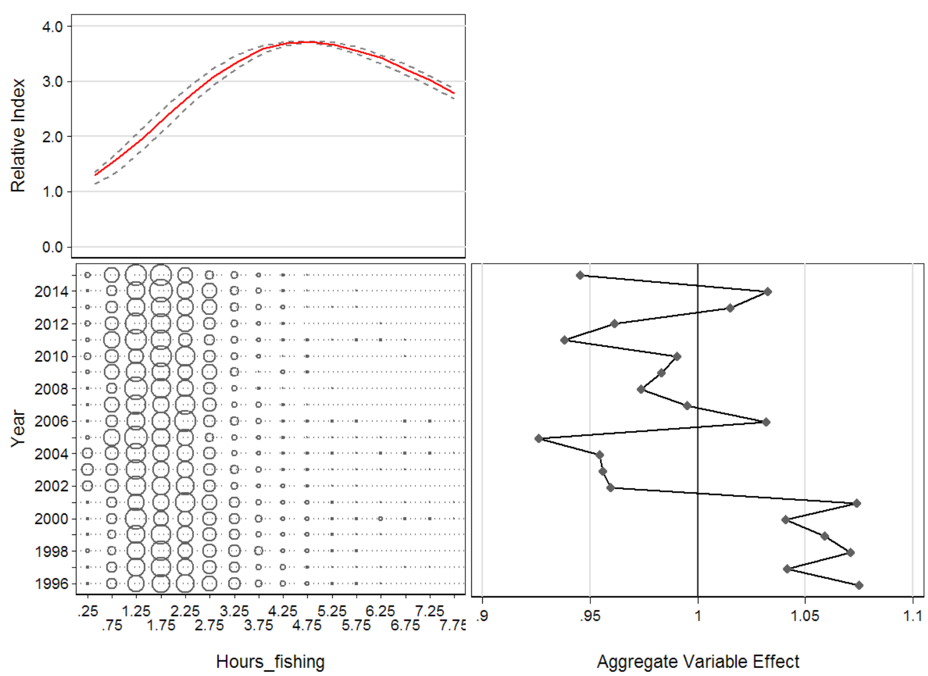

Figure C.16. CDI plot showing the effect of introducing the categorical variable [Hours_fished] to the lognormal regression model for Walleye Pollock in the 5CDE bottom trawl fishery. Each plot consists of subplots showing the effect by level of variable (top left), the relative distribution by year of variable records (bottom left), and the cumulative effect of variable by year (bottom right).

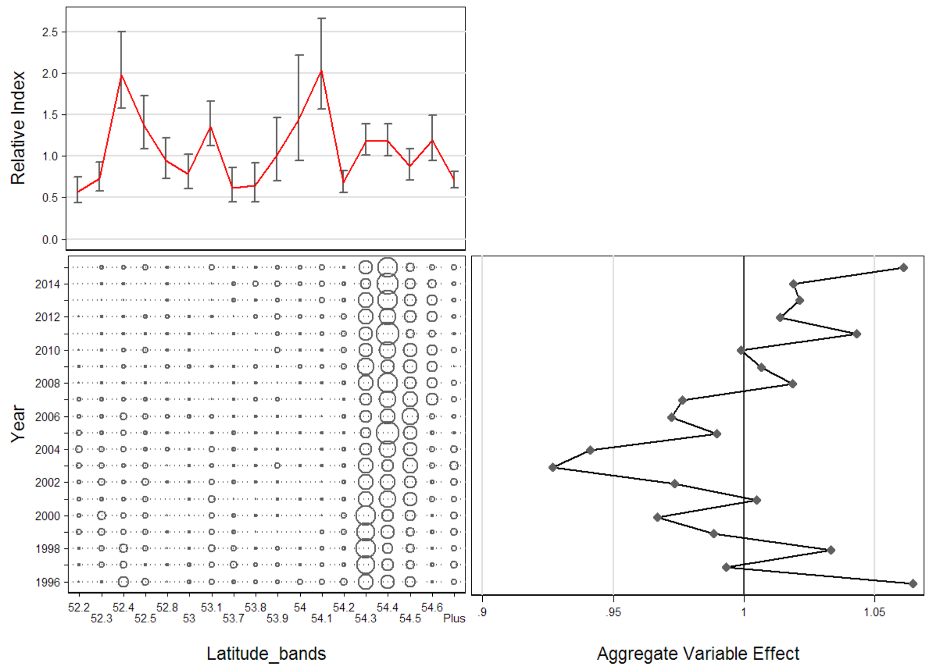

Figure C.17. CDI plot showing the effect of introducing the categorical variable [Latitude_bands] to the lognormal regression model for Walleye Pollock in the 5CDE bottom trawl fishery. Each plot consists of subplots showing the effect by level of variable (top left), the relative distribution by year of variable records (bottom left), and the cumulative effect of variable by year (bottom right).

C.4.1.3. Bottom trawl fishery: binomial logit model

The same variables used in the lognormal model were offered sequentially to this model, beginning with the year categorical variable, until the improvement in the model R^2 was less than 1% (Table C.10). This model drops in the first four years, followed by a period of little trend up to 2009, then shifts to a strong increase that peaks in 2014 (Figure C.18).

*Table C.10. Order of acceptance of variables into the binomial model of presence/absence of verified landings plus discards of Walleye Pollock in 5CDE bottom trawl fishery with the amount of explained deviance (R^2) for each variable. Variables accepted into the model are marked in bold with an *. Year was forced as the first variable.*

Variable	1	2	3	4	5	6
Year*	**0.0166**	-	-	-	-	-
DFO_locality*	0.1414	**0.1565**	-	-	-	-
Depth_bands*	0.0829	0.0968	**0.2015**	-	-	-
Month*	0.0273	0.0433	0.1803	**0.2224**	-	-
Latitude_bands*	0.1396	0.1547	0.1788	0.2143	**0.2349**	-
Hours_fished	0.0090	0.0250	0.1618	0.2120	0.2327	0.2447
Vessel	0.0122	0.0282	0.1699	0.2126	0.2327	0.2444
Improvement in deviance	0	0.1399	0.0451	0.0209	0.0124	0.0099

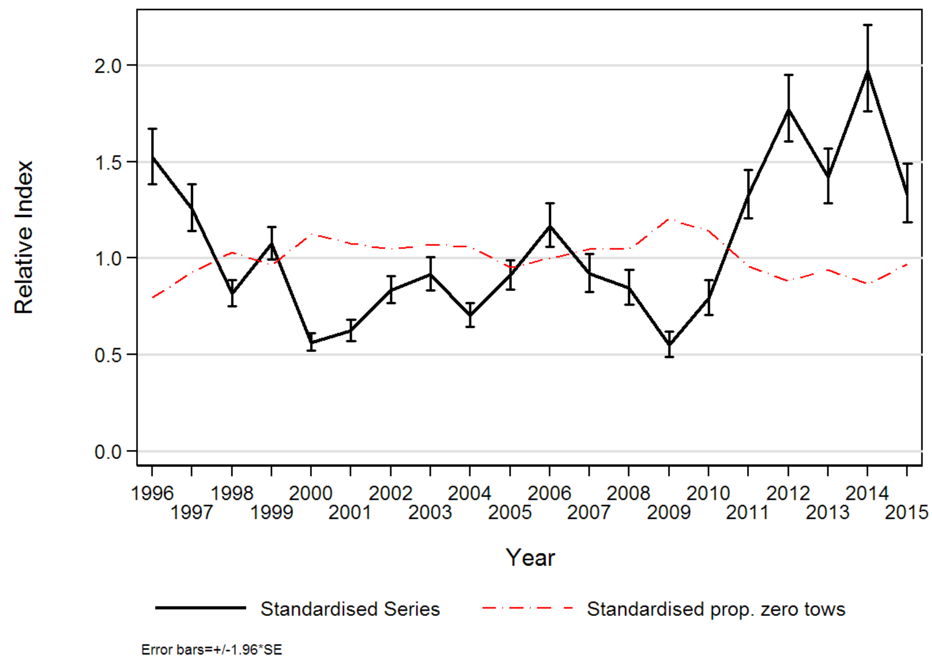

Figure C.18. Binomial index series for the 5CDE bottom trawl fishery also showing the trend in proportion of zero tows from the same data set.

C.4.1.4. Bottom trawl fishery: combined model

The combined model (Eq. C.4) initially drops, as seen in both the lognormal and binomial series, but then takes on a gradually increasing trend that more closely resembles the binomial series (Figure C.19), giving the series a slight "U" shape.

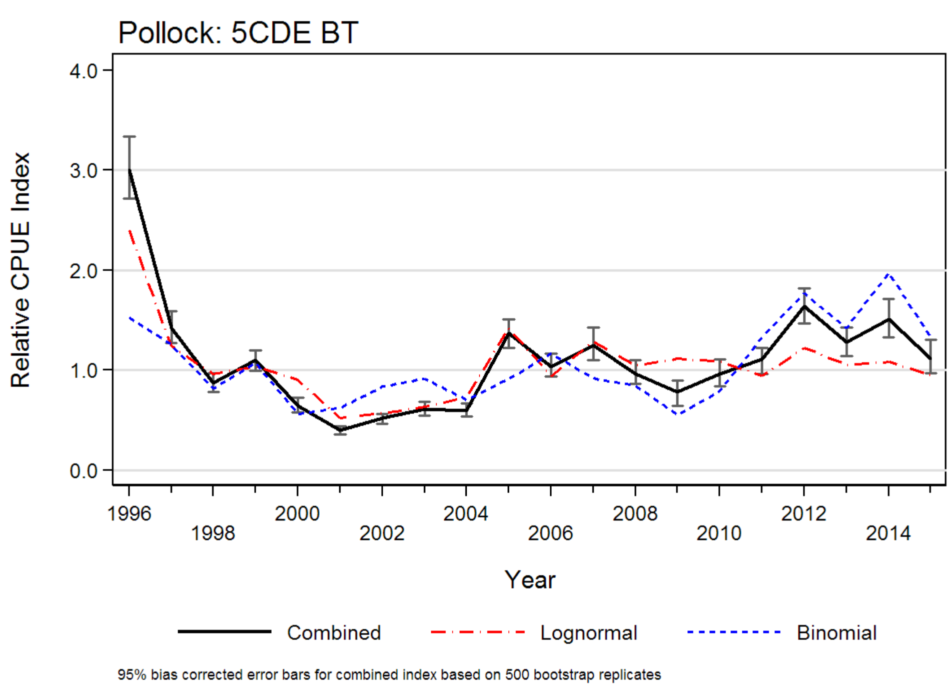

Figure C.19. Combined index series (Eq. C.4) for the 5CDE bottom trawl fishery also showing the contributing lognormal and binomial index series. Confidence bounds based on 500 bootstrap replicates.

C.4.2. Areas 3CD5AB + Minor Areas 12&20 (South)

C.4.2.1. Midwater trawl fishery

A standardised lognormal General Linear Model (GLM) analysis was performed on positive catch records from the midwater trawl tow-by-tow data set generated as described in Section C.3. Six explanatory variables (described in Section C.3 above) were offered to the model and *ln(catch)* was used as the dependent variable, where catch is the total by weight of landed plus discarded Walleye Pollock in each record (tow) (Eq. C.3). The resulting CPUE index series is presented in Figure C.20.

The **[Year]** categorical variable was forced as the first variable in the model without regard to its effect on the model deviance. The remaining five variables were offered sequentially, with a stepwise acceptance of the remaining variables with the best AIC. This process was continued until the improvement in the model R^2 was less than 1% (Table C.11). This model selected four of the five remaining explanatory variables, including **[0.1°Latitude_bands]**, **[DFO_locality]**, **[Month]**, and **[Hours_fished]** in addition to **[Year]**. The final lognormal model accounted for 66% of the total model deviance (Table C.11), with the year variable explaining 11% of the model deviance.

As seen in the 5CDE model, residuals do not fit the underlying lognormal distributional assumption very well, with considerable deviation at the tails and in the body of the residual distribution (Figure C.21).

A stepwise plot showing how the year indices change as each explanatory variable was introduced into the model shows a strong standardisation effect near the end of the series, beginning around 2010, with the main effect occurring with the addition of the initial **[0.1°Latitude_bands]** variable (Figure C.22).

CDI plots of the four explanatory variables introduced to the model in addition to **[Year]** show a strong, but variable with large swings between years, standardisation effect with the addition of the **[0.1°Latitude_bans]** variable (Figure C.23). This type of sharp shifts between years is not a desirable feature in this type of analysis because it indicates lack of stability in the underlying data. The explanatory variables **[DFO_Locality]** (Figure C.24), **[Month]** (Figure C.25) and **[Hours_fished]** (Figure C.26) all show similar behaviour in their contributions to the standardisation model. These substantial year-to-year changes indicate that this model is likely to be unstable.

The year indices show a rising index from the late-2000s (Figure C.20), but this model has poor residual diagnostics, abrupt annual shifts in the underlying data and is consequently not reliable.

*Table C.11. Order of acceptance of variables into the lognormal model of positive total mortalities (verified landings plus discards) of Walleye Pollock 3CD5AB+Minor Areas 12&20 midwater trawl fishery with the amount of explained deviance (R^2) for each variable. Variables accepted into the model are marked with an *. Year was forced as the first variable and vessel was not offered to this model.*

Variable	1	2	3	4	5	6
Year*	**0.1089**	-	-	-	-	-
Latitude_bands*	0.4481	**0.5996**	-	-	-	-
DFO_locality*	0.4628	0.5938	**0.6293**	-	-	-
Month*	0.2775	0.4054	0.6144	**0.6457**	-	-
Hours_fished	0.1159	0.2081	0.6131	0.6401	**0.6579**	-
Depth_bands*	0.2945	0.3620	0.6070	0.6375	0.6523	0.6656
Improvement in deviance	0	0.4907	0.0297	0.0164	0.0123	0.0076

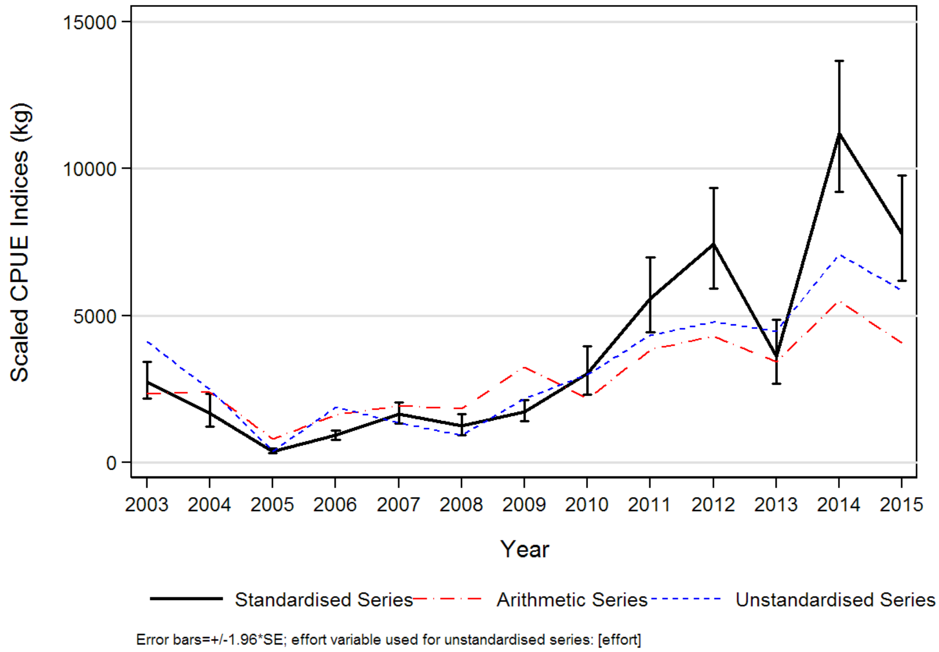

Figure C.20. Three CPUE series for Walleye Pollock from 2003 to 2015 in 3CD5AB+Minor Areas 12&20 midwater trawl fishery. The solid line is the standardised CPUE series from the lognormal model (Eq. C.3). The arithmetic series (Eq. C.1) and the unstandardised series (Eq. C.2) are also presented. All three series have been scaled to same geometric mean.

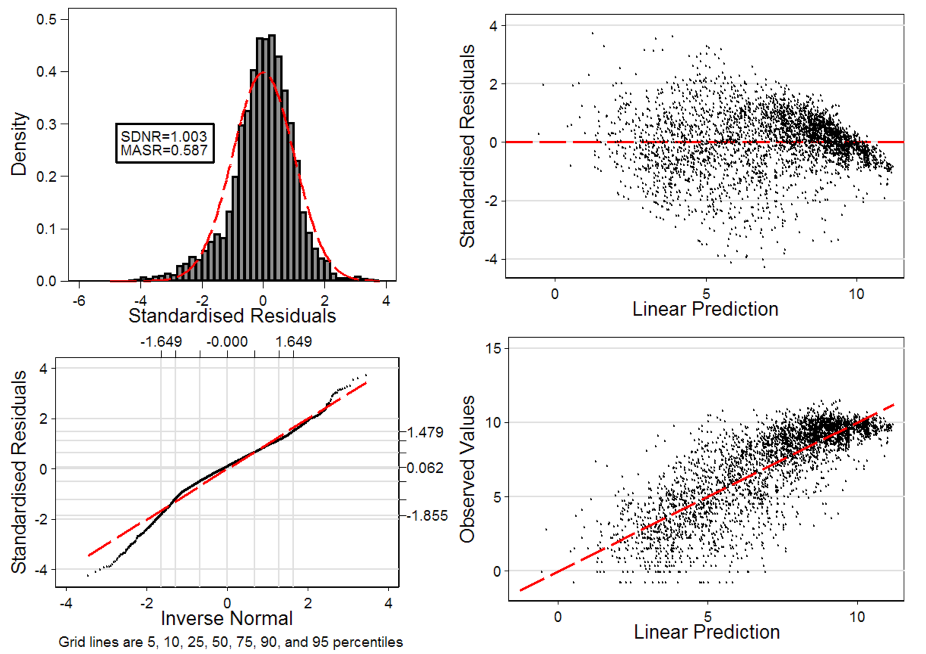

Figure C.21. Residual diagnostic plots for the GLM lognormal analysis for Walleye Pollock in 3CD5AB+Minor Areas 12&20 midwater trawl fishery. Upper left: histogram of the standardised residuals with overlaid lognormal distribution (SDNR = standard deviation of normalised residuals. MASR = median of absolute standardised residuals). Lower left: Q-Q plot of the standardised residuals with the outside horizontal and vertical lines representing the 5th and 95th percentiles of the theoretical and observed distributions. Upper right: standardised residuals plotted against the predicted CPUE. Lower right: observed CPUE plotted against the predicted CPUE.

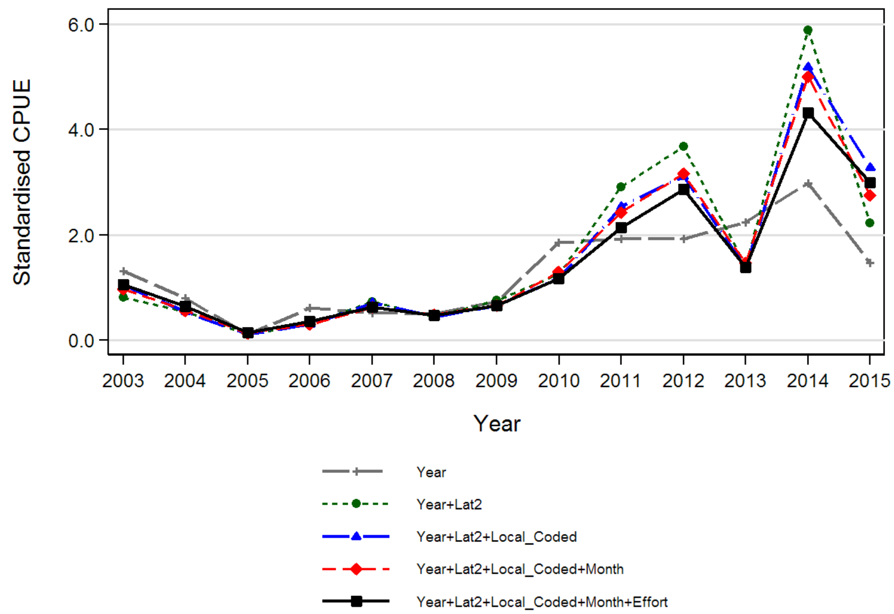

Figure C.22. Plot showing the year coefficients after adding each successive term of the standardised lognormal regression analysis for Walleye Pollock in the 3CD5AB+Minor Areas 12&20 midwater trawl fishery. The final model is shown with a thick solid black line. Each line has been scaled so that the geometric mean equals 1.0.

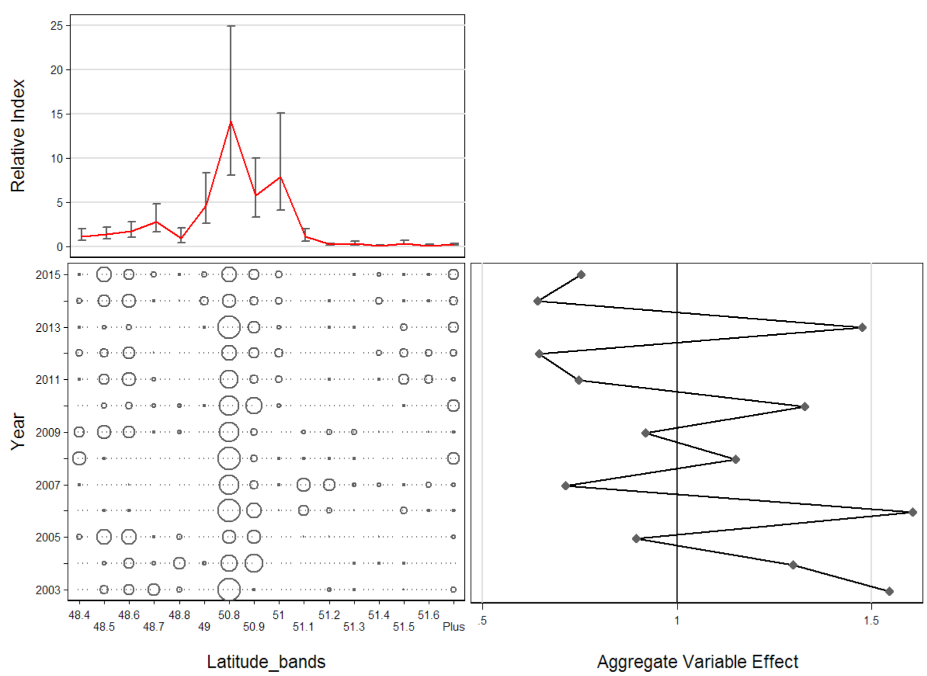

Figure C.23. CDI plot showing the effect of introducing the categorical variable [Latitude_bands] to the lognormal regression model for Walleye Pollock in the 3CD5AB+Minor Areas 12&20 midwater trawl fishery. Each plot consists of subplots showing the effect by level of variable (top left), the relative distribution by year of variable records (bottom left), and the cumulative effect of variable by year (bottom right).

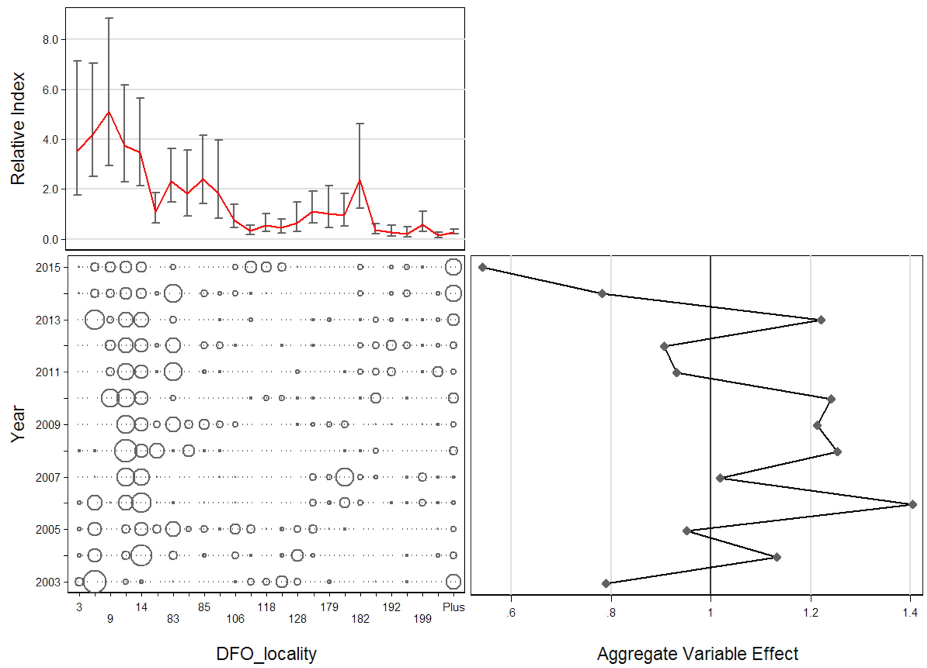

Figure C.24. CDI plot showing the effect of introducing the categorical variable [DFO_locality] to the lognormal regression model for Walleye Pollock in the 3CD5AB+Minor Areas 12&20 midwater trawl fishery. Each plot consists of subplots showing the effect by level of variable (top left), the relative distribution by year of variable records (bottom left), and the cumulative effect of variable by year (bottom right).

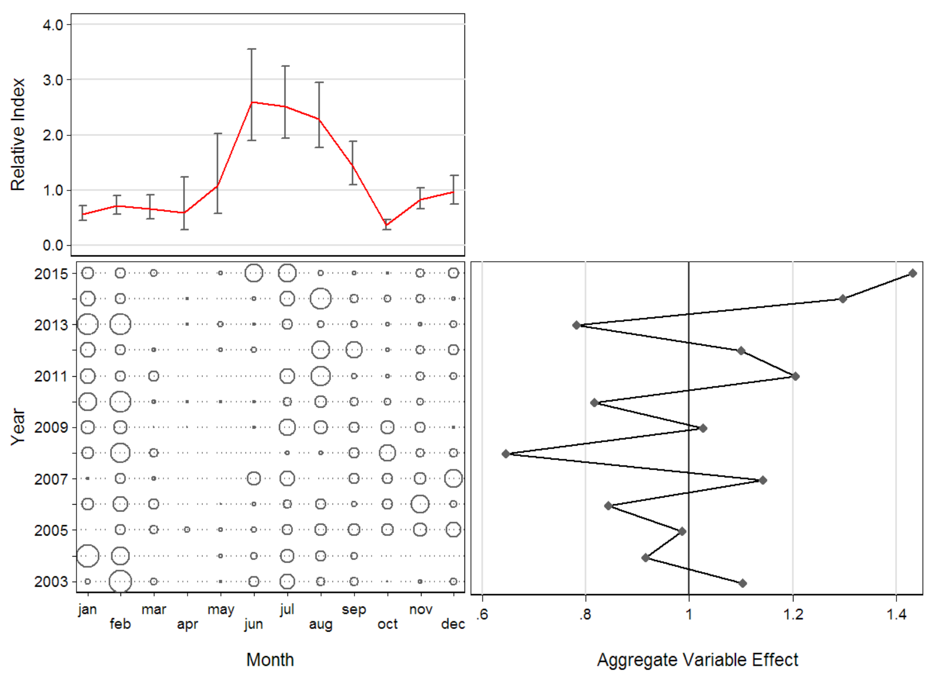

Figure C.25. CDI plot showing the effect of introducing the categorical variable [Month] to the lognormal regression model for Walleye Pollock in the 3CD5AB+Minor Areas 12&20 midwater trawl fishery. Each plot consists of subplots showing the effect by level of variable (top left), the relative distribution of variable records by year (bottom left), and the cumulative effect of variable by year (bottom right).

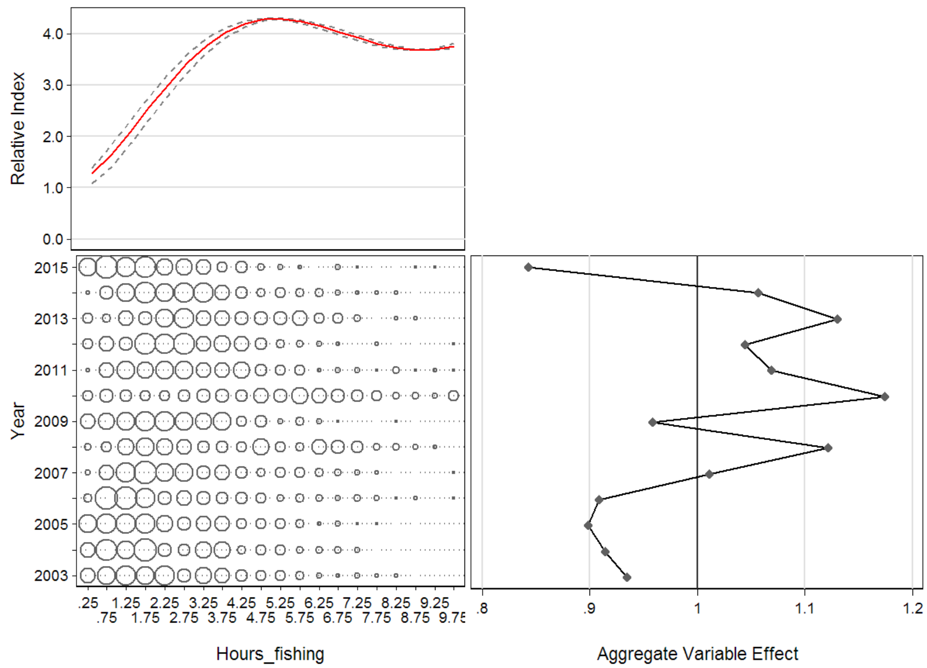

Figure C.26. CDI plot showing the effect of introducing the categorical variable [Hours_fished] to the lognormal regression model for Walleye Pollock in the 3CD5AB+Minor Areas 12&20 midwater trawl fishery. Each plot consists of subplots showing the effect by level of variable (top left), the relative distribution by year of variable records (bottom left), and the cumulative effect of variable by year (bottom right).

C.4.2.2. Bottom trawl fishery: positive lognormal model

A standardised lognormal General Linear Model (GLM) analysis was performed on positive catch records from the bottom trawl tow-by-tow data set generated as described in Section C.3. Seven explanatory variables (described in Section C.3 above) were offered to the model and *ln(catch)* was used as the dependent variable, where catch is the total by weight of landed plus discarded Walleye Pollock in each record (tow) (Eq. C.3). The resulting CPUE index series is presented in Figure C.27.

The **[Year]** categorical variable was forced as the first variable in the model without regard to its effect on the model deviance. The remaining six variables were offered sequentially, with a stepwise acceptance of the remaining variables with the best AIC. This process was continued until the improvement in the model R^2 was less than 1% (Table C.12). This model selected five of the six remaining explanatory variables, including **[DFO_locality]** , **[Month]**, **[Vessel]**, **[Hours_fished]** and **[Latitude_bands]** in addition to **[Year]**. The final lognormal model accounted for 24% of the total model deviance (Table C.12), with the year variable explaining only 3% of the model deviance.

Model residuals show an excellent fit with the underlying lognormal distributional assumption, with only a small deviation at the upper tail of the distribution and none in the lower tail or in the body of the residual distribution (Figure C.28).

A stepwise plot showing the effect on the year indices as each explanatory variable was introduced into the model shows that the standardisation procedure made small adjustments to the unstandardised series in 1996, 1997, 2000, 2005 and 2010, resulting in a relatively smooth annual trend (Figure C.29).

CDI plots of the five explanatory variables introduced to the model in addition to **[Year]** show reasonably strong standardisation effects at the beginning, the middle and the end of the series with the addition of **[DFO_locality]** variable (Figure C.30). The variables **[Month]** (Figure C.31), **[Vessel]** (Figure C.32), **[Hours_fished]** (Figure C.33) and **[Latitude_bands]** (Figure C.34) also impact the standardisation model, but the effects are relatively minor. A possible exception to this is a strong deviation in the vessel effect in 2001 (Figure C.32), but an examination of the shift in Figure C.29 shows little change in the 2001 year index when **[Vessel]** was added to the model.

The lognormal year indices show a declining trend at the beginning of the series, followed by a flat or slightly increasing trend towards the end of the series (Figure C.27). This model has excellent diagnostics and shows only small changes from the unstandardised series.

*Table C.12. Order of acceptance of variables into the lognormal model of positive total mortalities (verified landings plus discards) of Walleye Pollock 3CD5AB+Minor Areas 12&20 bottom trawl fishery with the amount of explained deviance (R^2) for each variable. Variables accepted into the model are marked in bold with an *. Year was forced as the first variable.*

Variable	1	2	3	4	5	6	7
Year*	**0.0318**	-	-	-	-	-	-
DFO_locality*	0.1366	**0.1675**	-	-	-	-	-
Month*	0.0486	0.0751	**0.1898**	-	-	-	-
Vessel	0.0412	0.0754	0.1900	**0.2121**	-	-	-
Hours_fished*	0.0155	0.0456	0.1828	0.2041	**0.2296**	-	-
Latitude_bands	0.1151	0.1449	0.1813	0.2025	0.2248	**0.2416**	-
Depth_bands	0.0185	0.0482	0.1740	0.1965	0.2194	0.2361	0.2479
Improvement in deviance	0	0.1358	0.0223	0.0224	0.0174	0.0120	0.0063

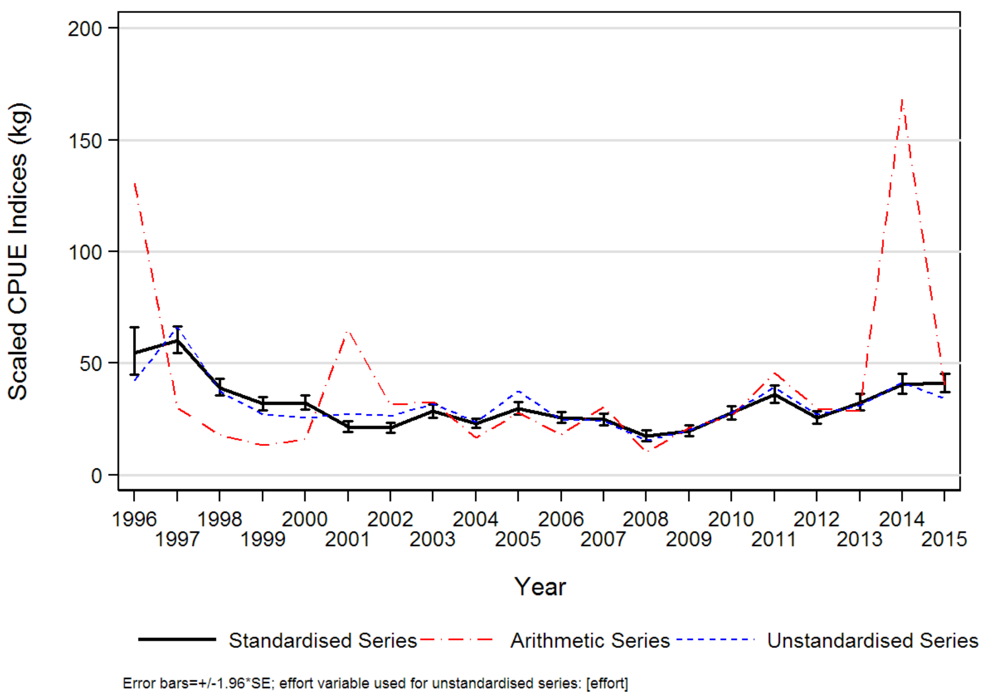

Figure C.27. Three CPUE series for Walleye Pollock from 1996 to 2015 in 3CD5AB+Minor Areas 12&20 bottom trawl fishery. The solid line is the standardised CPUE series from the lognormal model (Eq. C.3). The arithmetic series (Eq. C.1) and the unstandardised series (Eq. C.2) are also presented. All three series have been scaled to same geometric mean.

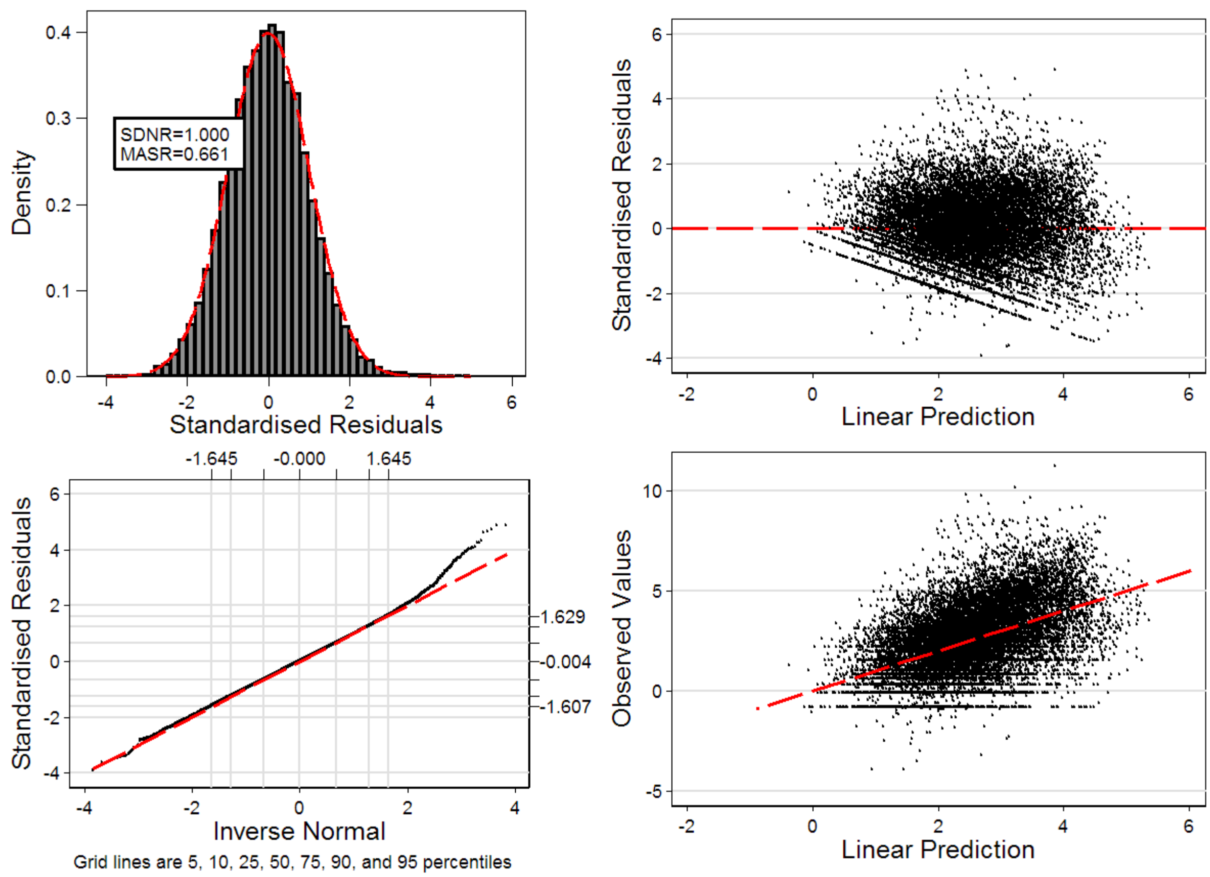

Figure C.28. Residual diagnostic plots for the GLM lognormal analysis for Walleye Pollock in 3CD5AB+Minor Areas 12&20 bottom trawl fishery. Upper left: histogram of the standardised residuals with overlaid lognormal distribution (SDNR = standard deviation of normalised residuals. MASR = median of absolute standardised residuals). Lower left: Q-Q plot of the standardised residuals with the outside horizontal and vertical lines representing the 5th and 95th percentiles of the theoretical and observed distributions. Upper right: standardised residuals plotted against the predicted CPUE. Lower right: observed CPUE plotted against the predicted CPUE.

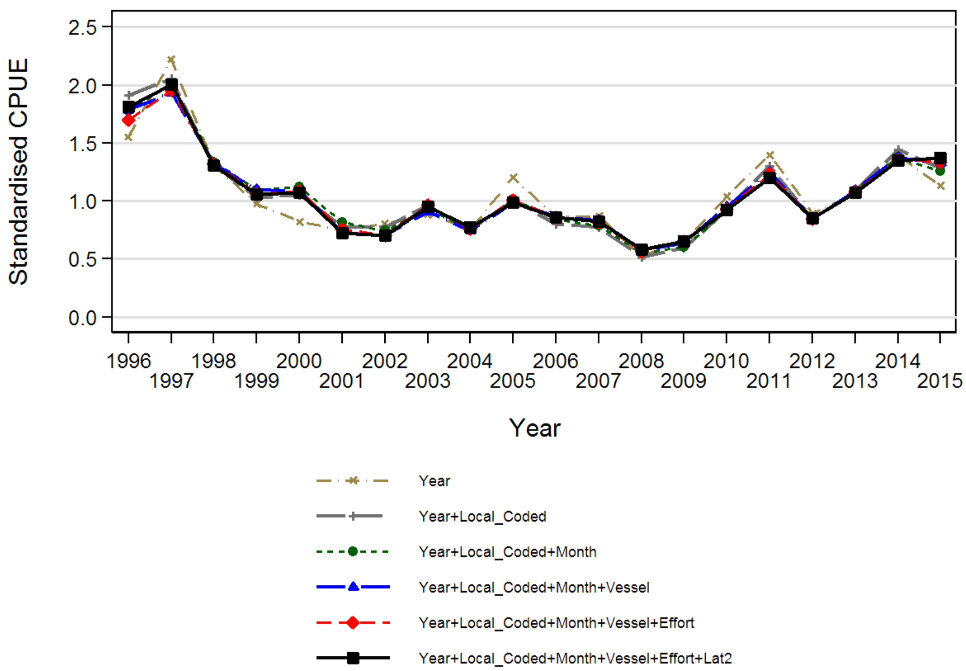

Figure C.29. Plot showing the year coefficients after adding each successive term of the standardised lognormal regression analysis for Walleye Pollock in the 3CD5AB+Minor Areas 12&20 bottom trawl fishery. The final model is shown with a thick solid black line. Each line has been scaled so that the geometric mean equals 1.0.

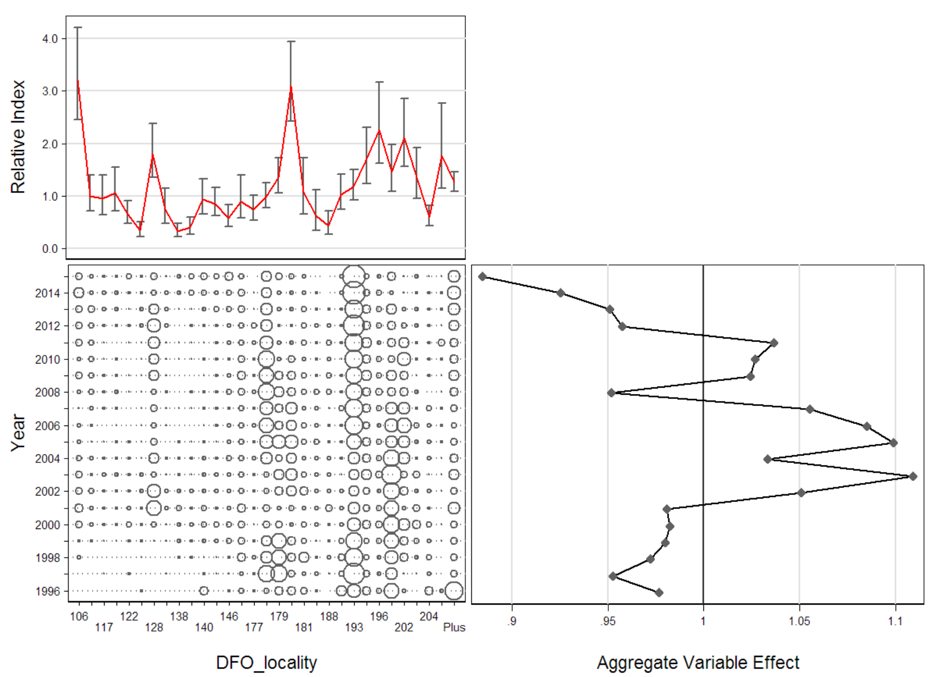

Figure C.30. CDI plot showing the effect of introducing the categorical variable [DFO_locality] to the lognormal regression model for Walleye Pollock in the 3CD5AB+Minor Areas 12&20 bottom trawl fishery. Each plot consists of subplots showing the effect by level of variable (top left), the relative distribution by year of variable records (bottom left), and the cumulative effect of variable by year (bottom right).

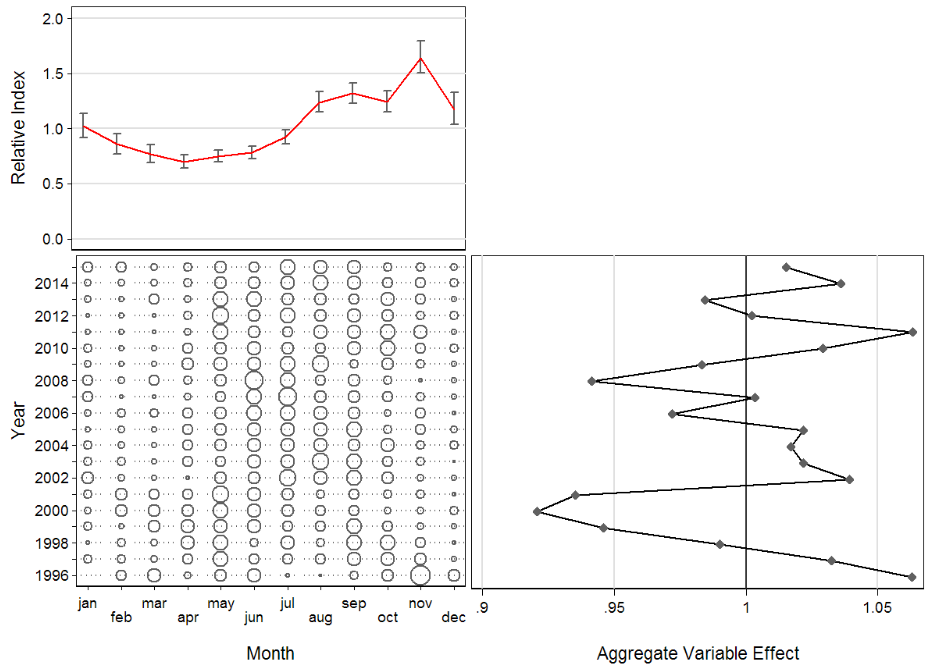

Figure C.31. CDI plot showing the effect of introducing the categorical variable [Month] to the lognormal regression model for Walleye Pollock in the 3CD5AB+Minor Areas 12&20 bottom trawl fishery. Each plot consists of subplots showing the effect by level of variable (top left), the relative distribution of variable records by year (bottom left), and the cumulative effect of variable by year (bottom right).

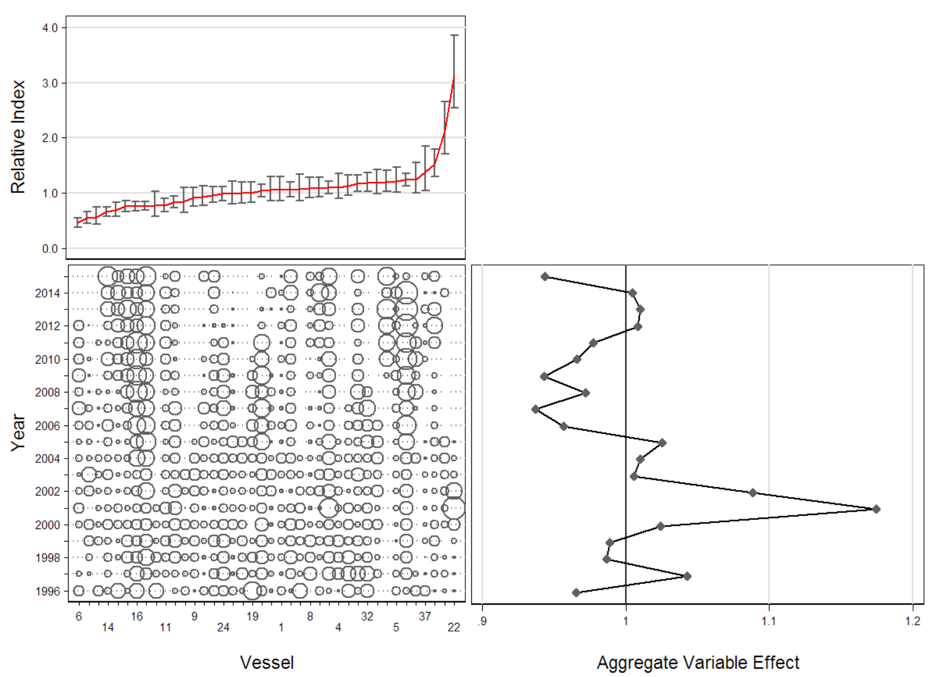

Figure C.32. CDI plot showing the effect of introducing the continuous variable [Vessel] to the lognormal regression model for Walleye Pollock in the 3CD5AB+Minor Areas 12&20 bottom trawl fishery. Each plot consists of subplots showing the effect by level of variable (top left), the relative distribution by year of variable records (bottom left), and the cumulative effect of variable by year (bottom right).

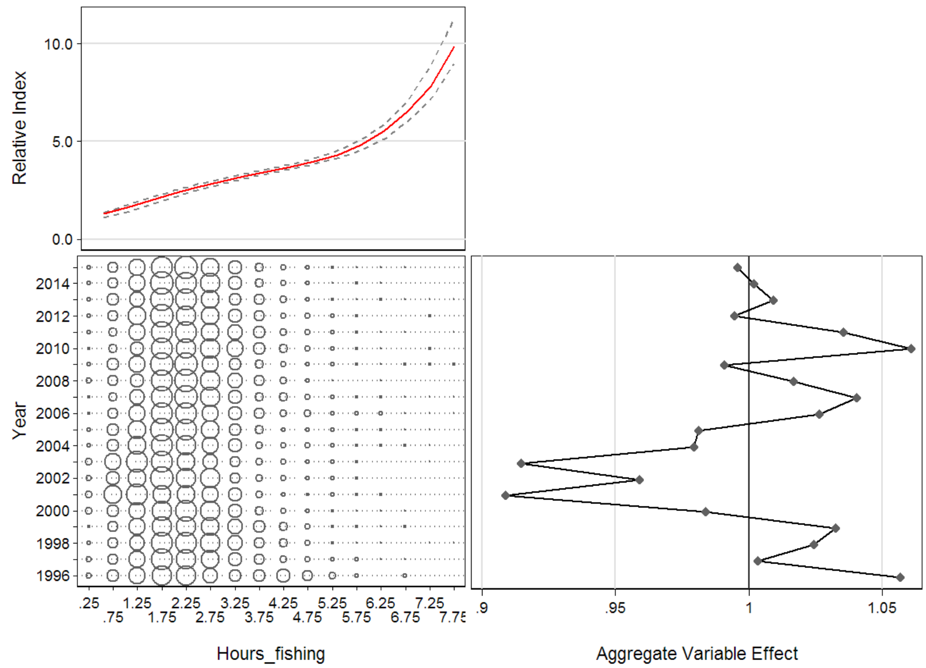

Figure C.33. CDI plot showing the effect of introducing the categorical variable [Hours_fished] to the lognormal regression model for Walleye Pollock in the 3CD5AB+Minor Areas 12&20 bottom trawl fishery. Each plot consists of subplots showing the effect by level of variable (top left), the relative distribution by year of variable records (bottom left), and the cumulative effect of variable by year (bottom right).

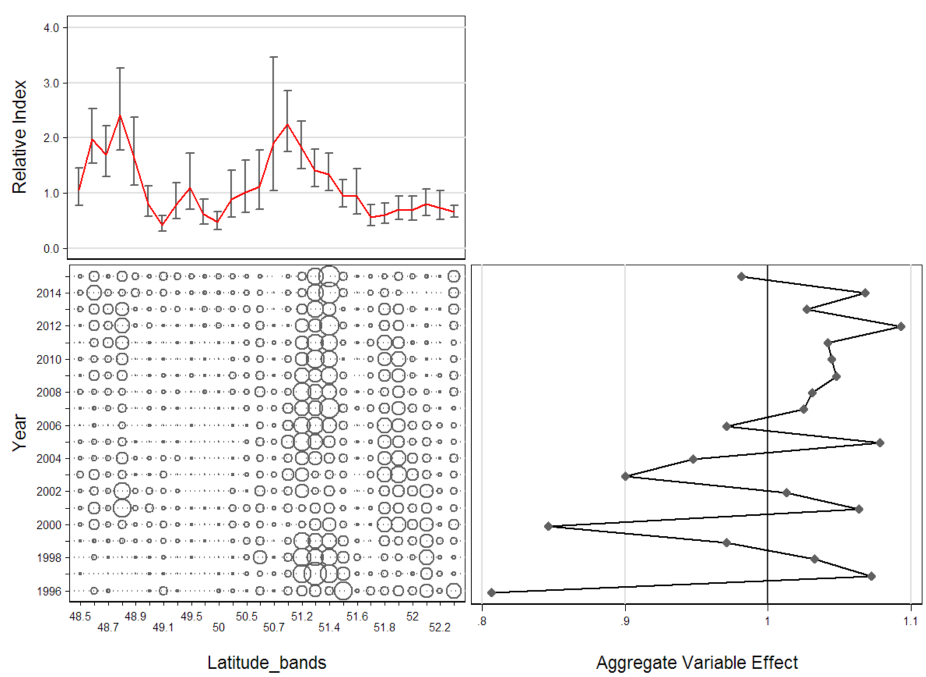

Figure C.34. CDI plot showing the effect of introducing the categorical variable [Latitude_bands] to the lognormal regression model for Walleye Pollock in the 3CD5AB+Minor Areas 12&20 bottom trawl fishery. Each plot consists of subplots showing the effect by level of variable (top left), the relative distribution by year of variable records (bottom left), and the cumulative effect of variable by year (bottom right).

C.4.2.3. Bottom trawl fishery: binomial logit model

The same variables used in the lognormal model were offered sequentially to this model, beginning with the year categorical variable, until the improvement in the model R^2 was less than 1% (Table C.13). This model shows no little trend up to about 2009 or 2010, but is then followed by a strong increase up to 2015 (Figure C.35).

*Table C.13. Order of acceptance of variables into the binomial model of presence/absence of verified landings plus discards of Walleye Pollock in 3CD5AB+Minor Areas 12&20 bottom trawl fishery with the amount of explained deviance (R^2) for each variable. Variables accepted into the model are marked in bold with an *. Year was forced as the first variable.*

Variable	1	2	3	4	5	6
Year*	**0.0149**	-	-	-	-	-
Latitude_bands	0.0921	**0.1075**	-	-	-	-
Depth_bands*	0.0541	0.0675	**0.1510**	-	-	-
DFO_locality*	0.0865	0.1042	0.1415	**0.1854**	-	-
Hours_fished *	0.0135	0.0277	0.1167	0.1673	**0.2000**	-
Vessel	0.0166	0.0306	0.1162	0.1591	0.1918	0.2072
Month	0.0098	0.0259	0.1111	0.1565	0.1890	0.2029
Improvement in deviance	0	0.0927	0.0435	0.0344	0.0146	0.0071

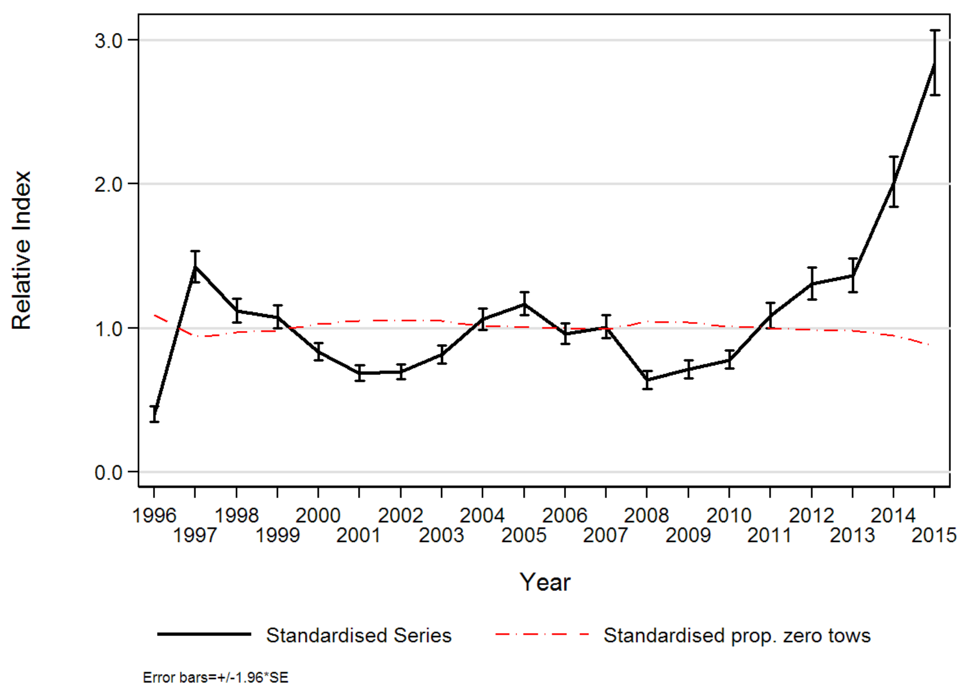

Figure C.35. Binomial index series for the 3CD5AB + Minor Areas 12&20 bottom trawl fishery also showing the trend in proportion of zero tows from the same data set.

C.4.2.4. Bottom trawl fishery: combined model

The combined model (Eq. C.4) shows an even stronger “U” pattern than did the 5CDE (North) model, with a declining trend to early 2000s, followed by a period of little change and increasing strongly to 2015, taking its signal from the binomial series (Figure C.36).

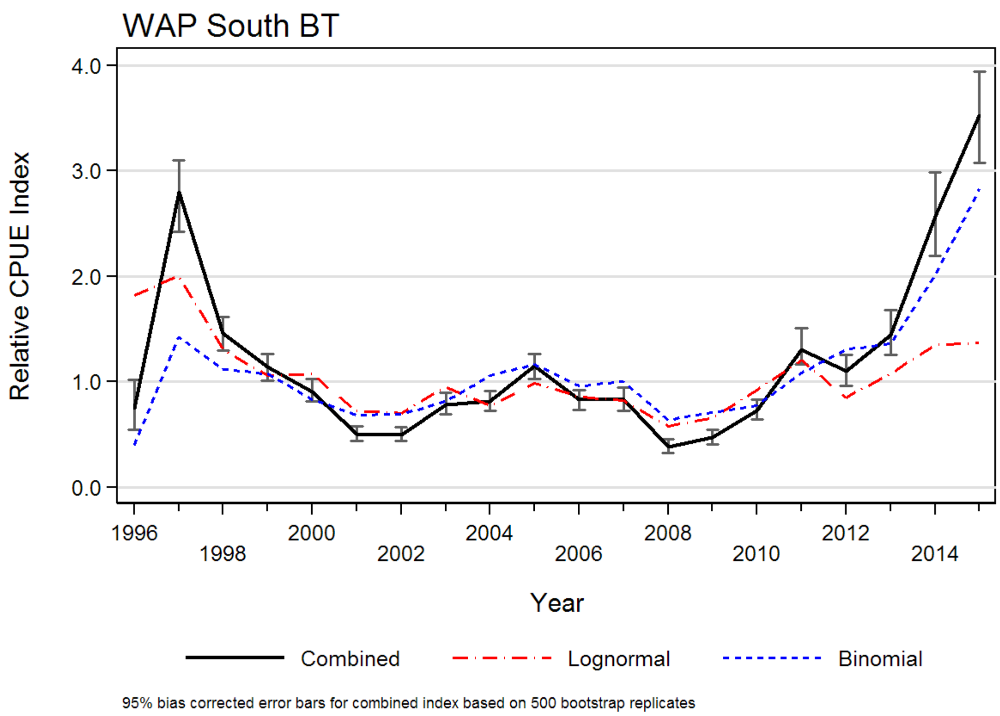

Figure C.36. Combined index series (Eq. C.4) for the 3CD5AB+Minor Areas 12&20 bottom trawl fishery also showing the contributing lognormal and binomial index series. Confidence bounds based on 500 bootstrap replicates.

C.5. COMPARISONS WITHIN AND AMONG STOCKS

Figure C.37 compares the lognormal midwater and bottom trawl indices for the defined 5CDE (North) WAP area, showing a strong increase in the midwater trawl CPUE beginning from 2008 while there was only a moderate increase in the bottom trawl CPUE in the mid-2000s, followed by a stable index over the last decade.

Figure C.38 compares the lognormal midwater and bottom trawl indices for the defined 3CD5AB+Minor Areas 12&20 (South) WAP area, showing an increasing trend in midwater trawl CPUE from the mid-2000s while the bottom trawl index is mainly stable over the same period, after dropping from a high level observed in the late 1990s.

Both lognormal midwater trawl indices (Figure C.39) increase, starting at the end of the 2000s. The overall level of increase is much greater for the South series, but this series also shows strong annual variations which are unlikely to be abundance driven. Given the poor residual diagnostics for both series (see Figure C.4 and Figure C.21) and the strong year-to-year variations observed in both series, neither can be considered sufficiently reliable for use as an indicator of abundance trends.

The two combined bottom trawl CPUE series show less annual variability than the midwater trawl series (Figure C.40) and show similar patterns up to the early 2010s, with both series declining from high levels in 1996 or 1997 and then maintaining a consistent level just below the series mean up to around 2012/2013. The large jump from 1996 to 1997 in the South series is unlikely to be abundance driven, especially given the small amount of data in 1996 (see Table C.7: 1996 has about one-quarter the number tows and less than half the trips of subsequent years). The North and South series diverge after about 2013, with the South series showing a strong increase to over three times the series mean while the North maintains a level just above the series mean (Figure C.40).

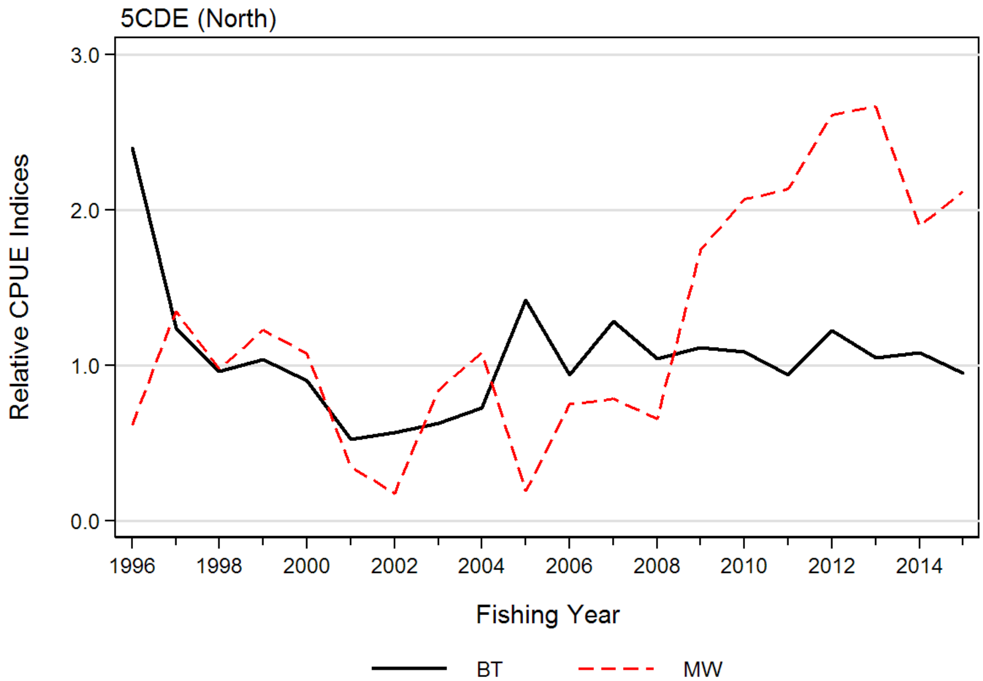

Figure C.37. Comparison of the lognormal bottom trawl and midwater CPUE index series for the 5CDE (North) WAP area.

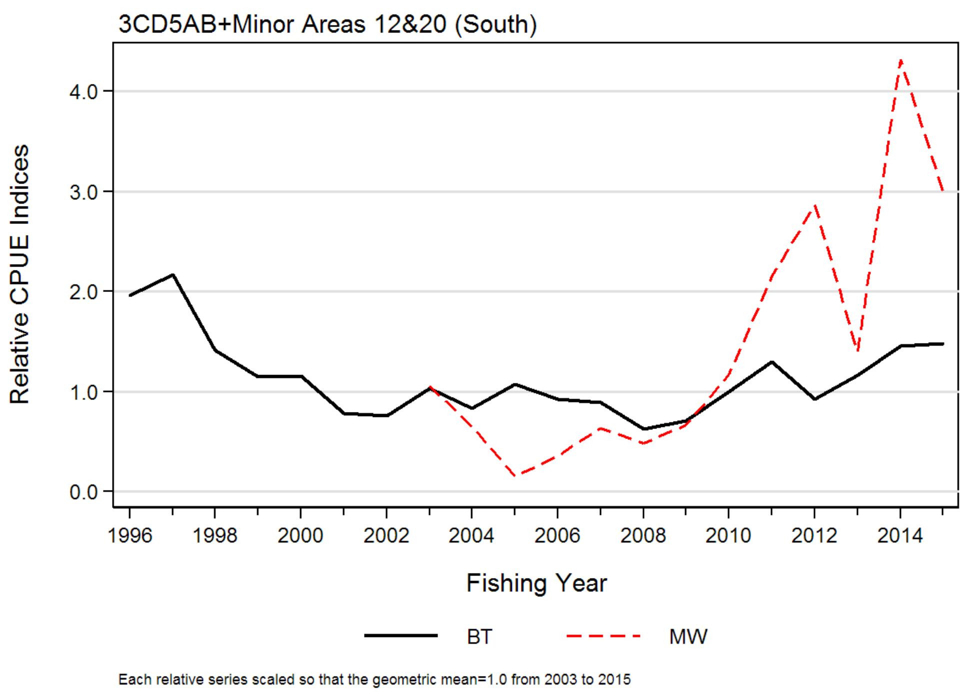

Figure C.38. Comparison of the lognormal bottom trawl and midwater CPUE index series for the 3CD5AB+Minor Areas 12&20 (South) WAP area.

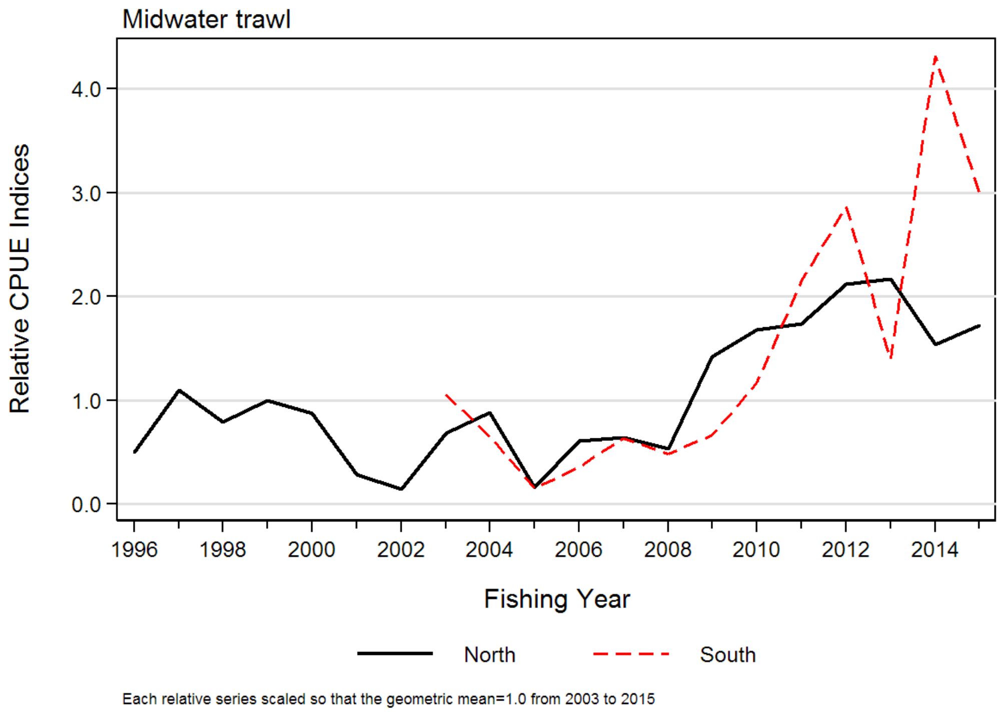

Figure C.39. Comparison of the lognormal midwater trawl CPUE index series for the North and South WAP area definitions.

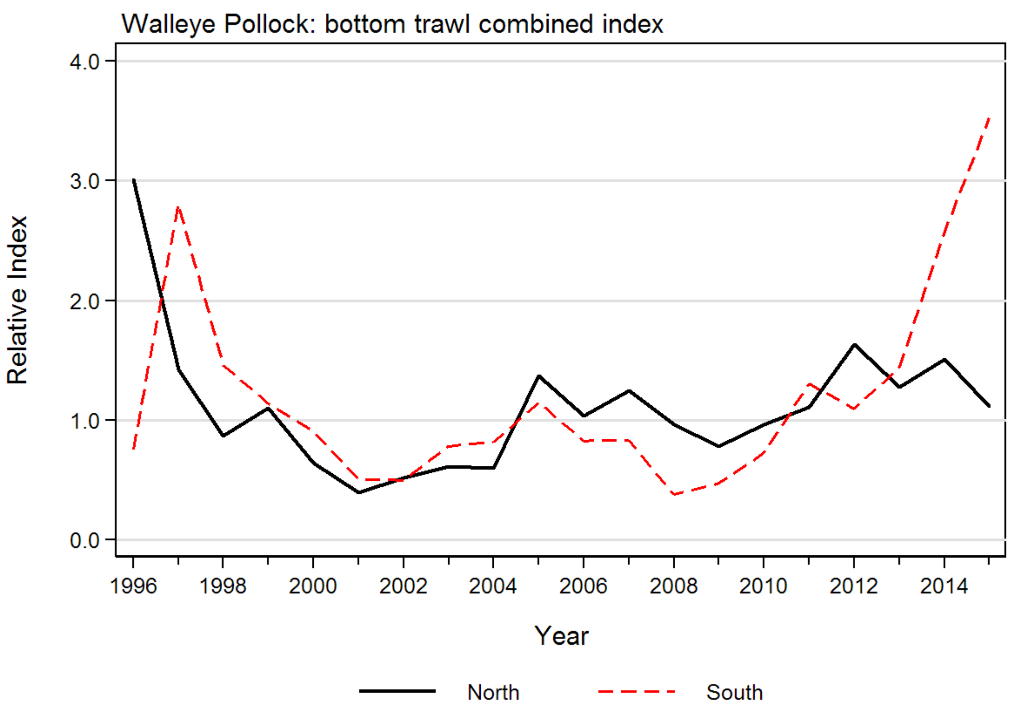

Figure C.40. Comparison of the combined (Eq. C.4) bottom trawl CPUE index series for the North and South WAP area definitions.

C.6. RELATIVE INDICES OF ABUNDANCE

Table C.14 to Table C.16 summarise the relative indices of abundance derived from the CPUE analyses for the two Walleye Pollock stocks. The midwater gear yields indices from 1996 to 2015 for BC North, but only from 2003 to 2015 for BC South (Table C.14). These indices were not used in the model because they rely on directed effort that is heavily influenced by fisher behaviour and management regulation.

CPUE indices used in the delay-difference model appear as the delta-lognormal (combined) indices from the bottom trawl data (BC North: Table C.15, BC South: Table C.16).
A fixed CV of 0.3 was applied to each CPUE index in the model, which iSCAM accepts as the inverse of CV: $v_{jt} = 1/c_{jt}$ = 1/0.3 = 3.333 (see Eqn E.29).

Table C.14. Relative indices of annual CPUE (kg/tow) from the arithmetic, geometric and lognormal models of non-zero catches of midwater trawl fishery for Walleye Pollock in the indicated sub-regions with associated standard error (SE) for the lognormal model. '–': indices not available.

	5CDE				3CD5AB+Minor Areas 12&20			
	Arithmetic (Eq. C.1)	Geometric (Eq. C.2)	Lognormal (Eq. C.3)	Standard error	Arithmetic (Eq. C.1)	Geometric (Eq. C.2)	Lognormal (Eq. C.3)	Standard error
1996	557	528	1,048	0.171	–	–	–	–
1997	2,446	3,402	2,286	0.206	–	–	–	–
1998	1,765	2,765	1,659	0.211	–	–	–	–
1999	2,171	3,901	2,086	0.164	–	–	–	–
2000	1,868	2,304	1,825	0.226	–	–	–	–
2001	492	422	597	0.276	–	–	–	–
2002	208	67	301	0.252	–	–	–	–
2003	2,825	1,638	1,425	0.195	2,355	4,119	2,742	0.116
2004	2,868	3,018	1,838	0.150	2,408	2,499	1,691	0.166
2005	845	278	328	0.187	816	387	395	0.096
2006	1,648	1,310	1,278	0.168	1,628	1,895	933	0.085
2007	1,534	1,363	1,334	0.114	1,934	1,356	1,654	0.110
2008	1,041	348	1,118	0.175	1,840	935	1,247	0.146
2009	3,084	3,391	2,961	0.143	3,255	2,185	1,730	0.106
2010	3,339	5,541	3,509	0.127	2,185	3,000	3,040	0.135
2011	3,339	2,906	3,621	0.183	3,846	4,336	5,575	0.116
2012	3,367	7,401	4,430	0.169	4,303	4,791	7,442	0.117
2013	2,206	4,152	4,525	0.176	3,427	4,476	3,618	0.150
2014	2,588	2,996	3,217	0.276	5,514	7,090	11,208	0.101
2015	3,251	7,179	3,596	0.254	4,059	5,861	7,777	0.117

Table C.15. Relative indices of annual CPUE from the arithmetic, unstandardised, lognormal models of non-zero bottom trawl catches of Walleye Pollock in 5CDE . Also shown are the indices from the binomial model of presence/absence in this fishery and the combined delta-lognormal model (Eq. C.4). All indices are scaled so that their geometric means equal 1.0. Upper and lower 95% confidence bounds and associated standard error (SE) are presented for the lognormal model, while bootstrapped upper and lower 95% confidence bounds are presented for the combined model.

Year	Arithmetic Index (Eq. C.1)	Geometric Index (Eq. C.2)	Lognormal (Eq. C.3)				Binomial Index (Eq. C.3)	Combined (Eq. C.4)		
			Index	Lower bound	Upper bound	SE		Index	Lower bound	Upper bound
1996	2.538	2.341	2.399	2.172	2.650	0.0497	1.522	3.005	2.721	3.336
1997	1.109	1.108	1.242	1.122	1.375	0.0509	1.258	1.423	1.269	1.593
1998	0.875	0.830	0.961	0.871	1.061	0.0495	0.817	0.869	0.778	0.974
1999	1.021	0.951	1.040	0.954	1.135	0.0436	1.074	1.098	0.995	1.197
2000	0.948	0.877	0.904	0.818	0.998	0.0498	0.564	0.644	0.574	0.729
2001	0.484	0.653	0.525	0.473	0.582	0.0520	0.622	0.399	0.358	0.440
2002	0.536	0.553	0.567	0.516	0.624	0.0474	0.835	0.520	0.462	0.564
2003	0.344	0.530	0.632	0.567	0.705	0.0546	0.915	0.611	0.549	0.686
2004	0.911	0.707	0.726	0.655	0.804	0.0511	0.704	0.598	0.534	0.667
2005	3.009	1.914	1.422	1.296	1.559	0.0463	0.912	1.370	1.223	1.510
2006	0.652	0.799	0.940	0.845	1.046	0.0534	1.167	1.036	0.933	1.165
2007	0.957	1.301	1.286	1.140	1.451	0.0604	0.918	1.245	1.102	1.424
2008	0.943	1.280	1.046	0.927	1.180	0.0603	0.846	0.966	0.862	1.098
2009	1.592	1.264	1.113	0.965	1.285	0.0716	0.550	0.779	0.641	0.894
2010	0.899	1.018	1.089	0.952	1.245	0.0670	0.792	0.966	0.843	1.108
2011	0.980	1.083	0.942	0.850	1.046	0.0519	1.327	1.108	0.961	1.220
2012	0.913	1.120	1.224	1.108	1.352	0.0497	1.770	1.636	1.470	1.819
2013	1.091	1.123	1.052	0.950	1.165	0.0510	1.421	1.277	1.143	1.426
2014	0.937	0.919	1.083	0.966	1.215	0.0574	1.973	1.512	1.332	1.716
2015	2.225	1.006	0.950	0.838	1.078	0.0630	1.331	1.119	0.969	1.307

Table C.16. Relative indices of annual CPUE from the arithmetic, unstandardised, lognormal models of non-zero bottom trawl catches of Walleye Pollock in 3CD5AB+Minor Areas 12&20 . Also shown are the indices from the binomial model of presence/absence in this fishery and the combined delta-lognormal model (Eq. C.4). All indices are scaled so that their geometric means equal 1.0. Upper and lower 95% confidence bounds and associated standard error (SE) are presented for the lognormal model, while bootstrapped upper and lower 95% confidence bounds are presented for the combined model.

Year	Arithmetic Index (Eq. C.1)	Geometric Index (Eq. C.2)	Lognormal (Eq. C.3)				Binomial Index (Eq. C.3)	Combined (Eq. C.4)		
			Index	Lower bound	Upper bound	SE		Index	Lower bound	Upper bound
1996	2.308	1.415	1.816	1.497	2.202	0.0985	0.399	0.753	0.548	1.021
1997	1.573	2.206	2.005	1.817	2.213	0.0503	1.424	2.803	2.427	3.105
1998	0.760	1.247	1.305	1.183	1.440	0.0500	1.118	1.457	1.297	1.614
1999	0.516	0.907	1.058	0.963	1.163	0.0483	1.074	1.138	1.008	1.260
2000	0.464	0.849	1.072	0.972	1.183	0.0500	0.833	0.906	0.811	1.028
2001	1.413	0.904	0.722	0.645	0.809	0.0577	0.684	0.506	0.439	0.577
2002	0.695	0.880	0.704	0.634	0.782	0.0533	0.693	0.499	0.439	0.570
2003	0.698	1.063	0.951	0.858	1.055	0.0528	0.813	0.785	0.691	0.896
2004	0.552	0.790	0.771	0.704	0.846	0.0470	1.058	0.817	0.723	0.910
2005	0.939	1.251	0.990	0.904	1.083	0.0460	1.166	1.149	1.025	1.267
2006	0.670	0.822	0.858	0.779	0.945	0.0491	0.958	0.829	0.737	0.924
2007	1.147	0.806	0.822	0.742	0.910	0.0521	1.005	0.830	0.728	0.945
2008	0.266	0.512	0.579	0.507	0.662	0.0681	0.638	0.379	0.327	0.451
2009	0.571	0.663	0.656	0.582	0.739	0.0609	0.710	0.476	0.406	0.546
2010	0.934	0.928	0.922	0.827	1.028	0.0554	0.776	0.728	0.639	0.829
2011	1.649	1.305	1.204	1.080	1.341	0.0552	1.085	1.306	1.163	1.511
2012	1.135	0.901	0.851	0.761	0.952	0.0572	1.305	1.097	0.962	1.258
2013	1.123	1.034	1.076	0.958	1.207	0.0588	1.361	1.441	1.256	1.680
2014	7.772	1.377	1.348	1.207	1.506	0.0565	2.010	2.574	2.194	2.989
2015	2.401	1.139	1.369	1.241	1.509	0.0500	2.833	3.525	3.075	3.945

C.7. REFERENCS – CPUE

Bentley, N., Kendrick, T.H., Starr, P.J., and Breen, P.A. 2012. Influence plots and metrics: tools for better understanding fisheries catch-per-unit-effort standardizations. ICES J. Mar. Sci. 69(1): 84-88.

Francis, R.I.C.C. 1999. The impact of correlations on standardised CPUE indices. N.Z. Fish. Ass. Res. Doc. 99/42: 30 pp.

Francis, R.I.C.C. 2001. Orange roughy CPUE on the South and East Chatham Rise. N.Z. Fish. Ass. Rep. 2001/26: 30 pp.

Quinn, T.R. and R.B. Deriso. 1999. Quantitative Fish Dynamics. Oxford University Press. 542 pp.

Thompson, J.M. 1981. Preliminary report on the population biology and fishery of walleye pollock (*Theragra chalcogramma*) off the Pacific coast of Canada. Can. Tech. Rep. Fish. Aquat. Sci. 1031: v + 157 pp.

Vignaux, M. 1994. Catch per unit effort (CPUE) analysis of west coast South Island and Cook Strait spawning hoki fisheries, 1987-93. N.Z. Fish. Ass. Res. Doc. 94/11: 29 pp.

APPENDIX D. BIOLOGICAL DATA

D.1. GROWTH AND MATURITY

This appendix describes the derivation of the length-weight relationship, von Bertalanffy growth relationship, maturity schedule, natural mortality and Walford parameters used in the Walleye Pollock (WAP) delay-difference stock assessment model. These analyses are based on Walleye Pollock biological data extracted from the Fisheries and Oceans Canada (DFO) Groundfish database "*GFBioSQL*" on Dec 13, 2016 (345,429 records). General data selection criteria for many analyses are summarized in Table D.1, though each analysis can vary the selection.

Table D.1. Data selection criteria for analyses of Walleye Pollock biological data for growth and length-weight analysis.

Field	Criterion	Notes
Trip type	[trip_type] == c(2, 3) [trip_type] == c(1, 4, 5)	Definition of research observations. Definition of commercial observations
Sample type	[sample_type] == c(1, 2, 6, 7)	Only random or total samples.
Ageing method	[agemeth]==3 | (==0 & [year]>=1980) or ==7 (fin rays)	Break & burn method, or unknown from 1980 onwards, assumed to be B&B.
Species category code	[SPECIES_CATEGORY_CODE] == 1 (or 3)	1 = Unsorted samples 3 = Sorted (keeper) samples
Sex code	[sex] == c(1, 2)	Clearly identified sex (1=male or 2=female).
Area code	[stock] select valid stock area observations	North (5CDE): PMFC major area codes 7:9 South (5AB3CD): PMFC major areas 5:6 (5AB) + minor 12 (Queen Charlotte Strait) + majors 3:4 (3CD) + minor 20 (Juan de Fuca Strait)
Tow status	select [Not_available_reason_code] == NULL	Not rejected, valid tow.

D.1.1. Length-Weight

A log-linear relationship with additive errors was fitted to females, males, and combined to all valid weight and length data pairs i, $\{W_i, L_i\}$:

$$\ln(W_i) = b\ln(L_i) + a + \varepsilon \qquad \text{(D.1)}$$

where a and b are the intercept and slope parameters.

Samples from gear types bottom trawl (Table D.2) and midwater trawl (Table D.3) were analysed separately, but not used in the assessment. As the delay-difference model was not sex-specific, males and females were combined for allometric relationships for stocks North (Figure D.1), South (Figure D.2), and coastwide (Figure D.3).

Table D.2. Length-weight parameter estimates, standard errors (SE) and number of observations (n) for Walleye Pollock (females, males and combined) for all research/charter and commercial samples from **bottom** trawls operating in stock areas 5CDE, 5AB, 3CD, and 4B from 1973 to 2015. $\bar{W}_{\text{pred}}$ = mean weight (in kg) from the fitted data set.

Stock	*n*	ln(*a*)	SE ln(*a*)	*b*	SE(b)	$\bar{W}_i$	SD W_i	min W_i	max W_i	$\bar{W}_{\text{pred}}$
5CDE+5AB+3CD (Research Survey)										
Females	5,209	-11.782	0.0178	3.0153	0.0050	0.5257	0.4457	0.016	2.744	0.6322
Males	3,363	-11.841	0.0227	3.0333	0.0067	0.3167	0.3065	0.016	1.927	0.4216
F+M	8,575	-11.801	0.0135	3.0210	0.0039	0.4437	0.4099	0.016	2.744	0.5433
5CDE+5AB+3CD (Commercial)										
Females	253	-10.359	0.2081	2.6726	0.0534	1.1168	0.3703	0.447	2.052	1.4237
Males	258	-10.373	0.2130	2.6741	0.0557	0.8995	0.2524	0.249	1.745	1.2031
F+M	511	-10.407	0.1413	2.6839	0.0366	1.0071	0.3342	0.249	2.052	1.3461
5CDE (Research Survey)										
Females	2,589	-11.691	0.0217	2.9889	0.0061	0.5689	0.5011	0.027	2.418	0.6395
Males	1,491	-11.852	0.0286	3.0362	0.0084	0.3565	0.3682	0.023	1.927	0.4820
F+M	4,080	-11.745	0.0168	3.0043	0.0048	0.4913	0.4683	0.023	2.418	0.5717
5CDE (Commercial)										
Females	181	-9.835	0.2172	2.5323	0.0562	1.0037	0.3423	0.447	2.052	1.3805
Males	214	-10.221	0.2159	2.6322	0.0567	0.8569	0.2427	0.249	1.745	1.2024
F+M	398	-9.981	0.1518	2.5695	0.0396	0.9277	0.3072	0.249	2.052	1.3139
5AB (Research Survey)										
Females	1,531	-12.010	0.0304	3.0881	0.0083	0.6254	0.4087	0.046	2.364	0.9322
Males	813	-12.214	0.0369	3.1484	0.0107	0.3738	0.3183	0.024	1.446	0.6126
F+M	2,345	-12.073	0.0225	3.1059	0.0063	0.5380	0.3982	0.024	2.364	0.8158
5AB (Commercial)										
Females	69	-10.176	0.7024	2.6399	0.1766	1.4060	0.2529	0.737	2.041	1.5211
Males	43	-10.681	1.1595	2.7638	0.2977	1.1056	0.1914	0.709	1.559	1.1787
F+M	113	-10.392	0.5231	2.6917	0.1325	1.2896	0.2721	0.709	2.041	1.4182
3CD (Research Survey)										
Females	1,093	-11.204	0.0553	2.8332	0.0161	0.2812	0.2002	0.016	2.744	0.3087
Males	1,053	-11.125	0.0564	2.8144	0.0168	0.2162	0.1217	0.016	0.82	0.1940
F+M	2,144	-11.137	0.0389	2.8159	0.0115	0.2495	0.1695	0.016	2.744	0.2554
4B (Research Survey)										
Females	413	-11.911	0.0509	3.0228	0.0150	0.3189	0.2657	0.009	1.207	0.4752
Males	353	-12.046	0.0463	3.0729	0.0141	0.2097	0.1697	0.008	1.165	0.3412
F+M	769	-11.950	0.0355	3.0387	0.0106	0.2680	0.2327	0.008	1.207	0.4158
4B (Commercial)										
Females	150	-12.653	0.1895	3.2713	0.0502	0.8797	0.5006	0.16	1.945	0.9751
Males	45	-13.105	0.3022	3.3963	0.0844	0.4700	0.3200	0.175	1.3	0.6547
F+M	195	-12.743	0.1495	3.2952	0.0401	0.7852	0.4956	0.16	1.945	0.9019

Table D.3. Length-weight parameter estimates, standard errors (SE) and number of observations (n) for Walleye Pollock (females, males and combined) for all research/charter and commercial samples from **midwater** trawls operating in stock areas 5CDE, 5AB, 3CD, and 4B from 1978 to 2015. $\bar{W}_{\text{pred}}$ = mean weight (in kg) from the fitted data set.

Stock	*n*	ln(*a*)	SE ln(*a*)	*b*	SE(b)	$\bar{W}_i$	SD W_i	min W_i	max W_i	$\bar{W}_{\text{pred}}$
5CDE+5AB+3CD (Research Survey)										
Females	2,021	-11.563	0.0394	2.9714	0.0103	0.9966	0.6098	0.027	4.654	0.8456
Males	1,671	-11.658	0.0411	3.0001	0.0110	0.8069	0.4869	0.046	2.875	0.6693
F+M	3,694	-11.592	0.0283	2.9806	0.0075	0.9106	0.5654	0.027	4.654	0.7644
5CDE+5AB+3CD (Commercial)										
Females	1,407	-11.934	0.0657	3.0738	0.0173	0.9101	0.4903	0.142	2.709	1.2227
Males	1,274	-11.777	0.0625	3.0400	0.0167	0.7874	0.3969	0.142	2.063	1.0096
F+M	2,675	-11.819	0.0449	3.0476	0.0119	0.8526	0.4526	0.142	2.709	1.1339

Stock	n	ln(a)	SE ln(a)	b	SE(b)	$\overline{W}_i$	SD W_i	min W_i	max W_i	$\overline{W}_{pred}$
5CDE (Research Survey)										
Females	1,567	-11.538	0.0512	2.9617	0.0132	1.1031	0.5640	0.031	2.667	1.0320
Males	1,322	-11.735	0.0488	3.0165	0.0129	0.8909	0.4750	0.046	2.875	0.7942
F+M	2,888	-11.618	0.0350	2.9838	0.0091	1.0056	0.5352	0.031	2.875	0.9149
5CDE (Commercial)										
Females	479	-10.037	0.1618	2.5916	0.0410	1.2674	0.3891	0.25	2.504	1.3768
Males	416	-10.033	0.1780	2.5898	0.0455	1.1515	0.3176	0.247	2.012	1.1830
F+M	895	-10.042	0.1184	2.5926	0.0301	1.2135	0.3621	0.247	2.504	1.2981
5AB (Research Survey)										
Females	76	-12.620	0.3905	3.2656	0.0985	1.5757	0.8348	0.38	4.654	0.9977
Males	39	-12.903	0.8839	3.3392	0.2269	1.1830	0.4557	0.484	2.313	0.6349
F+M	115	-12.659	0.3491	3.2759	0.0886	1.4425	0.7500	0.38	4.654	0.8401
5AB (Commercial)										
Females	551	-12.236	0.1151	3.1656	0.0301	0.9524	0.4240	0.142	2.709	1.0045
Males	588	-12.313	0.1209	3.1936	0.0323	0.7386	0.2755	0.142	2.063	0.7450
F+M	1,139	-12.158	0.0798	3.1488	0.0211	0.8417	0.3710	0.142	2.709	0.8745
3CD (Research Survey)										
Females	380	-12.175	0.0767	3.1530	0.0217	0.4437	0.3372	0.027	1.486	0.6422
Males	311	-12.479	0.0886	3.2508	0.0253	0.4037	0.2816	0.081	1.262	0.5475
F+M	691	-12.268	0.0594	3.1842	0.0169	0.4257	0.3138	0.027	1.486	0.6025
3CD (Commercial)										
Females	378	-9.850	0.1598	2.4750	0.0445	0.3944	0.1162	0.181	0.708	0.3754
Males	269	-10.305	0.1602	2.6065	0.0455	0.3351	0.0937	0.16	0.593	0.3365
F+M	645	-10.014	0.1095	2.5224	0.0308	0.3697	0.1113	0.16	0.708	0.3602
4B (Research Survey)										
Females	2,687	-10.643	0.0556	2.6923	0.0155	0.4183	0.2110	0.041	1.905	0.5454
Males	3,289	-10.926	0.0486	2.7655	0.0138	0.3283	0.1490	0.034	0.991	0.4533
F+M	5,979	-10.831	0.0360	2.7414	0.0101	0.3684	0.1842	0.015	1.905	0.4886
4B (Commercial)										
Females	542	-11.841	0.1569	3.0505	0.0431	0.5021	0.1728	0.138	1.47	0.6961
Males	809	-11.949	0.1193	3.0725	0.0337	0.3644	0.1222	0.118	0.87	0.5436
F+M	1,355	-12.043	0.0916	3.1017	0.0256	0.4193	0.1596	0.118	1.47	0.6173

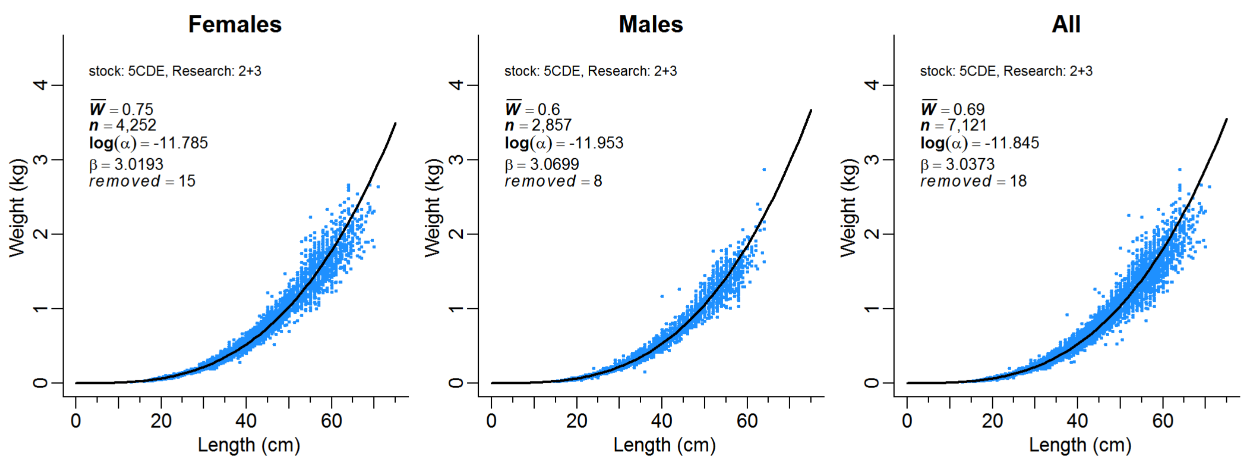

Figure D.1. Length-weight relationship for the North (5CDE) stock of Walleye Pollock – derived from randomly selected research survey samples, regardless of gear type. Records with absolute value of standardised residuals >3 (starting with a preliminary fit) were dropped, removing 18 observations for the combined-sex fit.

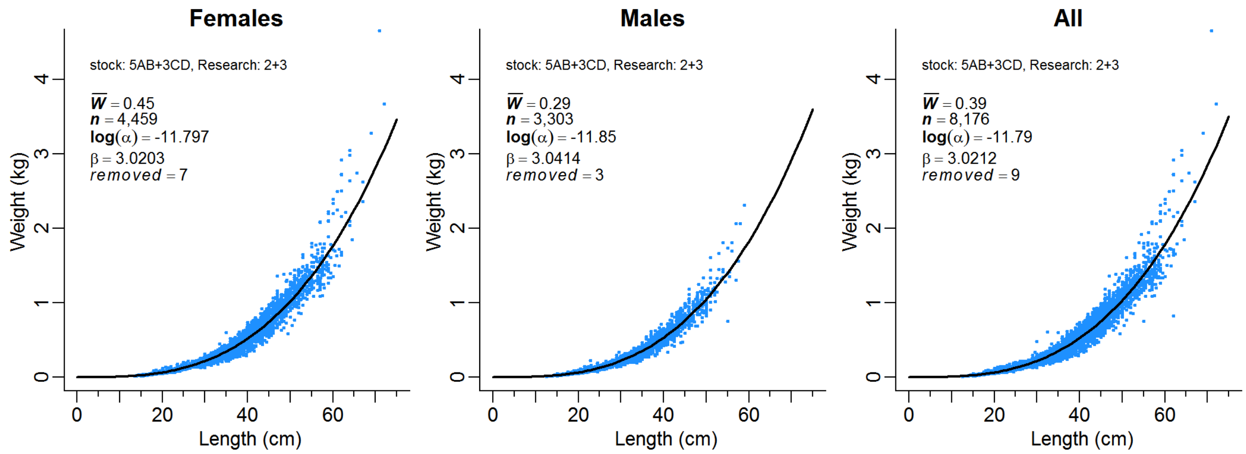

Figure D.2. Length-weight relationship for the South (5AB3CD) stock of Walleye Pollock – derived from randomly selected research survey samples, regardless of gear type. Records with absolute value of standardised residuals >3 (starting with a preliminary fit) were dropped, removing 9 observations for the combined-sex fit.

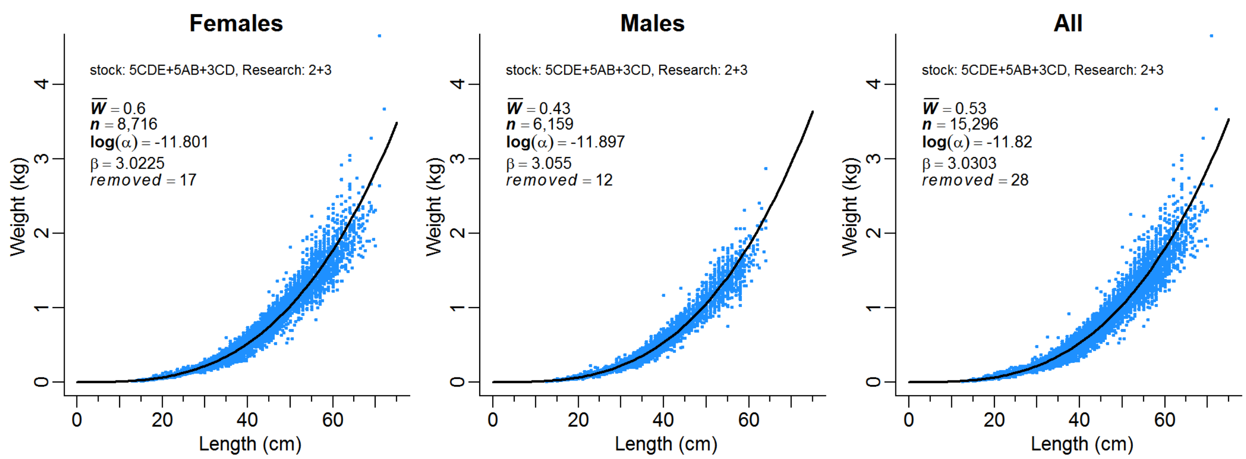

Figure D.3. Length-weight relationship for the combined North and South stocks of Walleye Pollock – derived from randomly selected research survey samples, regardless of gear type. Records with absolute value of standardised residuals >3 (starting with a preliminary fit) were dropped, removing 28 observations for the combined-sex fit.

For the assessment model input, the following procedure was followed to combine the length-weight information by sex into an interpolated unsexed length-weight relationship. This approach was used because it was felt that the sex ratio in the samples used to estimate the functions would not be representative of the population and that it was better to give equal weight to the length-weight model for each sex.

1. A combined sex weight W_i was calculated for every length i and sex m or f, using the sex-specific length-weight parameters calculated using (D.1) and (D.2), weighting equally between the estimated weight for each sex.
2. Parameters *a* and *b* were estimated such that the least-squares sum (D.3) between the averaged weight and an estimated weight was minimised.

The resulting function is the average of the sex-specific length-weight functions (Figure D.4).

$$W_i = 0.5\left(a_m L_i^{b_m}\right) + 0.5\left(a_f L_i^{b_f}\right) \qquad \text{(D.2)}$$

$$\sum_{i=10}^{100}\left(W_i - a\ L_i^b\right)^2 \qquad \text{(D.3)}$$

The allometric parameters (a,b) calculated using (D.2) were close to those estimated in Figure D.1 for BC North and Figure D.2 for BC South.

$$W_i = e^a L_i^b \begin{cases} \text{North: } a = \text{-}11.84492,\ b = 3.03728 \\ \text{South: } a = \text{-}11.78992,\ b = 3.02122 \end{cases}$$

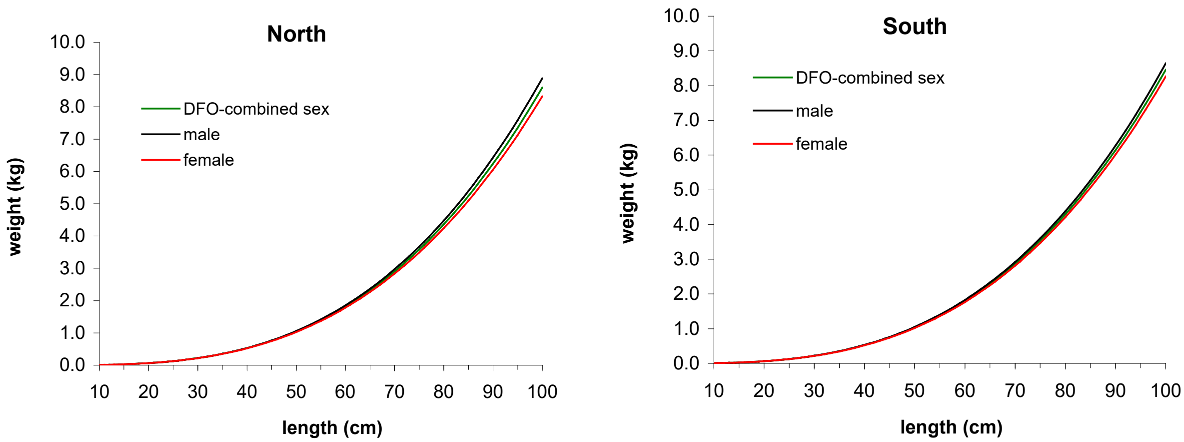

Figure D.4. Interpolated combined sex length-weight models used to estimate the Walford parameters used in the WAP delay-difference stock assessment model. [left panel]: North area model; [right panel]: South area model.

D.1.2. von Bertalanffy Growth

Paired observations i of length and age by sex, $\{L_{is}, a_{is}\}$, for $s = 1,2$ (males, females) were available using the break and burn method (MacLellan 1997) for only 17 specimens from commercial trips (16 otoliths in 5CDE and one otolith in 5AB). Otoliths aged by surface readings were more abundant (commercial: 230 otoliths in 5CDE and 399 otoliths in 5AB). The remaining samples come from research surveys but are aged using pectoral fin rays or an unknown method. Unfortunately, pectoral fin ageing is thought to be biased, especially at older ages (MacLellan et al. 1990), because fin ray deposition slows down or ceases at ages greater than ten. A summary of available age data in the GFBioSQL database by stock and ageing method appears in Table D.4. Also note the low number of samples from which these otoliths were collected.

Table D.4. Walleye Pollock number of ages available in GFBioSQL database by ageing method (accessed 2016-12-13). Number of samples appear in parentheses.

Stock	Otolith (surface)			Otolith (B&B)			Pectoral fin			Unknown		
	Female	Male	Total	Female	Male	Total	Female	Male	Total	Female	Male	Total
5CDE	165 (5)	65 (5)	230 (5)	14 (2)	2 (1)	16 (2)	0	0	0	0	0	0
5AB	210 (7)	189 (7)	399 (7)	0	1 (1)	1 (1)	305 (1)	144 (1)	449 (1)	0	0	0
3CD	0	0	0	0	0	0	100 (1)	89 (1)	189 (1)	123 (2)	87 (2)	210 (2)
4B	0	0	0	0	0	0	87 (2)	146 (2)	233 (2)	36 (2)	314 (2)	350 (2)

Growth was formulated as a von Bertalanffy model where lengths by sex, L_{is}, for fish $i = 1,\ldots,n_s$ are given by:

$$L_{is} = L_{\infty s}\left[1 - e^{-\kappa_s\left(a_{is} - t_{0s}\right)}\right] + \varepsilon_s, \quad \varepsilon_s \sim N\left(0, \sigma_s^2\right) \qquad \text{(D.4)}$$

where for each sex s,

$L_{\infty s}$ = the average length at maximum age of an individual,

κ_s = growth rate coefficient, and

t_{0s} = age at which the average size is zero.

The negative log likelihood for each sex s, used for minimisation is:

$$\ell\left(L_\infty, \kappa, t_0, \sigma\right) = n\ln\left(\sigma\right) + \frac{\sum_i^n \left(L_i - \hat{L}_i\right)^2}{2\sigma^2}, \qquad i = 1,\ldots,n.$$

The limited DFO data (Table D.4) did not yield satisfactory growth curves (Figure D.5 to Figure D.7) and were presumably biased by the ageing methods, which cannot resolve older ages. Therefore, we requested help from an Alaskan colleague, Martin Dorn (Research Fish Biologist, NOAA Fisheries, Sand Point, Seattle), who supplied us with 8,882 age-length pairs randomly selected from six biannual surveys conducted in the Gulf of Alaska (GoA) between 2005 and 2015. These fish had all been aged from otoliths prepared using the “break & burn” method and he advised us to use the specimens from the Eastern GoA only (n=847) as growth varied across the GoA. We used these data to estimate a growth function for use in this BC Pollock stock assessment (Figure D.8). The resulting function adequately fit the mean weight data for the BC North stock for all three of the credible knife-edge age at full selectivity assumptions (see all three panels in Figure D.9). However, we could not use this function for the BC South stock because fish sampled from Dixon Entrance were, on average, twice as large as those sampled from more southern BC waters. This North stock is likely to belong to a larger stock that includes Dixon Entrance, northern Hecate Strait, and waters off of Southeast Alaska (Gustafson et al. 2000). Consequently, we decided to divide BC Pollock into two stocks, with the North stock encompassing Dixon Entrance and upper Hecate Strait and the South stock including all Pollock from Moresby Gully to the US-Canada border.

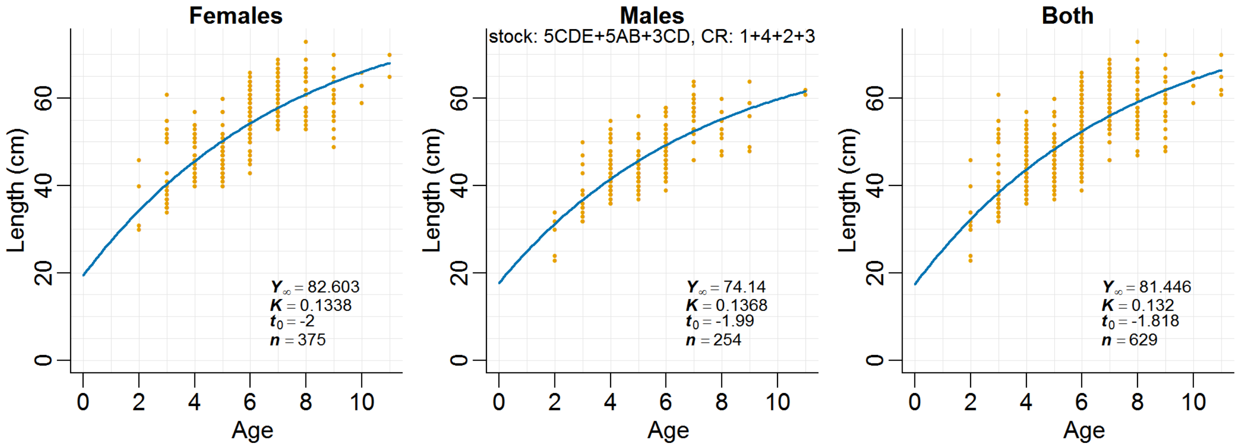

Figure D.5. von Bertalanffy fits to BC Walleye Pollock ages determined by surface-read otoliths.

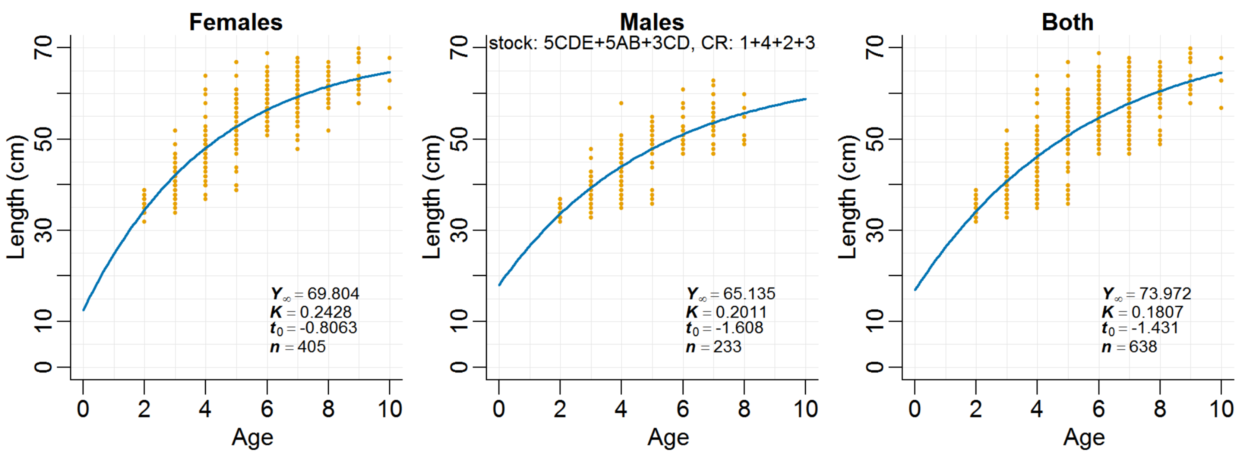

Figure D.6. von Bertalanffy fits to BC Walleye Pollock ages determined by pectoral fin rays.

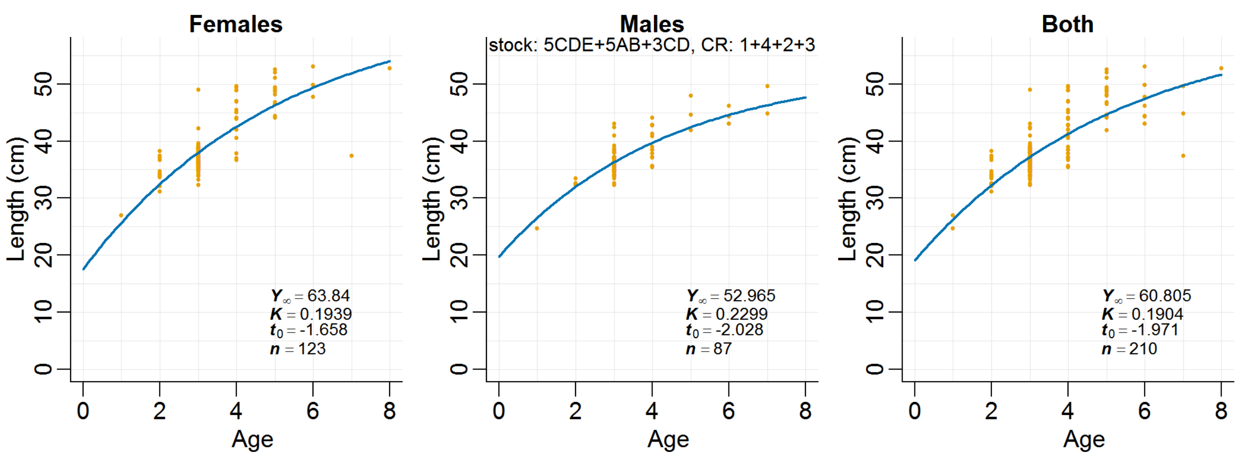

Figure D.7. von Bertalanffy fits to BC Walleye Pollock ages determined by unknown methods.

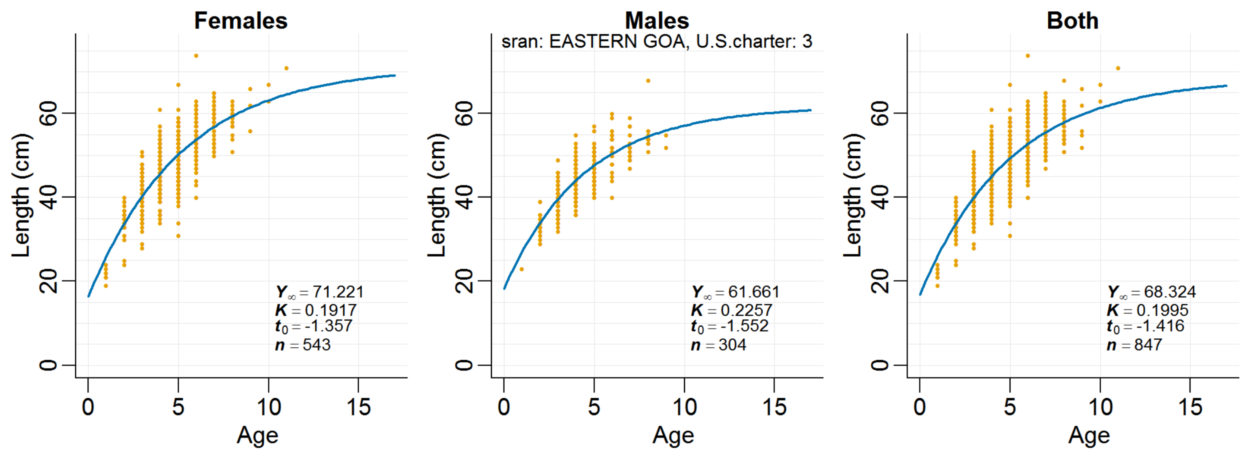

Figure D.8. von Bertalanffy fits to eastern Gulf of Alaska Walleye Pollock ages determined by broken-burnt otoliths.

For the BC South stock, the eastern GOA growth function did not provide a satisfactory fit to the mean weight data (either with knife-edge age=3 – see panel [a] Figure D.10 or knife-edge age=4, see panel [a] Figure D.11, so we turned to other sources (Table D.1). Growth functions based on fin ray ages published by Saunders et al. (1989) for the west coast of Vancouver Island (3CD) and the Strait of Georgia (apparently derived from age-length pairs not available in the general DFO database) were tested but featured growth rate coefficients (κ) that were so steep (0.31 and 0.91, respectively) that neither function could fit the South mean weight data satisfactorily when knife-edge age=4 (panels [b] and [c], Figure D.11. Even with knife-edge age=3, neither function gave good fits to the mean weight data (panels [b] and [c], Figure D.10. We also enquired with NOAA colleagues who were working on pelagic fish off the west coasts of Washington and Oregon who were able to provide us with sampled lengths for Pollock from their fisheries, but were unable to provide us with age-length pairs. In the end, we found a growth function published by Janusz and Horbowy (1997) for Walleye Pollock in the Sea of Okhotsk (L_∞ = 50.827, κ = 0.199, t_0 = -1.790, ages from otoliths), which provided satisfactory fits to the observed South mean weight data for both knife-edge age=3 (panel [d],Figure D. 10) and knife-edge age=4 (panel [d], Figure D.11.) We have no reason to believe that the Sea of Okhotsk relationship represents BC South other than the estimated growth was consistent with our mean weight data. We also noted that some authors have suggested similarities between Pollock populations in disconnected regions. For example, Thompson (1981) noted that populations of Pollock from the Strait of Georgia were more similar to those from the Bering Sea than they were to those in Dixon Entrance.

The following procedure was followed to combine the von-Bertalanffy growth model by sex into an interpolated unsexed growth model. This approach was used because it was felt that the sex ratio in the samples used to estimate the growth functions would not be representative of the population and that it was better to give equal weight to the growth model for each sex.

1. A combined sex length L_i is calculated for every age i and sex m or f, using the sex-specific growth model parameters calculated using (D.4) and (D.5), weighting equally between the estimated length for each sex.
2. Parameters L_∞, κ, t_0 are estimated such that the least-squares sum (D.6) between the averaged length and an estimated length is minimised.

The resulting function is the average of the sex-specific growth functions (Figure D.12). There is no evidence that these data show changes in size at age over time (Table D.5).

$$L_i = 0.5\left(L_{\infty m} e^{\left(-\kappa_m\left[a_{im}-t_{0m}\right]\right)}\right) + 0.5\left(L_{\infty f} e^{\left(-\kappa_f\left[a_{if}-t_{0f}\right]\right)}\right) \quad \text{(D.5)}$$

$$\sum_{i=1}^{50}\left(L_i - L_{\infty} e^{\left(-\kappa\left[a_i-t_0\right]\right)}\right)^2 \quad \text{(D.6)}$$

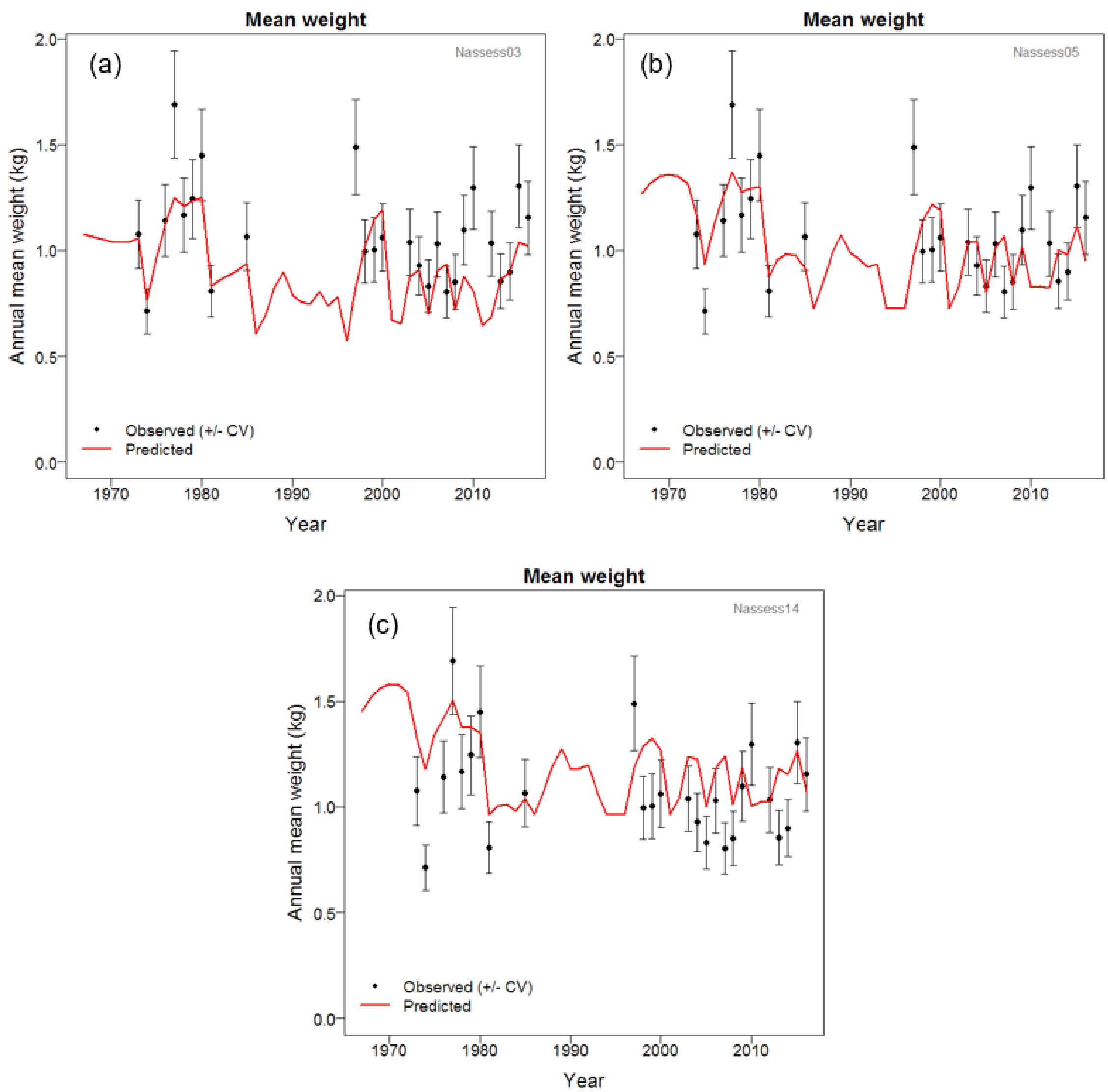

Figure D.9. Comparison of fits to the mean weight data for the BC North stock (Section D.2.2) under three knife-edge age assumptions. All three panels use the Eastern GoA growth function (Table D.6) and assume M=0.3. NLL=negative log likelihood provided for each fit; (a): knife-edge age=3 (NLL=0.059); (b) knife-edge age=4 (NLL=-5.97); (c) knife-edge age=5 (NLL=2.95).

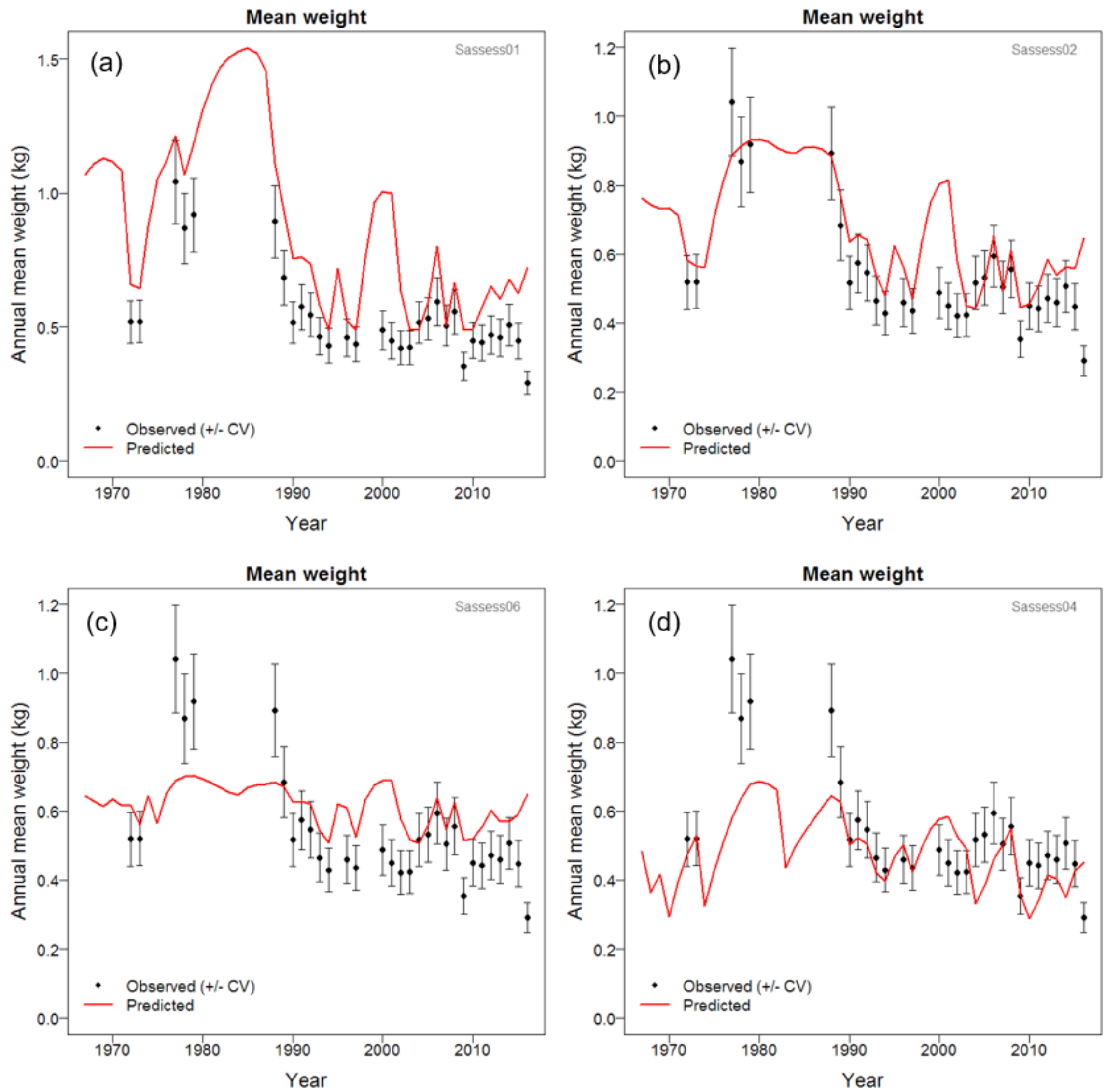

Figure D.10. Comparison of fits to the mean weight data for the BC South stock (Section D.2.2) under four growth rate assumptions (Table D.6), assuming the same age=3 at knife-edge selectivity and M=0.3. NLL=negative log likelihood provided for each fit; (a): E. GoA (NLL=50.5); (b) WCVI (NLL=10.0); (c) SG (NLL=17.3); (d) OS (NLL=10.8).

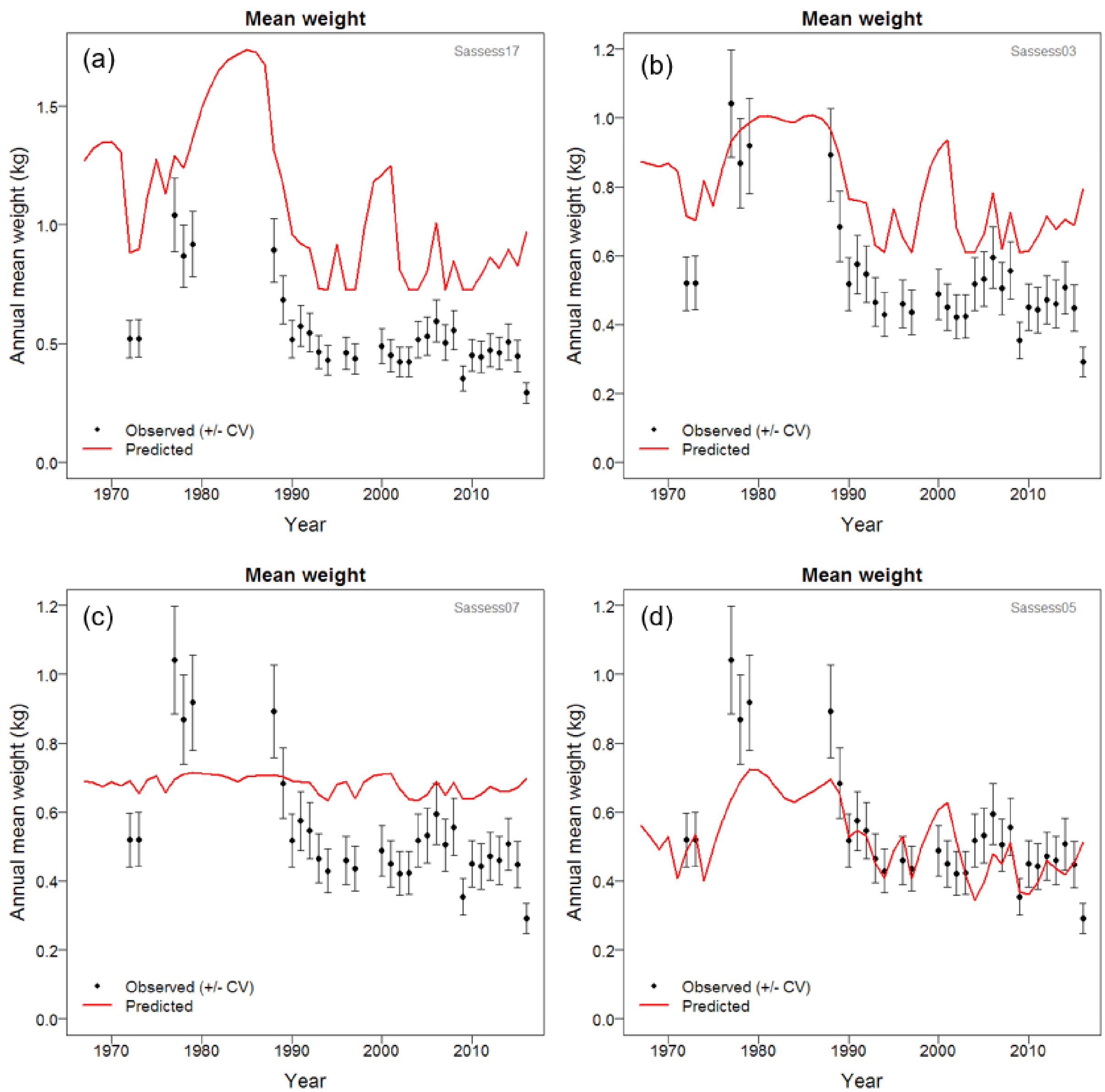

Figure D.11. Comparison of fits to the mean weight data for the BC South stock (Section D.2.2) under four growth rate assumptions (Table D.6), assuming the same age=4 at knife-edge selectivity and M=0.3. NLL=negative log likelihood provided for each fit; (a): E. GoA (NLL=204); (b) WCVI (NLL=76.1); (c) SG (NLL=58.9); (d) OS (NLL=0.58).

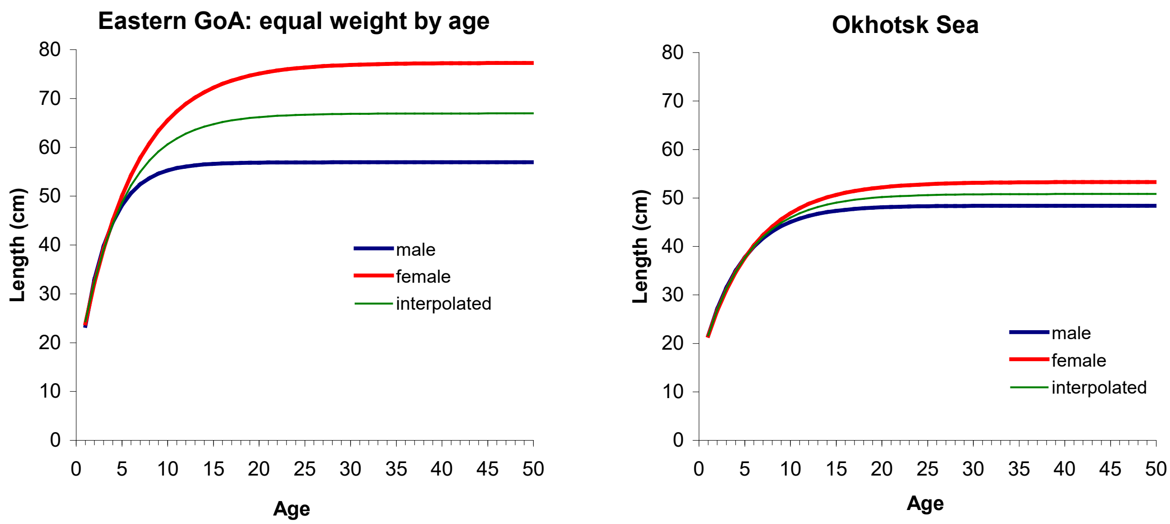

Figure D.12. Interpolated combined sex growth models used to estimate the Walford parameters used in the WAP delay-difference stock assessment model. [left panel]: Eastern Gulf of Alaska model; [right panel]: Okhotsk Sea model.

Table D.5. Mean length (cm) of Walleye Pollock, based on number of fish in brackets, by age and year for survey data from the Eastern Gulf of Alaska (Martin Dorn, pers. comm.).

Age	2005	2007	2009	2011	2013	2015	Total
0	5.0 [1]	7.0 [6]	---	---	--- ---	8.0 [2]	7.0 [9]
1	19.5 [190]	18.8 [40]	19.8 [97]	19.6 [99]	18.6 [103]	19.3 [28]	19.4 [557]
2	30.7 [51]	31.9 [28]	33.1 [62]	31.0 [56]	33.3 [8]	32.1 [24]	31.8 [229]
3	39.7 [202]	38.1 [73]	42.3 [96]	40.6 [57]	40.8 [39]	38.3 [100]	39.9 [567]
4	42.9 [128]	41.5 [36]	48.6 [38]	47.3 [29]	47.7 [41]	42.7 [26]	44.5 [298]
5	45.1 [108]	48.1 [16]	53.9 [32]	48.9 [52]	51.6 [30]	50.1 [21]	48.3 [259]
6	49.8 [29]	50.4 [10]	55.0 [14]	56.4 [19]	55.2 [14]	54.2 [26]	53.3 [112]
7	52.8 [11]	53.7 [7]	57.5 [8]	59.6 [13]	56.0 [5]	55.1 [8]	56.0 [52]
8	56.3 [8]	51.0 [1]	58.0 [4]	---	57.6 [7]	58.3 [8]	57.2 [28]
9	52.0 [1]	---	57.7 [3]	66.0 [1]	--- ---	--- ---	58.2 [5]
10	65.0 [2]	---	---	---	--- ---	--- ---	65.0 [2]

Table D.6. Walleye Pollock growth parameters by sex from von Bertalanffy fits (D.4); estimated parameters from a combined-sex, interpolated model (D.5) for the non-DFO sources were used in the delay-difference model (shaded). DFO parameters for the coastwide population are included for comparison only. E.GoA = eastern Gulf of Alaska, WCVI = west coast Vancouver Is., SG = Strait of Georgia, OS = Okhotsk Sea, DFO =Dept. Fisheries & Oceans Canada.

Source	Assess	Ageing Method	Females			Males			Combined		
			L_∞	κ	t_0	L_∞	κ	t_0	L_∞	κ	t_0
E.GoA (Dorn pers.comm.)	North	Otoliths (B&B)	71.221	0.192	-1.357	61.661	0.226	-1.552	66.944	0.212	-1.136
WCVI (Saunders et al. 1989)	South	Pectoral fins	56.500	0.300	-0.960	50.500	0.320	-0.970	53.499	0.309	-0.968
SG (Sauders et al. 1989)	South	Pectoral fins	46.500	0.835	0.559	42.500	0.997	0.590	44.498	0.905	0.572
OS (Janusz & Horbowy (1997)	South	Otoliths	53.300	0.177	-1.930	48.400	0.231	-1.560	50.827	0.199	-1.790
DFO (GFBioSQL 2017-12-13)	Coast	Pectoral fins	69.804	0.243	-0.806	65.135	0.201	-1.608	73.972	0.181	-1.431
DFO (GFBioSQL 2017-12-13)	Coast	Otoliths (sfc)	82.603	0.134	-2.000	74.140	0.137	-1.990	81.446	0.132	-1.818

D.1.3. Maturity

Maturity data for Walleye Pollock were obtained from GFBioSQL on Dec 13, 2016. Ages were scarce for this species and so data filtering was minimal for the maturity analysis. The following summary characterises the distribution of the 977 maturity data records used:

- stock – 3CD (385), 5AB (497), 5CDE (95)
- sex – males (405), females (572)
- trip type – non-observed commercial (394), charter (583)
- sample type – total catch (98), random(879)
- sampled catch – unsorted (583), sorted labelled as “keepers” (394)
- ageing method – unknown (210), surface otoliths (382), broken-burnt otoliths (12), pectoral fins (373)
- maturity codes – 1 (75), 2 (188), 3 (69), 4 (218) 5 (12), 6 (6), 7 (28), 10 (1), 12 (380)

In the GFBioSQL database, Walleye Pollock uses maturity convention 25 (Hake-Pollock, 7-stages), but may also have been using maturity convention 2 (Hake 1977+, 12-stages) as maturity codes 10 and 12 appeared. For the analysis, all stages 3 and higher were assumed to be mature, and a maturity ogive (Figure D.14) was fit to otolith and pectoral fin data using a double-normal model:

$$m_{as} = \begin{cases} e^{-(a-\nu_s)^2/\rho_{sL}}, & a \le \nu_s \\ 1, & a > \nu_s \end{cases} \qquad \text{(D.7)}$$

where, m_{as} = maturity at age a for sex s (combined),

ν_s = age of full maturity for sex s,

ρ_{sL} = variance for the left limb of the maturity curve for sex s.

The ages at 50% and full maturity are estimated at 3.6 y and 4.6 y, respectively, for otolith-aged fish and 2.4 y and 3.4 y, respectively, for fin-aged fish (Figure D.13). There appears to be a consistent difference between these two ageing methods, although the fit to these sparse data can be influenced by the initial values offered to the minimization of (D.7).

All commercial data comprise sorted fish and all charter data comprise unsorted fish (see maturity data composition bullets above). Comparing maturity ogives for sorted and unsorted catches (Figure D.14) unfortunately means lumping ages determined by surface-read otoliths and broken-burnt otoliths for the sorted ogive and pectoral fins and unknown methods for the unsorted ogive. The results are presented for comparison only.

The maturity schedules presented here (Table D.7) are not used in this assessment because the knife-edge selectivity assumption (*k* = 3 or 4 y) used by the delay-difference model assumes that maturity matches selectivity, i.e., all recruited fish are mature. This analysis shows that the estimated age at maturity for Walleye Pollock is similar to that for knife-edge recruitment investigated in the population model.

Alternative maturity ogives by length are shown in Figure D.15. Length data are more abundant than age data. The estimated length at full maturity from unsorted catch samples is 56.6 cm for the commercial fishery and 49.7 cm for research surveys. For sorted catch samples, the length at full maturity for the commercial fishery is 57.3 cm (no sorted samples from surveys).

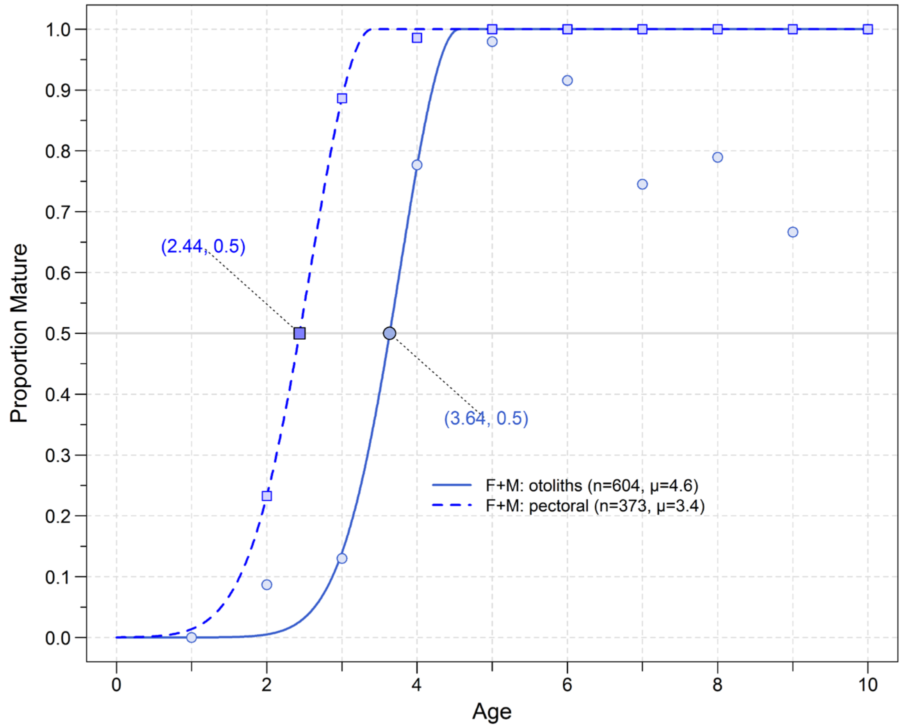

Figure D.13. Maturity-at-age ogives by ageing method for BC Walleye Pollock (data from Dec 13, 2016, GFBioSQL) as double-normal fits using (D.7) for both sexes combined, where maturity is defined by stages ≥ 3. Solid blue line shows fit to otolith data; blue dashed line indicates fit to pectoral fin data.

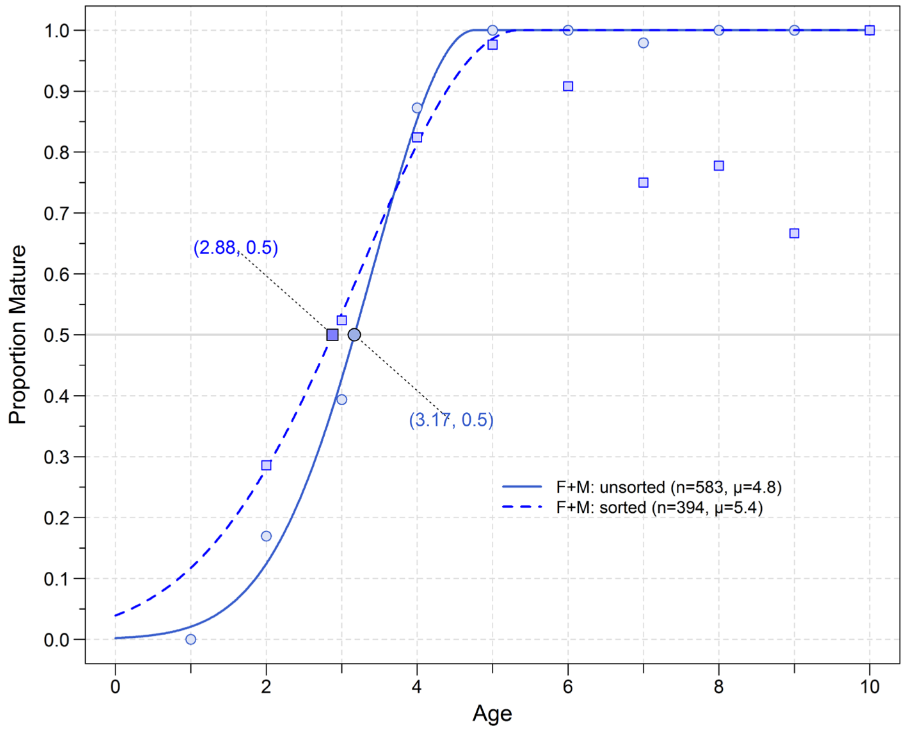

Figure D.14. Maturity-at-age ogives by catch sorting for BC Walleye Pollock (data from Dec 13, 2016, GFBioSQL) as double-normal fits using (D.7) for both sexes combined, where maturity is defined by stages ≥ 3. Solid blue line shows fit to otolith data; blue dashed line indicates fit to pectoral fin data.

Table D.7. Proportion of Walleye Pollock mature at each age (m_a) up to age 10y. Maturity stages 1 and 2 describe immature fish while stages 3 to 12 are considered mature. Model fits are presented for the binomial logit (BL, comparison only) and the double normal (DN).

Age	# Fish	Obs. m_a	BL m_a	DN m_a	Age	# Fish	Obs. m_a	BL m_a	DN m_a
		Otoliths					Pectoral		
1	2	0	0.07347	0.00004	1	0	0	0.01474	0.01388
2	23	0.08696	0.16830	0.00500	2	43	0.23256	0.24427	0.23256
3	154	0.12987	0.34053	0.13948	3	88	0.88636	0.87475	0.88636
4	139	0.77698	0.56854	0.77461	4	71	0.98592	0.99342	1
5	99	0.97980	0.77078	1	5	43	1	0.99969	1
6	107	0.91589	0.89563	1	6	58	1	0.99999	1
7	51	0.74510	0.95633	1	7	45	1	1.00000	1
8	19	0.78947	0.98242	1	8	17	1	1	1
9	9	0.66667	0.99304	1	9	5	1	1	1
10	1	1	0.99726	1	10	3	1	1	1
		Unsorted					Sorted		
1	2	0	0.01658	0.02087	1	0	0	0.73652	0.11727
2	59	0.16949	0.10180	0.12429	2	7	0.28571	0.76385	0.28038
3	221	0.39367	0.43247	0.42829	3	21	0.52381	0.78915	0.53463
4	102	0.87255	0.83669	0.85370	4	108	0.82407	0.81241	0.81302
5	58	1	0.97179	1	5	84	0.97619	0.83364	0.98603
6	67	1	0.99570	1	6	98	0.90816	0.85291	1
7	48	0.97917	0.99936	1	7	48	0.75000	0.87029	1
8	18	1	0.99990	1	8	18	0.77778	0.88589	1
9	5	1	0.99999	1	9	9	0.66667	0.89983	1
10	3	1	1.00000	1	10	1	1	0.91224	1

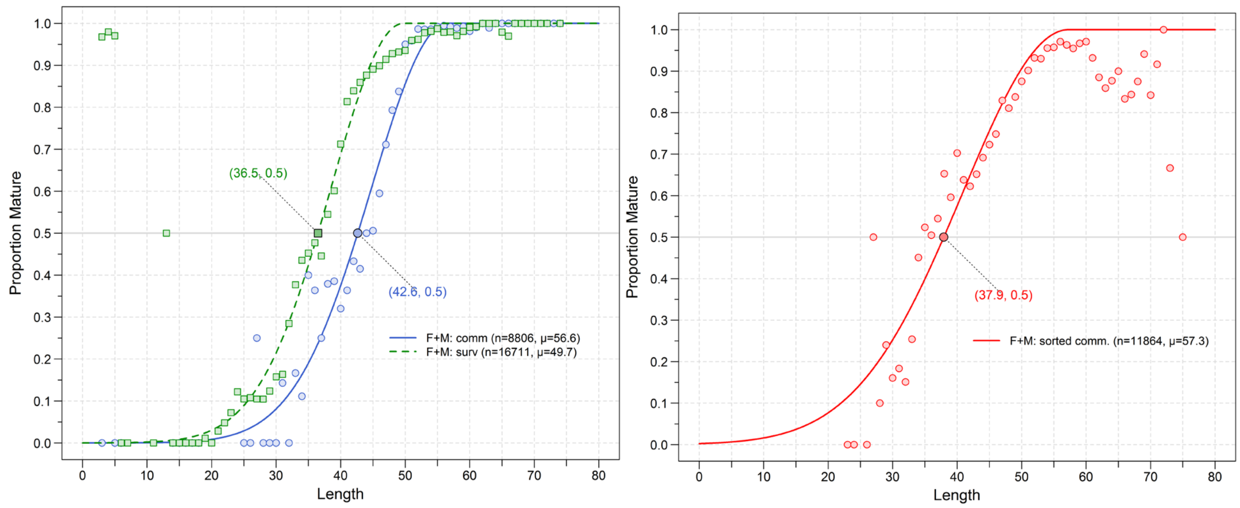

Figure D.15. Maturity-at-length ogives for BC Walleye Pollock: (left) unsorted samples from the commercial fishery (trip types 1,4,5 combined in blue) and research surveys (trip types 2,3 combined in green); (right) sorted samples from the commercial fishery (red). Curves depict double-normal fits using (D.7) for both sexes combined, where maturity is defined by stages ≥ 3.

D.1.4. Natural Mortality

Although the Alaskan fisheries stock assessments use age-specific mortality rates for Walleye Pollock, the underlying assumption is that M = 0.30 for age at full maturity (Dorn et al. 2015). Age-specific M values of 0.90, 0.45, and 0.30 for ages 1, 2 and 3+, respectively, have been used in Alaskan Eastern Bering Sea catch-age models since 1982 (Ianelli et al. 2015). The delay-difference model used for the BC population assumes that maturity matches selectivity, i.e., all recruited fish are mature, and by extension, all mature fish have a natural mortality rate of 0.30, which is the value adopted by this assessment. Sensitivity runs were made with M=0.25 and M=0.35 to bracket plausible values for this parameter.

In the DFO database GFBioSQL, the maximum age is 11 years for two female and two male specimens caught at depths between 106 and 381 m in PMFC area 5CD, specifically in Moresby Gully; however the mean age is 5.0 y (n=1494) and the 0.99 quantile is 9 y. McFarlane and Beamish (1990) reported a maximum age of 28 y from the Bering Sea using a burnt otolith section method. These authors generally found that the burnt otolith method produced higher estimates of age when comparing them to ages from fin rays (Beamish and McFarlane 1995, and see Figure D.13).

The current assessment does not use catch-at-age information as the data are insufficient and potentially biased by the ageing methodology. However, natural mortality (M) can be estimated using Quinn and Deriso (1999, p.361) based on Hoenig (1983):

$$M = -\ln(0.01)/t_m \qquad \text{(D.8)}$$

where, t_m = maximum observed age reach by 1% of the population.

Using the maximum age observed in the DFO database t_m = 11 y, M = 0.419, which seems high compared to M =0.30 adopted for use in the delay-difference model. However, using t_m = 28 y, natural mortality M = 0.164, which seems low for this species.

Then et al. (2015) revisited various natural mortality estimators and recommended the use of an updated Hoenig estimator based on nonlinear least squares:

$$M_{\text{est}} = 4.899\, t_{\max}^{-0.916} \qquad \text{(D.9)}$$

where $t_{\max}$ = maximum age. For WAP with a maximum age of 11 y (GFBio) or 28 y (McFarlane and Beamish 1990), the updated Hoenig estimator suggests that *M* = 0.55 or 0.23, respectively.

D.1.5. Knife-edge Selectivity and Walford Plot

Dorn et al. (2012) provide a range of selectivity ogives for the GoA fisheries and surveys, with the median age selected to these commercial fisheries ranging from age 3 to age 5 (see columns 5 to 7 in Table D.8). Based on the ogives in this table, ages 3 and 4 were selected as the most likely ages to use for the age of knife-edge recruitment in the WAP delay-difference model. Knife-edge selectivity at age 5 was also run as an additional sensitivity for both stock definitions. Growth and length-weight parameters appropriate were used to prepare Walford plots (Figure D.16) which provide the growth parameter values used as input to the WAP delay-difference model. The Walford parameters are calculated from the knife-edge recruitment age to 30 y for the Section D.1.2 growth model. The Walford parameters will vary slightly with changing age assumptions at knife-edge recruitment for both growth models. Table D.9 presents the Walford parameters used in the stock assessment for both growth models along with the mean length and mean weight associated with each of the knife-edge age at recruitment assumptions. Equilibrium mean weights assuming *M*=0.3 are also presented for comparative purposes.

Table D.8. Table 1.17 taken from Dorn et al. (2012) showing various selectivity ogives estimated for Gulf of Alaska pollock fisheries and surveys.

Table I.17 Estimated selectivity at age for Gulf of Alaska Pollock fisheries and survey. The fisheries and surveys were modeled using double logistic functions.

Age	*POP fishery (1964-71)*	*Foreign (1972-81)*	*Foreign and JV (1982-1988)*	*Domestic (1989-2000)*	*Domestic (2001-2006)*	*Recent domestic (2007-2012)*	*Acoustic survey*	*Bottom trawl survey*	*ADF&G bottom trawl*
1	0.000	0.002	0.016	0.004	0.029	0.030	0.584	0.358	0.011
2	0.000	0.020	0.082	0.022	0.102	0.171	0.974	0.202	0.039
3	0.003	0.187	0.399	0.110	0.304	0.578	0.933	0.314	0.131
4	0.438	0.727	0.771	0.405	0.632	0.902	0.870	0.478	0.358
5	1.000	0.977	0.989	0.796	0.881	0.984	0.778	0.692	0.673
6	0.793	1.000	1.000	0.964	0.981	0.998	0.657	0.905	0.884
7	0.504	0.966	0.859	1.000	1.000	1.000	0.519	1.000	0.966
8	0.254	0.820	0.528	0.985	0.938	0.998	0.380	0.904	0.991
9	0.108	0.476	0.202	0.836	0.628	0.930	0.259	0.690	0.998
10	0.042	0.159	0.056	0.374	0.188	0.323	0.168	0.477	1.000

Table D.9. Age varying biological parameters used in the WAP delay-difference stock assessment using two growth models.

	Age at knife-edge recruitment			
	GoA growth model (North)		**Okhotsk Sea growth model (South)**	
Parameter	**3**	**4**	**3**	**4**
α_g	0.347	0.372	0.144	0.153
ρ_g	0.867	0.856	0.871	0.861
length (cm) at W_k	39.1	44.4	31.2	34.8
W_k (kg)	0.493	0.727	0.249	0.344
$\bar{W}_0$ (kg)[1]	1.076	1.269	0.483	0.561

[1] assumes *M*=0.3 for comparative purposes.

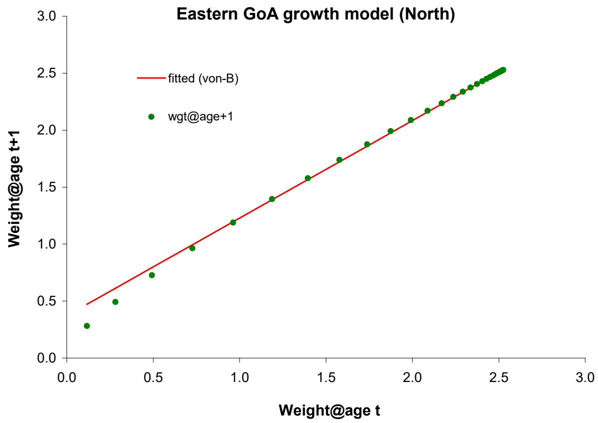

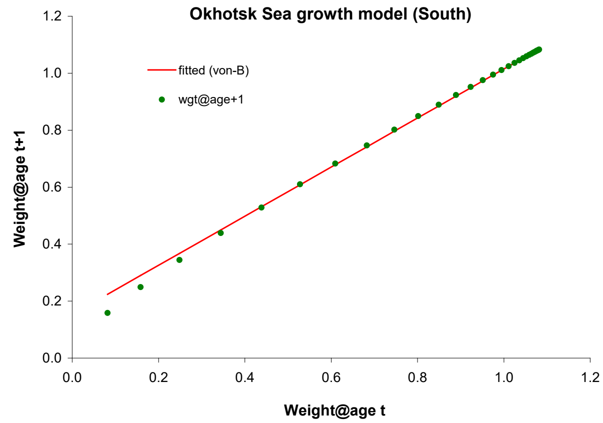

Figure D.16. Walford plot for WAP using age=4y as the knife-edge recruitment assumption: [left panel]: Eastern GoA growth model (North); [right panel]: Okhotsk Sea growth model (South). Plotted points are the estimated weight-at-age from the growth model and the line is the fitted Walford plot to the points.

D.2. MEAN WEIGHT

Data used to estimate the mean weight by year for this stock assessment were selected following the relevant guidelines in Table D.1. The biological data for WAP (downloaded from the GFBio database, Dec 13, 2016) yielded 345,429 records which were filtered as follows:

- year = 1967:2016 {modern} 344,377 records
- stock = c("3CD","5AB","5CDE") {outer coast} 218,136 records
- trip type = c(1,4,5) {comm. incl. JV Hake} 102,254 records
- sample type = c(1,2,6,7) {random} 100,596 records
- gear type = c(1,6) {trawl: BW + MW} 98,292 records
- spp. category = 1 {unsorted} 50,998 records

or

- spp. category = 3 {keepers = sorted} 46,769 records

This process resulted in 50,998 biological records for unsorted samples, all containing length data but only 266 records with weight data, and 46,769 records for sorted (keeper) samples, all but one with length data and 2,750 records with weight data. Weights, missing or otherwise, were calculated from the measured lengths using the length-weight regression (D.1) described in Section D.1.1, specifically $W = e^a L^b = e^{-11.82032} L^{3.03028}$.

D.2.1. GLM method – unsorted vs. sorted samples (coastwide)

To remove some of the variance due to influential factors in the data, an additive lognormal model (Schnute et al. 2004) was used to adjust the annual index of fish weight for minor PMFC area:

$$w_{ij} = \mu + \alpha_i + \beta_j + \sigma\varepsilon_{ijm} \qquad \text{(D.10)}$$

where, μ = the overall mean;

α_i = year effect (with missing years)

unsorted: i_1 = 1972, i_N = 2016, where N = 38 available years,

sorted: i_1 = 1975, i_N = 2009, where N = 31 available years;

β_j	=	minor PMFC area effect
		unsorted: (1, 2, 3, 4, 5, 6, 7, 8, 11, 12, 20, 21, 23, 35),
		sorted: (0, 1, 2, 3, 4, 5, 8, 11, 12, 20, 21, 23);
m	=	number of fish weight values;
σ	=	standard deviation of the model; and
ε_{ijm}	=	independent residuals assumed to be standard normal N(0,1).

The fitted unsorted-catch model had a residual standard error of 0.2984 on 50,947 degrees of freedom (multiple R^2 = 0.6695, adjusted R^2 = 0.6691, Figure D.17). The fitted sorted-catch model had a residual standard error of 0.3682 on 46,727 degrees of freedom (multiple R^2 = 0.4458, adjusted R^2 = 0.4453, Figure D.18).

The main purpose of the GLM fit was to adjust for trend in the annual indices of weight; however, the process rendered the scale of the indices relative. To transform the relative indices back to absolute, they were multiplied by the ratio of the geometric mean of the non-standardised annual indices (0.7606 kg/fish) to the geometric mean of the standardised (and sometimes normalized) indices (1 kg/fish); see results in Table D.10.

$$w_{ai} = w_{si}\left[\left(\prod_{i_1}^{i_N} w_{ui}\right)^{1/N} \middle/ \left(\prod_{i_1}^{i_N} w_{si}\right)^{1/N}\right] \qquad \text{(D.11)}$$

where, $i_{1,\ldots,N}$ = annual index (unsorted: *N*=38 years, sorted: *N*=31 years),

w_{ui} = unstandardized annual mean weights (kg/fish),

w_{si} = GLM-standardized annual mean weights (kg/fish), and

w_{ai} = adjusted GLM-standardized annual mean weights (kg/fish).

The standardization removed substantial spatial effects from area, specifically PMFC minor area (Figure D.17, Figure D.18). Additional effects (e.g., season, depth, sex) were explored but their effects on the annual index series were minimal and consequently not used. Only season could have been used without losing annual indices; data for the other effects were not universally available for all years. The mean weight of unsorted fish (0.67989 kg/fish, Table D.10) was lower than that for sorted (kept) fish (1.09049 kg/fish, Table D.11). The delay-difference model assumes that signals in mean weight trend result from recruitment, not spatial movement of the fishery.

*Table D.10. Annual mean weight (kg) per Walleye Pollock using samples of **unsorted** catch aboard commercial trawlers: w_{ui} = non-standardized (non-std), w_{si} = GLM-standardized (glm-std), w_{ai} = adjusted GLM-standardized (adj glm-std); numbers of fish used for annual mean calculations are also reported. Final row reports geometric mean weight of all years with data.*

Year	# Fish	Fish wt. (non-std)	Fish wt. (glm-std)	Fish wt. (adj glm-std)	Year	# Fish	Fish wt. (non-std)	Fish wt. (glm-std)	Fish wt. (adj glm-std)
1972	140	0.87075	1.00025	0.67990	1998	152	0.96381	0.92997	0.63212
1973	2324	1.00374	0.75808	0.51529	1999	610	1.17332	1.09209	0.74232
1974	77	0.83167	1.29147	0.87784	2000	1502	0.83841	1.04592	0.71094
1976	593	1.36151	1.48094	1.00663	2001	3074	0.24238	0.95541	0.64941
1977	1308	1.27842	2.02779	1.37834	2002	293	0.25857	0.79753	0.54210
1978	6071	1.29251	1.32626	0.90149	2003	732	0.62835	0.80124	0.54463
1979	5350	1.38308	1.27879	0.86922	2004	547	0.73322	0.94263	0.64073
1980	1204	0.82737	1.49355	1.01520	2005	340	0.93635	0.91294	0.62054
1981	908	1.10047	0.82731	0.56234	2006	1440	0.64403	1.00675	0.68431

Year	# Fish	Fish wt. (non-std)	Fish wt. (glm-std)	Fish wt. (adj glm-std)	Year	# Fish	Fish wt. (non-std)	Fish wt. (glm-std)	Fish wt. (adj glm-std)
1985	255	1.43418	1.08711	0.73894	2007	867	0.76250	0.86537	0.58821
1988	3598	0.70947	1.51776	1.03166	2008	104	0.74438	0.95243	0.64739
1989	3527	0.43554	1.29587	0.88084	2009	470	0.78158	0.81327	0.55280
1990	719	0.54339	0.97948	0.66577	2010	562	0.75736	0.94711	0.64378
1991	337	0.48092	1.08684	0.73875	2011	592	0.50006	0.87682	0.59599
1992	3340	0.33721	1.03111	0.70087	2012	1190	0.53003	0.79461	0.54012
1993	1336	0.27738	0.88058	0.59855	2013	610	0.72040	0.78201	0.53155
1994	60	0.37424	0.81273	0.55244	2014	1276	0.49386	0.86495	0.58793
1996	3942	0.27973	0.87060	0.59177	2015	384	0.92280	0.80019	0.54391
1997	924	0.45531	0.82335	0.55965	2016	240	0.82869	1.00191	0.68102
-	-	-	-	-	-	Σ = 50998	$\prod^{1/N}$ = 0.67972	$\prod^{1/N}$ = 1.00000	$\prod^{1/N}$ = 0.67972

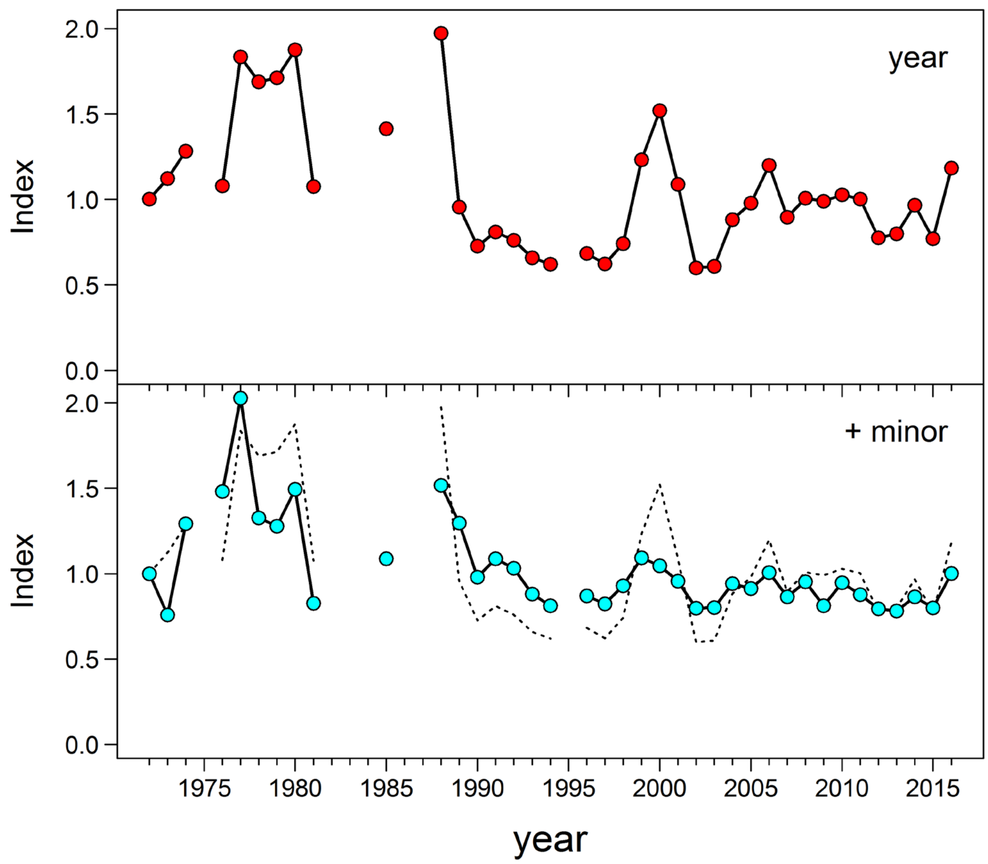

*Figure D.17. Normalised mean weight (kg/fish) of WAP coastwide estimated from (D.10) using data from sampling **unsorted** catch (original geometric mean = 0.680 kg/fish). Panels from top to bottom show how the annual indices change as residual variance from each factor (in this case, only PMFC minor area) is removed. Broken lines show the index series in the panel above (using the factor accepted just prior to that depicted in the current panel).*

*Table D.11. Annual mean weight (kg) per Walleye Pollock from samples of **sorted** (coded as "keepers") catch aboard commercial trawlers coastwide: see Table D.10 caption for details.*

Year	# Fish	Fish wt. (non-std)	Fish wt. (glm-std)	Fish wt. (adj glm-std)	Year	# Fish	Fish wt. (non-std)	Fish wt. (glm-std)	Fish wt. (adj glm-std)
1975	475	1.11523	1.00740	1.09016	1994	1997	1.29558	1.36343	1.47544
1976	1408	1.34492	0.81094	0.87757	1995	3871	1.31178	1.20889	1.30821
1977	699	1.31660	1.09264	1.18241	1996	2282	1.55122	1.25881	1.36223
1978	3106	1.29478	1.09655	1.18665	1997	554	1.19400	1.46935	1.59007
1979	1623	1.42501	1.10631	1.19720	1998	548	1.16599	1.16118	1.25658
1980	1233	0.97085	1.13920	1.23280	1999	2552	1.18719	0.89451	0.96800
1981	1469	1.12347	0.76335	0.82607	2000	1707	1.12938	0.92542	1.00145
1982	3404	1.20553	0.90398	0.97825	2001	2000	0.39071	0.91688	0.99221
1983	2095	1.24211	0.92093	0.99659	2002	768	0.29984	0.72025	0.77943
1984	868	1.10698	0.96721	1.04667	2003	1749	0.83749	0.79294	0.85808
1985	3296	1.30633	0.86806	0.93938	2004	983	0.53450	0.99397	1.07563
1986	251	1.50615	1.06892	1.15674	2005	750	0.72745	0.65608	0.70999
1990	1047	1.27638	1.32541	1.43431	2006	350	0.77008	0.85718	0.92760
1991	438	1.53763	1.14233	1.23618	2007	500	1.12009	0.73788	0.79851
1992	2587	1.39607	1.32153	1.43010	2009	200	1.48541	0.86547	0.93657
1993	1958	1.35347	1.29682	1.40336	-	-	-	-	-
-	-	-	-	-	-	Σ = 46768	$\prod^{1/N}$ = 1.08216	$\prod^{1/N}$ = 1.00000	$\prod^{1/N}$ = 1.08216

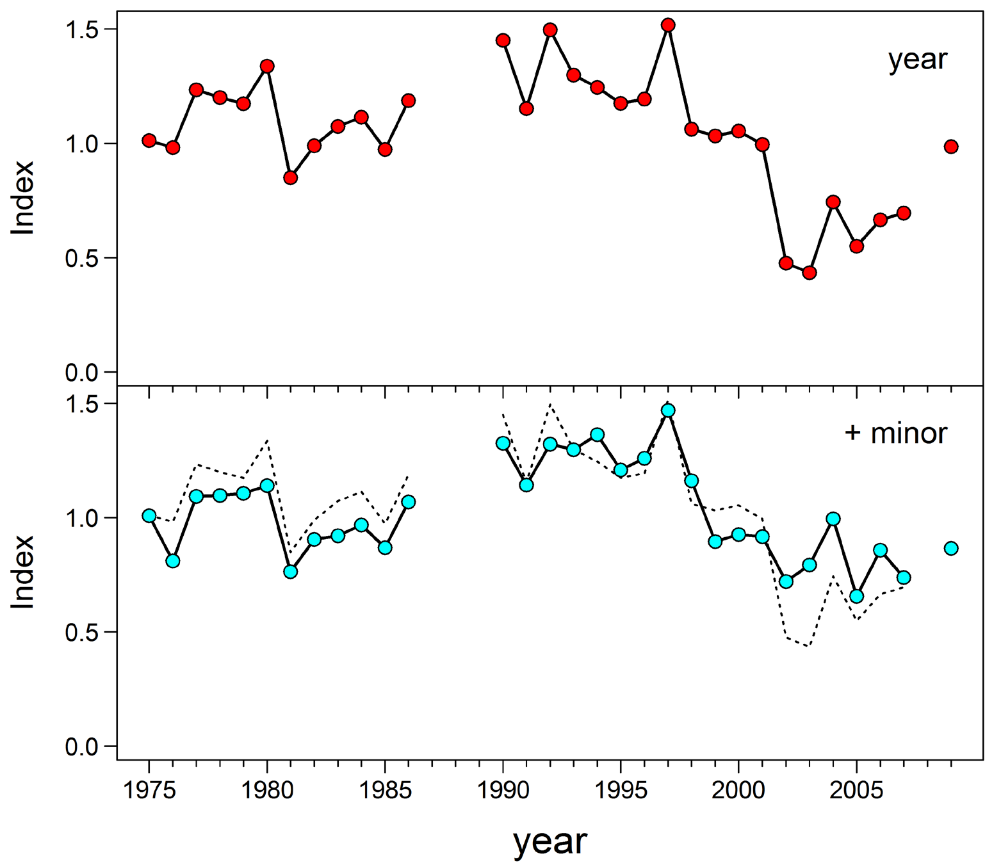

*Figure D.18. Normalised mean weight (kg/fish) of WAP coastwide estimated from (D.10) using data from sampling **sorted** (keepers) catch (original geometric mean = 1.082 kg/fish). See Figure D.17 caption for additional detail.*

D.2.2. North vs. South (unsorted)

The same GLM standardisation (D.10) and (D.11) using PMFC minor area as a factor was applied to the North and South stocks of Walleye Pollock to derive stock-specific mean weight series. Only unsorted samples were used for these analyses. The most striking feature between the North and the South is that fish are roughly twice as large in the North with a geometric mean weight of 1.056 kg/fish vs. 0.521 kg/fish in the South. The mean weight series for the North appears in Table D.12 and Figure D.19 and for the South in Table D.13 and Figure D.20.

While coastwide mean weights were used in the exploratory phase of the assessment, only mean weights from the North and South were used in the delay-difference model results in Appendix F.

Table D.12. Annual mean weight (kg) per Walleye Pollock using unsorted samples from the ***North*** *stock caught aboard commercial trawlers: : w_{ui} = non-standardized (non-std), w_{si} = GLM-standardized (glm-std), w_{ai} = adjusted GLM-standardized (adj glm-std); number of samples and fish used for annual mean calculations are also reported. Final row reports geometric mean weight of all years with data..*

Year	# Samp	# Fish	Fish wt. (non-std)	Fish wt. (glm-std)	Fish wt. (adj glm-std)	Year	# Samp	# Fish	Fish wt. (non-std)	Fish wt. (glm-std)	Fish wt. (adj glm-std)
1973	4	666	0.44522	1.01932	1.07634	2003	2	125	1.01387	0.98346	1.03847
1974	1	77	0.83361	0.67685	0.71471	2004	3	219	0.85789	0.87875	0.92790
1976	4	593	1.36630	1.08168	1.14219	2005	3	193	1.06979	0.78859	0.83270
1977	10	738	1.19360	1.59989	1.68938	2006	2	109	0.82390	0.97472	1.02924
1978	26	5293	1.26248	1.10469	1.16649	2007	3	170	0.88071	0.76224	0.80487
1979	34	5150	1.40211	1.17811	1.24401	2008	1	51	1.22924	0.80679	0.85192
1980	6	1204	0.82942	1.37333	1.45015	2009	4	187	1.35303	1.03832	1.09641
1981	4	908	1.10393	0.76645	0.80933	2010	4	230	1.12128	1.22896	1.29770
1985	1	255	1.43928	1.00857	1.06498	2012	2	122	0.99180	0.97924	1.03401
1997	2	97	1.08712	1.41041	1.48931	2013	5	206	0.96015	0.81048	0.85582
1998	3	152	0.96654	0.94375	0.99655	2014	4	204	1.07054	0.85253	0.90022
1999	5	610	1.17708	0.95078	1.00397	2015	5	331	0.99307	1.23533	1.30443
2000	11	923	1.14732	1.00518	1.06140	2016	1	60	1.61203	1.09369	1.15487
-	-	-	-	-	-	-	Σ = 150	Σ = 18873	$\prod^{1/N}$ = 1.05594	$\prod^{1/N}$ = 1.00000	$\prod^{1/N}$ = 1.05594

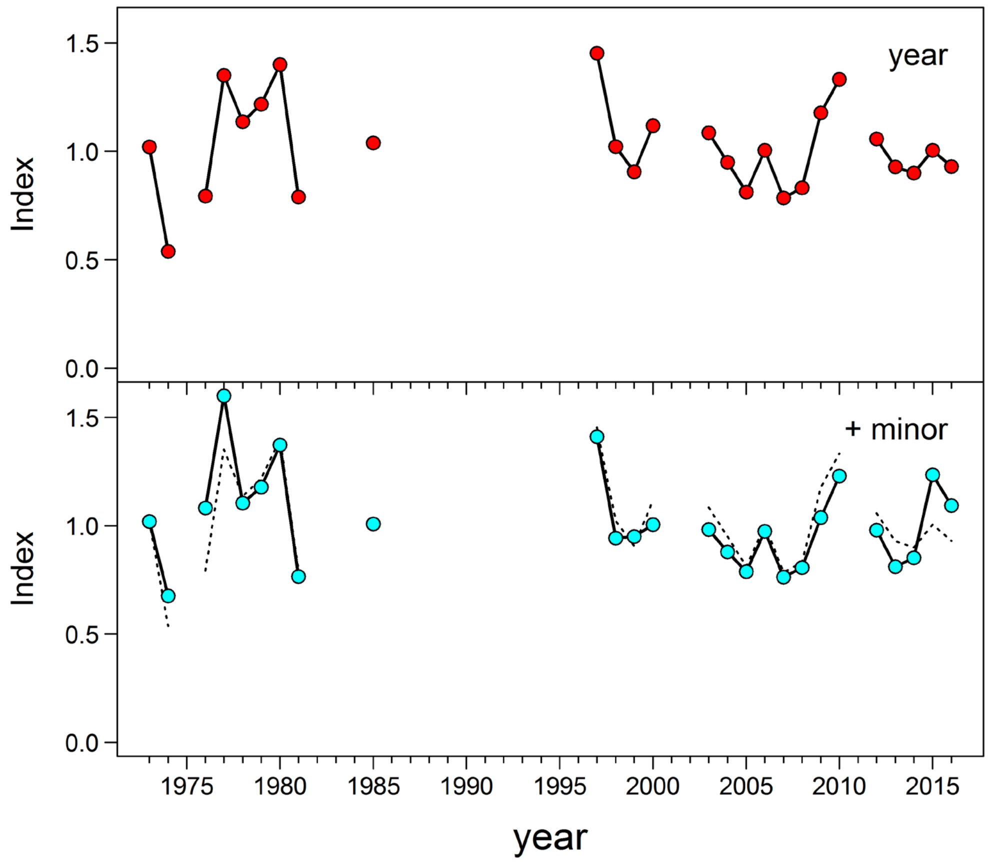

*Figure D.19. Normalised mean weight (kg/fish) of WAP **North** estimated from (D.10) using data from sampling unsorted catch (original geometric mean = 1.056 kg/fish). Panels from top to bottom show how the annual indices change as residual variance from each factor (in this case, only PMFC minor area) is removed. Broken lines show the index series in the panel above (using the factor accepted just prior to that depicted in the current panel).*

*Table D.13. Annual mean weight (kg) per Walleye Pollock using unsorted samples from the **South** stock caught aboard commercial trawlers: see Table D.12 caption for details.*

Year	# Samp	# Fish	Fish wt. (non-std)	Fish wt. (glm-std)	Fish wt. (adj glm-std)	Year	# Samp	# Fish	Fish wt. (non-std)	Fish wt. (glm-std)	Fish wt. (adj glm-std)
1972	2	140	0.86657	0.99684	0.51888	2002	2	293	0.25799	0.81064	0.42196
1973	9	1658	1.22141	1.00120	0.52115	2003	9	607	0.54768	0.81378	0.42359
1977	4	570	1.38474	1.99986	1.04098	2004	5	328	0.64893	0.99373	0.51726
1978	4	778	1.51574	1.66741	0.86793	2005	4	147	0.76201	1.02091	0.53141
1979	1	200	1.01578	1.76370	0.91805	2006	21	1331	0.62708	1.14122	0.59403
1988	13	3598	0.70662	1.71509	0.89274	2007	9	697	0.73123	0.96939	0.50459
1989	18	3527	0.43429	1.31448	0.68422	2008	1	53	0.28124	1.06983	0.55687
1990	4	719	0.54164	0.99494	0.51789	2009	4	283	0.40613	0.67862	0.35324
1991	2	337	0.47957	1.10330	0.57429	2010	6	332	0.50607	0.86530	0.45041
1992	50	3340	0.33660	1.04748	0.54524	2011	11	592	0.49856	0.84970	0.44229
1993	24	1336	0.27704	0.89481	0.46577	2012	18	1068	0.47613	0.90615	0.47167
1994	1	60	0.37348	0.82553	0.42971	2013	8	404	0.59731	0.88366	0.45997
1996	53	3942	0.27940	0.88310	0.45968	2014	17	1072	0.38372	0.97481	0.50741
1997	16	827	0.38079	0.83661	0.43547	2015	1	53	0.49991	0.85971	0.44750
2000	10	579	0.35104	0.93747	0.48797	2016	3	180	0.56772	0.56092	0.29197
2001	42	3074	0.24218	0.86350	0.44947	-	-	-	-	-	-
-	-	-	-	-	-	-	Σ = 372	Σ = 32125	$\prod^{1/N}$ = 0.52052	$\prod^{1/N}$ = 1.00000	$\prod^{1/N}$ = 0.52052

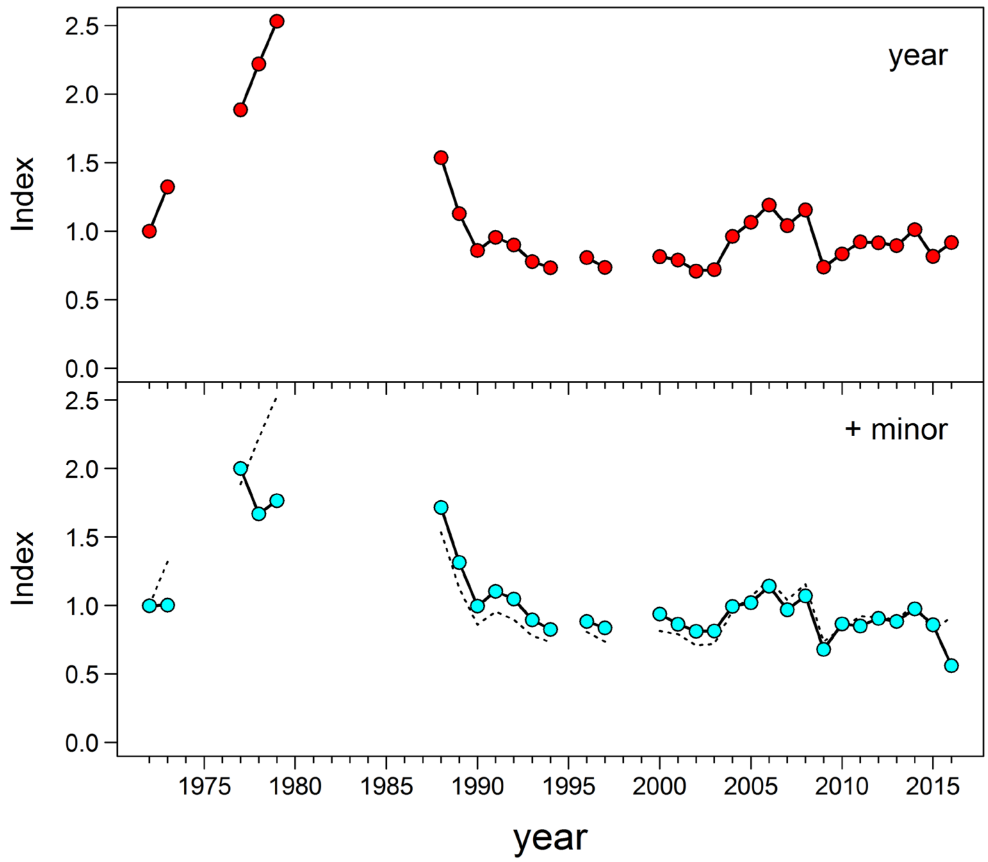

Figure D.20. Normalised mean weight (kg/fish) of WAP ***South*** *estimated from (D.10) using data from sampling unsorted catch (original geometric mean = 0.521 kg/fish). See Figure D.19 caption for additional detail.*

D.3. HABITAT

Walleye Pollock is ubiquitous along the BC coast, with an estimated area of occupancy ranging from ~50,200 km^2 using trawl occurrence (Figure A.2) to ~72,400 km^2,using bathymetry limits (Figure D.21). The estimated bathymetry limits are derived from the distribution of this species captured in observer log trawl tows (bottom and midwater), which spans depths 62 to 448 m 98% of the time (Figure D.22). Species caught concurrently in coastwide observer log tows that captured at least one Walleye Pollock, herein referred to as "pollock tows" (Figure D.23), are dominated by Walleye Pollock (25% of total catch) and include significant amounts of Arrowtooth Flounder *Atheresthes stomias* (16%), Pacific Ocean Perch *Sebastes alutus* (14%), and Pacific Hake *Merluccius productus* (13%).

Regional variations in depth distributions of pollock tows occur along the BC coast, and species caught concurrently also vary. In addition to the BC offshore stock assessed, we present three PMFC combinations that are typically used by managers of this species – 5CDE (Hecate Strait, Dixon Entrance, west coast Haida Gwaii), 5AB (Queen Charlotte Sound, Queen Charlotte Strait), and 3CD (west coast Vancouver Island and mouth of Juan de Fuca Strait).

The 5CDE region is dominated by shallow trawl effort (Figure D.24), which presumably indicates the targeting of flatfish in Hecate Strait. Pollock tows occur a little deeper than this and are dominated by catches of Arrowtooth Flounder (27% of total catch), Walleye Pollock (20%), and

Dover Sole (7%), amongst an assemblage of rockfish, flatfish, and skates (Figure D.25, Table D.14).

Region 5AB contains three important gullies – Goose Island Gully, Mitchell's Gully, and Moresby Gully. The effort of the trawl fleet in this region appears to be limited to depths shallower than 400 m with a mode at 100 m (Figure D.26), whereas the depth of pollock tows shows a mode at ~200 m. While this region is highly important to the POP fishery, the inclusion of PMFC minor area 12 increases the catch contribution of Walleye Pollock in pollock tows Figure D.27 to equal that of POP (both ~27% of total catch). This region has the highest percentage of Walleye Pollock in depths where it is caught (Table D.14). The next greatest contributor to catch is Arrowtooth Flounder at only 10%.

Region 3CD (excluding PMFC minor area 20) has traditionally been fished to great depths (>700 m, not shown) due to favourable bathymetry but the shallow mode of the fleet effort distribution has always been the greatest (Figure D.28, which includes minor area 20). The pollock tows follow the shallow fleet effort with a peak at ~150 m. The species that occur in pollock tows appear in Figure D.29. The dominant concurrent species in this region are Pacific Hake (40%), followed by Walleye Pollock (30%) and Yellowtail Rockfish *Sebastes flavidus* (8%). Catches of other concurrent species appear in Table D.14.

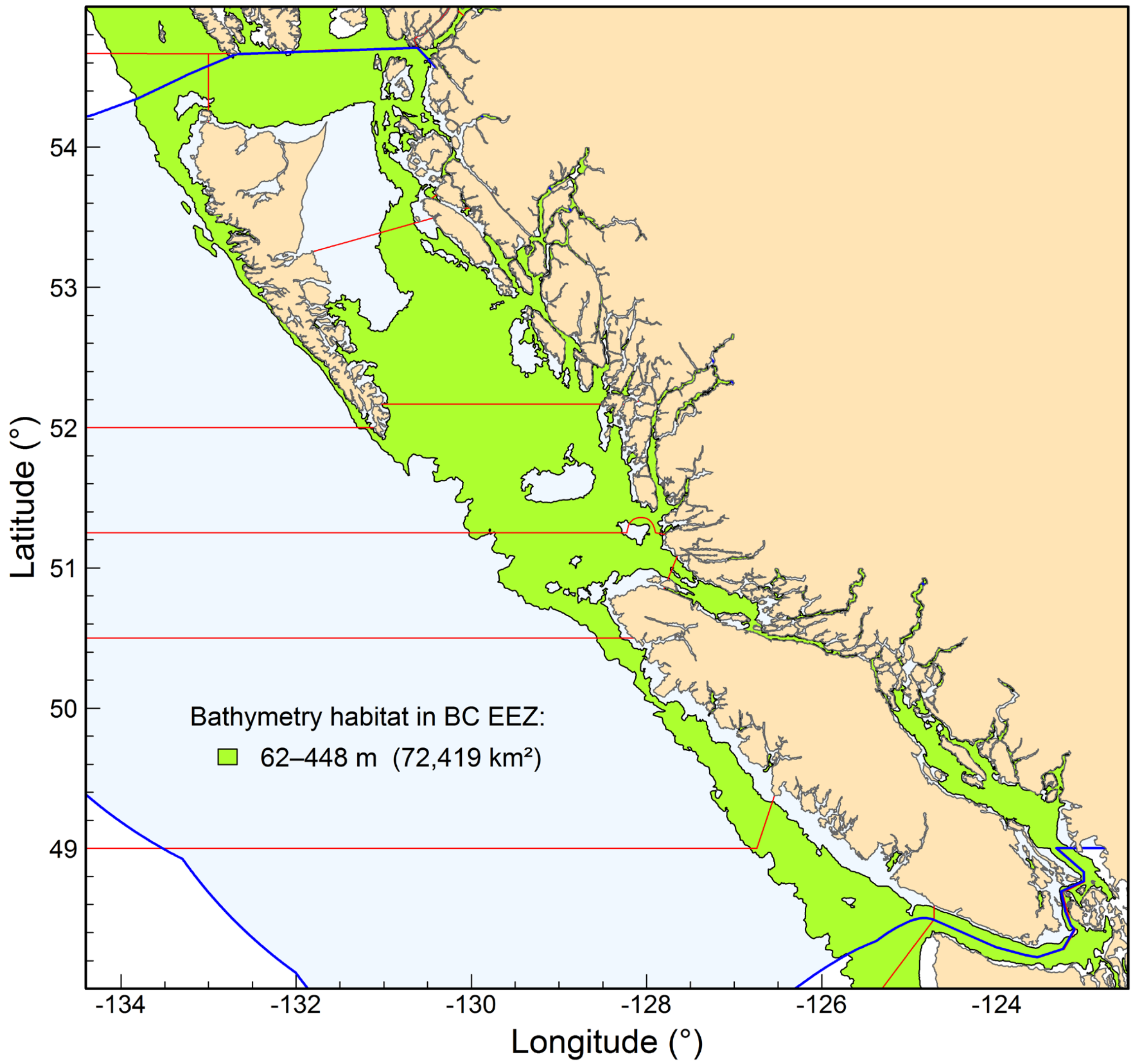

Figure D.21. Highlighted bathymetry (green) between 62 and 448 m serves as a proxy for benthic habitat for Walleye Pollock along the BC coast. Within Canada's exclusive economic zone (EEZ, blue highlighted area), the green highlighted region covers 72,419 km². The boundaries in red delimit the PMFC areas.

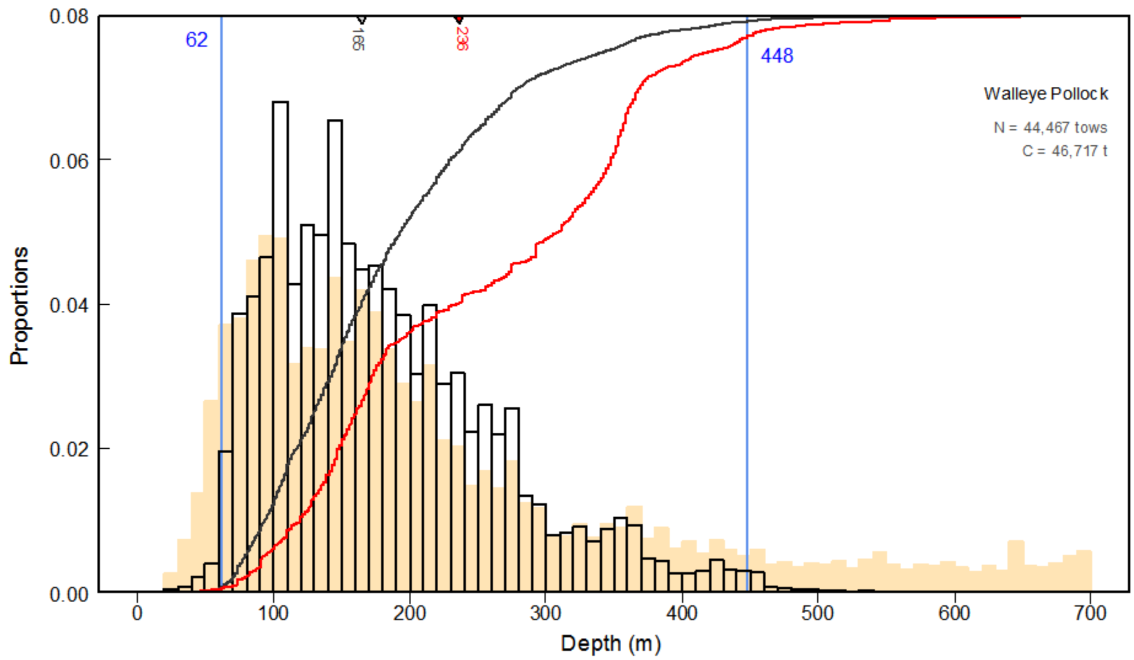

Figure D.22. BC Offshore – Depth frequency of bottom tows that captured Walleye Pollock (WAP) from commercial trawl logs (1996-2007 in PacHarvest, 2007-2016 in GFFOS) in areas outside the Strait of Georgia (transparent histogram). The vertical solid lines denote the 1% and 99% quantiles. The black curve shows the cumulative frequency of tows that encounter WAP while the red curve shows the cumulative catch of WAP at depth (scaled from 0 to 1). The median depths of WAP encounters (inverted grey triangle) and of cumulative catch (inverted red triangle) are indicated along the upper axis. 'N' reports the total number of tows; 'C' reports the total catch (t). The shaded histogram in the background reports the relative trawl effort on all species offshore down to 700 m.

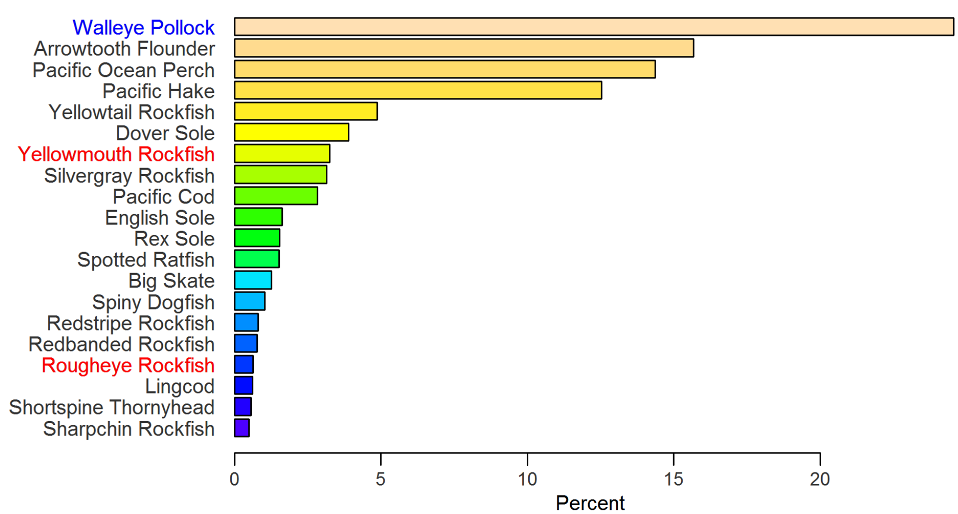

Figure D.23. BC Offshore – Distribution of catch weights summed over the period February 1996 to January 2017 for important finfish species in bottom and midwater trawl tows that caught at least one Walleye Pollock coastwide. Tows were selected over a depth range between 62 and 448 m (the 1% and 99% quantile range, see Figure D.22). Relative concurrence is expressed as a percentage by species relative to the total catch weight summed over all finfish species in the specified period. Walleye Pollock is indicated in blue on the y-axis; other species of interest to SARA are indicated in red.

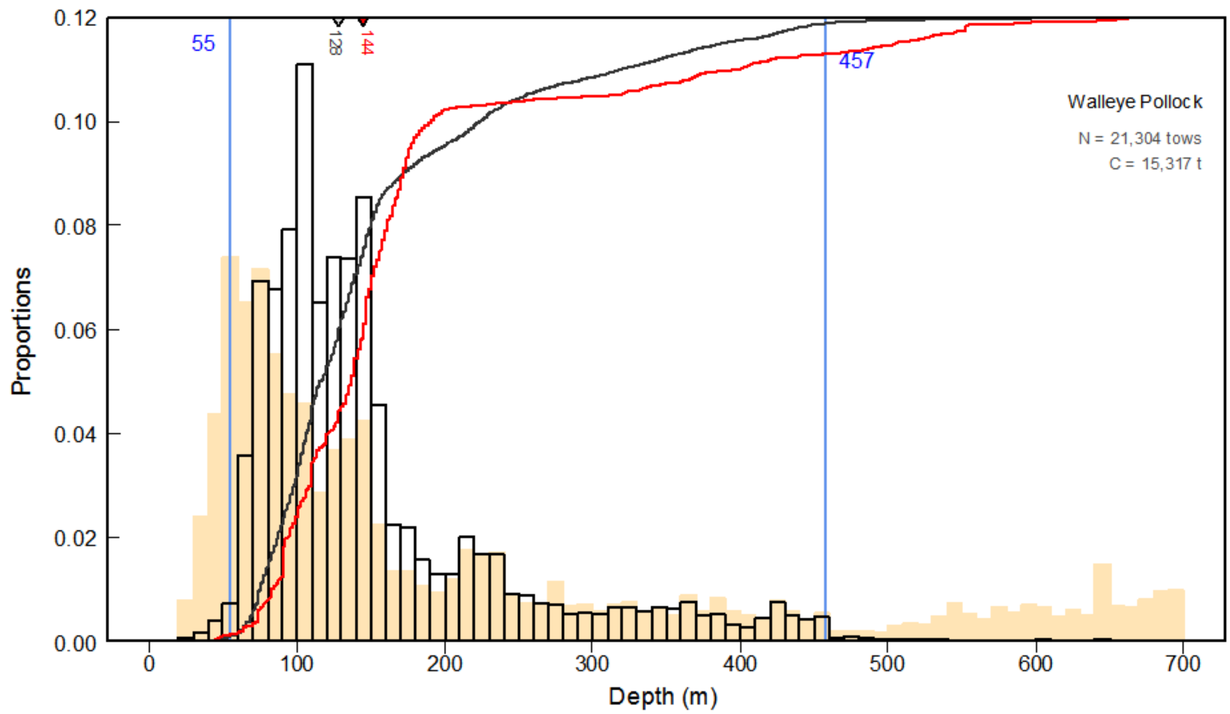

Figure D.24. 5CDE – Depth frequency of bottom and midwater trawl tows that captured Walleye Pollock (WAP) from commercial trawl logs (1996-2007 in PacHarvest, 2007-2016 in GFFOS) in PMFC major areas 5CDE (transparent histogram). The shaded histogram in the background reports the relative trawl effort on all species in 5CDE down to 700 m. Plot details appear in Figure D.22.

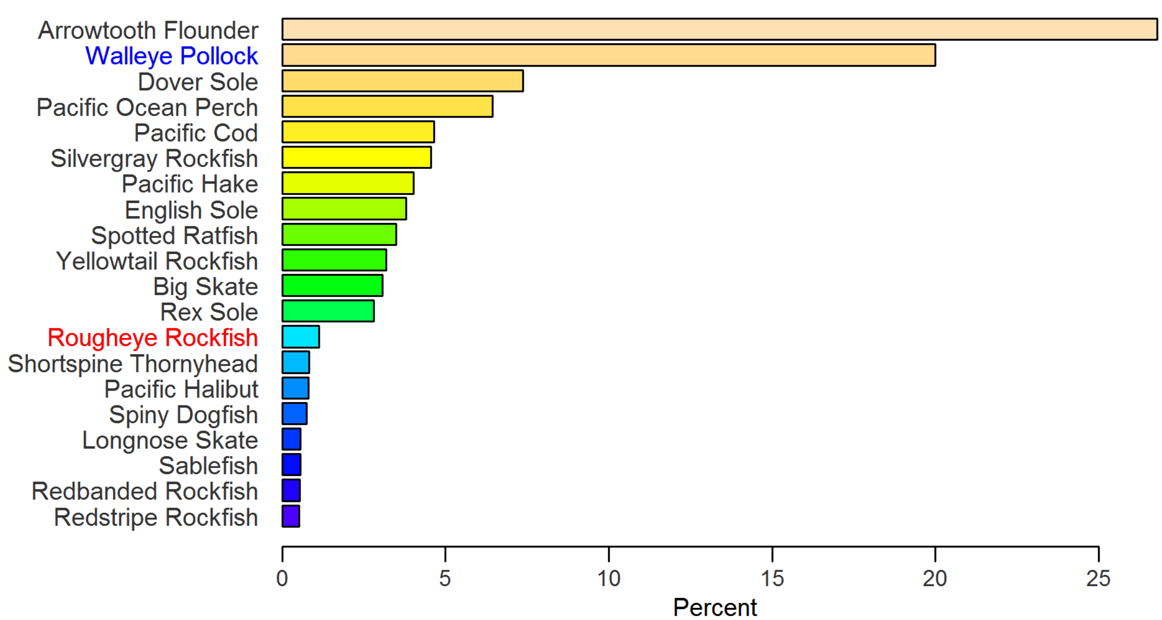

Figure D.25. 5CDE – Distribution of catch weights summed over the period February 1996 to January 2017 for important finfish species in bottom and midwater trawl tows that caught at least one Walleye Pollock off Haida Gwaii and in Dixon Entrance. Tows were selected over a depth range between 55 and 457 m (the 1% and 99% quantile range, see Figure D.24). Plot details appear in Figure D.23.

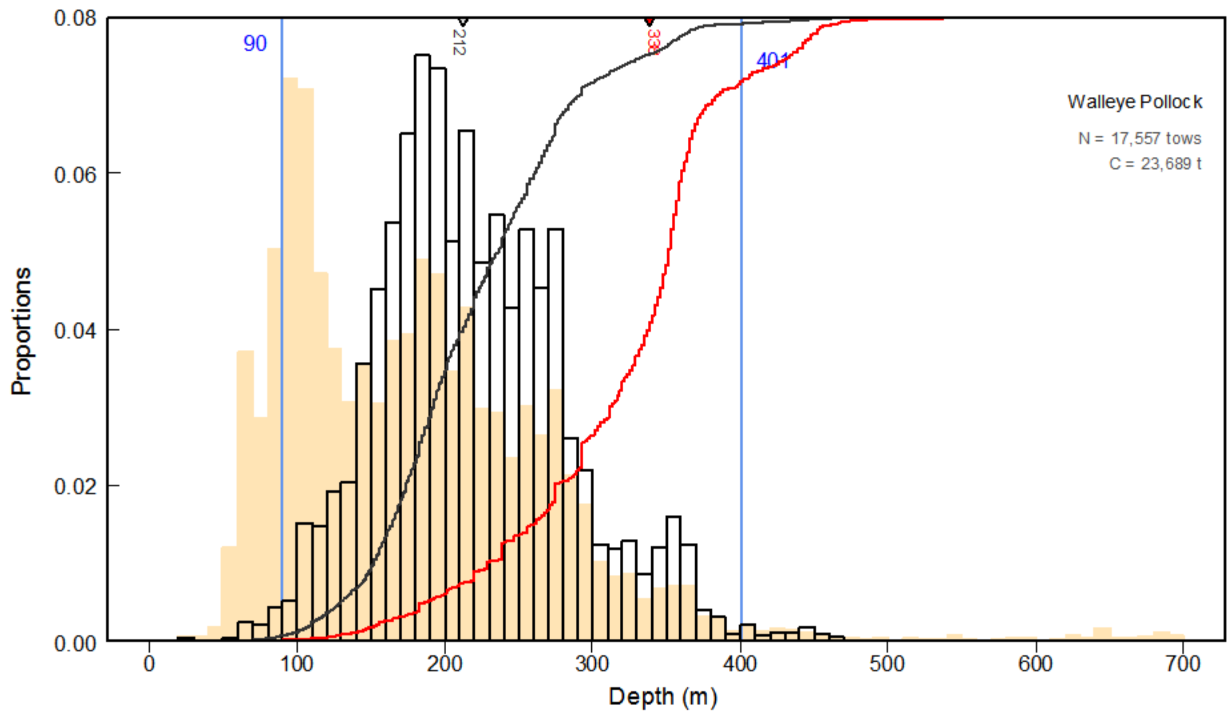

Figure D.26. 5AB – Depth frequency of bottom and midwater trawl tows that captured Walleye Pollock (WAP) from commercial trawl logs (1996-2007 in PacHarvest, 2007-2016 in GFFOS) in PMFC major areas 5AB (transparent histogram). The shaded histogram in the background reports the relative trawl effort on all species in 5AB down to 700 m. Plot details appear in Figure D.22.

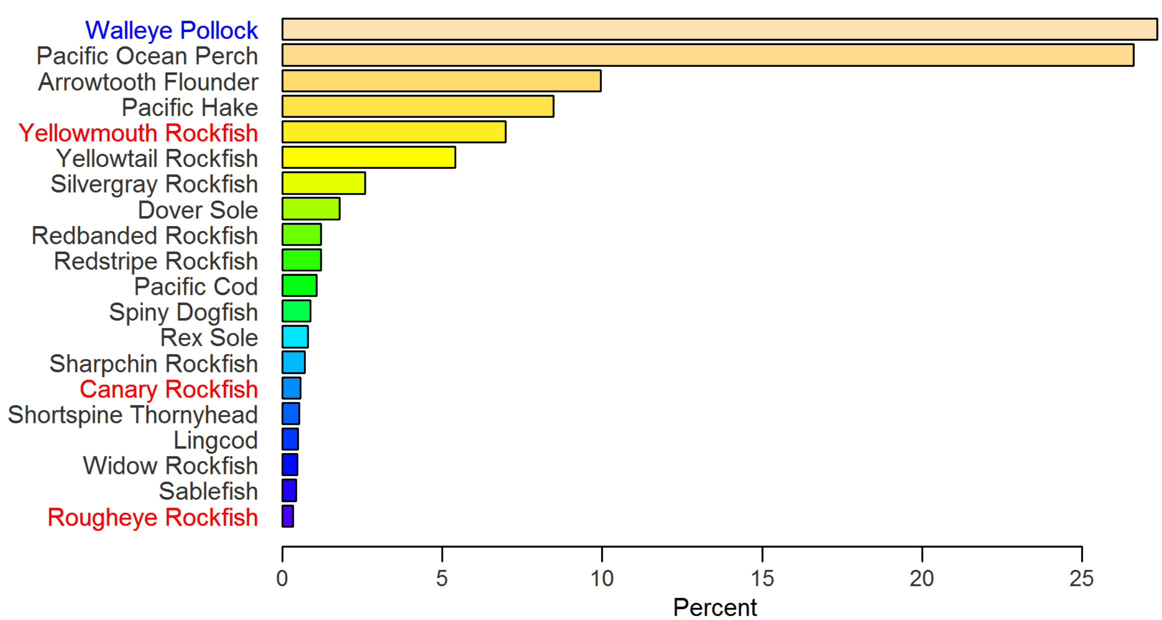

Figure D.27. 5AB – Distribution of catch weights summed over the period February 1996 to January 2017 for important finfish species in bottom and midwater trawl tows that caught at least one Walleye Pollock in Queen Charlotte Sound and Strait. Tows were selected over a depth range between 90 and 401 m (the 1% and 99% quantile range, see Figure D.26). Plot details appear in Figure D.23.

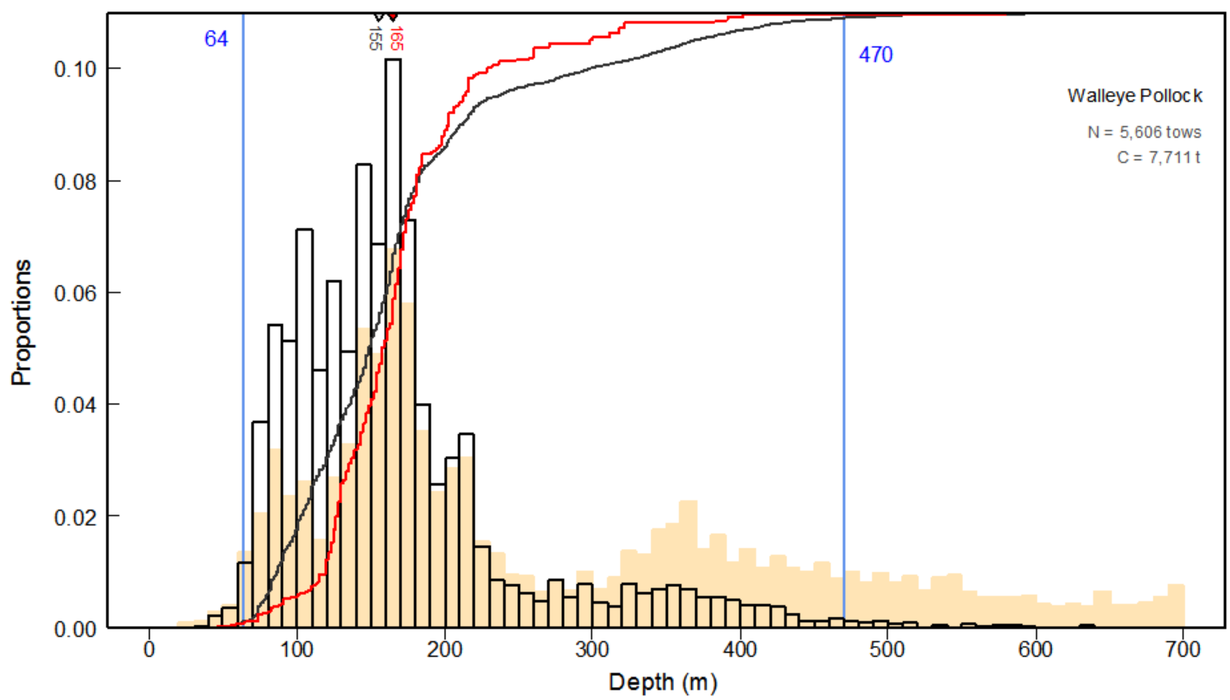

Figure D.28. 3CD – Depth frequency of bottom and midwater trawl tows that captured Walleye Pollock (WAP) from commercial trawl logs (1996-2007 in PacHarvest, 2007-2016 in GFFOS) in PMFC major areas 3CD (transparent histogram). The shaded histogram in the background reports the relative trawl effort on all species in 3CD down to 700 m. Plot details appear in Figure D.22.

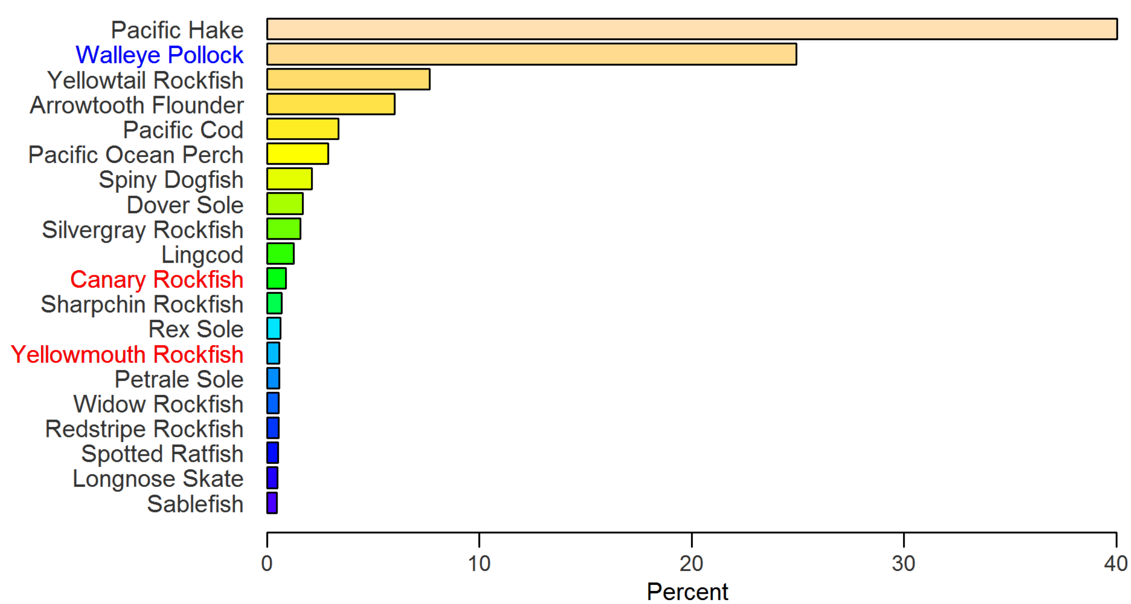

Figure D.29. 3CD – Distribution of catch weights summed over the period February 1996 to January 2017 for important finfish species in bottom and midwater trawl tows that caught at least one Walleye Pollock off the west coast of Vancouver Island and at the mouth of Juan de Fuca Strait. Tows were selected over a depth range between 64 and 470 m (the 1% and 99% quantile range, see Figure D.28). Plot details appear in Figure D.23.

Table D.14. Top 20 species by catch weight (sum of landed + discarded from Feb,1996 to Jan,2016, observer logs only) that co-occur in Walleye Pollock bottom and midwater trawl tows along the BC coast, in PMFC 5DE, in PMFC 5AB + minor 12, and in PMFC 3CD + minor 20. Rockfish species of interest to COSEWIC appear in red font, target species (occurs in every tow) appears in blue font.

Code	Species	Latin Name	Catch (t)	Catch (%)
Coast				
228	Walleye Pollock	*Theragra chalcogramma*	44,553	24.562
602	Arrowtooth Flounder	*Atheresthes stomias*	28,435	15.676
396	Pacific Ocean Perch	*Sebastes alutus*	26,060	14.367
225	Pacific Hake	*Merluccius productus*	22,724	12.528
418	Yellowtail Rockfish	*Sebastes flavidus*	8,840	4.873
626	Dover Sole	*Microstomus pacificus*	7,073	3.899
440	Yellowmouth Rockfish	*Sebastes reedi*	5,887	3.245
405	Silvergray Rockfish	*Sebastes brevispinis*	5,723	3.155
222	Pacific Cod	*Gadus macrocephalus*	5,149	2.839
628	English Sole	*Parophrys vetulus*	2,943	1.623
610	Rex Sole	*Errex zachirus*	2,791	1.539
066	Spotted Ratfish	*Hydrolagus colliei*	2,778	1.532
056	Big Skate	*Raja binoculata*	2,299	1.268
044	Spiny Dogfish	*Squalus acanthias*	1,872	1.032
439	Redstripe Rockfish	*Sebastes proriger*	1,467	0.809
401	Redbanded Rockfish	*Sebastes babcocki*	1,399	0.771
394	Rougheye Rockfish	*Sebastes aleutianus*	1,157	0.638
467	Lingcod	*Ophiodon elongatus*	1,130	0.623
451	Shortspine Thornyhead	*Sebastolobus alascanus*	1,029	0.567
450	Sharpchin Rockfish	*Sebastes zacentrus*	888	0.490
5CDE				
602	Arrowtooth Flounder	*Atheresthes stomias*	19,014	26.797
228	Walleye Pollock	*Theragra chalcogramma*	14,180	19.985
626	Dover Sole	*Microstomus pacificus*	5,235	7.379
396	Pacific Ocean Perch	*Sebastes alutus*	4,575	6.447
222	Pacific Cod	*Gadus macrocephalus*	3,303	4.655
405	Silvergray Rockfish	*Sebastes brevispinis*	3,230	4.552
225	Pacific Hake	*Merluccius productus*	2,860	4.030
628	English Sole	*Parophrys vetulus*	2,689	3.790
066	Spotted Ratfish	*Hydrolagus colliei*	2,471	3.482
418	Yellowtail Rockfish	*Sebastes flavidus*	2,263	3.189
056	Big Skate	*Raja binoculata*	2,178	3.069
610	Rex Sole	*Errex zachirus*	1,987	2.800
394	Rougheye Rockfish	*Sebastes aleutianus*	803	1.131
451	Shortspine Thornyhead	*Sebastolobus alascanus*	581	0.818
614	Pacific Halibut	*Hippoglossus stenolepis*	577	0.813
044	Spiny Dogfish	*Squalus acanthias*	534	0.753
059	Longnose Skate	*Raja rhina*	403	0.567
455	Sablefish	*Anoplopoma fimbria*	400	0.563
401	Redbanded Rockfish	*Sebastes babcocki*	383	0.540
439	Redstripe Rockfish	*Sebastes proriger*	369	0.520
5AB				
228	Walleye Pollock	*Theragra chalcogramma*	21,148	27.355
396	Pacific Ocean Perch	*Sebastes alutus*	20,569	26.606
602	Arrowtooth Flounder	*Atheresthes stomias*	7,693	9.951
225	Pacific Hake	*Merluccius productus*	6,548	8.470
440	Yellowmouth Rockfish	*Sebastes reedi*	5,391	6.974
418	Yellowtail Rockfish	*Sebastes flavidus*	4,186	5.415
405	Silvergray Rockfish	*Sebastes brevispinis*	2,007	2.596

Code	Species	Latin Name	Catch (t)	Catch (%)
626	Dover Sole	*Microstomus pacificus*	1,383	1.789
401	Redbanded Rockfish	*Sebastes babcocki*	941	1.217
439	Redstripe Rockfish	*Sebastes proriger*	931	1.204
222	Pacific Cod	*Gadus macrocephalus*	833	1.077
044	Spiny Dogfish	*Squalus acanthias*	683	0.883
610	Rex Sole	*Errex zachirus*	621	0.803
450	Sharpchin Rockfish	*Sebastes zacentrus*	540	0.698
437	Canary Rockfish	*Sebastes pinniger*	442	0.571
451	Shortspine Thornyhead	*Sebastolobus alascanus*	417	0.539
467	Lingcod	*Ophiodon elongatus*	386	0.499
417	Widow Rockfish	*Sebastes entomelas*	360	0.465
455	Sablefish	*Anoplopoma fimbria*	340	0.440
394	Rougheye Rockfish	*Sebastes aleutianus*	269	0.348
3CD				
225	Pacific Hake	*Merluccius productus*	12,266	40.053
228	Walleye Pollock	*Theragra chalcogramma*	7,638	24.941
418	Yellowtail Rockfish	*Sebastes flavidus*	2,344	7.654
602	Arrowtooth Flounder	*Atheresthes stomias*	1,843	6.017
222	Pacific Cod	*Gadus macrocephalus*	1,029	3.359
396	Pacific Ocean Perch	*Sebastes alutus*	883	2.882
044	Spiny Dogfish	*Squalus acanthias*	644	2.103
626	Dover Sole	*Microstomus pacificus*	513	1.676
405	Silvergray Rockfish	*Sebastes brevispinis*	481	1.571
467	Lingcod	*Ophiodon elongatus*	385	1.257
437	Canary Rockfish	*Sebastes pinniger*	275	0.897
450	Sharpchin Rockfish	*Sebastes zacentrus*	209	0.682
610	Rex Sole	*Errex zachirus*	194	0.632
440	Yellowmouth Rockfish	*Sebastes reedi*	182	0.595
607	Petrale Sole	*Eopsetta jordani*	174	0.570
417	Widow Rockfish	*Sebastes entomelas*	173	0.566
439	Redstripe Rockfish	*Sebastes proriger*	166	0.543
066	Spotted Ratfish	*Hydrolagus colliei*	161	0.526
059	Longnose Skate	*Raja rhina*	152	0.496
455	Sablefish	*Anoplopoma fimbria*	142	0.465

D.4. REFERENCES – BIOLOGY

Beamish, R.J. and McFarlane, G.A. 1995. A discussion of the importance of aging errors, and an application to walleye pollock: the world's largest fishery. In D. H. Secor, J. M. Dean and S. E. Campana, eds., Recent Developments in Fish Otolith Research, The Belle W. Baruch Library in Marine Science 19, p. 545-565. University of South Carolina Press, Columbia, SC.

Dorn, M., Aydin, K., Barbeaux, S., Jones, D., Spalinger, K. and Palsson, W. 2012. Chapter 1. Assessment of the Walleye Pollock stock in the Gulf of Alaska. In NPFMC Gulf of Alaska SAFE, p. 53-182. North Pacific Fisheries Management Council.

Dorn, M., Aydin, K., Jones, D., McCarthy, A., Palsson, W. and Spalinger, K. 2015. Chapter 1. Assessment of the Walleye Pollock stock in the Gulf of Alaska. In NPFMC Gulf of Alaska SAFE, p. 49-172. North Pacific Fisheries Management Council.

Gustafson, R.G., Lenarz, W.H., McCain, B.B., Schmitt, C.C., Grant, W.S., Builder, T.L. and Methot, R.D. 2000. Status review of Pacific Hake, Pacific Cod, and Walleye Pollock from Puget Sound, Washington. NOAA Technical Memorandum NMFS-NWFSC-44: 275 pp.

Hoenig, J.M. 1983. Empirical use of longevity data to estimate mortality rates. Fish. Bull. 82(1): 898-903.

Ianelli, J.N., Honkalehto, T., Barbeaux, S. and Kotwicki, S. 2015. 1. Assessment of the walleye pollock stock in the Eastern Bering Sea. In NPFMC Bering Sea and Aleutian Islands SAFE, p. 53-152. North Pacific Fisheries Management Council.

Janusz, J. and Horbowy, J. 1997. The state of the walleye pollock in the northern part of the Okhotsk Sea, North Pacific. Fish. Res. 30(1-2): 87-102.

MacLellan, S.E. 1997. How to age rockfish (*Sebastes*) using *S. alutus* as an example – the otolith burnt section technique. Can. Tech. Rep. Fish. Aquat. Sci. 2146: 39 pp.

McFarlane, G.A. and Beamish, R.J. 1990. An examination of age determination structures of Walleye Pollock (*Theragra chalcogramma*) from five stocks in the Northeast Pacific Ocean. In Proceedings of the Symposium on Application of Stock Assessment Techniques to Gadids, Seattle, WA, Oct 31-Nov 1, 1989, INPFC Bulletin 50, p. 37-56. International North Pacific Fisheries Commission.

Quinn, T.J.I. and Deriso, R.B. 1999. Quantitative Fish Dynamics. Oxford University Press, New York, NY.

Saunders, M.W., McFarlane, G.A. and Shaw, W. 1989. Delineation of Walleye Pollock (*Theragra chalcogramma*) stocks off the Pacific Coast of Canada. In Proc. Int. Symp. Biol. Mgmt. Walleye Pollock, Anchorage, AK, Nov 14-16, 1988, Lowell Wakefield Fisheries Symposia Series 7, Alaska Sea Grant Rep. 89-1, p. 379-401. Alaska Sea Grant College Program, University of Alaska, Fairbanks, AK.

Schnute, J.T., Haigh, R., Krishka, B.A., Sinclair, A. and Starr, P.J. 2004. The British Columbia Longspine Thornyhead fishery: analysis of survey and commercial data (1996-2003). DFO Can. Sci. Advis. Sec. Res. Doc. 2004/059. iii + 75 p.

Then, A.Y., Hoenig, J.M., Hall, N.G. and Hewitt, D.A. 2015. Evaluating the predictive performance of empirical estimators of natural mortality rate using information on over 200 fish species. ICES J. Mar. Sci. 72(1): 82-92.

Thompson, J.M. 1981. Preliminary report on the population biology and fishery of walleye pollock *Theragra chalcogramma* off the Pacific Coast of Canada. Can. Tech. Rep. Fish. Aquat. Sci. 1031: v + 157 pp.

APPENDIX E. MODEL EQUATIONS

E.1. INTRODUCTION

The software used in this stock assessment of Walleye Pollock (WAP) is a variant of the integrated Statistical Catch Age Model (iSC∀M), developed by Steven Martell (Martell 2010) and modified by Robyn Forrest in 2015 to run a delay-difference (DD) model for Pacific Cod (*Gadus macrocephalus*) on the west code of Canada (Forrest et al. 2015). The DD model was written in AD Model Builder template code (Fournier et al. 2012) and was compiled for WAP using the PBSadmb package (Schnute et al. 2017).

The original iSC∀M code for Pacific Cod has been modified several times – in 2015 for Shortspine Thornyhead (*Sebastolobus alascanus*, Starr and Haigh 2017) and in 2017 for Walleye Pollock (*Theragra chalcogramma*):

1. The parameter R_0 (equilibrium unfished age-0 recruits) was estimated while $\bar{R}$ (average annual recruitment) was tethered to equal R_0. In the code, this entailed forcing theta(4) = theta(1). There seems to be some difference of opinion on how these parameters should be handled.
2. The analytical method for MSY implemented in the original code gave results that did not appear to be correct. We adapted code from Awatea, used to model populations of Pacific Ocean Perch (*Sebastes alutus*), to estimate MSY and B_{MSY} through a brute-force method by projecting forward under constant F policies and finding the F that gave the greatest yield (MSY). The associated biomass is B_{MSY}. This method was crude but effective.
3. The original version of the model assumed that the mean weight data vector is continuous by year for a given range. An un-interrupted series was not available for Walleye Pollock so we recoded the input routine to accept a matrix with year and mean weight. Other model components (e.g., mean weight likelihood) were re-coded accordingly. This revision allows the use of annual mean weight data with missing years.

E.2. DELAY-DIFFERENCE MODEL

Note: The text and equations below are taken from Forrest et al. (2015), and modified as needed.

Delay difference models represent an intermediate approach between aggregated surplus production models and age-structured models. The delay-difference structure tracks the effects of recruitment, survival and growth on biomass, without requiring an age-structured framework, and can perform well as long as its major assumptions are met (Hilborn and Walters 1992). Difference equations, which allow for a time-delay between spawning and recruitment, are used to build population models in discrete time-steps (generally 1 year), in which the surviving biomass for next year is predicted from the surviving biomass from last year, after adjusting for growth and adding next year's recruitment. An advantage of delay difference models over simpler production models is that they do not assume constant recruitment over time.

The key assumptions of the delay difference model are:

- Growth in mean body weight W_a follows the linear relationship described by the Ford-Walford equation (E.1); see Section D.1.4.

$$W_a = \alpha_g + \rho_g W_{a-1} \tag{E.1}$$

- Knife-edge selectivity, i.e., all fish aged k and older, are equally vulnerable to the fishing gear. A corollary to the assumption of knife-edge selectivity is that maturity is also knife-edge and the same as selectivity. This means that all fish in the model are mature and fully selected; and
- Mortality at age remains constant, i.e., all fish aged k and older have the same mortality rate.

The delay difference model collapses all the equations needed to fully describe the population's age structure into equations for the biomass (B_t), total numbers (N_t), and survival (S_t) at time t:

$$B_t = S_{t-1}(\alpha_g N_{t-1} + \rho_g B_{t-1}) + w_k R_t \tag{E.2}$$

$$N_t = S_{t-1} N_{t-1} + R_t \tag{E.3}$$

$$S_t = e^{-(M+F_t)} \tag{E.4}$$

where:

k = the age at which fish are assumed to become fully vulnerable to fishing;

M = the instantaneous natural mortality rate;

F_t = the instantaneous fishing mortality rate at time t;

(α_g, ρ_g) = the intercept and slope of the Ford-Walford equation for all ages $\geq k$;

w_k = the weight at age k; and

R_t = is the number of recruits at time t calculated by the stock-recruit function, here constrained to conform to a Beverton-Holt relationship with constants a and b (E.26).

We assume that recruitment to the fishery and surveys occurs at age $k \in \{3, 4, 5\}$ for both stocks in the various alternative cases.

A list of model parameters is given in Table E.1. Equilibrium and dynamic equations are given in Tables E.2 and E.3, respectively. Variance parameters and likelihood components of the objective function are given in Table E.4.

E.2.1. Objective function components

Variance parameters and objective function components are listed in Table E.4. The objective function $f(\theta)$ in the delay-difference model contains five major components:

1. the negative log-likelihood for the relative abundance data (E.33);
2. the negative log-likelihood for the catch data (E.35);
3. the negative log-likelihood for the mean weight data (E.37);
4. the prior distributions for model parameters, and
5. three penalty functions that:
    a. constrain the estimates of annual recruitment to conform to a Beverton-Holt stock-recruit function;
    b. weakly constrain the log recruitment deviations to a normal distribution; and
    c. weakly constrain estimates of log fishing mortality to a normal distribution, N (ln(0.2), 4.0), to prevent estimates of catch from exceeding estimated biomass.

E.2.2. Variance components and weighting of index data

The iSC$\forall$M modelling framework (Martell 2010) partitions the variance using an errors in variables approach. Total variance ϑ can be fixed or estimated, and was fixed for the Walleye Pollock delay-difference model (as it was for the Shortspine Thornyhead model, Starr and Haigh 2017). Total variance is partitioned by the model into observation and process error components (E.27 and E.28, respectively) using the parameter ρ, which represents the proportion of the total variance that is due to observation error (Punt and Butterworth 1993; Deriso et al. 2007). The process error component (E.28) of the total variance is applied to the estimated recruitments as shown in equation (E.39).

Two variance control parameters in the model were fixed ($\rho = 0.1, \vartheta = 2.5$) for Walleye Pollock. The formulae for model observation and process error, respectively, are: $\sigma = \sqrt{\rho} \cdot \sqrt{1/\vartheta}$ and $\tau = \sqrt{1-\rho} \cdot \sqrt{1/\vartheta}$. In the Shortspine Thornyhead assessment, sensitivities to σ and τ were examined through runs that fixed the variance control parameters at alternative values; the sensitivities showed only small effects on model outcome.

The standard deviation used when fitting the survey and CPUE abundance index data is given in equation (E.27), with each index value weighted by the inverse of the CV associated with that index, as shown in equation (E.29). The index variance is added to the total likelihood as shown in (E.33). Five surveys and one CPUE index series were fitted in this model. The relative sampling error or CV (c_{jt}) associated with each survey index value was used without adding additional survey process error c'_j. A relative error of 0.3 was assumed for each CPUE index value. We did not attempt to alter the relative weights of the component data series (Francis 2011), instead using the observation error CVs estimated by the surveys without modification.

Note that after the assessment model was accepted, some of the calculations for the variance components: (σ, τ) = $(\sqrt{\rho} \cdot \varphi, \sqrt{1-\rho} \cdot \varphi)$, appear to have been incorrectly specified as $(\sqrt{\rho}/\varphi, \sqrt{1-\rho}/\varphi)$ in the model code `iscamdelaydiff.tpl` (dated 2017-01-03). These potential errors appear on lines 2054 (likelihood for stock-recruitment relationship in `calc_objective_function`) and 2513-14 (in `simulation_model` function). In these instances (σ, τ) = $(0.5, 1.5)$ instead of the correct values $(0.2, 0.6)$. We don't anticipate that these errors would change the model outcomes substantially.

E.3. REFERENCES POINTS, PROJECTIONS AND ADVICE TO MANAGERS

Typically, advice to managers is given with respect to three reference points based on maximum sustainable yield (MSY). The provisional reference points of the DFO Precautionary Approach (DFO 2006), namely $0.4B_{\mathrm{MSY}}$ and $0.8B_{\mathrm{MSY}}$, comprise the primary benchmarks for advice, where B_{MSY} is the estimated equilibrium spawning biomass at MSY. The third reference point is u_{MSY}, the harvest rate at MSY, and is derived from the instantaneous fishing mortality at MSY: $u_{\mathrm{MSY}} = (1 - e^{-F_{MSY}})$. However, exploration on the treatment of R_0 and $\bar{R}$, i.e., (i) estimating R_0 and setting $\bar{R} = R_0$, (ii) estimating $\bar{R}$ and setting $R_0 = \bar{R}$, and (iii) estimating R_0 and $\bar{R}$ independently, uncovered instabilities in the trajectory of spawning biomass, specifically in the start and end points, B_0 and B_{2017}, respectively. Unfortunately, these two points are critical in assessing stock status using MSY-based criteria.

For these reasons, we adopted historical reference points (HRP) to assess stock status and to provide advice to managers in the form of decision tables. As a proxy for B_{MSY}, we use average B_t (B_{avg}), where $t = 1967, ..., 2016$; similarly, u_{avg} acts as a proxy for u_{MSY}. For the limit reference point (LRP) we adopt B_t from year t in which biomass was at a minimum and subsequently recovered to exceed B_{avg}. The minimum year is determined for each MCMC sample, and the biomass from this year is denoted B_{min}. Consequently, there are 1000 B_{min} values with a distribution of years in which they occur. The upper stock reference (USR) is simply $2B_{\mathrm{min}}$.

Projections were made for only 2 years due to the model's inherent uncertainty and its lack of associated age structure, starting with the biomass calculated for the start of 2017, across a range of constant catch strategies. For each strategy, projections were performed for each of the 1000 MCMC samples (resulting in posterior distributions of future spawning biomass).

Recruitments for the projections were randomly generated from lognormal recruitment deviations applied to the deterministic recruitment estimate from the Beverton-Holt stock-recruitment function, using randomly generated values of $\epsilon_t \sim$ Normal$(0, \sigma_R^2)$. For each of the 1000 MCMC samples a time series of $\{\epsilon_t\}$ was generated. For each MCMC sample, the same time series of $\{\epsilon_t\}$ was used for every catch strategy so that, for a given MCMC sample, all catch strategies experienced the same recruitment stochasticity in projections using (E.2).

Decision tables comprise probabilities calculated as the proportion of the 1000 MCMC samples for which $B_{t=2017,...,2019}$ is greater than a reference point (B_{2017}, B_{min}, $2B_{\mathrm{min}}$, B_{avg}, u_{avg}), and is expressed as P$(B_t > B_{\mathrm{ref}})$ or P$(u_{t-1} > u_{\mathrm{ref}})$.

Table E.1. Notation for the iSC$\forall$M delay-difference model used for Walleye Pollock. The term 'log' refers to natural logarithms (base e) herein.

Symbol	Description	North	South
	Indices (subscripts)		
t	Model year, where $t = 1980, 1981, ..., 2015$;		
	and $t = 1980$ represents unfished equilibrium conditions		
j	Gear (catch, surveys, CPUE)		
g	Ford-Walford identifier		
	Fixed input parameters		
k	Age at knife-edge recruitment	3	3
L_∞	Theoretical maximum length (cm)	66.944	50.827
κ	von Bertalanffy growth rate	0.2118	0.1991
t_0	Theoretical age at length = 0 cm	-1.136	-1.790
α	Scaling parameter of the length-weight relationship	7.102E-6	7.354E-6
β	Exponent of the length-weight relationship	3.042	3.030
α_g	Intercept of the Ford-Walford plot, for all ages > k	0.3475	0.1444
ρ_g	Slope of the Ford-Walford plot, for all ages > k	0.8668	0.8706
W_k	Weight at age of recruitment k	0.4929	0.2488
M	Natural mortality (estimated in log space)	ln(0.30)	ln(0.30)

Symbol	Description	North	South
	Annual input data		
C_{jt}	Catch (metric tonnes) for gear j=1 (total commercial) at time t		
W_t	Mean weight (kg) of individuals i in population at time t		
	where all weights are calculated from lengths: $W_i = \alpha L_i^\beta$		
I_{jt}	Indices of abundance for gear j at time t in BC North, where		
	j=2 – GB Reed (or GIG) rockfish survey series		
	j=3 – Hecate Strait Assemblage survey series		
	j=4 – Hecate Strait synoptic survey series		
	j=5 – West Coast Haida Gwaii synoptic survey series		
	j=6 – commercial WAP North CPUE series		
I_{jt}	Indices of abundance for gear j at time t in BC South, where		
	j=2 – GB Reed (or GIG) rockfish survey series		
	j=3 – West Coast Vancouver Island synoptic survey series		
	j=4 – Queen Charlotte Sound synoptic survey series		
	j=5 – commercial WAP South CPUE series		
c$_{jt}$	Annual coefficients of variation (CV) for I_{jt}		
	Time-invariant parameters		
R_0	Equilibrium unfished age-0 recruits (est. in log space)		
h	Steepness of the stock-recruit relationship		
χ	Recruitment compensation ratio (CR)		
a	Slope of the stock-recruit function at the origin		
b	Scaling parameter of the stock-recruit function		
N_0	Equilibrium unfished number of fish		
B_0	Equilibrium unfished biomass (t)		
S_0	Equilibrium unfished survival rate		
$\overline{W}_0$	Equilibrium unfished mean weight (kg)		
c'_j	Additional process error in abundance indices I_{jt} for gear j		
n_j	Number of abundance indices for gear j		
	Time-varying parameters (at time t)		
ω_t	Recruitment deviations (est. in log space)		
F_t	Fishing mortality (est. in log space) by the commercial fishery		
S_t	Survival rate		
N_t	Numbers of fish		
R_t	Recruits (1000s fish)		
B_t	Biomass (tonnes)		
$\overline{W}_t$	Predicted mean weight (kg)		

Symbol	Description	North	South
	Likelihood components		
ϑ	Total variance of the total error	2.5	2.5
φ	Precison as square root of inverse variance ϑ	$\sqrt{0.4}$	$\sqrt{0.4}$
ρ	Proportion of total variance due to observation error	0.1	0.1
σ_O	Overall standard deviation of observation residuals	0.2	0.2
σ_R	Standard deviation of ln-recruitment deviations	0.6	0.6
σ_W	Standard deviation of mean weight	0.15	0.15
σ_C	Standard deviation of catch		
σ_{jt}	Annual standard deviation of observation residuals for each survey		
q_j	Constant of proportionality in indices of catchability (est. in log space)		
d_{jt}^2	Residual log difference for I_{jt} indices of abundance		
$d_{C_t}^2$	Residual log difference for catch data		
$d_{W_t}^2$	Residual log difference for mean weight data		
	Fishery reference points		
MSY	Maximum sustainable yield (t)		
B_{MSY}	Long-term fixed spawning biomass at MSY		
F_{MSY}	Long-term fixed fishing mortality that produces MSY		
u_{MSY}	Long-term fixed harvest rate that produces MSY ($1 - e^{-F_{\mathrm{MSY}}}$)		
B_{avg}	Average spawning biomass (t) over a specified number of years (1967-2016)		
B_{min}	Minimum annual spawning biomass (t) from which the biomass recovered to B_{avg}		

Table E.2. Summary of equilibrium equations for the delay-difference model.

Description	Equations	
Initialization at equilibrium with $F = 0$		
Unfished survival	$S_0 = e^{-M}$	(E.5)
Unfished mean weight	$\overline{W}_0 = \dfrac{S_0\alpha_g + W_k(1 - S_0)}{1 - \rho_g S_0}$	(E.6)
Unfished numbers	$N_0 = \dfrac{R_0}{1 - S_0}$	(E.7)
Unfished biomass	$B_0 = N_0\overline{W}_0$	(E.8)
Recruitment compensation ratio (CR)	$\chi = \dfrac{4h}{1 - h}$	(E.9)
Stock-recruit parameters	$a = \chi\dfrac{R_0}{B_0}; \quad b = \dfrac{\chi - 1}{B_0}$	(E.10)
Initialization at equilibrium with $F_e > 0$		
Survival at F_e	$S_e = e^{-(M+F_e)}$	(E.11)
Mean weight at F_e	$\overline{W}_e = \dfrac{S_e\alpha_g + W_k(1 - S_e)}{1 - \rho_g S_e}$	(E.12)
[1]Biomass at F_e	$B_e = -\dfrac{\left(-\overline{W}_e + S_e\alpha_g + S_e\rho_g\overline{W}_e + W_k a\overline{W}_e\right)}{b\left(-\overline{W}_e + S_e\alpha_g + S_e\rho_g\overline{W}_e\right)}$	(E.13)
Fisheries reference points at equilbrium fishing mortality F_e		
Fishing mortalities	$\gamma = \{0.01, 0.02, ..., 1.0\}$	
Years to equilibrium	$t = \{2017, ..., T\}$, where $T = 2017 + 200$	
Biomass	$B_{\gamma t} = S_{\gamma,t\text{-}1}\rho_g B_{\gamma,t\text{-}1} + \alpha_g N_{\gamma,t\text{-}1} + W_k R_{\gamma t}$	(E.14)
Numbers	$N_{\gamma t} = S_{\gamma,t\text{-}1} N_{\gamma,t\text{-}1} + R_{\gamma t}$	(E.15)
Survival	$S_{\gamma t} = e^{-(M+\gamma)}$	(E.16)
Long-term yield	$Y_{\gamma T} = \left(1 - e^{-\gamma}\right) B_{\gamma T}$	(E.17)
MSY	$Y_e = \max\left\{Y_{\gamma T}\right.$	(E.18)
Biomass at MSY	$B_e = B_{\gamma T}, \quad \text{for } \gamma \text{ when } Y_e = Y_{\gamma T}$	(E.19)
Fishing mortality at MSY	$F_e = F_{\gamma T}, \quad \text{for } \gamma \text{ when } Y_e = Y_{\gamma T}$	(E.20)

[1] Steven Martell (Sea State Inc., Seattle WA, pers. comm.)

Table E.3. Time-dynamic equations and likelihood components for the delay-difference model.

Description	Equations	
Time-dynamic equations		
Survival rate	$S_t = e^{-M+F_t}$	(E.21)
Biomass	$B_t = S_{t-1}\left(\alpha_g N_{t-1} + \rho_g B_{t-1}\right) + W_k R_t$	(E.22)
Recruits	$R_t = R_0\, e^{\omega_t - 0.5\sigma_R^2}$	(E.23)
Predicted variables used in objective function		
Predicted catch	$\widehat{C}_t = B_t \frac{F_t}{(F_t + M)}\left(1 - e^{-(F_t+M)}\right)$	(E.24)
Predicted mean weight	$\widehat{W}_t = \frac{B_t}{N_t}$	(E.25)
Predicted recruits	$\widehat{R}_t = \frac{aB_{t-k+1}}{1 + bB_{t-k+1}}$	(E.26)

Table E.4. Calculation of variance parameters, residuals, and likelihoods.

Description	Equations	
Variance parameters (SD = standard deviation)		
SD of abundance index residuals	$\sigma_O = \sqrt{\frac{\rho}{\vartheta}} = \sqrt{\rho} \cdot \varphi$	(E.27)
SD of recruitment residuals	$\sigma_R = \sqrt{\frac{1-\rho}{\vartheta}} = \sqrt{1-\rho} \cdot \varphi$	(E.28)
SD of abundance index observations	$\sigma_{jt} = \frac{I_{jt}}{v_{jt}}; \quad \text{where } v_{jt} = \frac{1}{c_{jt}}$	(E.29)
Indices of abundance		
Residuals	$z_{jt} = \log(I_{jt}) - \log(q_j) + \log\left(\widehat{B}_{jt}\right)$	(E.30)
	$\bar{z}_j = \frac{1}{n_j} \sum_{t=1}^{n_j} z_{jt}$	(E.31)
	$d_{jt} = z_{jt} - \bar{z}_j$	(E.32)
Log likelihood	$L_{jt} = \log\left(\sigma_{jt}^2\right) + \frac{d_{jt}^2}{2\sigma_{jt}^2}$	(E.33)
Catch		
Residuals	$d_{C_t} = \log(C_t) - \log\left(\widehat{C}_t\right)$	(E.34)
Log likelihood	$L_t = \log\left(\sigma_C^2\right) + \frac{d_{C_t}^2}{2\sigma_C^2}$	(E.35)
Mean weight		
Residuals	$d_{W_t} = \log\left(\overline{W}_t\right) - \log\left(\widehat{\overline{W}}_t\right)$	(E.36)
Log likelihood	$L_t = \log\left(\sigma_W^2\right) + \frac{d_{W_t}^2}{2\sigma_W^2}$	(E.37)
Recruitment		
Residuals	$d_{R_t} = \log(R_t) - \log\left(\widehat{R}_t\right)$	(E.38)
Log likelihood	$L_t = \log\left(\sigma_R^2\right) + \frac{d_{R_t}^2}{2\sigma_R^2}$	(E.39)

E.4. REFERENCES – MODEL EQUATIONS

Deriso, R.B., Maunder, M.N. and Skalski, J.R. 2007. Variance estimation in integrated assessment models and its importance for hypothesis testing. Can. J. Fish. Aquat. Sci. 64(2): 187–197.

DFO. 2006. A harvest strategy compliant with the precautionary approach. DFO Can. Sci. Advis. Sec. Res. Doc. 2006/023.

Forrest, R.E., Rutherford, K.L., Lacko, L., Kronlund, A.R., Starr, P.J. and McClelland, E.K. 2015. Assessment of Pacific Cod (*Gadus macrocephalus*) for Hecate Strait (5CD) and Queen Charlotte Sound (5AB) in 2013. DFO Can. Sci. Advis. Sec. Res. Doc. 2015/052: xii + 197 p.

Fournier, D.A., Skaug, H.J., Ancheta, J., Ianelli, J., Magnusson, A., Maunder, M.N., Nielsen, A. and Sibert, J. 2012. AD Model Builder: using automatic differentiation for statistical inference of highly parameterized complex nonlinear models. Optim. Methods Softw. 27: 233–249.

Francis, R.I.C.C. 2011. Data weighting in statistical fisheries stock assessment models. Can. J. Fish. Aquat. Sci. 68(6): 1124–1138.

Hilborn, R. and Walters, C.J. 1992. Quantitative Fisheries Stock Assessment: Choice, Dynamics and Uncertainty. Chapman and Hall, New York NY.

Martell, S. 2010. Integrated Statistical Catch Age Model (*i*SCAM). GitHub.

Punt, A.E. and Butterworth, D.S. 1993. Variance estimates for fisheries assessment: their importance and how best to evaluate them. In S. J. Smith, J. J. Hunt and D. Rivard, eds., Risk evaluation and biological reference points for fisheries management, vol. 120 of *Can. Spec. Pub. Fish. Aquat. Sci.*, p. 145–162. Fisheries and Oceans Canada.

Schnute, J.T., Haigh, R. and Couture-Beil, A. 2017. PBSadmb: ADMB for R Using Scripts or GUI. R package version 1.0.0.

Starr, P.J. and Haigh, R. 2017. Stock assessment of the coastwide population of Shortspine Thornyhead (*Sebastolobus alascanus*) in 2015 off the British Columbia coast. DFO Can. Sci. Advis. Sec. Res. Doc. 2017/015: ix + 174 p.

APPENDIX F. MODEL RESULTS

F.1. INTRODUCTION

This appendix describes the results from the application of a delay-difference model (see Appendix E for equations, see Schnute 1985 for model framework) to a suite of survey data (Appendix B), CPUE series (Appendix C) and time series of mean weight estimates (Appendix D) pertaining to two biological stocks of BC Walleye Pollock (WAP). The modelling was done in two stages: initially the best fit to the data was found by finding the mode of the posterior distribution (MPD), which minimised the negative log-likelihood when fitting to the data including the prior penalties (Eqs. E.33, E.35, E.37 and E.39). Fits to the data, model estimates and comparative negative log-likelihoods are presented for all models. A Bayesian second step was adopted, with a Markov chain Monte Carlo (MCMC) search across plausible parameter combinations initialised from the MPD fit. MCMC diagnostics are presented, along with estimated parameters and derived parameters for 12 model runs for the BC North stock and 11 model runs for the BC South stock. All final advice and major outputs are based on the MCMC results. Estimates of major quantities and advice to management (such as decision tables) appearing here are also presented in the main document.

Biological data (weights converted from lengths) from DFO sources suggested that two stocks of Walleye Pollock occur along the outer coast of BC, with fish on average twice as large in the north (mainly Dixon Entrance – 1.056 kg/fish) compared to those in the south (beginning in the lower parts of Hecate Strait – 0.521 kg/fish). This information is presented in detail in Appendix D. The BC North stock probably represents the southern extreme of a larger SE Alaska population, which may provide a rescue effect for any over-harvesting in BC (Gustafson et al. 2000). Consequently, biomass levels for the BC North stock appear to be relatively small and variable. In contrast, the BC South stock is estimated to be much larger ($\sim$ 10x) than the BC North stock, and has two apparent main population centres – Juan de Fuca Strait and Queen Charlotte Strait.

No reliable DFO data (e.g., ages by broken/burnt otoliths) exist to estimate growth models for either stock; therefore, these stock assessment models use a growth model estimated from eastern Gulf of Alaska (GoA) survey data (Martin Dorn, NOAA Fisheries, Sand Point, Seattle, pers. comm.) for the BC North stock and a published growth model based on data from the Sea of Okhotsk (Janusz and Horbowy 1997), which lies between the eastern Russian mainland and Kamchatka Peninsula, just west of the Bering Sea, for the BC South stock. The growth models in Saunders et al. (1989) for the west coast Vancouver Island and the Strait of Georgia were based on ages derived from fin ray sections, with the published growth rate coefficients not capable of matching the observed mean lengths, especially at higher ages of selectivity ($k > 3$), because of the extremely fast growth at young ages (see Figures D.10 and D.11).

Model runs are reported for each stock which span a range of fixed values for $M \in \{0.25, 0.30, 0.35\}$ and $k \in \{3, 4, 5\}$. We selected these values to include the most plausible values for these important parameters. Some other sensitivities were also tried, such as excluding the GIG survey (BC North) and the commercial fishery CPUE series.

This range of model exploration was undertaken because there is substantial uncertainty in specifying the productivity of this stock (as represented by M and the growth model), as well as selecting the age at full knife-edge recruitment (k), assumptions that are mandatory when using a delay difference model. Because the available data are not informative with respect to these key model parameters, it is not possible to objectively rule out these alternate hypotheses. Initially, after covering a range of plausible values for the key parameter assumptions, we chose model runs for advice based on a subjective ranking of the MCMC diagnostics (1 = good, 2 = acceptable, 3 = poor), selecting only those runs that ranked $\leq$2 (using the mean ranking across both authors). The regional peer review (RPR) participants were concerned about runs with high values of $F_{\max}$, and so choices based on F were first identified before considering the MCMC diagnostics:

- use model runs where median $F_{\max}$ across MCMC samples is < 2 (three runs each in BC North and BC South);
- add model runs where median annual F_t is > 2 only once (one run in BC North, three in BC South);
- remove one model run from BC North with poor diagostics;
- keep two BC South model runs with diagnostics flagged as poor but ranked as acceptable by at least one of the authors.

This stock assessment adopted a “Model Averaging” (MA) approach, using the selection process above to yield three model runs for BC North and six for BC South, that represent a range of plausible hypotheses to construct a “Model Average Composite” for each stock to provide advice to managers (Sections F.2.3. and F.3.3.).

F.1.1. Historical Reference Points

The Sustainable Fisheries Framework (SFF, DFO 2009) established provisional reference points to guide management and assess harvest in relation to sustainability. These reference points are the Limit Reference Point (LRP, limit below which biological harm occurs) of 0.4B_{MSY} and the upper stock reference point (USR, limit at which management needs to consider conservation action) of 0.8B_{MSY}, which have not been adopted in this assessment due to concerns about the stability of estimating B_0 and B_{2017} using the iSC∀M delay-difference model (see Appendix E for discussion). In their stead, this assessment adopted historical reference points (HRPs): B_{avg} (average spawning biomass from 1967–2016) as a proxy for B_{MSY}, and $B_{\min}$ (spawning biomass in the year when the reconstructed biomass reached a minimum from which it subsequently recovered to B_{avg}) in place of 0.4B_{MSY}. The term “spawning biomass” used in this Walleye Pollock assessment is interchangeable with “mature exploitable biomass (males and females)”.

The determination of $B_{\min}$ required an algorithm that could be applied to each MCMC sample (matrix row) or MPD vector:

1. Calculate B_{avg} for years spanning 1967–2016;
2. Identify a set of candidate $B_{\min}$ points using the 0.005 quantile;
3. For consecutive-year lows (if any), identify the lowest point to represent the group by the low year;
4. Remove any candidate low that occurs in the final year;
5. Using these candidates (+ the final year) as break points, create vectors of B_t between and including the break points;
6. Determine which vectors of B_t increase to equal or exceed B_{avg};
7. Of the successful candidates in the previous step, choose the one that started from the minimum B_t to represent $B_{\min}$;

8. If none of the B_t vectors reach B_{avg}, increase the quantile for candidate selection and repeat the above from step 2 until a valid B_{min} is found.

As the assessment uses B_{avg} as a recovery point from a low at B_{min}, there is little likelihood that a recovery to B_{avg} cannot be identified. However, certain trajectories, like a constantly decreasing population from B_0, will not yield an identifiable B_{min} using the above algorithm.

In this assessment, the following reference points are used to determine the probabilty of projected B_t exceeding them:

- Current spawning biomass B_{2017}
- Limit Reference Point (LRP): B_{min}
- Upper Stock Reference (USR): $2B_{\mathrm{min}}$
- Average spawning biomass: B_{avg} (average over the years 1967-2016)
- Average harvest rate: u_{avg} (average over the years 1967-2016)

F.2. BC NORTH STOCK

F.2.1. Example Case – North

An example model run for BC North stock is presented to show representative detail in the results. This model is based on a growth model derived from eastern Gulf of Alaska data supplied by Martin Dorn (pers. comm.) and included the following elements:

- instantaneous natural mortality M fixed at 0.30;
- knife-edge recruitment at age k = 3 y;
- steepness h beta prior (mean=0.7, SD=0.15);
- 1973-2016 standardised unsorted mean weights ($\bar{w}$ = 1.05594 kg);
- length-weight allometry: α = 7.1018E-06, β = 3.0415;
- Brody parameters: α_g = 0.3475 kg, ρ_g = 0.8668, w_k = 0.4929 kg;
- growth parameters: L_∞ = 66.9436 cm, κ = 0.211778, t_0 = -1.13642 y;
- errors: observation σ_O = 0.2, recruitment σ_R = 0.6, mean weight σ_W = 0.15;
- uniform priors on q from -10 to 0;
- Walleye Pollock CPUE indices (uniform -10 to 0);
- catch series (GFFOS accessed 2016-09-12);
- equilibrium start in 1967 (use all of GIG historical, including 1995)
- equal-weight for each age class when estimating von Bertalanffy model parameters by sex, combined-sex model interpolated between sexes;
- estimate $\ln(R_0)$ (uniform prior) and fix $\ln(\bar{R})$ and $\ln(R_{\mathrm{init}})$ to $\ln(R_0)$;
- version `iscam-delaydiff.exe`: built 2017-01-03.

F.2.1.1. MPD results – example (north)

The mode of the posterior distribution (MPD) for this model (reported in Table F.1) is estimated by minimising the objective function (components summarised in Section E.2.1). The results are presented to show the fits by the model to the observed data and are used as the starting point for the MCMC simulations. MPD fits are shown for the abundance indices (Figure F.1), the annual mean weights and annual recruitment (Figure F.2). The fits to the survey and CPUE indices are generally reasonable although the model is incapable of fitting the abrupt changes in some series.

The model is not capable of fitting the high values of mean weight that occur throughout the series (Figure F.2). Instead it fluctuates near the mean of the series, effectively ignoring four or five recurring upward shifts in the data. Recruitment events exceed the long-term mean of the series 13 times; the 1974 event is roughly seven times higher than the long-term mean. Fits to the catch data are not presented because the model is parameterised so that it always fits the catch closely.

F.2.1.2. MCMC results – example (north)

The MCMC procedure performed 60,000,000 iterations, sampling every 50,000 to give 1200 draws (1000 samples after dropping the first 200, including the MPD start point, as burn-in). The 1000 samples were used to estimate parameters and quantities of interest, including stock status by year and the probabilities of being above reference points.

MCMC traces show good convergence properties (no trend with increasing sample number) for the leading estimated parameters (Figure F.3), as does a diagnostic analysis that splits the samples into three segments, checking for consistency along the length of the chain (Figure F.4). Autocorrelation appears to be minimal with some periodicty over 100 lags (Figure F.5). Pairs plots of the estimated parameters (Figure F.6) show no undesirable correlation between the two primary parameters, ln(R_0) and h, though all the q parameters were highly correlated with ln(R_0) and with each other, as would be expected. MCMC quantiles for parameters, biomass, and status with respect to historical reference points are summarised in Table F.1.

Marginal posterior distributions, along with the corresponding priors for the estimated parameters, are shown in Figure F.7. Only the steepness parameter used an informative prior, with its posterior distribution largely reflecting the prior. This indicates that there was relatively little information in this model to inform this parameter and it is unlikely that it could be estimated without using a prior.

The plot of estimated spawning biomass (Figure F.8) shows a large increase in the mid 1970s followed by a decline to a low point in 1986. Since then, spawning biomass has fluctuated at levels below the average biomass calculated from 1967-2016. Assuming a catch policy of 1000 t/y, which is close to the 5-y average catch and lower than the current TAC of 1320 t/y, the projected biomass declines precipitously under conditions of average recruitment.

This model run estimates a few strong recruitment pulses in 1974, 1996, and 2012 (Figure F.9), likely to fit drops in mean weight. The first strong recruitment occurs in absence of fishing pressure and so spawing biomass increases substantially (Figure F.8). Thereafter, strong fishing pressure dampens any benefits from strong recruitment (Figure F.10). Fishing mortality peaks in 1993 at a median F value of 0.652 y^{-1} and declines thereafter until it reaches 0.334 y^{-1} in 2016. The median value (and the 5th and 95th percentiles in parentheses) for the estimated level of biomass depletion (B_t/B_{avg}) at the end of the final year of the reconstruction is 0.57 (0.35, 0.83), with the MPD value of 0.52 lying close to the median of the posterior distribution of this quantity (Figure F.10).

The use of historical reference points is illustrated in Figure F.11. Under an assumed catch policy of 1000 t/y, B_{2019} lies considerably below B_{2017}, and both lie below B_{avg}. The current year biomass B_{2017} lies between the LRP and the USR and the median lies just below the median USR. While the current fishing mortality rate F_{2016} is higher than both the average F and the minimum F that occurred in 2001, it is not as high as the maximum fishing mortlaity rates experienced over the assessment time period. The phase plot (Figure F.12) also indicates that the current stock status lies between the LRP and the USR, and the current mid-year harvest rate u_{2016} lies above the average harvest rate over the time series.

Table F.1. BC North: The 5th, 50th, and 95th percentiles of MCMC-derived parameter estimates and quantities from 1,000 MCMC samples for the example model run. Some fixed parameters are reported as MPD only. See Appendix E for paramater definitions. Subscripts 1-4 on q refer to the fishery-independent surveys, subscript 5 refers to the commercial trawl CPUE series. Other definitions: B_{2017} – biomass at the start of 2017, u_{2016} – exploitation rate (ratio of total catch to vulnerable biomass) in the middle of 2016, B_{avg} – average biomass from 1967 to 2016, LRP (limit reference point) – minimum median estimated biomass in the time series, USR (upper stock reference) – twice the LRP biomass. All biomass values are in tonnes. For reference, the average catch over the last 5 years (2011-2015) is 992 t.

	5%	50%	95%	MPD
Parameters				
R_0	565	831	1,266	939
h	0.482	0.736	0.922	0.788
M				0.3
q_1	0.132	0.199	0.291	0.204
q_2	0.0905	0.136	0.202	0.157
q_3	0.169	0.249	0.349	0.287
q_4	0.00451	0.00676	0.0097	0.00789
q_5	0.000132	0.000194	0.000275	0.000225
HRP-based				
B_{2017}	2,145	4,297	8,045	3,544
B_{avg}	5,349	7,568	11,033	6,816
$\mathrm{LRP} = B_{2001}$	1,154	2,333	3,866	2,249
$\mathrm{USR} = 2B_{2001}$	2,308	4,665	7,732	4,498
$B_{2017}/B_{\mathrm{avg}}$	0.353	0.573	0.834	0.52
B_{2017}/B_{2001}	1.19	1.88	3.12	1.58
$B_{2017}/2B_{2001}$	0.594	0.942	1.56	0.788
u_{avg}	0.0964	0.142	0.207	0.157
$u_{2016}/u_{\mathrm{avg}}$	1.55	2.01	2.63	2.12

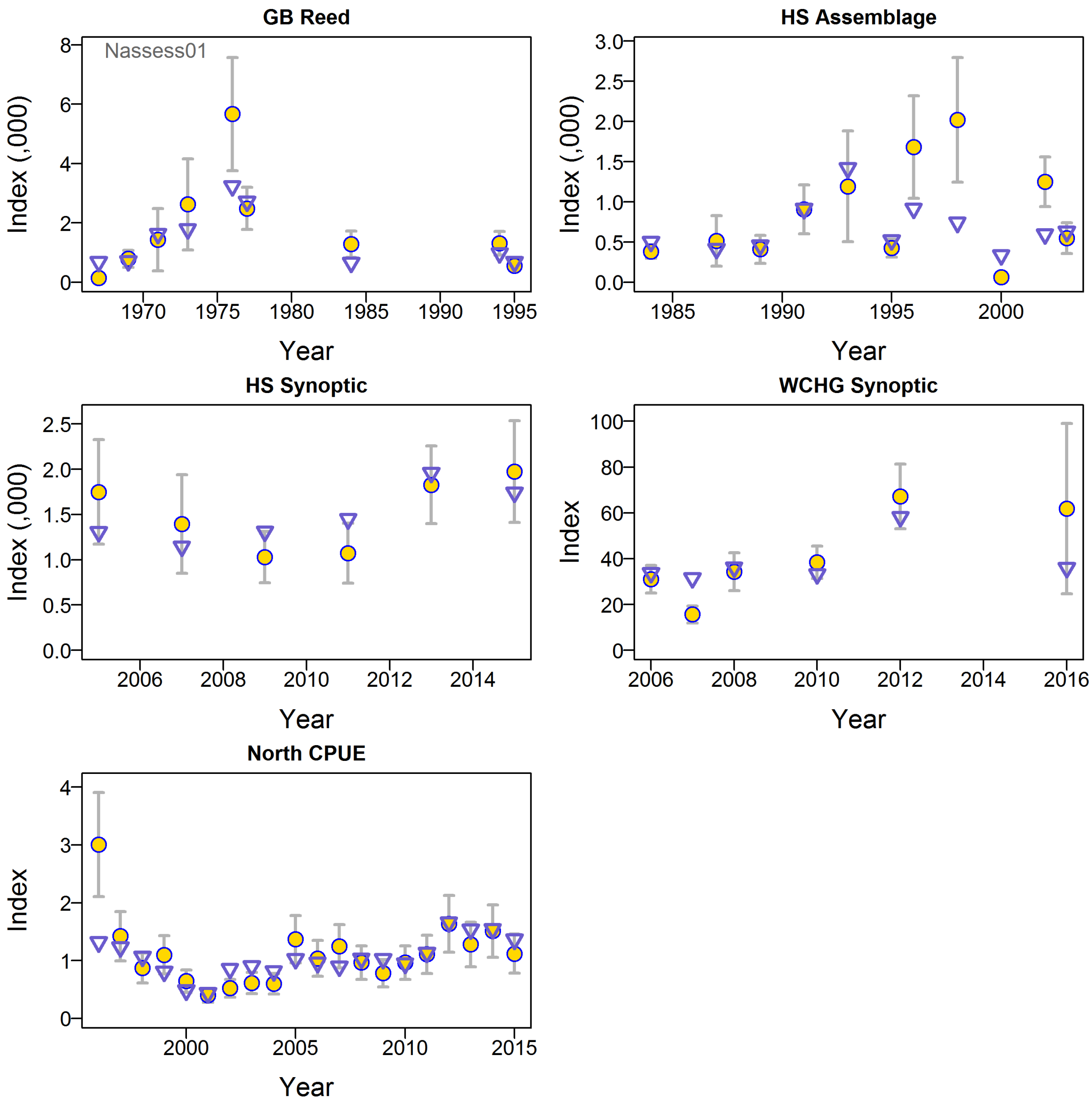

Figure F.1. BC North: MPD index fits to relative abundance indices for the example model run. Circles represent observed indices with associated CVs; squares represent the model fit. Surveys: (1) GIG (Goose Island Gully) Historical, (2) HS (Hecate Strait) Assemblage, (3) HS Synoptic, (4) WCHG (west coast Haida Gwaii) Synoptic, and (5) commercial trawl catch per unit effort of Walleye Pollock.

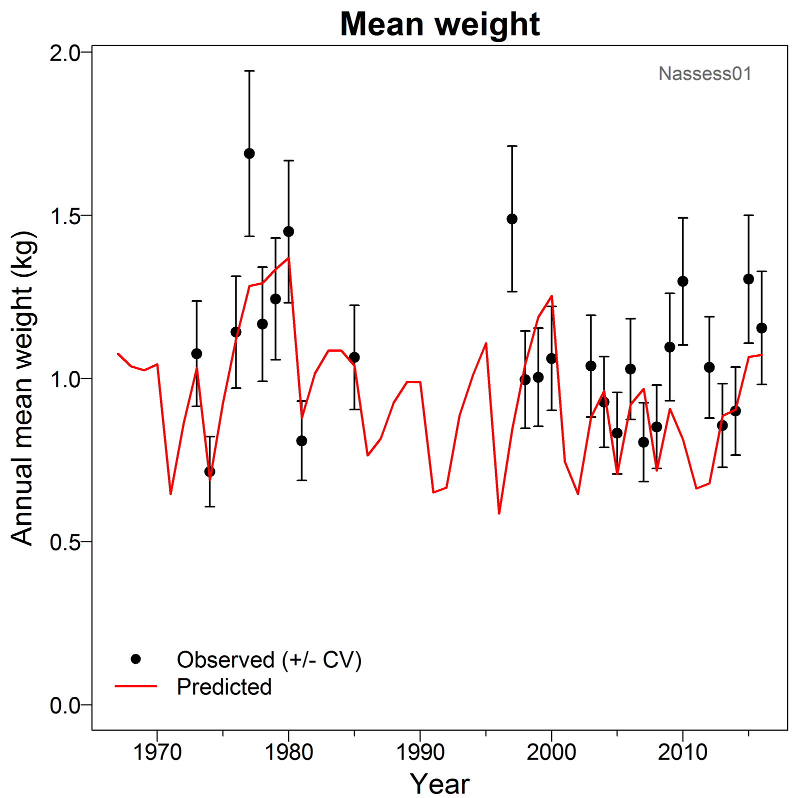

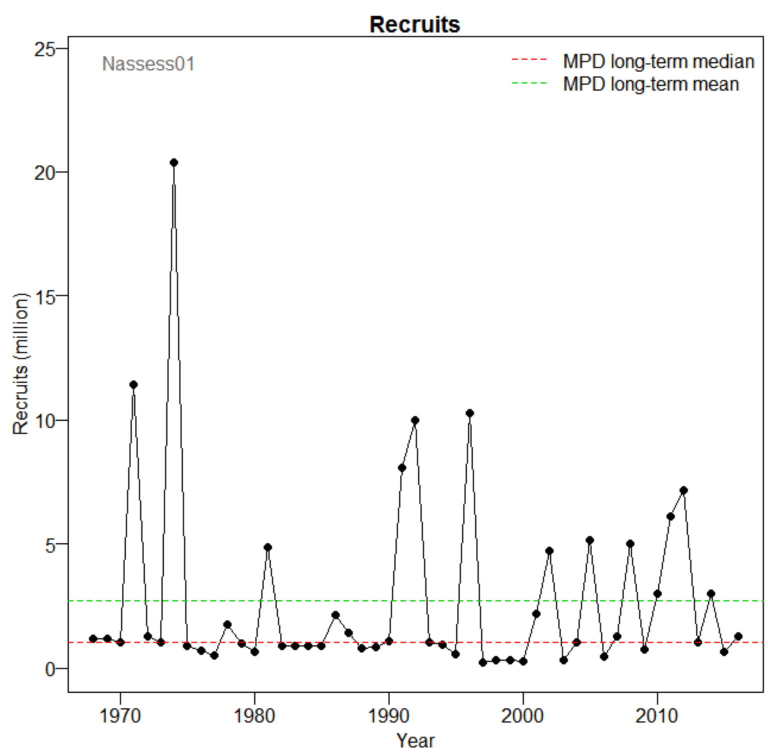

Figure F.2. BC North: **[Top]** *MPD fit to the mean weight data for the example model run. Predicted mean weights are shown as a red line and observations are shown as points. Error bars on mean weight observations represent a fixed CV using σ_W = 0.15.* **[Bottom]** *MPD recruitment in thousands of age-3 individuals in year t for example model run.*

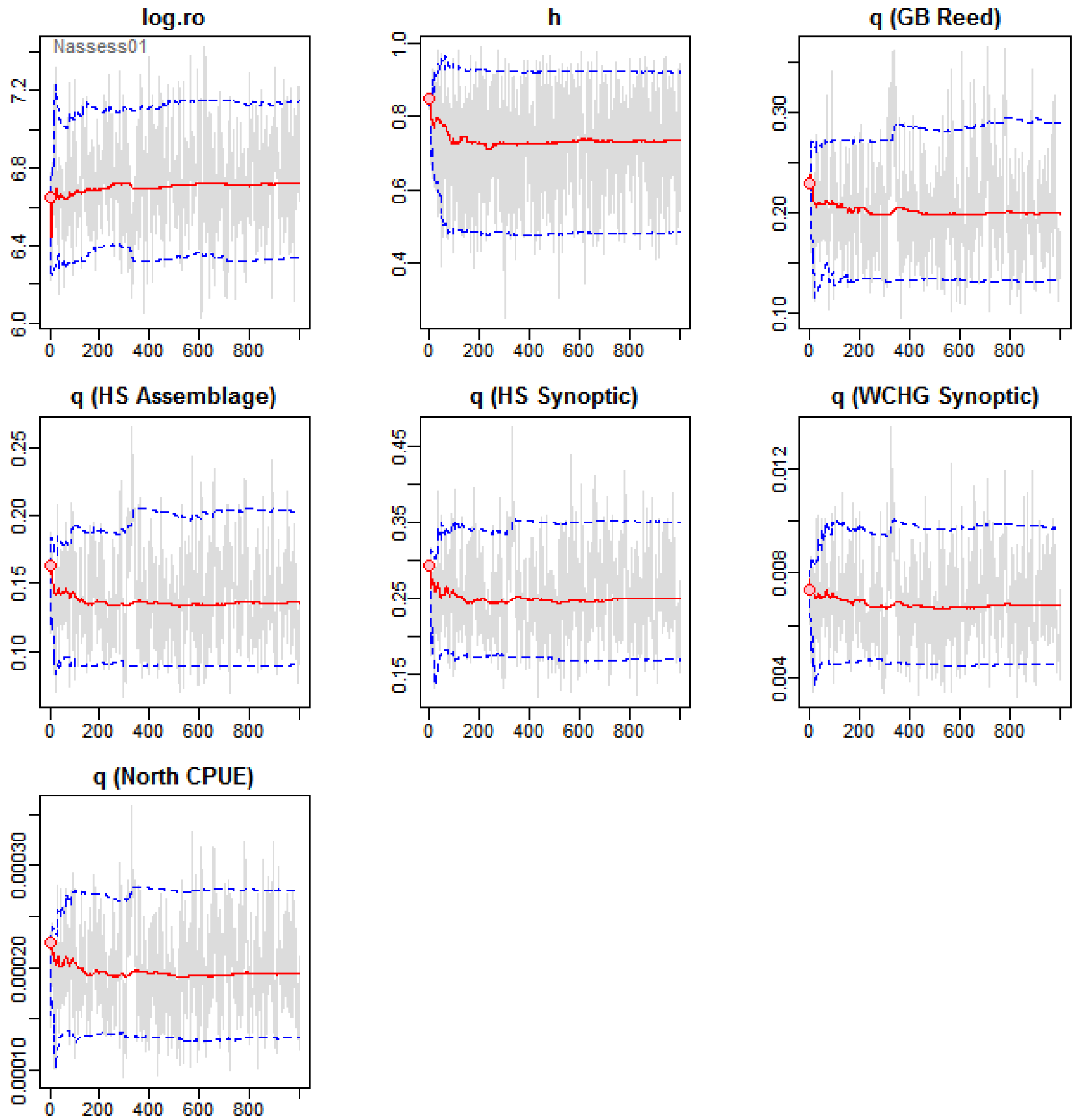

Figure F.3. BC North: Trace plots for MCMC output of estimated parameters in the example model run. The MCMC run shows 1000 MCMC samples after removing 200 samples. Parameters log.ro (natural log of unfished equilibrium recruitment), h (steepness), and q (catchability) for the surveys outlined in Figure F.1. Grey lines show the 1000 samples for each parameter, solid lines show the cumulative median (up to that sample), and dashed lines show the cumulative 2.5 and 97.5 quantiles. Red circles are the MPD estimates.

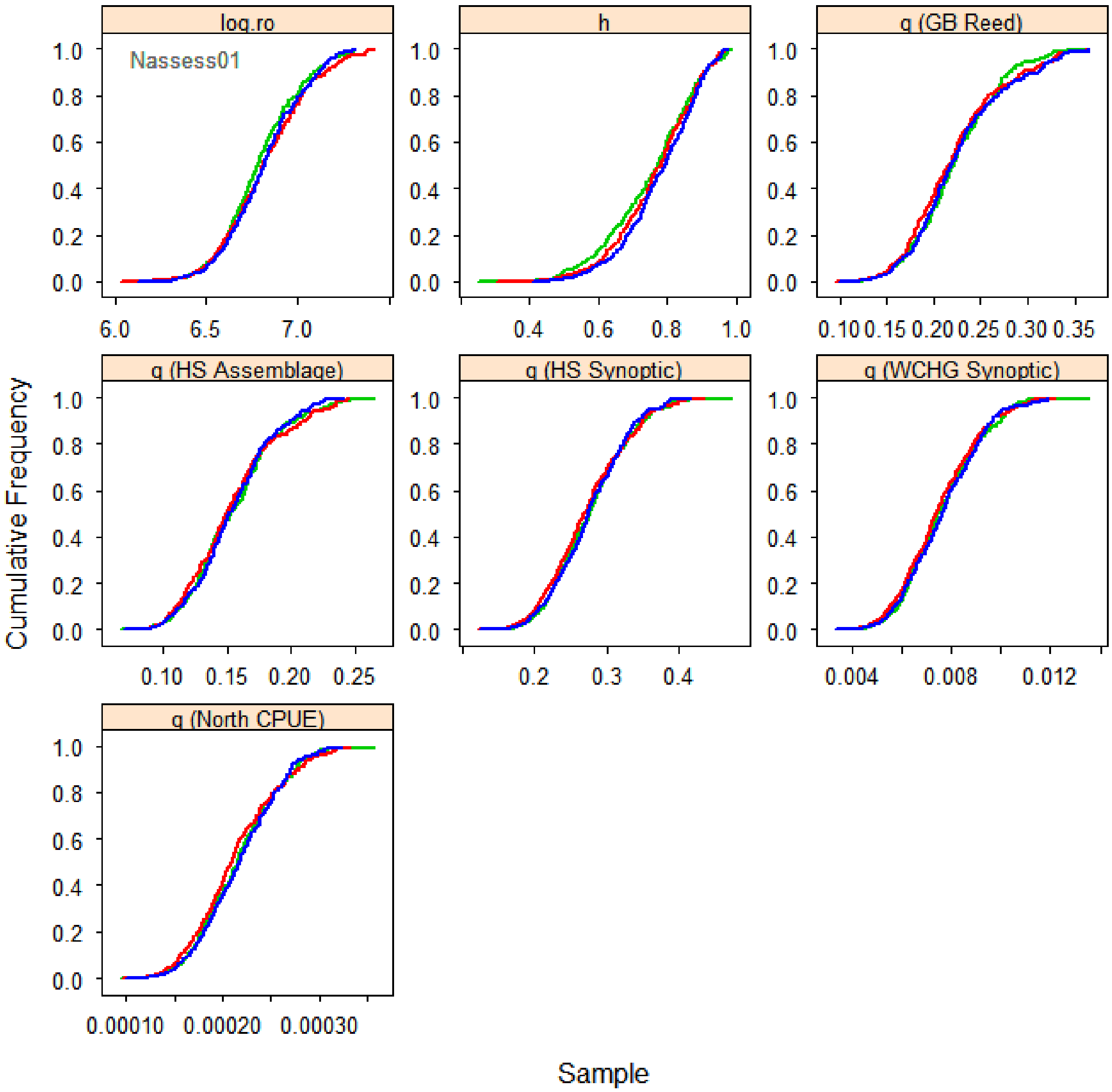

Figure F.4. BC North: Diagnostic plot for the example model run obtained by dividing the MCMC chain of 1000 samples into three segments and over-plotting the cumulative distributions of the first segment (green), second segment (red), and final segment (blue).

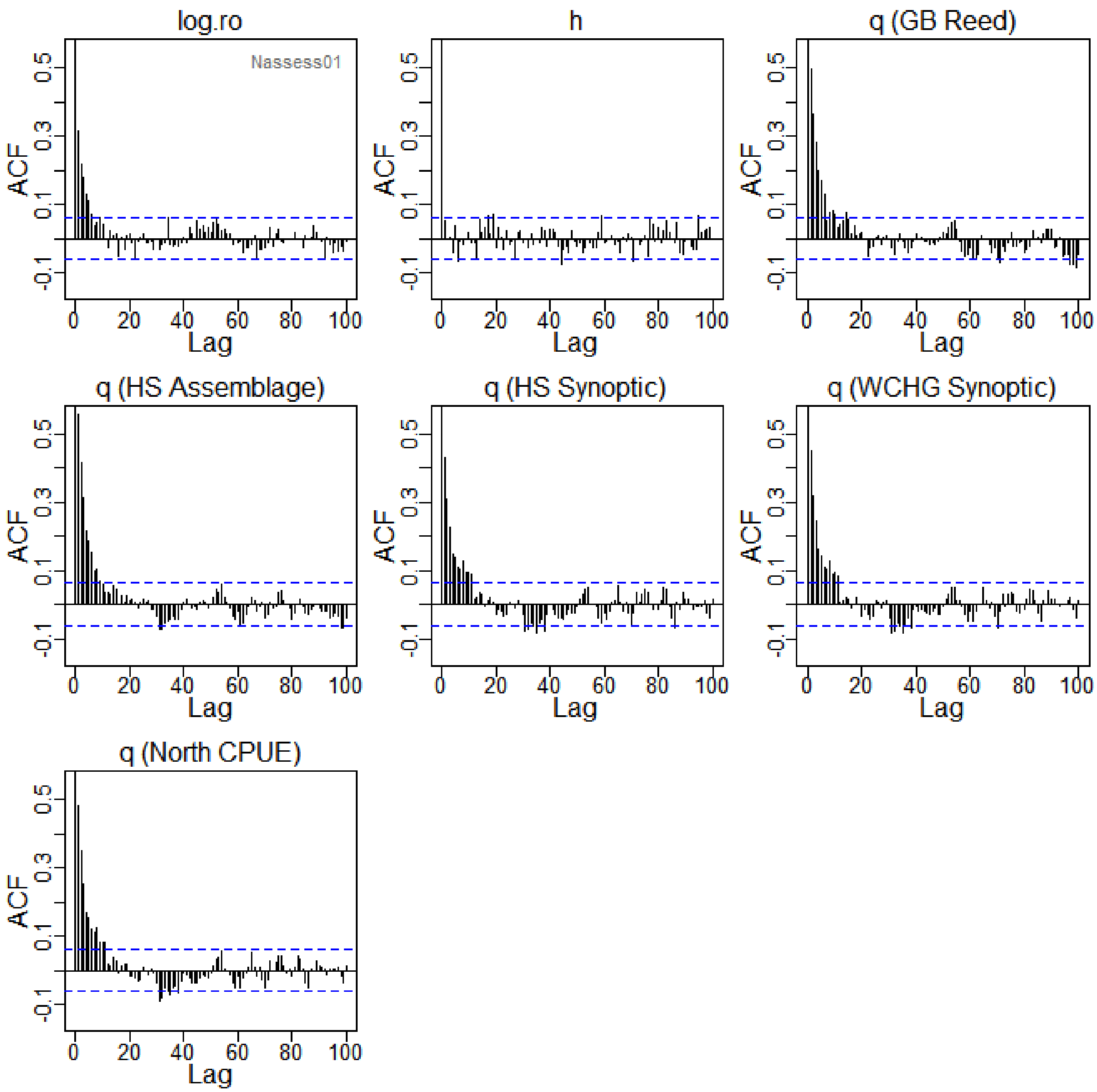

Figure F.5. BC North: Autocorrelation plots for MCMC output of estimated parameters in the example model run. See Figure F.3 for parameter descriptions.

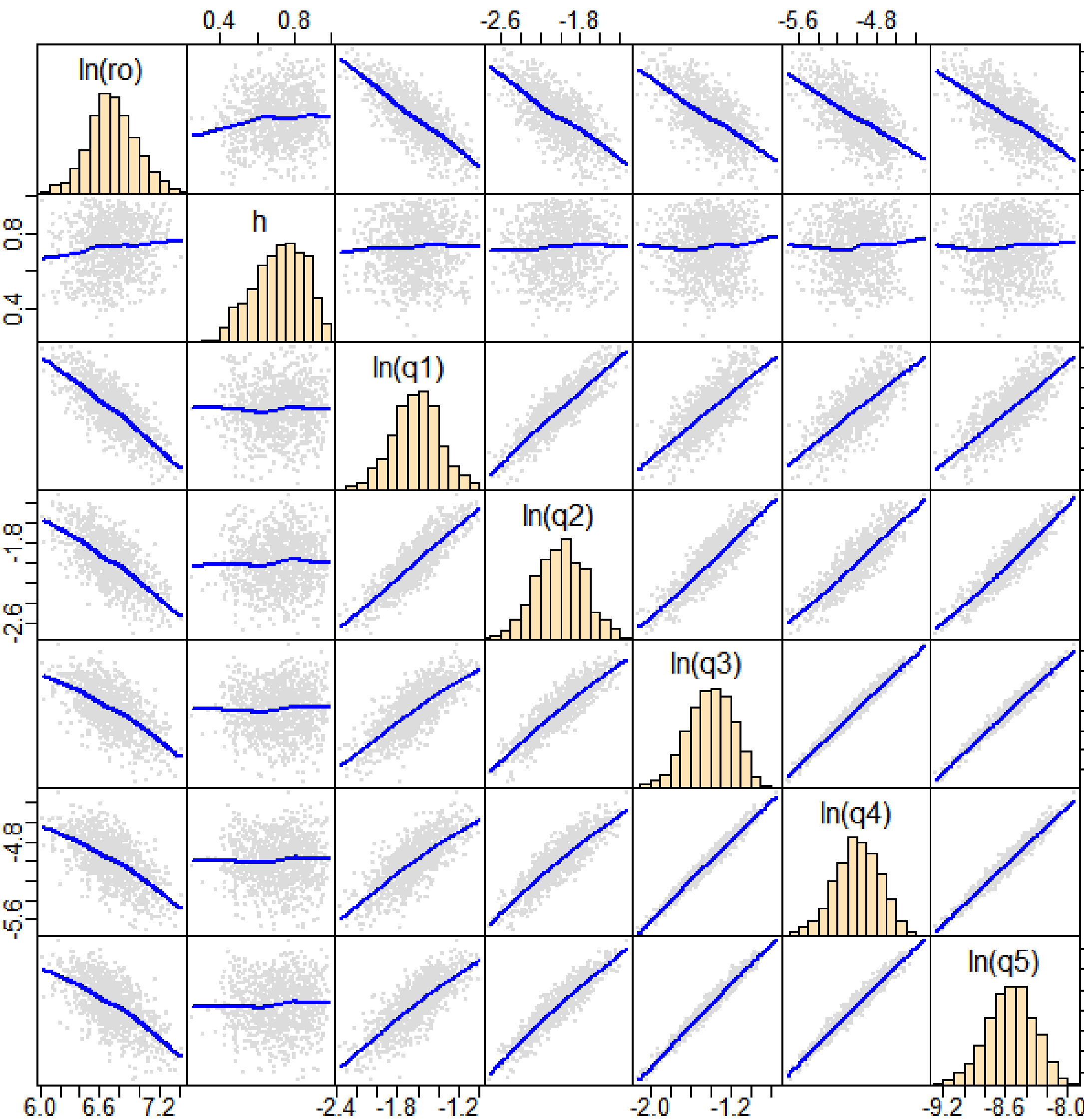

Figure F.6. BC North: Pairs plot from the northern BC region of 1000 MCMC samples for the estimated parameters of the example model run. The diagonal shows the frequency distribution of each posterior.

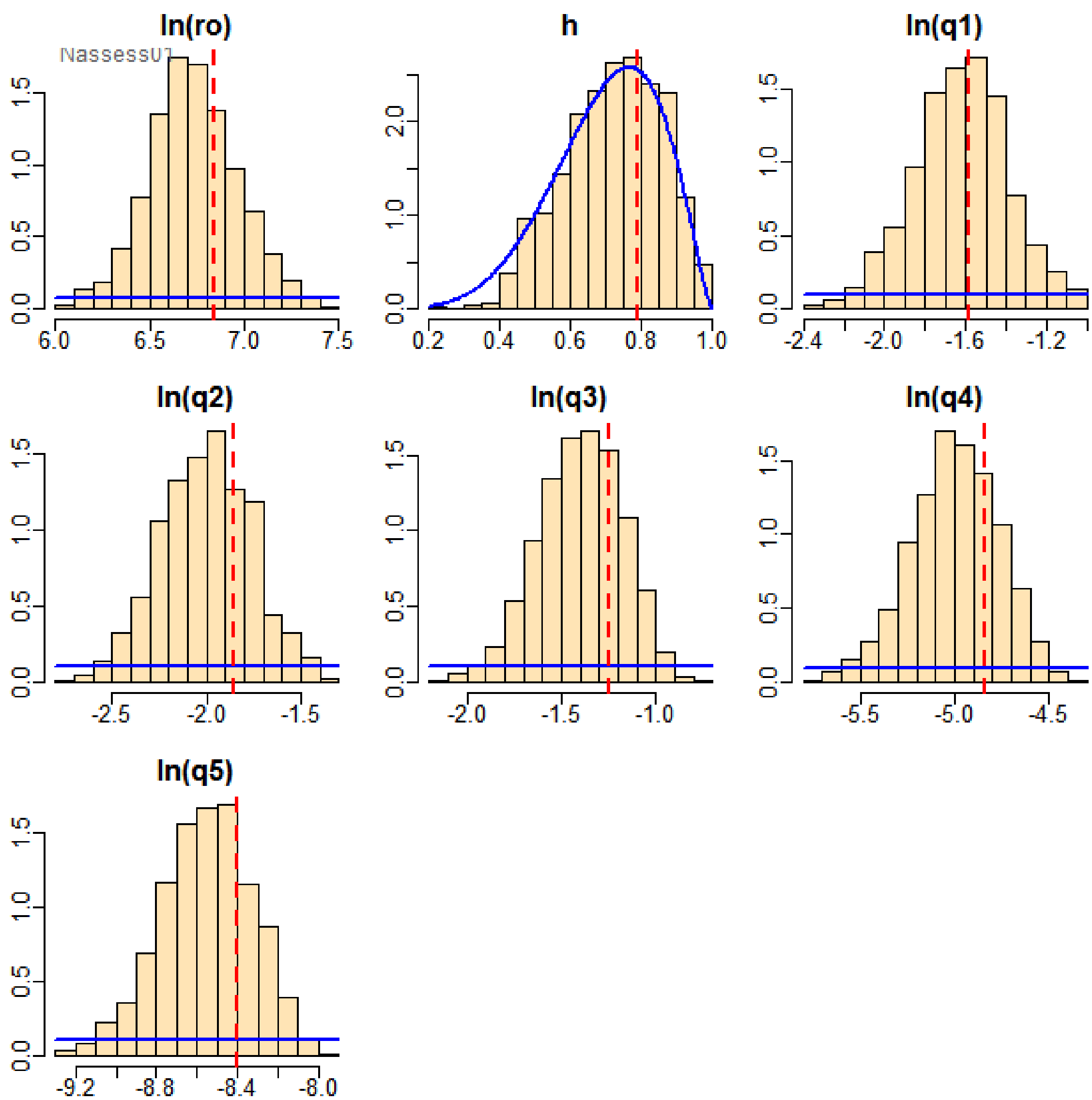

Figure F.7. BC North: Prior probability distributions (blue lines) used in the example model run and the comparative posterior histograms. Parameters q_j represent catchability of the various surveys j as defined in Figure F.3. The dashed red vertical lines show the MPD estimates.

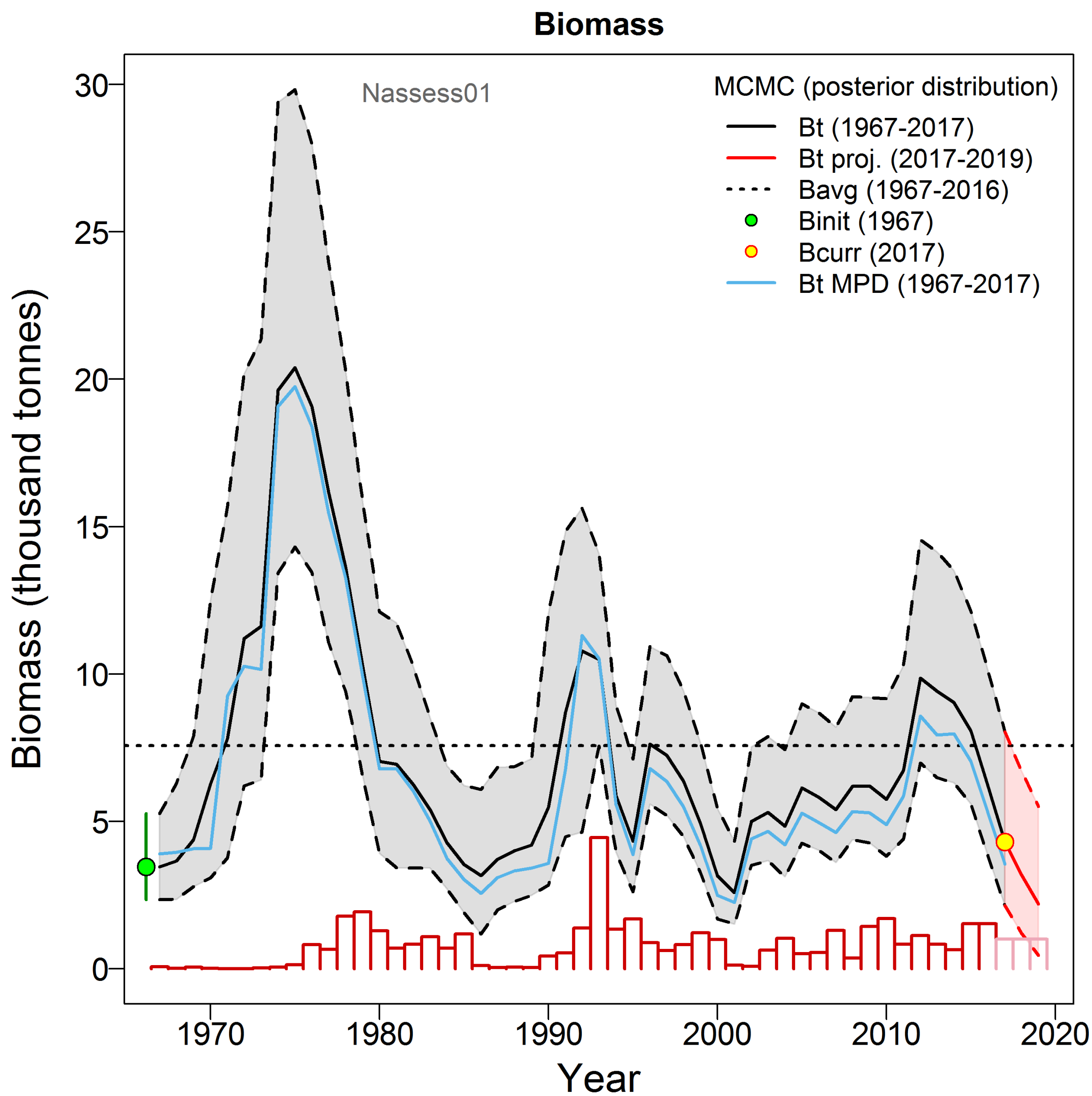

Figure F.8. BC North: Posterior estimates of spawning biomass (1000 t) for the example model run with 95% credibility intervals in grey. The current year biomass (2017, yellow point) and projected biomass (2018-2022, red line), assuming a constant catch policy of 1000 t/y, are enclosed by a 95% credibility interval shaded pink. The median posterior estimate of B_0 is shown as a green point (with 95% credibility range) to the left of the time series. The MPD estimate is shown as a blue line. The total catch is shown along the bottom as red bars, with assumed TAC catch in pink.

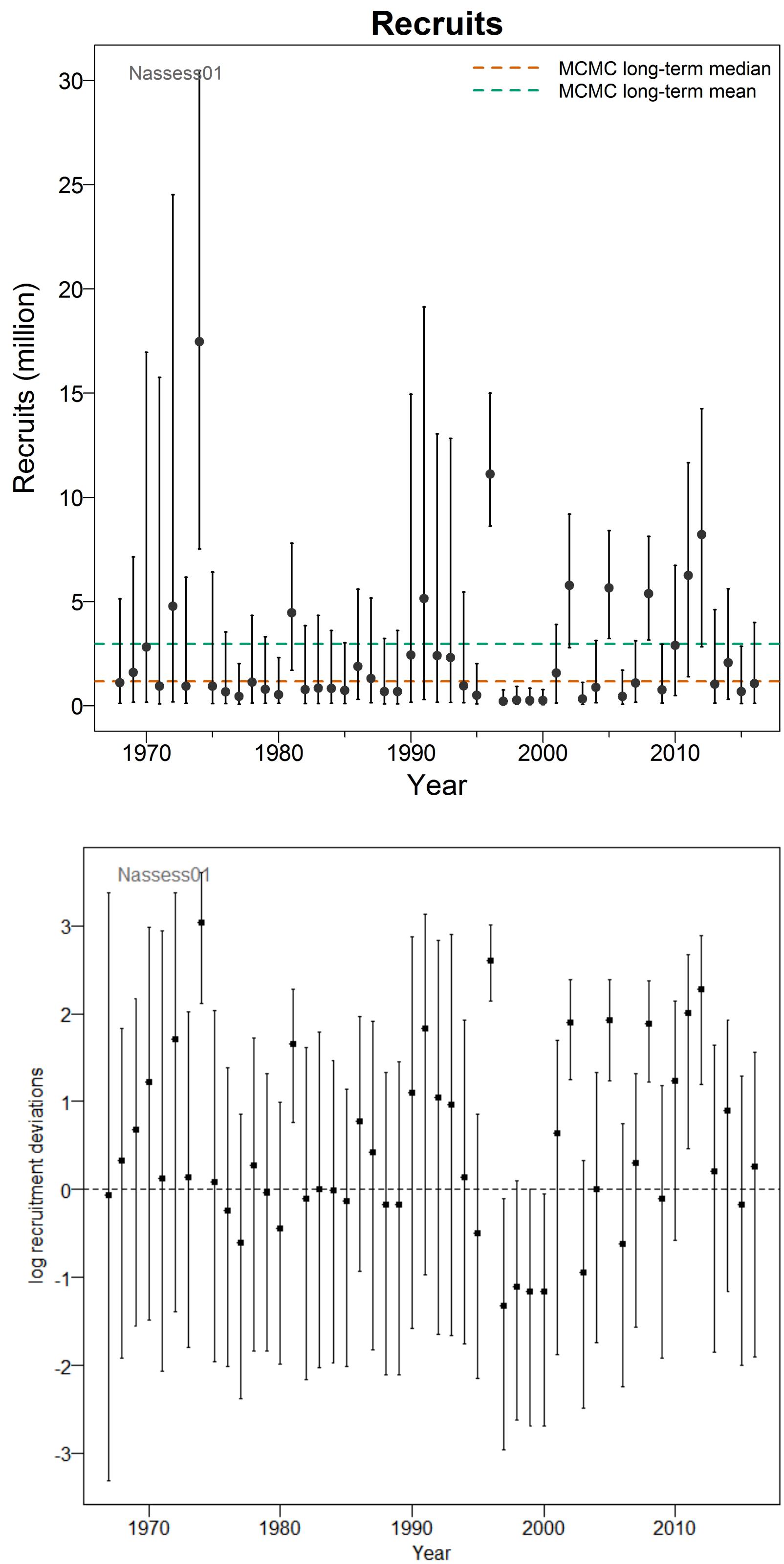

Figure F.9. BC North: **[Top]** *Posterior estimates of age-3 recruits for the example model run.* **[Bottom]** *Log recruitment deviations for the example model run with 95% credibility intervals.*

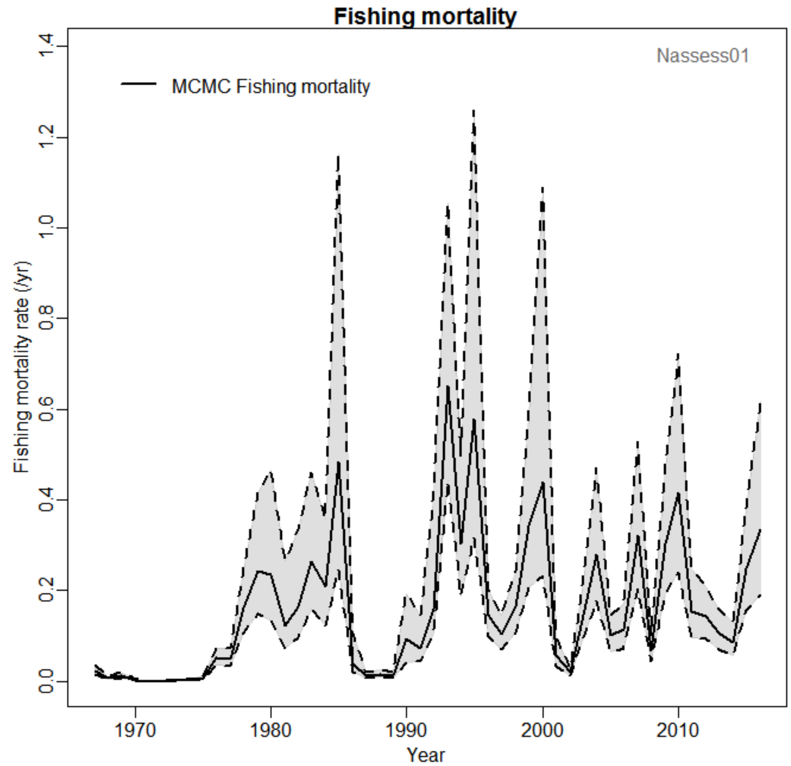

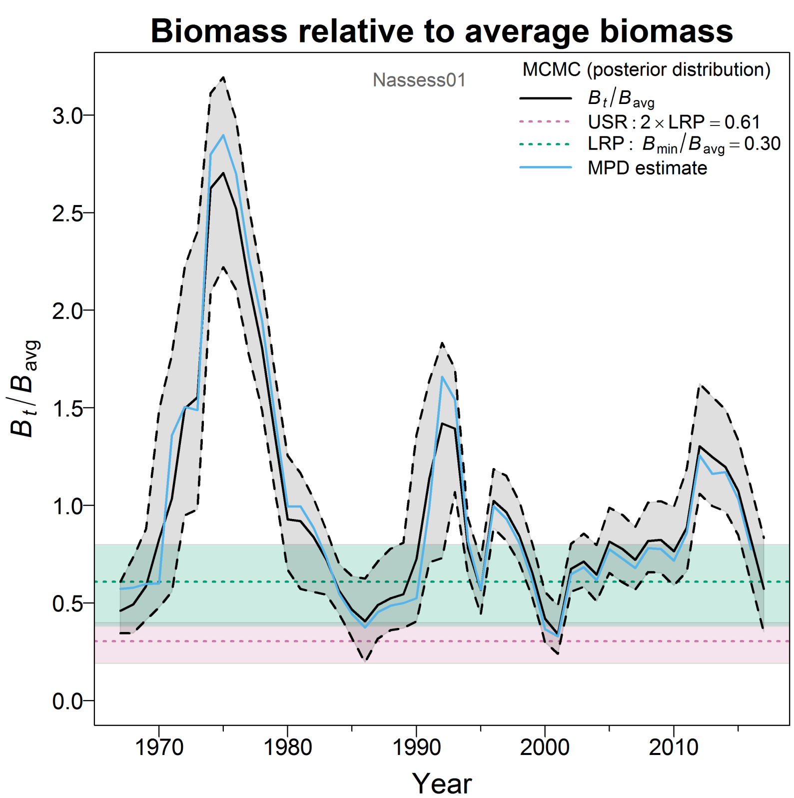

Figure F.10. BC North: **[Top]** *Posterior estimates of fishing mortality for the example model run.* **[Bottom]** *Biomass depletion, i.e. B_t/B_{avg}, for the example model run with 95% credibility intervals. Also displayed on the depletion figure is the MPD estimate (blue line) and the reference points B_{min} (red dashed line) and $2B_{\mathrm{min}}$ (green dashed line).*

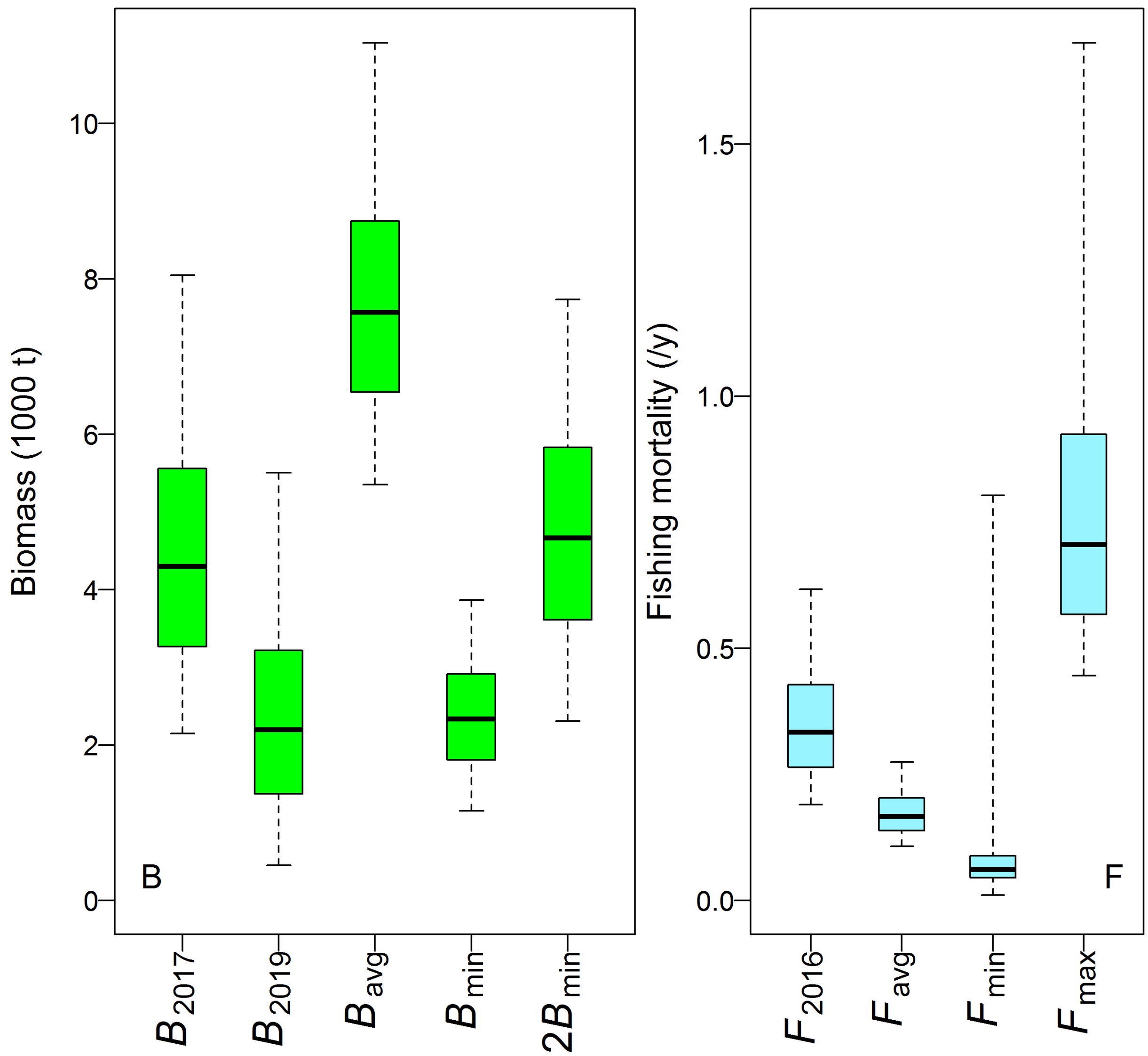

Figure F.11. BC North: Posterior estimates of spawning biomass- and harvest-based reference points for the example model run. **[Left]** *The current-year biomass B_{2017}, the projected-year biomass B_{2019}, B_{avg} = average biomass from 1967 to 2016, the limit reference biomass (or B_{min}) = biomass in 2001, and the upper stock biomass set at $2B_{2001}$.* **[Right]** *The current-year fishing mortality rate F_{2016}, the average fishing mortality rate F_{avg} from 1967 to 2016, the fishing mortality rate in the year of minimum biomasss F_{2001}, and the maximum fishing mortality experience over the time series F_{max}. Box delimiter and limits represent quantiles at 0.5 (median), 0.25 and 0.75 quantiles, respectively, and the whiskers delimit the 0.05 and 0.95 quantiles. Outliers are not shown.*

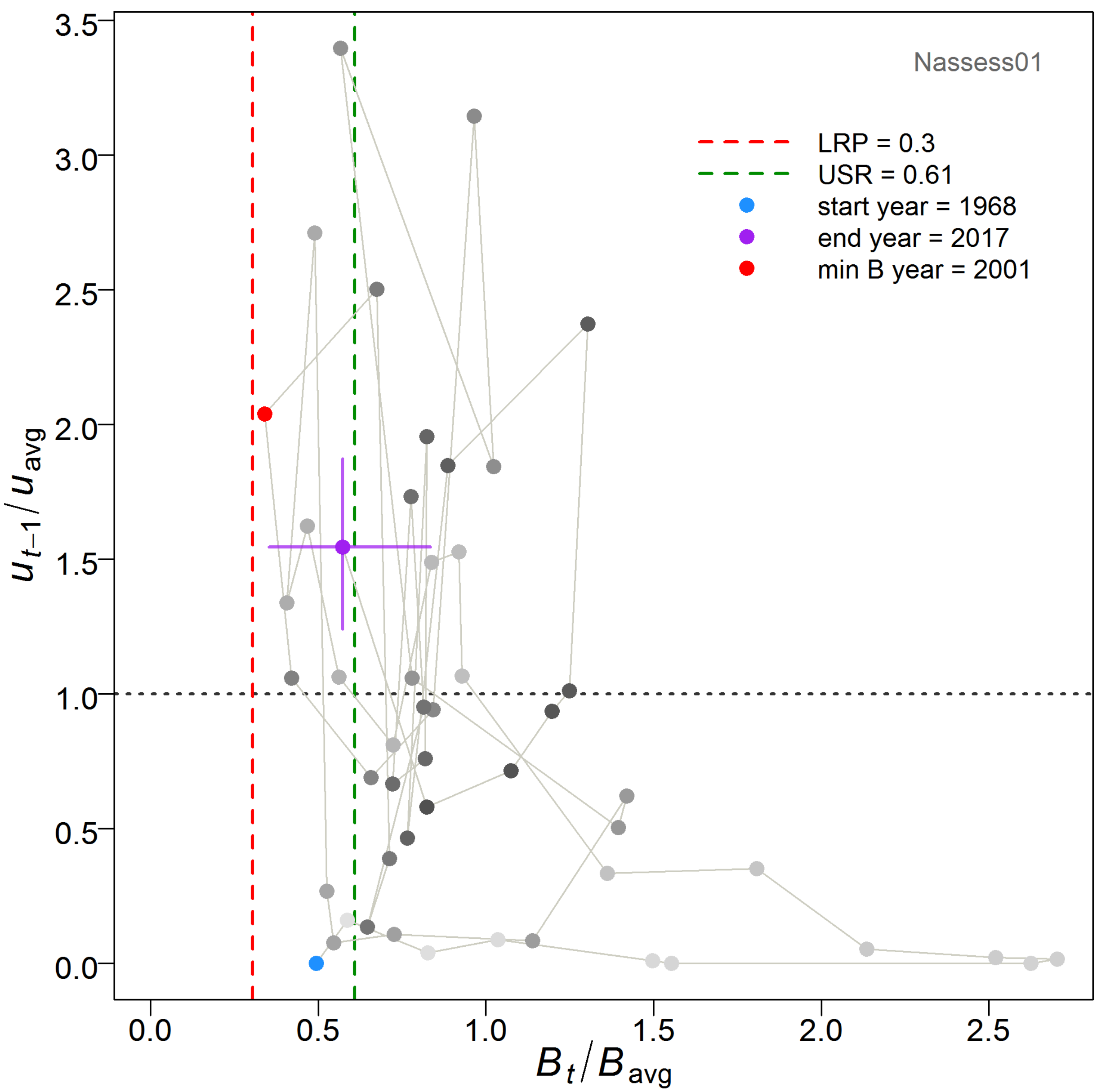

Figure F.12. BC North: Phase plot through time for the example model run of the medians of the ratios B_t/B_{avg} (the biomass in year t relative to B_{avg}) and u_{t-1}/u_{avg} (the exploitation rate in year $t-1$ relative to u_{avg}). Blue filled circle is the starting year 1967. Years then proceed from light grey through to dark grey with the final year 2017 as a filled purple circle with limit lines represent the 0.05 and 0.95 quantiles of the posterior distributions for the final year. Vertical dashed lines indicate the historical limit (red) and upper stock reference (green) points (see legend for values), and horizontal dotted line indicates u_{t-1} at u_{avg}.

F.2.2. Alternative Cases – North

A necessary component to this stock assessment was testing the sensitivity of the results and the associated advice to key uncertainties in the underlying stock assessment model. Therefore, we ran a total of 12 alternative runs (Table F.2) (including the example run above), using the derived growth model from the eastern Gulf of Alaska (see Appendix D) to test the robustness of the results to uncertainties in:

- natural mortality (M);
- age at knife-edge recruitment (k);
- use of the GIG historical survey series; and
- use of the CPUE index series.

We tested a range of sensible values for M and k because these parameters control key assumptions made by the delay-difference model, given that the data available to the model are not very informative with respect to these parameters. We also tested combinations of M and k for the last two alternative categories (removing index series).

Although the Alaskan stock assessments use age-specific natural mortality rates for Walleye Pollock, the underlying assumption is that M = 0.30 for age at full maturity (Dorn et al. 2015). The delay-difference model assumes that maturity matches selectivity, i.e., all recruited fish are mature, and by extension, all mature fish will have a single natural mortality rate. Alternative runs were made with $M \in \{0.25, 0.30, 0.35\}$ to bracket plausible values for this parameter (Table F.2) that are consistent with the Alaskan stock assessment assumption for this species.

The delay-difference assumption of knife-edge selectivity at a specific age k is a strong assumption that is difficult to test without age information from the fishery. However, if such information were available, it is likely that another form of model would have been used. Dorn et al. (2012) provide a range of selectivity ogives for the GoA fisheries and surveys, with the median age selected to these commercial fisheries ranging from age 3 to age 5 (see columns 5 to 7 in Table D.7). Based on the ogives in this table, ages 3 and 4 were selected as the most likely ages to use for the age of knife-edge recruitment in the BC North Walleye Pollock delay-difference model (Table F.2).

The parameterisation of the iSC∀M delay-difference model combines observation and process error into a single total variance parameter ϑ. This variable is partitioned into observation and process error components through the parameter ρ (see Equations E.27 and E.28). Experimentation with a higher value for ρ when using the same model to assess Shortspine Thornyhead (Starr and Haigh 2017) showed that increasing the error term led to greater uncertainty but did not appreciably affect the overall conclusions. Consequently, it was decided to leave out sensitivities to this component of the model for this assessment. These parameters were fixed in all model runs such that the overall observation error (σ_O) was 0.2 and the recruitment process error (σ_R) was 0.6, the latter being a common value used as a default for teleost finfish. A further variance component σ_W sets the weight used to fit the mean weight observations, which was fixed at $\sigma_W = 0.15$ for all model runs to ensure a strong fit to the mean weight series.

Five of the alternative runs (including the example case) used all the abundance index series and paired $k = 3$ with $M \in \{0.25, 0.30, 0.35\}$ and $k = 4$ with $M \in \{0.30, 0.35\}$. Five alternative runs dropped the GIG historical survey and paired $k = 3$ with $M \in \{0.25, 0.30\}$ and $k = 4$ with

$M \in \{0.25, 0.30, 0.35\}$. This was done because, strictly speaking, the GIG survey did not operate in the stock definition area for the BC North stock. However, because this series is the only set of early abundance information, two blocks of runs were made, one with and one without this survey. The final two sensitivities dropped the CPUE index series as well as the GIG survey series and paired $M = 0.3$ with $k \in \{3, 4\}$. Again, this was done because there is uncertainty as to whether fishery-dependent data track abundance.

All 12 alternative runs were taken to the MCMC level. Each MCMC search was started at the "best fit" MPD parameter set, run for 60 million iterations, and sampled every 50,000 for 1200 samples. The first 200 samples were dropped as burn-in to yield a total posterior sample of 1000 draws.

F.2.2.1. MPD results – alternatives (north)

This large number of alternative runs shows that the data available to this model do not allow much discrimination between the range of hypotheses tested. While there were differences in the fits to the available biomass indices and to the mean weight data, these differences tended to be small and probably could not distinguish between hypotheses except in the most extreme cases. As an example, none of the models were able to fit the high mean weights observed in the late 1970s or near the end of the time series (Figure F.13), which may be attributable to misspecification of the growth model. While the delay-difference model uses the mean weight data to scale the overall biomass and to obtain recruitment deviation information, it is likely that only an age-structured model would have sufficient flexibility to fit the entire mean weight series. The model also did not fit high points in the HS Assemblage survey or in the CPUE times series (Figures F.14 and F.17). However, despite these difficulties, the overall fit to most abundance indices was acceptable.

In an attempt to make such comparisons more quantitative, the negative log-likelihoods for the fits to each data component of the model are summarised for the 12 alternative runs in Table F.3. Comparisons of the whole model can only be made among those runs that shared the same estimated components:

- Cases S00 to S04 – S04 had the lowest objective function value of these five cases and offered the best model fit in the first group;
- Cases S05 to S09 – S09 offered the best fit in the second group; and
- Cases S10 to S11 – S11 offered the best fit in the third group.

The three best-fit models all featured $k = 4$ and $M \in \{0.35, 0.30\}$, which likely reflects the growth model used for this population of large Walleye Pollock. Case S11 also showed the best fit to the mean weight component, and most of the $k = 4$ models showed better fits than those where $k = 3$. This observation tended to be true for the survey components as well.

Table F.2. Summary of the analyses performed to test the sensitivity of the delay-difference model to variations in natural mortality M, knife-edge recruitment age k. All runs for the BC North stock use the eastern Gulf of Alaksa growth function (Martin Dorn, pers.comm.). The column marked 'Rank' provides a subjective ranking of the MCMCs, where 1 = good, 2 = acceptable, and 3 = poor.

Case	Run ID	Run #	M	k	Rank
S00	M.30+k3	1	0.3	3	1.25
Four surveys + CPUE time series					
S01	M.25+k3	16	0.25	3	3
S02	M.30+k4	4	0.3	4	2.5
S03	M.35+k3	2	0.35	3	1.5
S04	M.35+k4	12	0.35	4	1.5
Remove the GIG survey					
S05	M.25+k3-GIG	9	0.25	3	3
S06	M.25+k4-GIG	7	0.25	4	2
S07	M.30+k3-GIG	3	0.3	3	3
S08	M.30+k4-GIG	5	0.3	4	1.5
S09	M.35+k4-GIG	10	0.35	4	1.25
Remove both GIG survey and CPUE					
S10	M.30+k3-GIG-CPUE	8	0.3	3	2
S11	M.30+k4-GIG-CPUE	6	0.3	4	2

Table F.3. BC North MPD negative log likelihoods from the 12 alternative cases documented in Table F.2 for each data component used in the model.

Case	Catch	GIG Hist	HS Assem	HS Synop	WCHG Synop	North CPUE	Recruits	Mean Weight	ObFn Value
S00: M.30+k3	-101.355	19.734	48.086	-0.694	7.464	9.000	80.902	-1.100	198.860
S01: M.25+k3	-101.135	22.087	47.223	-0.354	7.910	11.075	82.006	-1.465	204.633
S02: M.30+k4	-101.465	23.916	32.534	-2.655	2.898	4.975	81.486	-6.832	171.551
S03: M.35+k3	-101.532	17.715	48.824	-0.982	7.038	7.171	80.259	-0.596	194.482
S04: M.35+k4	-101.535	22.377	30.236	-2.781	2.494	5.077	80.540	-7.329	165.332
S05: M.25+k3-GIG	-101.116	—	40.897	-0.115	7.654	11.390	72.901	-0.288	164.739
S06: M.25+k4-GIG	-101.336	—	32.827	-2.160	3.413	4.403	72.644	-4.646	138.121
S07: M.30+k3-GIG	-101.322	—	42.312	-0.425	7.229	9.237	72.718	0.059	163.199
S08: M.30+k4-GIG	-101.433	—	30.338	-2.325	3.022	4.311	72.005	-5.972	132.711
S09: M.35+k4-GIG	-101.510	—	28.094	-2.469	2.626	4.319	71.733	-6.578	128.908
S10: M.30+k3-GIG-CPUE	-101.389	—	26.508	1.652	3.586	—	72.920	-6.654	130.290
S11: M.30+k4-GIG-CPUE	-101.202	—	23.382	-0.348	0.452	—	71.339	-7.695	118.341

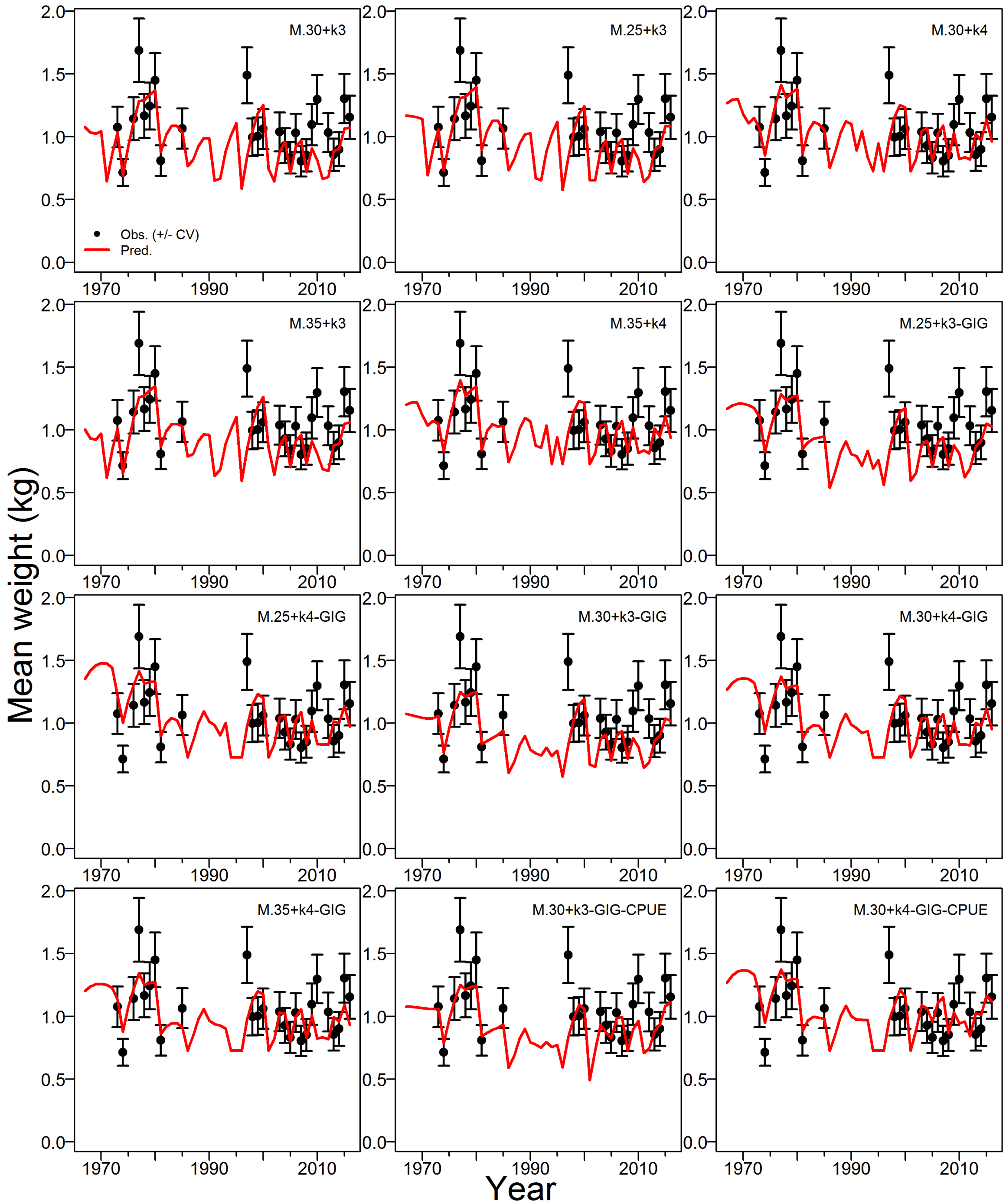

Figure F.13. BC North: MPD fit to the mean weight data for the 12 alternative runs. Predicted mean weights are shown as red lines and observations are shown as points. Error bars on mean weight observations represent a fixed CV using $\sigma_W = 0.15$.

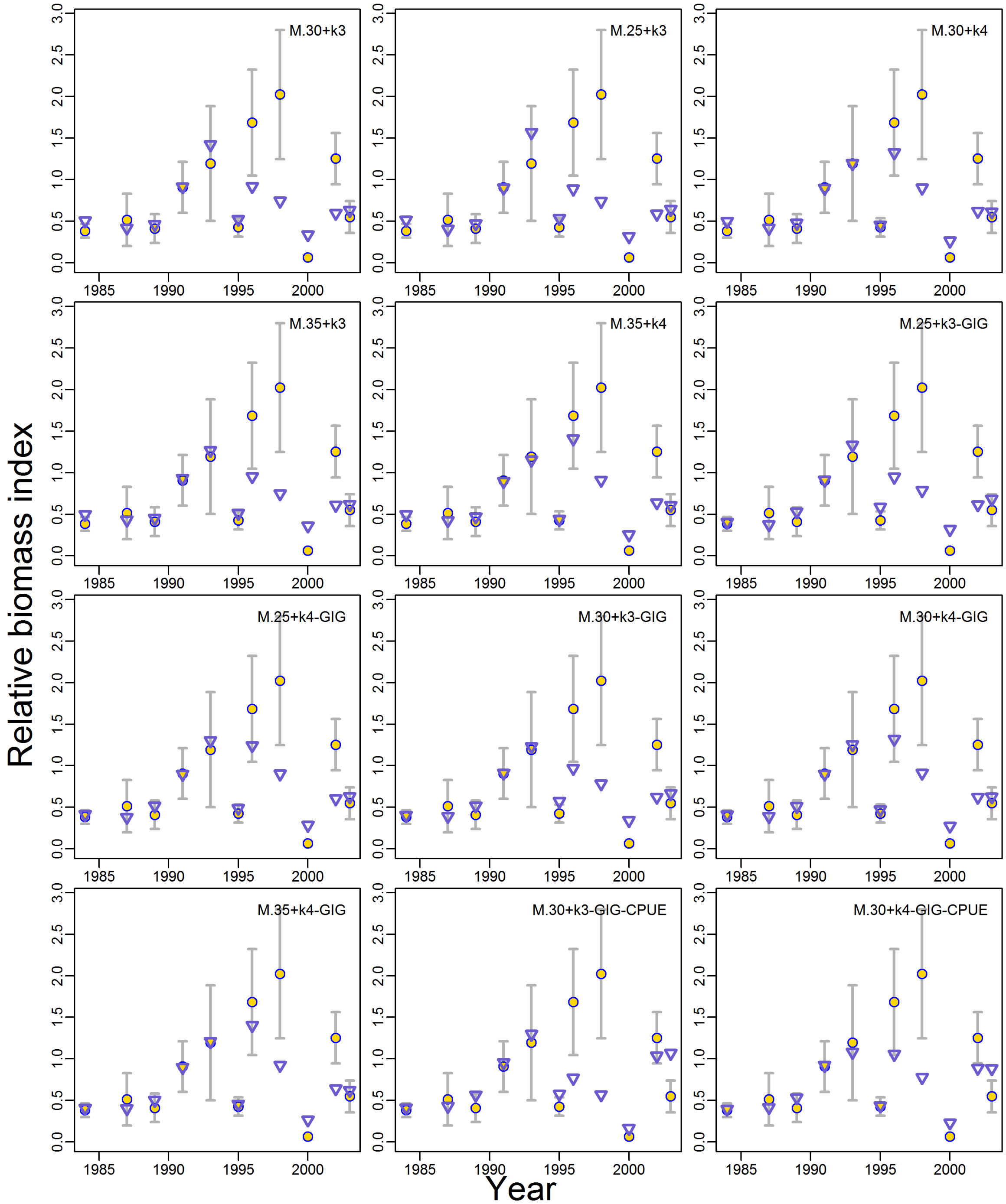

Figure F.14. BC North: MPD index fits (12 alternative runs) for the HS (Hecate Strait) assemblage survey relative abundance indices. Circles represent observed indices with associated CVs, triangles represent the model fit.

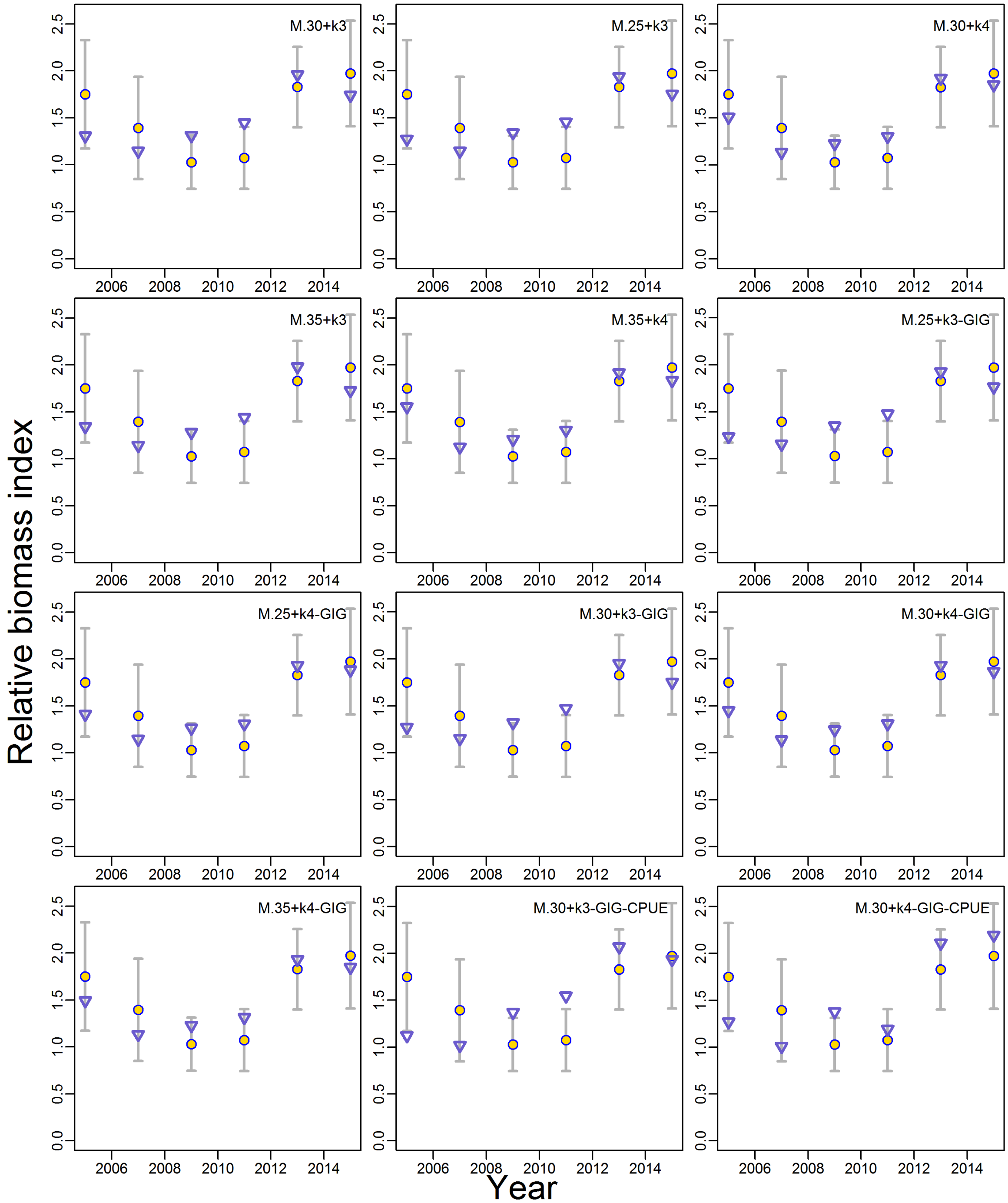

Figure F.15. BC North: MPD index fits (12 alternative runs) for the HS (Hecate Strait) synoptic survey relative abundance indices. Circles represent observed indices with associated CVs, triangles represent the model fit.

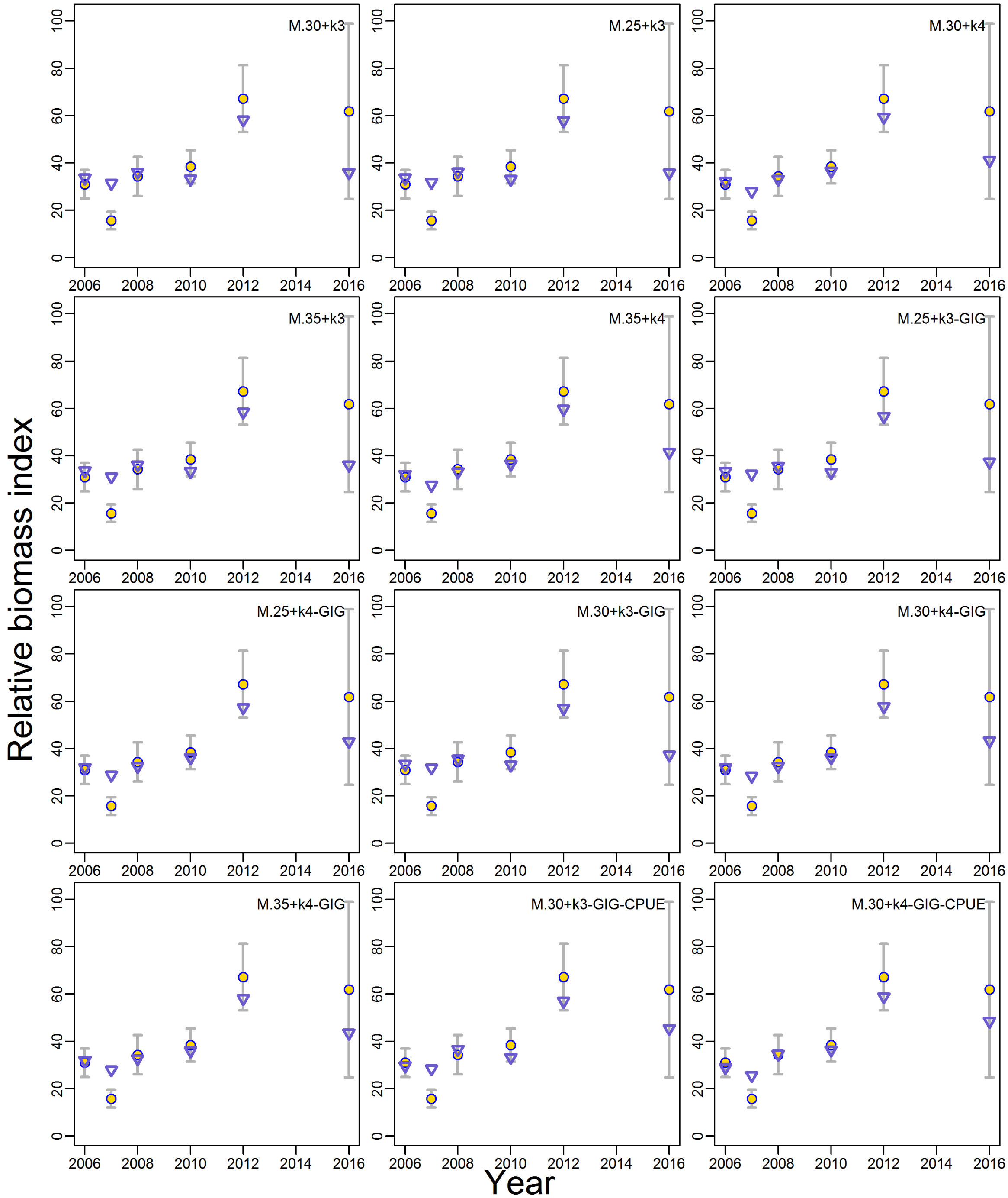

Figure F.16. BC North: MPD index fits (12 alternative runs) for the WCHG (west coast Haida Gwaii) synoptic survey relative abundance indices. Circles represent observed indices with associated CVs, triangles represent the model fit.

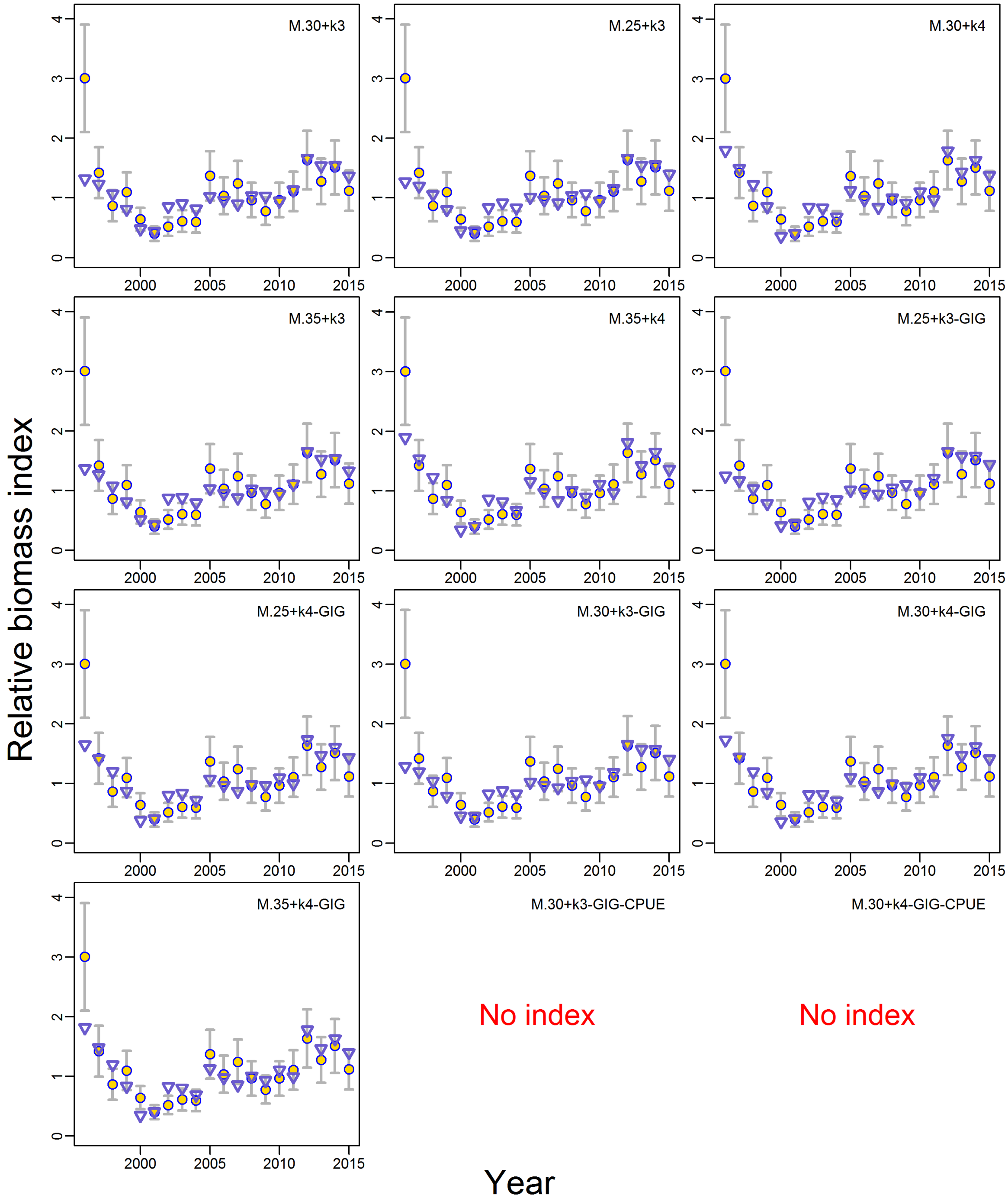

Figure F.17. BC North: MPD index fits (12 alternative runs) for the commercial trawl Walleye Pollock CPUE relative abundance indices. Circles represent observed indices with associated CVs, triangles represent the model fit.

F.2.2.2. MCMC results – alternatives (north)

Median estimates for current biomass B_{2017} lie below the average biomass B_{avg} for all alternative cases except the two that remove the CPUE and GIG index series (Table F.4). Additionally, the year in which median spawning biomass reached a minimum is not stable across the suite of runs. The maximum fishing mortality F estimated in the MCMC samples exceeded realistic levels (F>2) in some years for all but three cases. This is likely to be the result of the failure of the knife-edge recruitment assumption (particularly when it is k=4), which leaves too few fish in the population in some years to support the observed level of catch. The alternative cases do not model population trajectories consistently such that the minimum biomass occurs in the same year.

Table F.5 shows for each alternative run the probabilities of projected biomass in two years at 1000 t/y (at the level of recent average catch) exceeding various reference points . Only runs S10 and S11 (which omit the CPUE series) show high probabilities of B_{2019} exceeding the limit reference point B_{min}. All other scenarios are fairly pessimistic, although it should be noted that 2-year projections using this delay-difference model are unreliable and uncertain. That is because these models, like a surplus production model and unlike an age-structured model, only project using the stock-recruitment function, which has little predictive power.

Most of the trace plots for R_0 look acceptable but a few show an increasing trend in the median while others show large-scale shifts in the trace mean (Figure F.18). Autocorrelation plots for R_0 highlight other problems (Figure F.19), with strong significant positive serial corrleation in S01, S05, and S07, all of which feature $k = 3$. The ranks assigned to the quality of MCMCs appear in Table F.2. While there is no statistical basis for selecting among these hypotheses, these MCMC results suggest that a selection of the runs with the best diagnostics can be used to model this Pollock stock. Consequently, this stock assessment used the subjective MCMC quality rankings to construct a Model Average posterior to provide advice to managers (Section F.2.3.), with a rank $\leq$2 used as the quality cutoff criterion.

Quantile plots compare B_{avg}, $B_{2017}/B_{\mathrm{avg}}$, $u_{2016}/u_{\mathrm{avg}}$ and $u_{\mathrm{avg}}B_{\mathrm{avg}}$ of the example run to alternative runs grouped by category:

- $M \in \{0.25, 0.30, 0.35\}$ and $k \in \{3, 4\}$ using all abundance indices (Figure F.20);
- $M \in \{0.25, 0.30, 0.35\}$ and $k \in \{3, 4\}$ after dropping the GIG survey (Figure F.21); and
- $M = 0.30$ and $k \in \{3, 4\}$ after dropping both the GIG survey and the CPUE series (Figure F.22).

These plots show that M and k interact to change the perceived size of the stock (e.g, B_{avg}), but the estimated stock status $B_{2017}/B_{\mathrm{avg}}$ is relatively consistent across these runs (Figure F.20). Removing the GIG survey abundance index estimates a lower average biomass (B_{avg}) with higher mean removals relative to average biomass ($u_{\mathrm{avg}}B_{\mathrm{avg}}$); however, estimated stock status ($B_{2017}/B\mathrm{avg}$) remains similar across all these runs and to that of the example case (Figure F.21). Removing the GIG survey and the commercial CPUE series does change estimated stock status (higher than that for the example case) even though average removal rates are a lot higher (Figure F.22).

Table F.4. BC North median values for select MCMC-derived parameters and quantities for 12 alternative runs from the BC North stock. The value for B_{2019} is that assuming a TAC of 1000 t/y. Model senstivity details appear in Table F.2.

Run	h	B_{avg}	$\frac{B_{2017}}{B_{\mathrm{avg}}}$	$\frac{B_{2019}}{B_{\mathrm{avg}}}$	$\mathrm{Yr}_{\mathrm{min}}$	$\frac{B_{2017}}{B_{\mathrm{min}}}$	F_{max}	u_{avg}	$\frac{u_{2016}}{u_{\mathrm{avg}}}$
S00: M.30+k3	0.74	7,568	0.57	0.29	2001	1.9	0.71	0.14	2.0
S01: M.25+k3	0.75	4,962	0.48	0.12	1986	2.3	1.7	0.21	2.0
S02: M.30+k4	0.78	3,377	0.44	0.11	1986	3.1	19	0.35	1.7
S03: M.35+k3	0.73	10,270	0.60	0.36	2001	1.9	0.51	0.11	2.0
S04: M.35+k4	0.77	3,695	0.46	0.13	1986	3.1	16	0.33	1.6
S05: M.25+k3-GIG	0.78	4,628	0.54	0.27	1986	2.7	10	0.26	1.8
S06: M.25+k4-GIG	0.81	3,272	0.51	0.24	1986	2.9	19	0.36	1.6
S07: M.30+k3-GIG	0.77	5,325	0.65	0.42	1986	3.7	8.0	0.24	1.6
S08: M.30+k4-GIG	0.80	3,438	0.58	0.30	1986	3.5	19	0.35	1.5
S09: M.35+k4-GIG	0.80	3,725	0.62	0.36	1986	3.5	17	0.34	1.5
S10: M.30+k3-GIG-CPUE	0.75	6,986	1.3	0.90	2000	9.9	18	0.20	0.80
S11: M.30+k4-GIG-CPUE	0.80	4,248	1.1	0.74	1986	8.9	20	0.31	0.87

Table F.5. BC North: Assuming a constant catch policy of 1000 t/y, the probability that B_{2019} (or u_{2018}) is greater than reference points used in this assessment for 12 alternative runs. Model senstivity details appear in Table F.2. For reference, the average catch over the last 5 years (2011-2015) is 992 t.

Run	P$\left(\frac{B_{2019}>}{B_{2017}}\right)$	P$\left(\frac{B_{2019}>}{B_{\min}}\right)$	P$\left(\frac{B_{2019}>}{2B_{\min}}\right)$	P$\left(\frac{B_{2019}>}{B_{\text{avg}}}\right)$	P$\left(\frac{u_{2018}>}{u_{\text{avg}}}\right)$
S00: M.30+k3	0	0.46	0.03	0	1
S01: M.25+k3	0	0.39	0.12	0	1
S02: M.30+k4	0.05	0.46	0.25	0	0.99
S03: M.35+k3	0.01	0.66	0.06	0	1
S04: M.35+k4	0.04	0.52	0.28	0	0.99
S05: M.25+k3-GIG	0.07	0.64	0.35	0.01	0.98
S06: M.25+k4-GIG	0.12	0.66	0.36	0.02	0.94
S07: M.30+k3-GIG	0.08	0.87	0.59	0.03	0.94
S08: M.30+k4-GIG	0.12	0.75	0.48	0.04	0.91
S09: M.35+k4-GIG	0.14	0.81	0.53	0.05	0.90
S10: M.30+k3-GIG-CPUE	0.03	1	0.99	0.37	0.22
S11: M.30+k4-GIG-CPUE	0.06	0.98	0.92	0.25	0.44

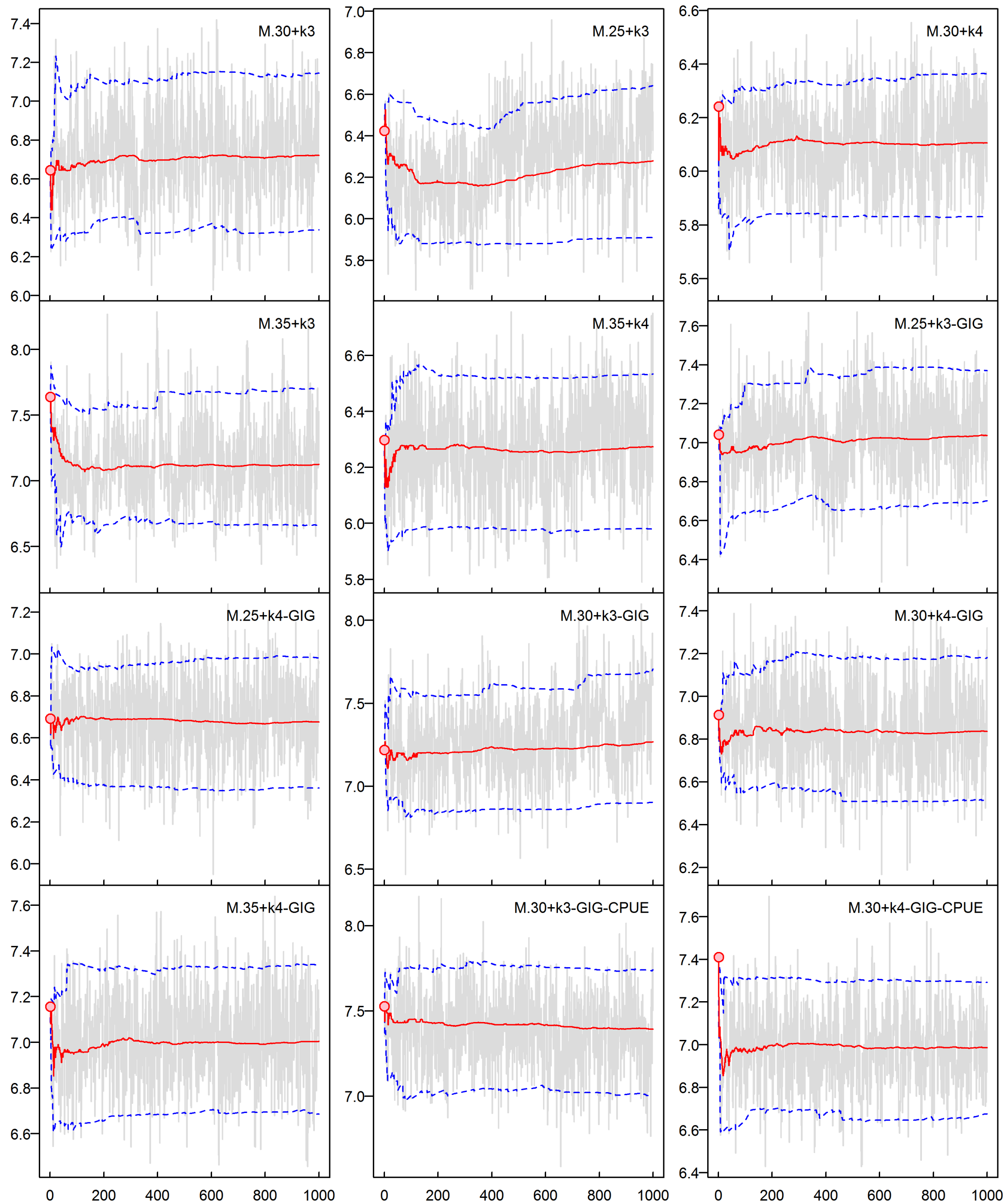

Figure F.18. BC North: Trace plots (12 alternative runs) for MCMC samples of $\log(R_0)$ (natural log of unfished equilibrium recruitment). The MCMC run had chain length 60 million and a sample taken at every 50,000$^{\text{th}}$ iteration to yield 1,000 MCMC samples after a removing a burn-in of 200 samples. Grey lines show the 1000 samples for each parameter, solid lines show the cumulative median (up to that sample), and dashed lines show the cumulative 2.5 and 97.5 quantiles. Red circles are the MPD estimates.

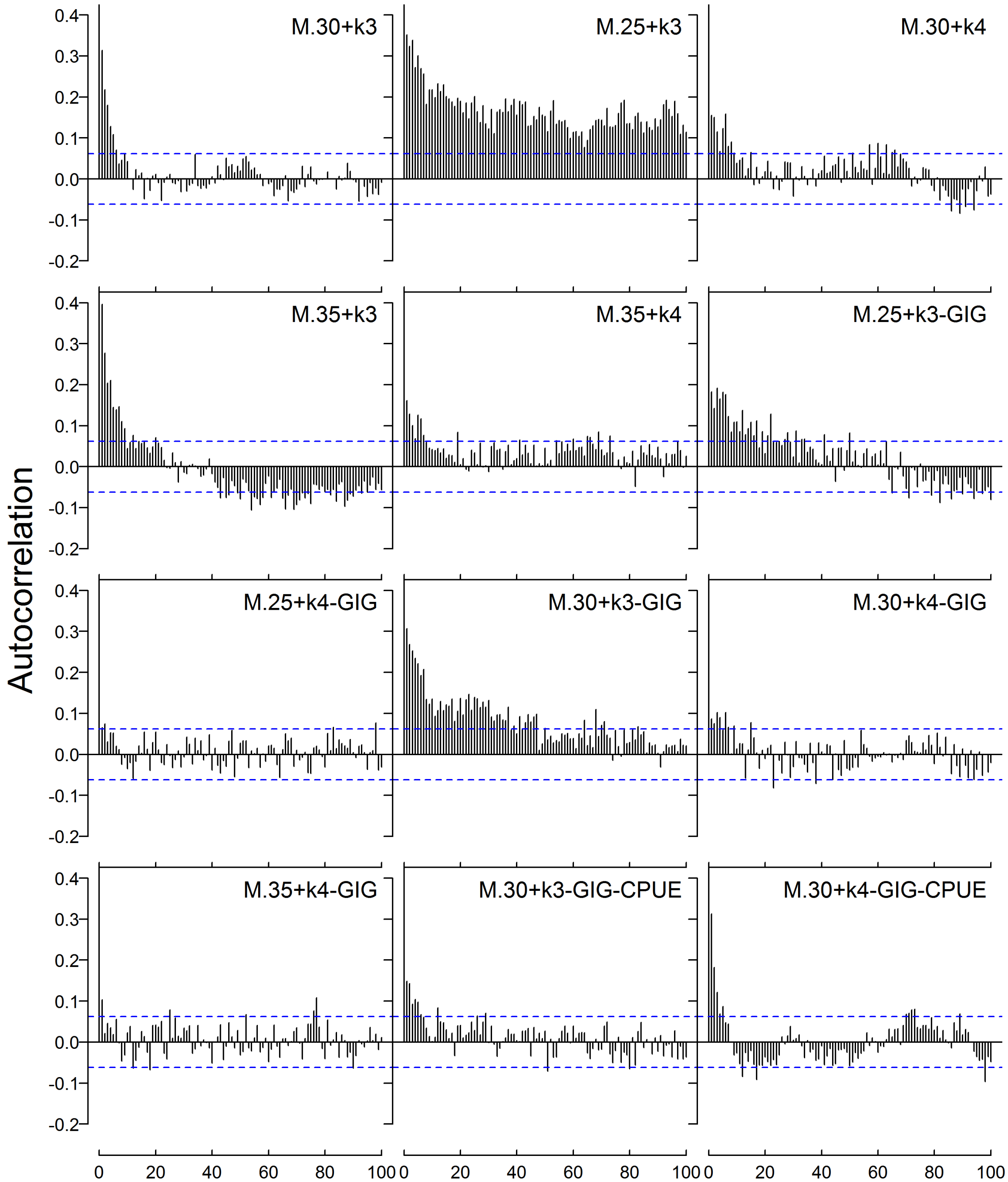

Figure F.19. BC North: Autocorrelation plots (12 alternative runs) for MCMC samples of $\log(R_0)$ *(natural log of unfished equilibrium recruitment). The MCMC runs had 1,000 MCMC samples each.*

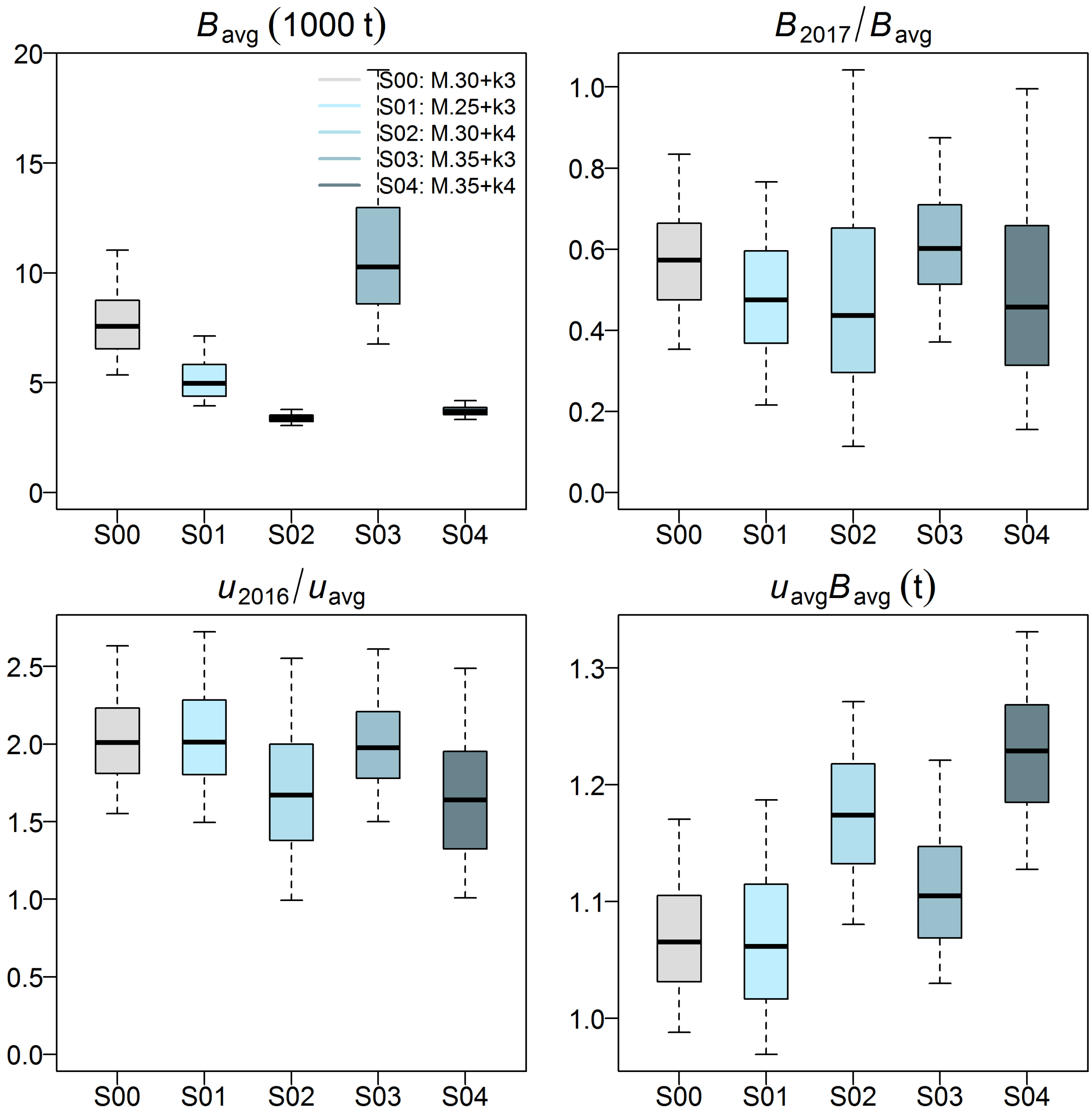

Figure F.20. BC North: Quantile plots comparing the example model case (S00 with M=0.30 and k=3 using the eastern Gulf of Alaska growth model) to alternative runs that vary natural mortality, where M = 0.25, 0.30, 0.35, and knife-edge recruitment age k, where k=3,4. Box delimiter and limits represent quantiles at 0.5 (median), 0.25 and 0.75 quantiles, respectively, and the whiskers delimit the 0.05 and 0.95 quantiles. Outliers are not shown.

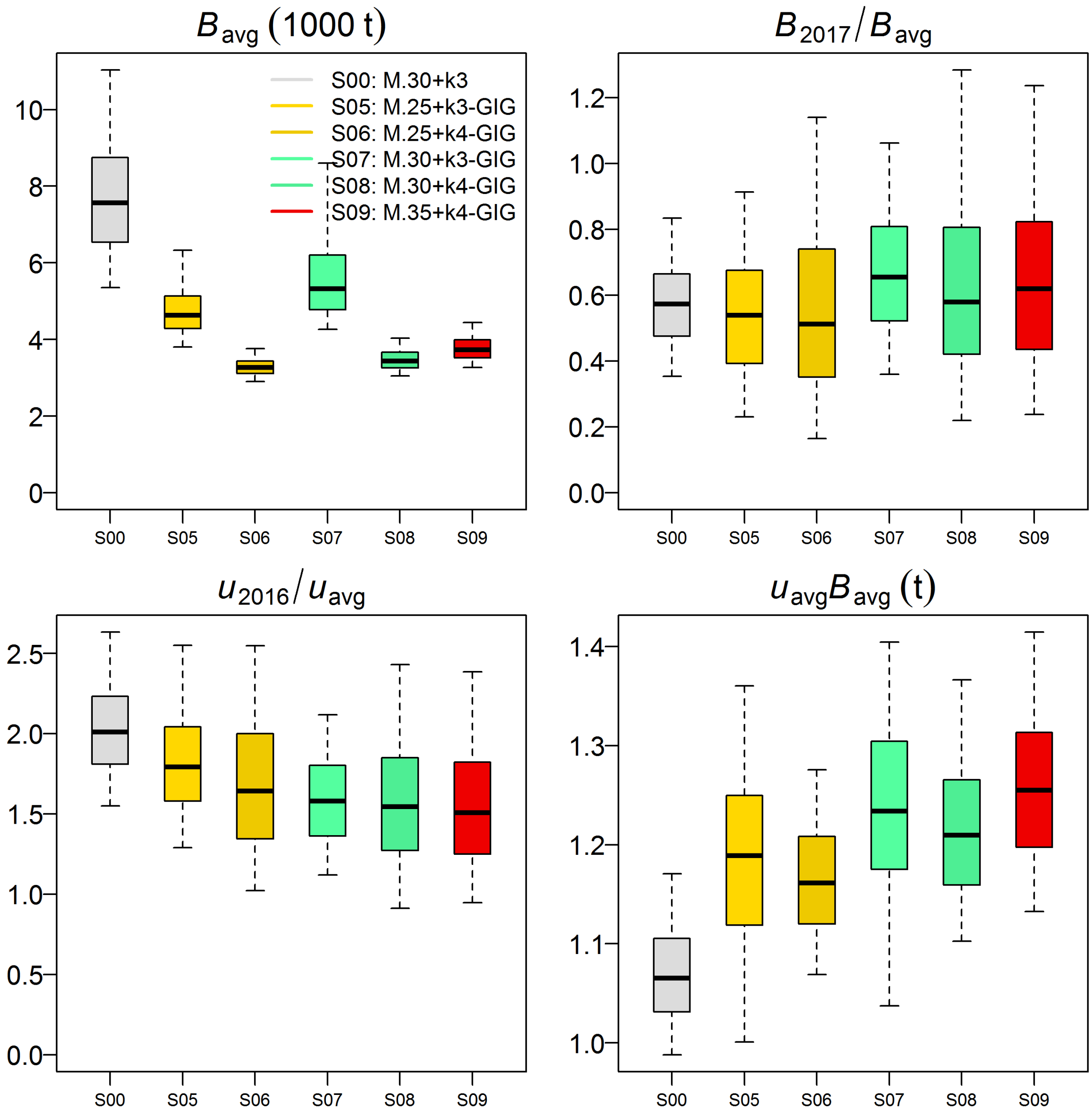

Figure F.21. BC North: Quantile plots comparing the example reference case S00 to alternative runs that do not use the GIG (Goose Island Gully) historical surveys. Quantile box delimiters are detailed in Figure F.20.

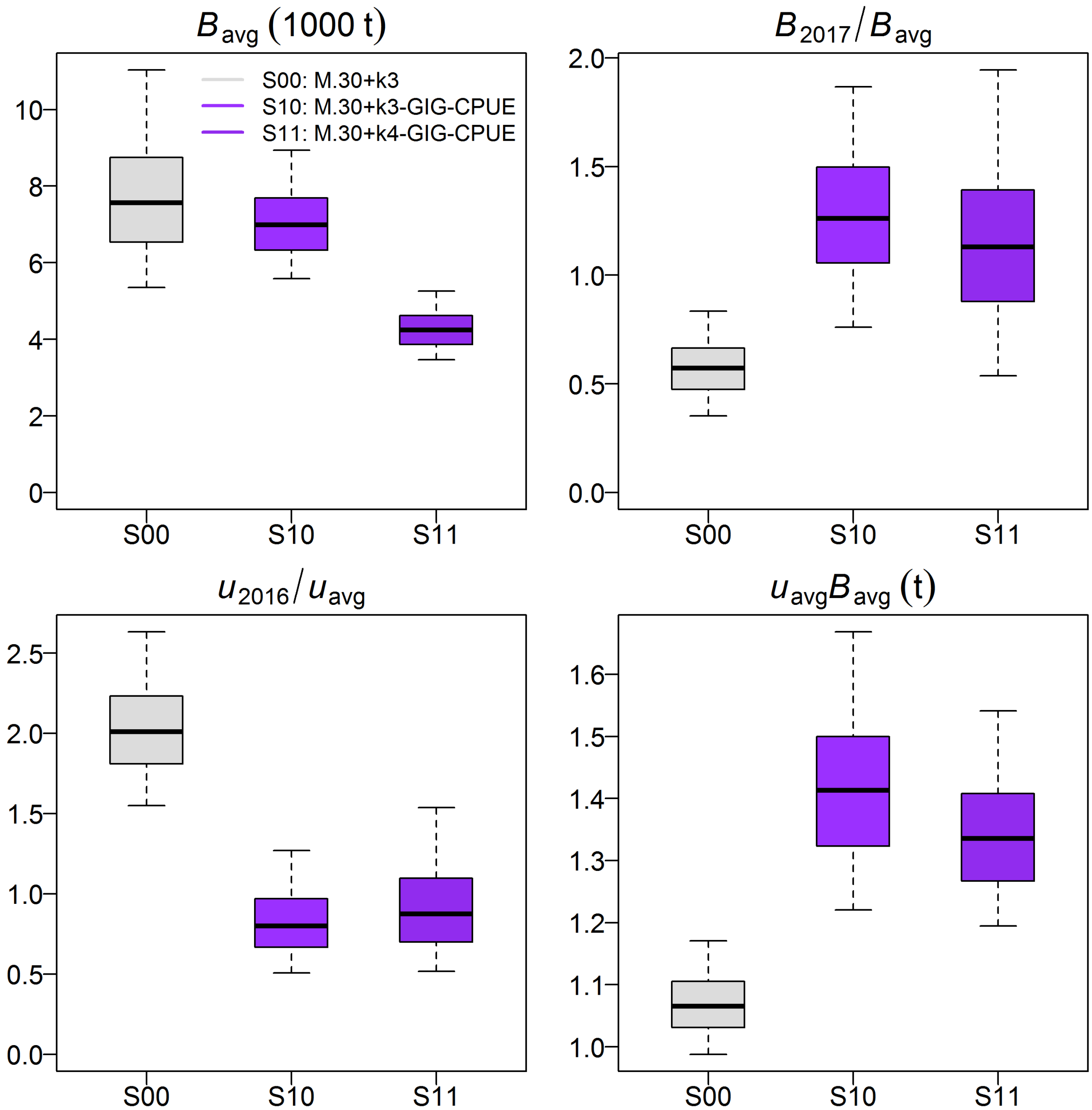

Figure F.22. BC North: Quantile plots comparing the example reference case S00 to alternative runs that do not use the GIG survey series or the commercial trawl CPUE series. Quantile box delimiters are detailed in Figure F.20.

F.2.3. Model Average Composite – North

Three alternative BC North runs were selected for inclusion to the Model Average posterior based on the following criteria (see Tables F.2 and F.4):

- use model runs where the median $F_{\max}$ across MCMC samples was < 2;
- add model runs where median annual F_t was > 2 only once;
- remove model runs with poor diagnostics (rank > 2).

For the BC North stock, these criteria selected 3 out of 12 models:

- S00: M.30+k3 (rank=1.25, med.$F_{\max}$=0.71, no.yrs med.$F_t > 2$ =0)
- S03: M.35+k3 (rank=1.50, med.$F_{\max}$=0.51, no.yrs med.$F_t > 2$ =0)
- S10: M.30+k3-GIG-CPUE (rank=2.00, med.$F_{\max}$=18.4, no.yrs med.$F_t > 2$ =1)

Table F.6 gives the model-based and HRP-based quantities (0.05, 0.50, and 0.95 quantiles) from the model average posterior based on 3000 pooled MCMC samples. Table F.8 gives the decision table for this Model Average Composite scenario, showing the probabilities that B_{2019} will exceed various reference points. Figure F.23 shows the stock status B_{2017}/B_{avg} of the Model Average Composite scenario and the 3 models that contribute to the composite model. Finally, Tables F.9–F.11 show the 2-y decision tables for scenarios contributing to the composite.

Table F.6. BC North: The 5th, 50th, and 95th percentiles of MCMC-derived quantities from 3000 MCMC samples comprising the Model Average Composite scenario. Definitions: B_{2017} – current year spawning biomass, B_{avg} – average biomass from 1967 to 2016, $B_{\min}$ – minimum biomass that acts as the LRP (and USR = 2LRP), u_{2016} – harvest rate (ratio of total catch to vulnerable biomass) in the middle of 2016, and u_{avg} – average harvest rate from 1967 to 2016. All biomass values are in tonnes. For reference, the average catch over the last 5 years (2011-2015) is 992 t.

	5%	50%	95%
Model-based			
B_{2017}	2,621	6,185	13,927
B_{avg}	5,634	7,837	14,626
B_{2017}/B_{avg}	0.385	0.683	1.62
u_{2016}	0.106	0.214	0.406
HRP-based			
$B_{\min}$	654	2,051	4,818
$2B_{\min}$	1,307	4,101	9,636
$B_{\min}/B_{\text{avg}}$	0.0921	0.270	0.388
$2B_{\min}/B_{\text{avg}}$	0.184	0.540	0.775
$B_{2017}/B_{\min}$	1.29	2.31	16.1
u_{avg}	0.0744	0.150	0.234
u_{2016}/u_{avg}	0.602	1.79	2.52

Table F.7. BC North: Decision table for the Model Average Composite scenario for 5 reference points – the current year spawning biomass, the limit reference point $B_{\min}$, the upper stock reference $2B_{\min}$, the average spawning stock biomass from 1967 to 2016, and the average harvest rate over the same time period – for projection-year biomass B_{2018} and mid-year harvest rate u_{2017} for a range of constant catch strategies (in tonnes). Each value is the probability that projected biomass or harvest rate is greater than the indicated reference point. The probabilities are the proportion of MCMC samples from 3 pooled scenarios chosen for their well-behaved MCMC diagnostics. The probabilities that current-year spawning biomass (or harvest rate) is greater than the reference points are: P($B_{2017} > B_{\min}$) = 0.99, P($B_{2017} > 2B_{\min}$) = 0.62, P($B_{2017} > B_{\text{avg}}$) = 0.27, and P($u_{2016} > u_{\text{avg}}$) = 0.74. For reference, the average catch over the last 5 years (2011-2015) is 992 t.

Catch	P$\left(\frac{B_{2018}>}{B_{2017}}\right)$	P$\left(\frac{B_{2018}>}{B_{\min}}\right)$	P$\left(\frac{B_{2018}>}{2B_{\min}}\right)$	P$\left(\frac{B_{2018}>}{B_{\text{avg}}}\right)$	P$\left(\frac{u_{2017}>}{u_{\text{avg}}}\right)$
0	0.23	0.99	0.58	0.26	0
100	0.17	0.99	0.56	0.26	0
200	0.12	0.98	0.54	0.25	0
300	0.10	0.98	0.53	0.24	0.01
400	0.08	0.97	0.51	0.24	0.08
500	0.07	0.96	0.50	0.23	0.24
600	0.06	0.95	0.48	0.22	0.45
700	0.05	0.94	0.47	0.22	0.58
800	0.04	0.93	0.46	0.21	0.65
900	0.03	0.91	0.45	0.21	0.68
1000	0.03	0.90	0.43	0.20	0.70
1200	0.02	0.87	0.42	0.18	0.74
1400	0.01	0.84	0.40	0.18	0.80
1600	0.01	0.80	0.39	0.16	0.85
1800	0.01	0.76	0.38	0.15	0.90
2000	0.01	0.71	0.37	0.13	0.93
2500	0	0.62	0.35	0.11	0.98
3000	0	0.54	0.34	0.09	0.99
3500	0	0.48	0.32	0.07	1
4000	0	0.43	0.30	0.05	1
4500	0	0.40	0.28	0.04	1
5000	0	0.37	0.26	0.03	1

Table F.8. BC North: Decision table for the Model Average Composite scenario for 5 reference points – the current year spawning biomass, the limit reference point B_{min}, the upper stock reference $2B_{\mathrm{min}}$, the average spawning stock biomass from 1967 to 2016, and the average harvest rate over the same time period – for projection-year biomass B_{2019} and mid-year harvest rate u_{2018} for a range of constant catch strategies (in tonnes). Each value is the probability that projected biomass or harvest rate is greater than the indicated reference point. The probabilities are the proportion of MCMC samples from 3 pooled scenarios chosen for their well-behaved MCMC diagnostics. The probabilities that current-year spawning biomass (or harvest rate) is greater than the reference points are: P($B_{2017} > B_{\mathrm{min}}$) = 0.99, P($B_{2017} > 2B_{\mathrm{min}}$) = 0.62, P($B_{2017} > B_{\mathrm{avg}}$) = 0.27, and P($u_{2016} > u_{\mathrm{avg}}$) = 0.74. For reference, the average catch over the last 5 years (2011-2015) is 992 t.

Catch	P$\left(\frac{B_{2019}>}{B_{2017}}\right)$	P$\left(\frac{B_{2019}>}{B_{\mathrm{min}}}\right)$	P$\left(\frac{B_{2019}>}{2B_{\mathrm{min}}}\right)$	P$\left(\frac{B_{2019}>}{B_{\mathrm{avg}}}\right)$	P$\left(\frac{u_{2018}>}{u_{\mathrm{avg}}}\right)$
0	0.23	0.99	0.54	0.24	0
100	0.17	0.98	0.51	0.23	0
200	0.13	0.96	0.48	0.22	0
300	0.09	0.95	0.46	0.21	0.03
400	0.07	0.93	0.44	0.20	0.17
500	0.05	0.89	0.42	0.19	0.41
600	0.04	0.86	0.40	0.17	0.58
700	0.04	0.82	0.39	0.16	0.65
800	0.02	0.79	0.38	0.15	0.69
900	0.02	0.74	0.37	0.14	0.71
1000	0.02	0.71	0.36	0.12	0.74
1200	0.01	0.63	0.35	0.11	0.81
1400	0.01	0.55	0.34	0.09	0.88
1600	0	0.51	0.33	0.07	0.93
1800	0	0.46	0.32	0.06	0.96
2000	0	0.42	0.30	0.05	0.98
2500	0	0.36	0.26	0.03	1
3000	0	0.30	0.22	0.01	1
3500	0	0.26	0.18	0.01	1
4000	0	0.22	0.14	0.01	1
4500	0	0.20	0.11	0	1
5000	0	0.17	0.08	0	1

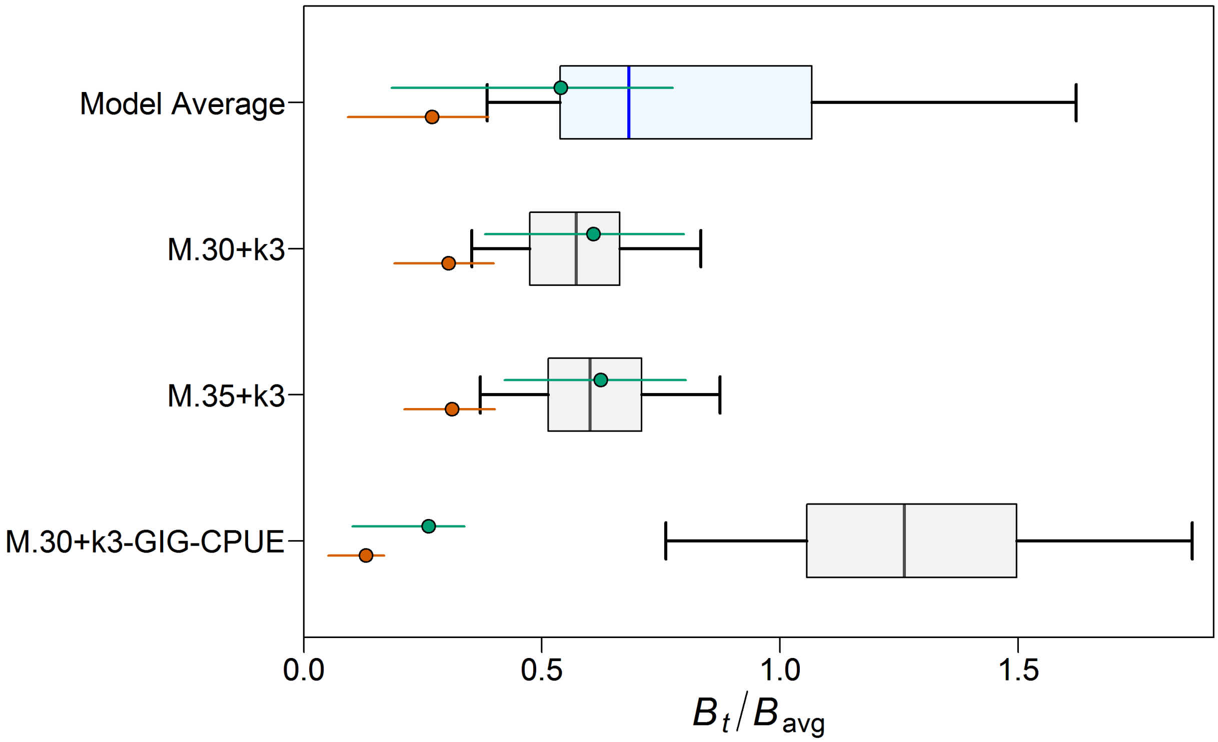

Figure F.23. BC North: Status of the current stock B_{2017} relative to B_{avg} with the dashed lines showing historical reference points ($B_{\mathrm{min}}/B_{\mathrm{avg}}$, $2B_{\mathrm{min}}/B_{\mathrm{avg}}$) that mimic DFO Precautionary Approach provisional MSY-based reference points. Stock status is shown for the Model Average Composite scenario comprising 3 pooled model runs and for each of the 3 model runs (see Table F.2) for definitions of these model runs). Boxplots show the 5, 25, 50, 75 and 95 percentiles from the MCMC results. M = instantaneous natural mortality (y^{-1}); k = age (y) at knife-edge recruitment.

Table F.9. BC North: Decision table for case S00: M.30+k3 for 5 reference points – the current year spawning biomass, the limit reference point $B_{\min}$, the upper stock reference $2B_{\min}$, the average spawning stock biomass from 1967 to 2016, and the average harvest rate over the same time period – for projection-year biomass B_{2019} and mid-year harvest rate u_{2018} for a range of constant catch strategies (in tonnes). Each value is the probability that projected biomass or harvest rate is greater than the indicated reference point. The probabilities that current-year spawning biomass (or harvest rate) is greater than the reference points are: P($B_{2017} > B_{\min}$) = 0.98, P($B_{2017} > 2B_{\min}$) = 0.41, P($B_{2017} > B_{\mathrm{avg}}$) = 0.01, and P($u_{2016} > u_{\mathrm{avg}}$) = 1. For reference, the average catch over the last 5 years (2011-2015) is 992 t.

Catch	P$\left(\frac{B_{2019}>}{B_{2017}}\right)$	P$\left(\frac{B_{2019}>}{B_{\min}}\right)$	P$\left(\frac{B_{2019}>}{2B_{\min}}\right)$	P$\left(\frac{B_{2019}>}{B_{\mathrm{avg}}}\right)$	P$\left(\frac{u_{2018}>}{u_{\mathrm{avg}}}\right)$
0	0.28	0.98	0.34	0	0
100	0.20	0.97	0.29	0	0
200	0.13	0.95	0.24	0	0
300	0.08	0.92	0.18	0	0.05
400	0.05	0.88	0.15	0	0.29
500	0.03	0.82	0.12	0	0.67
600	0.02	0.76	0.09	0	0.90
700	0.02	0.68	0.07	0	0.97
800	0.01	0.62	0.06	0	0.99
900	0.01	0.54	0.05	0	1
1000	0	0.46	0.03	0	1
1200	0	0.34	0.02	0	1
1400	0	0.22	0.01	0	1
1600	0	0.14	0.01	0	1
1800	0	0.09	0	0	1
2000	0	0.07	0	0	1
2500	0	0.03	0	0	1
3000	0	0.01	0	0	1
3500	0	0.01	0	0	1
4000	0	0.01	0	0	1
4500	0	0.01	0	0	1
5000	0	0	0	0	1

Table F.10. BC North: Decision table for case S03: M.35+k3 for 5 reference points – the current year spawning biomass, the limit reference point B_{min}, the upper stock reference $2B_{\mathrm{min}}$, the average spawning stock biomass from 1967 to 2016, and the average harvest rate over the same time period – for projection-year biomass B_{2019} and mid-year harvest rate u_{2018} for a range of constant catch strategies (in tonnes). Each value is the probability that projected biomass or harvest rate is greater than the indicated reference point. The probabilities that current-year spawning biomass (or harvest rate) is greater than the reference points are: P($B_{2017} > B_{\mathrm{min}}$) = 0.99, P($B_{2017} > 2B_{\mathrm{min}}$) = 0.45, P($B_{2017} > B_{\mathrm{avg}}$) = 0.02, and P($u_{2016} > u_{\mathrm{avg}}$) = 1. For reference, the average catch over the last 5 years (2011-2015) is 992 t.

Catch	P$\left(\frac{B_{2019}>}{B_{2017}}\right)$	P$\left(\frac{B_{2019}>}{B_{\mathrm{min}}}\right)$	P$\left(\frac{B_{2019}>}{2B_{\mathrm{min}}}\right)$	P$\left(\frac{B_{2019}>}{B_{\mathrm{avg}}}\right)$	P$\left(\frac{u_{2018}>}{u_{\mathrm{avg}}}\right)$
0	0.16	0.98	0.27	0	0
100	0.12	0.97	0.24	0	0
200	0.09	0.94	0.22	0	0
300	0.07	0.93	0.20	0	0.04
400	0.06	0.90	0.16	0	0.20
500	0.04	0.86	0.14	0	0.56
600	0.04	0.82	0.12	0	0.83
700	0.03	0.79	0.10	0	0.94
800	0.02	0.76	0.08	0	0.98
900	0.02	0.70	0.06	0	1
1000	0.01	0.66	0.06	0	1
1200	0.01	0.56	0.04	0	1
1400	0	0.44	0.04	0	1
1600	0	0.39	0.03	0	1
1800	0	0.30	0.02	0	1
2000	0	0.24	0.01	0	1
2500	0	0.14	0	0	1
3000	0	0.09	0	0	1
3500	0	0.06	0	0	1
4000	0	0.03	0	0	1
4500	0	0.02	0	0	1
5000	0	0.02	0	0	1

Table F.11. BC North: Decision table for case S10: M.30+k3-GIG-CPUE for 5 reference points – the current year spawning biomass, the limit reference point $B_{\min}$, the upper stock reference $2B_{\min}$, the average spawning stock biomass from 1967 to 2016, and the average harvest rate over the same time period – for projection-year biomass B_{2019} and mid-year harvest rate u_{2018} for a range of constant catch strategies (in tonnes). Each value is the probability that projected biomass or harvest rate is greater than the indicated reference point. The probabilities that current-year spawning biomass (or harvest rate) is greater than the reference points are: P($B_{2017} > B_{\min}$) = 1, P($B_{2017} > 2B_{\min}$) = 1, P($B_{2017} > B_{\text{avg}}$) = 0.80, and P($u_{2016} > u_{\text{avg}}$) = 0.23. For reference, the average catch over the last 5 years (2011-2015) is 992 t.

Catch	P$\left(\frac{B_{2019}>}{B_{2017}}\right)$	P$\left(\frac{B_{2019}>}{B_{\min}}\right)$	P$\left(\frac{B_{2019}>}{2B_{\min}}\right)$	P$\left(\frac{B_{2019}>}{B_{\text{avg}}}\right)$	P$\left(\frac{u_{2018}>}{u_{\text{avg}}}\right)$
0	0.23	1	1	0.73	0
100	0.19	1	1	0.69	0
200	0.16	1	1	0.66	0
300	0.13	1	1	0.62	0
400	0.10	1	1	0.60	0
500	0.08	1	1	0.56	0.01
600	0.07	1	1	0.51	0.02
700	0.06	1	1	0.47	0.04
800	0.05	1	0.99	0.44	0.08
900	0.04	1	0.99	0.41	0.13
1000	0.03	1	0.99	0.37	0.22
1200	0.02	1	0.98	0.32	0.43
1400	0.02	0.99	0.97	0.26	0.64
1600	0.02	0.99	0.96	0.22	0.79
1800	0.01	0.98	0.93	0.18	0.89
2000	0.01	0.97	0.89	0.14	0.95
2500	0	0.90	0.78	0.08	0.99
3000	0	0.81	0.66	0.04	1
3500	0	0.72	0.53	0.02	1
4000	0	0.63	0.42	0.02	1
4500	0	0.56	0.32	0.01	1
5000	0	0.49	0.25	0.01	1

F.3. BC SOUTH STOCK

F.3.1. Example Case – South

An example model run for the BC South stock is presented to show more detail in the results. This model is based on the eastern Bering Sea Okhotsk growth model from Janusz and Horbowy (1997) and included the following elements:

- instantaneous natural mortality M fixed at 0.30;
- knife-edge recruitment at age k = 3 y;
- steepness h beta prior (mean=0.7, SD=0.15);
- 1972-2016 standardised unsorted mean weights ($\bar{w}$ = 0.52052 kg);
- length-weight allometry: α = 7.3536E-06, β = 3.030278;
- Brody parameters: α_g = 0.14441 kg, ρ_g = 0.87063, w_k = 0.24875 kg;
- growth parameters: L_∞ = 50.82725 cm, κ = 0.199054, t_0 = -1.78968 y;
- errors: observation σ_O = 0.2, recruitment σ_R = 0.6, mean weight σ_W = 0.15;
- uniform priors on q from -10 to 0;
- Walleye Pollock CPUE indices (uniform -10 to 0);
- catch series (GFFOS accessed 2016-09-12);
- equilibrium start in 1967 (use all of GIG historical, including 1995);
- equal-weight for each age class when estimating von Bertalanffy model parameters by sex, combined-sex model interpolated between sexes;
- estimate $\ln(R_0)$ (uniform prior) and fix $\ln(\bar{R})$ and $\ln(R_{\text{init}})$ to $\ln(R_0)$;
- version `iscam-delaydiff.exe`: built 2017-01-03.

F.3.1.1. MPD results – example (south)

The mode of the posterior distribution (MPD) for this model (reported in Table F.12) is estimated by minimising the objective function (components summarised in Section E.2.1). The results are presented to show the fits by the model to the observed data and are used as the starting point for the MCMC simulations. MPD fits are shown for the abundance indices (Figure F.24), the annual mean weights and annual recruitment (Figure F.25). The fits to the survey and CPUE indices are generally reasonable although the model is incapable of fitting the abrupt changes in some series. The model is also not capable of fitting the high values of mean weight that occur at the beginning of the series (Figure F.25). Instead it fluctuates near the mean of the series, with a general dome-shaped trend that tries to fit the high values in the 1970s and 1980s. Recruitment events exceed the long-term median of the series 10 times; the 1975 event is roughly 11 times higher than the long-term median. Fits to the catch data are not presented because the model is parameterised so that it always fits the catch closely.

F.3.1.2. MCMC results – example (south)

The MCMC procedure performed 60,000,000 iterations, sampling every 50,000 to give 1200 draws (1000 samples after dropping the first 200, including the MPD start point, as burn-in). The 1000 samples were used to estimate parameters and quantities of interest, including stock status by year and the probabilities of being above reference points.

MCMC traces show good convergence properties (no trend with increasing sample number) for the leading estimated parameters (Figure F.26); however, a diagnostic analysis that splits the samples into three segments, checking for consistency along the length of the chain (Figure F.27), indicates some instability over time. The autocorrelation plots (Figure F.28) confirm this with some periodicity over 100 lags and significant serial correlation for the first 5-10 lags for all parameters except h. Pairs plots of the estimated parameters (Figure F.29) show no undesirable correlation between the two primary parameters, ln(R_0) and h, though all the q parameters were highly correlated with ln(R_0) and with each other, as would be expected. MCMC quantiles for parameters, biomass, and status with respect to historical reference points are summarised in Table F.12.

Marginal posterior distributions along with the corresponding priors for the estimated parameters are shown in Figure F.30. Only the steepness parameter used an informative prior, with its posterior distribution largely reflecting the prior. This indicates that there was relatively little information in this model to inform this parameter and it is unlikely that it could be estimated without using a prior.

The plot of estimated spawning biomass (Figure F.31) shows a large increase in the mid 1970s followed by a decline to a low point in 2008. Since then, spawning biomass has increased and the median B_{2017} lies very close to the average biomass B_{avg}. Assuming a catch policy of 3250 t/y, which is almost double the current TAC of 1790 t/y in 5AB but close to the 5-y average catch of 3256 t in the BC South region, the projected biomass declines under conditions of average recruitment.

This model run estimates a few strong recruitment pulses in 1970, 1974, and 2014 (Figure F.32). The first strong recruitment occurs in the absence of fishing pressure and so spawing biomass increases substantially (Figure F.31). Thereafter, strong fishing pressure brings the population to a minimum in 2008, but after this point fishing does not appear to dampen lacklustre recruitment (Figure F.33). Fishing mortality peaks in 2003 at a median F value of 0.275 y^{-1} and declines thereafter until it reaches 0.028 y^{-1} in 2016. The median value (and the 5th and 95th percentiles in parentheses) for the estimated level of biomass depletion (B_t/B_{avg}) at the end of the final year of the reconstruction is 1.02 (0.68, 1.4), with the MPD value of 1 lying well above the median of the posterior distribution of this quantity (Figure F.33).

The use of historical reference points is illustrated in Figure F.34. Under an assumed catch policy of 3250 t/y, B_{2019} lies lower than B_{2017} and B_{avg}. All three biomass estimates lie above the LRP and the USR, with the median of B_{2017} slightly above the median of average biomass B_{avg}. The current fishing mortality rate F_{2016} is lower than the average F, the minimum F that occurred in 2008, and the maximum fishing mortlaity rates experienced over the assessment time period. The phase plot (Figure F.35) confirms that the current stock status lies well above the LRP and the USR, and the current mid-year harvest rate u_{2016} lies below the average harvest rate over the time series.

Table F.12. BC South: The 5th, 50th, and 95th percentiles of MCMC-derived parameter estimates and quantities from 1,000 MCMC samples for the example model run. Some fixed parameters are reported as MPD only. See Appendix E for paramater definitions. Subscripts 1-3 on q refer to the fishery-independent surveys, subscript 4 refers to the commercial trawl CPUE series. Other definitions: B_{2017} – biomass at the start of 2017, u_{2016} – exploitation rate (ratio of total catch to vulnerable biomass) in the middle of 2016, B_{avg} – average biomass from 1967 to 2016, LRP (limit reference point) – minimum median estimated biomass in the time series, USR (upper stock reference) – twice the LRP biomass. All biomass values are in tonnes. For reference, the average catch over the last 5 years (2011-2015) is 3256 t.

	5%	50%	95%	MPD
Parameters				
R_0	7,614	13,738	36,627	13,347
h	0.505	0.751	0.926	0.792
M				0.3
q_1	0.00562	0.0146	0.0252	0.0191
q_2	0.0019	0.00561	0.0109	0.00779
q_3	0.00806	0.0244	0.0468	0.0335
q_4	0.00001	0.000031	0.00006	0.000043
HRP-based				
B_{2017}	43,736	91,200	280,228	67,025
B_{avg}	50,723	89,549	244,104	66,878
$\mathrm{LRP} = B_{2008}$	7,296	16,655	50,664	10,239
$\mathrm{USR} = 2B_{2008}$	14,593	33,309	101,328	20,478
$B_{2017}/B_{\mathrm{avg}}$	0.679	1.02	1.4	1
B_{2017}/B_{2008}	2.59	5.82	8.11	6.55
$B_{2017}/2B_{2008}$	1.29	2.91	4.06	3.27
u_{avg}	0.0127	0.0383	0.0696	0.0511
$u_{2016}/u_{\mathrm{avg}}$	0.582	0.735	0.946	0.739

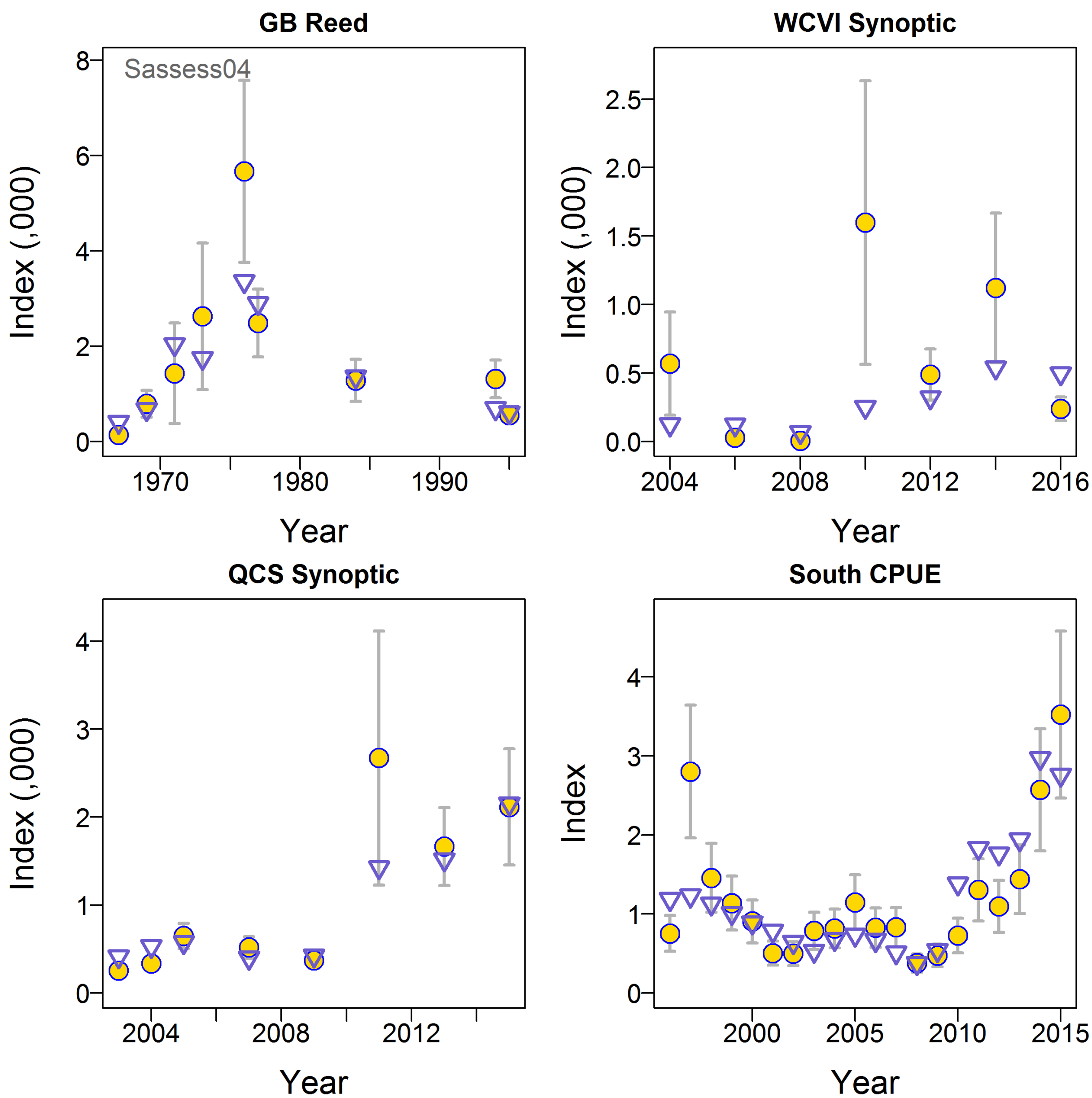

Figure F.24. BC South: MPD index fits to relative abundance indices for the example model run. Circles represent observed indices with associated CVs; squares represent the model fit. Surveys: (1) GIG (Goose Island Gully) Historical, (2) WCVI (west coast Vancouver Island) Synoptic, (3) QCS (Queen Charlotte Sound) Synoptic, (4) commercial trawl catch per unit effort of Walleye Pollock.

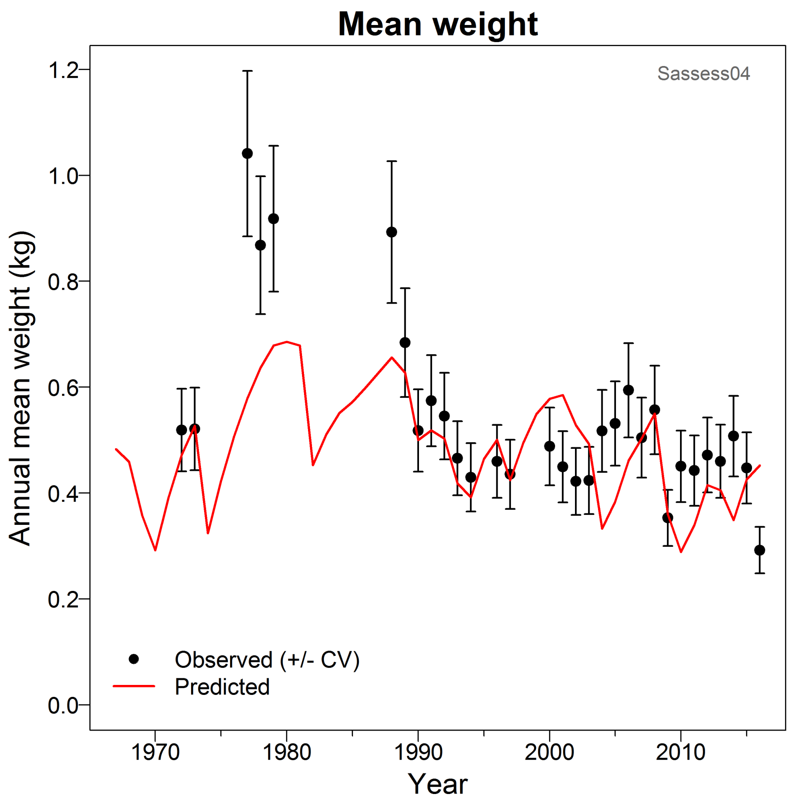

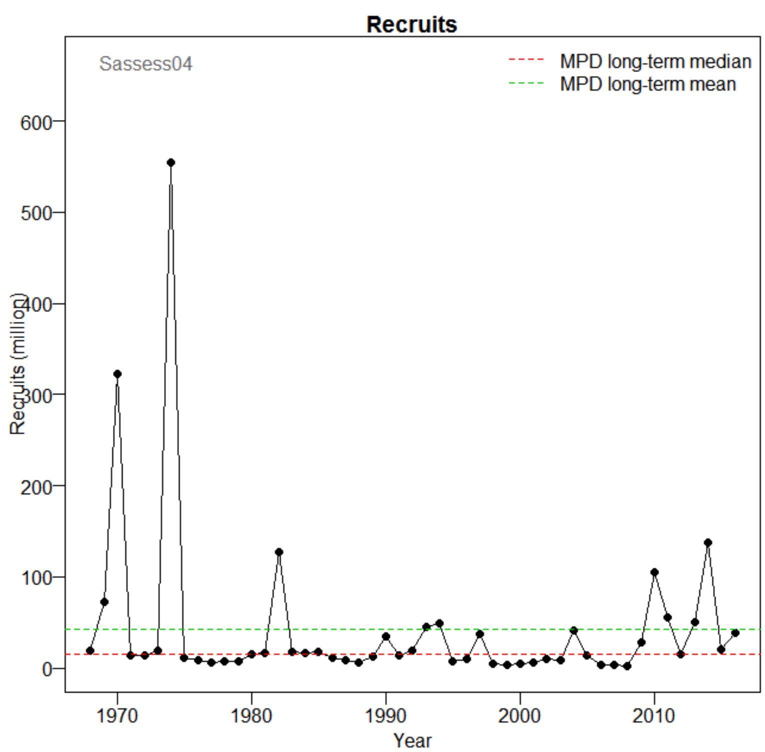

Figure F.25. BC South: **[Top]** *MPD fit to the mean weight data for the example model run. Predicted mean weights are shown as a red line and observations are shown as points. Error bars on mean weight observations represent a fixed CV using* $\sigma_W = 0.15$. **[Bottom]** *MPD recruitment in thousands of age-3 individuals in year* t *for example model run.*

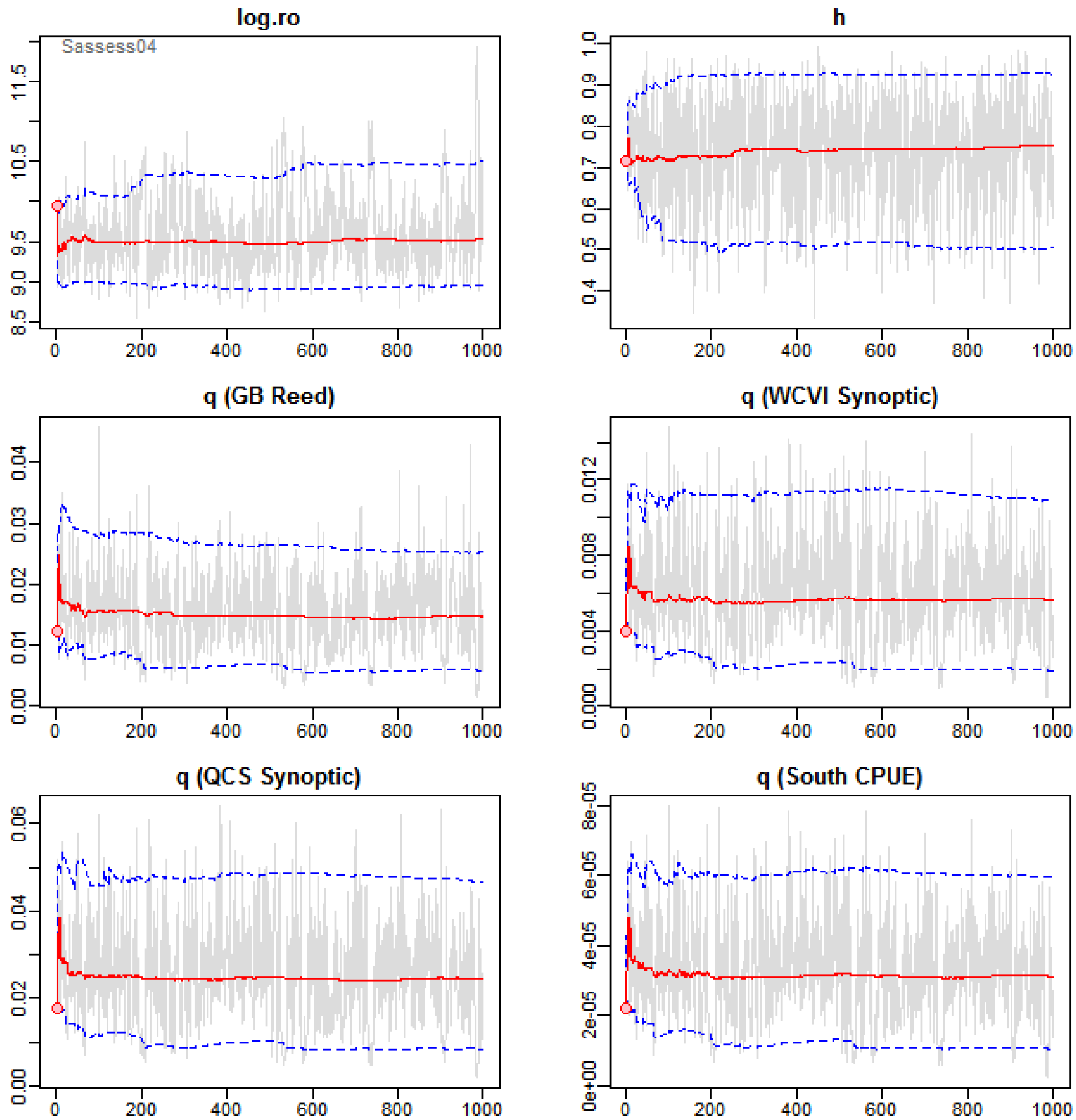

Figure F.26. BC South: Trace plots for MCMC output of estimated parameters in the example model run. The MCMC run shows 1000 MCMC samples after removing 200 samples. Parameters log.ro (natural log of unfished equilibrium recruitment), h (steepness), and q (catchability) for the surveys outlined in Figure F.24. Grey lines show the 1000 samples for each parameter, solid lines show the cumulative median (up to that sample), and dashed lines show the cumulative 2.5 and 97.5 quantiles. Red circles are the MPD estimates.

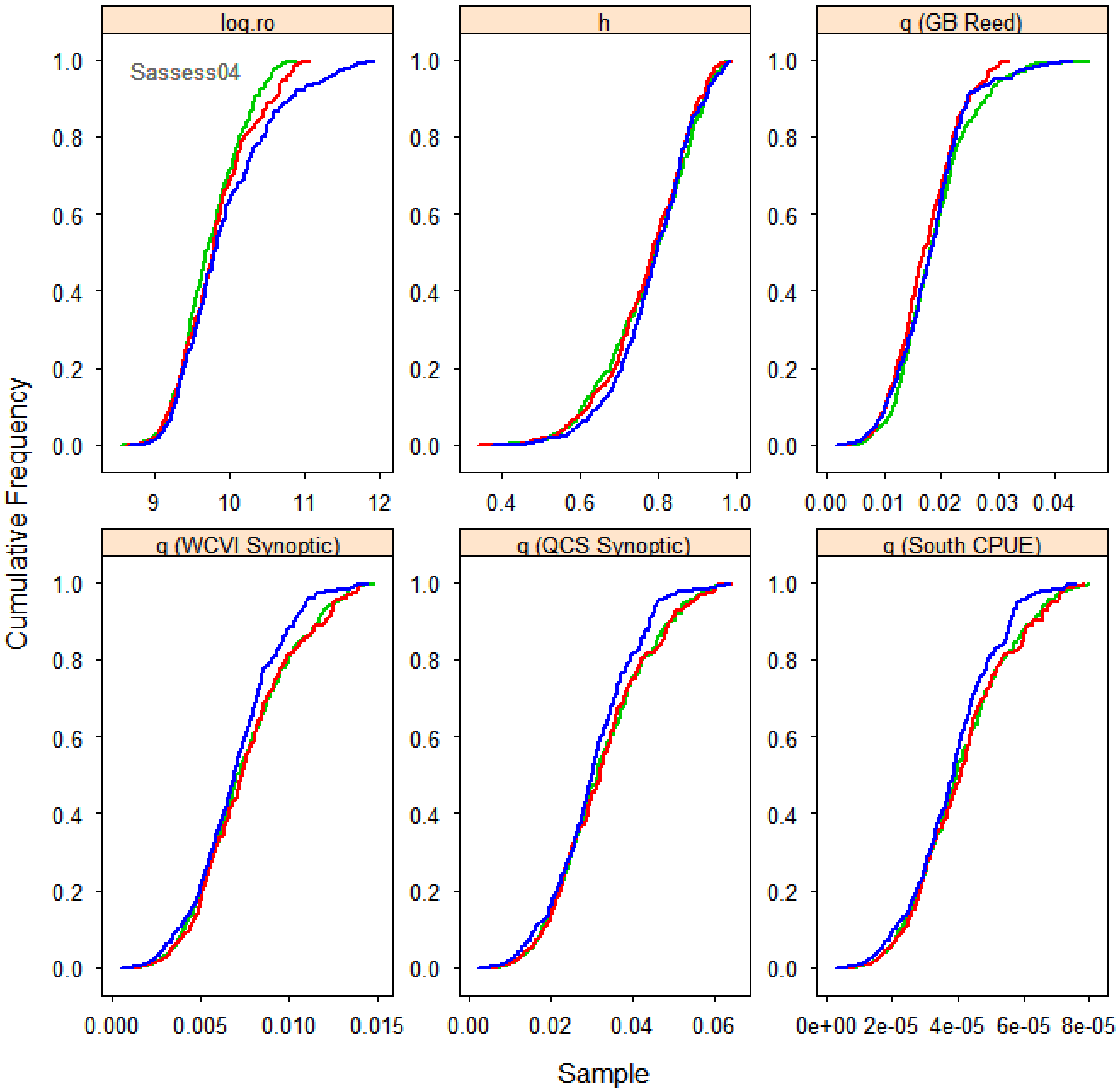

Figure F.27. BC South: Diagnostic plot for the example model run obtained by dividing the MCMC chain of 1000 samples into three segments and over-plotting the cumulative distributions of the first segment (green), second segment (red), and final segment (blue).

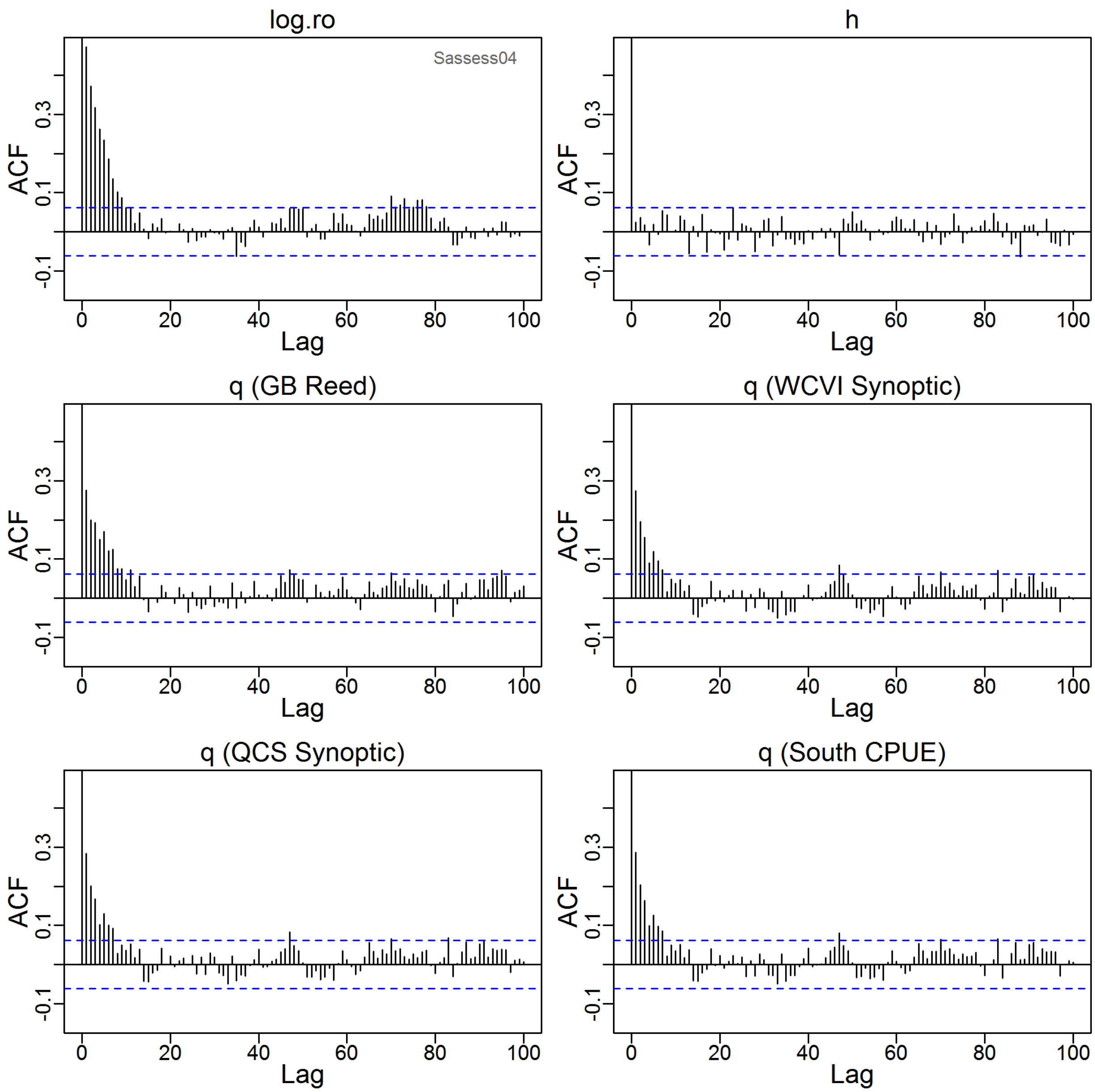

Figure F.28. BC South: Autocorrelation plots for MCMC output of estimated parameters in the example model run. See Figure F.26 for parameter descriptions.

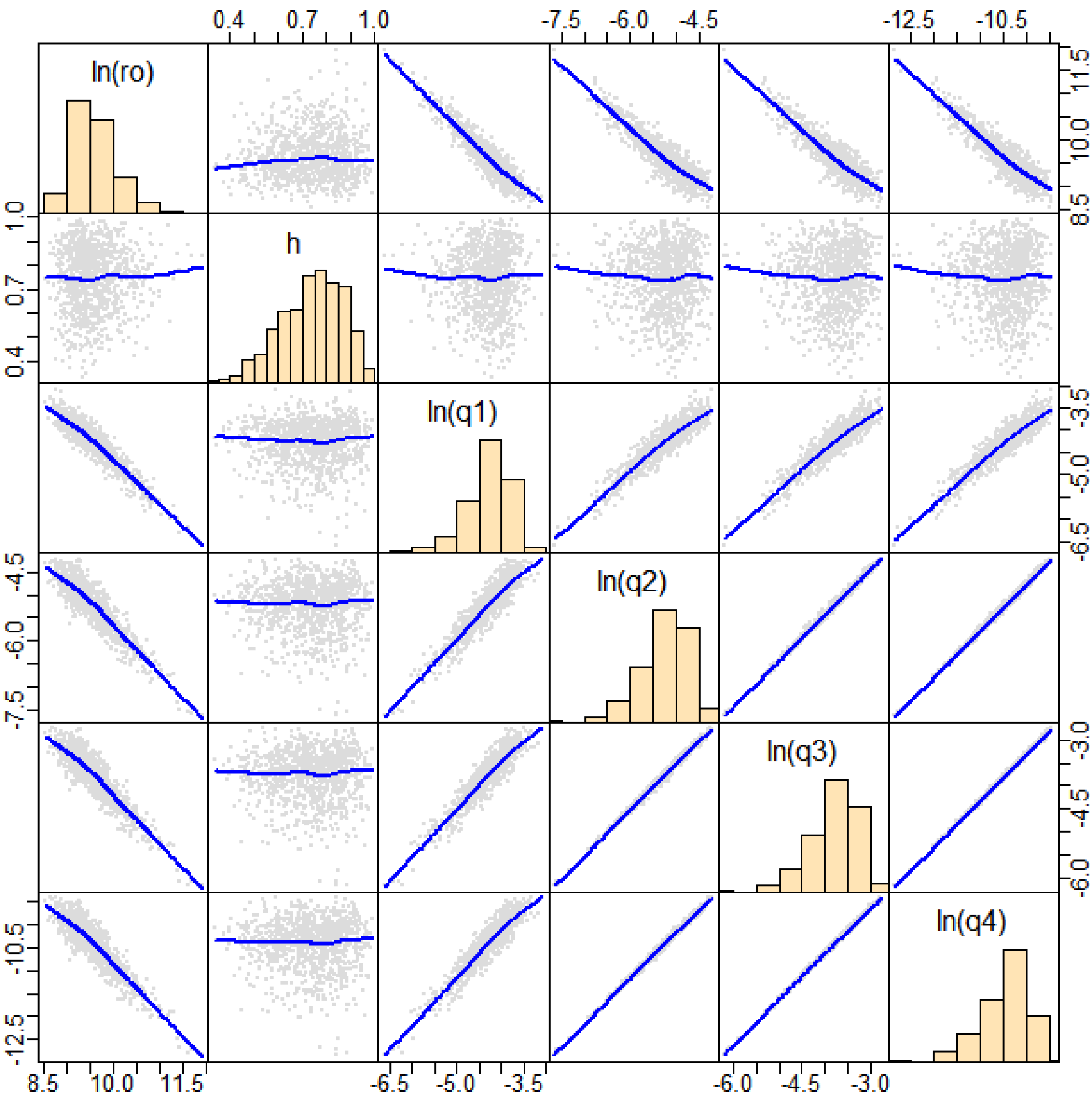

Figure F.29. BC South: Pairs plot from the southern BC region of 1000 MCMC samples for the estimated parameters of the example model run. The diagonal shows the frequency distribution of each posterior.

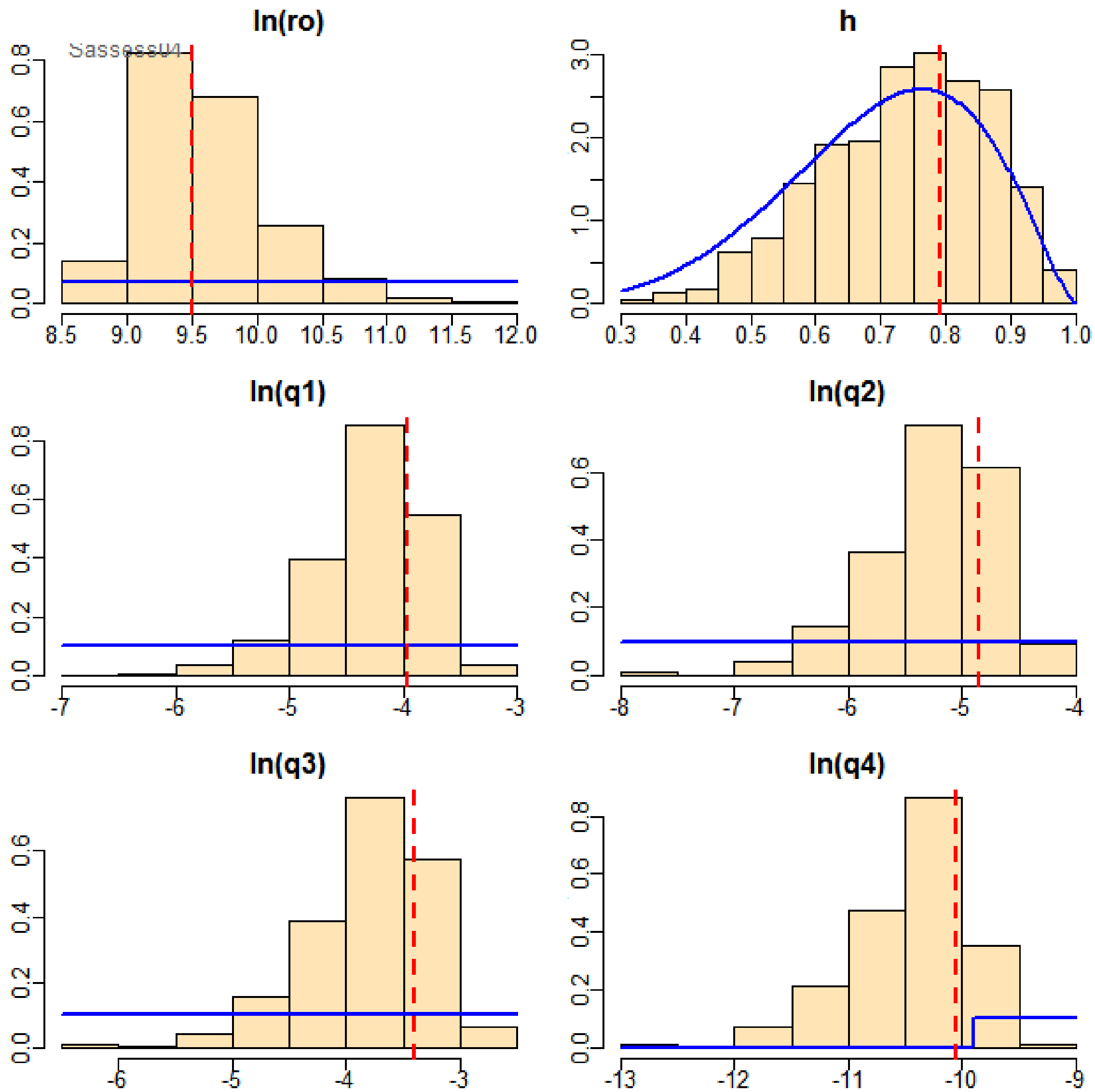

Figure F.30. BC South: Prior probability distributions (blue lines) used in the example model run and the comparative posterior histograms. Parameters q_j represent catchability of the various surveys j as defined in Figure F.26. The dashed red vertical lines show the MPD estimates.

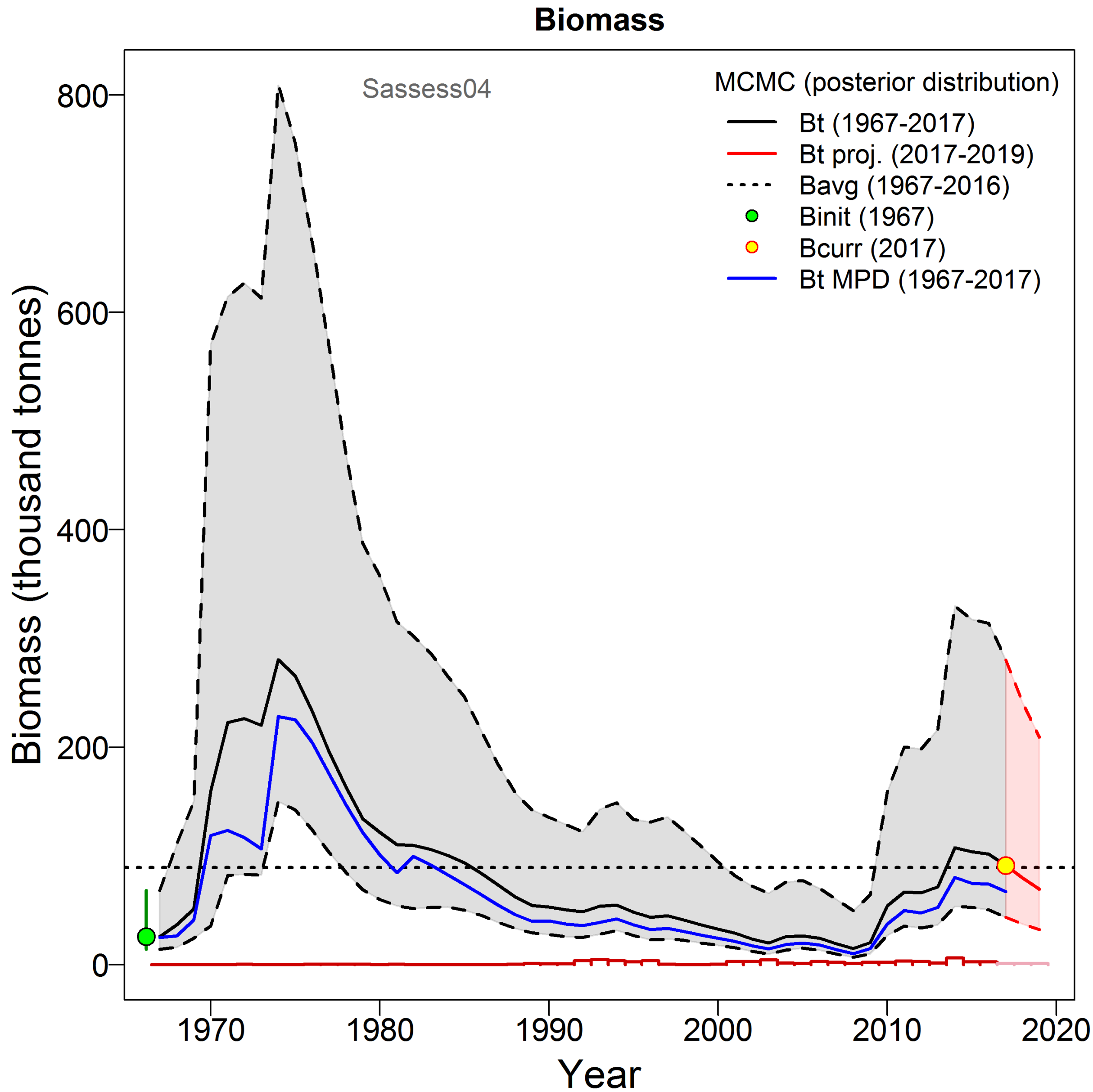

Figure F.31. BC South: Posterior estimates of spawning biomass (1000 t) for the example model run with 95% credibility intervals in grey. The current year biomass (2017, yellow point) and projected biomass (2018-2022, red line), assuming a constant catch policy of 3250 t/y, are enclosed by a 95% credibility interval shaded pink. The median posterior estimate of B_0 is shown as a green point (with 95% credibility range) to the left of the time series. The MPD estimate is shown as a blue line. The total catch is shown along the bottom as red bars, with assumed TAC catch in pink..

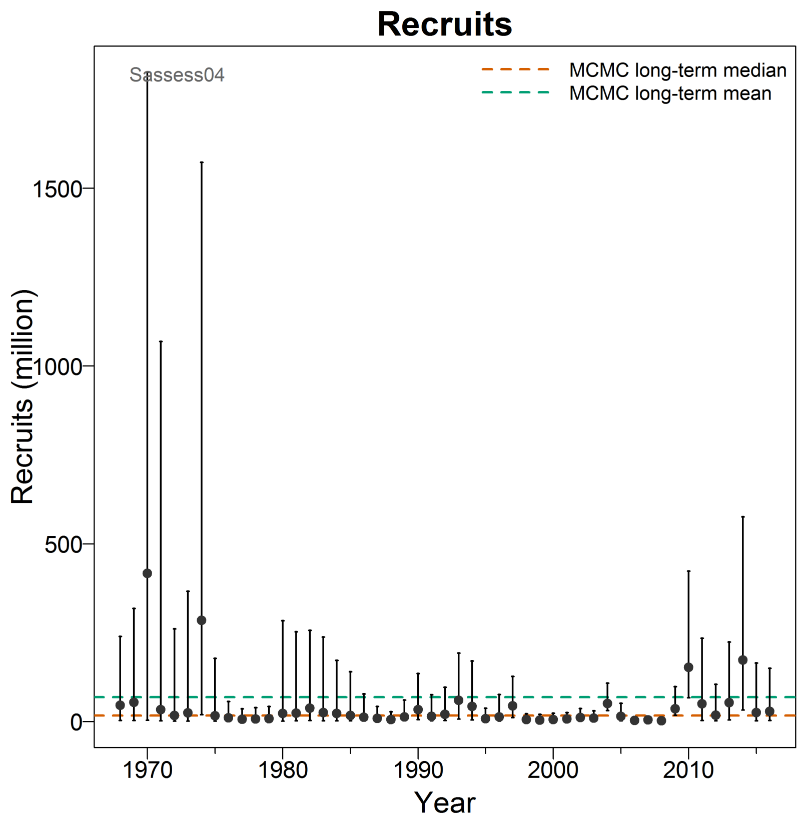

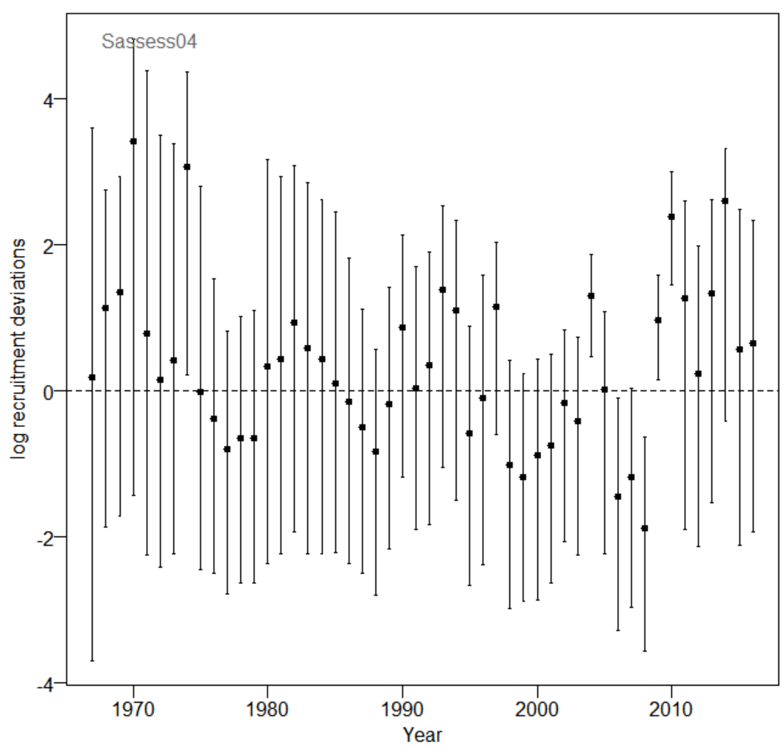

Figure F.32. BC South: **[Top]** *Posterior estimates of age-3 recruits for the example model run.* **[Bottom]** *Log recruitment deviations for the example model run with 95% credibility intervals.*

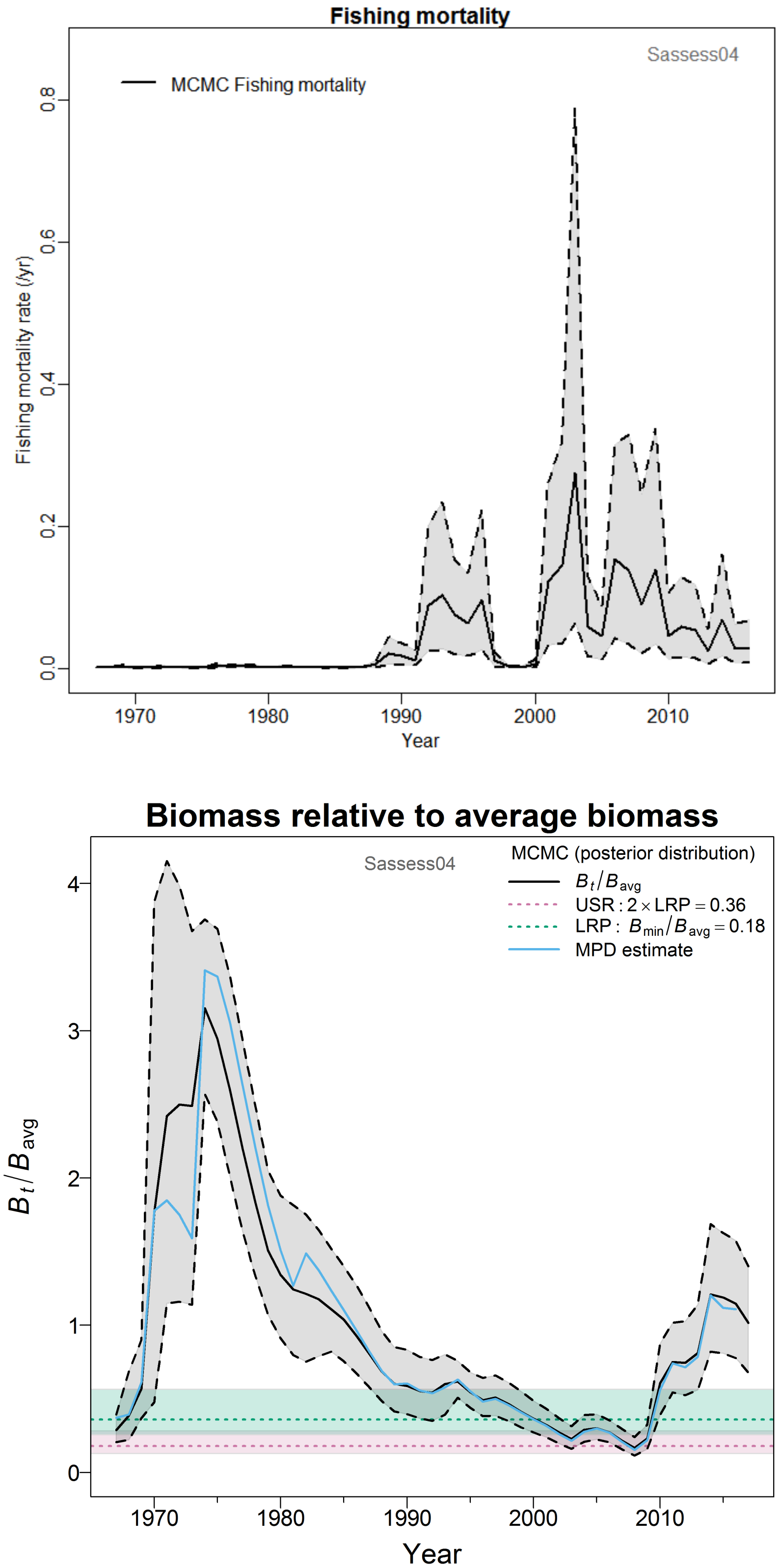

Figure F.33. BC South: **[Top]** *Posterior estimates of fishing mortality for the example model run.* **[Bottom]** *Biomass depletion, i.e. $B_t/B_{\rm avg}$, for the example model run with 95% credibility intervals. Also displayed on the depletion figure is the MPD estimate (blue line) and the reference points $B_{\rm min}$ (red dashed line) and $2B_{\rm min}$ (green dashed line).*

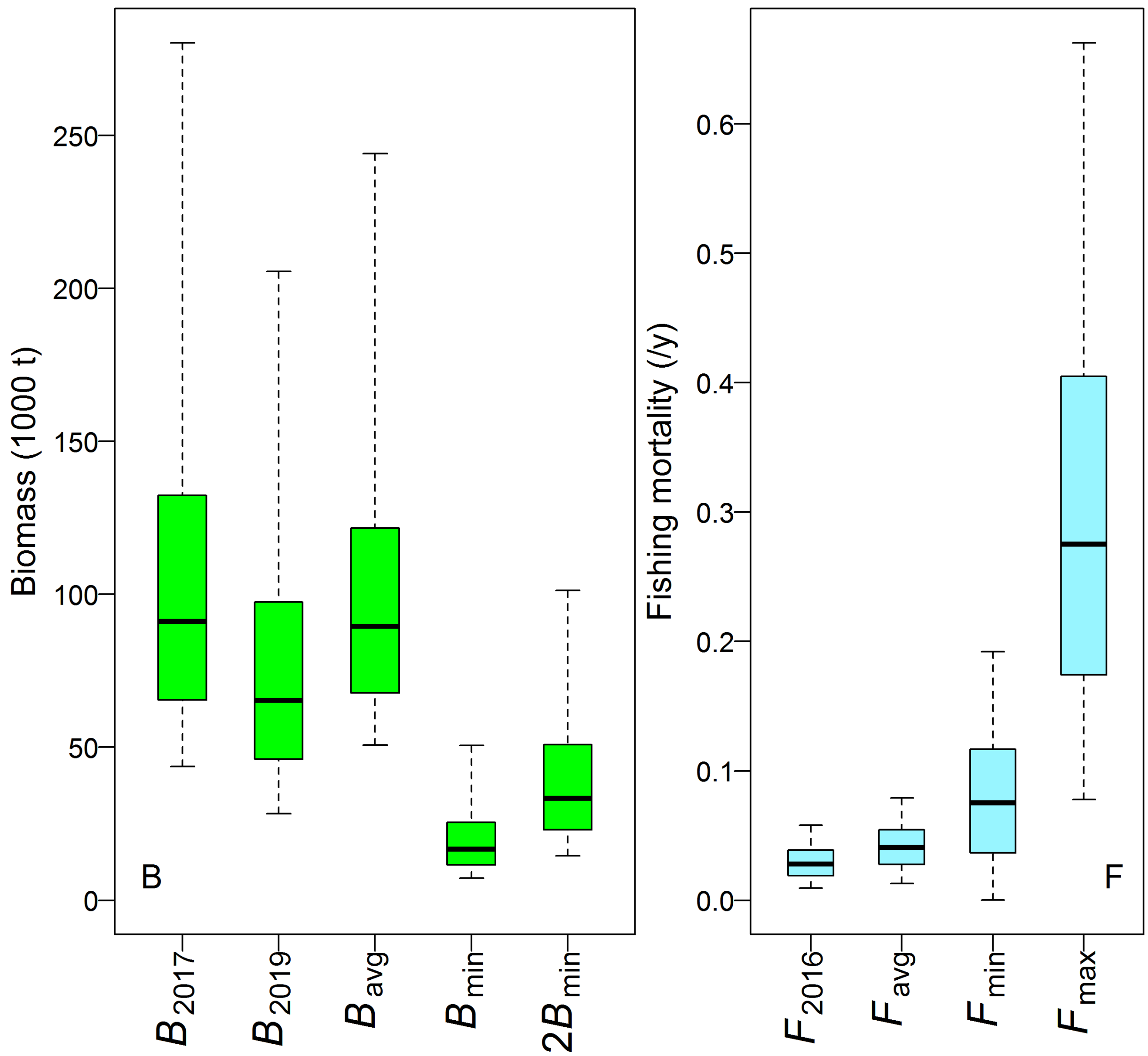

Figure F.34. BC South: Posterior estimates of spawning biomass- and harvest-based reference points for the example model run. **[Left]** *The current-year biomass B_{2017}, the projected-year biomass B_{2019}, B_{avg} = average biomass from 1967 to 2016, the limit reference biomass (or B_{min}) = biomass in 2008, and the upper stock biomass set at $2B_{2008}$.* **[Right]** *The current-year fishing mortality rate F_{2016}, the average fishing mortality rate F_{avg} from 1967 to 2016, the fishing mortality rate in the year of minimum biomasss F_{2008}, and the maximum fishing mortality experience over the time series F_{max}. Box delimiter and limits represent quantiles at 0.5 (median), 0.25 and 0.75 quantiles, respectively, and the whiskers delimit the 0.05 and 0.95 quantiles. Outliers are not shown.*

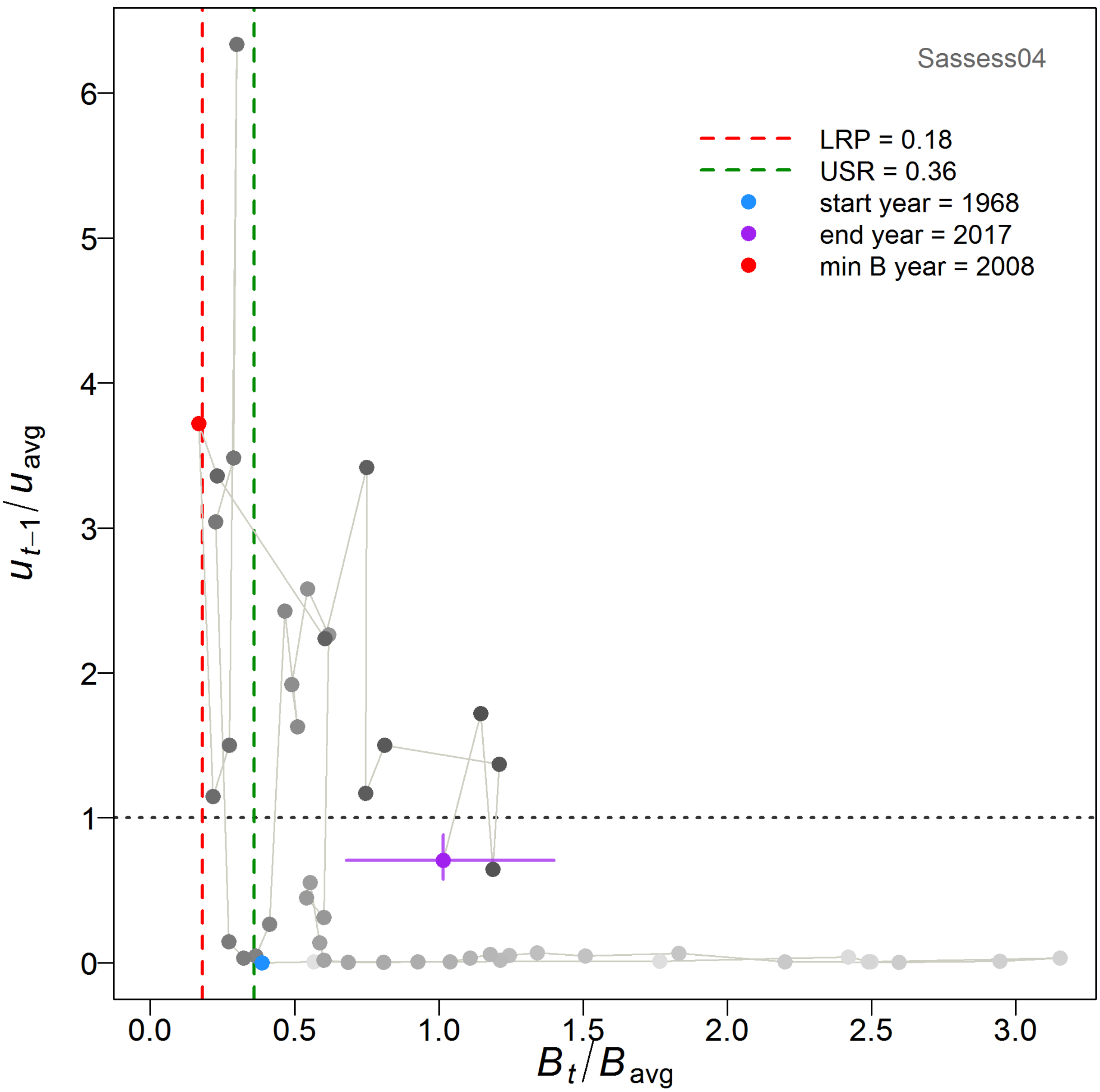

Figure F.35. BC South: Phase plot through time for the example model run of the medians of the ratios B_t/B_{avg} *(the biomass in year* t *relative to* B_{avg}*) and* u_t/u_{avg} *(the exploitation rate in year* t *relative to* u_{avg}*). Blue filled circle is the starting year 1967. Years then proceed from light grey through to dark grey with the final year 2017 as a filled orange circle with limit lines represent the 0.05 and 0.95 quantiles of the posterior distributions for the final year. Vertical dashed lines indicate the historical limit (red) and upper stock reference (green) points (see legend for values), and horizontal dotted line indicates* u_t *at* u_{avg}.

F.3.2. Alternative Cases – South

For the BC South stock, we ran a total of 11 alternative runs (Table F.13) (including the example run above) using the growth model published by Janusz and Horbowy (1997) for the Sea of Okhotsk (off Russia's east coast and west of the Bering Sea) to test the robustness of the results to uncertainties in:

- natural mortality (M);
- age at knife-edge recruitment (k);
- the use of the CPUE index series.

We tested a range of sensible values for M and k because these parameters control key assumptions made by the delay-difference model when the data available to the model are not very informative with respect to these parameters. We also tested combinations of M and k for the last alternative category (removing CPUE index series).

The delay-difference model assumes that maturity matches selectivity, i.e., all recruited fish are mature, and by extension, all mature fish have a single natural mortality rate. Alternative runs for the BC South stock were made with $M \in \{0.25, 0.30, 0.35\}$ to bracket plausible values for this single parameter (Table F.13). We use $k \in \{3, 4, 5\}$ for the BC South stock guided by ogive information in Table D.7 of Dorn et al. (2012). We added k=5 to the suite of alternative values for this parameter because of the lower maximum size in this growth model. Nine of the alternative runs (including the example case) used all the abundance index series and paired $k \in \{3, 4, 5\}$ with $M \in \{0.25, 0.30, 0.35\}$. Two of the alternative runs dropped the CPUE index series and paired $M = 0.3$ with $k \in \{3, 4\}$.

All 11 alternative runs were taken to the MCMC level. Each MCMC search was started at the "best fit" MPD parameter set, run for 60 million iterations, and sampled every 50,000 for 1200 samples. The first 200 samples were dropped as burn-in to yield a total posterior sample of 1000 draws.

F.3.2.1. MPD results – alternatives (south)

Visual inspection of fits from these alternative runs suggests that the data available to this model did not allow much discrimination between the range of hypotheses tested. While there were differences in the fits to the available biomass indices and to the mean weight data, these differences tended to be small and probably could not distinguish between hypotheses except in the most extreme cases. As an example, none of the models were able to fit the high mean weights observed in the late 1970s and in the late 1980s (Figure F.36), which may be attributable to misspecification of the growth model. While the delay-difference model uses the mean weight data to scale the overall biomass and to obtain recruitment deviation information, it is likely that only an age-structured model would have sufficient flexibility to fit the entire mean weight series. The model also did not fit some of the high points in the survey series or the CPUE times series (Figures F.37–F.40), but generally most index points were acceptably fitted. The model seemed to have the most difficulty fitting the WCVI survey series (Figure F.38).

In an attempt to make such comparisons more quantitative, the negative log-likelihoods for the fits to each data component of the model are summarised for the 11 alternative runs in Table F.14. Comparisons of the whole model can only be made among those runs that share the same estimated components:

- Cases S00 to S08 – S08 had the lowest objective function value of these nine cases and offered the best model fit in the first group;
- Cases S09 to S10 – S10 offered the better fit in the second group.

The two best-fit models featured high values for M paired with high values of k, which likely reflects the growth model used for this population of smaller Walleye Pollock. Case S08 (M=0.35, k=5) also had the best fit to the mean weight component, and most of the $k \in \{4, 5\}$ models showed much better fits than those where $k = 3$.

Table F.13. Summary of the analyses performed to test the sensitivity of the delay-difference model to variations in natural mortality M, knife-edge recruitment age k. All runs for the BC South stock use the Okhotsk Sea growth function (Janusz and Horbowy 1997). The column marked 'Rank' provides a subjective ranking of the MCMCs, where 1 = good, 2 = acceptable, and 3 = poor.

Case	Run ID	Run #	M	k	Rank
S00	M.30+k3	4	0.3	3	2
Sensitivity to k at M=0.30					
S01	M.30+k4	5	0.3	4	2
S02	M.30+k5	15	0.3	5	2
Sensitivity to k at M=0.25					
S03	M.25+k3	11	0.25	3	1
S04	M.25+k4	9	0.25	4	1.5
S05	M.25+k5	14	0.25	5	2
Sensitivity to k at M=0.35					
S06	M.35+k3	12	0.35	3	2
S07	M.35+k4	13	0.35	4	2
S08	M.35+k5	16	0.35	5	2
Removal of commercial CPUE					
S09	M.30+k3-CPUE	10	0.3	3	1
S10	M.30+k4-CPUE	8	0.3	4	3

Table F.14. BC South MPD negative log likelihoods from the 11 alternative cases documented in Table F.13 for each data component used in the model.

Case	Catch	GIG Hist	WCVI Synop	QCS Synop	South CPUE	Recruits	Mean Weight	ObFn Value
S00: M.30+k3	-103.746	12.417	77.426	12.888	24.692	81.712	10.980	254.232
S01: M.30+k4	-103.424	12.807	67.805	7.540	20.435	80.728	0.580	223.310
S02: M.30+k5	-102.609	12.418	65.330	11.370	14.403	81.524	-0.916	218.626
S03: M.25+k3	-103.645	14.049	75.907	13.553	28.263	80.874	10.145	256.383
S04: M.25+k4	-103.278	14.357	68.264	8.702	23.549	81.285	0.001	229.967
S05: M.25+k5	-102.339	14.152	65.824	12.677	17.421	82.400	0.711	228.370
S06: M.35+k3	-103.805	10.913	78.441	12.100	21.326	82.190	13.178	252.633
S07: M.35+k4	-103.521	11.083	67.216	6.615	17.741	80.980	1.440	218.596
S08: M.35+k5	-102.823	10.721	64.767	10.251	11.978	81.093	-2.125	210.788
S09: M.30+k3-CPUE	-103.089	12.146	35.993	13.843	—	82.603	22.418	202.150
S10: M.30+k4-CPUE	-102.837	12.806	36.614	8.391	—	80.376	-1.323	170.736

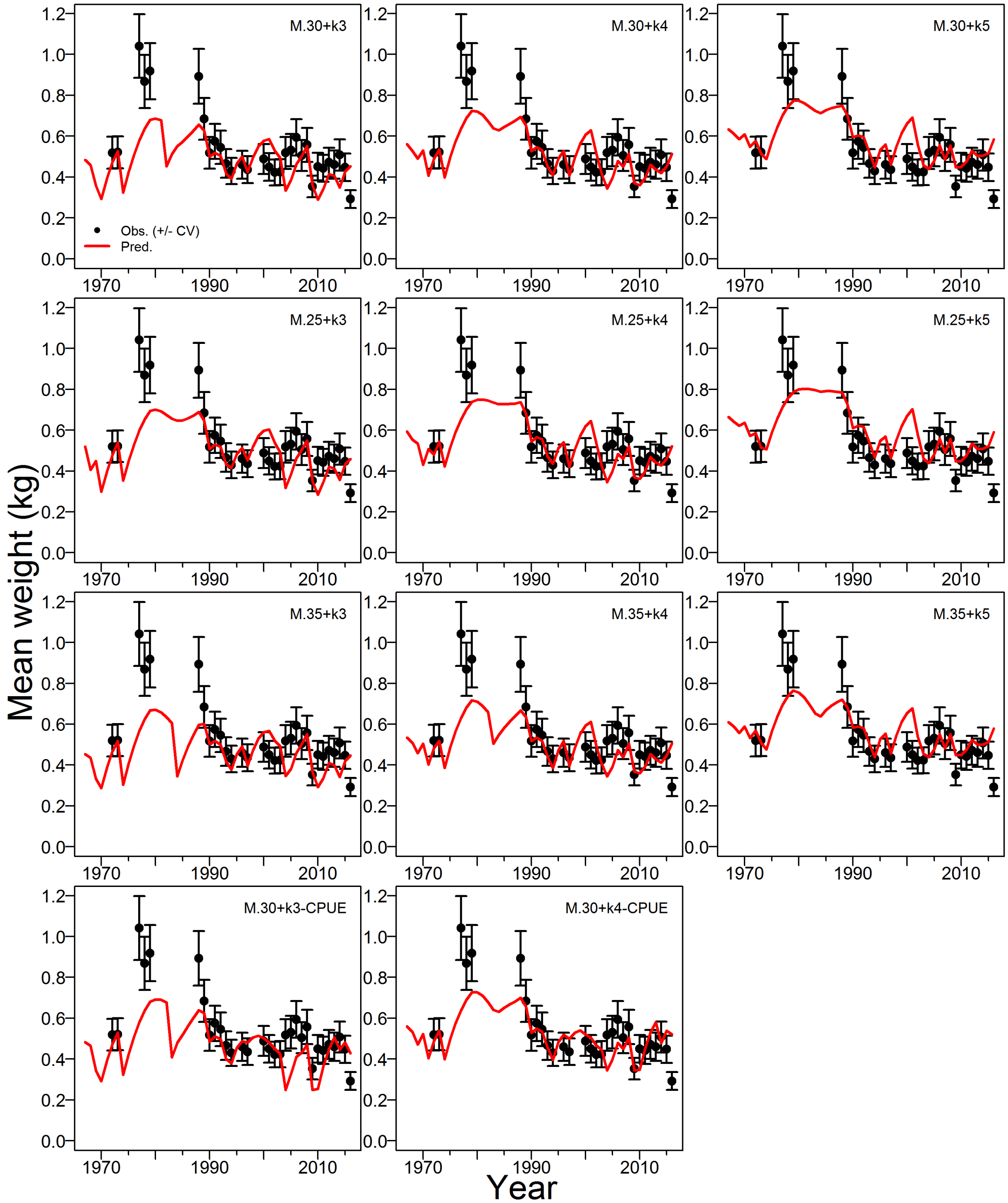

Figure F.36. BC South: MPD fit to the mean weight data for the 11 alternative runs. Predicted mean weights are shown as red lines and observations are shown as points. Error bars on mean weight observations represent a fixed CV using $\sigma_W = 0.15$.

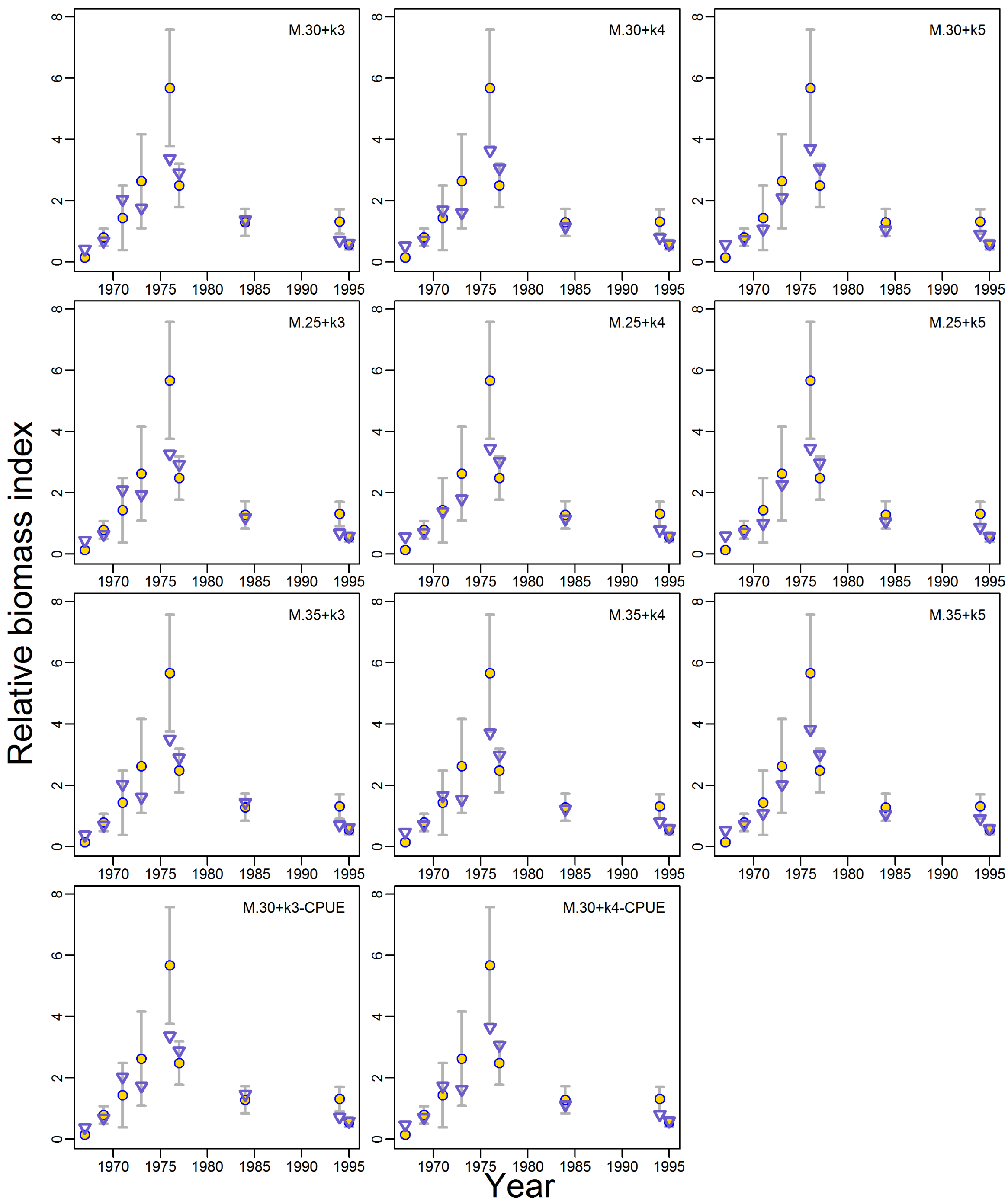

Figure F.37. BC South: MPD index fits (11 alternative runs) for the GIG (Goose Island Gully) historical rockfish survey relative abundance indices. Circles represent observed indices with associated CVs, triangles represent the model fit.

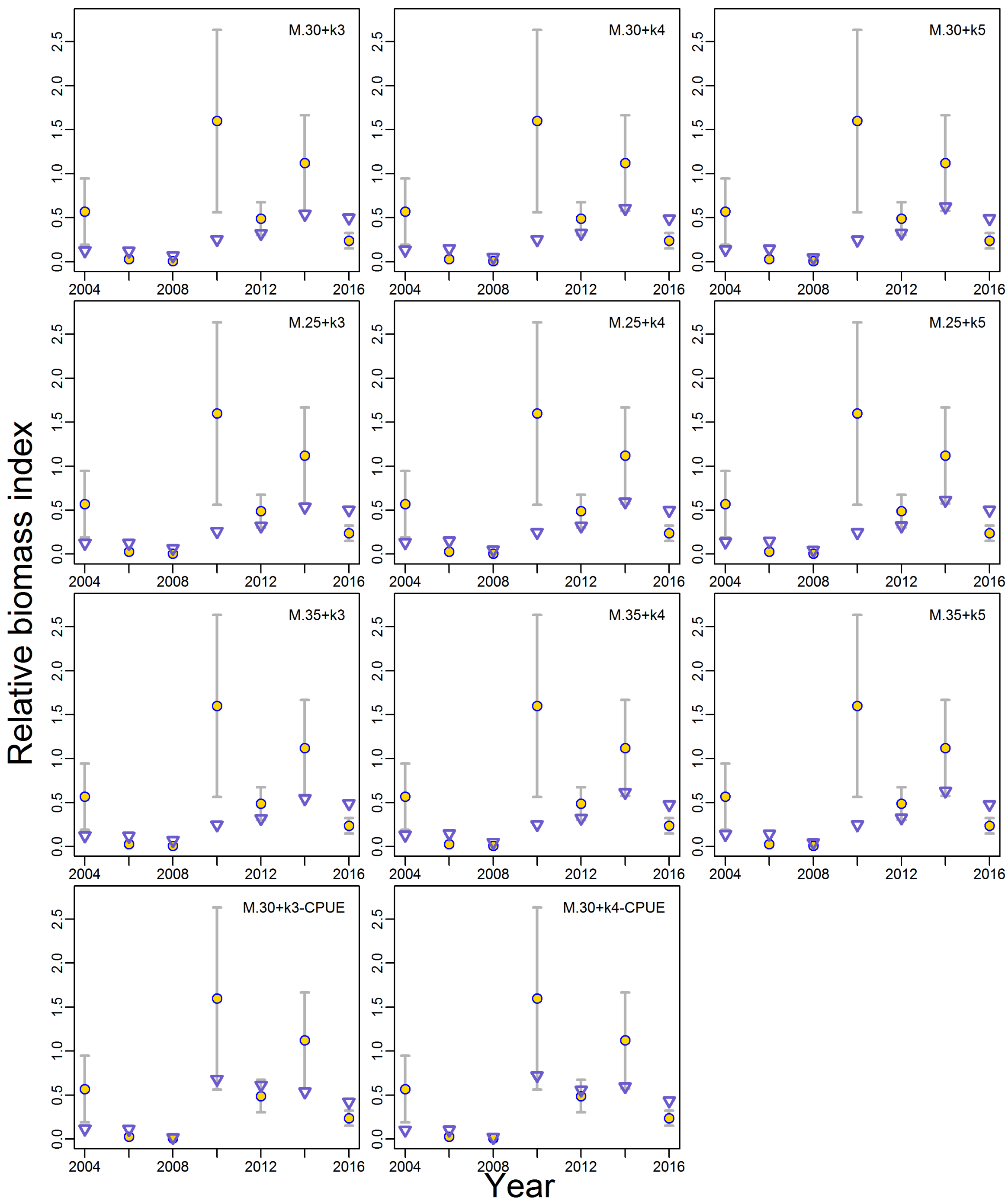

Figure F.38. BC South: MPD index fits (11 alternative runs) for the WCVI (west coast Vancouver Island) synoptic survey relative abundance indices. Circles represent observed indices with associated CVs, triangles represent the model fit.

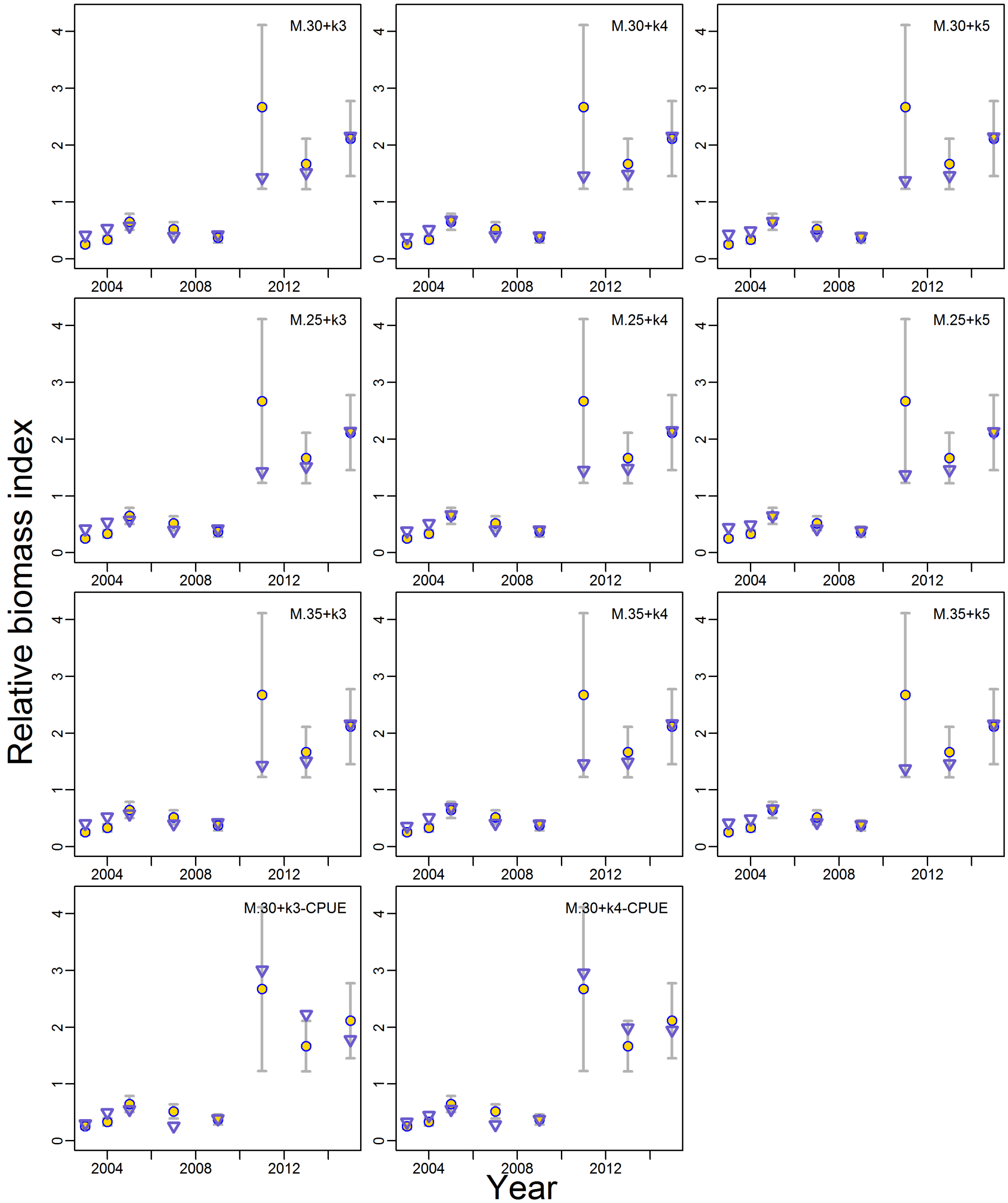

Figure F.39. BC South: MPD index fits (11 alternative runs) for the QCS (Queen Charlotte Sound) synoptic survey relative abundance indices. Circles represent observed indices with associated CVs, triangles represent the model fit.

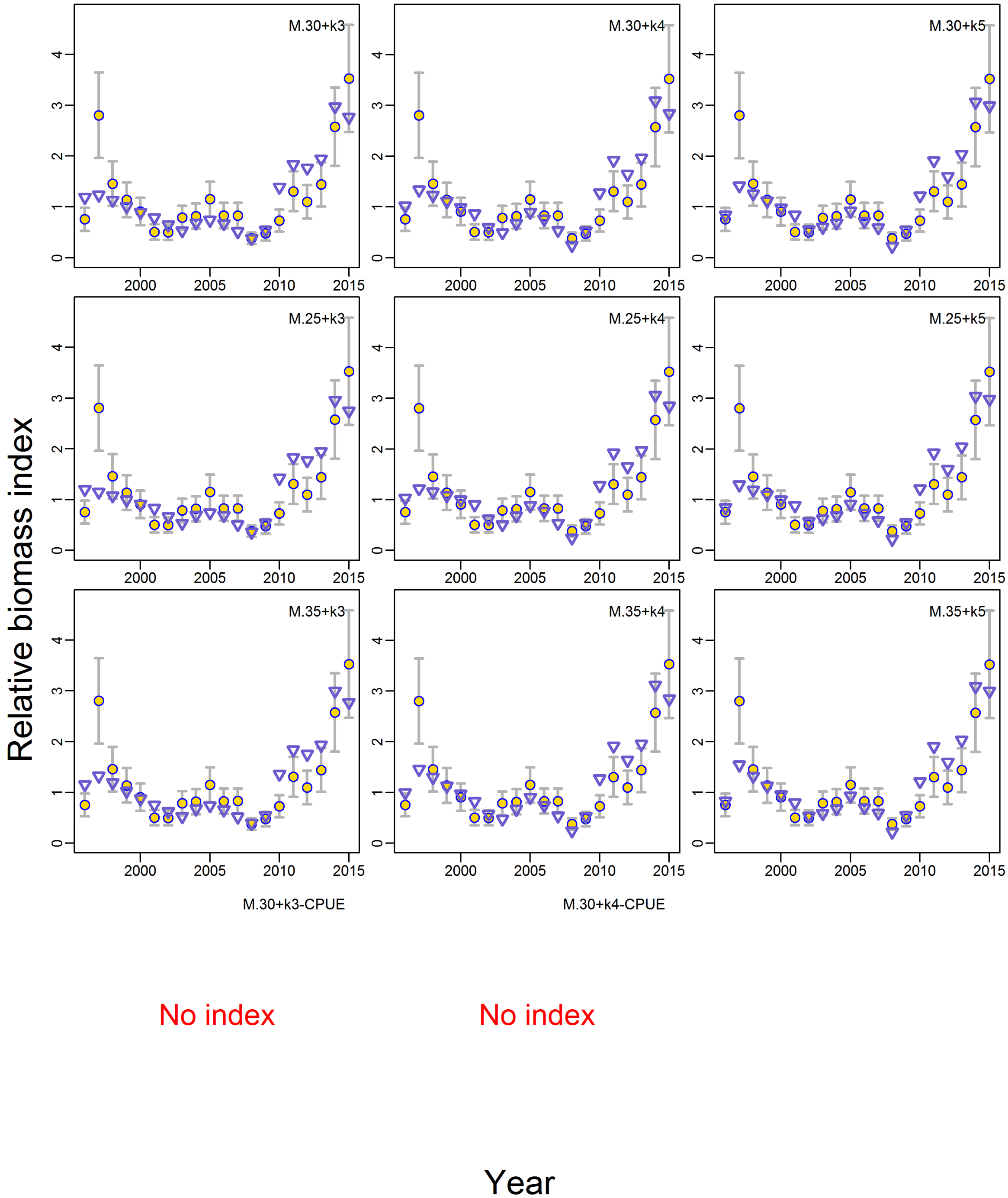

Figure F.40. BC South: MPD index fits (11 alternative runs) for the commercial trawl Walleye Pollock CPUE relative abundance indices. Circles represent observed indices with associated CVs, triangles represent the model fit.

F.3.2.2. MCMC results – alternatives (south)

Median estimates for current biomass B_{2017} lie at or below the average biomass B_{avg} for all alternative cases(Table F.15). Unlike the alternative case for the BC North stock, the year in which median spawning biomass reached a minimum is stable across all runs, occurring in 2008. Despite this apparent stability, the maximum fishing mortality F estimated in the MCMC samples exceeded realistic levels (F>2) in some years for all but three cases. This is likely to be the result of the failure of the knife-edge recruitment assumption (particularly when it is k=4 or k=5), which leaves too few fish in the population in some years to support the observed level of catch. However, the alternative cases model population trajectories consistently such that the minimum biomass occurs in the same year.

Table F.16 shows for each alternative run the probabilities of projected biomass in two years at 3250 t/y (at the level of recent average catch) exceeding various reference points . All runs except S08 show high probabilites of B_{2019} exceeding the limit reference point B_{min}. All scenarios project B_{2019} to fall below B_{avg} and B_{2017}, although it should be noted that 2-year projections using this delay-difference model are unreliable and uncertain. That is because these models, like a surplus production model and unlike an age-structured model, only project using the stock-recruitment function, which has little predictive power.

Most of the trace plots for R_0 look acceptable but a few show large-scale shifts in the trace mean (Figure F.41). Autocorrelation plots for R_0 highlight other problems (Figure F.42), with high levels of serial correlation in seven of the 11 alternative runs. The runs featuring low M and k values show the least autocorrelation, but these are the runs with the higher negative log-likelihood fits (Table F.14). The ranks assigned to the quality of MCMCs appear in Table F.13. While there is no statistical basis for selecting among these hypotheses, these MCMC results suggest that a selection of the runs with the best diagnostics can be used to model this Pollock stock. Consequently, this stock assessment used the subjective MCMC quality rankings to construct a Model Average posterior to provide advice to managers (Section F.3.3.), with a rank $\leq$2 used as the quality cutoff criterion.

Quantile plots compare B_{avg}, $B_{2017}/B_{\mathrm{avg}}$, $u_{2016}/u_{\mathrm{avg}}$ and $u_{\mathrm{avg}}B_{\mathrm{avg}}$ of the example run to alternative runs grouped by category:

- $M = 0.30$ and $k \in \{3, 4, 5\}$ – comparing all the medium M alternatives (Figure F.43);
- $M = 0.25$ and $k \in \{3, 4, 5\}$ – comparing all the low M alternatives (Figure F.44); and
- $M = 0.35$ and $k \in \{3, 4, 5\}$ – comparing all the high M alternatives (Figure F.45).

These plots show that M and k interact to change the perceived size of the stock (e.g, B_{avg}), but the estimated stock status is much more consistent among the runs (Figure F.43).

Note that runs S00, S03 and S06, all runs where $k = 3$ (but include the CPUE series), have the largest estimated B_{avg} and consequently the lowest F_{max}. All other runs estimate smaller average biomass levels and consequent maximum exploitation rates that are not credible. This is likely to be the result of the strong assumption of knife-edge recruitment that is made by the delay-difference model, resulting in insufficient biomass to accommodate catch levels in some years when k>3. This is a model misspecification resulting from data limitations (i.e., the lack of ageing data), leading to a cautious interpretation of these runs but probably not to outright rejection. The two runs which discard the CPUE series also estimate levels of biomass that result in unacceptable estimates for F_{max}, even for runs with k=3.

Table F.15. BC South median values for select MCMC-derived parameters and quantities for 11 alternative runs from the BC South stock. The value for B_{2019} is that assuming a TAC of 3250 t/y. Model senstivity details appear in Table F.13.

Run	h	B_{avg}	$\frac{B_{2017}}{B_{\mathrm{avg}}}$	$\frac{B_{2019}}{B_{\mathrm{avg}}}$	$\mathrm{Yr}_{\mathrm{min}}$	$\frac{B_{2017}}{B_{\mathrm{min}}}$	F_{max}	u_{avg}	$\frac{u_{2016}}{u_{\mathrm{avg}}}$
S00: M.30+k3	0.75	89,549	1.0	0.75	2008	5.8	0.28	0.038	0.73
S01: M.30+k4	0.77	21,257	0.79	0.50	2008	8.0	18	0.16	0.82
S02: M.30+k5	0.79	14,835	0.72	0.38	2008	8.3	18	0.24	0.82
S03: M.25+k3	0.76	54,998	1.0	0.73	2008	6.4	0.49	0.062	0.74
S04: M.25+k4	0.78	20,412	0.85	0.46	2008	8.5	18	0.16	0.80
S05: M.25+k5	0.81	13,022	0.84	0.47	2008	8.7	19	0.24	0.82
S06: M.35+k3	0.74	183,563	1.0	0.72	2008	5.5	0.12	0.018	0.74
S07: M.35+k4	0.78	21,814	0.75	0.36	2008	7.6	14	0.17	0.82
S08: M.35+k5	0.79	14,623	0.72	0.24	2008	7.9	20	0.23	0.85
S09: M.30+k3-CPUE	0.75	33,336	0.62	0.36	2008	18	19	0.14	0.81
S10: M.30+k4-CPUE	0.76	19,971	0.90	0.44	2008	17	18	0.18	0.69

Table F.16. BC South: Assuming a constant catch policy of 3250 t/y, the probability that B_{2019} (or u_{2018}) is greater than reference points used in this assessment for 11 alternative runs. Model senstivity details appear in Table F.13. For reference, the average catch over the last 5 years (2011-2015) is 3256 t.

Run	P$\left(\frac{B_{2019}>}{B_{2017}}\right)$	P$\left(\frac{B_{2019}>}{B_{\min}}\right)$	P$\left(\frac{B_{2019}>}{2B_{\min}}\right)$	P$\left(\frac{B_{2019}>}{B_{\mathrm{avg}}}\right)$	P$\left(\frac{u_{2018}>}{u_{\mathrm{avg}}}\right)$
S00: M.30+k3	0	1	0.94	0.10	0.08
S01: M.30+k4	0	0.97	0.92	0	0.58
S02: M.30+k5	0	0.96	0.93	0	0.81
S03: M.25+k3	0	1	0.91	0.09	0.93
S04: M.25+k4	0	0.95	0.91	0	0.99
S05: M.25+k5	0	0.98	0.96	0	0.72
S06: M.35+k3	0	1	0.97	0.08	0.11
S07: M.35+k4	0	0.94	0.88	0	1
S08: M.35+k5	0	0.90	0.67	0	1
S09: M.30+k3-CPUE	0	0.94	0.88	0	0.99
S10: M.30+k4-CPUE	0	1	1	0.01	0.97

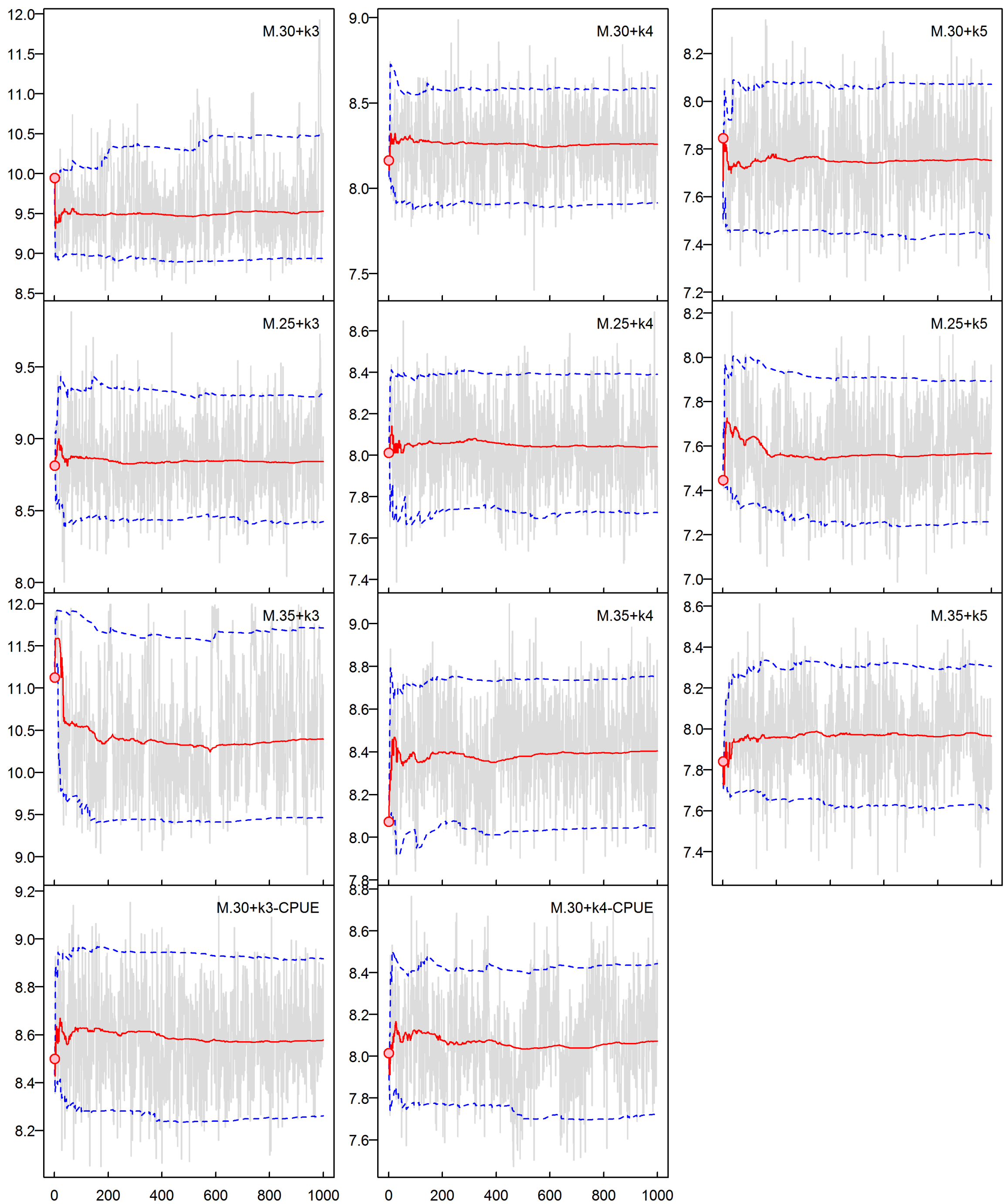

Figure F.41. BC South: Trace plots (11 alternative runs) for MCMC samples of $\log(R_0)$ (natural log of unfished equilibrium recruitment). The MCMC run had chain length 60 million and a sample taken at every 50,000$^{\text{th}}$ iteration to yield 1,000 MCMC samples after a removing a burn-in of 200 samples. Grey lines show the 1000 samples for each parameter, solid lines show the cumulative median (up to that sample), and dashed lines show the cumulative 2.5 and 97.5 quantiles. Red circles are the MPD estimates.

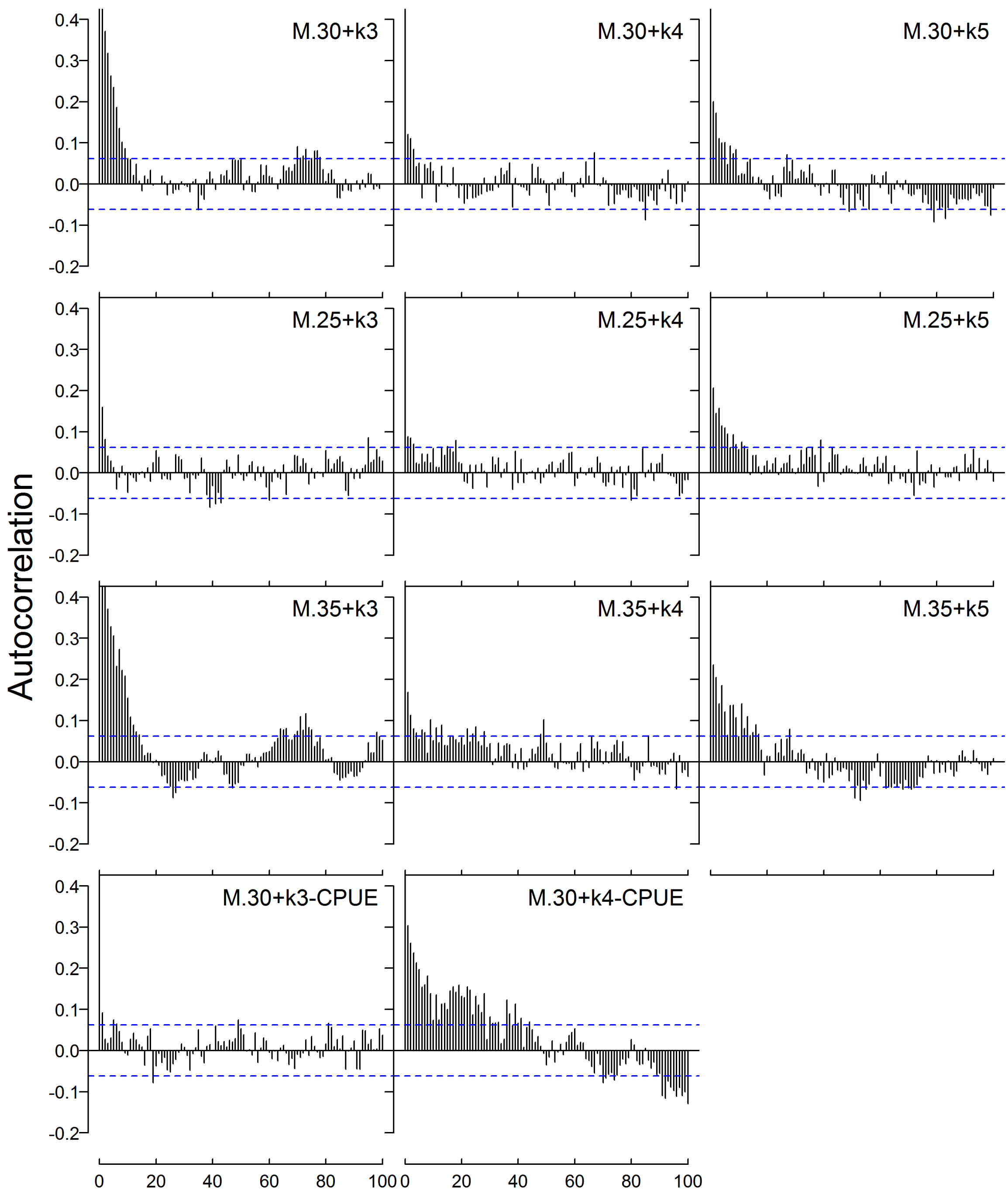

Figure F.42. BC South: Autocorrelation plots (11 alternative runs) for MCMC samples of $\log(R_0)$ (natural log of unfished equilibrium recruitment). The MCMC runs had 1,000 MCMC samples each.

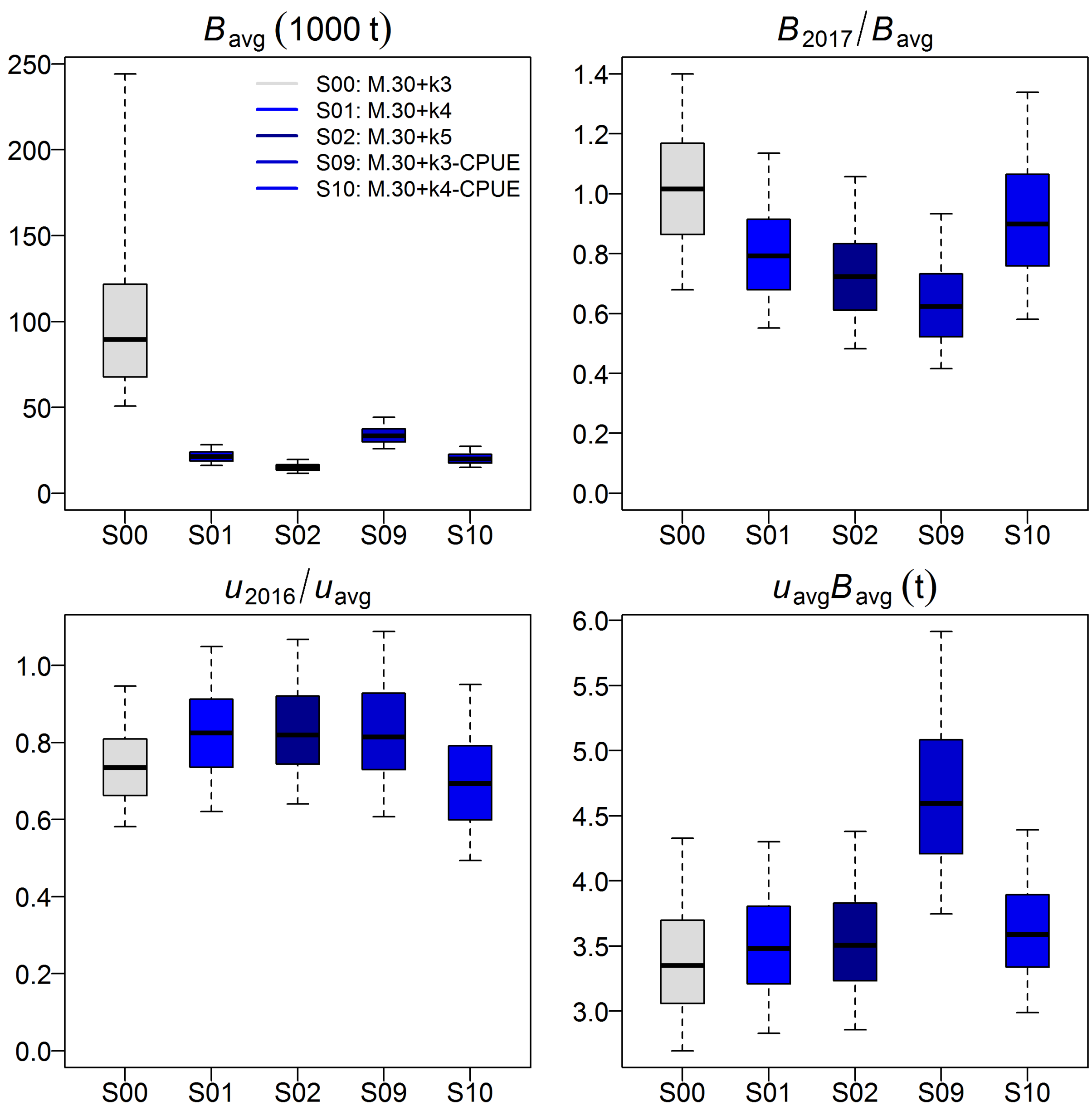

Figure F.43. BC South: Quantile plots comparing the base case (S00 with M=0.30 and k=3 using the Okhotsk Sea (OS) growth model) to alternative runs (all with M=0.30 and using OS growth) that vary by by knife-edge recruitment age k, where $k \in \{3, 4, 5\}$. Additionally, S09 and S10 were fit after dropping the commercial CPUE data. Box delimiter and limits represent quantiles at 0.5 (median), 0.25 and 0.75 quantiles, respectively, and the whiskers delimit the 0.05 and 0.95 quantiles. Outliers are not shown.

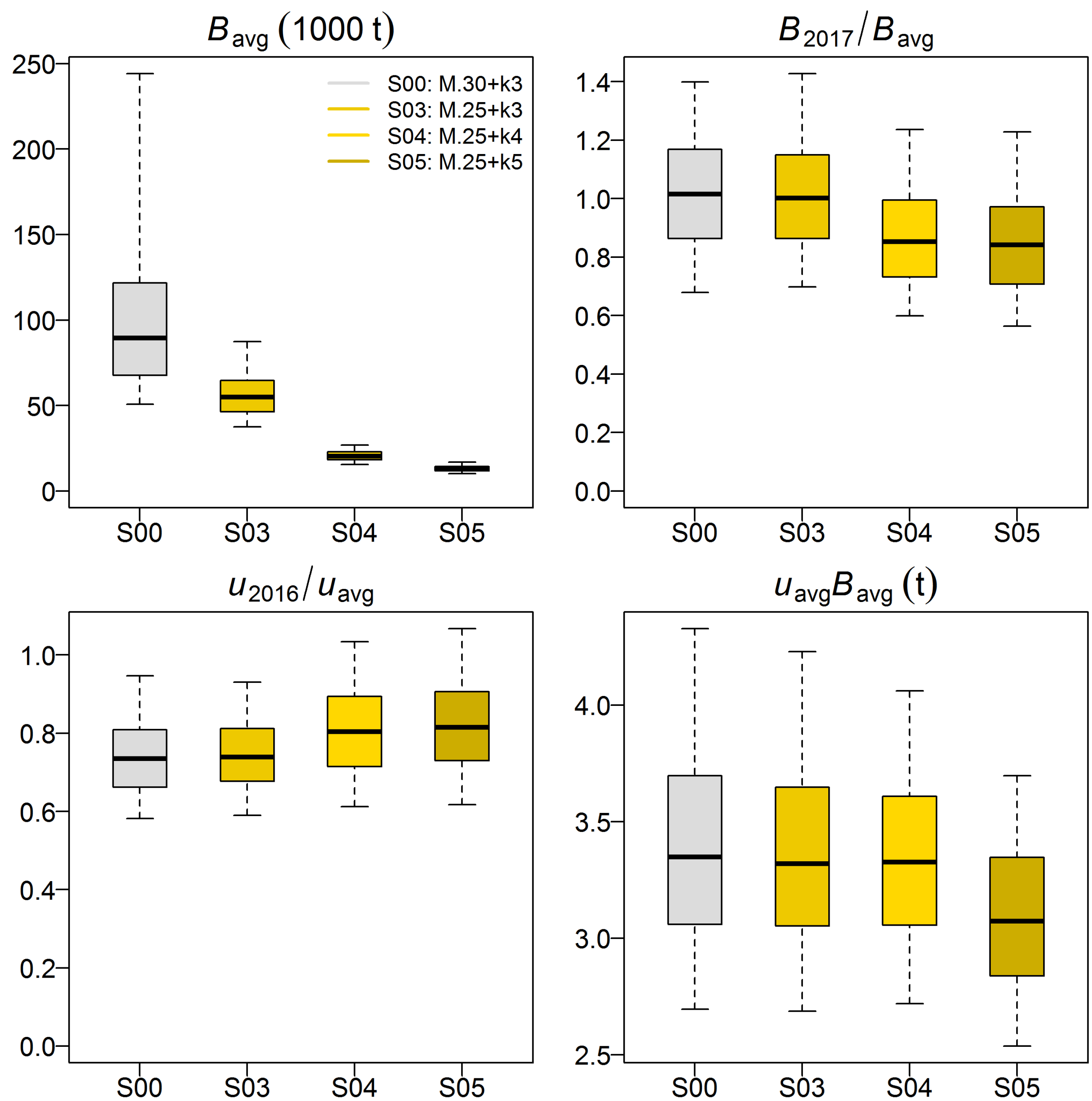

Figure F.44. BC South: Quantile plots comparing the base case to alternative runs (all with M=0.25 and using OS growth) that vary by knife-edge recruitment age k, where $k \in \{3, 4, 5\}$. Quantile box delimiters are detailed in Figure F.43.

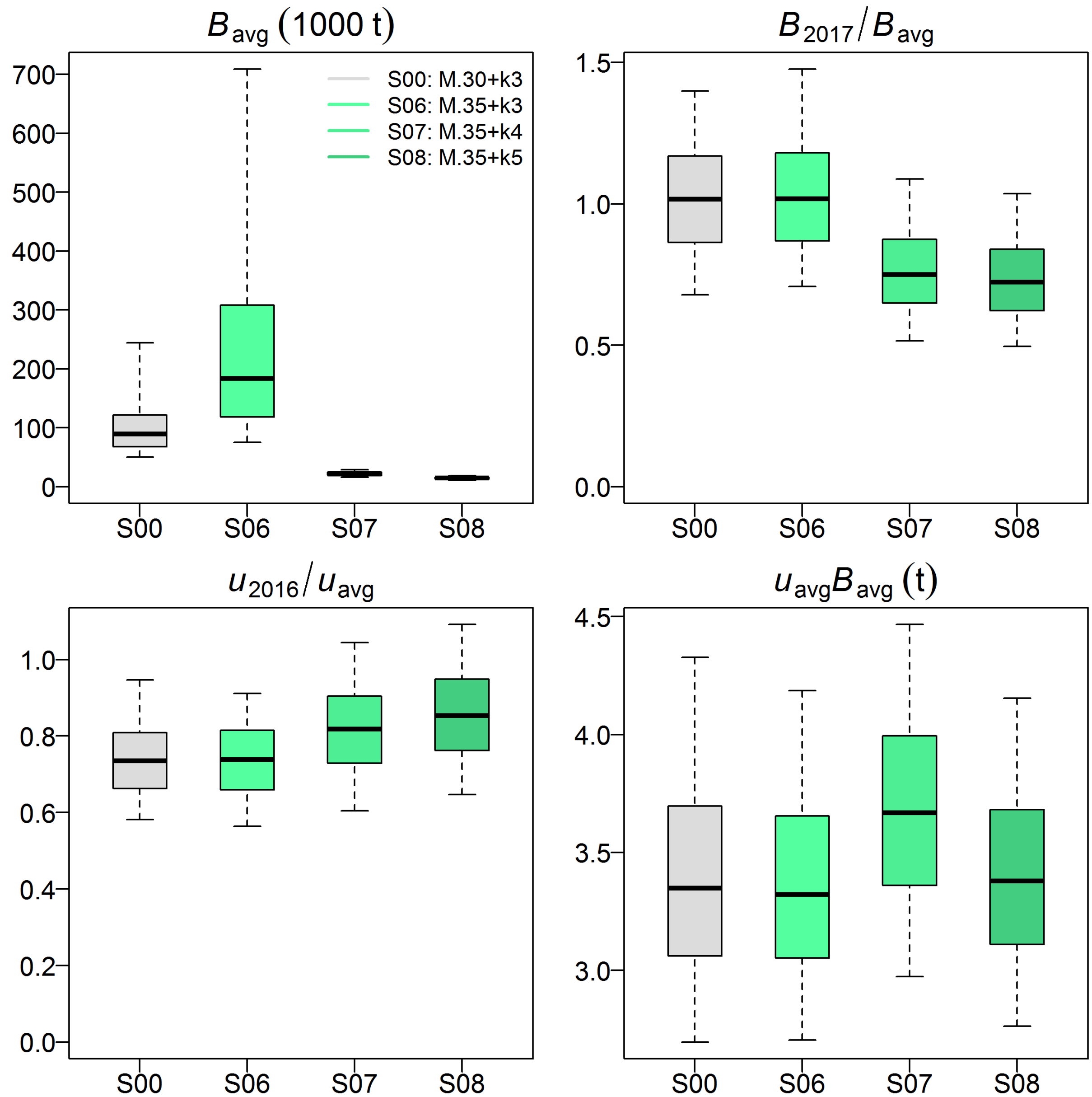

Figure F.45. BC South: Quantile plots comparing the base case to alternative runs (all with M*=0.35 and using OS growth) that vary by knife-edge recruitment age* k*, where* $k \in \{3, 4, 5\}$*. Quantile box delimiters are detailed in Figure F.43.*

F.3.3. Model Average Composite – South

Six alternative BC South runs were selected for inclusion to the Model Average posterior based on the following criteria (see Tables F.13 and F.15):

- use model runs where the median $F_{\max}$ across MCMC samples was < 2;
- add model runs where median annual F_t was > 2 only once;
- remove model runs with poor diagnostics (rank > 2).

For the BC South stock, these criteria selected 6 out of 11 models:

- S00: M.30+k3 (rank=2.0, med.$F_{\max}$=0.28, no.yrs med.$F_t > 2$ =0)
- S01: M.30+k4 (rank=2.0, med.$F_{\max}$=18.3, no.yrs med.$F_t > 2$ =1)
- S03: M.25+k3 (rank=1.0, med.$F_{\max}$=0.49, no.yrs med.$F_t > 2$ =0)
- S04: M.25+k4 (rank=1.5, med.$F_{\max}$=18.3, no.yrs med.$F_t > 2$ =1)
- S06: M.35+k3 (rank=2.0, med.$F_{\max}$=0.12, no.yrs med.$F_t > 2$ =0)
- S07: M.35+k4 (rank=2.0, med.$F_{\max}$=14.2, no.yrs med.$F_t > 2$ =1)

Table F.17 gives the model-based and HRP-based quantities (0.05, 0.50, and 0.95 quantiles) from the model average posterior based on 6000 pooled MCMC samples. Table F.19 gives the decision table for this Model Average Composite scenario, showing the probabilities that B_{2019} will exceed various reference points. Figure F.46 shows the stock status B_{2017}/B_{avg} of the Model Average Composite scenario and the 6 models that contribute to the composite model. Finally, Tables F.20–F.25 show the 2-y decision tables for scenarios contributing to the composite.

Table F.17. BC South: The 5th, 50th, and 95th percentiles of MCMC-derived quantities from 6000 MCMC samples comprising the Model Average Composite scenario. Definitions: B_{2017} – current year spawning biomass, B_{avg} – average biomass from 1967 to 2016, $B_{\min}$ – minimum biomass that acts as the LRP (and USR = 2LRP), u_{2016} – harvest rate (ratio of total catch to vulnerable biomass) in the middle of 2016, and u_{avg} – average harvest rate from 1967 to 2016. All biomass values are in tonnes. For reference, the average catch over the last 5 years (2011-2015) is 3256 t.

	5%	50%	95%
Model-based			
B_{2017}	12,737	28,923	317,629
B_{avg}	16,938	33,487	292,976
B_{2017}/B_{avg}	0.589	0.899	1.35
u_{2016}	0.00787	0.0829	0.171
HRP-based			
$B_{\min}$	1,543	6,520	58,110
$2B_{\min}$	3,086	13,041	116,219
$B_{\min}/B_{\text{avg}}$	0.0753	0.138	0.296
$2B_{\min}/B_{\text{avg}}$	0.150	0.277	0.593
$B_{2017}/B_{\min}$	2.33	6.77	10.8
u_{avg}	0.0113	0.119	0.195
u_{2016}/u_{avg}	0.589	0.772	1.00

Table F.18. BC South: Decision table for the Model Average Composite scenario for 5 reference points – the current year spawning biomass, the limit reference point $B_{\min}$, the upper stock reference $2B_{\min}$, the average spawning stock biomass from 1967 to 2016, and the average harvest rate over the same time period – for projection-year biomass B_{2018} and mid-year harvest rate u_{2017} for a range of constant catch strategies (in tonnes). Each value is the probability that projected biomass or harvest rate is greater than the indicated reference point. The probabilities are the proportion of MCMC samples from 6 pooled scenarios chosen for their well-behaved MCMC diagnostics. The probabilities that current-year spawning biomass (or harvest rate) is greater than the reference points are: P($B_{2017} > B_{\min}$) = 1, P($B_{2017} > 2B_{\min}$) = 0.96, P($B_{2017} > B_{\text{avg}}$) = 0.34, and P($u_{2016} > u_{\text{avg}}$) = 0.05. For reference, the average catch over the last 5 years (2011-2015) is 3256 t.

Catch	P$\left(\frac{B_{2018}>}{B_{2017}}\right)$	P$\left(\frac{B_{2018}>}{B_{\min}}\right)$	P$\left(\frac{B_{2018}>}{2B_{\min}}\right)$	P$\left(\frac{B_{2018}>}{B_{\text{avg}}}\right)$	P$\left(\frac{u_{2017}>}{u_{\text{avg}}}\right)$
0	0.05	1	0.96	0.20	0
500	0.03	1	0.95	0.19	0
1000	0.02	1	0.95	0.18	0
1500	0.01	1	0.95	0.16	0
1750	0.01	1	0.95	0.16	0.02
2000	0.01	1	0.95	0.16	0.07
2250	0.01	1	0.95	0.15	0.20
2500	0.01	1	0.95	0.15	0.38
2750	0.01	0.99	0.95	0.15	0.56
3000	0	0.99	0.95	0.14	0.73
3250	0	0.99	0.95	0.14	0.85
3500	0	0.99	0.95	0.13	0.93
4000	0	0.99	0.95	0.13	0.99
4500	0	0.99	0.94	0.12	1
5000	0	0.98	0.94	0.11	1
5500	0	0.98	0.94	0.11	1
6000	0	0.98	0.93	0.10	1
6500	0	0.97	0.93	0.10	1
7000	0	0.97	0.93	0.10	1
8000	0	0.97	0.91	0.09	1
9000	0	0.96	0.87	0.09	1
10000	0	0.94	0.82	0.08	1

Table F.19. BC South: Decision table for the Model Average Composite scenario for 5 reference points – the current year spawning biomass, the limit reference point B_{min}, the upper stock reference $2B_{\mathrm{min}}$, the average spawning stock biomass from 1967 to 2016, and the average harvest rate over the same time period – for projection-year biomass B_{2019} and mid-year harvest rate u_{2018} for a range of constant catch strategies (in tonnes). Each value is the probability that projected biomass or harvest rate is greater than the indicated reference point. The probabilities are the proportion of MCMC samples from 6 pooled scenarios chosen for their well-behaved MCMC diagnostics. The probabilities that current-year spawning biomass (or harvest rate) is greater than the reference points are: P($B_{2017} > B_{\mathrm{min}}$) = 1, P($B_{2017} > 2B_{\mathrm{min}}$) = 0.96, P($B_{2017} > B_{\mathrm{avg}}$) = 0.34, and P($u_{2016} > u_{\mathrm{avg}}$) = 0.05. For reference, the average catch over the last 5 years (2011-2015) is 3256 t.

Catch	P$\left(\frac{B_{2019}>}{B_{2017}}\right)$	P$\left(\frac{B_{2019}>}{B_{\mathrm{min}}}\right)$	P$\left(\frac{B_{2019}>}{2B_{\mathrm{min}}}\right)$	P$\left(\frac{B_{2019}>}{B_{\mathrm{avg}}}\right)$	P$\left(\frac{u_{2018}>}{u_{\mathrm{avg}}}\right)$
0	0.04	1	0.95	0.09	0
500	0.02	1	0.94	0.08	0
1000	0.01	1	0.94	0.07	0
1500	0	0.99	0.94	0.06	0.04
1750	0	0.99	0.94	0.05	0.15
2000	0	0.99	0.93	0.05	0.32
2250	0	0.98	0.93	0.05	0.52
2500	0	0.98	0.93	0.05	0.70
2750	0	0.98	0.93	0.04	0.84
3000	0	0.98	0.92	0.04	0.93
3250	0	0.97	0.92	0.04	0.97
3500	0	0.97	0.91	0.04	0.99
4000	0	0.96	0.89	0.04	1
4500	0	0.95	0.84	0.03	1
5000	0	0.94	0.79	0.03	1
5500	0	0.91	0.73	0.03	1
6000	0	0.87	0.67	0.03	1
6500	0	0.81	0.63	0.02	1
7000	0	0.76	0.58	0.02	1
8000	0	0.69	0.52	0.02	1
9000	0	0.63	0.48	0.02	1
10000	0	0.59	0.46	0.02	1

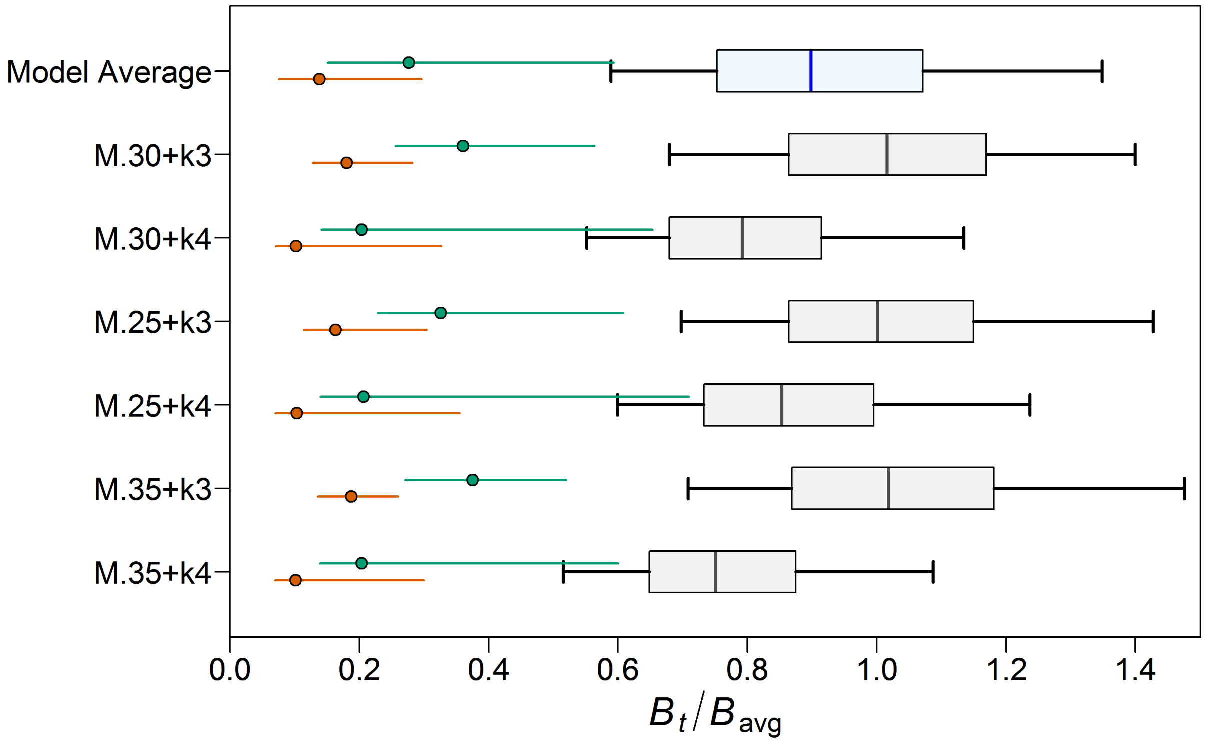

Figure F.46. BC South: Status of the current stock B_{2017} relative to B_{avg} with the dashed lines showing historical reference points ($B_{\mathrm{min}}/B_{\mathrm{avg}}$, $2B_{\mathrm{min}}/B_{\mathrm{avg}}$) that mimic DFO Precautionary Approach provisional MSY-based reference points, and 0.4B_{avg} as a proxy for 0.4B_0. Stock status is shown for the Model Average Composite scenario comprising 6 pooled model runs and for each of the 6 model runs (see Table F.13) for definitions of these model runs). Boxplots show the 5, 25, 50, 75 and 95 percentiles from the MCMC results. M = instantaneous natural mortality (y^{-1}); k = age(y) at knife-edge recruitment.

Table F.20. BC South: Decision table for case S00: M.30+k3 for 5 reference points – the current year spawning biomass, the limit reference point $B_{\min}$, the upper stock reference $2B_{\min}$, the average spawning stock biomass from 1967 to 2016, and the average harvest rate over the same time period – for projection-year biomass B_{2019} and mid-year harvest rate u_{2018} for a range of constant catch strategies (in tonnes). Each value is the probability that projected biomass or harvest rate is greater than the indicated reference point. The probabilities that current-year spawning biomass (or harvest rate) is greater than the reference points are: P($B_{2017} > B_{\min}$) = 1, P($B_{2017} > 2B_{\min}$) = 0.99, P($B_{2017} > B_{\text{avg}}$) = 0.53, and P($u_{2016} > u_{\text{avg}}$) = 0.02. For reference, the average catch over the last 5 years (2011-2015) is 3256 t.

Catch	P$\left(\frac{B_{2019}>}{B_{2017}}\right)$	P$\left(\frac{B_{2019}>}{B_{\min}}\right)$	P$\left(\frac{B_{2019}>}{2B_{\min}}\right)$	P$\left(\frac{B_{2019}>}{B_{\text{avg}}}\right)$	P$\left(\frac{u_{2018}>}{u_{\text{avg}}}\right)$
0	0	1	0.96	0.12	0
500	0	1	0.95	0.11	0
1000	0	1	0.95	0.10	0
1500	0	1	0.94	0.10	0
1750	0	1	0.94	0.10	0.01
2000	0	1	0.94	0.10	0.08
2250	0	1	0.94	0.09	0.24
2500	0	1	0.93	0.08	0.49
2750	0	1	0.93	0.08	0.71
3000	0	1	0.93	0.08	0.86
3250	0	1	0.93	0.08	0.95
3500	0	1	0.93	0.07	0.99
4000	0	1	0.92	0.07	1
4500	0	1	0.92	0.06	1
5000	0	0.99	0.92	0.06	1
5500	0	0.99	0.91	0.05	1
6000	0	0.99	0.91	0.05	1
6500	0	0.99	0.90	0.04	1
7000	0	0.99	0.90	0.04	1
8000	0	0.99	0.89	0.04	1
9000	0	0.98	0.88	0.03	1
10000	0	0.97	0.86	0.03	1

Table F.21. BC South: Decision table for case S01: M.30+k4 for 5 reference points – the current year spawning biomass, the limit reference point $B_{\min}$, the upper stock reference $2B_{\min}$, the average spawning stock biomass from 1967 to 2016, and the average harvest rate over the same time period – for projection-year biomass B_{2019} and mid-year harvest rate u_{2018} for a range of constant catch strategies (in tonnes). Each value is the probability that projected biomass or harvest rate is greater than the indicated reference point. The probabilities that current-year spawning biomass (or harvest rate) is greater than the reference points are: P($B_{2017} > B_{\min}$) = 1, P($B_{2017} > 2B_{\min}$) = 0.94, P($B_{2017} > B_{\text{avg}}$) = 0.14, and P($u_{2016} > u_{\text{avg}}$) = 0.10. For reference, the average catch over the last 5 years (2011-2015) is 3256 t.

Catch	P$\left(\frac{B_{2019}>}{B_{2017}}\right)$	P$\left(\frac{B_{2019}>}{B_{\min}}\right)$	P$\left(\frac{B_{2019}>}{2B_{\min}}\right)$	P$\left(\frac{B_{2019}>}{B_{\text{avg}}}\right)$	P$\left(\frac{u_{2018}>}{u_{\text{avg}}}\right)$
0	0.07	1	0.92	0.03	0
500	0.03	1	0.92	0.02	0
1000	0.02	0.99	0.92	0.01	0
1500	0.01	0.98	0.92	0.01	0.06
1750	0	0.98	0.92	0	0.29
2000	0	0.97	0.92	0	0.58
2250	0	0.97	0.92	0	0.81
2500	0	0.96	0.92	0	0.92
2750	0	0.96	0.92	0	0.97
3000	0	0.95	0.91	0	0.99
3250	0	0.94	0.90	0	1
3500	0	0.94	0.89	0	1
4000	0	0.92	0.85	0	1
4500	0	0.90	0.78	0	1
5000	0	0.88	0.66	0	1
5500	0	0.82	0.53	0	1
6000	0	0.74	0.41	0	1
6500	0	0.62	0.32	0	1
7000	0	0.53	0.24	0	1
8000	0	0.38	0.12	0	1
9000	0	0.28	0.07	0	1
10000	0	0.21	0.04	0	1

Table F.22. BC South: Decision table for case S03: M.25+k3 for 5 reference points – the current year spawning biomass, the limit reference point $B_{\min}$, the upper stock reference $2B_{\min}$, the average spawning stock biomass from 1967 to 2016, and the average harvest rate over the same time period – for projection-year biomass B_{2019} and mid-year harvest rate u_{2018} for a range of constant catch strategies (in tonnes). Each value is the probability that projected biomass or harvest rate is greater than the indicated reference point. The probabilities that current-year spawning biomass (or harvest rate) is greater than the reference points are: P($B_{2017} > B_{\min}$) = 1, P($B_{2017} > 2B_{\min}$) = 0.98, P($B_{2017} > B_{\text{avg}}$) = 0.50, and P($u_{2016} > u_{\text{avg}}$) = 0.02. For reference, the average catch over the last 5 years (2011-2015) is 3256 t.

Catch	P$\left(\frac{B_{2019}>}{B_{2017}}\right)$	P$\left(\frac{B_{2019}>}{B_{\min}}\right)$	P$\left(\frac{B_{2019}>}{2B_{\min}}\right)$	P$\left(\frac{B_{2019}>}{B_{\text{avg}}}\right)$	P$\left(\frac{u_{2018}>}{u_{\text{avg}}}\right)$
0	0	1	0.95	0.20	0
500	0	1	0.95	0.18	0
1000	0	1	0.94	0.15	0
1500	0	1	0.93	0.14	0
1750	0	1	0.93	0.13	0
2000	0	1	0.93	0.12	0.05
2250	0	1	0.93	0.11	0.19
2500	0	1	0.92	0.11	0.43
2750	0	1	0.92	0.10	0.67
3000	0	1	0.91	0.10	0.83
3250	0	1	0.91	0.09	0.93
3500	0	1	0.91	0.09	0.97
4000	0	1	0.90	0.08	0.99
4500	0	1	0.90	0.07	1
5000	0	0.99	0.90	0.06	1
5500	0	0.99	0.89	0.05	1
6000	0	0.99	0.88	0.05	1
6500	0	0.99	0.88	0.04	1
7000	0	0.98	0.87	0.04	1
8000	0	0.97	0.86	0.03	1
9000	0	0.95	0.84	0.02	1
10000	0	0.93	0.80	0.02	1

Table F.23. BC South: Decision table for case S04: M.25+k4 for 5 reference points – the current year spawning biomass, the limit reference point $B_{\min}$, the upper stock reference $2B_{\min}$, the average spawning stock biomass from 1967 to 2016, and the average harvest rate over the same time period – for projection-year biomass B_{2019} and mid-year harvest rate u_{2018} for a range of constant catch strategies (in tonnes). Each value is the probability that projected biomass or harvest rate is greater than the indicated reference point. The probabilities that current-year spawning biomass (or harvest rate) is greater than the reference points are: P($B_{2017} > B_{\min}$) = 1, P($B_{2017} > 2B_{\min}$) = 0.94, P($B_{2017} > B_{\text{avg}}$) = 0.24, and P($u_{2016} > u_{\text{avg}}$) = 0.07. For reference, the average catch over the last 5 years (2011-2015) is 3256 t.

Catch	P$\left(\frac{B_{2019}>}{B_{2017}}\right)$	P$\left(\frac{B_{2019}>}{B_{\min}}\right)$	P$\left(\frac{B_{2019}>}{2B_{\min}}\right)$	P$\left(\frac{B_{2019}>}{B_{\text{avg}}}\right)$	P$\left(\frac{u_{2018}>}{u_{\text{avg}}}\right)$
0	0.07	1	0.93	0.08	0
500	0.03	1	0.93	0.06	0
1000	0.01	0.99	0.92	0.04	0
1500	0.01	0.98	0.92	0.02	0.03
1750	0	0.98	0.92	0.01	0.17
2000	0	0.98	0.92	0.01	0.44
2250	0	0.97	0.92	0.01	0.66
2500	0	0.97	0.92	0	0.83
2750	0	0.97	0.92	0	0.94
3000	0	0.96	0.92	0	0.98
3250	0	0.95	0.91	0	0.99
3500	0	0.95	0.91	0	1
4000	0	0.94	0.89	0	1
4500	0	0.93	0.83	0	1
5000	0	0.90	0.74	0	1
5500	0	0.86	0.63	0	1
6000	0	0.79	0.52	0	1
6500	0	0.68	0.43	0	1
7000	0	0.58	0.33	0	1
8000	0	0.43	0.16	0	1
9000	0	0.27	0.07	0	1
10000	0	0.18	0.03	0	1

Table F.24. BC South: Decision table for case S06: M.35+k3 for 5 reference points – the current year spawning biomass, the limit reference point $B_{\min}$, the upper stock reference $2B_{\min}$, the average spawning stock biomass from 1967 to 2016, and the average harvest rate over the same time period – for projection-year biomass B_{2019} and mid-year harvest rate u_{2018} for a range of constant catch strategies (in tonnes). Each value is the probability that projected biomass or harvest rate is greater than the indicated reference point. The probabilities that current-year spawning biomass (or harvest rate) is greater than the reference points are: P($B_{2017} > B_{\min}$) = 1, P($B_{2017} > 2B_{\min}$) = 1, P($B_{2017} > B_{\text{avg}}$) = 0.53, and P($u_{2016} > u_{\text{avg}}$) = 0.01. For reference, the average catch over the last 5 years (2011-2015) is 3256 t.

Catch	P$\left(\frac{B_{2019}>}{B_{2017}}\right)$	P$\left(\frac{B_{2019}>}{B_{\min}}\right)$	P$\left(\frac{B_{2019}>}{2B_{\min}}\right)$	P$\left(\frac{B_{2019}>}{B_{\text{avg}}}\right)$	P$\left(\frac{u_{2018}>}{u_{\text{avg}}}\right)$
0	0	1	0.98	0.09	0
500	0	1	0.97	0.09	0
1000	0	1	0.97	0.09	0
1500	0	1	0.97	0.08	0
1750	0	1	0.97	0.08	0.02
2000	0	1	0.97	0.08	0.11
2250	0	1	0.97	0.08	0.36
2500	0	1	0.97	0.07	0.60
2750	0	1	0.97	0.07	0.79
3000	0	1	0.97	0.07	0.90
3250	0	1	0.97	0.07	0.95
3500	0	1	0.97	0.07	0.98
4000	0	1	0.97	0.06	1
4500	0	1	0.97	0.06	1
5000	0	1	0.97	0.06	1
5500	0	1	0.96	0.06	1
6000	0	1	0.96	0.06	1
6500	0	1	0.96	0.06	1
7000	0	1	0.96	0.05	1
8000	0	1	0.96	0.05	1
9000	0	1	0.96	0.05	1
10000	0	1	0.95	0.04	1

Table F.25. BC South: Decision table for case S07: M.35+k4 for 5 reference points – the current year spawning biomass, the limit reference point $B_{\min}$, the upper stock reference $2B_{\min}$, the average spawning stock biomass from 1967 to 2016, and the average harvest rate over the same time period – for projection-year biomass B_{2019} and mid-year harvest rate u_{2018} for a range of constant catch strategies (in tonnes). Each value is the probability that projected biomass or harvest rate is greater than the indicated reference point. The probabilities that current-year spawning biomass (or harvest rate) is greater than the reference points are: P($B_{2017} > B_{\min}$) = 1, P($B_{2017} > 2B_{\min}$) = 0.94, P($B_{2017} > B_{\text{avg}}$) = 0.11, and P($u_{2016} > u_{\text{avg}}$) = 0.09. For reference, the average catch over the last 5 years (2011-2015) is 3256 t.

Catch	P$\left(\frac{B_{2019}>}{B_{2017}}\right)$	P$\left(\frac{B_{2019}>}{B_{\min}}\right)$	P$\left(\frac{B_{2019}>}{2B_{\min}}\right)$	P$\left(\frac{B_{2019}>}{B_{\text{avg}}}\right)$	P$\left(\frac{u_{2018}>}{u_{\text{avg}}}\right)$
0	0.07	1	0.93	0.02	0
500	0.03	0.99	0.93	0.01	0
1000	0.02	0.99	0.93	0.01	0
1500	0.01	0.98	0.93	0.01	0.13
1750	0.01	0.97	0.93	0	0.38
2000	0.01	0.96	0.93	0	0.66
2250	0.01	0.96	0.93	0	0.84
2500	0	0.95	0.92	0	0.93
2750	0	0.95	0.91	0	0.98
3000	0	0.94	0.90	0	0.99
3250	0	0.94	0.88	0	1
3500	0	0.94	0.86	0	1
4000	0	0.92	0.79	0	1
4500	0	0.89	0.68	0	1
5000	0	0.85	0.57	0	1
5500	0	0.77	0.46	0	1
6000	0	0.69	0.36	0	1
6500	0	0.59	0.27	0	1
7000	0	0.50	0.19	0	1
8000	0	0.37	0.12	0	1
9000	0	0.29	0.07	0	1
10000	0	0.24	0.05	0	1

F.4. REFERENCES – MODEL RESULTS

DFO. 2009. A fishery decision-making framework incorporating the Precautionary Approach. (Accessed 18 March 2015).

Dorn, M., Aydin, K., Barbeaux, S., Jones, D., Spalinger, K. and Palsson, W. 2012. Chapter 1. Assessment of the Walleye Pollock stock in the Gulf of Alaska. In NPFMC Gulf of Alaska SAFE, p. 53–182. North Pacific Fisheries Management Council.

Dorn, M., Aydin, K., Jones, D., McCarthy, A., Palsson, W. and Spalinger, K. 2015. Chapter 1. Assessment of the Walleye Pollock stock in the Gulf of Alaska. In NPFMC Gulf of Alaska SAFE, p. 49–172. North Pacific Fisheries Management Council.

Gustafson, R.G., Lenarz, W.H., McCain, B.B., Schmitt, C.C., Grant, W.S., Builder, T.L. and Methot, R.D. 2000. Status review of Pacific Hake, Pacific Cod, and Walleye Pollock from Puget Sound, Washington. NOAA Technical Memorandum NMFS-NWFSC-44: 275 p.

Janusz, J. and Horbowy, J. 1997. The state of the walleye pollock in the northern part of the Okhotsk Sea, North Pacific. Fish. Res. 30(1-2): 87–102.

Saunders, M.W., McFarlane, G.A. and Shaw, W. 1989. Delineation of Walleye Pollock (*Theragra chalcogramma*) stocks off the Pacific Coast of Canada. In Proc. Int. Symp. Biol. Mgmt. Walleye Pollock, Anchorage, AK, Nov 14-16, 1988, Lowell Wakefield Fisheries Symposia Series 7, Alaska Sea Grant Rep. 89-1, p. 379–401. Alaska Sea Grant College Program, University of Alaska, Fairbanks, AK.

Schnute, J. 1985. A general theory for analysis of catch and effort data. Can. J. Fish. Aquat. Sci. 42(3): 414–429.

Starr, P.J. and Haigh, R. 2017. Stock assessment of the coastwide population of Shortspine Thornyhead (*Sebastolobus alascanus*) in 2015 off the British Columbia coast. DFO Can. Sci. Advis. Sec. Res. Doc. 2017/015: ix + 174 p.